



UNIVERSIDAD DE CHILE
FACULTAD DE CIENCIAS FÍSICAS Y MATEMÁTICAS
DEPARTAMENTO DE GEOLOGÍA

EVOLUCIÓN TECTÓNICA Y CONFIGURACIÓN ACTUAL DE LOS ANDES CENTRALES DEL SUR ($34^{\circ}45'$ - $35^{\circ}30'$ S)

TESIS PARA OPTAR AL GRADO DE DOCTOR EN CIENCIAS, MENCIÓN
GEOLOGÍA

FELIPE FERNANDO TAPIA SILVA

PROFESOR GUÍA
MARCELO FARÍAS THIERS

MIEMBROS DE LA COMISIÓN
REYNALDO CHARRIER GONZÁLEZ
CÉSAR ARRIAGADA ORTEGA
ANDRÉS FOLGUERA

SANTIAGO DE CHILE,
MARZO 2015

RESUMEN DE LA TESIS PARA
OPTAR AL GRADO DE DOCTOR
EN CIENCIAS MENCIÓN GEOLOGÍA

Por: Felipe Tapia Silva
Fecha: 24/03/2015
Prof. Guía: Marcelo Farías Thiers

Evolución tectónica y configuración actual de los Andes Centrales del sur (34°45'-35°30'S)

La evolución neógena de los Andes Centrales al sur del segmento de subducción plana ha sido ampliamente estudiada aunque sin haberse logrado un consenso acerca del origen de las variaciones en el estilo estructural, la edad de la deformación, el espesor cortical y la cantidad de acortamiento, entre otros, que muestra el orógeno a lo largo del rumbo. Mediante análisis cronoestratigráficos y estructurales, el presente estudio persigue caracterizar los períodos de deformación que experimentaron los Andes desde el Mesozoico hasta el presente, entre 34°45' y 35°30'S, con el fin de establecer su influencia en la construcción neógena del orógeno y en las diferencias que presenta este a lo largo del rumbo.

Los resultados muestran que la deformación contraccional durante el Neógeno se caracterizó tanto por la reactivación de estructuras normales previas como por la generación de nuevas fallas. Estas estructuras involucraron el basamento en la deformación, desarrollando un estilo de piel gruesa favorecido por la presencia de fallas normales asociadas a las cuencas extensionales que caracterizaron la evolución de este segmento de los Andes durante el Mesozoico y Cenozoico.

Asimismo, se pudieron reconocer dos pulsos de deformación contraccional previos al Neógeno que afectaron a esta región durante el Cretácico Superior y el Paleoceno. Sin embargo, no se pudo cuantificar la cantidad de acortamiento acomodado durante estos períodos, lo que imposibilita reconocer su influencia en períodos de deformación posteriores.

Durante la deformación de la vertiente occidental de la cordillera (20-11 Ma), cerca de 18 km de acortamiento fueron acomodados en la corteza superior, mientras que la faja plegada y corrida de Malargüe acomodó 30 km, implicando una variación mínima con el acortamiento acomodado por la Cordillera Principal a los 33°30'S. No obstante, el porcentaje de acortamiento disminuye hacia el sur debido a que la deformación se distribuyó en una región más amplia. De esta forma, se establece que la disminución de acortamiento hacia el sur que presenta el orógeno, se originaría por la ausencia de la Cordillera Frontal al sur de 34°40'S, lo cual sería consecuencia directa de la menor cantidad de deformación que experimentó la corteza.

Esta menor cantidad de deformación y acortamiento tendría implicancias directas en la forma en cómo se deforma la corteza. Es así como el acortamiento acomodado por la corteza superior ha sido transformado en engrosamiento cortical in-situ implicando un modo de deformación en cizalle puro, contrastando con el modo de cizalle simple que dominaría al norte de 35°S.

Finalmente, si bien, la evolución y arquitectura previa influye sobre el estilo de deformación de la corteza, la cantidad de deformación que experimenta el continente es la responsable de que la segmentación de los Andes, quedando aún por dilucidar si esto depende de la cantidad de deformación que puede acomodar la placa superior o a variaciones a lo largo de la placa subductada.

*“El aspecto más triste de la vida actual
es que la ciencia gana en conocimiento
más rápidamente que la sociedad en sabiduría”*

(Isaac Asimov)

AGRADECIMIENTOS

Quisiera comenzar agradeciendo a todas las personas que me escucharon pelar el cable durante estos 5 años. Siempre es necesario verbalizar los pensamientos para ordenar las ideas.

A Marcelo, gracias por todo. Por la amistad, la paciencia, la dedicación y sobre toda la confianza que siempre me brindaste para realizar mi trabajo. Al profesor Reynaldo con quien compartí innumerables conversaciones y donde aprendí de los Andes más que en cualquier libro. Asimismo un agradecimiento a Maximiliano Naipauer con quien tuve el agrado de trabajar. También agradecer a César Arriagada y Andrés Folguera por participar del jurado de esta tesis.

Una mitad del trabajo en Santiago. Mis agradecimientos a todos los que pasaron por la sala de postgrado en estos 5 años, a los antiguos amigos y a los nuevos amigos. A mis amigos-compañeros de doctorado Feña, Pablo y Viole con quienes compartí el parto de esta tesis, así como un montón de ideas, discusiones, “comete un paper”, almuerzos, cervezas y otras cosas. Al dani, la pita, junior, la feñi, al boyce, shorty, el pelao, la vale, el vladi, el mumo y muchos más. Perdón que no los nombre a todos, pero sepan todos los que lean estas palabras, que en esa sala es donde se vive el día a día del quehacer científico, que son los integrantes de esa sala la punta de la flecha de la ciencia que se hace en la universidad. También agradecer a Marcia, Daniel, Juanito, Atax, Pajaro por sus comentarios, discusiones y apoyo.

La otra mitad en Baires. En la UBA conocí a grandes personas con las cuales espero seguir compartiendo algunos años más. A todos los chicos de la 101, Jony, Bruno, Miguelito y Guido, por recibirme y darme un espacio de trabajo cuando me aparecía por allá. A Tito, Dani, Jere, Lucas, Andrés y toda la gente buena onda con quien disfruté estos últimos años.

Nada de esto podría ser posible sin la ayuda de mi familia. Gracias a mis padres por el apoyo incondicional en todas las ideas y proyectos que he emprendido. A mi hermano, la Vicky y la Fran, por su ayuda, amor y apoyo. A mis tíos y tíos, abuelas, primos, gracias a todos.

Por último agradecer a Lú, mi compañera en toda esta travesía que decidimos emprender hace algunos años atrás. Gracias por la paciencia, la comprensión y por tu amor. Todo este trabajo fue mucho más alegre y fácil porque tú estabas ahí.

Y como dijo una amiga hace un par de años, y que reafirmó otro amigo hace muy poco en sus agradecimientos, gracias a todos los que luchan.

Este trabajo de tesis fue financiado por los proyectos Fondecyt 11085022 y 1120272.

TABLA DE CONTENIDO

CAPÍTULO I: INTRODUCCIÓN

I.1	Motivación y Presentación	1
I.2	LOS ANDES DE CHILE Y ARGENTINA CENTRAL: EVOLUCIÓN Y PROBLEMÁTICA.....	3
I.2.1	Rasgos generales y evolución de los Andes Centrales del sur	3
I.2.2	Exposición del Problema.....	6
I.3	Objetivos y metodologías	7
I.3.1	Objetivos del estudio.....	7
I.3.2	Metodología y actividades	8

CAPÍTULO II: LA CUENCA DE ABANICO: ARQUITECTURA Y EVOLUCIÓN DE UNA CUENCA DE INTRA-ARCO 10

II.1	Introducción.....	10
II.2	El Basamento de la Cuenca de Abanico.....	12
II.2.1	BRCU	16
II.2.2	Unidad Guanaco	19
II.3	Formación Abanico y la extensión paleógena.....	67
II.4	Inversión de la Cuenca de Abanico: Estructura actual de Cordillera Principal occidental	24
II.5	Modelo estructural de la Cordillera Principal occidental a 35°S	33
II.6	Análisis complementario: El Cretácico Tardío en la Cordillera Principal occidental y sus implicancias regionales	35

CAPÍTULO III: LA FAJA PLEGADA Y CORRIDA DE MALARGÜE Y LA INFLUENCIA DE ESTRUCTURAS PREVIAS EN SU EVOLUCIÓN 43

III.1	Introducción.....	43
III.2	Arquitectura Previa: La Extensión mesozoica	44
III.2.1	Resultados	46
III.2.2	Interpretación de los resultados: Áreas de aporte e implicancias para la evolución jurásica	50
III.2.3	Modelo evolutivo para el Triásico Tardío al Jurásico Tardío	51

III.3 Evolución neógena. Artículo: "Controls of the overriding plate architecture inthe along-strike Andean segmentations: insight into the Malargüe fold-and-thrusts belt, southern Central Andes."	54
--	----

CAPÍTULO IV: EVOLUCIÓN DE LA REGIÓN AXIAL DE LA CORDILLERA PRINCIPAL 93

IV.1 Introducción.....	93
IV.2 Artículo: "Late Cenozoic contractional evolution of the current arc region along the southern Central Andes (35°20'S)"	94

CAPÍTULO V:LA CONSTRUCCIÓN DEL ORÓGENO ANDINO: SÍNTESIS Y DISCUSIÓN

V.1 Evolución estructural de los Andes a 35°S	129
V.2 Análisis comparativo a lo largo de los Andes de Chile central y el oeste de Argentina.....	1133
V.2.1 La arquitectura cortical y modo de deformación	133
V.2.2 Diferencias latitudinales en la cantidad de deformación y el acortamiento	144

CAPÍTULO VI: CONCLUSIONES GENERALES 150

BIBLIOGRAFÍA 152

ANEXO I: Publicaciones de coautor

ANEXO II: Resúmenes presentados a congresos y reuniones científicas

ANEXO III: Datos analíticos de dataciones U-Pb en circón

ANEXO IV: Material suplementario Tapia et al. Aceptado

ANEXO V: Ubicación muestras datadas

ÍNDICE DE FIGURAS

CAPÍTULO I

- Fig. I.1. Mapa geológico de los Andes entre 31 y 37°S 4

CAPÍTULO II

- Fig. II.1. Mapa geológico del área del valle del río Tinguiririca..... 4
- Fig. II.2. Diagramas de concordia para resultados analíticos de dataciones U-Pb en circones detríticos del BRCU 15
- Fig. II.3. Diagrama de concordia para los resultados analíticos de dataciones U-Pb en circones detríticos de la Fm. Colimapu en el sector del río Volcán 17
- Fig. II.4. Evidencias de fallas normales en la Unidad Guanaco 18
- Fig. II.5. Columnas estratigráficas de la Unidad Guanaco en la ladera norte y sur del valle del río Tinguiririca 20
- Fig. II.6. Columnas estratigráficas del Miembro Oriental y Occidental de la Fm. Abanico 22
- Fig. II.7. Estratos de crecimiento en la Fm. Abanico 23
- Fig. II.8. Bloque diagrama mostrando la arquitectura de la Cuenca de Abanico 25
- Fig. II.9. Deformación a lo largo del río Tinguiririca..... 27
- Fig. II.10. Deformación del miembro oriental del Fm. Abanico 28
- Fig. II.11. Columna estratigráfica de la Fm. Farellones en el cerro Alto del Padre 29
- Fig. II.12. Estratos de crecimiento Fm. Farellones 30
- Fig. II.13. Deformación del miembro superior de la Fm. Farellones en el cerro Alto del Padre .. 32
- Fig. II.14. Tren de pliegues sinclinal al oeste del río Azufre 33
- Fig. II.15. Perfil estructural a lo largo del valle del Tinguiririca..... 36
- Fig. II.16. Comparación entre las fms. del Gr. Neuquén y BRCU-Areniscas de Pichuante 39
- Fig. II.17. Evolución geológica y paleogeográfica del Cretácico Tardío a 35°S 41

CAPÍTULO III

- Fig. III.1. Mapa geológico simplificado de los Andes Centrales del sur 44

Fig. III.2. Mapa Geológico del área de estudio y ubicación de las 8 muestras analizadas.....	45
Fig. III.3. Diagramas de concordia para resultados analíticos de dataciones U-Pb en circones detríticos para las muestras de las fms. Lotena, La Manga, Río Damas y Tordillo	47
Fig. III.4. Histogramas de frecuencia y probabilidad relativa de las edades U-Pb en circón detrítico de las muestras de las fms. La Manga, Lotena, Río Damas y Tordillo.....	49
Fig. III.5. Principales áreas de proveniencia de sedimentos para las rocas del Jurásico Medio y Tardío en la porción norte de la Cuenca Neuquina	51
Fig. III.6 Evolución geológica y paleogeográfica en perfiles esquemáticos en torno a 35°S desde el Triásico Tardío hasta Cretácico Temprano.....	53

CAPÍTULO V

Fig. V.1. Cuadro comparativo de la evolución neógena de los Andes de Chile central y el oeste de Argentina	130
Fig. V.2. Arquitectura cortical de los Andes Centrales del sur entre 33° y 36°S.....	134
Fig. V.3. Espesor cortical de los Andes Centrales del Sur entre 30° y 40°S.....	135
Fig. V.4. Modelo evolutivo del engrosamiento cortical de los Andes Centrales del sur a 35°S. .	139
Fig. V.5. Sección esquemática del margen occidental de Sudamérica.....	148

ÍNDICE DE TABLAS

CAPÍTULO III

Tabla. III.1. Muestras estudiadas y cantidad de análisis realizados y rechazados para cada una de ellas.....	46
--	----

CAPÍTULO V

Tabla V.1. Calculo del engrosamiento y el espesor inicial de los dominios estructurales de la Cordillera Principal a partir de los valores de acortamiento estimados.	137
Tabla V.2. Comparación del acortamiento tectónico entre 33°30'S y 35°S.....	144

CAPÍTULO I.

INTRODUCCIÓN

I.1 Motivación y presentación

Los Andes son una cadena montañosa activa formada en un margen convergente, el cual se caracteriza por la subducción de la placa oceánica de Nazca bajo la placa continental Sudamericana. Una de las principales características del orógeno andino corresponde a la segmentación estructural que presenta latitudinal, longitudinal y temporalmente. Dicha segmentación queda de manifiesto al observar la variación de estilos estructurales, mecanismos de deformación, espesor cortical, altura o ancho de la cordillera, entre otros, implicando cambios en la arquitectura cortical a lo largo de la cordillera.

Es ampliamente aceptado que la evolución y segmentación de los Andes tiene una relación de primer orden con las variaciones espaciales y temporales de los parámetros que definen la dinámica de la subducción y la transmisión de los esfuerzos a la placa Sudamericana. Sin embargo, existen otros factores, de segundo orden, que controlan de forma local la construcción de la cordillera, y que aún son materia de discusión. *¿Son las características intrínsecas de la placa subductada el principal control en la dinámica de subducción?, ¿Cuál es el papel real que juegan las características de la placa continental en las variaciones de la dinámica de subducción?* Cualquier investigación que se refiera a estos temas, en primer lugar, debe considerar la identificación de los cambios en la dinámica de la subducción para así determinar las variables que controlan el sistema. En este sentido, el estudio de la evolución estructural de la corteza continental permite asociar las variaciones presentes en el desarrollo del orógeno y los cambios en los parámetros involucrados en la dinámica de subducción, debido a las implicancias directas que tiene ésta en la deformación de la placa superior.

En este contexto, los Andes Centrales del sur, considerados como el segmento andino comprendido entre los 27° y 40°S, presentan diversas características que evidencian variaciones en los procesos que controlaron la construcción del orógeno en esta región: (1) el cambio de orientación de la fosa y la cadena andina, lo que marca el desarrollo del oroclino del Maipo, (2) una disminución hacia el sur de la altura de la cordillera,(3) del acortamiento tectónico de la corteza, y (4) del espesor cortical. Estas características hacen de los Andes Centrales del sur una región

propicia para el estudio de los factores que controlaron la arquitectura del orógeno debido a la fuerte segmentación y variabilidad estructural que existe dentro de esta zona de los Andes.

La presente Tesis de Doctorado se aboca al estudio de la evolución estructural de los Andes Centrales del sur durante el Neógeno y como la impronta de procesos ocurridos previamente a este periodo ha determinado este desarrollo. Con este fin, se estudió la estructura de la vertiente occidental y oriental de la cordillera entre $34^{\circ}45'$ y $35^{\circ}30'S$. En los últimos años numerosos trabajos han sugerido que existen diferencias en la evolución y arquitectura del orógeno, al norte y sur del segmento comprendido entre 35° y $36^{\circ}S$: al sur de este segmento, la evolución estaría controlada por la somerización y empinamiento de la losa oceánica durante el Mioceno, mientras que al norte este proceso no ha sido reconocido (Ramos et al., 2014 y referencias ahí). Esto sugiere que esta zona es clave para comprender las diferencias en la evolución a lo largo de los Andes. Adicionalmente, los múltiples trabajos realizados en la vertiente argentina de la cordillera a estas latitudes constituyen una base para la construcción de modelos estructurales en el lado chileno de los Andes. Este trabajo se enmarca dentro de los proyectos FONDECYT 11085022 y 1120272.

Esta tesis se organiza en 6 capítulos. En las secciones siguientes a la presente introducción se presenta un resumen de la evolución de los Andes desde el Paleozoico hasta la actualidad. Posteriormente, y en base a lo anterior, se plantea la problemática en la cual se enfoca este estudio.

En particular, el área de estudio se enmarca dentro de lo que corresponde a la cordillera de Chile y Argentina entre $\sim 35^{\circ}$ y $35^{\circ}30'S$. Este sector se caracteriza por presentar dos dominios estructurales muy marcados: la Cuenca de Abanico y la faja plegada y corrida de Malargüe. En este sentido, en los Capítulos II y III se presentan los resultados obtenidos a partir del estudio de la evolución de los dos dominios estructurales mencionados anteriormente. Estos capítulos están enfocados principalmente en entender cómo, cuándo y cuánto se deformó la corteza en esas regiones. El Capítulo IV trata sobre la deformación en la región axial de la cordillera, la cual corresponde a la zona de transición entre la Cuenca de Abanico y la faja plegada y corrida de Malargüe, además es donde está ubicado el actual arco volcánico.

Finalmente, en el Capítulo V se integran todos los resultados obtenidos en este estudio para compararlos con otras regiones de los Andes, con el objeto de establecer cuáles pueden ser los principales factores que controlaron la segmentación andina, y en consecuencia, que intervienen durante la construcción de un orógeno en un margen de subducción, como lo son los Andes de Chile y Argentina central.

I.2 Los Andes de Chile y Argentina Central: Antecedentes y problemáticas

I.2.1 Rasgos generales y evolución de los Andes Centrales del Sur¹

Los Andes Centrales del Sur corresponden al segmento comprendido entre la zona de subducción horizontal (*ca* 27 y 33°S) y 40°S (Gansser, 1973). En esta región, el relieve andino está compuesto por diferentes unidades morfoestructurales dispuestas en franjas paralelas al margen continental y con una orientación N-S, desde los 33°S al norte, y NNE-SSW, al sur de los 34°S (Fig. I. 1). A lo largo de la región que comprende este estudio se pueden reconocer de oeste a este: Cordillera de la Costa, Depresión Central, Cordillera Principal, Cordillera Frontal, y el antepaís ubicado en territorio argentino (Fig. I. 1).

La Cordillera de la Costa no sobrepasa los 2200 m s.n.m y entre los ríos Tinguiririca y Bío-Bío tiene alturas máximas que oscilan entre 500-700 m s.n.m. Está conformada por granitoides y basamento metamórfico del Paleozoico Superior en su flanco occidental y por secuencias volcánicas y sedimentarias Mesozoicas en la parte más oriental (Fig. I.1) (Sellés y Gana, 2001; Sernageomin, 2003; Wall et al., 1999).

La Depresión Central se extiende desde los *ca.* 33°S por más de 1000 km, hasta los 40°S. Corresponde a un valle que contiene depósitos aluviales y volcánicos principalmente pleistocenos a holocenos (Fig. I. 1) (Farías et al., 2008; Thiele, 1980).

La Cordillera Principal se encuentra formada por rocas cenozoicas de las formaciones Abanico y Farellones, y por rocas mesozoicas fuertemente deformadas. Las primeras afloran tanto en la franja occidental como en la oriental de la Cordillera Principal, mientras que las otras se encuentran principalmente en la vertiente oriental de la misma, dispuestas en una dirección preferente N-S a NNE-SSW (Fig. I. 1) (Charrier et al., 2002, 2007, Farías et al., 2008, 2010; Fock et al., 2006).

La Cordillera Frontal corresponde a una provincia tectónica compuesta principalmente por rocas intrusivas y volcánicas del Pérmico-Triásico que afloran en territorio argentino al sur de 31 °S (Fig. I. 1).

El antepaís andino se presenta como el piedemonte oriental de la Cordillera de los Andes en esta región. Su elevación fluctúa entre los 900 a 1000 m s.n.m a 33°S, aumentando a 1300 m a los 36°S. El antepaís andino entre los 33°30' y 36°S se encuentra disectado por el Bloque de San Rafael, un bloque de basamento mesoproterozoico-paleozoico exhumado (Fig. I.1).

¹ Ver Charrier, R., Ramos, V., Tapia, F., Sagripanti, L., 2014. *Tectono-stratigraphic evolution of the Andean Orogen between 31 and 37°(Chile and Western Argentina)*, en: Sepúlveda, S.A., Giambiagi, L.B., Moreiras, S.M., Pinto, L., Tunik, M., Hoke, G.D. y Farías, M. (Eds), Geodynamics Processes in the Andes of Central Chile y Argentina. Geol. Soc. London, Spec. Publ. 399, doi 10.1144/SP399.20 (Anexo I) para una detallada descripción de la evolución de los Andes Centrales del Sur.

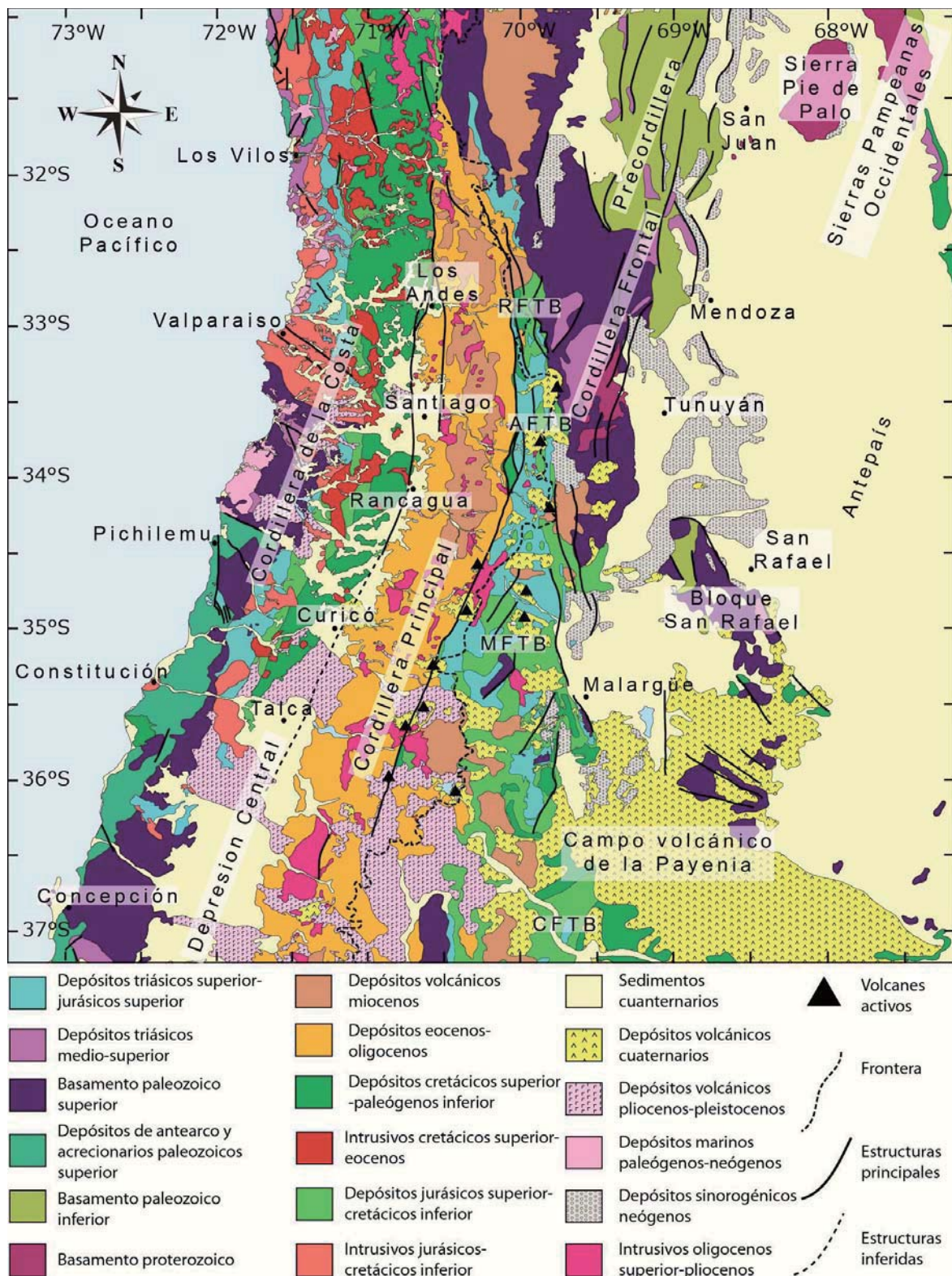


Fig. I. 1. Mapa geológico de los Andes entre 31 y 37°S. RFTB: Faja plegada y corrida de La Ramada; AFTB: Faja plegada y corrida de Aconcagua; MFTB: Faja plegada y corrida de Malargüe; CFTB: Faja plegada y corrida de Chos-Malal (Tomado de Charrier et al. 2014).

La evolución tectónica de los Andes Centrales del sur comienza ya durante el Paleozoico, cuando una serie de diferentes terrenos fueron acrecionados al borde occidental de gondwánico y terminando con un intenso periodo de tectónica compresiva conocido como la orogenia San Rafael (Charrier et al., 2007). Cabe mencionar que la evolución paleozoica, e incluso anterior, también pudo haber ejercido algún control sobre los periodos de deformación posteriores. Sin embargo, los escasos afloramientos de rocas paleozoicas en la región de estudio impiden una detallada caracterización de la evolución pre-mesozoica impidiendo determinar cualitativa y cuantitativamente el control que pudo haber ejercido.

Posteriormente la evolución triásica de esta región se caracteriza por la ausencia de un arco magmático lo que ha sido interpretado como un periodo con una velocidad de subducción cero, apoyado por el hecho que los datos paleomagnéticos muestran que la deriva continental fue casi nula. Durante este periodo dominó una tectónica extensional que produjo una serie de depocentros con una orientación NW (Charrier et al., 1979), lo cual ha sido asociado a un fuerte control de las debilidades previas producto de la acreción de terrenos. Este periodo muestra desarrollo de depocentros correspondientes a grábenes y hemigrábenes llenos de depósitos sedimentarios y volcánicos acumulados durante alternancia de periodos de subsidencia termal o tectónica (Charrier et al., 2007).

El Jurásico temprano y Cretácico medio también se caracterizó por una tectónica extensional, pero que a diferencia del periodo anterior, se desarrolló un arco magmático asociado a subducción, ubicado en lo que corresponde a la actual Cordillera de la Costa, y cuencas de tras-arco al este del mismo, siendo la más importante en la región de estudio la Cuenca Neuquina. Esta cuenca se caracteriza por la presencia de graben y hemigrábenes llenos con depósitos marinos y continentales relacionados a transgresiones y regresiones marinas.

Para el Cretácico tardío al Eoceno Temprano la tectónica cambió, dominando una deformación contraccional que marca el inicio de la construcción del orógeno andino (Boyce et al., 2014; DiJulio et al., 2012; Tunik et al., 2010). Este periodo se caracterizo por la deformación y alzamiento de la Cordillera de la Costa junto la transformación de la cuenca de tras-arco en una cuenca de antepaís donde fueron acumulados los depósitos sinorogénicos asociados a la erosión del relieve que se formaba (Mpodozis y Ramos, 1989). Durante el Eoceno Medio al Mioceno temprano la deformación a lo largo de los Andes Centrales del sur fue diferente al norte y al sur de los 31°S. En particular, al sur de esta latitud domino la extensión, evidenciado por el desarrollo de la Cuenca de Abanico, una cuenca de intra-arco donde se acumularon depósitos volcánicos asociados al arco magmático y depósitos sedimentarios (Charrier et al., 2002, 2005).

Ya para el Mioceno temprano-Plioceno la compresión dominó a lo largo de todo el orógeno correspondiendo al principal periodo de construcción de los Andes, al menos al sur de 31°S (e.g. Farías et al., 2010). Durante este periodo se produjo la inversión de la Cuenca de Abanico, así como la formación de las fajas plegadas y corridas que caracterizan el borde oriental de la cordillera (Charrier et al., 2007). Durante este periodo se desarrollo el segmento de subducción plana al norte de los 33°S (Fig. I.1). Otro aspecto que caracterizó este periodo fue la rotación del margen del continente sudamericano en sentido horario originando así el Oroclino del Maipo a partir de los 12 Ma (Arriagada et al., 2013).

La evolución de los Andes Centrales del Sur durante el Mioceno-Plioceno muestra que la deformación fue migrando al este. Esta migración al sur de los 34°S fue acompañada de una migración del volcanismo de arco hasta 500 km de la fosa (Ramos et al., 2014 y referencias ahí), lo cual ha sido asociado a una somerización de la losa oceánica durante el Mioceno medio-tardío (Kay et al., 2006). A partir de los 2 Ma, el retroarco al sur de los 34° habría experimentado extensión, contrariamente a lo que pasaba al norte de dicha latitud, y el desarrollo de un magmatismo basáltico alcalino asociado a una fuente mantélica (Kay et al., 2006). Lo anterior ha sido asociado al posterior empinamiento de la losa oceánica lo cual produjo el flujo de la astenosfera hacia el oeste, produciendo el volcanismo alcalino y la extensión en el retroarco (Kay et al., 2006, Ramos et al., 2014).

I.2.2 Exposición del Problema

De acuerdo con la revisión presentada en la sección anterior, los Andes al sur de 33°S son el resultado de la tectónica compresiva que ha experimentado el borde occidental de la placa Sudamericana durante el Neógeno. La construcción orogénica se caracterizó por un engrosamiento cortical producto principalmente del acortamiento tectónico ocurrido durante un evento contraccional mioceno, responsable de la organización actual de los Andes de Chile y Argentina central.

En el último tiempo se han presentado modelos cinemáticos contrastantes para explicar el estilo estructural de la vertiente oriental de la cordillera al sur de 34°S. Por un lado existen modelos que plantean la inversión de fallas normales como el mecanismo principal a través del cual se incorpora el basamento en la deformación (Charrier et al., 2014; Giambiagi et al., 2009, 2008; Kozlowsky et al., 1993; Manceda and Figueroa, 1995; Mescua et al., 2014; Ramos et al., 1996); mientras que en el otro extremo, la generación y apilamiento de fallas inversas de bajo ángulo del tipo “Laramide” serían el mecanismo que explicaría el alzamiento estructural del basamento (Dimieri, 1997; Turienzo, 2010; Turienzo et al., 2012). Una diferencia fundamental entre estos dos modelos corresponde a la cantidad de acortamiento que acomoda uno u otro, lo que tiene implicancias directas en la estimación del engrosamiento cortical, alzamiento tectónico, además de la cantidad de deformación que se traspasa desde la subducción de placas al continente.

Así también, se han propuesto distintos modelos para la arquitectura del orógeno. El modelo más aceptado corresponde al que presentan diversos autores en el que la deformación es traspasada desde el contacto intra-placa a través de un nivel de despegue profundo que se someriza hacia el este (*cf.* Farías et al., 2010; Giambiagi et al., 2012; Ramos et al., 2004). Contrariamente, Armijo et al. (2010) propusieron que el *backstop* del sistema correspondería al basamento paleozoico-neoproterozoico ubicado hacia el este. En este caso el empuje sería hacia el oeste deformando las rocas mesozoicas y cenozoicas estableciendo así un transporte tectónico hacia el oeste, dirección contraria a los modelos propuestos anteriormente.

Otro aspecto a considerar al momento de intentar entender la construcción del orógeno andino corresponde a las variaciones latitudinales en su evolución, las cuales se evidencian al comparar las regiones al norte y sur de 35°S. Las principales diferencias radican en la migración al este de la deformación y volcanismo de arco que presenta el segmento sur respecto al norte durante la

evolución neógena. Como se desprende de la sección anterior, estas variaciones evolutivas serían, además consecuencia de un periodo de somerización de la losa oceánica desde el Mioceno tardío. El cambio de ángulo de la subducción implicó un aumento del área de contacto entre las placas generando un mayor acople entre ellas, y en consecuencia, una transferencia de esfuerzos más eficiente (*e.g.* Martinod et al., 2010).

Si bien un periodo de somerización de la placa explicaría la evolución geológica al sur de 35°S, el origen de este proceso aún no ha sido identificado existiendo variadas hipótesis. En efecto, Mescua et al. (2014) propusieron que la migración de la deformación y magmatismo podrían ser explicadas a través de un modelo de cuña de Coulomb. En este modelo, la dinámica de la deformación se caracteriza por el desarrollo de fallas en secuencia, controlado por las características intrínsecas de las rocas que componen la corteza (Dahlen et al., 1984; Davis et al., 1983), las cuales explicarían las diferencias evolutivas entre los segmentos, al norte y sur de 35°S. La consideración de uno u otro modelo implican condiciones distintas de la dinámica de la subducción y, por lo tanto, diferencias en la cantidad de deformación que se traspasaría al continente.

A pesar de los numerosos trabajos realizados en los Andes de Chile central y del oeste de Argentina, aún existe una serie de interrogantes sobre la construcción del orógeno, lo que impide un análisis más detallado de los procesos que caracterizan la dinámica de la subducción y su control en la orogénesis de un margen convergente. En este sentido, aún falta por precisar cuál es *el rol de la arquitectura de la corteza continental*, particularmente *la influencia real de estructuras antiguas en la construcción de los Andes y cómo influye en la dinámica de la subducción de placas*.

I.3 Objetivos y metodologías

I.3.1 Objetivos del estudio

Este estudio tiene como objetivo principal "*Determinar la evolución estructural y los mecanismos que controlaron la configuración actual de los Andes Centrales del sur entre 35°S y 35°30'S*".

En términos generales, por medio de este estudio, se espera:

- (1) Comprender el control de la arquitectura previa de la corteza continental durante la deformación contraccional neógena.
- (2) Comprender la forma en la cual los diferentes mecanismos de deformación han controlado el desarrollo tectónico de los Andes Centrales del sur entre 33°S y 36°S.
- (3) Determinar un modelo de la arquitectura cortical de los Andes Centrales del sur a 35°S, para su comparación con otros sectores de la cadena andina con el fin de identificar variaciones en los parámetros que controlan la dinámica de la subducción y la transferencia de los estreses a la corteza continental.

Para conseguir estos objetivos, es necesario:

- (1) Determinar los rasgos estructurales previos a la fase compresiva neógena
- (2) Determinar la paleogeografía asociada a cada evento de deformación.
- (3) Determinar cuáles son los mecanismos de deformación a lo largo y ancho de la cordillera.
- (4) Establecer el grado de influencia de las estructuras previas en los distintos mecanismos de deformación reconocidos.
- (5) Establecer la cantidad de deformación asociada a cada fase tectónica previa.
- (6) Determinar la edad de la deformación para cada periodo de deformación reconocido.
- (7) Determinar las características de los depósitos asociados a cada periodo de deformación identificado

I.3.2 Metodología y actividades

- Se realizaron campañas de terreno las que consisten en el uso de uso de técnicas estándar de geología de campo con énfasis en la geología estructural y estratigrafía. Los terrenos tuvieron como finalidad definir unidades estratigráficas y reconocer estructuras y unidades claves que permitan la separación de las diferentes fases tectónicas. La información obtenida

se compiló en mapas geológicos y secciones estructurales preliminares a escalas 1:100.000 o 1:150.000, las cuales incluyen datos de cartografía de estudios previos.

- La determinación de la cronología de los eventos de deformación requiere de un sólido control estratigráfico el cual se basó en dataciones radioisotópicas U-Pb en niveles guías. Además se realizaron análisis sedimentario de proveniencia basado en petrografía y dataciones U-Pb en circón detrítico. De esta manera, se espera poder identificar las áreas de aporte, la roca fuente de los sedimentos, discordancias y los depósitos sin-tectónicos de cada etapa, para así establecer la temporalidad de diferentes fases tectónicas y así caracterizar de mejor manera la deformación durante cada etapa. Este estudio cuenta con la colaboración de investigadores argentinos expertos en este tipo de análisis.
- El detallado análisis geométrico y cinemático de las estructuras permitió la confección de secciones estructurales balanceadas tanto locales como regionales. las cuales fueron restauradas por etapa correspondiendo la base para la identificación y separación de las distintas fases tectónicas, además del reconocimiento de los diferentes estilos estructurales y la cuantificación de la cantidad de deformación. Lo anterior también sienta la base para comparar la geología de la vertiente chilena con la vertiente argentina de modo de integrarlas de manera acuciosa. Esto último cuenta con la colaboración y participación de investigadores argentinos que han trabajado a estas latitudes en la vertiente oriental de la Cordillera de los Andes. Los perfiles estructurales fueron realizados por métodos clásicos propios de la geología estructural, además de la ayuda del software MOVE (© Midland Valley), el cual es una plataforma especializada en la construcción de modelos estructurales en 2D y 3D.

CAPÍTULO II.

LA CUENCA DE ABANICO: ARQUITECTURA Y EVOLUCIÓN DE UNA CUENCA DE INTRA-ARCO

II.1 Introducción

En los últimos 60 años, variados han sido los estudios realizados para comprender las características y evolución de los Andes de Chile Central ($33^{\circ}30'S$ - $37^{\circ}S$) (e.g. Aguirre, 1960; Charrier, 1973; Charrier et al., 2012, 2002, 1996; Davidson y Vicente, 1973; Farías et al., 2010, 2008; Flynn et al., 2003; Fock et al., 2006; González y Vergara, 1962; Jordan et al., 2001; Klohn, 1960; Thiele, 1980; Wyss et al., 1996, 1994). La geología de la Cordillera Principal de los Andes de Chile central está principalmente caracterizada por el desarrollo de la Cuenca de Abanico, una cuenca extensional de intra-arco desarrollada entre el Eoceno tardío y el Mioceno temprano e invertida posteriormente durante el evento compresivo neógeno temprano (Charrier et al., 2009, 2005, 1996), durante el cual se estructuró la arquitectura actual de la Cordillera de los Andes al sur de la actual zona de subducción plana. Por lo tanto, determinar la evolución y estructura de la Cuenca de Abanico se hace imprescindible para establecer el control que ésta ejerció durante la posterior fase de contracción y, en consecuencia, entender la evolución de los Andes de Chile Central. Es por esto que en este capítulo se presenta un estudio realizado a lo largo del valle del río Tinguiririca ($35^{\circ}S$), desde la frontera con Argentina, por el este, hasta el área de confluencia de los ríos Tinguiririca, Claro y Clarillo, por el oeste, que aporta nuevos antecedentes en ese sentido.

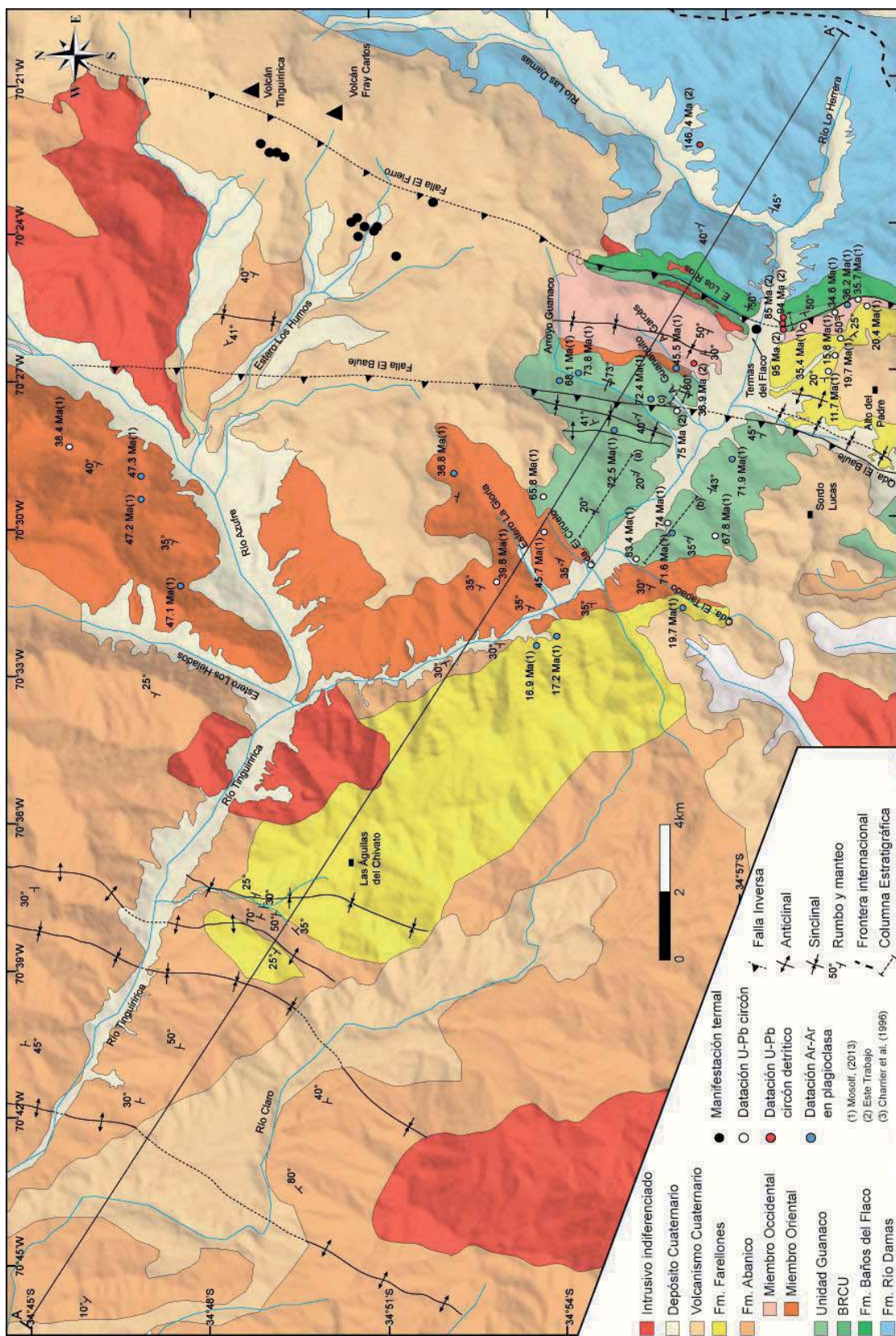


Fig.II.1. Mapa geológico del área del valle del río Tinguiririca. Perfil A-A' en figura II.15.

Este capítulo consta de 6 secciones, en las 3 primeras se presentan las características de los periodos previos, contemporáneos y posteriores al desarrollo de la cuenca. Es así como, en la sección II.2 se caracterizan y exponen antecedentes sobre el basamento de la cuenca y la deformación que éste habría sufrido, en forma previa a la extensión del Paleógeno tardío. La sección II.3 analiza a partir de información de superficie y nuevos datos geocronológicos la arquitectura y evolución de la Cuenca de Abanico. En la sección II.4 se analiza la inversión tectónica y la arquitectura actual de los depósitos acumulados en la cuenca para luego, en la sección II.5, presentar un modelo estructural de la Cordillera Principal occidental. Finalmente, en la sección II.6 se discute acerca de los nuevos antecedentes de los depósitos del Cretácico Tardío y sus implicancias regionales en la evolución cretácica tardía.

II.2 El basamento de la Cuenca de Abanico

El basamento de la cuenca está constituido por las rocas depositadas en forma previa al Eoceno medio, correspondiendo principalmente a las secuencias sedimentarias y volcánicas mesozoicas que llenaron la Cuenca Neuquina, tanto en su etapa extensional como compresiva. Estas secuencias mesozoicas afloran inmediatamente al este y oeste de la Cuenca de Abanico donde se encuentran en contacto por falla o discordancia con la Fm. Abanico (Charrier et al., 2002; Fock et al., 2006). La ausencia del basamento dentro de la cuenca ha impedido conocer la continuidad lateral de los depósitos mesozoicos además de impedir la caracterización de la deformación previa a la extensión durante el Paleógeno superior. Sin embargo, aquí se presentan nuevos antecedentes del basamento posterior al Cretácico Temprano y previo a la Fm. Abanico, que ayudarán a la comprensión de la evolución andina a estas latitudes. Las rocas previas al Cretácico Temprano serán abordadas en el Capítulo III de este trabajo, debido a que ellas se enmarcan dentro de la evolución del dominio estructural de la faja plegada y corrida de Malargüe.

II.2.1 BRCU

Frente al poblado de Termas del Flaco (Fig. II.1) aflora la unidad BRCU (Charrier et al., 1996), una secuencia continental compuesta por una brecha sedimentaria basal, constituida mayoritariamente por clastos de caliza pertenecientes a la formación que lo sobreyace, conglomerados y areniscas conglomerádicas alternando con niveles más finos de lutitas y areniscas finas (Fig. II.2c) (Charrier et al., 1996; Zapatta, 1995). Presenta un espesor máximo de 230 m (Fig. II.2c) sobreyciendo en aparente concordancia la Fm. Baños del Flaco (Charrier et al., 1996; Zapatta, 1995), y subyaciendo discordantemente a la Fm. Abanico (Fig. II.1) (Zapatta, 1995). De acuerdo con esto, su edad estaría acotada entre el Cretácico Tardío y Eoceno medio. Charrier et al. (1996) acotan esta unidad al Cretácico Tardío basándose en la presencia de un hueso de dinosaurio y correlacionándola así con el Grupo Neuquén. La presencia del BRCU, una sucesión granodecreciente y estrato decreciente con una brecha sedimentaria en la base que, y de la Fm. Baños del Flaco del Jurásico Tardío, permitió a esos autores concluir que faltan los términos cretácicos de la Fm. Baños del Flaco y toda la Fm. Colimapu.

Con el objeto de establecer detalladamente la edad del BRCU, se realizaron 3 dataciones U-Pb en circones detríticos por el método LA-ICP-MS de 3 muestras del BRCU (FD12-03, FD12-04, FD12-05), recolectadas frente al pueblo de Termas del Flaco (Fig. II.1), y 1 muestra (FD12-02) tomada en el sector de la Laguna del Teno perteneciente a la unidad Areniscas de Pichuante (Klohn, 1960), secuencia sedimentaria roja a la cual se le ha atribuido una edad Cretácico Tardío (Klohn, 1960) y se ha correlacionado con el BRCU (Parada, 2008) (ver en Anexo III la metodología y los resultados analíticos de las edades U-Pb)

Un total de 96 circones fueron analizados para la muestra FD12-03, de los cuales se obtuvieron 96 edades, todas con un porcentaje de discordancia menor al 10% (Fig. II.2a). El espectro de edades muestra que los valores principales pertenecen al Cretácico con 4 *peaks* principales centrados en torno a 94, 105, 111 y 123 Ma (94% en total). El resto de las edades son Jurásicas representando solo el 6% de la población.

Para la muestra FD12-04 se analizaron 96 circones y se obtuvieron 93 edades. Se desecharon 3 debido a su alta incerteza (Fig. II.2b). Así también fueron desechados 49 análisis debido a que el porcentaje de discordancia era mayor a 15% (Fig. II.2b). Las edades concordantes obtenidas se distribuyen entre 84 y 130 Ma, con dos edades aisladas de 287 y 299 Ma. La curva de probabilidad relativa muestra varios *peaks* máximos de edades Cretácicas tales como 85, 93, 98, 108 y 119 Ma (Fig. II.2d).

De la muestra FD12-05 se analizaron 99 circones, de los cuales 68 no fueron considerados debido a que presentan una discordancia mayor al 15% y un alto grado de incerteza (Fig. II.2b). Los 31 análisis concordantes muestran edades entre 94 y 149 Ma con tres edades aisladas de 294, 297 y 342 Ma (Fig. II.2d). El diagrama de probabilidades relativas de edades entrega un *peak* principal de 95 Ma y una serie de *peaks* secundarios entre 100 y 125 Ma junto con un *peak* Jurásico de 148 Ma (Fig. II.2d).

Por último, para la muestra FD12-02 se consideraron 24 circones de los analizados ya que los otros presentan un alto porcentaje de discordancia (Fig. II.2a). La curva de probabilidad relativa muestra un espectro multimodal donde los *peaks* principales se centran en torno a 90, 94, 100 y 111 Ma (Fig. II.2d). También se observan *peaks* secundarios en torno a los 133, 140 y 181 Ma.

La datación de circones detríticos ha sido ampliamente utilizada para determinar la edad máxima del depósito basándose principalmente en el circón más joven de la muestra (Dickinson y Gehrels, 2009). Considerando lo anterior, el circón más joven para cada muestra del BRCU corresponde a $89,8 \pm 2,5$, $84,6 \pm 0,8$, y $94,8 \pm 1,2$ Ma para las muestras FD12-03, FD12-04 y FD12-05, respectivamente (error con $\pm 2\sigma$). De esta forma, se establece que la edad máxima de depósito para el BRCU se encontraría entre 96 y 83,8 Ma.

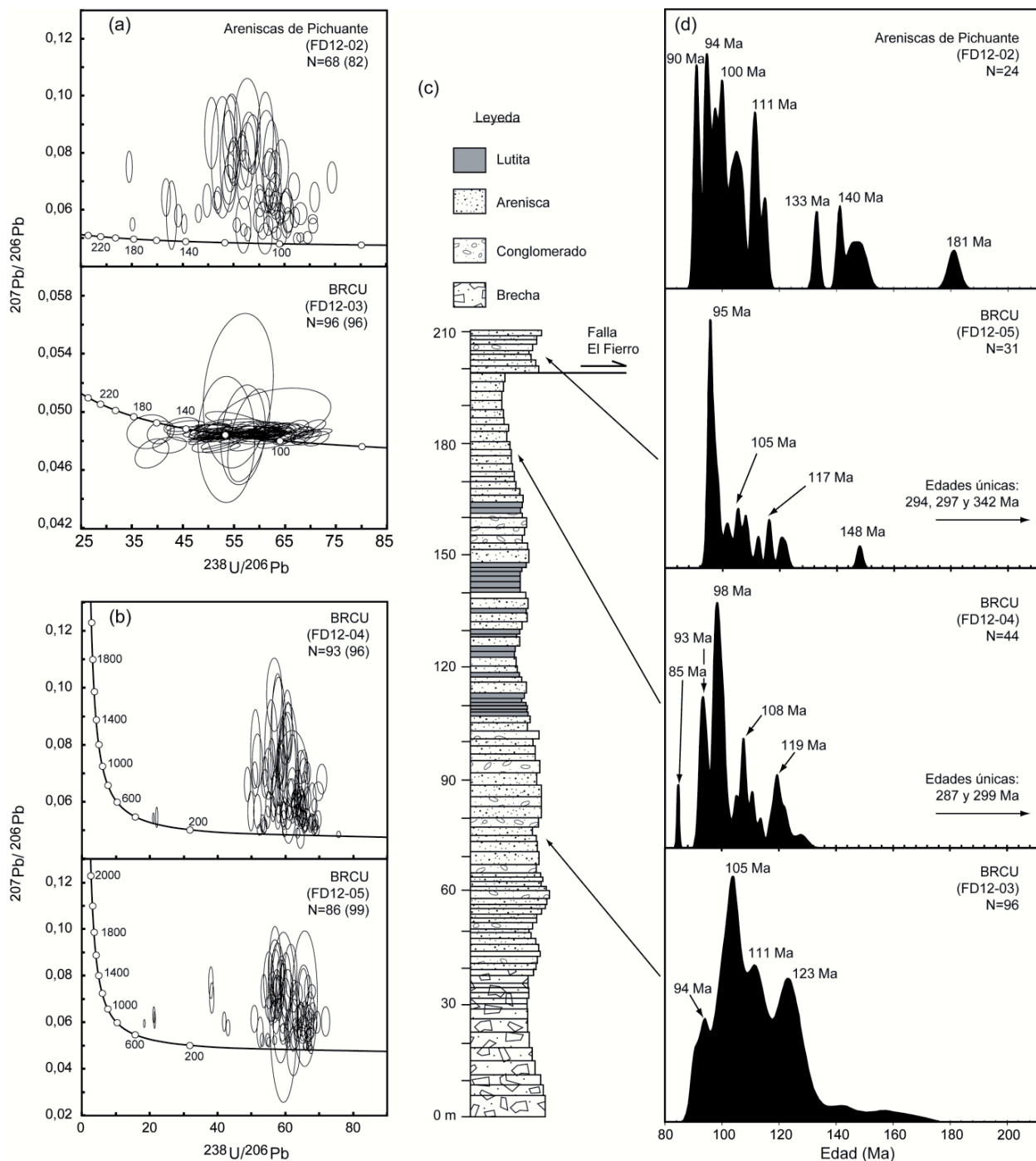


Fig. II.2: (a) Diagramas de concordia para resultados analíticos de dataciones U-Pb en circones detriticos de las muestras FD12-02 y FD12-03, de las unidades Areniscas de Pichuante y BRCU, respectivamente. (b) Diagramas de concordia para resultados analíticos de dataciones U-Pb en circones detriticos de las muestras FD12-04 y FD12-05, de la unidad BRCU. (c) Columna estratigráfica de la unidad BRCU en la ladera sur del valle del Tinguiririca (modificada de Zapatta, 1995) con la ubicación de las muestras datadas. (d) Curvas de probabilidad relativa para las edades U-Pb en circones detriticos de las unidades BRCU (muestra FD12-03, 04 y 05) y Areniscas de Pichuante (muestra FD12-02).

Cabe mencionar que las 3 edades más jóvenes obtenidas para las 3 muestras coinciden con su posición estratigráfica. Es así como la muestra FD12-04 posee la edad más joven y la posición más alta en la columna respecto a la muestra FD12-03 que tiene una edad 5 m.a. mayor. Por otro lado, la muestra FD12-05 posee la edad más antigua, lo cual podría estar evidenciando una repetición del BRCU producida por la presencia de la falla El Fierro (Fig. II.1), ya que esta muestra se ubica directamente sobre la falla (Fig. II.2c). Lo anterior, sin embargo, es discutible debido a que los análisis en circones detriticos no son concluyentes para las edades absolutas de cada nivel.

Esta edad máxima de depósito estimada para el BRCU pone en evidencia la discordancia erosiva y el *hiatus* en el registro estratigráfico con la subyacente Fm. Baños del Flaco, así como también el *hiatus* y discordancia angular previamente establecido con la sobreycacente Fm. Abanico (Charrier et al., 1996).

En la muestra de la unidad Areniscas de Pichuante se obtiene una edad máxima de depósito de 90 ± 1.6 ($\pm 2\sigma$) Ma la cual es se encuentra dentro del intervalo definido para la edad máxima del depósito del BRCU.. De acuerdo con lo anterior y en base a la litología, posición estratigráfica y las edades obtenidas en este trabajo, se propone que el BRCU y las Areniscas de Pichuante son equivalentes cronológicos y litoestratigráficos, y que, por lo tanto, se habrían depositado durante las mismas condiciones tectónicas. Sin embargo, la caracterización geología del sector del río Teno donde aflora esta unidad no fue realizada en esta tesis, para establecer las relaciones de contacto con las unidades sub- y suprayentes y de esa forma establecer una correlación estratigráfica más detallada entre las Areniscas de Pichuante y el BRCU.

Finalmente, se realizó una datación U-Pb en circones detriticos en una muestra de la parte superior de la Fm. Colimapu recolectada en el sector del río Volcán, al este de Santiago, con el objeto de establecer una posible correlación entre los afloramientos que en esa localidad fueron atribuidos a la Fm. Colimapu y el BRCU, como ha sido propuesto por otros autores (*cf.* Charrier et al., 2007, 2014). De acuerdo con los resultados obtenidos, la edad máxima del depósito para el techo de la Fm. Colimapu correspondería a $73,8 \pm 4,2$ ($\pm 2\sigma$) Ma (Fig. II.3), la cual es más joven que la edad máxima de depósito determinada para el BRCU y las Areniscas de Pichuante. De la misma forma que para las Areniscas de Pichuante, no es posible establecer una edad máxima de depósito que sea representativa para toda la unidad que aflora en el río Volcán, dado que se dispuso de una sola muestra. Sin embargo, se puede inferir que estos depósitos no pertenecen a la Fm. Colimapu (*s.s.* Klohn, 1960).

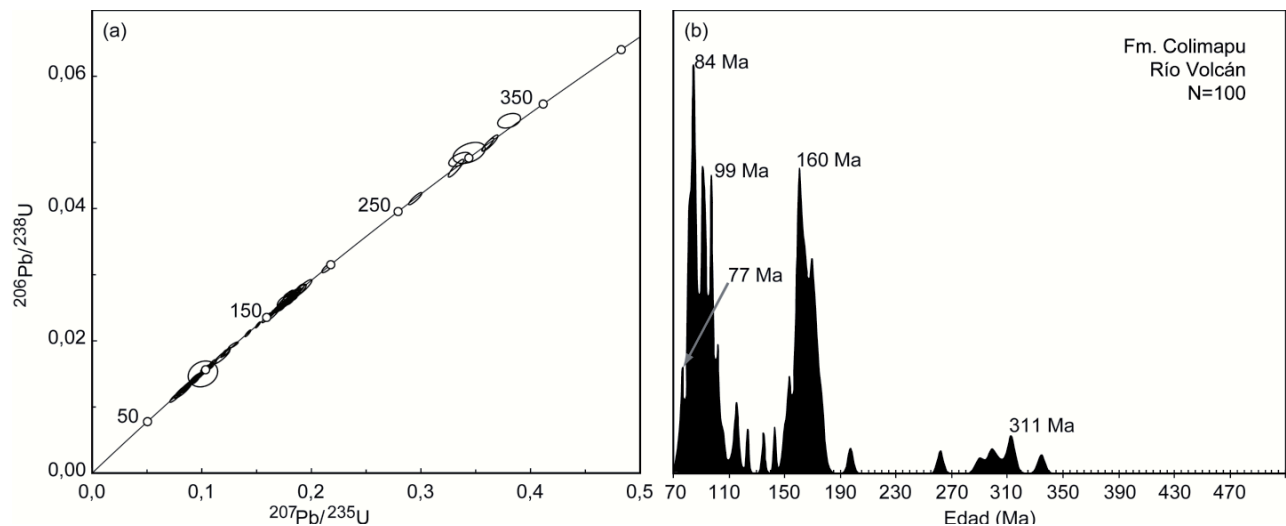


Fig. II.3. (a) Diagrama de concordia para los resultados analíticos de dataciones U-Pb en circones detríticos de la Fm. Colimapu en el sector del río Volcán, al este de la ciudad de Santiago. (b) Curva de probabilidad relativa para las edades U-Pb en circones detríticos para la muestra de la Fm. Colimapu, en el río Volcán.

II.2.2 Unidad Guanaco

Esta unidad informal fue definida a lo largo del valle del Tinguiririca entre el arroyo Garcés y la quebrada El Ciruelo (Fig. II.1). La Unidad Guanaco corresponde a una secuencia volcánica y volcanoclástica de marcada coloración rojiza, de al menos 1800 m de espesor anteriormente asignada a la Fm. Abanico (*cf.* Charrier et al., 1996; Zapatta, 1995). Está compuesta de andesitas, brechas volcánicas y tobas con intercalaciones de conglomerados y areniscas cubiertas discordantemente por la Fm. Abanico, mientras que su base no se encuentra expuesta.

En los afloramientos de la Unidad Guanaco a lo largo del valle del Tinguiririca se reconocieron fallas normales de escala centimétrica a decamétrica, acomodando espacio para el depósito de esta unidad (Fig. II.4). En la ladera sur del río Tinguiririca, 5 km al oeste de la localidad de Termas del Flaco, una falla de más de 300 m de desplazamiento normal acomoda una secuencia roja de lavas y tobas pertenecientes a la Unidad Guanaco (Fig. II.4a). El espesor de la secuencia sobre el bloque yacente supera al menos en 2 veces el espesor acumulado sobre el bloque colgante (Fig. II.4a) evidenciando que la falla estuvo activa durante la acumulación de los depósitos volcánicos. De la misma manera, en la quebrada Guanaquito se pueden observar fallas normales de 30 cm de rechazo acomodando el depósito de estratos volcados de tobas rojas (Fig. II.4b y c). Las implicancias de estas fallas normales en la evolución de los Andes serán analizadas en la sección II.6.

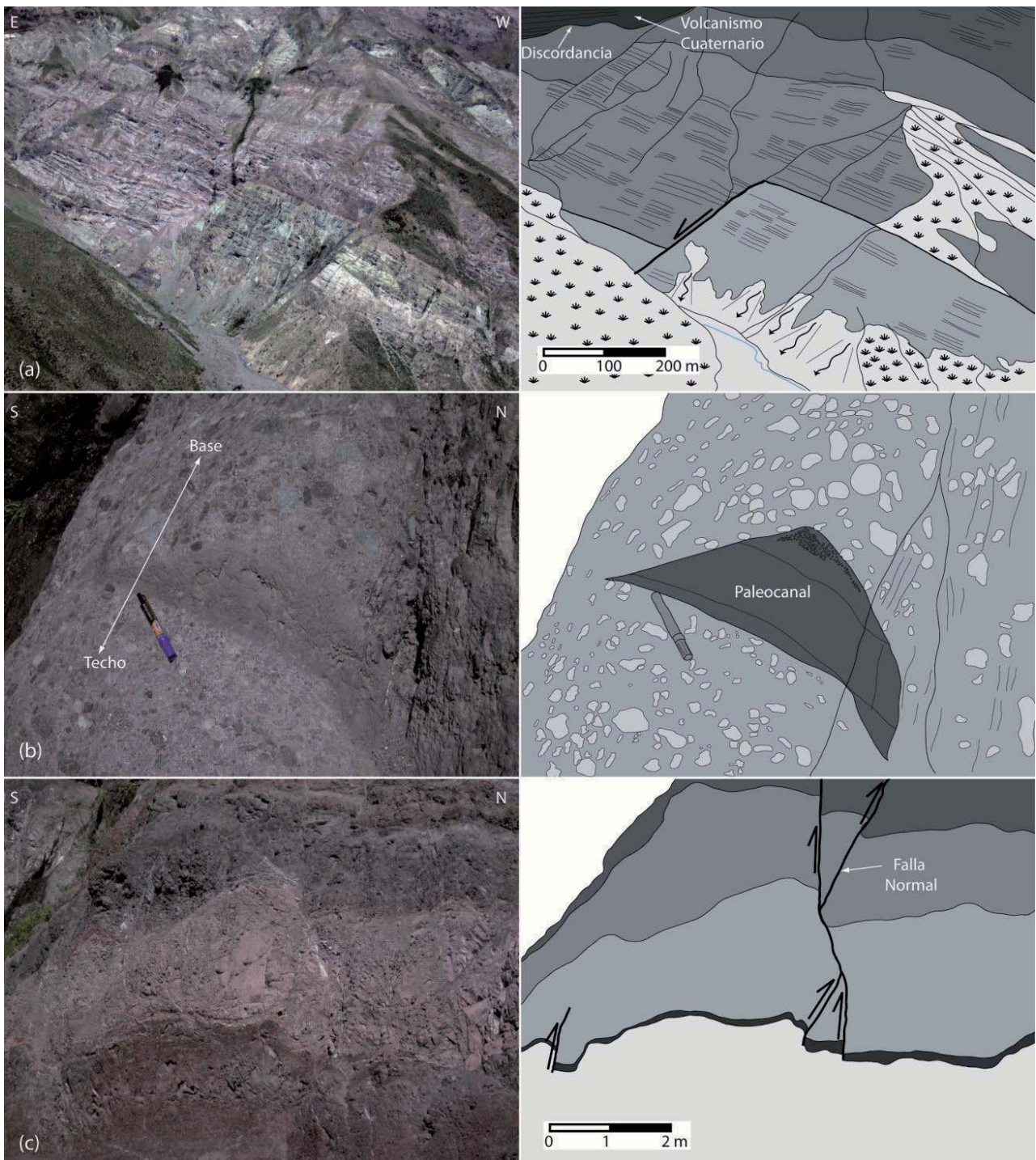


Fig. II.4: Evidencias de fallas normales en la Unidad Guanaco. (a) Fotografía de la ladera sur del valle del río Tinguiririca, al oeste de la quebrada El Baule. Al lado de ésta se encuentra la interpretación donde se muestra como al este de la falla el espesor de la secuencia aumenta. (b) Fotografía e interpretación de un paleocanal en secuencias volcadas de la Unidad Guanaco en el arroyo Guanaquito, que muestra la base y el techo de los estratos. (c) Fotografía de estratos volcados de la Unidad Guanaco en la ladera oeste del arroyo Guanaquito. A la derecha se muestra la interpretación donde se puede observar fallas normales con desplazamiento de centímetros activas durante el depósito de la secuencia.

En la ladera occidental del valle del arroyo Guanaco (Fig. II.1), las rocas de la Unidad Guanaco se encuentran involucradas en un sistema anticlinal-sinclinal, el cual es intruido por diques de 38,4 Ma (Ar- Ar, Mosolf, 2013). Esto evidencia un periodo de deformación contraccional previo a 38,4 Ma, lo cual es anterior a la extensión Paleógena relacionada con la formación de la Cuenca de Abanico. Las implicancias de estas evidencias serán abordadas en la sección de discusión de este capítulo.

Con el fin de determinar la edad de la Unidad Guanaco se colectó una muestra (FD13-01) de un nivel de toba expuesto en la ladera este del arroyo Guanaquito (Fig. II.1) a la cual se le realizó una datación U-Pb en circón (Ver resultados del análisis en Anexo III). A nivel microscópico, la toba muestra fragmentos de cristales de feldespatos potásicos (Fig. II.5f y 5h), anfíbolas alteradas a biotitas y fiammes (Fig. II.5g y 5i), inmersos en una matriz vítreo amorfado (Fig. II.5h). Se realizaron 32 análisis en la misma cantidad de circones, los cuales presentan un porcentaje de discordancia menor al 2% (Fig. II.5d). Los resultados muestran un espectro de edades con 3 *peaks* principales entorno a 75, 78 y 81 Ma además de 4 *peaks* aislados cercanos a 88, 162, 170 y 1053 Ma (Fig. II.5e). Considerando lo anterior, se puede plantear que el *peak* cercano a 75 Ma corresponde a la edad del depósito y que las otras edades corresponden a circones provenientes de rocas más antiguas como el BRCU con edades de 85 y 88 Ma (Fig. II.2d). De acuerdo con su litología y edad, esta unidad correspondería a los depósitos asociados al arco volcánico de edad Campaniano-Maastrichtiano, pudiendo correlacionarse temporal y litológicamente con la Fm. Lo Valle (Thomas, 1958) que aflora en la Depresión Central y Cordillera de la Costa, al norte de 34°S.

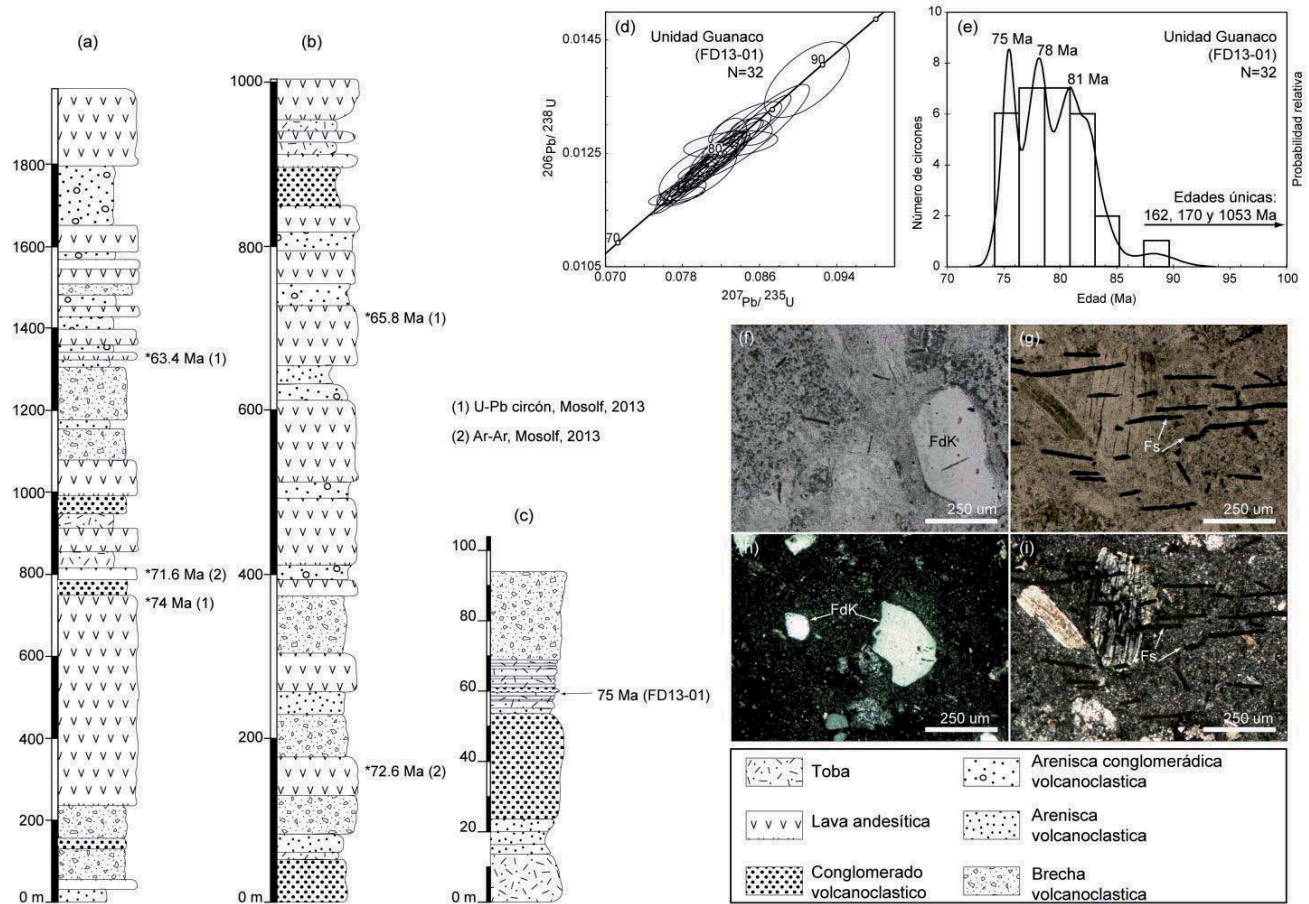


Fig. II.5. (a) y (b) Columnas estratigráficas de la Unidad Guanaco en la ladera norte y sur del valle del río Tinguiririca realizadas por Mosolf (2013). (c) Columna estratigráfica de la Unidad Guanaco en la quebrada Guanaquito (ver ubicación de las columnas en la Fig. II.1). (d) Diagrama de concordia para los resultados analíticos de dataciones U-Pb en circones de la muestra FD13-01 de la Unidad Guanaco (ver ubicación de la muestra en la Fig. II.1). (e) Curva de probabilidad relativa e histograma para las edades U-Pb en circones de la muestra FD13-01, datada en este estudio. (f) y (g) Microfotografía a nícoles paralelos de la muestra FD13-01. Notar las fiammes alineadas en la microfotografía (g). (h) e (i) Microfotografía a nícoles cruzados de la muestra FD13-01. Notar la matriz vítreos y los cristales fragmentados de feldespato potásico que indican un origen volcánico para el depósito.

II.3 Formación Abanico y la extensión paleógena

La Fm. Abanico corresponde a una secuencia volcánica y volcanoclástica (Aguirre, 1960; Klhon, 1960; González y Vergara, 1962; Charrier, 1973, Thiele, 1980) acumulado durante la deformación extensional que dio origen a la Cuenca de Abanico (Charrier et al., 2002). Esta unidad se expande por una región muy amplia desde $32^{\circ}30'$ a 36° S abarcando casi en su totalidad la vertiente occidental de la Cordillera Principal.

Un reciente estudio realizado por Mosolf (2013) entregó una serie de nuevas edades U-Pb en circón, Ar- Ar en plagioclasas y roca total para la Fm. Abanico a lo largo del curso superior del río Tinguiririca (Fig. II.1). Las edades reportadas por este autor junto con los datos recolectados durante esta tesis permitieron establecer las condiciones de sedimentación y la evolución de la cuenca.

Las edades presentadas por Mosolf et al. (2011) y Mosolf (2013) abarcan un rango entre 46 y 20 Ma, concordantemente con lo reportado anteriormente al norte y sur de 35° S (e.g. Fock, 2005; Piquer et al., 2010; Radic, 2010). El registro de edades a lo largo del área de estudio muestra un patrón decreciente hacia el este debido a que las edades entre 46 y 36 Ma se encuentran principalmente entre el río Azufre y la quebrada El Tapado (Fig. II.1) salvo una edad Ar-Ar en el arroyo Garcés de 45,5 Ma (Fig. II.1), mientras que las edades entre 36 y 20 Mase distribuyen en el área de las Termas del Flaco (Fig. II.1). Esta distribución cronológica ya había sido identificada por Zapatta (1995) quien definió un miembro occidental y uno oriental basándose principalmente en un criterio temporal basado en el contenido fósil de cada miembro.

De acuerdo con los antecedentes expuestos, en este trabajo se mantendrá el criterio temporal de Zapatta (1995) para separar en dos miembros a la Fm. Abanico en esta región (miembros Oriental y Occidental), los cuales geográficamente se encuentran separados por los afloramientos de la Unidad Guanaco (Fig. II.1). Hacia el oeste del río Azufre no fue posible establecer esta subdivisión ya que no se cuenta con dataciones suficientes, las cuales son el único criterio de separación debido a la similitud litológica entre ambos miembros. El Miembro Occidental corresponde a rocas de la Fm. Abanico con edades entre 46 y 36 Ma. Se distribuye al oeste del estero El Ciruelo con un espesor mínimo de 400 m (Fig. II.6a), el cual aumenta hacia el oeste y disminuye hacia el este (Fig. II.1). Hacia la base se encuentra en contacto con la Unidad Guanaco, lo que representa un *hiatus* de ~ 20 m.a. (63 a 46 Ma) en el registro estratigráfico. Este miembro también aflora a lo largo de la ladera oeste del río Azufre, lo cual ha sido puesto en evidencia por dataciones entre 47,3 y 38,4 Ma (Fig. II.1 y II.6a, Mosolf et al., 2011). Así mismo, en el arroyo Garcés, una serie de estratos rojos y blancos datados en 46,5 Ma (Fig. II.7b) (Ar-Ar en plagioclasas, Mosolf et al., 2011), y dispuestos sobre la Unidad Guanaco, muestran estratos de crecimiento y fallas normales que controlan el depósito (Fig. II.7a), evidenciando la existencia de un régimen extensional en un estadío inicial de la acumulación de la Fm. Abanico. Estos niveles corresponden a los afloramientos más orientales del Miembro Occidental. Finalmente, otra característica de este miembro es que presenta un contenido fósil de mamíferos pertenecientes a la Fauna El Tapado (Wyss et al., 1994; Zapatta, 1995), el grupo de fósiles de mamíferos más antiguo de la región.

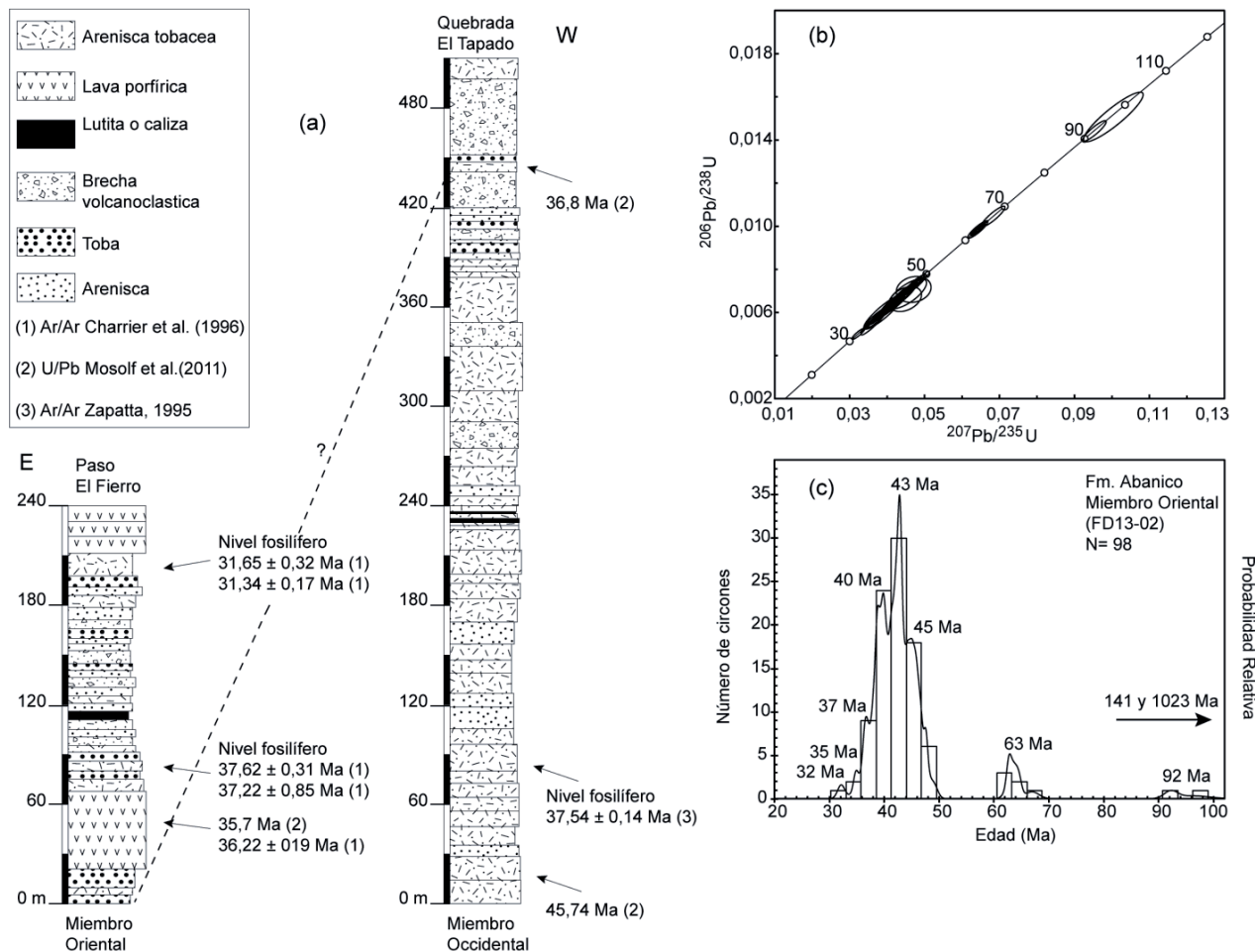


Fig. II.6. (a) Columnas estratigráficas del Miembro Oriental y Occidental de la Fm. Abanico, en el Paso El Fierro y quebrada el Tapado, respectivamente (Modificadas de Zapatta, 1995 y Mosolf, 2013). Además se indican las dataciones previas a este trabajo para ambos miembros (ver ubicación de las dataciones en Fig. II.1). (b) Diagrama de concordia para los resultados analíticos de dataciones U-Pb en circones de la muestra FD13-02 del Miembro Oriental (ver ubicación de la muestra en la Figs. II.1 y II.7). (c) Curva de probabilidad relativa e histograma para las edades U-Pb en circones de la muestra FD13-02.

El Miembro Oriental aflora en la ladera norte y sur del valle del Tinguiririca, en las cercanías del poblado de Termas del Flaco (Fig. II.1). Este miembro presenta un espesor mínimo de ~300 m y está compuesto por una sucesión volcánica y volcanoclástica más joven que 36 Ma (Fig. II.6a). En el arroyo Garcés se la observa sobre un nivel de tobas blancas del Miembro Occidental (Fig. II.7b), mientras que en el sector del Paso el Fierro y el estero Los Ríos se dispone sobre el BRCU o la Fm. Baños del Flaco (Fig. II.1). En este sector, el Miembro Oriental presenta restos fósiles de mamíferos pertenecientes a la Fauna Tinguiririca, una fauna fósil de mamíferos más joven que la Fauna del Tapado, pero de importancia mundial debido a sus implicancias estratigráficas y evolutivas (Charrier et al., 2012; Flynn et al., 2012; Wyss et al., 1994). Dataciones en la base del Miembro Oriental, cercano al contacto con el BRCU y la Fm. Baños del Flaco muestran que el depósito de este miembro habría comenzado posteriormente a 37 Ma, terminando

en el Mioceno temprano con el depósito de la Fm. Farellones que se dispone sobre él en el área del cerro Alto del Padre (Fig. II.1).

A lo largo del arroyo Garcés, niveles basales, correspondientes a areniscas y tobas del Miembro Oriental, muestran estratos de crecimiento que indican un aumento del espesor de la secuencia hacia el este (Fig. II.7.b). Si bien no se encontró ningún antecedente concreto que evidenciara la causa para el desarrollo de estos estratos de crecimiento, aquí se infiere que el Miembro Oriental también se depositó bajo una tectónica extensional al igual que el Miembro Occidental. Esto se sustenta en el hecho que las características y edades del Miembro Oriental se correlacionan con las de las rocas de la Fm. Abanico al norte y al sur de 35°S, cuyo depósito fue controlado por fallas normales asociadas a la tectónica extensional que afectó el área de la Cordillera Principal durante el Paleógeno tardío (Charrier et al., 2002; Farías et al., 2010; Fock, 2005; Radic, 2010).

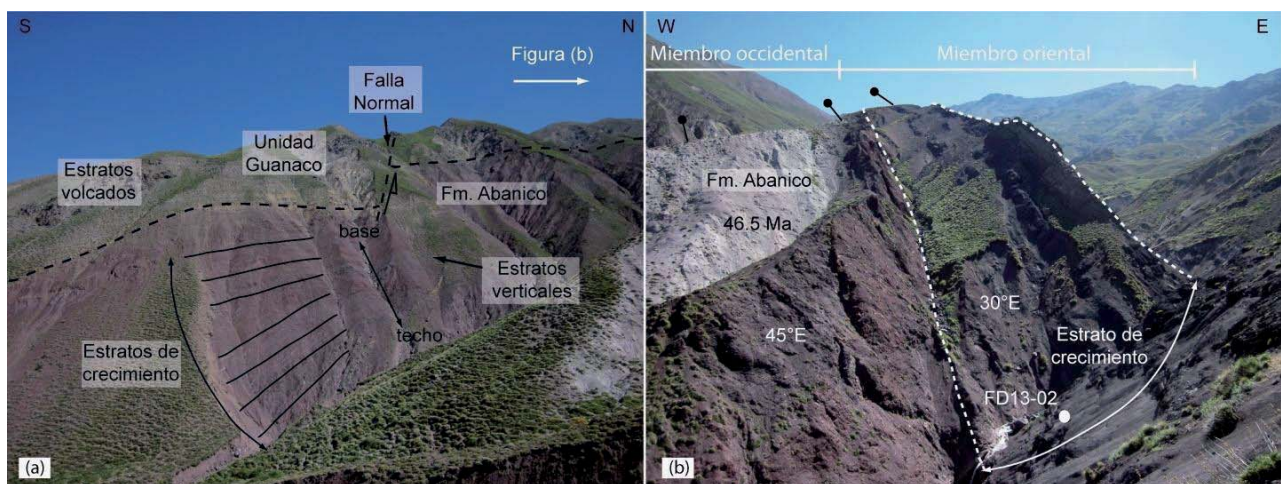


Fig. II.7. Estratos de crecimiento en la Fm. Abanico. (a) Vista de la ladera oeste del arroyo Garcés donde se desarrollan estratos de crecimiento en niveles de areniscas del Miembro Occidental, dispuestos verticalmente, ubicados sobre estratos volcados de la Unidad Guanaco. (b) Estratos de crecimiento al este en tobas del Miembro Oriental en la ladera este del arroyo Garcés sobre estratos pertenecientes al miembro occidental. Se muestra la ubicación de la muestra FD13-02.

Con el objeto de establecer la edad y las áreas fuentes de los depósitos que constituyen los estratos de crecimiento en el Miembro Oriental (Fig. II.7b), se realizó una datación de U-Pb en circones detríticos a una muestra (FD13-02) colectada en la ladera este del arroyo Garcés (ver ubicación en Fig.II.1). Los resultados muestran una concentración mayor de circones entre 32 y 49 Ma (90%), además de poblaciones menores de 60-70 Ma (6%), 90-95 Ma (2%) y 2 edades aisladas de 141 y 1023 Ma (Fig. II.6c). La edad máxima de depósito quedaría acotada por el *peak* de 35 Ma, lo cual es consistente con la edad de 45 Ma de los niveles ubicados por debajo (ver Fig. II.7b, Mosolf, 2013) y con el rango de edad determinado para el Miembro Oriental.

En cuanto a las áreas de aporte, del análisis realizado se desprende que la población de circones más jóvenes que 37 Ma tendría su origen en la actividad volcánica contemporánea. Por otra parte, las poblaciones comprendidas entre 37 y 49 Ma provendrían de la erosión del Miembro Occidental el cual se erosionaría producto de la exhumación causada por el régimen tectónico

extensional contemporáneo al depósito del Miembro Oriental (Fig. II.8). Así mismo, las poblaciones de 60-70 Ma y 90-95 Ma corresponderían a circones provenientes de la erosión del BRCU y de la Unidad Guanaco. De esta manera, el análisis de las áreas fuentes pone en evidencia que todo el aporte de sedimentos para el Miembro Oriental estaría supeditado a la erosión de las rocas circundantes a la cuenca, una característica recurrente en las cuencas extensionales de intraarco (Busby y Bassett, 2007; Busby et al., 2013; Centeno-Garcia et al., 2011)

De acuerdo con lo expuesto, la evolución de la Cuenca de Abanico habría comenzado con un primer periodo de deformación extensional que habría afectado principalmente a su región occidental a partir de los 46 Ma (Fig. II.8). Durante este periodo se habría depositado el Miembro Occidental, desarrollándose los depocentros más profundos hacia el oeste, evidenciado por el aumento del espesor en esa dirección que presenta el Miembro Occidental (Fig.II.8). Posteriormente, la extensión habría afectado a la región más oriental de la cuenca a partir de los 36 Ma, depositándose en este periodo el Miembro Oriental (Fig. II.8), lo cual se evidencia por la ausencia de rocas de este miembro al oeste de la Unidad Guanaco. De esta forma se puede proponer que la deformación extensional fue migrando al este, lo que explicaría la presencia de depósitos volcánicos del Mioceno temprano más al este, en territorio argentino, los que también se habrían acumulado en depocentros extensionales (Spagnuolo et al., 2012b).

En relación a la geometría de la cuenca a lo largo del curso superior del río Tinguiririca, se puede establecer la existencia de un depocentro mayor al oeste cercano a la confluencia de los ríos Tinguiririca y Azufre, donde el espesor del Miembro Occidental es máximo (Fig. II.8). Basado en el crecimiento al oeste que presenta el Miembro Occidental y su menor espesor en la ladera oeste del arroyo Garcés (Fig. II.1), dicho depocentro correspondería a un hemigraben controlado por una falla normal inclinada al este (Fig. II.8). Hacia el este, el hemigraben estaría limitado por un alto topográfico correspondiente a la parte del anticlinal de *roll-over* más alejada de la falla normal maestra (Fig. II.8), el cual estaría constituido por la Unidad Guanaco y por rocas del Miembro Occidental. Al este del alto de basamento, se encontraría un hemigraben, de menor escala que el ubicado al oeste, con una falla maestra manteando al oeste (Fig. II.8) evidenciado por el crecimiento al este que muestra las secuencias del Miembro Oriental en el arroyo Garcés (Fig. II.7b). Para el sector al oeste del río Azufre, no se tienen datos precisos que evidencien la arquitectura de lo cuenca. Sin embargo, basado en el gran espesor de la Fm. Abanico, se infiere que en este sector se habría desarrollado un hemigraben con una falla normal inclinada al oeste (Fig. II.8). De acuerdo con lo anterior, el estudio detallado del borde occidental de la Cuenca de Abanico, aún es un tema de investigación abierto.

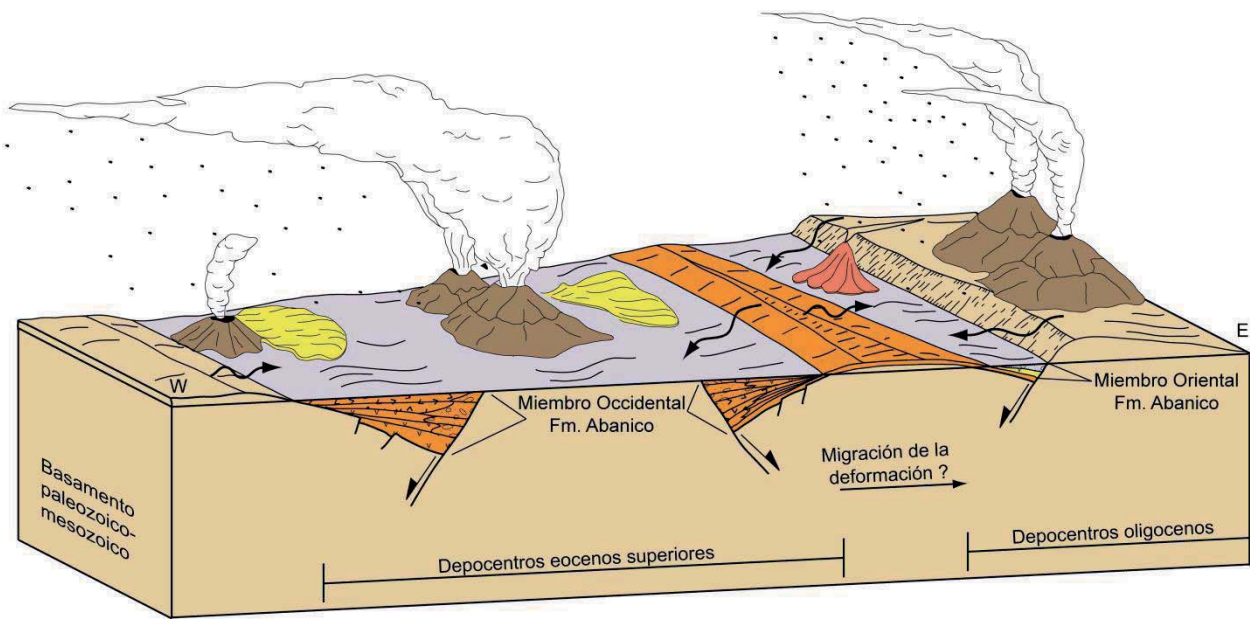


Fig. II.8: Bloque diagrama mostrando la arquitectura de la Cuenca de Abanico previo al Mioceno temprano, a lo largo del valle del río Tinguiririca, entre el valle del Azufre y el límite fronterizo.

El modelo arquitectural para la evolución extensional contrasta con lo propuesto para la región por otros autores quienes propusieron una arquitectura constituida por una serie de hemigrábenes definidos por fallas maestras inclinando al oeste (*cf.* Parada, 2008; Piquer et al., 2010). Estos trabajos consideraron a la Unidad Guanaco dentro de la Fm. Abanico lo que aumentaba su espesor y, en consecuencia, influyó en la concepción de los modelos geométricos. Esto pone en evidencia que la discriminación e identificación del substrato se hace indispensable para poder establecer concluyentemente la geometría de la Cuenca de Abanico a lo largo de su eje. Esto permitirá una mejor comprensión de la influencia de las estructuras previas durante las fases compresivas neógenas y, en consecuencia, un más detallado entendimiento de la construcción y arquitectura de los Andes a estas latitudes.

II.4 Inversión de la Cuenca de Abanico: Estructura actual de Cordillera Principal occidental

En el sector más oriental de la Cuenca de Abanico se observa el contacto entre la Fm. Abanico y las secuencias sedimentarias mesozoicas deformadas, lo cual corresponde en esta región a la parte interna de la faja plegada y corrida de Malargüe. En el curso superior del río Tinguiririca, las fms. Río Damas y Baños del Flaco junto con el BRCU se encuentran inclinadas al oeste (Fig. II.1, II.9a y b), configurando el limbo dorsal de un anticlinal de vergencia al este, con una longitud de 10 km y un limbo delantero corto e inclinando fuertemente al este ($60\text{-}70^\circ$) (Mescua et al., 2014). En el núcleo de la estructura afloran secuencias sedimentarias del Jurásico Temprano y Medio intensamente falladas y plegadas internamente, las cuales, junto con la Fm. Río Damas, muestran una fuerte disminución del espesor hacia el este (Mescua et al., 2014). Debido a esto y a la geometría que muestra la estructura, el anticlinal se ha asociado a la inversión de una falla normal previa, de manteo al oeste y que habría controlado el depósito de las rocas mesozoicas durante el Jurásico (Mescua et al., 2014). La falla normal se habría reactivado inversamente durante el Cretácico Tardío y luego durante el Mioceno, como lo muestran los depósitos sinorogénicos de esas edades que se encuentran por delante del limbo frontal y en el limbo dorsal del anticlinal (Mescua et al., 2014, 2013).

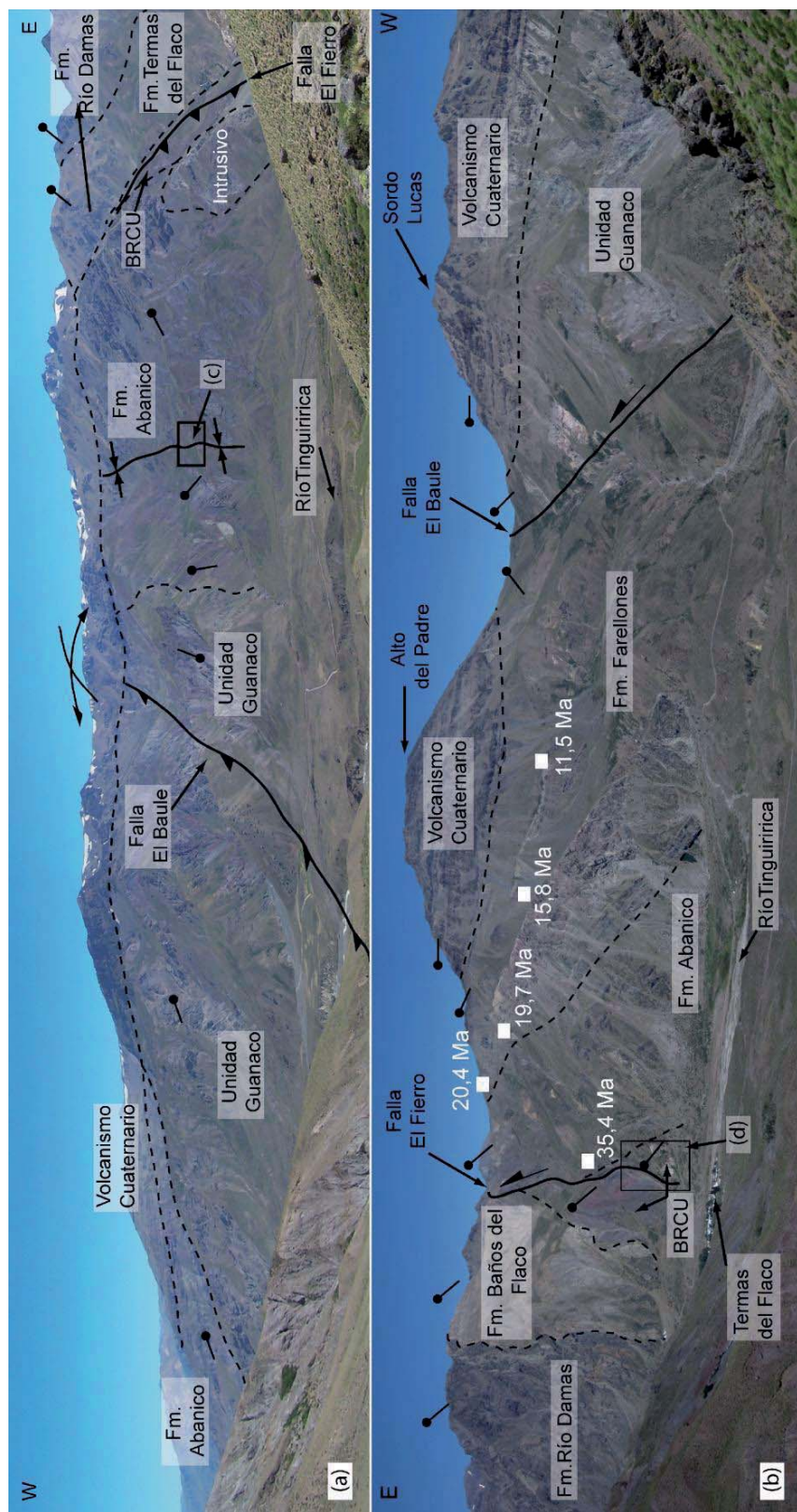


Fig. II.9. Deformación a lo largo del río Tinguiririca. (a) y (b) Fotos panorámicas de la laderas norte y sur del valle del Tinguiririca, respectivamente, mostrando las principales estructuras presentes.

Al oeste de la localidad de Termas del Flaco y a lo largo de la ladera norte del valle del Tinguiririca, aflora un anticlinal de 9 km de longitud constituido por la Unidad Guanaco en su núcleo, el Miembro Occidental y el Oriental, de la Fm. Abanico, en el limbo dorsal y frontal, respectivamente (Figs. II.1 y II.9a). Se caracteriza por un limbo trasero largo con manteos de 20° a 30° W y un limbo frontal corto con estratos verticales, lo que muestra una vergencia al este para esta estructura. A lo largo del arroyo Guanaco, la falla El Baule (Fig. II.1), una falla inversa de vergencia al este, corta el anticlinal fallando las rocas inclinadas de la Unidad Guanaco, basculando el limbo trasero hacia el oeste. Lo anterior indica que la falla El Baule estuvo activa con posterioridad a la formación del anticlinal. En el limbo frontal afloran los estratos de crecimiento de ambos miembros de la Fm. Abanico, observados en el arroyo Garcés (Fig. II.7a y b). En la ladera este del arroyo, las rocas del Miembro Oriental de la Fm. Abanico se encuentran deformadas, conformando lo que corresponde a un sinclinal. Este pliegue presenta una geometría asimétrica, limbo occidental manteando suavemente al este, mientras el limbo oriental inclina más de 50° al oeste (Fig. II.10a), y de acuerdo con su ubicación (Fig. II.1), se le puede identificar como el sinclinal de pie asociado a la formación del anticlinal ubicado hacia el oeste.

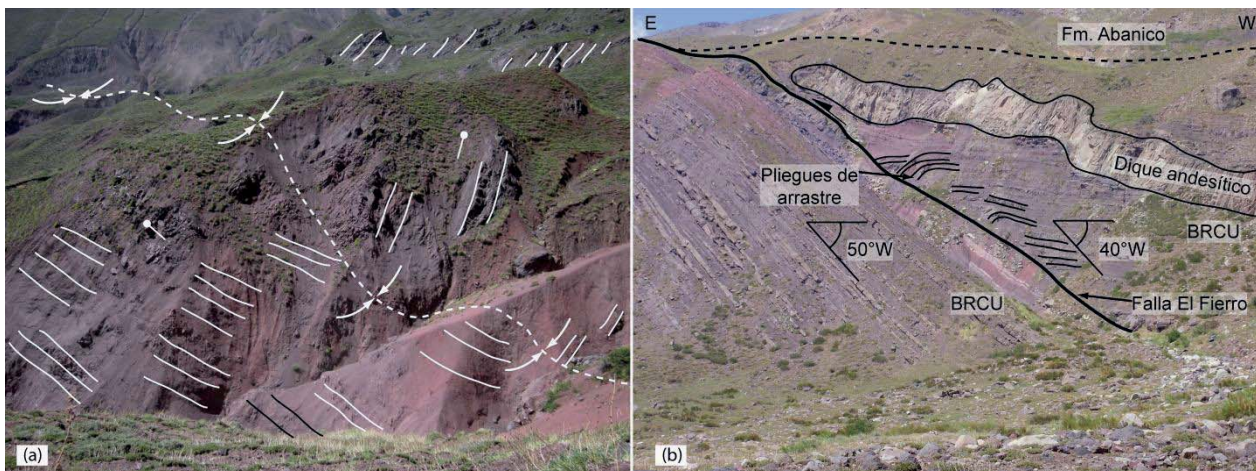


Fig. II.10. Deformación del miembro oriental del Fm. Abanico. (a) Vista al norte del sinclinal desarrollado al frente del limbo frontal del anticlinal que aflora en la ladera norte del valle. (b) Fotografía con vista al sur de la deformación asociada a la falla El Fierro. Se puede ver como la falla produce la repetición del BRCU.

En contraste a lo anterior, en la ladera sur del valle del Tinguiririca, la Unidad Guanaco y la Fm. Abanico conforman un homoclinal de 9 km que presenta inclinaciones entre 40° y 30° W (Fig. II.9b). El homoclinal se encuentra limitado al este por la falla El Baule (Fig. II.1 y II.9b), la cual monta a la Unidad Guanaco sobre las secuencias volcánicas y sedimentarias de la Fm. Farellones que afloran bajo las lavas pleistocena del cerro Alto del Padre (Fig. II.1).

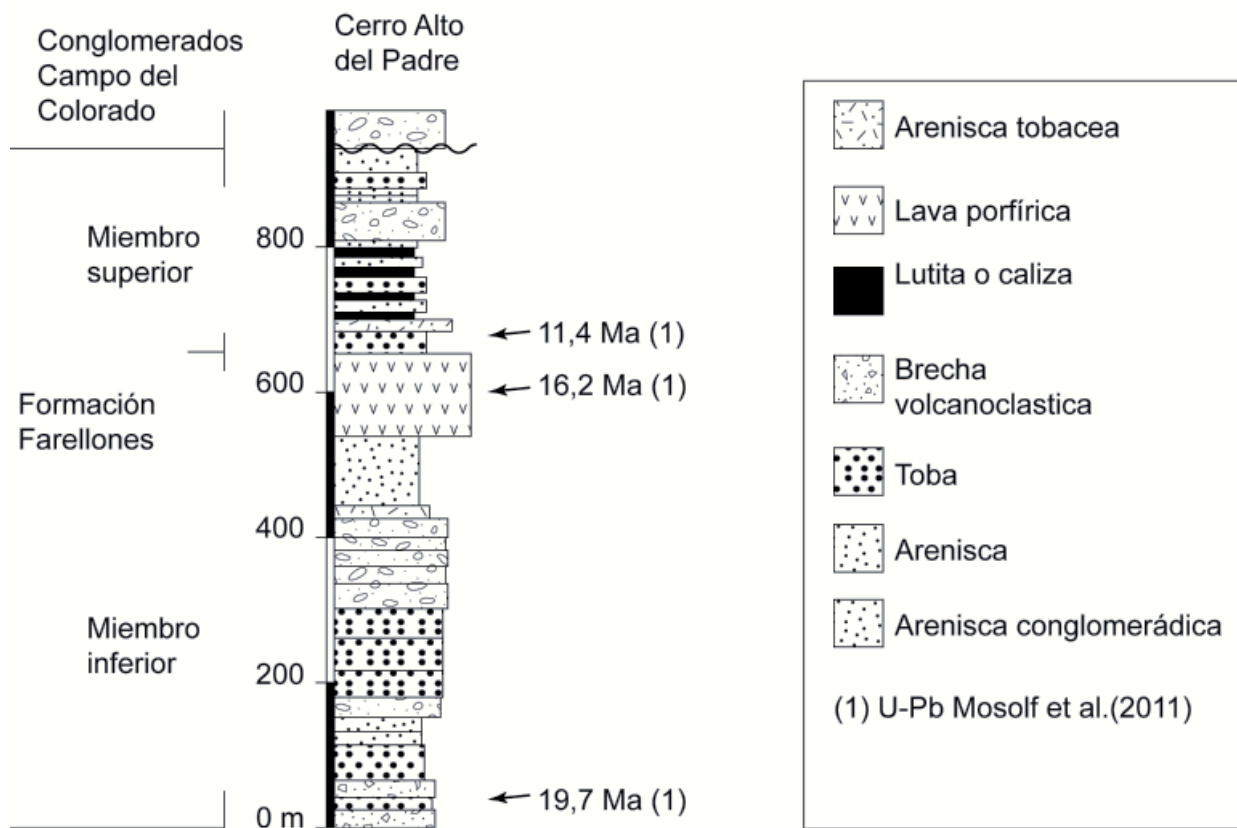


Fig. II. 11. Columna estratigráfica de la Fm. Farellones en el cerro Alto del Padre. Modificada de González (2008), Mosolf (2013) y Zapatta (1995).

La Fm. Farellones corresponde a una secuencia volcánica reconocida al norte de 35°S que se habría depositado durante la inversión de la Cuenca de Abanico en el Mioceno temprano y continuado hasta el Mioceno medio (*cf.* Fock, 2005). En esta área, se caracteriza por presentar un predominio de tobas y andesitas hacia la base, con algunas intercalaciones de areniscas, areniscas conglomerádicas, y potentes capas conglomerádicas, mientras hacia el techo dominan los niveles sedimentarios más finos como areniscas, calizas y limolitas, con intercalaciones esporádicas de niveles volcánicos (Fig. II.11). Estos niveles superiores han sido asociados a un ambiente lacustre de baja energía que favoreció el depósito de sedimentos finos y la precipitación de carbonatos (González, 2008), contrastando con la parte inferior de la Fm. Farellones, donde el predominio de facies volcánicas con intercalaciones de conglomerados indican condiciones de alta energía y un ambiente subaéreo aluvial con desarrollo fluvial e interrupciones debido a actividad volcánica. Con el objeto de una mejor comprensión sobre del periodo inversión de la Cuenca de Abanico, se propone definir para esta área, dos miembros informales dentro de la Fm. Farellones: el miembro inferior y el miembro superior, basado en las características anteriormente descritas.



Fig. II.12. Estratos de crecimiento Fm. Farellones. (a) Fotografía al sur del cerro Alto del Padre mostrando las discordancias progresivas del miembro inferior de la Fm. Farellones y el contacto discordante con el volcanismo Cuaternario. Además se incluyen las edades de Mosolf (2013). (b) y (c) Estratos de crecimiento y discordancias progresivas de la Fm. Farellones en el cerro Las Águilas del Chivato.

La Fm. Farellones en el sector de Termas del Flaco posee un espesor de ~750 m y se encuentra limitada por las fallas El Baule y El Fierro por el oeste y este, respectivamente (Fig. II.9b). Se apoya sobre el Miembro Oriental de la Fm. Abanico y está cubierta discordantemente por los Conglomerados Campo del Colorado, sucesión sedimentaria dominada por niveles de conglomerados con intercalaciones de areniscas finas y una edad comprendida entre 4 y 1,7 Ma (González, 2008). En el área del cerro Alto del Padre, se desarrollan estratos de crecimiento y discordancias progresivas hacia el oeste, en niveles de tobas y areniscas conglomerádicas del miembro inferior (Fig. II.12a), las cuales anteriormente habían sido asignadas a la Fm. Abanico y asociadas a sedimentación sintectónica en depocentros extensionales (Zapatta, 1995).

Mosolf (2013) realizó 3 dataciones U-Pb en circón en distintos niveles del miembro inferior de la Fm. Farellones (Fig. II.11) obteniendo edades entre 20,4 y 11,4 Ma, lo que permite acotar el depósito de este miembro entre el Mioceno temprano y, al menos, el Mioceno superior. Estas edades, además, acotan el inicio de la Fm. Farellones al Mioceno temprano, en forma consistente con lo propuesto al norte de 35°S (Charrier et al., 2005, 2002; Farías et al., 2010, 2008; Fock, 2005).

En la ladera este de la quebrada El Baule, un sinclinal-anticlinal deforma al miembro superior de la Fm. Farellones. Estas estructuras se extienden hacia la ladera sur del cerro Alto del Padre donde corresponden a pliegues apretados, con una amplitud de 200 y 400 m de longitud de onda de anticlinal-sinclinal definiendo así un estilo de deformación de piel fina de vergencia este y oeste (Fig. II.13) (González, 2008). De acuerdo con lo anterior, esta deformación habría ocurrido entre el Mioceno superior y el Plioceno, con posterioridad al depósito de la Fm. Farellones y anterioridad al depósito de los Conglomerados Campo del Colorado.

Las diferencias en las condiciones de sedimentación entre el miembro inferior y superior junto con las diferencias en el estilo estructural de la deformación que afecta a ambos miembros, sugieren que luego de la acumulación sinorogénica del miembro inferior hubo un cese en la deformación posibilitando condiciones ambientales de baja energía, a las cuales está asociado el depósito del miembro superior. Posteriormente, la contracción habría vuelto a deformar a la Fm. Farellones y, tal vez, se habría desarrollado en ese momento la falla El Baule.

La falla más oriental que aflora en el área, corresponde a la Falla el Fierro (Davidson, 1971), una falla inversa con manteo de 40° W, rumbo NNE-SSW, vergencia al este y cuya traza se reconoce a través del estero Los Ríos y el Paso del Fierro, pasando por la localidad de Termas del Flaco (Fig. II.1). Además de deformar estratos del BRCU y repetir parte de esta unidad en el sector sur del valle, frente al pueblo de Termas del Flaco (Fig. II.1 y II.10b), la falla El Fierro cabalga a la Fm. Abanico sobre la Fm. Baños del Flaco (Fig. II.1).

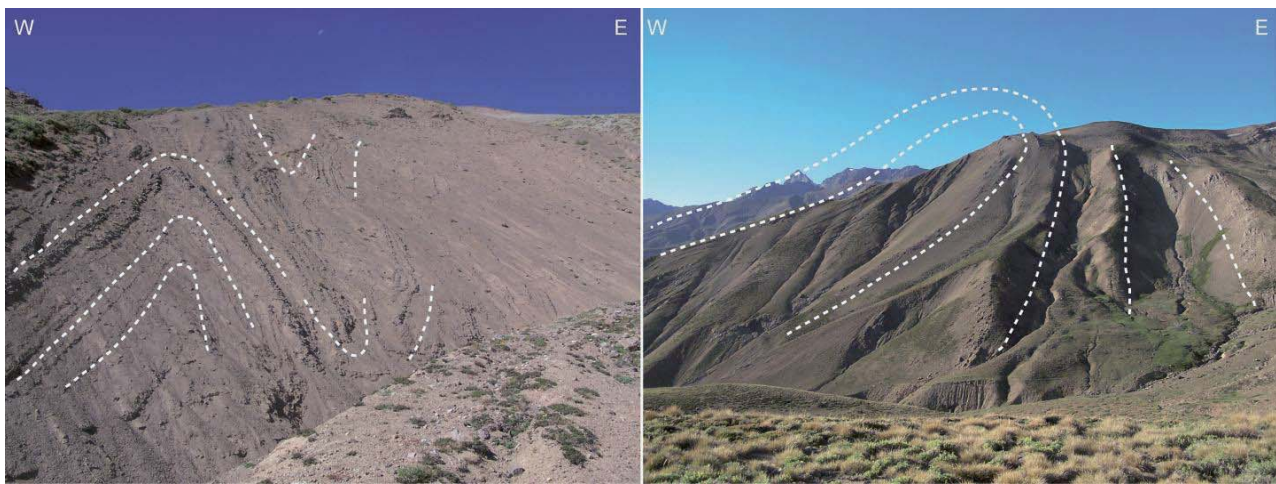


Fig. II.13. Deformación del miembro superior de la Fm. Farellones en el cerro Alto del Padre. Fotografías de Reynaldo Charrier.

La falla El Fierro pertenece a un sistema de falla regional (Charrier et al., 2005, Farías et al., 2010) que ha sido reconocido desde 33°30'S hasta 36°S (Astaburuaga, 2014; Charrier, 1973; Fock, 2005; Tapia, 2010) separando las rocas de la Fm. Abanico de las secuencias sedimentarias mesozoicas, ubicadas estas últimas al este de la estructura. Debido a las relaciones de contacto y a la ausencia de Fm. Abanico al este de estructura regional, la falla El Fierro, y todo el sistema estructural, ha sido interpretada como parte del sistema extensional del borde oriental de la Cuenca de Abanico, invertido durante el Mioceno temprano a medio (Charrier et al., 2005, 2002, 1996). Sin embargo, el Miembro Oriental de la Fm. Abanico en el área de cerro Alto del Padre, donde mejor se encuentra expuesta, no presenta un crecimiento de su espesor contra la falla El Fierro, sino que se apoya en *onlap* sobre el basamento mesozoico (Charrier et al., 1996), lo que invalidaría la proposición de la falla El Fierro como el borde de la cuenca. Considerando lo anterior junto con que la falla El Fierro tiene una inclinación menor que las secuencias mesozoicas cortadas por ella y que en la ladera sur del valle del Tinguiririca cabalga al BRCU sobre sí mismo, se puede plantear que la falla El Fierro correspondería a una falla fuera de secuencia, respecto al evento de deformación contraccional del Mioceno temprano, que cortó a través de rocas deformadas basculando las secuencias ubicadas en el bloque colgante.

La geología hacia el oeste de la Cordillera Principal presenta dificultades adicionales a las que se encuentran en las regiones fronterizas debido a la mayor vegetación y al desarrollo de las zonas urbanas, lo que frecuentemente impide el acceso en sectores cercanos a las ciudades. A pesar de eso, se intenta a continuación realizar una actualización de la geología al oeste del río Azufre para caracterizar la deformación a lo ancho de la Cuenca de Abanico y, en consecuencia, de la Cordillera Principal occidental a 35°S.

La principal estructura de esta área corresponde a un anticlinal de 10 km, con un limbo dorsal largo y un limbo frontal corto, en el que las capas de la Fm. Abanico inclinan 20°W y 70°E, respectivamente (Fig. II.1), indicando una vergencia este para esta estructura. Al este de este anticlinal se desarrolla un tren de pliegues sinclinal-anticlinal-sinclinal de 4 km de largo (Fig. II.14) y limitados al este por el cerro Las Águilas del Chivato (Fig. II.1). En la ladera oeste de este cerro,

se puede observar estratos de crecimiento al este y discordancias progresivas en niveles volcánicos y sedimentarios, los cuales muestran manteos de 70°E, que hacia el este y hacia el techo de la columna sistemáticamente disminuyen hasta 10°E (Fig. II.12b y c) evidenciando un carácter sinorogénico para el depósito de la secuencia. Considerando la litología de las capas, los estratos de crecimientos y el acuñamiento de la secuencia hacia el limbo frontal de la estructura compuesto por la Fm. Abanico, se infiere que esta secuencia corresponde a la Fm. Farellones. Esto también es consistente con lo reportado en la ladera norte del río Tinguiririca, donde sucesiones volcánicas ubicadas en la parte superiores de los cerros fueron asignadas a la Fm. Farellones (Malbran, 1986). Correlacionado estos depósitos de la Fm. Farellones con los ubicados al este, se puede inferir que las estructuras en el sector oeste se habrían formado al menos durante el Mioceno temprano.



Fig. III.14. Tren de pliegues sinclinal-anticlinal-sinclinal al oeste del río Azufre y a lo largo del valle del Tinguiririca. Nótese que el limbo oeste del sinclinal de la izquierda de la fotografía corresponde al limbo frontal del anticlinal de más de 10 km de largo que aflora más al oeste. Ver texto para mayor detalle.

En particular, los afloramientos de la Fm. Farellones en esta región occidental de la Cordillera Principal se correlacionarían, con los encontrados más al sur en el sector de la Corona del Fraile, a lo largo del río Teno (González y Vergara, 1962) recientemente datados por Hevia (2014), lo cual junto con lo reportado por Malbran (1986) en el estudio del área inmediatamente al norte del cerro Águilas del Chivato, conforman una alineación N-S, sugiriendo la existencia de un depocentro tectónico hacia el borde de la Cuenca de Abanico, en los cuales se acumularon depósitos sinorogénicos desde el Mioceno temprano.

En resumen, se pudieron identificar 2 períodos de deformación compresiva durante la inversión de la Cuenca de Abanico. El primero habría ocurrido durante el Mioceno temprano (~20 Ma) en el cual se habrían comenzado a formar los grandes anticlinales que caracterizan la estructura a lo largo del valle del Tinguiririca. Durante este periodo se depositó la Fm. Farellones tal como lo muestran los estratos de crecimiento en la base de esta unidad. El siguiente periodo de deformación de la región occidental de la Cordillera Principal habría ocurrido durante el Mioceno tardío-Plioceno (5 Ma?). Aquí se habrían desarrollado las fallas El Baule y El Fierro junto con los pliegues que deforman el miembro superior de la Fm. Farellones. Este periodo está limitado por el depósito de los conglomerados Campo del Colorado los cuales sellan la deformación. En la región del cerro Águilas del Chivato no se observaron evidencias de este último periodo compresivo que afectó a la Cuenca de Abanico, lo que permite inferir que la deformación del sector oriental de la cuenca se

correlacionaría con los eventos fuera de secuencia que afectaron la parte interna de la Cordillera de los Andes al norte y sur de 35°S (Folguera y Ramos, 2009; Giambiagi et al., 2003; Godoy et al., 1999; Tapia et al., en prensa; Rojas-Vera et al., 2014). Esto será analizado en el capítulo V de este trabajo.

II.5 Modelo estructural de la Cordillera Principal occidental a 35°S

A partir de los datos presentados anteriormente se confeccionó una sección estructural balanceada a lo largo del valle del río Tinguiririca, la cual fue restaurada hasta el Mioceno temprano, previo a la tectónica compresiva Neógena (Fig. II.15).

El modelo propuesto consta de tres anticlinales relacionados a fallas profundas arraigadas en un nivel de despegue profundo, el cual es consistente con los modelos propuestos para los Andes Centrales del sur (Farías et al., 2010; Giambiagi et al., 2012; Mescua et al., 2014; Rojas Vera et al., 2014; Turienzo et al., 2012).

El anticlinal más oriental se formó por la reactivación inversa de la falla normal mesozoica Río del Cobre (Mescua et al., 2014). Se puede observar que al restaurar parte de la Fm. Abanico que se dispone entre las fallas El Baule y El Fierro a una posición horizontal (Fig. II.1 y II.15), el limbo dorsal del anticlinal no se horizontaliza, evidenciando la deformación que tenían las rocas mesozoicas previo a la extensión paleógena y depósito de la Fm. Abanico. En el modelo se propuso una falla normal invertida de vergencia opuesta a la falla Río del Cobre, para explicar los fuertes manteos al oeste que muestran las secuencias sedimentarias.

El anticlinal más occidental fue interpretado como un anticlinal de inversión asociado a la inversión de una falla normal que mantea al oeste. La interpretación se sustenta principalmente en la geometría y la escala de la estructura, así como también en los grandes espesores de la Fm. Abanico en esa región (>1500 m), lo que sugiere un control tectónico en el depósito. El grado de inversión de la falla sería total (en el sentido de Williams et al., 1989) favorecido por el desarrollo de un nivel de despegue en la Unidad Guanaco que originó el cabalgamiento de los depósitos *syn-rift* paleógenos (Fm. Abanico) sobre el *pre-rift*. El tren de pliegues por delante del anticlinal de inversión fue modelado como un pliegue por flexura de falla (Suppe, 1983), con una rampa que va desde el nivel de despegue en la Unidad Guanaco hasta el contacto de esta unidad con la Fm. Abanico (Fig. II.15).

La parte central del modelo está dominado por el anticlinal conformado por la Unidad Guanaco y la Fm. Abanico, el cual fue modelado como un pliegue asociado a una falla inversa profunda y de manteo al oeste. Asociadas a esta estructura se encuentran las fallas El Baule y el Fierro, las cuales corresponderían a fallas tipo *by-pass* y *short-cut*, respectivamente, cortando y deformando el bloque colgante y yacente, respectivamente, las cuales se formaron posteriormente a la formación del anticlinal asociado a la falla inversa principal (Fig. II.15).

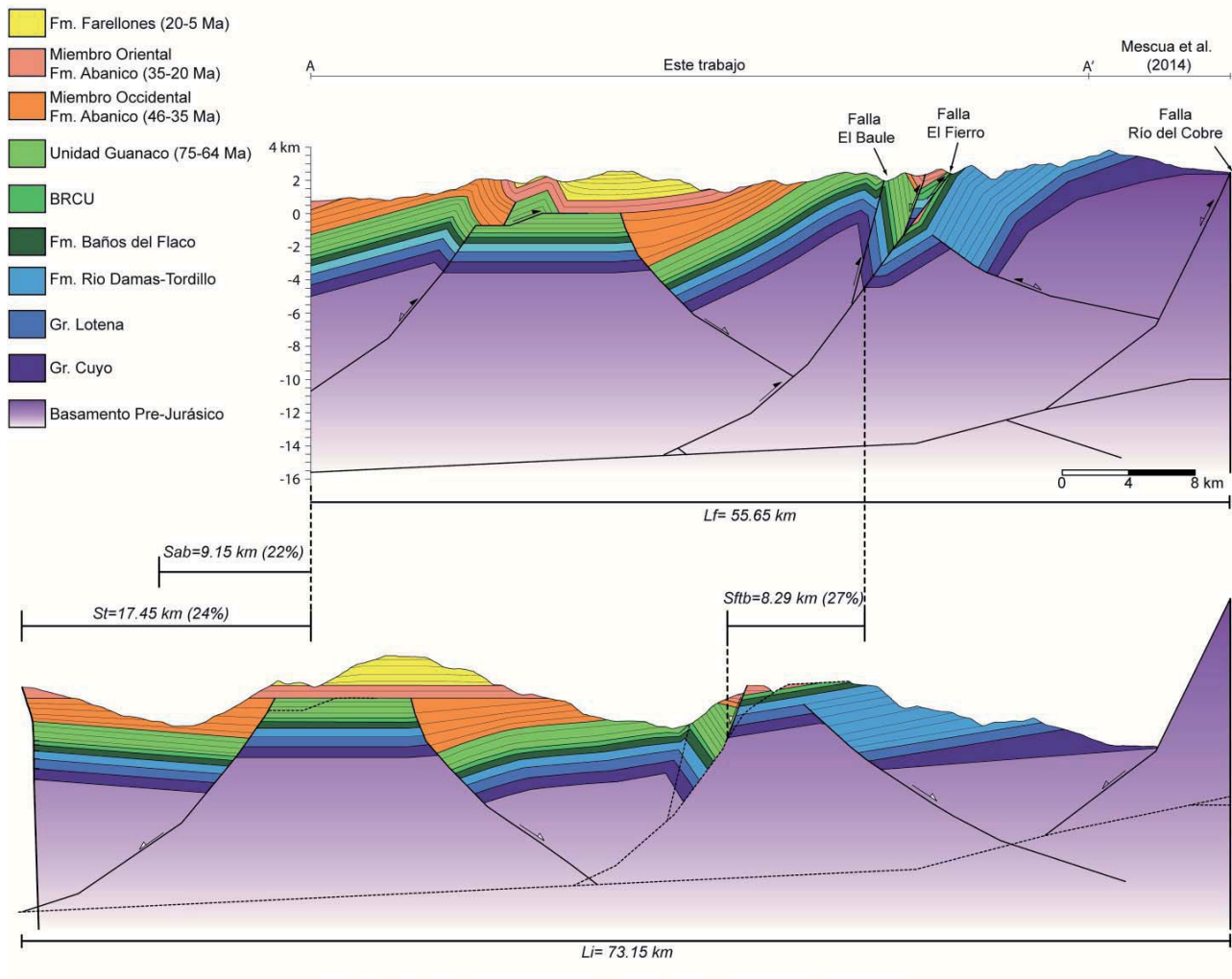


Fig. II.15. Perfil estructural A-A' a lo largo del valle del Tinguiririca y su reconstrucción palinspástica al Mioceno temprano (Ver la traza del perfil en Fig. II.1).

En superficie, esta estructura profunda, ubicada entre las fallas El Baule y El Fierro (Fig. II.15), coincide con la falla normal asociada al desarrollo de los estratos de crecimientos del Miembro Oriental de la Fm. Abanico, en el sector de arroyo Garcés. Esto podría sugerir que la estructura profunda corresponde a una falla normal invertida y no a una falla inversa nueva. Sin embargo, de acuerdo con el espesor estimado para el Miembro Oriental en esta región ($< 300\text{m}$), la falla extensional tiene un movimiento normal de centenas de metros, por lo que su movimiento inverso no podría explicar la geometría de 9 km de media longitud de onda del anticlinal ubicado al oeste de la falla (Fig. II.15). Se propone entonces, que en los últimos metros, cercano a la superficie, la *tip-line* de la falla inversa aprovechó el plano de la falla normal previo para canalizar el desplazamiento y la deformación a través de ella. No obstante, considerando el carácter sin-extensional de la Unidad Guanaco, esa falla profunda podría corresponder a una estructura normal invertida, heredada del Cretácico Tardío y aprovechada durante la extensión paleógena y durante la contracción neógena.

Por otra parte, la falla inversa propuesta también coincide con el límite hasta donde se habría depositado la Unidad Guanaco, ya que hacia el este de la estructura, el Miembro Oriental de la Fm. Abanico se encuentra apoyado discordantemente sobre el BRCU, evidenciando un *hiatus* en el registro estratigráfico y el no depósito de la Unidad Guanaco sobre el BRCU. Esto podría sugerir que la falla inversa corresponde a una falla normal previa del Cretácico Superior que controló el depósito de la Unidad Guanaco, consistentemente con las estructuras extensionales encontradas en esta unidad (Fig. II.4). Sin embargo, se requieren más estudios acerca del volcanismo y la tectónica durante el Cretácico Tardío para establecer la naturaleza de esta estructura profunda.

De acuerdo con la información y el modelo presentado se puede establecer que la Cordillera Principal occidental a 35°S presenta un estilo estructural de piel gruesa, en el que el basamento está involucrado a través de la generación de fallas nuevas o por la inversión de fallas previas. El acortamiento estimado total corresponde a 17,45 km, que equivale al 24%. Al descomponer la cantidad de acortamiento de la región abarcada por este se obtiene un acortamiento de 9,15 km (22%) para el dominio referido a la Cuenca de Abanico y 8,29 km (27%) para la estructura más oriental perteneciente a la faja plegada y corrida de Malargüe.

En particular, el valor de acortamiento obtenido para la Cuenca de Abanico es menor al estimado por otros autores a esta latitud 35°S (Mescua et al., 2014), debido principalmente a que este estudio no abarcó el ancho completo de la cuenca. Si se considera los 15-20 km de acortamiento estimados por Mescua et al. (2014) para la Cuenca de Abanico a esta latitud, junto con que el ancho de la cuenca son 64 km, medida perpendicularmente a las estructuras que la limitan, se puede establecer que el porcentaje de acortamiento es 18,9-23,8 %. Estos valores coinciden con los 22% de acortamiento estimados en este trabajo y a 36°S (Astaburuaga, 2014). Si consideramos la porción no considerada en este estudio (30 km), el acortamiento total correspondería a 18 km para toda la cuenca, consistente con los 16 km de Farías et al. (2010) y lo estimado por Mescua et al. (2014) para 33°30'S y 35°S, respectivamente.

II.6 Análisis complementario: El Cretácico Tardío en la Cordillera Principal occidental y sus implicancias regionales

Las edades de circones detríticos presentados en este trabajo para los depósitos del Cretácico Superior, tales como el BRCU y las Areniscas de Pichuante, evidencian casi una exclusiva fuente de sedimentos del Cretácico Temprano y Tardío. Posibles zonas fuentes de este rango de edad corresponden a los rocas ígneas de la Cordillera de la Costa que representan el arco magmático del periodo Cretácico (Charrier et al., 2014). Por otra parte, recientes dataciones U-Pb en circones detríticos de depósitos marinos y continentales del Cretácico Temprano en el área del Maule (Astaburuaga, 2014), muestran poblaciones de edades entre 121-134 Ma sugiriendo que el depósito de estas rocas fue previo al Cretácico Superior y que su posterior erosión podría haber aportado sedimentos las secuencias del Cretácico Superior, tales como el BRCU. De esta manera, se puede inferir que el BRCU habría tenido un principal aporte de sedimentos desde el oeste y desde regiones aledañas a los lugares de acumulación.

Por otra parte, el BRCU ha sido correlacionado con los depósitos del Gr. Neuquén ubicados en Argentina (Charrier et al., 2014, 2007). Al comparar las edades del BRCU con las del Gr. Neuquén se puede establecer que: (1) el BRCU es más joven que los depósitos de la Fm. Candeleros de la base del Gr. Neuquén (Fig. II.16) asignada al Cenomaniano-Turoniano (Tunik et al., 2010); (2) el BRCU se puede correlacionar con los depósitos de la parte media y superior del Gr. Neuquén, fms. Huincul, Portezuelos y Bajo de La Carpa. En particular, una datación de $88 \pm 3,9$ Ma en trazas de fisión en circón realizada en un nivel de toba de la Fm. Huincul acotan la edad máxima del depósito de esta formación en el Turoniano-Coniaciano (*cf.* Tunik et al., 2010), lo cual se correlaciona con el BRCU. Por otra parte, la edad máxima de las Fms. Portezuelos y Bajada de La Carpa no fue determinada ya que los *peaks* más jóvenes en los diagramas de distribución son más antiguos que la edad estratigráfica que se les asigna (Fig. II.16) (Di Giulio et al., 2012; Tunik et al., 2010). Lo anterior ha sido interpretado como un cambio de oeste a este en las áreas de aporte entre la base y el techo del Gr. Neuquén debido al alzamiento del bulbo periférico del sistema de antepaís del Cretácico Tardío lo cual permitiría la erosión de rocas del basamento de edad Mesoproterozoico-Paleozoico temprano ubicadas hacia el este (Di Giulio et al., 2012).

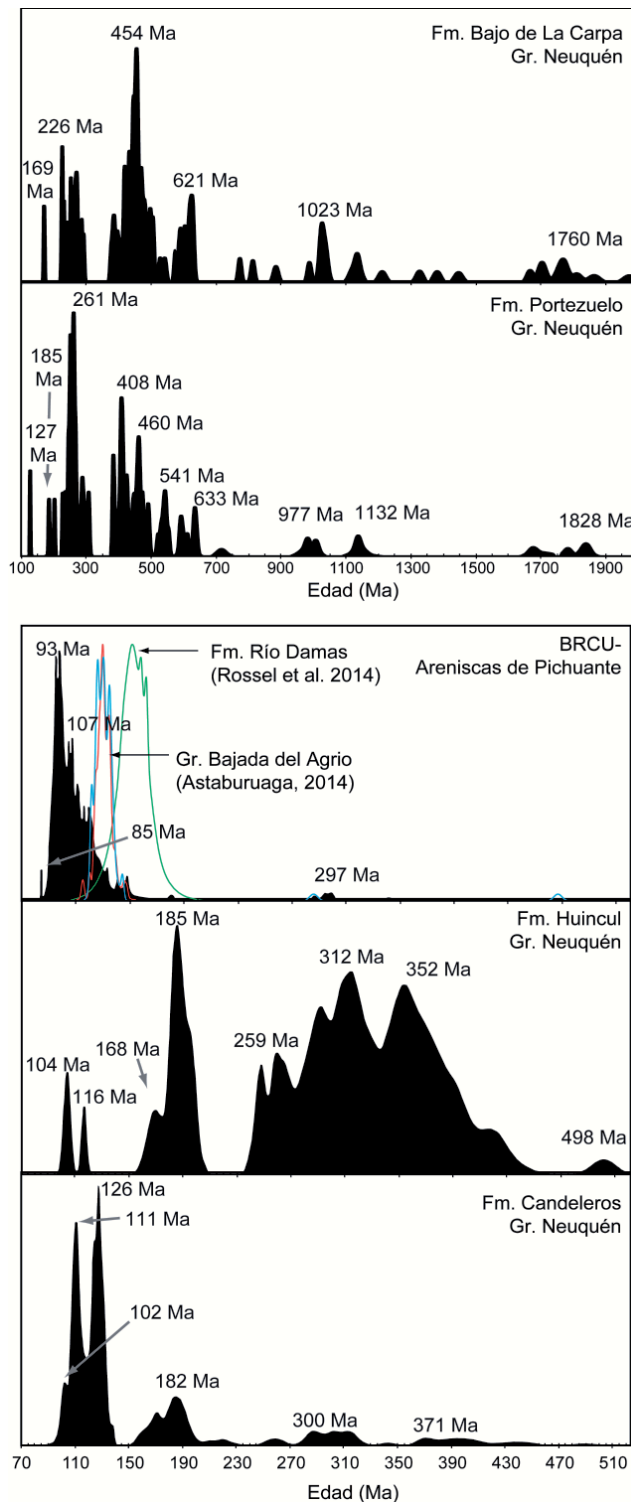
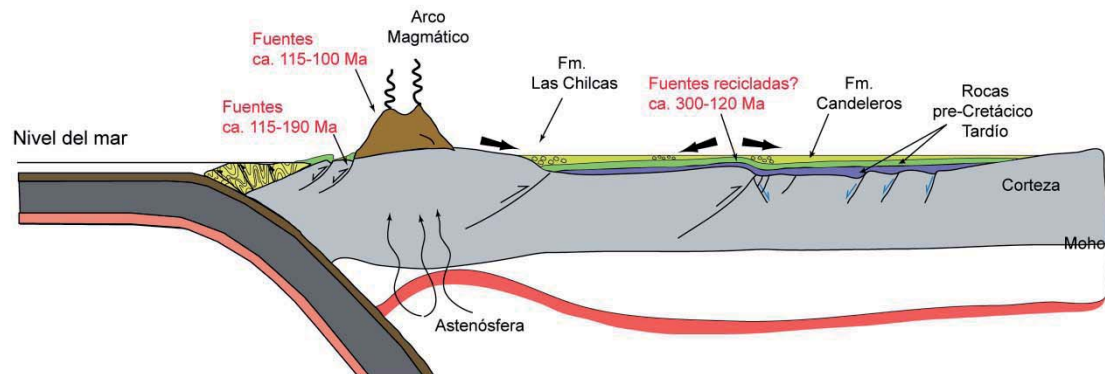


Fig. II.16. Comparación entre las formaciones del Gr. Neuquén y BRCU-Areniscas de Pichuante, basado en las curvas de probabilidad relativa de los análisis U-Pb de circones detriticos. Las curvas de probabilidad relativa del Gr. Neuquén fueron tomados de (Di Giulio et al., 2012; Tunik et al., 2010). En el gráfico correspondiente al BRCU-Areniscas de Pichuante se agregaron las curvas de probabilidad relativa de una muestra de la Fm. Río Damas, en el río de Las Damas (Rossel et al., 2014) y de dos muestras del Gr. Bajada del Agrio (Fm. Colimapu en el sentido de Klohn, 1960), en el río Maule (Astaburuaga, 2014).

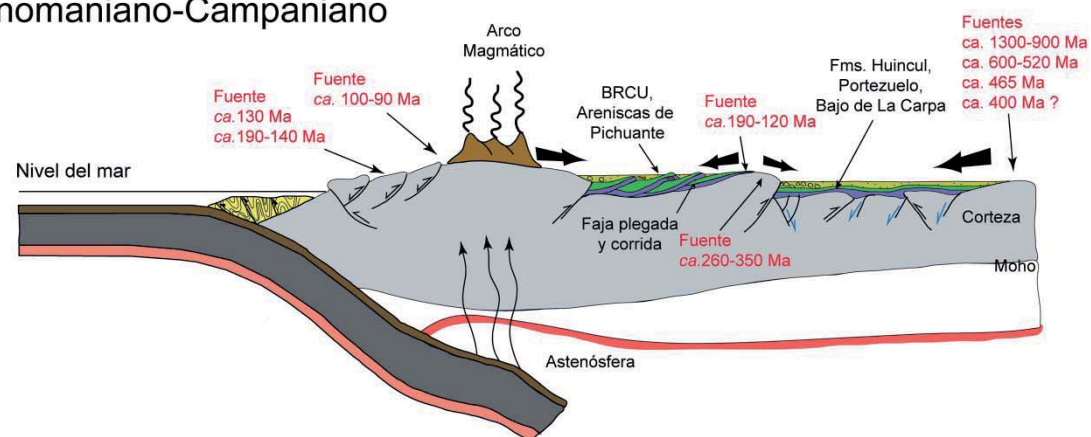
De esta manera, de acuerdo con las dataciones y nuevos estudios en los depósitos sinorogénicos del Cretácico Tardío, la deformación durante el Albiano-Cenomaniano estuvo caracterizada por el depósito del miembro Pitipeumo de la Fm. Las Chilcas, en el borde oriental de la Cordillera de la Costa (Fig. II.17a) (Boyce et al., 2014) y por el depósito de la Fm. Candeleros, que se estima habría tenido una ubicación distal respecto al orógeno (Fig. II.17a), de acuerdo con su posición actual respecto a la Cordillera de la Costa que habría correspondido a la región que experimentaba deformación y alzamiento (Boyce et al., 2014; Di Giulio et al., 2012; Tunik et al., 2010 y referencias ahí), pero lo cual no puede ser demostrado con los resultados mostrados en esta Tesis.

La correlación temporal establecida entre el BRCU y las fms. Huincul, Portezuelos y Bajo de la Carpa, indicaría que los depósitos continentales del Cretácico Tardío ubicados en la Cordillera Principal al sur de 33°30'S se habrían acumulado en un sistema de cuenca de antepaís, al igual que los términos más jóvenes del Gr. Neuquén durante el Cenomaniano-Campaniano (Fig. II.17b) (Di Giulio et al., 2012; Tunik et al., 2010). Sin embargo, la comparación del registro de edades U-Pb en circones detríticos de estas unidades evidenciaría variaciones en las áreas fuentes de los sedimentos. Por un lado las fms. Huincul, Portezuelo y Bajo de la Carpa presentan un amplio registro de circones jurásicos, triásicos, paleozoicos e incluso proterozoicos y una nula presencia de circones más jóvenes que 100 Ma. Tunik et al. (2010) y Di Giulio et al. (2012) propusieron que los circones jurásicos en estas formaciones provendrían desde la Cordillera de la Costa ubicada al oeste, sin embargo, la ausencia de edades jurásicas en el BRCU, desecharían esta hipótesis considerando que el BRCU se encuentra más cerca de la Cordillera de la Costa. Una fuente alternativa para los circones jurásicos en el Gr. Neuquén podría corresponder al reciclaje de las secuencias sedimentarias jurásicas acumuladas en la Cuenca Neuquina y que durante el Cretácico Tardío fueron involucradas en la deformación y estructuración de las fajas plegadas y corridas de Chos-Malal y del Agrio (Fig. II.17b) (Zamora Valcarce y Zapata, 2009; Zamora Valcarce et al., 2006; Zapata y Folguera, 2005). De acuerdo con lo anterior, se infiere que esta fase de estructuración de las fajas plegadas y corridas habría constituido una barrera paleogeográfica impidiendo el paso de circones más jóvenes que 100 Ma desde el oeste (Fig. II.17b), como lo evidencian los registros de edades detríticas de las fms. Huincul, Portezuelos y Bajo de la Carpa. Así mismo, esta barrera habría truncado el paso de circones paleozoicos y proterozoicos desde el este hacia el oeste, provenientes del basamento ubicado al este de la Cuenca Neuquina (Fig. II.17b). Por lo tanto, el inicio de la formación de las fajas plegadas y corridas que caracterizan la vertiente oriental de los Andes Centrales del sur habría sido previo a los 90 Ma de acuerdo con las edades del BRCU. De la misma manera, se puede establecer que el BRCU se depositó en la parte más occidental de la cuenca de antepaís segmentada y compartimentalizada, en lo que podría corresponder a una parte del *wedge-top* del sistema (Fig. II.17b) (DeCelles y Giles, 1996). De acuerdo a Di Giulio et al. (2012), las Fms. Huincul, Portezuelo y Bajo de la Carpa se habrían depositado en el *foredeep*, una posición más cercana al bulbo periférico, el cual sería la región fuente para los circones de edad pre-mesozoico (Fig. II.17b). Sin embargo, recientes trabajos han mostrado que el Gr. Neuquén también se habría depositado en el *wedge-top* de la cuenca y no en el *foredeep* (Fennell et al., 2014).

(a) Albiano-Cenomaniano



(b) Cenomaniano-Campaniano



(c) Campaniano-Paleógeno temprano

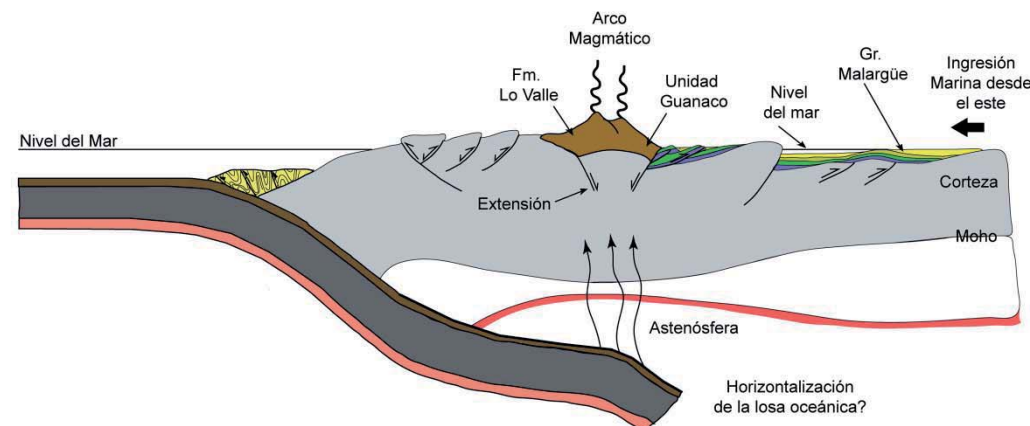


Fig. II.17. Evolución geológica y paleogeográfica del Cretácico Tardío a 35°S. (a) Inicio de la deformación compresiva correspondiendo al primer periodo de construcción de los Andes. (b) Estructuración de las fajas plegadas y corridas junto con la acumulación de depósitos sinorogénicos. (c) Estadio final de la fase compresiva, caracterizada por la migración del arco hacia el este, dominado por una deformación extensional, ingresión marina desde el este y depósito del Gr. Malargüe.

Las edades obtenidas por Mosolf (2013) y las realizadas en este estudio permiten señalar que la Unidad Guanaco representa el primer registro de rocas volcánicas de edad Campaniano-Daniano a lo largo de la Cordillera Principal, al sur de 34°S (Fig. II.17c). Su identificación y caracterización ayudará a profundizar el conocimiento de la evolución de los Andes previo al depósito de las rocas volcánicas Cenozoicas, las cuales obliteraron cualquier evidencia de deformación del Cretácico Tardío en la región cordillerana de Chile Central. De acuerdo con las edades presentadas aquí, la Unidad Guanaco se depositó contemporáneamente con el Gr. Malargüe ubicado en la ladera oriental del orógeno cretácico Tardío-paleógeno (Fig. II.17c). Esta correlación temporal entre los depósitos volcánicos del oeste con las sucesiones sedimentarias continentales y marinas del este, evidencian la existencia del proto-orógeno Andino el cual actuó de barrera ante la ingresión marina del este, proveniente del Atlántico (Fig. II.17c).

En particular, las fallas normales en los depósitos volcánicos de la Unidad Guanaco podían corresponder a estructuras extensionales rotacionales originadas como respuesta a la flexura de la corteza debido a la carga ejercida por el orógeno construido (Scisciani et al., 2001). El fallamiento normal generaría el espacio necesario para la acumulación de depósitos volcánicos o sedimentarios dentro de un contexto de cuenca de antepaís en el inicio de la construcción de los Andes, durante el Cretácico Tardío. Por otra parte, el periodo de depósito de la Unidad Guanaco coincide también con una disminución de la velocidad absoluta al oeste de placa Sudamericana (Silver, 1998). Esta coincidencia temporal sugiere una posible relación causa/efecto entre la disminución de la velocidad de convergencia de la placa y la extensión en la corteza superior, tal como ha sido propuesto para la formación de la Cuenca de Abanico (Jordan et al., 2001; Somoza y Ghidella, 2005). La disminución de la velocidad de la placa originaría un colapso o relajamiento extensional del reciente orógeno reactivándose negativamente fallas inversas previas junto con la creación de nuevas estructuras.

Otro punto a considerar corresponde la deformación presente en la Unidad Guanaco y reportada por Mosolf (2013), la cual quedaría acotada entre los 64 y 46 Ma. De acuerdo con esto, el origen de la deformación podría estar relacionada, tanto con la fase compresiva K-T como con la Incaica (*cf.* Charrier et al., 2014. Capítulo 2). Si bien no se tienen suficientes datos para restringir e identificar la fase de deformación, los datos reportados aquí y por Mosolf, (2013) indican que este periodo de deformación habría ocurrido entre 63-46 Ma, correspondiendo a las primeras evidencias de deformación contraccional durante el Paleógeno, al sur de 33°S.

Finalmente, la identificación de la Unidad Guanaco al este de los depósitos del arco del Cretácico Temprano (*cf.* Charrier et al., 2014), evidenciaría una migración del volcanismo durante el Cretácico Tardío desde la Cordillera de la Costa hacia el este (Fig. II.17). De acuerdo con los modelos propuestos para este periodo al sur de 36°S, la migración del volcanismo y la deformación se podría haber originado por una somerización de la placa subductada durante el Cretácico Tardío (Spagnuolo et al., 2012a). Sin embargo, se hace imprescindible un estudio más detallado y una actualización de la geología de la cordillera para profundizar el conocimiento de la evolución andina y así establecer un modelo geodinámico más detallado para el Cretácico Tardío-Paleógeno.

CAPÍTULO III.

LA FAJA PLEGADA Y CORRIDA DE MALARGÜE Y LA INFLUENCIA DE ESTRUCTURAS PREVIAS EN SU EVOLUCIÓN

III.1 Introducción

La faja plegada y corrida de Malargüe se desarrolla a lo largo de la vertiente oriental de la Cordillera Principal entre 34° y 37°S (Fig. III. 1). Presenta un estilo de deformación híbrida que incluye fallas inversas de alto ángulo, las que corresponderían a la reactivación de estructuras previas formadas durante la fase extensional Mesozoica e invertidas durante la contracción del Cretácico Tardío (Orts y Ramos, 2006; Mescua et al., 2013, Fennell et al., 2014) y Mioceno (Giambiagi et al., 2009, 2008; Kozlowsky et al., 1993).

Considerando lo anterior, se hace necesaria la caracterización de la arquitectura extensional mesozoica para comprender el desarrollo y construcción de la faja plegada y corrida de Malargüe dado el control que ejercen las estructuras previas en la evolución y construcción de los Andes según el registro reportado por numerosos trabajos desarrollados no solo en el este sector de la cadena, sino en general a lo largo de toda ella (e.g. Giambiagi y Ramos, 2002; Giambiagi et al., 2009, 2008; Kozlowsky et al., 1993; Manceda y Figueroa, 1995; Mescua et al., 2014; Orts et al., 2012; Yagupsky et al., 2008).

En particular, la arquitectura del borde occidental de la Cuenca Neuquina ha sido poco estudiada, lo que ha impedido un estudio continuo de la geología a través de la Cordillera Principal. En ese sentido, este capítulo presenta nuevos antecedentes de la paleogeografía mesozoica de la parte oeste de la Cuenca Neuquina y la influencia de ésta en el posterior desarrollo de la faja plegada y corrida de Malargüe. En la primera sección de este capítulo se expone un estudio de proveniencia para las secuencias del Jurásico Medio y Tardío mediante dataciones U-Pb en circones detríticos. Esto permitió establecer áreas de aporte y zonas de acumulación de sedimentos así como un modelo evolutivo desde el Triásico Tardío al Cretácico Temprano. La última sección del capítulo, corresponde a la propuesta de un artículo en el que se analiza como la paleogeografía mesozoica influyó en la evolución de la faja plegada y corrida de Malargüe, junto con una discusión de sus implicancias en la construcción del orógeno Andino.

III.2 Arquitectura Previa: La extensión mesozoica

El borde occidental de Gondwana durante el Jurásico se caracterizó por una tectónica extensional en la cual se desarrolló un arco magmático, en lo que actualmente corresponde a la Cordillera de la Costa en Chile, junto con una cuenca de tras-arco al este, denominada en la región de estudio como la Cuenca Neuquina (ver Charrier et al., 2014 y referencias ahí). Recientes trabajos a lo largo del borde oriental de la Cuenca Neuquina han reconocido tres principales áreas fuentes para el relleno jurásico de la cuenca: Grupo Choiyoi (290-240 Ma), volcanismo Precuyano (230-200 Ma) y el arco magmático jurásico (200-145 Ma) (Naipauer et al., 2014).

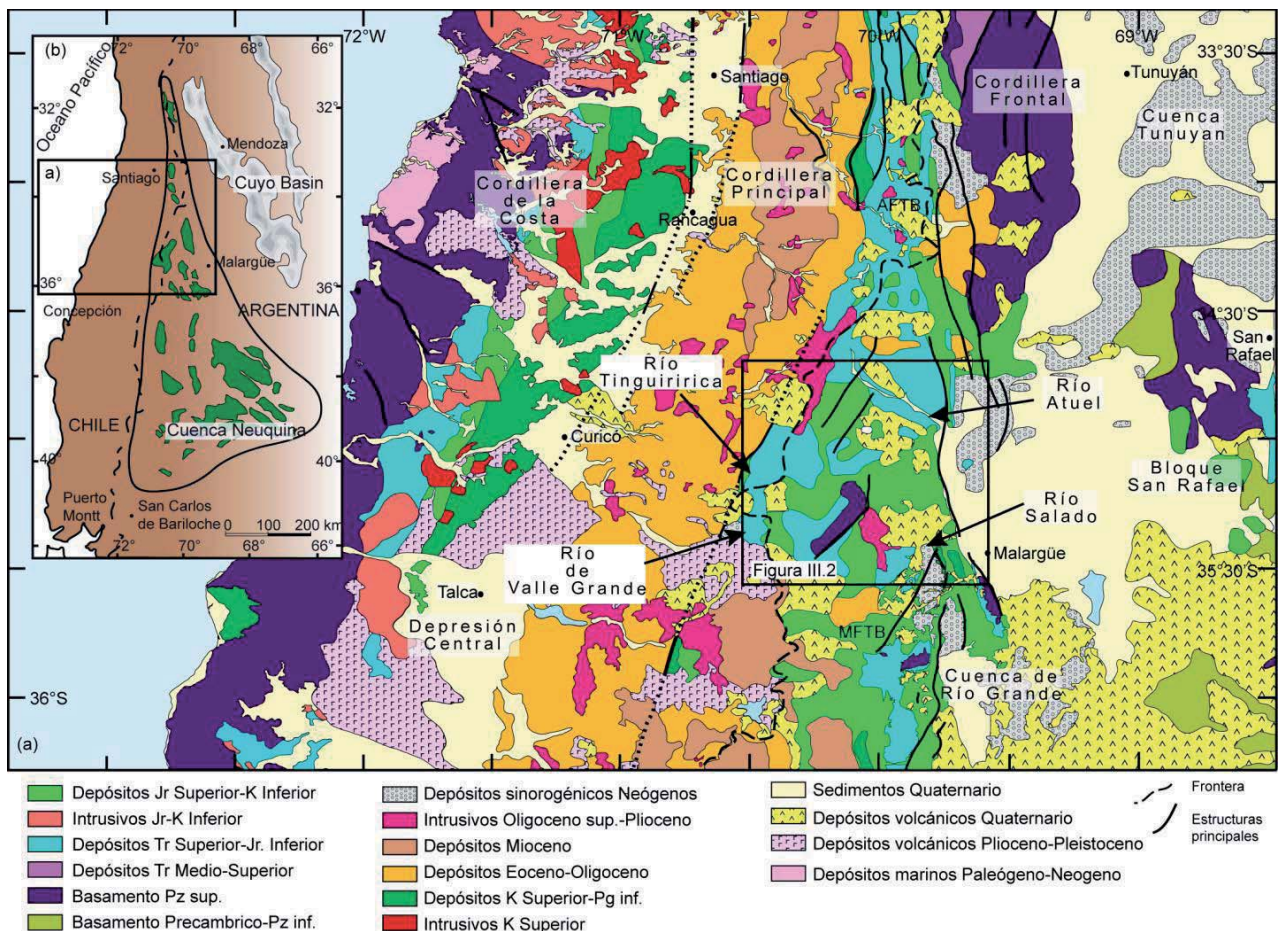


Fig. III. 1. (a) Mapa geológico simplificado de los Andes Centrales del sur mostrando la ubicación de los sitios de origen de las muestras presentadas en esta sección: Río Tinguiririca, Atuel, Salado y Valle Grande. AFTB: Faja plegada y corrida de Aconcagua; MFTB: Faja plegada y corrida de Malargüe. (b) Ubicación de la Cuenca Neuquina. En verde se muestran los depocentros reconocidos dentro de la cuenca.

Con el objeto de reconocer variaciones en las áreas fuentes de los sedimentos entre la parte oeste y este de la cuenca durante el Jurásico y así determinar la paleogeografía durante este periodo, se realizaron análisis de edades U-Pb en circones detríticos en ocho muestras obtenidas en secuencias jurásicas del borde occidental y oriental de la Cuenca Neuquina. Se recolectaron tres muestras pertenecientes a las formaciones Lotena, La Manga y Río Damas, esta última equivalente a la Fm. Tordillo, en la región del río Valle Grande, Chile (Fig. III.2); una muestra de la Fm. Río Damas, en el sector del río de las Damas, Chile (Fig. III.2); dos muestras de la Fm. Tordillo en el

área del río Atuel, Argentina (Fig. III.2); y dos muestras de la Fm. Tordillo en la región del río Salado, Argentina (Fig. III.2). Todos los resultados analíticos se encuentran en el Anexo III.

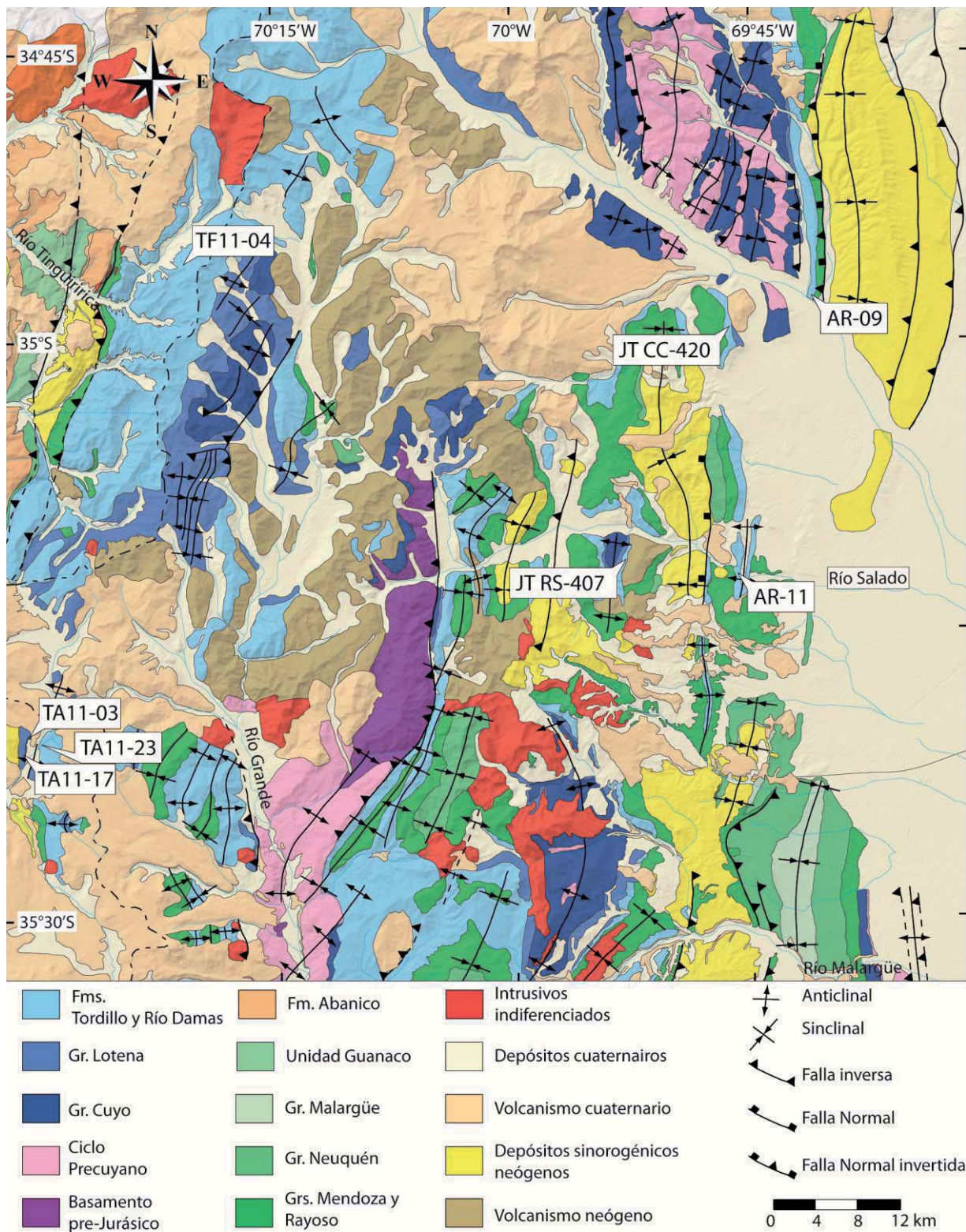


Fig. III.2. Mapa Geológico del área de estudio y ubicación de las 8 muestras analizadas. Basado en Giambiagi et al. (2009) y (2008).

III.2.1 Resultados

La Tabla III.1 muestra el número de análisis realizados para cada muestra junto con los que fueron rechazados, ya sea por una alta incerteza o por que presentaban un porcentaje de discordancia muy elevado ($>15\%$) (Fig. III.3). Además, se indica para cada muestra su ubicación dentro de la Cuenca Neuquina, la unidad estratigráfica a la cual pertenece y la localidad geográfica de donde fue recolectada

Tabla III-1. Muestras estudiadas y cantidad de análisis realizados y rechazados para cada una de ellas.

	Muestra	Formación	Localidad	Cantidad de Análisis	Cantidad de Análisis descartados
Borde Occidental	TA11-03	Lotena	Valle Grande	52	0
	TA11-17	La Manga	Valle Grande	98	1
	TA11-23	Río Damas	Valle Grande	85	44
	TF11-04	Río Damas	Tinguiririca	100	11
Borde Oriental	AR-11	Tordillo	Salado	82	41
	JTRS-407	Tordillo	Salado	85	41
	JTRS-429	Tordillo	Atuel	81	28
	AR-09	Tordillo	Atuel	81	37

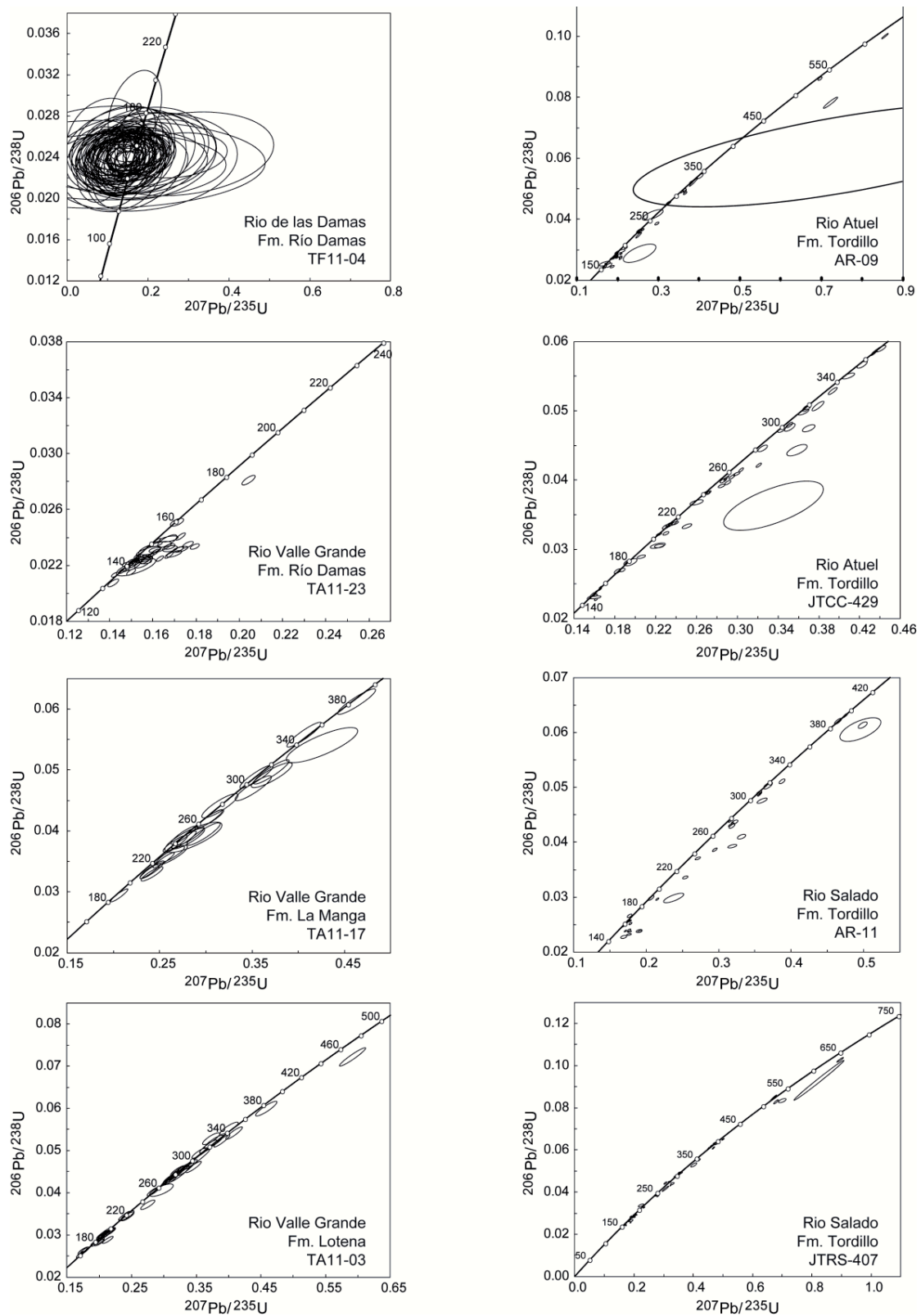


Fig. III. 3. Diagramas de concordia para resultados analíticos de dataciones U-Pb en circones detriticos para las muestras de las fms. Lotena, La Manga, Río Damas y Tordillo (ver Fig. III.2 para la ubicación de muestras).

Las muestras del borde occidental pertenecientes a las formaciones Lotena y La Manga muestran una distribución de edades multimodal con los *peaks* máximos correspondientes a las edades asociadas al arco jurásico (162-200 Ma), destacando de forma secundaria edades entre 200-220 Ma, 220-300 Ma y 300-330 Ma (Fig. III.4). Con menor representatividad se observan edades mayores a 330 Ma (Fig. III.4) pertenecientes al basamento magmático-metamórfico del Paleozoico que aflora al este de la Cuenca Neuquina (Fig. III.1). En las muestras de la Formación Tordillo en los ríos Atuel y Salado, en el borde oriental de la Cuenca Neuquina, también se observan histogramas multimodales en los que la mayor frecuencia se concentran en edades asociadas al arco jurásico (149-200 Ma) y con *peaks* secundarios de edades de el ciclo Precuyano (200-227 Ma), provincia magnética Choiyoi (227-300 Ma) y magmatismo del Carbonífero (300-350 Ma) (Fig. III.4). Por el contrario, las muestras de la Fm. Río Damas de los ríos de las Damas y Valle Grande en la parte oeste, presentan una distribución unimodal con edades que representan el magmatismo de arco jurásico, con un rango comprendido entre 142-170 Ma.

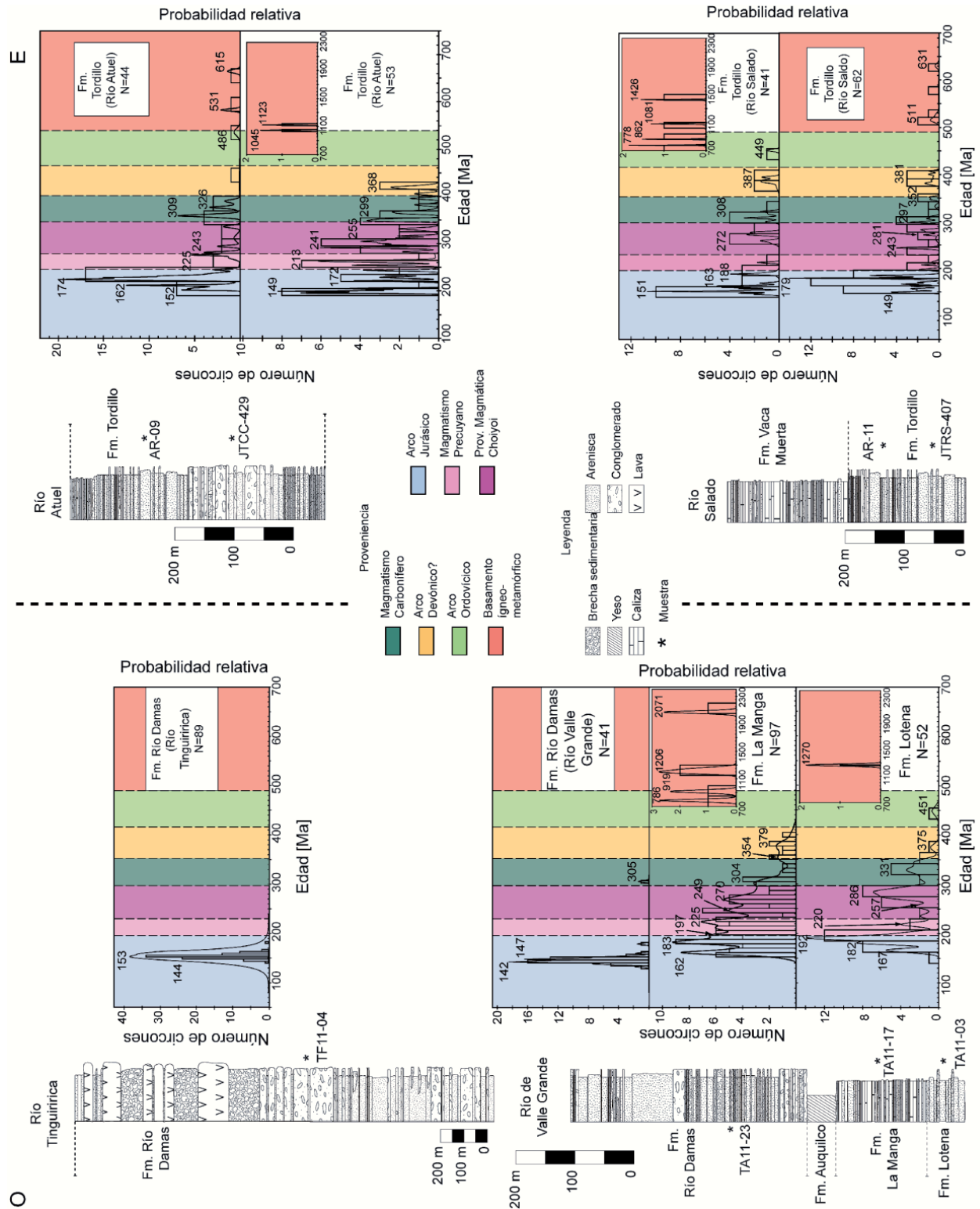


Fig. III.4. Histogramas de frecuencia y probabilidad relativa de las edades U-Pb en cirón detrítico de las muestras de las fms. La Manga, Lotena, Río Damas y Tordillo recolectadas en este estudio. Además se presentan columnas estratigráficas esquemáticas que incluye la posición de las muestras.

III.2.2 Interpretación de los resultados: Áreas de aporte e implicancias para la evolución jurásica

A partir de los resultados obtenidos se puede establecer que en todas las muestras los circones más jóvenes tienen edades jurásica, lo que representa aportes desde el arco magmático ubicado al oeste (Fig. III.5). Por otro lado, los circones asociados al ciclo Precuyano provendrían de la erosión de altos de basamento desarrollados a lo largo de la cuenca. En particular, a 35°S se reconoce el Alto Dedos de Silla (Fig. III.5), una estructura formada por rocas intrusivas del Pérmico-Triásico y rocas volcánicas y sedimentarias del Triásico Tardío que establecieron un alto geográfico durante el Jurásico (Manceda y Figueroa, 1995). Este relieve positivo se continúa hacia el norte donde fue reconocido con el nombre Alto del Tordillo (Davidson y Vicente, 1973; Legarreta y Kozlowsky, 1984). Además de estos altos de basamento, otra fuente para los circones asociados a la provincia magmática del Choiyoi (227-300 Ma) sería la Cordillera Frontal (Fig. III.5), la cual está compuesta por rocas del Pérmico y Triásico, junto con depósitos del Carbonífero y Devónico (Fig. III.1) (Heredia et al., 2012 y referencias ahí); y el Bloque San Rafael ubicado al este de la Cuenca Neuquina (Fig. III.5) donde además de las rocas volcánicas del Grupo Choiyoi afloran rocas con una edad mayor a 300 Ma (Fig. III.1) (Japas et al., 2008 y referencias ahí).

El área de proveniencia para los circones del Pensilvaniano (Carbonífero tardío) correspondería al Batolito Paleozoico ubicado en la Cordillera de la Costa (Fig. III.5), el cual presenta edades U-Pb en circón entre 300 y 320 Ma (Deckart et al., 2014; Hervé et al., 2013) y de acuerdo con edades de trazas de fisión en el complejo de subducción Paleozoico que intruye (Willner et al., 2005), habría sido exhumado durante la extensión mesozoicas. Por último, los circones con edades mayores a 330 Ma provendrían desde el sector más al este de la Cuenca Neuquina donde aflora el basamento paleozoico (Fig. III.1) (Azcuy et al., 1999; Baldis y Peralta, 1999; Bordonaro, 1999).

Por otro lado, al comparar los histogramas de las muestras ubicadas en la región oeste de la Cuenca Neuquina se puede establecer una variación en el aporte de sedimentos. La Fm. Río Damas muestra una exclusividad de aporte desde el arco jurásico lo que contrasta con las muestras de las formaciones previas como Lotena y La Manga (Fig. III.4). Esta variación también se ve reflejada en los histogramas de las muestras de la Fm. Tordillo (Fig. III.4), ubicadas en el sector oriental de la cuenca, los cuales indican variabilidad en la proveniencia de sedimentos.

La exclusividad de circones provenientes del arco magmático para la Fm. Río Damas evidenciarían que para el final del Jurásico, los centros volcánicos se habrían ubicado muy próximos a lo que hoy corresponde el borde occidental de la Cuenca Neuquina, en la Cordillera Principal. La ubicación de este volcanismo podría corresponder a: 1) la expansión y/o migración del arco magmático respecto de la ubicación en la Cordillera de la Costa para el Jurásico Inferior y Medio (Charrier et al., 2014), o bien a 2) un volcanismo de tras-arco al este del arco magmático contemporáneo, similar a lo propuesto para la Cuenca de Tarapacá, en el norte de Chile (Oliveros et al., 2012). Sin embargo, recientes trabajos demostraron que el volcanismo de la Fm Río Damas muestra una signatura geoquímica con afinidad calcoalcalina lo cual estaría asociado a un arco magmático formado en un ambiente de subducción (Rossel et al., 2014) implicando entonces una expansión y/o migración del arco volcánico al sur de 33°30'S durante el Jurásico Superior.

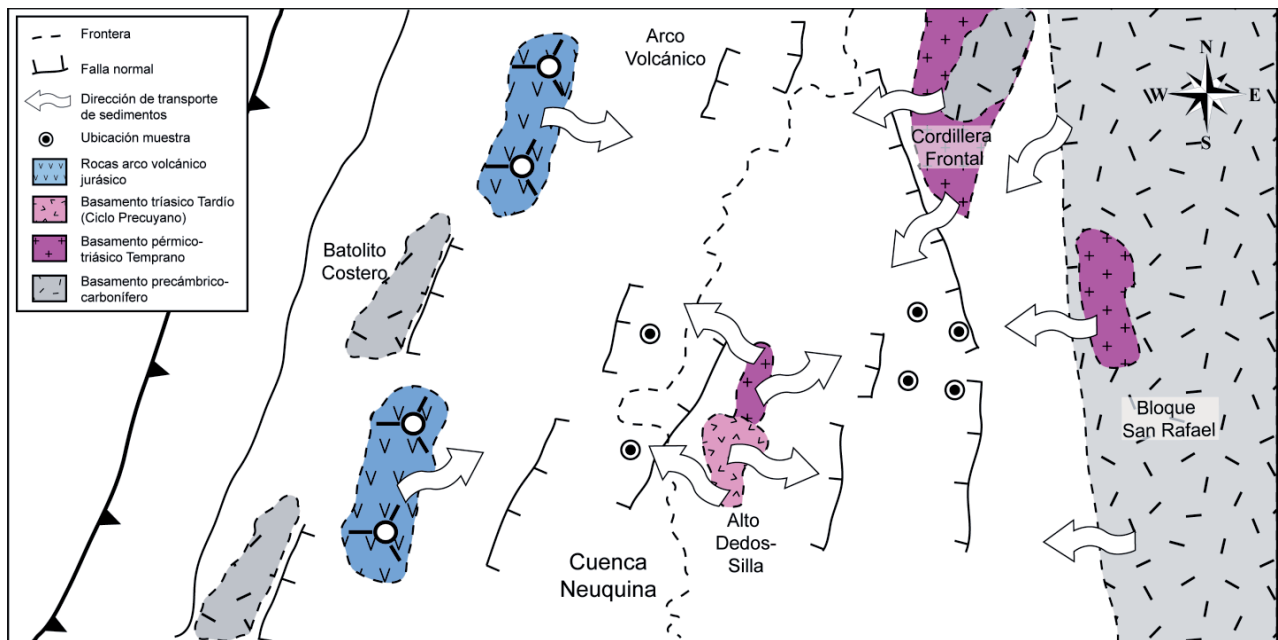


Fig. IV.5. Principales áreas de proveniencia de sedimentos para las rocas del Jurásico Medio y Tardío en la porción norte de la Cuenca Neuquina.

III.2.3 Modelo evolutivo para el Triásico Tardío al Jurásico Tardío

Considerando todos los datos y discusiones presentadas con anterioridad, se presenta un modelo paleogeográfico evolutivo en torno a 35°S. Este modelo consta de periodos que son descritos a continuación.

- **Triásico Tardío a Jurásico Temprano:** Este periodo corresponde al ciclo Precuyano durante el cual comienza a estructurarse la Cuenca Neuquina. Se caracteriza por el desarrollo de depocentros extensionales aislados donde se acumularon los depósitos volcánicos y sedimentarios de las formaciones Remoredo y El Freno (Fig. III.6a). Los altos de basamento corresponderían a las regiones que separarían y delimitarían los depocentros, estableciéndose como las áreas fuentes de sedimentos (Fig. III.6a). El volcanismo estuvo controlado por la ubicación y el desarrollo de fallas normales (Fig. III.6a), lo que explicaría su distribución discreta a lo largo de los Andes. De acuerdo con la edad de la Fm. Remoredo (215 Ma, Andesita de Cerro Negro, Naipauer et al., 2014) y las edades reportadas para los depósitos de este periodo (Naipauer et al., 2014; Schiuma y Llambías, 2008), el ciclo Precuyano se correlacionaría con la segunda etapa del ciclo tectónico Pre-Andino (Charrier et al., 2014), lo que es consistente con el desarrollo de depocentros aislados llenados con depósitos volcánicos, marinos y continentales de acuerdo con su distancia con el océano ubicado en el borde occidental de Gondwana (Charrier, 1979; Charrier et al., 2007).
- **Jurásico Temprano a Jurásico Medio:** Durante este periodo se estableció un arco magmático al oeste de la Cuenca Neuquina, lo que evidenciaría el retorno de la subducción al margen occidental de Gondwana, y el inicio de una transgresión marina desde el oeste (Fig. III.6b) (Charrier et al., 2014). La cuenca adquiere una posición de tras-arco, se produce

un mayor desarrollo de depocentros los cuales terminaron conectándose a través de la unión de fallas normales (*cf.* Bechis et al., 2014, 2010; Giambiagi et al., 2005). La primera parte de este periodo se caracteriza por una sedimentación *syn-rift*, durante la cual se acumularon los depósitos de la parte inferior del Grupo Cuyo (Fig. III.6b), y una posterior sedimentación *post-rift* relacionada a la parte superior del Grupo Cuyo y al Grupo Lotena (Fig. III.6b), aunque en algunas partes estos depósitos tendrían un carácter *syn-rift* asociados a la actividad de fallas normales locales (ver sección III-3). En este periodo se habrían desarrollado altos de basamentos como los altos del Tordillo (Davidson y Vicente, 1973; Davidson, 1971) y Dedos de Silla (Manceda y Figueroa, 1995), los cuales estaban limitados a ambos lados por fallas normales (Fig. III.6b) (Mescua et al., 2014).

- **Jurásico Tardío:** Se caracteriza por una regresión generalizada, sucedida por un nuevo pulso extensional y la expansión hacia el este del arco magmático (Fig. III.6c). Durante este periodo se depositaron las formaciones Río Damas y Tordillo, las cuales presentan los mayores espesores en lugares donde se formaron o reactivaron fallas normales, como en el depocentro Río del Cobre (Mescua et al., 2014). A nivel local, los altos de basamento, tales como el Alto del Tordillo y Dedos de Silla, habrían actuado como barrera impidiendo el paso de sedimentos de este a oeste de acuerdo con el análisis de proveniencia de edades U-Pb en circones detriticos, dejando aislado el lado oeste de la cuenca, el cual solo recibió aporte desde el arco volcánico. Este escenario parece continuar hasta 33°30'S ya que los histogramas de dataciones de circones detriticos en la Fm. Río Damas a esta latitud también muestran una distribución unimodal de edades en torno a 144 Ma (Aguirre et al., 2009). Además, en este periodo se habría expandido el arco magmático hacia el este (Fig. III-5), tal como indicarían las facies volcánicas andesíticas con signatura de arco que caracterizan a la Fm. Río Damas (Rossel et al., 2014)
- **Cretácico Temprano:** Se produce una nueva ingresión marina desde el oeste inundando toda la cuenca. Se depositan las formaciones Baños del Flaco, Vaca Muerta y El Agrio, y el arco volcánico pareciera volver a una posición más occidental de acuerdo con los afloramientos de intrusivos de esta edad en la actual Cordillera de la Costa (Fig. III. 1) (*cf.* Charrier et al., 2014), aún cuando se reconocen intercalaciones volcánicas en los depósitos marino de trasarco de este periodo (*e.g.* Vennari et al., 2014). De acuerdo con las edades U-Pb en circones detriticos reportadas por Astaburuaga (2014) en niveles del techo de la Fm. Baños del Flaco, la principal fuente de sedimentos para los depósitos marinos del borde occidental de la Cuenca Neuquina correspondería al arco volcánico (ver Fig. II.16).

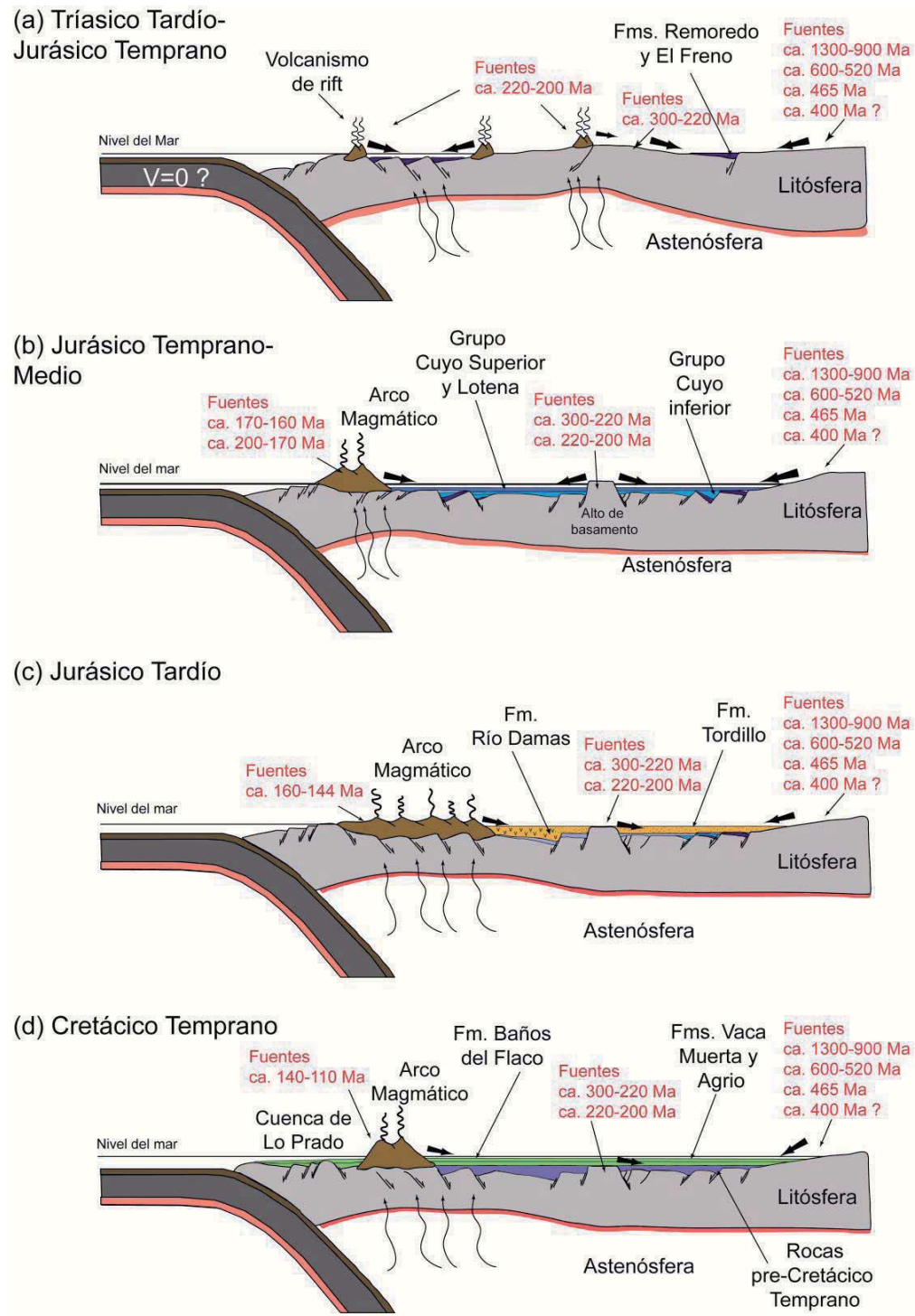


Fig. III.6. Evolución geológica y paleogeográfica en perfiles esquemáticos en torno a 35°S desde el Triásico Tardío hasta Cretácico Temprano. (a) Ciclo Precuyano e inicio de la formación de la Cuenca Neuquina. (b) Mayor desarrollo de depocentros extensionales y ampliación de la Cuenca Neuquina junto con el inicio del magmatismo de subducción. (c) Expansión del arco magmático y depósito de las fms. Tordillo y Río Damas durante un nuevo periodo extensional. (d) Ingresión marina y desarrollo de la Cuenca de Lo Prado al oeste del arco magmático

III.3 Evolución neógena. Artículo: "Controls of the overriding plate architecture in the along-strike Andean segmentations: insight into the Malargüe fold-and-thrust belt, southern Central Andes."

Controls of the overriding plate architecture in the along-strike Andean segmentations: insight into the Malargüe fold-and-thrust belt, southern Central Andes.²

Felipe Tapia^a, Marcelo Fariñas^a, Jose Mescua^b, Laura Giambiagi^b, Maximiliano Naipauer^c, Reynaldo Charrier^{a,d}

^aDepartamento de Geología, Universidad de Chile, Plaza Ercilla 803, Santiago, Chile

^bCentro Científico y Tecnológico CCT-Mendoza, Consejo Nacional de Ciencia y Tecnología (CONICET), Parque San Martín s/n, 5500 Mendoza, Argentina

^cInstituto de Estudios Andinos “Don Pablo Groeber”, Departamento de Ciencias Geológicas, FCEN, Universidad de Buenos Aires-CONICET, Buenos Aires, Argentina

^dEscuela de Ciencias de la Tierra, Universidad Andres Bello, Campus República, Salvador Sanfuentes 2357, Santiago, Chile

²

Artículo en preparación

Abstract

The Andes show remarkable latitudinal variations in their maximum mean elevation, width and crustal shortening produced by changes of the inter-plate dynamics. This phenomenon has been mainly attributed to variations along the subducting plate neglecting the role of the overriding plate features. Here, we explore the influence of the overriding plate architecture in the crustal structural style across the Malargüe foreland fold-and-thrust belt and its consequences in the mountain building processes. Through a newly balanced cross section of the Malargüe fold-and-thrust belt at 35°S, we show that the inversion of the previous normal faults of the Neuquén Basin is the main basement deformational mechanism defining a thick-skinned structural style in the eastern Principal Cordillera at this latitude and thus evidencing the influence of the Mesozoic extensional architecture over the Cenozoic contraction. Although the tectonic inversion characterizes the Malargüe fold-and-thrust belt, the generation of new Andean faults also occurred along the orogen. Comparison of the estimated shortening of 30 km (23.7%) with that reported between 33°30' and 36° S indicates (1) a minimum shortening variation but (2) shortening-percentage southward decreases along the eastern Principal Cordillera. The inverted faults of the thick-skinned fold-and-thrust belt absorb less shortening than low-angle thrusts of the northern thin-skinned fold-and-thrust belt, however, the deformed zone is wider thus accommodating a similar shortening as the northern region. Consequently, the Cordillera is lower and wider in the south respect to that observed north of 34°30'S reflected in the fact that crustal roots are deeper and narrower in the thin-skinned segment respect to the thick-skinned zone. Our results indicate that the previous architecture of the overriding-plate crust is critical for the understanding the Andean segmentation at in this segment of the southern Central Andes suggesting a key role of the overriding plate in the inter-plate dynamics along the Andean subduction.

Keyword: Tectonic inversion, Southern Central Andes, Malargüe fold-and-thrust belt, Paleogeography, Balanced cross-section, Neuquén Basin.

1 Introduction

The Andes are the example of an orogenic system formed in an ocean-continent subduction margin. Along strike, the orogen shows a segmentation evidenced by variations in structural style, crustal thickness and tectonic shortening (*e.g.* Jordan et al., 1983, Kley et al., 1999; Ramos et al., 2004). In particular, the segmentation in the southern Central Andes located south of the current Pampean flat-slab region (Fig 1a) is accompanied by a southward decrease of the mean topographic elevation and maximum crustal thickness attained during the Cenozoic contractional tectonics (*e.g.* Farías et al., 2010; Ramos et al., 1996). Some authors have proposed that the Andean segmentation is controlled by subduction dynamics as well as variations either in the subducting angle or age of the plate along with the presences of discontinuities in the subducting plate, which have been invoked to explain along-strike variations of the Andes (Arriagada et al., 2013; Jordan et al., 1983; Ramos et al., 2014; Schellart, 2008; Sobolev et al., 2006; Yáñez and Cembrano, 2004). Although changes in the subducting angle were proposed to the Neogene evolution of the Andean segment between 34° and 37°S (Kay et al., 2006; Ramos et al., 2014 and references therein), the only variation along the subducting Nazca plate in the southern Central Andes corresponds to the alleged more buoyant ocean crust to the south due to the younger age of the plate (Yáñez et al., 2001).

However, a negligible correlation exists between the age of the subducting plate and the overriding plate deformation along the Andean subduction zone (Schellart, 2008). On the other hand, inherited architecture of the overriding plate has been invoked to explain variations in structural orientations, structural styles, and the amount of accumulated shortening along the Andean orogen (Allmendinger et al., 1983; Kley et al., 1999; Ramos et al., 2004, 1996). Particularly, south of 34°30'S, the deformation front of the Malargüe fold-and-thrust belt in the eastern flank of the Andes coincides with the eastern limit of the major extensional back-arc basins developed in Mesozoic times (Figs. 1b, 2a and b). Moreover, the southward widening of the orogen coincides with the major grade of development of the extensional basin to the south of flat-slab segment according to the 1.29-1.48 crustal attenuation factor (β) estimated to south of 36°S (Sigismondi, 2011) (Figs. 1a and b).

It is widely accepted that crustal shortening is responsible for crustal thickening, defining the height and width of the range. Consequently, the amount of shortening and the features of the structural systems that accommodate deformation are determinant in the resulting shape of the mountain belt. Along strike shortening variations are controlled by the structural styles characteristics of a determined region: a thin-skinned style shows shortening values of 40-70%, the thick-skinned shorten 20-35% and basement thrusts less than 10% (Kley et al., 1999). For these reasons, determining the structural styles is necessary to comprehend what would effectively have controlled the variations of shortening along the southern Central Andes.

In order to address this issue, we examine the structure of the southern Central Andes (33°-36°) constructing a cross section along the eastern Principal Cordillera at 35°30'S. Through with this study, we seek answer three main questions (1) which are the structural styles and the amount of the shortening, (2) what controlled the structural styles, and (3) which has been its influence in mountain building. This study is based on detailed field mapping and U-Pb ages on zircons. Based on our findings, we show major changes on the structural style that would be linked to an inherited architecture. We finally discuss the implications of structural variations in the construction of the mountain belt and the role of the South America overriding plate in the Andean segmentation.

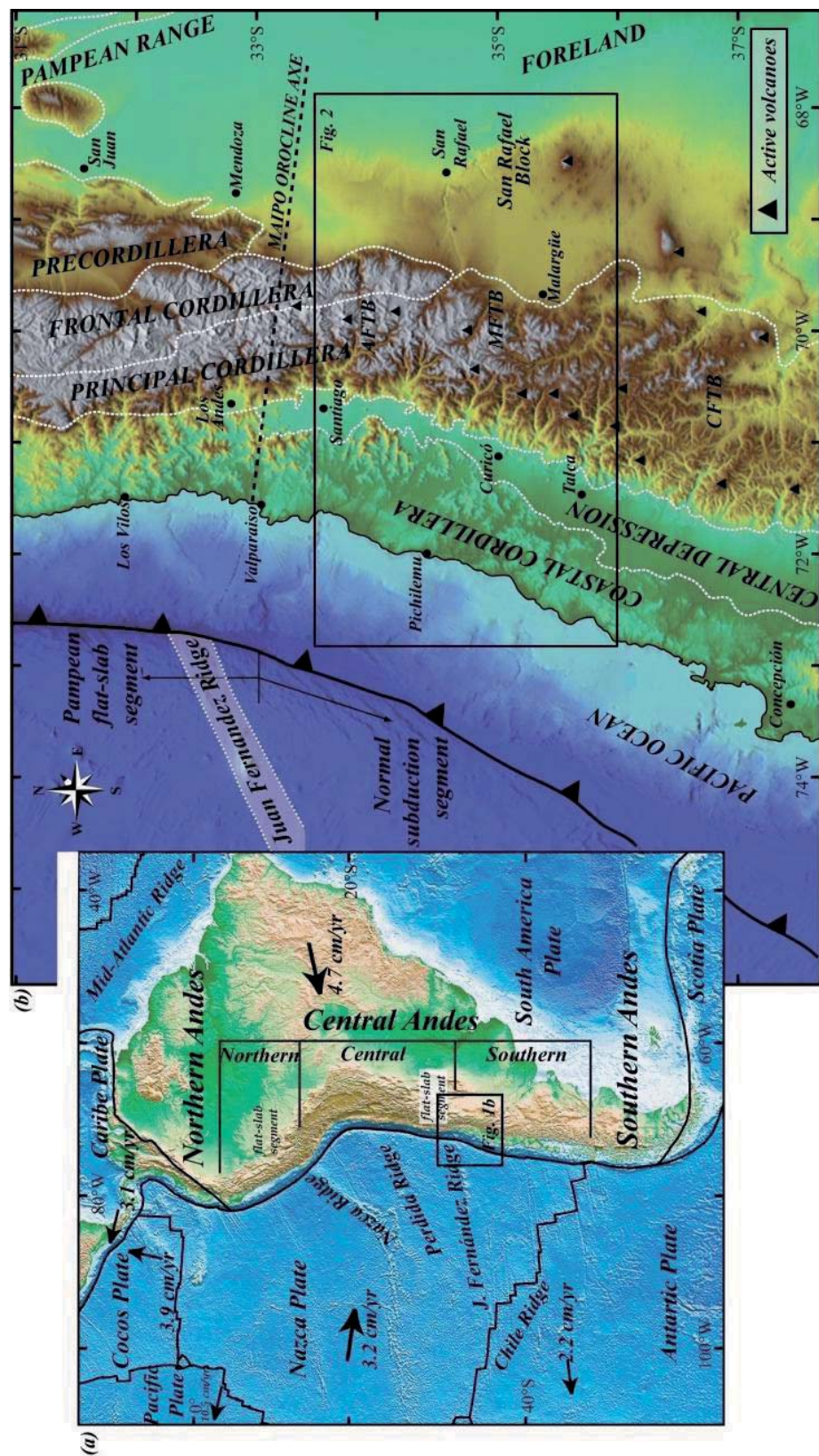


Figure 1. (a) Tectonic framework of the Andean margin. The arrows indicate the absolute velocity of the plate. (b) Main tectonic and morphological features of the Andes of central Chile and western Argentina.

2 Geological Setting

2.1 Tectonic framework

The Andean region between $33^{\circ}30'S$ and $36^{\circ}S$ comprises five major continental morphostructural units (Figure 1b), from west to east: Coastal Cordillera, Central Depression, Principal Cordillera, Frontal Cordillera, which disappears to south of $34^{\circ}40'S$, and the foreland. These morphostructural units consist of igneous, metamorphic and sedimentary rocks formed along of the pre-Andean and Andean evolution (Figs. 1b and 2b) (Charrier et al., 2007).

In this work, the Principal Cordillera has been subdivided into a western and an eastern domain according to the outcropping rocks. The western Principal Cordillera is mainly composed of Cenozoic rocks while the eastern Principal Cordillera is mostly made up by Mesozoic rocks (Fig. 2). The limit between them corresponds to a regional east-vergent reverse fault system associated with basin inversion (named as El Fierro fault system by Farías et al., 2010), which produces the overriding of Mesozoic rocks by Cenozoic rocks.

The tectonic and geological evolution of the western margin of South America has been related to an almost continuous subduction regime. Modern subduction resumed in the western margin of Gondwana during the Mesozoic after a period of terranes accretion during the Proterozoic-Paleozoic and Triassic rifting. Between the Early Jurassic and the middle Cretaceous, the evolution of the Andes was characterized by the development of a magmatic arc in the current Coastal Cordillera (Fig. 1b) and a back-arc basin to the east, dominated by extensional tectonics (Charrier et al., 2007; Ramos, 2000). Since the Late Cretaceous until Present, different pulses of contraction and uplift alternated with extensional episodes controlled the evolution of the southern Central Andes (Charrier et al., 2007).

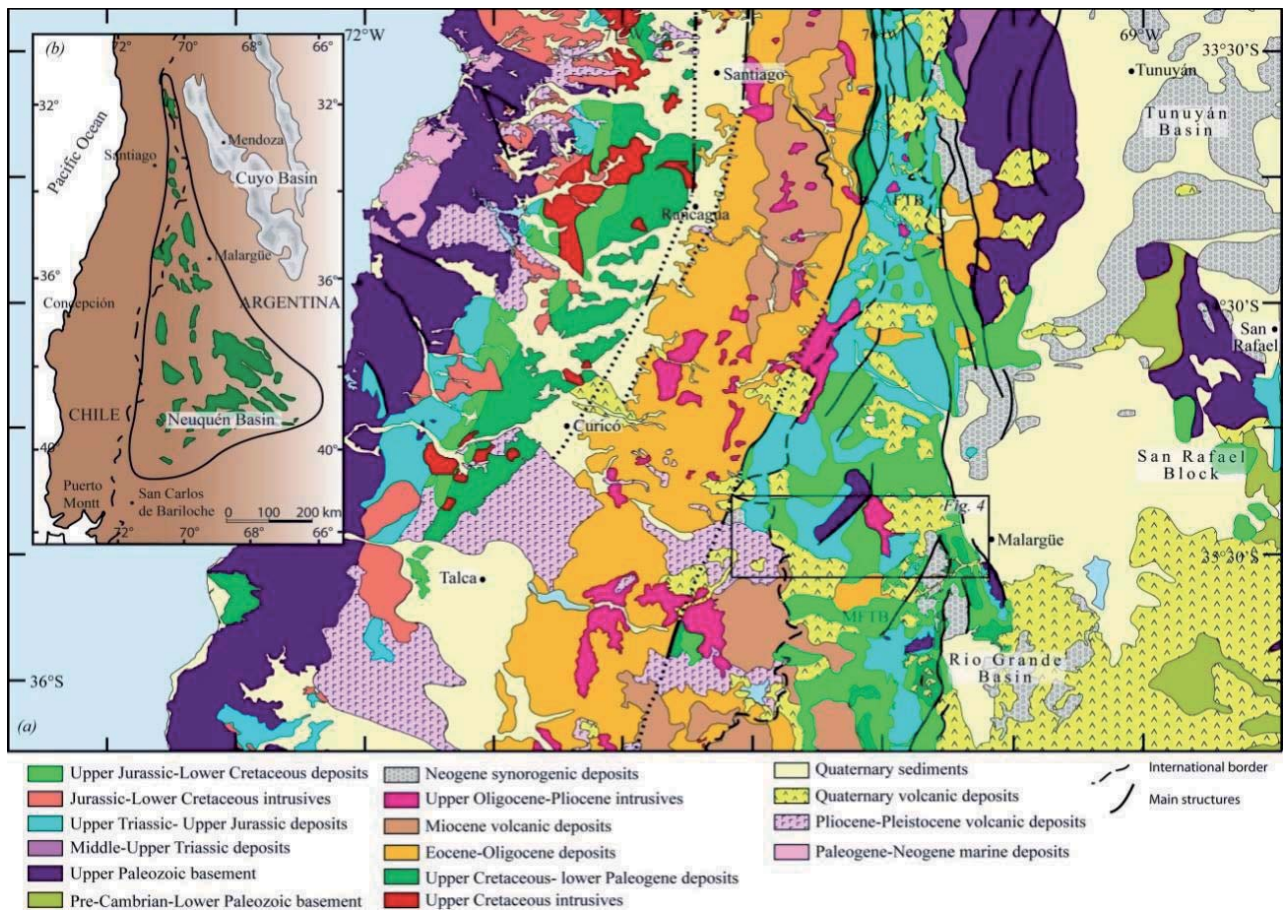


Figure 2. (a) Simplified geological map (modified after Argentino, 1997; Farías et al., 2010; Giambiagi et al., 2009a; Servicio Nacional de Geología y Minería, 2002). AFTB: Aconcagua fold and-thrust belt; MFTB: Malargüe fold-and-thrust belt. (b) Location of the Neuquén Basin.

Particularly, during the Mesozoic developed the Neuquén basin, a large basin located on the eastern side of the current Andes of central Argentina and Chile (Fig. 2a), where more than 4000 m of marine and continental sedimentary rocks accumulated in an extensional setting (Howell et al., 2005; Legarreta and Uliana, 1996; Manceda and Figueroa, 1995). Basin evolution records a history that includes a Late Triassic-Early Jurassic rift stage, followed by a long period of thermal subsidence since Middle Jurassic to Lower Cretaceous (Franzese et al., 2003; Franzese and Spalletti, 2001; Howell et al., 2005; Vergani et al., 1995). The sedimentation continued with an extensional stage during Late Jurassic to Early Cretaceous (Mescua et al., 2008; Vergani et al., 1995). Subsequently, the Neuquén Basin as a whole underwent again a contractional episode after 100 Ma (Ramos and Folguera, 2005; Zamora Valcarce et al., 2006; Zapata and Folguera, 2005; Tunik et al., 2010). During the Late Cretaceous, the contractional deformation was focused in the Coastal Cordillera with the deformation and uplift of late Paleozoic and Mesozoic rocks (Charrier et al., 2014 and references there in) (Di Giulio et al., 2012; Tunik et al., 2010) as indicated by petrological and thermochronological data (Parada et al., 2005) (Fig. 2b). Then, shortening migrated to the east, accompanied by the migration of the magmatic arc (Folguera and Ramos, 2011; Folguera et al., 2011). During this time, deformation was associated with the first development phase of fold-and-thrust belts in the eastern slope of the southern Central Andes (Figs. 1b and 2b).

(Folguera et al., 2011; Mescua et al., 2013, 2012; Ramos and Folguera, 2005; Zamora Valcarce et al., 2006; Zapata and Folguera, 2005). Shortening and magmatic arc remained in the foreland area until the Eocene, when the arc retreated to west (Kay et al., 2006; Zamora Valcarce et al., 2006) and a period of extension affected the western flank of the Andes (Charrier et al., 2007, 2005, 2002; Godoy et al., 1999), forming the Abanico basin and some extensional depocenters in the eastern slope of the Principal Cordillera in Argentina (Alvarez Cermedo et al., 2013; Spagnuolo et al., 2012). Contractual tectonics recommenced at the southern Central Andes with the inversion of the Abanico basin in the early Miocene (Charrier et al., 2005, 2002; Farías et al., 2010; Fock et al., 2006). Subsequently occurred the main phase of the shortening of the Neuquén Basin region with the development of the eastern fold-and-thrust belts that characterized this Andean segment, particularly the Malargüe fold and thrust belt at the latitudes of this study (Giambiagi et al., 2008; Kozlowsky et al., 1993; Silvestro and Atencio, 2009; Silvestro and Kraemer, 2005).

2.2 Stratigraphic background

The study region is characterized by sedimentary and volcanic rocks deposited since the Paleozoic up to the present. According to previous studies developed in this region, such as González and Vergara (1962), Burckhardt, (1900) and Groeber, (1947), the lithostratigraphic units can be grouped into: (1) a basement, composed of volcanic rocks of the Choiyoi Group and Late Paleozoic intrusive bodies; (2) Triassic to Late Cretaceous marine and continental sedimentary rocks of the Neuquén Basin; and (3) Cenozoic rocks. The nomenclature, lithology, age and tectonic setting of all these groups are summarized in the Fig. 3 and their distribution is shown in Figs. 2b and 4. Next, we describe these groups.

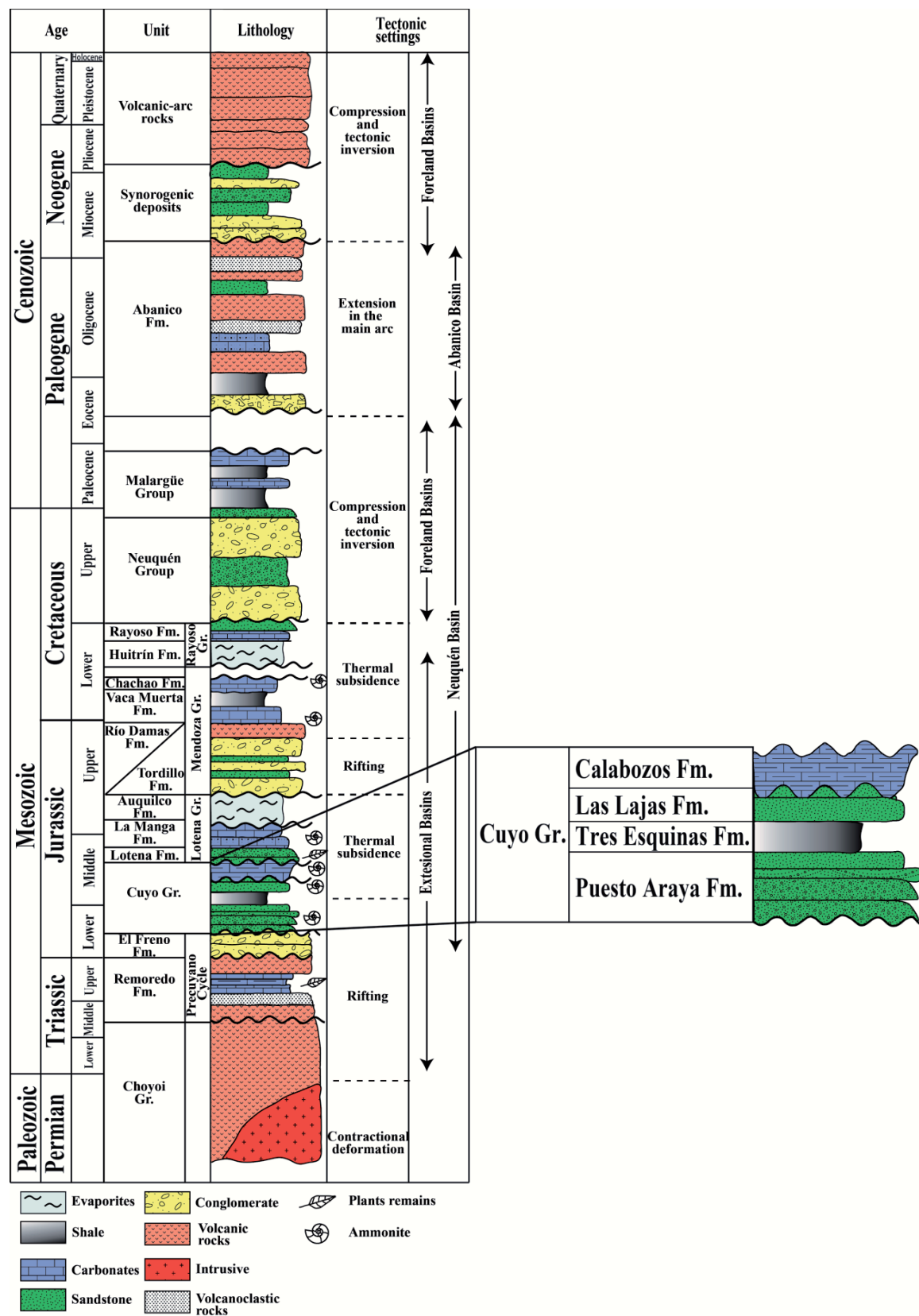


Figure 3. Generalized stratigraphic column including the lithology, age and tectonic setting of the units present in the studied area.

2.2.1 Basement rocks

The basement consists of Permian-Triassic volcanic and intrusive rocks of the Choiyoi Group, a large silicic volcanic province that extends from 23° to 42°S (Kleiman and Japas, 2009; Mpodozis and Kay, 1992). Choiyoi magmatism represents the transitional sequences between Carboniferous-Early Permian calc-alkaline I-type magmatism (Hervé, 1988) and bimodal suites erupted during the Triassic rifting, a period of arrested or very slow subduction (Charrier et al., 2014 and references there in). To south of 34°S, the Choiyoi Group crops out along of the Frontal Cordillera and in uplifted basement blocks.

2.2.2 Neuquén Basin infill

The Neuquén Basin contains several thousand meters of Late Triassic to Early Cretaceous marine and continental sequences accumulated under variable sedimentary and tectonic conditions (Fig. 3). The older record of the Neuquén Basin infill corresponds to rocks of the Precuyano cycle, a term used commonly for the Late Triassic-Early Jurassic volcano-sedimentary sequences deposited in a series of fault-bounded isolated depocenters during the initial syn-rift stage of the Neuquén Basin (Franzese and Spalletti, 2001 and references therein). During this period, the lower part of the Cuyo Group also was accumulated (Lanés et al., 2008).

After the initial syn-rift phase, a thermal subsidence stage (Toarcian-middle Callovian) affected the region. During this time, the sedimentation was marked by the marine deposits and a widely extended flooding episode (Leanza et al., 2013), represented by the upper half of the Cuyo Group. It consists of pelites, sandstones, conglomerates and evaporites that represent deep to shallow marine environments and a complete transgressive-regressive second order cycle (Franzese et al., 2003) grouped in upper part of the Tres Esquinas, Lajas, Calabozos and Tábanos formations. A regional unconformity separates the Cuyo Group from the overlying Lotena Group (Gulisano, 1981; Leanza, 2009).

The Lotena Group consists of deltaic to shallow- marine deposits represented by conglomerates, sandstones and shales, as well as continental sandstones and conglomerates deposited in a fluvial environment (Gulisano et al., 1984; Leanza, 1993, 1990). The sedimentation of this sequence began in the Callovian and ended with both thick evaporites deposits and another paleogeographic reorganization that precedes the profound paleogeographic changes during the Oxfordian-Kimmeridgian (Arregui et al., 2011). The thick clastic red-bed succession at the base of Mendoza Group indicates a progradation of continental facies over marine deposits as a consequence of the paleogeographic changes in the Late Jurassic. These continental rocks show a predominance of volcanic materials in the Chilean side of the Principal Cordillera, which interfinger with the red deposits of the Argentine slope characterized by the predominance of the basement clasts. Based on this, these deposits are named the Río Damas and Tordillo formations in Chile and Argentina respectively.

The continental deposits were followed by the accumulation of Tithonian black shales, Valanginian richly fossiliferous limestones and deep-water black shales indicating an important marine transgression (Vergani et al., 1995). Barremian-Albian evaporites and clastic sedimentary

rocks constitute the Rayoso Group, accumulated in a continental environment and evidencing the end of the marine connection between the Pacific Ocean and the back-arc Neuquén Basin.

Since the Late Cretaceous, the active depositional systems within the Neuquén Basin were strongly controlled by the compressive regime. Uplift and tectonic inversion led to the deposition of more than 2000 m of continental deposits of the Neuquén Group (Di Giulio et al., 2012; Legarreta and Uliana, 1999, 1991; Tunik et al., 2010; Vergani et al., 1995). From Late Cretaceous to Paleocene, very high global sea levels and orogenic flexural subsidence in the foreland resulted in the first marine transgression from the Atlantic represented by the Malargüe Group (Aguirre-Urreta et al., 2011). However, in Chile this period is represented by a large unconformity between the latest Cretaceous and the middle Eocene, and no evidence of compressive tectonics has been reported.

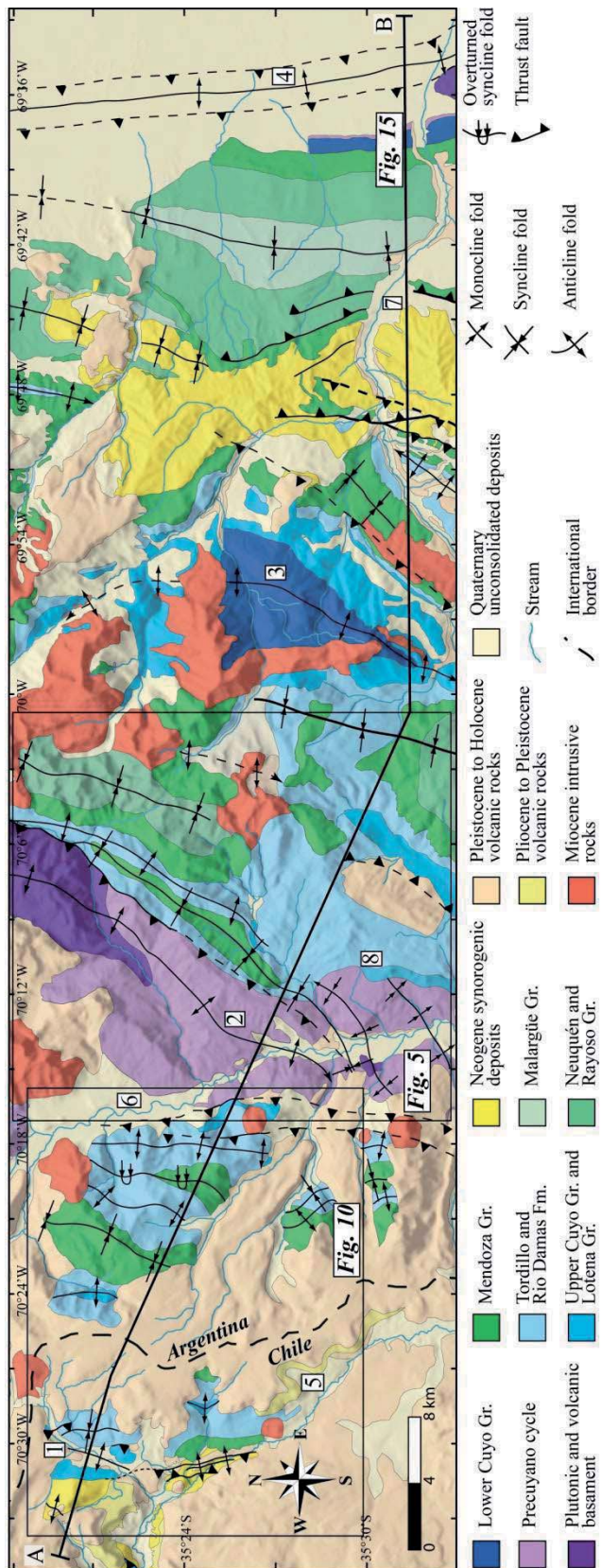


Figure 4. Simplified geological map of the Malargüe fold-and-thrust belt to 33°30'S, showing major structural features and location of the cross section in Fig. 15. Boxes indicate location of the Figs. 5 and 10. Modified after Giambiagi et al., (2009a) and Groeber, (1947) and our own observations. Numbers within white rectangles correspond to the following locations: (1) Valle Grande anticline; (2) Dedos-Silla block; (3) La Valenciana-Torrecilla anticline; (4) Malargüe anticline; (5) Colorado river; (6) Río Grande valley; (7) Malargüe river; (8) Tricolor mount.

2.2.3 Cenozoic rocks

The stratigraphic record shows a hiatus between the Paleocene and the middle Eocene north of 36°S, after deposition of the Malargüe Group, which is even larger in the Chilean slope. This hiatus is interrupted by the volcanic and volcaniclastic rocks deposited during an extensional regime that affected first the arc and then retro-arc since middle Eocene to early Miocene (Charrier et al., 2002; Kay and Ramos, 2006; Fariñas et al., 2010; Spagnuolo et al., 2012). The volcanic activity continued during the Miocene until Pliocene characterized for the eastern migration of the volcanism with arc signature, 500 km away from the trench (Folguera and Ramos, 2011).

Coeval with the volcanism, synorogenic sediments accumulated during the Neogene contractional event identified as the main Cenozoic mountain building event in the southern Central Andes (Charrier et al., 2007; Ramos, 2000; Ramos et al., 2004). These rocks were deposited in different depocenters within a foreland basin system and subsequently were cannibalized and integrated to the orogenic wedge during the eastern migration of the deformation (Giambiagi et al., 2003b; Manceda and Figueroa, 1995; Silvestro and Atencio, 2009; Silvestro and Kraemer, 2005)

3 Structure of the internal zone of the Malargüe fold-and-thrust belt

The study region is located in the eastern side of the Principal Cordillera, from the eastern Chilean part of the belt near the international boundary between Chile and Argentina, up to the foreland (Fig 1), corresponding to a transect nearly 85 km long across strike the southern Central Andes. This region corresponds to the internal or inner region of the Malargüe fold and thrust belt, which is characterized by a deformed belt of Paleozoic, Mesozoic and Cenozoic rocks. Basement-involved in the deformation is the main characteristic across of the south part of the Malargüe fold-and-thrust belt. Large half-wavelengths and outcrops of Triassic and Lower to Middle Jurassic syn-extensional deposits, among other observations, evidence the basement participation in areas where it does not crop out (Manceda and Figueroa, 1995; Mescua and Giambiagi, 2012).

Description of the main structures was performed from a detailed field mapping work and photo-interpretation based on aerial photographs (1:50.000) and LANDSAT satellite images. In order to comprehend how the basement involved in the deformation, balanced geologic cross-section were made and tested using the academic license for 2D-MOVE software (© Midland Valley Exploration Ltd.) to project data on the cross-section and to draw the dip domains. The section was constrained by bedding orientation data and stratigraphic thickness variations across the fold-and-thrust belt. In restoration, we assumed: (1) line-length balance; (2) area-balanced for the basement; and (3) deformation by plane strain with no movement out of the plane of the section.

3.1 Dedos-Silla block

3.1.1 Stratigraphy

The Dedos de Silla block is mainly constituted by the Remoredo Formation, the syn-rift deposits of the Late Triassic-Early Jurassic rifting stage of the Neuquén Basin (Franzese and Spalletti, 2001). It crops out in the SW part of the study region, exhibiting thickness variations across the region (Lanés and Salani, 1998).

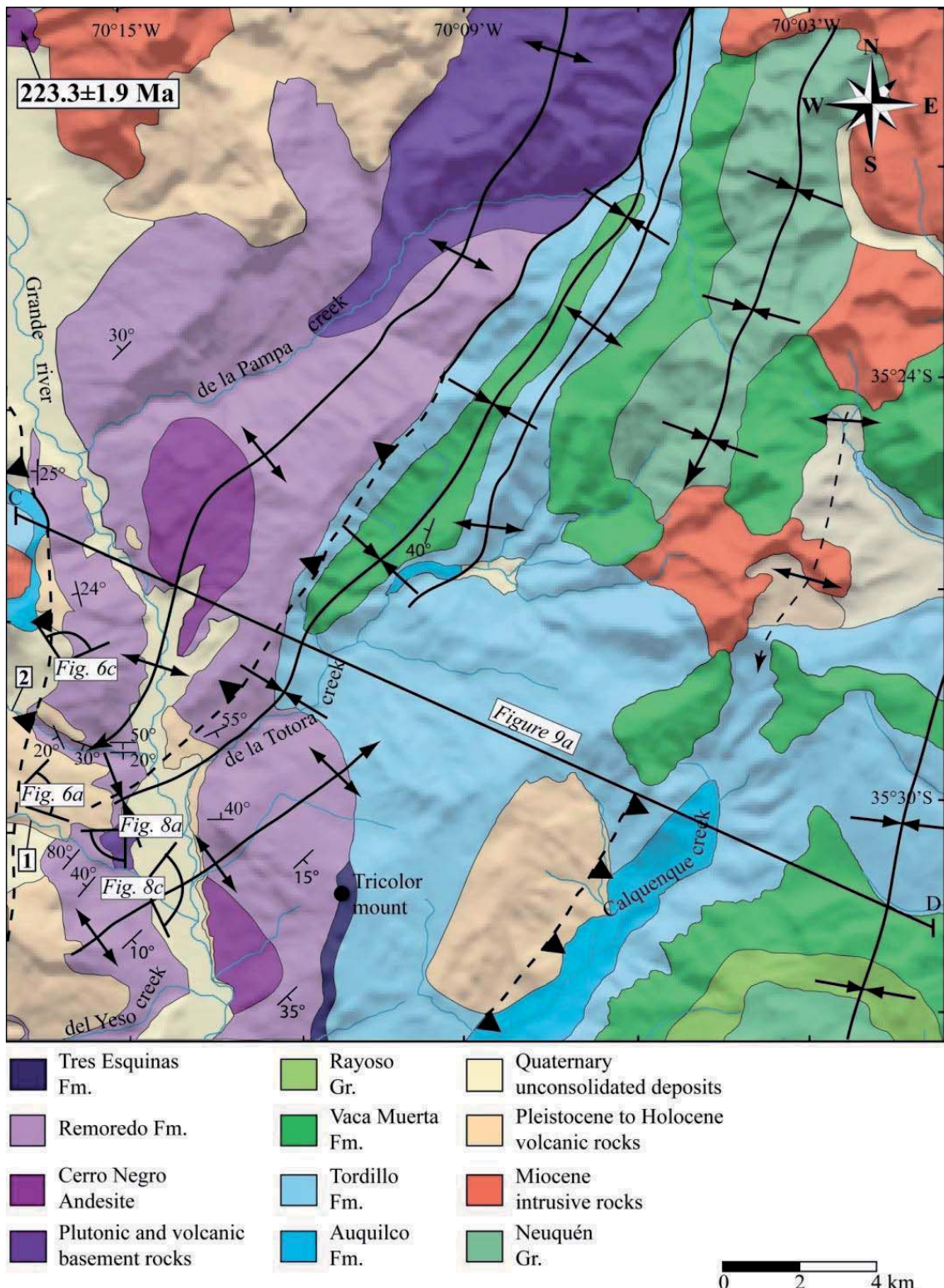


Figure 5. Detailed geologic map of the Dedos-Silla block based on new field observation and previous studies carried out by Groeber, (1947). See location on Fig. 4. See section C-D in Fig. 9. Number in rectangle: (1) Montañez creek.; (2) Montañecito creek

The Remoredo Formation is a pyroclastic succession with intercalations of lacustrine sandstones and limestones deposited relatively close to its respective volcanic centers (Lanés and Palma, 1998; Lanés and Salani, 1998). Lanés and Salani (1998) recognized that lithic fragments of the tuff layers of the Remoredo Formation show the same petrography of an andesitic intrusive named as the Cerro Negro Andesite. The porphyric andesitic intrusive is a green fenoandesite that intrudes the Choiyoi Group and unconformably underlies the Remoredo Formation. It was interpreted as the volcanic necks of the emission center of the pyroclastic flow (Lanés and Palma, 1998), as well as the source of the lithics of the volcanoclastic rocks of the Remoredo Formation (Lanés and Salani, 1998).

The Remoredo Formation uncomfortably overlies the Cerro Negro Andesite (Fig. 5), while to the south in the Tricolor mount (Fig. 5), the Remoredo Formation underlies marine rocks of the Aalenian-Bajocian (Westermann and Riccardi, 1982), correlated with the Tres Esquinas and Las Lajas formations (Fig. 3). This fact reflects the existence of a hiatus due to the non-deposition of the early jurassic successions (Fig. 3). North of the Montañez creek, in the western slope of the Río Grande valley (Fig. 5), oxfordian gypsum layers of the Auquilco Formation overlie the volcanoclastic rocks of the Remoredo Formation (Fig. 6d).

Recently, U-Pb radiometric dating provides an age of 223.3 ± 1.9 Ma to the Cerro Negro Andesite (Naipauer et al., 2015), which allows assigning along with the contact relationship a Late Triassic age to the Remoredo Formation.

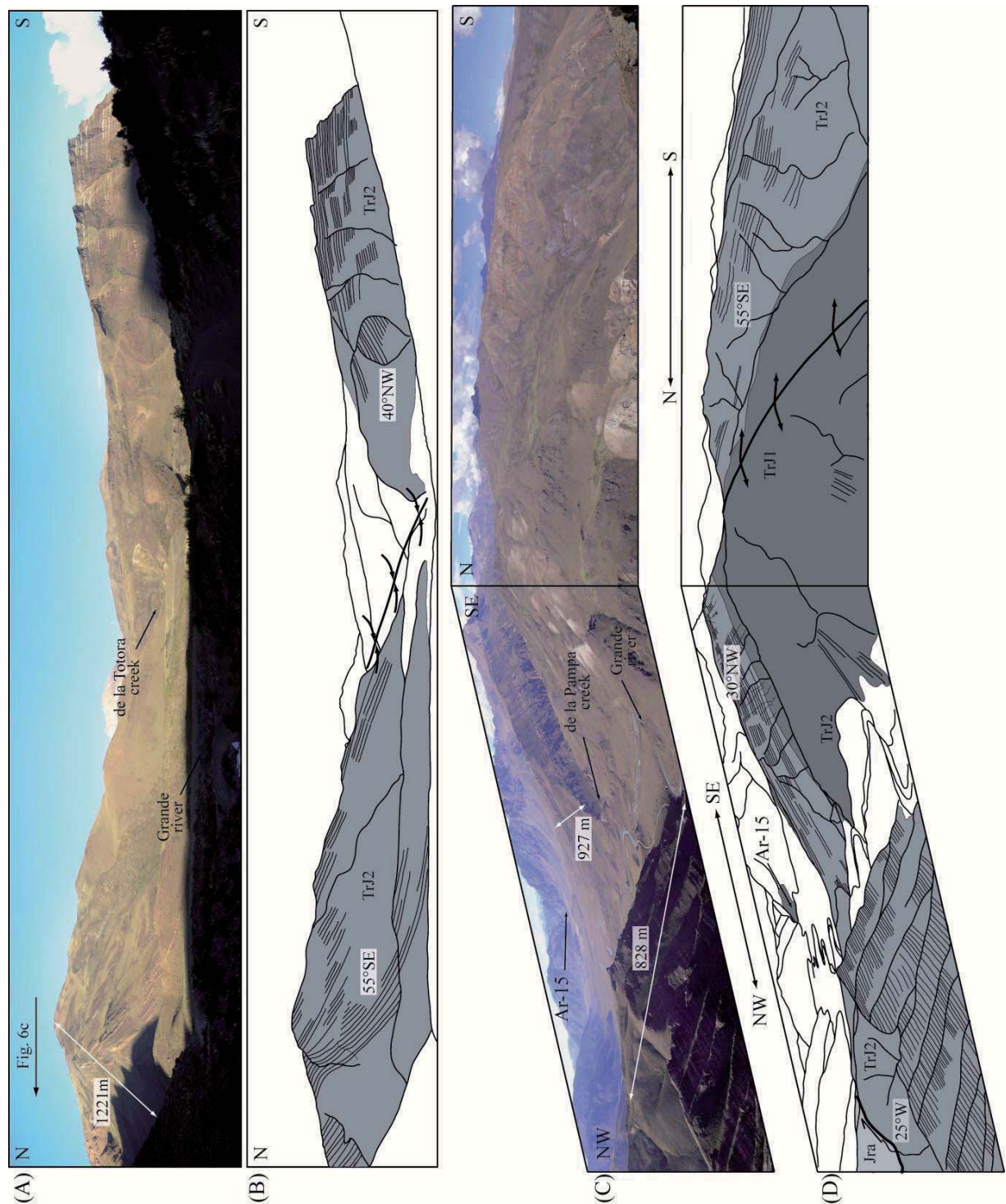


Figure 6. (a) Panoramic view of the syncline separating the northern and southern anticlines of the Dedos de Silla block. (b) Line-drawing picture interpretation. The fold is a broad syncline with the Remoredo Formation (TrJ2) in its limbs. (c) Panoramic view of the northern anticline of the Dedos de Silla block. (d) line-drawing picture interpretation. The Cerro Negro Andesite (TrJ1) is in the core of the anticline as the stratified rocks of the Remoredo Formation are in the limbs. Note the difference in the dip of the back- and fore-limb. In the NW, there is the tectonic contact between Remoredo Formation and Auquilco Formation (Jra). See the location of the Ar-15 sample.

3.1.2 Structure

The Dedos-Silla block is a basement involved anticline defined by Manceda and Figueroa (1995). These authors recognized this basement block as a topographic high, to the west of the Lower Jurassic La Valenciana extensional depocenter (Fig. 4) based in thickness changes of the early-middle Jurassic successions. This situation has been also documented north of this region in the Portezuelo Ancho area at 35°S (Davidson and Vicente, 1973; Legarreta and Kozlowsky, 1984) where the Tordillo Ridge, the northern prolongation of the Dedos-Silla block, splits the Atuel and La Valenciana depocenters from the western depocenters of the Neuquén Basin.

The Dedos-Silla block is a complex structure composed by two anticlines involving rocks of the Choiyoi Group, Remoredo Formation and jurassic successions (Fig. 5). The northern anticline is an NE-SW trending southeast-verging fold plunging to the NE with a gently dipping backlimb and very steeply dipping forelimb (Fig. 6d). The back-limb shows variations in the strike, changing the NW in the La Pampa creek area to NS and then E-W in the Rio Grande valley and Montañez creek (Fig. 5). This fold is flanked to the east by an east-verging thrust which NE trace accommodates the overthrusting of the Choiyoi Group over the folded Mendoza Group (Fig. 5) evidencing not only the contractional late evolution of this fold, but also out-of-sequence thrusting after the growth of the northern anticline. The referred fault is the southern prolongation of the Las Leñas fault described farther north at *ca.* 35°S (Mescua et al., 2014), which also shows out-of-sequence thrusting. The fault loses expression to south-west, where a symmetric syncline separates the northern and southern anticlines (Figs. 5 and 6a). Across the northern anticline, the Remoredo Formation exhibits changes of thickness from 900 m in the back limb to 1200 m in the front limb. Immediately next to the front limb of the northern anticline, along the Montañez creek, the Remoredo Formation unconformably overlies rocks of the Choiyoi groups and its thickness decreases to 290 m (Fig. 7e and f).

The southern anticline is a broad asymmetrical SE-verging fold that plunges to the north-east (Fig 5). In the Montañecito creek area (Fig. 5), the structure involves rocks of the Remoredo Formation (Fig. 7a and b) and the Choiyoi Group outcropping in its limbs and core, respectively (Fig. 5). On the other hand, to the south-east, it involves rocks of the Remoredo Formation together with part of the Jurassic sequences (Fig. 7c and d). In the Calquenque creek, a NW-verging fault produces the thrusting of the rocks of the Auquilco Formation over the Tordillo Formation (Fig. 5). East of the former thrust, a syncline involving rocks of the Mendoza, Rayoso and Neuquén groups divides the Dedos-Silla block from the La Valenciana anticline (Fig. 5). Similarly to the other anticline, the thickness of the Remoredo Formation also varies. Thereby, toward the south-east the thickness is 400 m (Fig. 7c), whereas along the Montañecito creek exceeds the 800 m (Fig. 7a).

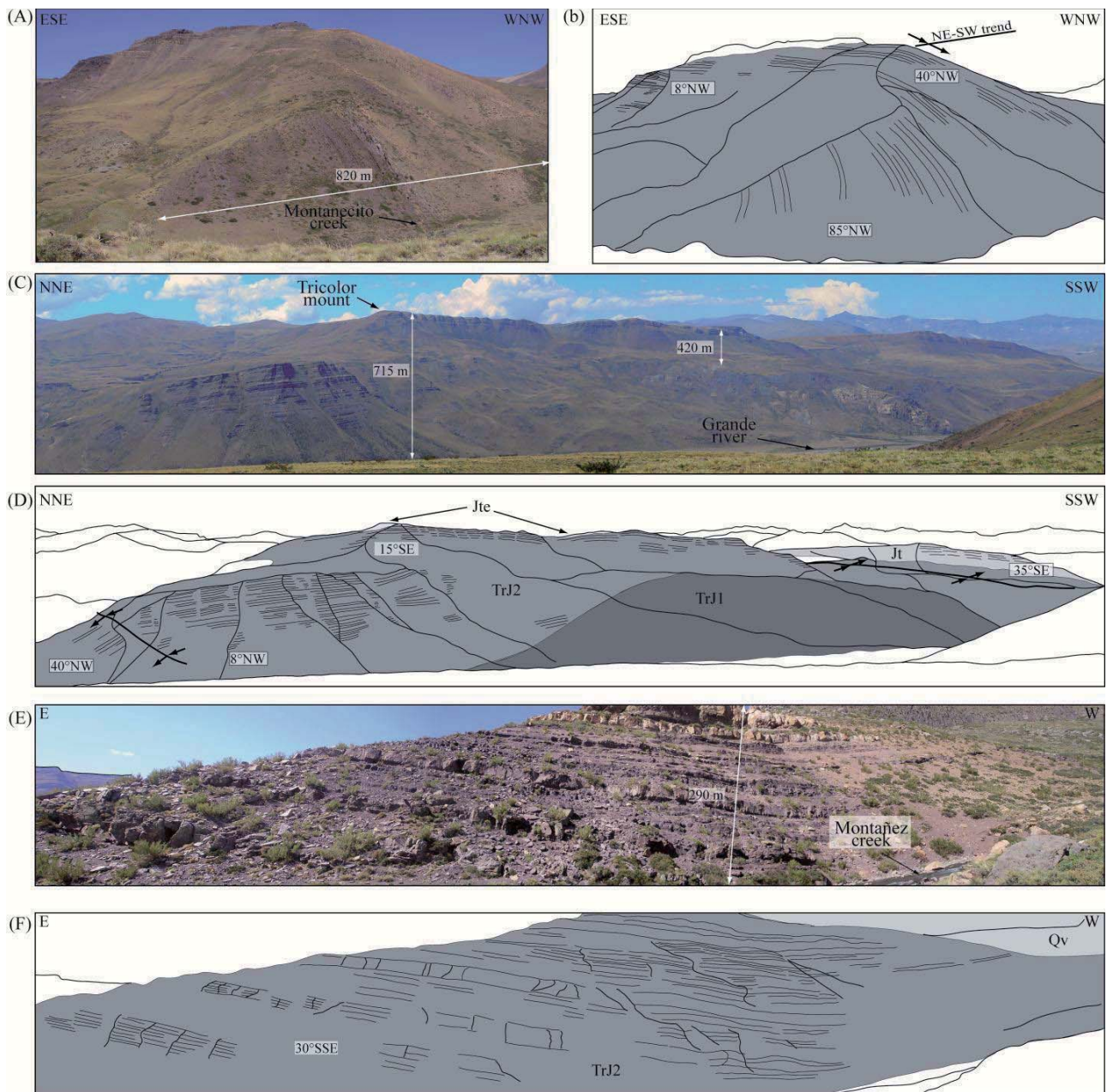


Figure 7. (a) SSW view of the NW flank of the southern anticline in the Montañecito creek. (b) Line-drawing picture interpretation. (c) Panoramic view of the southern anticline of the Dedos de Silla block. (d) Line-drawing picture interpretation. Rocks correlated to Cerro Grande Andesite (TrJ1) out-crop in the core of the anticline. To the SSW, the Tordillo (Jt) and Remoredo formations make up the SE flank of the fold. The Tres Esquinas Formation (Jte) out-crops in the Tricolor Mount in the central area of the structure. (e) South view of the syncline separating the northern and southern anticline. Note the minimum thickness of the Remoredo Formation compared to the thickness across the both northern and southern anticlines. (f) Lin-drawing picture interpretation.

3.1.3 Interpretation

The thickness growth in both northern and southern anticlines, as well as the regional syn-rift nature of the Remoredó Formation (see Franzese and Spalletti, 2001) suggests a tectonic control during the deposition of the late triassic deposits. Based on the growing direction, we infer the presence of two depocenters consisting of two NNE-trending antithetic master faults forming two half-grabens and a horst geometry (Fig. 8b). According to the age of the Remoredó Formation, this extensional system would have been active during the Late Triassic whereas during the Early Jurassic it acts as a topographic high evidenced for the non-deposition of the syn-rift part of the Cuyo Gr. and the condensed thickness of both Tres Esquinas and Las Lajas formations.

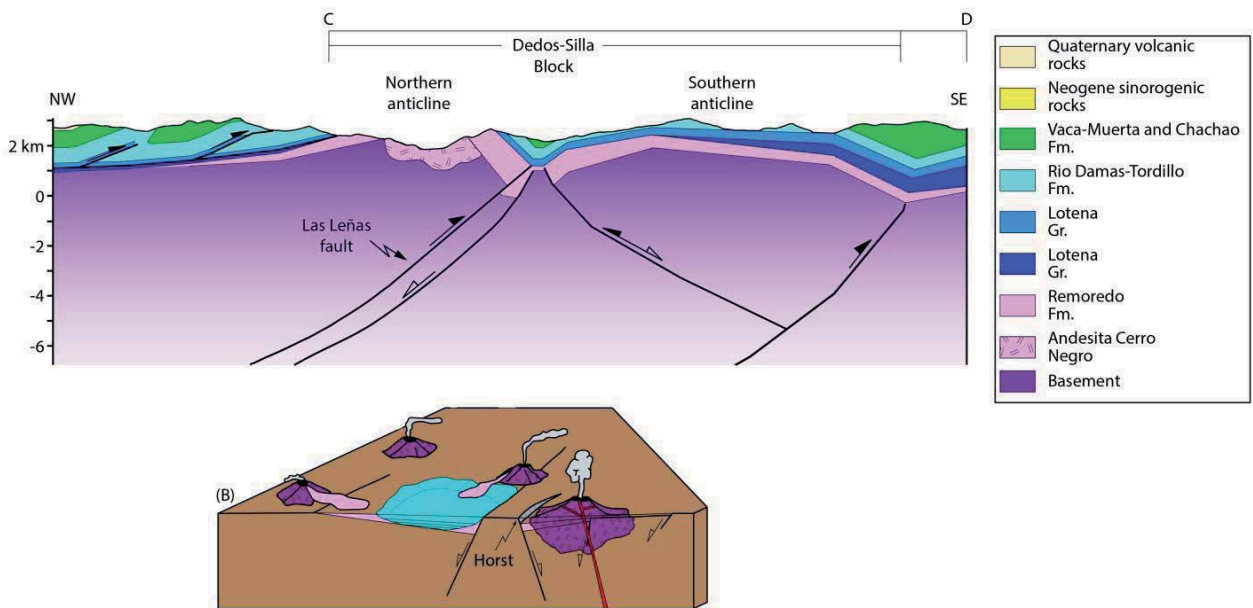


Figure 8. (a) Cross-section of the Rio Grande area. See Fig. 5 for location. The Dedos-Silla block is composed by two anticlines with opposite vergence. (b) 3D block of the configuration of the Dedos-Silla block during Late Triassic.

Although the master normal fault of the northern half-graben dips to the north-west and that the northern anticline exhibits an eastward vergence, the contractional folding of the Late Triassic syn-rift Remoredó Formation would be associated with the generation of a new east-verging thrust instead of the inversion of a pre-existing normal fault. This structure corresponds to the Las Leñas fault (Fig. 8a) which acts as a by-pass of the master normal fault.

The geometry of the southern anticline would be associated to the presence of two faults the opposite vergence (Fig. 8a). The NW-growing thickness of the syn-rift sequences of the Remoredó Formation suggest that the inversion of the SE-dipping master normal fault could be the origin of folding along the Monatañecito and La Totora creeks (Fig. 5 and 7a). On the other hand, the kinematic model of the inversion of the normal fault does not explain the folding of the southeastern limb of the southern anticline and the development of the syncline along the Calquenque creek, which separate the La Valanciana anticline from the Dedos-Silla block (Fig. 4). In this way, we infer the presence of the blind NW-dipping fault (Fig. 8a).

3.2 Valle Grande and Debia Anticlines

3.2.1 Stratigraphy

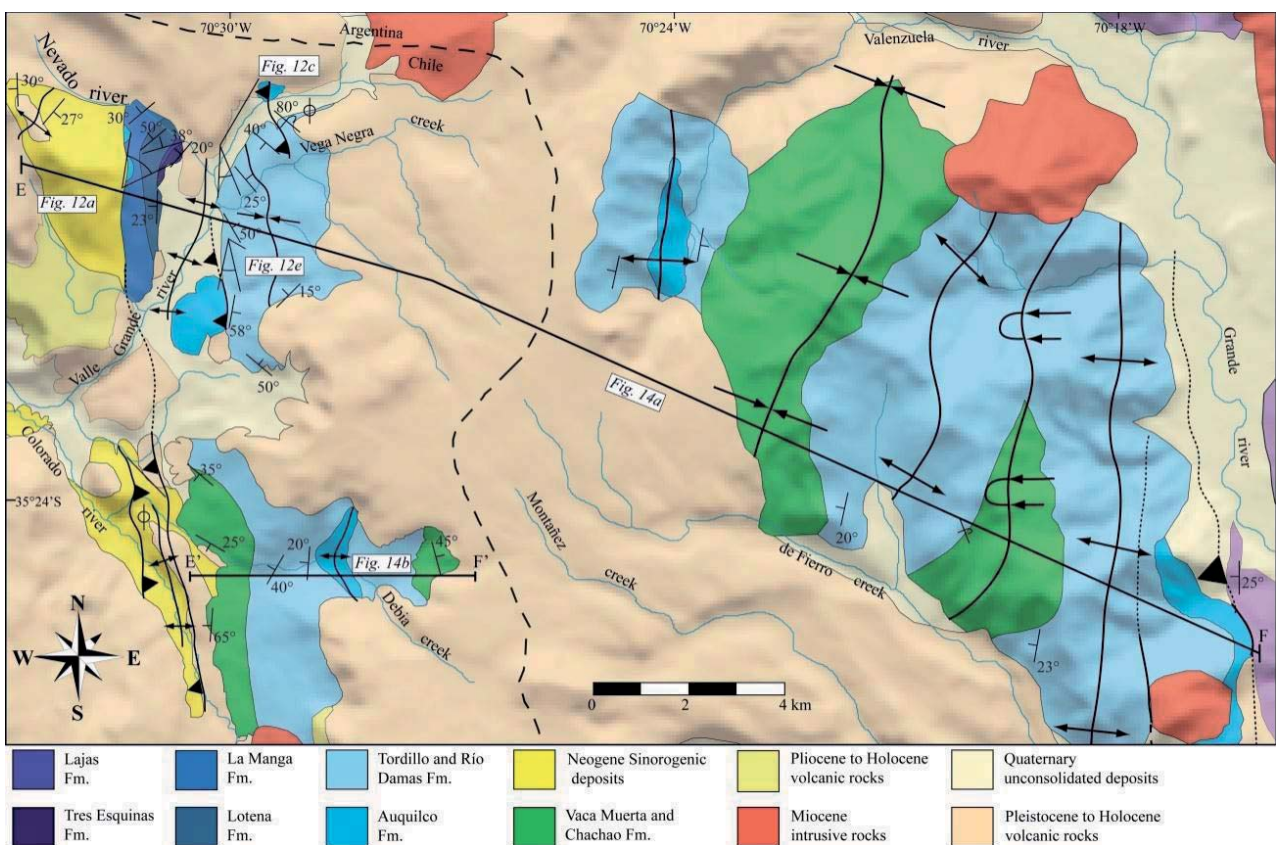


Figure 9. Geologic map of the western sector of the Malargüe fold-and-thrust belt in this study, showing the main structural features in this region. See location in Fig. 4. See cross-section E-F in Fig. 13.

In contrast to the features described in the Río Grande valley, a more complete Middle-Upper Jurassic sequence crops out along the Valle Grande river in Chile. According to the lithology and fossil content, the oldest outcropping rocks belong to the Tres Esquinas Formation of the Cuyo Group (Fig. 3 and 9), which consists of black fossiliferous shale layers with limestone intercalations. It has a maximum observed thickness of *ca.* 30 m, even though its base is not exposed (Fig. 10). An erosional contact separates the Tres Esquinas shales from the sandstones of the overlying Lajas Formation. The Lajas Formation consists of 60 m of the red sandstone with sandy breccias. To the base, limestone and shale clasts evidence the erosion and recycling of the underlying Tres Esquina Formation and the change on sedimentary conditions: The Lajas Formation shows current ripples with different directions, reflecting variable flow direction likely related to a shallow and proximal marine environment.

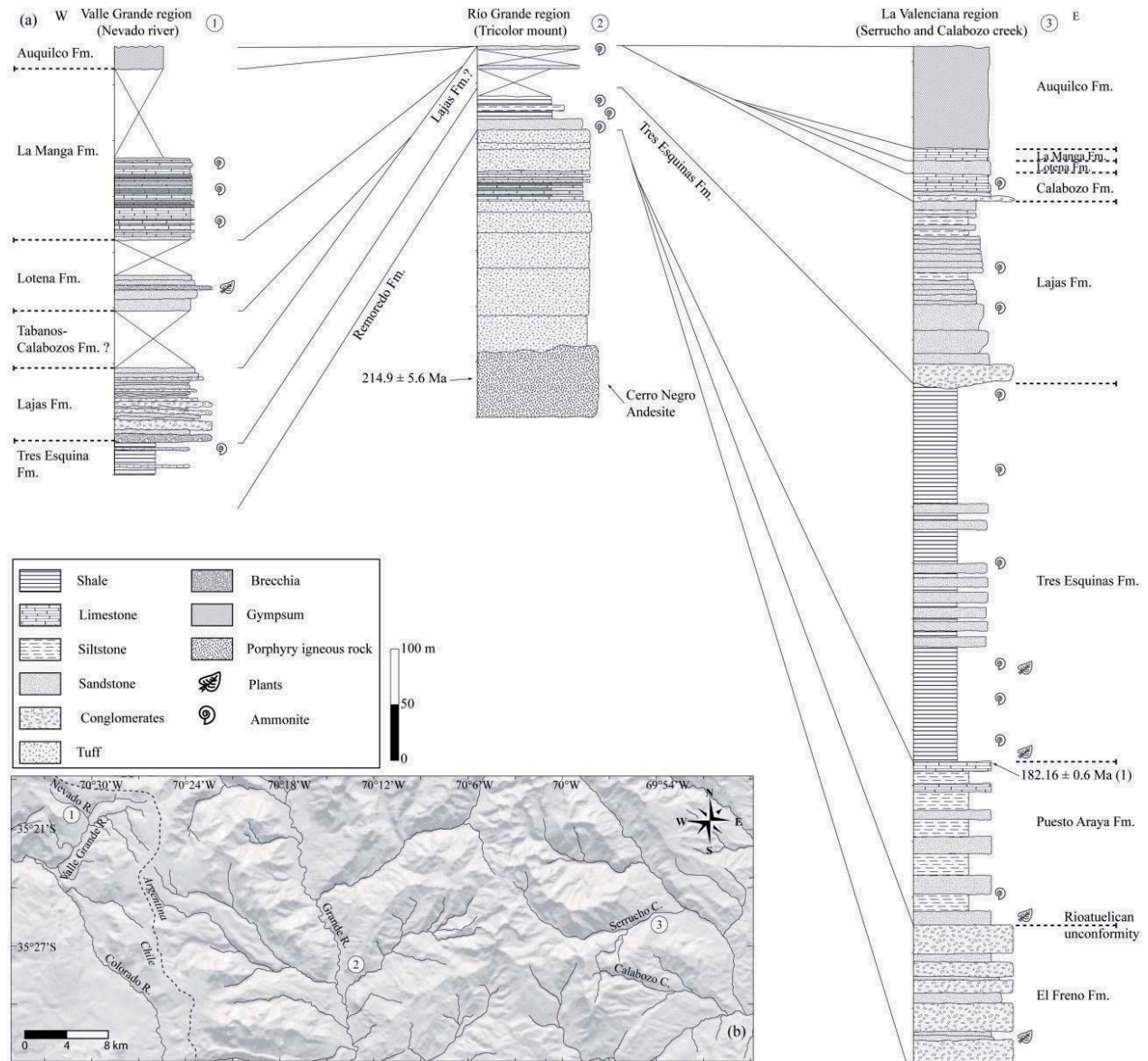


Figure 10. (a) Lithological correlation of the stratigraphic columns of Valle Grande, Río Grande and La Valenciana regions. The Rio Grande and La Valenciana stratigraphic columns are based in Westermann and Riccardi (1982) and Gulisano and Gutiérrez Pleimling (1995), respectively. The age in the La Valenciana column after Mazzini et al (2010). (b) Location of stratigraphic columns.

The Lotena Formation unconformably overlies the Lajas Formation. This unit consists of about 50 m of greenish and reddish coarse sandstones and conglomeratic sandstones with plants remains and desiccation cracks (Fig. 10) evidencing a non marine environment. It presents levels of monomictic breccias with calcareous clasts. To the top, the grain size of the sandstones decreases and the deposits progressively increases in calcareous sandstones and shales layers. This gradual change marks the onset of marine sedimentation with the deposition of the overlying La Manga Formation. The later unit reaches a thickness of *ca.* 200 m in the western slope of the Valle Grande river (Fig. 9) and consists of a sequence of fossiliferous mudstones, limestones and sandstones (Fig. 10).

3.2.2 Structure

The Valle Grande anticline is a north-south trending structure with ~6 km half-wavelength and asymmetric folds plunging to the north, involving rocks of the Cuyo and Lotena groups in its western limb, and rocks of the Lotena and Mendoza groups in its eastern limb (Fig. 9). The fold is exposed along the Valle Grande river with a gently dipping west-limb (Fig. 11b) and a very steep east-limb (Fig. 11d), which is indicative of its east vergence. In its front, the rocks of the Río Damas Formation (lower Mendoza Gr.) are folded into a broad syncline with a 20°W dipping eastern limb (Fig. 9), indicating the location of another structure responsible for the westward tilting toward the east. In the eastern slope of the Valle Grande valley the NNW-striking Valle Hermoso fault produces the overriding of the Auquilco Formation (upper Lotena Gr.) over the Río Damas Formation (Fig. 11f), producing the subsequently breakthrough anticline thrusting within the Valle Grande anticline.

Along the Debia Creek, the NS-trending Debia anticline exhibits the Río Damas, Vaca Muerta and Chachao Formations in its limbs and the Auquilco Formation in its core (Fig. 9). It is a broad and symmetric fold covered to north and south by Pliocene-Quaternary volcanic rocks. A NW-trending anticline involving rocks of the Mendoza Group joins the Valle Grande and Debia anticlines (Fig. 9).

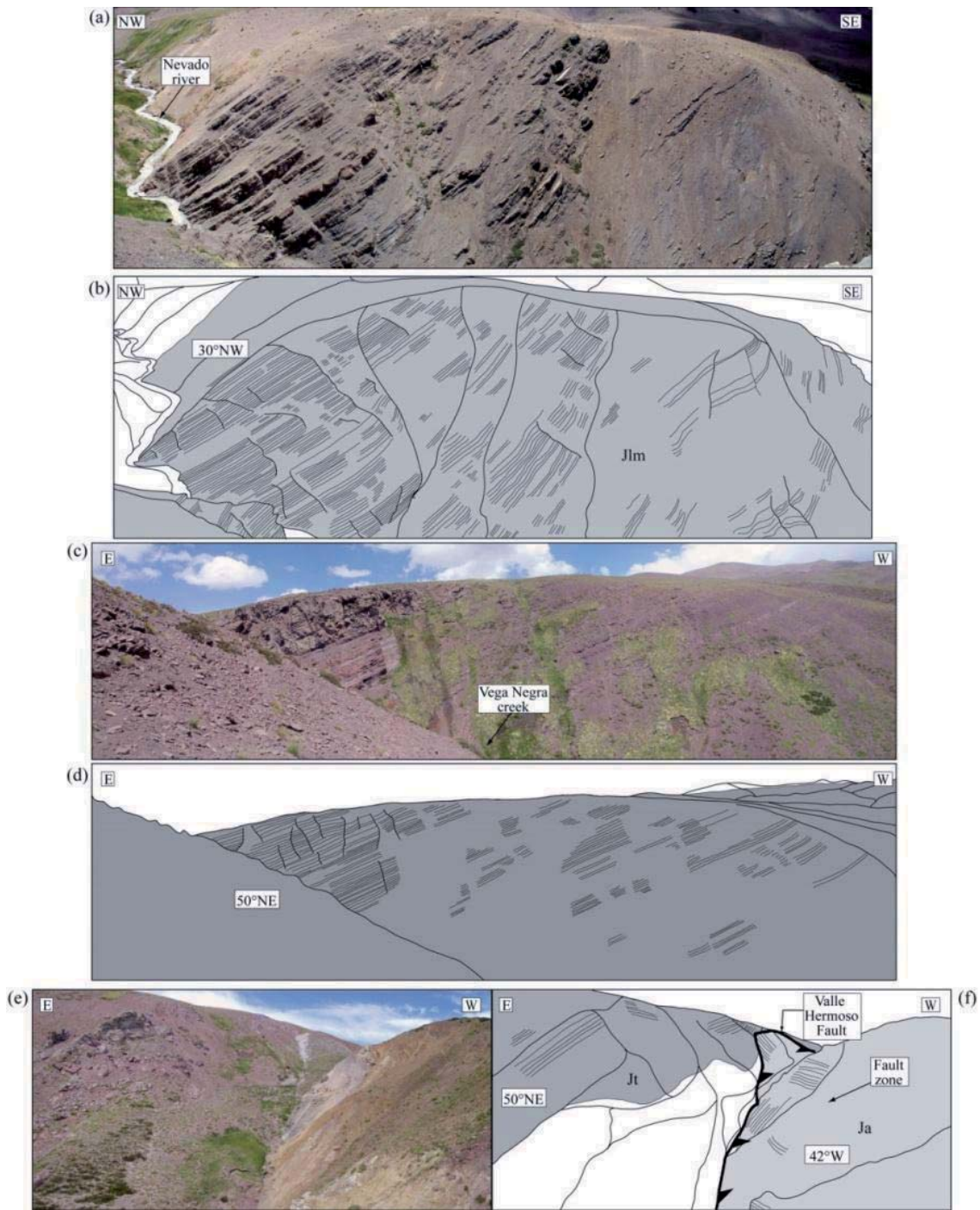


Figure 11. (a) View of the Valle Grande anticline back-limb at the Nevado river. (b) Line-drawing picture interpretation. The back-limb dips between 20° and 30° NW and involves La Manga (Jlm), Lotena, Lajas and Tres Esquinas formations. (c) Panoramic photograph of the Valle Grande anticline fore-limb (eastern flank). (d) Line-drawing picture interpretation. This limb is made up by the Rio Damas Formation (Jra) dipping between 50° and 60° E. (e) View to the south of the Valle Hermoso fault. (f) Line-drawing picture interpretation. The Valle Hermoso fault puts the Auquilco Formation (Ja) over Río Damas Formation (Jra).

3.2.3 Interpretation

The asymmetric geometry developed in the hanging wall and the 6 km of half-wavelength of the Valle Grande anticline is consistent with the presence of a deep thrust involving the basement. Furthermore, the greater thickness of the Jurassic succession in the Valle Grande relative to the Río Grande area (Fig. 10) indicates that the Valle Grande region was a depocenter located west of the Dedos-Silla block at least until the Middle Jurassic. This is consistent with the proposition of Davidson and Vicente (1972) and Legarreta and Gulisano (1984) for the existence of a topographic high located north of the study area based on thickness differences in the Jurassic to Early Cretaceous sequence. In fact, the Cuyo and Lotena group reaches up 300 m of thickness in the Valle Grande area, contrasting with the 80 m in the Río Grande valley (Fig. 10).

The Valle Grande depocenter is located <30 km to southwest of the Río del Cobre depocenter, a Jurassic depocenter characterized for the developed of a half-graben with a W-dipping normal fault (Mescua et al., 2014). This suggest that the former is the southern prolongation of the Río del Cobre depocenter although in the Valle Grande depocenter there are not evidences of a normal fault controlling the deposition of the mesozoic sequences.

The geometry of the Valle Grande anticline is originated by the generation of a new reverse fault folding the mesozoic and cenozoic sequences (Fig. 12). Likewise, we interpret the Debia anticline as a structure formed by a short-cut of the main reverse fault that controlled the Valle Grande anticline formation (Fig. 12).

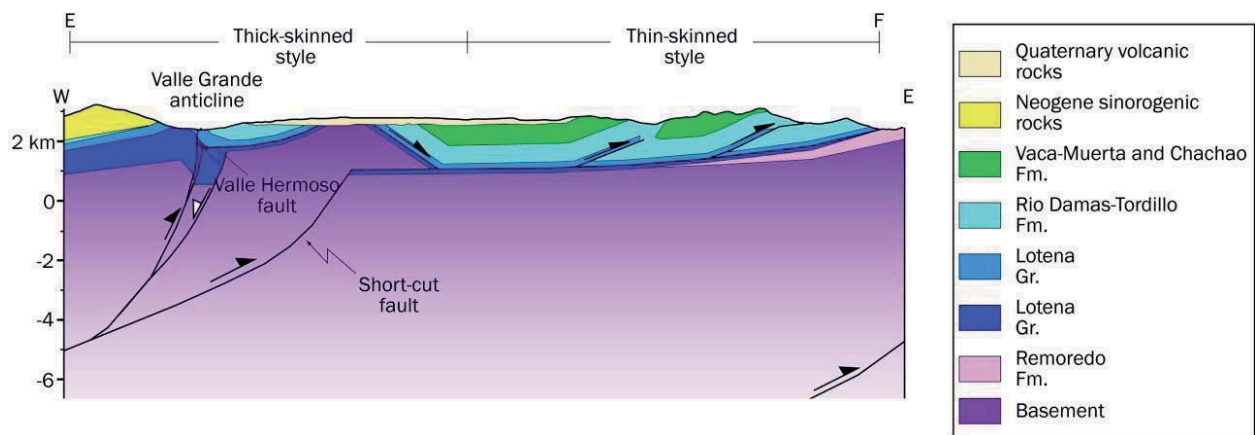


Figure 12. (a) Cross-section through Valle Grande area. See location in Fig. 9 (E-F section). The Valle Grande anticline is interpreted as a result of inversion of Early Jurassic half-grabens. A short-cut structure would be associated with the inversion of a normal fault.

4 Structure and evolution of the Malargüe fold-and-thrust belt

4.1 Balanced cross section

The main structural relationships described before are here considered for constructing a 96.6 km long regional cross-section (Fig. 13). The section runs across all the eastern Principal Cordillera (A-B, Fig 4) incorporating all available information and thus allowing a full analysis of the structure and evolution of the Malargüe fold-and-thrust belt at the latitude of this study. The western side of the cross-section includes our own new results, while to the east it is supported by previous works (Giambiagi et al., 2009a).

The balanced cross-section was constructed considering dip angles of the strata and the thickness of the stratigraphic units. Two-dimensional area-balancing forward models were performed to obtain a balanced and palinspastic-restored cross section using the software 2D Move (© Midland Valley Exploration Ltd.), analyzing the folding mechanisms for each fault related fold following the proposition of Giambiagi et al. (2009). This analyze allowed us to conclude that the best mechanisms correspond to inclined shear and flexural slip algorithms to restore the thick-skinned structures, while fault-parallel flow and trishear are the best algorithms for the thin-skinned deformation, in a similar way as used by Giambiagi et al. (2009).

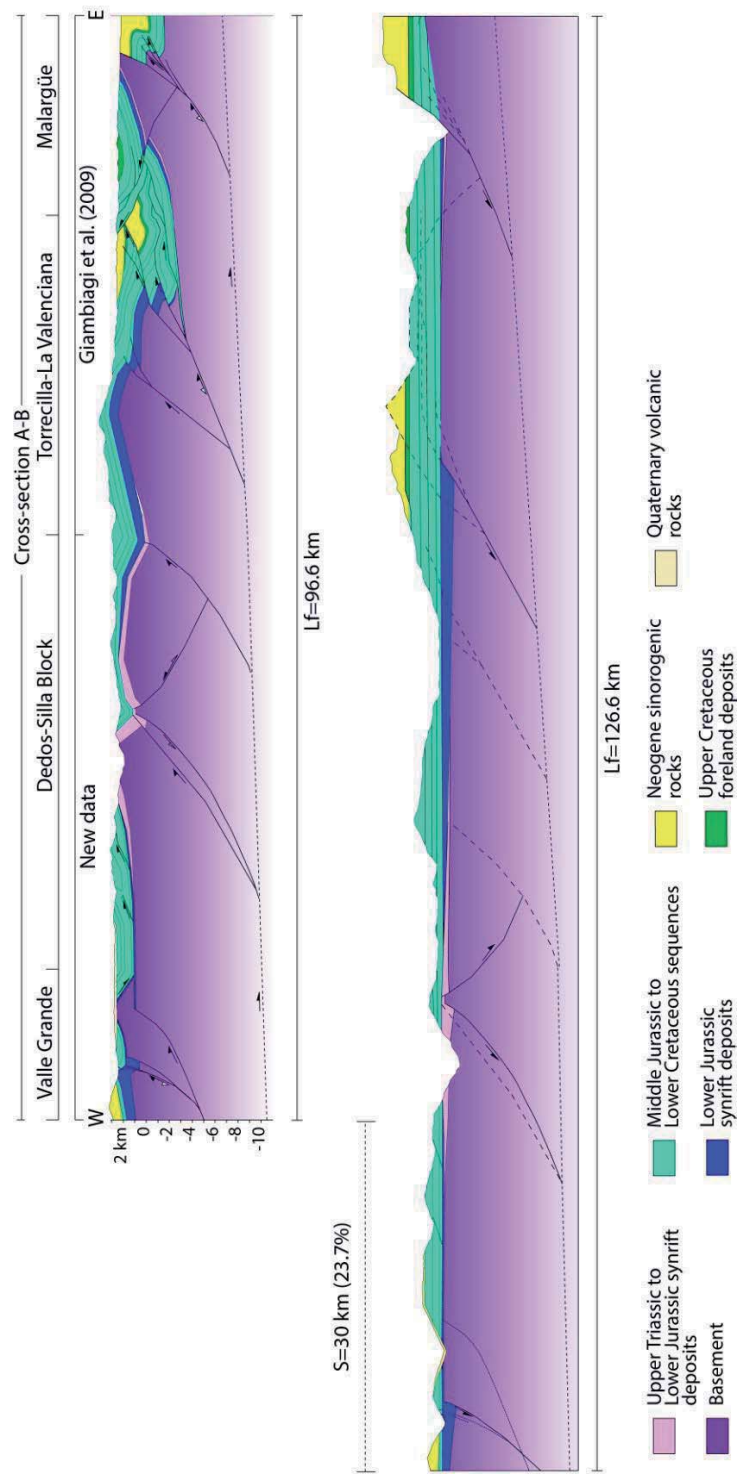


Figure 13. Balanced regional cross-section A-B of the Malargüe at 35°30'S and its restoration. See location in Fig. 4. The cross section shows a thick-skinned style with a thin-skinned style limited for basement structures. The inversion of the Mesozoic depocenter is accompanied by short-cut, by-pass and back-thrust structures, considered as a result of interaction between previous extensional faulting and subsequent contractional structures.

The western part of the regional balanced cross section was built according to the assumptions made for the Dedos-Silla block and the Valle Grande cross sections described previously in section 3. The features presented in the Dedos-Silla and Valle Grande sectors permit conclude that both sectors are characterized by the presence of normal faults controlling the deposition of sedimentary sequences during the Mesozoic. These normal faults would have not been inverted during both late cretaceous and miocene contractional episodes according to the absence of the inversion evidences.

After the modelling procedure, we assumed a basal detachment at the western part of the study area at *ca.* 10 km depth. A 2°W dip for this detachment leads to similar depths as those proposed by both Giambiagi et al. (2009) and Farías et al. (2010) for the eastern and western Principal Cordillera. Thus the regional section (Fig. 13) would show the hybrid structural style proposed for the Malargüe fold-and-thrust belt: the basement is involved through both the inversion of the pre-existing normal faults and new reverse fault rooted in a westward-dipping basal detachment level, and the development of thin-skinned folding in front of basement-involved anticlines is due to the transference of the deformation to the cover.

The palinspastic restoration reveals a dominated east-vergence for the contractional deformation. A total accumulated shortening *ca.* 30 km (23.7 %) (Fig. 13) was estimated corresponding to a minimum value because the high exhumation of the western part precludes analyze adequately the complete sedimentary succession.

4.2 Timing of deformation

The age of the deformation in the eastern sector of the Malargüe fold-and-thrust belt has been accurately determined (Giambiagi et al., 2008; Silvestro and Kraemer, 2005) in contrast with the western zone of the thrust-belt where the chronology of the events is still unclear. In order to constrain the evolution of the study area, we analyzed the timing of the deformation based on structural relationships and radiometric ages reported in other studies.

Growth strata within the Miocene synorogenic deposits in the back-limb of the Valle Grande and Debia anticlines (Tapia et al., 2015) evidences a Miocene activity for the westernmost zone of the thrust-belt. The provenance analysis of the synorogenic deposits indicates multiple source areas currently eroded. These sources mostly correspond to late Miocene plutons and volcanic deposits present in the area, an eastern Tordillo-Río Damas Formation, and the western volcanic-volcanoclastic Abanico Formation. The latter deposited within an extensional intra-arc basin, inverted from 23 and 20 Ma north of the study region (Charrier et al., 2002; Farías et al., 2008, Muñoz-Saez et al., 2014). Thus the main activity within the Valle Grande and Debia anticlines occurred simultaneously or immediately after the Abanico Basin inversion. Then contractional deformation migrated to the east and returned to this area in the late Miocene during an out-of-sequence thrusting period (*c.f.* Giambiagi et al., 2003b). According to the detritic age of the top of the synorogenic sequence, outh-of-sequence thrusting occurred after 7 Ma up to Present (Tapia et al., 2015), which is consistent with the age of the synorogenic rocks and the thrusting of the Pliocene-Pleistocene Loma Seca Formation and recent moraines (Tapia et al., 2015).

The Dedos-Silla block shows two main periods of shortening. The first stage would correspond to inversion-related deformation of the southern anticline. During this period, the Neuquén Group would have deposited between the Dedos-Silla block and the La Valenciana anticline. These rocks correspond to the westernmost outcrops of the Upper Cretaceous Neuquén Group (Fig. 3), evidencing the position of the orogenic front in the Late Cretaceous. This is consistent with the proposition made by Mescua et al. (2013) and Tunik et al. (2010) for the area just northeast and south of the study region at 35°S and between 36° and 37°S, respectively. The second stage would be associated with the contractional growth of the northern anticline and the subsequent thin-skinned deformation developed to the east of its front. This period ended with an out-sequence thrusting along the Las Leñas fault and a later eastward migration of deformation. We propose that this stage occurred between 20 and 16 Ma, that is, after the development of the Valle Grande anticline and before the growth of the La Valenciana anticline.

Finally, the easternmost inversion-related structures, La Valenciana and Malargüe anticlines (Fig.13), developed at 18 and 5 Ma respectively (Silvestro and Atencio, 2009; Silvestro and Kraemer, 2005).

5 Discussion

5.1 Inversion in the Malargüe fold-and-thrust belt

We present data evidencing a strong control of pre-existing extensional structures in the structural style, orientation and fault distribution in the fold-and-thrust belt which played an important role during the tectonic inversion of the western Neuquén Basin. Although the reactivation of normal faults is a common feature in the Malargüe fold-and-thrust belt, the magnitude of inversion varies across the deformation belt. According to Giambiagi et al. (2009a) and Manceda and Figueroa, (1995), the La Valenciana and Malargüe depocenters would show a total inversion, whereas our interpretation for the half-grabens in the Dedos-Silla block and Valle Grande region indicates either just partial inversion (Figs. 8 and 12) (*sensu* Williams et al., 1989) or null inversion. The geometries of the northern and southern anticlines of the Dedos-Silla block and of the Valle Grande anticline would be linked to the development of fault-propagating folding (Suppe and Medwedeff, 1990) with the tip point of reverse movement in the bottom segment of the former normal faults. These cases are common in listric fault geometries, where the upper segment of the fault is steeper than the lower part, resulting in a partial inversion and thus impeding the reactivation in a steeper segment.

Reactivation of the NE-trending normal faults in the Dedos-Silla block could be prevented by its oblique orientation respect to the ESE or ENE convergence direction recorded during both the Late Cretaceous and the Miocene, which would represent the direction of the maximum horizontal stress (Somoza and Ghidella, 2012). The models of Yagupsky et al.,(2008) show that inversion of oblique half-grabens within the Neuquén Basin occurs in fault sectors just close to high competence contrasts, such as those given by the presence of basement. This would explain the reactivation that only occurred in the southern normal fault of the Dedos-Silla block. However, deeper studies are necessary to understanding the inversion of the Dedos-Silla block due to late Miocene clockwise

tectonic rotation reported between 34° to 36°S (Arriagada et al., 2013) which could change the extensional architecture and orientation within this depocenter.

Although inversion tectonic seems to be the main deformational mechanism in this Andean segment, there are regions in the Malargüe fold-and-thrust belt where the generation of the basement-involved thrust controls the accommodation of shortening and the resulting structural style. For example, a non-inversion-related structural style has been proposed for the Diamante river at 34°30'S (Turienzo, 2010; Turienzo et al., 2009), in region in which the Neuquén Basin becomes narrower and had a less-evolved depocenter than the southern region (Fig. 2a).

To sum up, inversion tectonics is the main basement-involved deformational mechanism across the Malargüe fold-and-thrust belt at 36°S, consistent with the reported to both the north (Giambiagi et al., 2012, 2009b, 2003a; Kozlowsky et al., 1993; Manceda and Figueroa, 1995; Mescua et al., 2014) and south (Orts et al., 2012; Rojas Vera et al., 2014; Valcarce and Zapata, 2009; Yagupsky et al., 2008; Zamora Valcarce et al., 2006). However, there are some inhibiting factors along the thrust-belt that would have favored the formation of new thrusts during the contractional phase. These factors would explain the differences in the basement deformational mechanism reported along the Malargüe fold-and-thrust belt.

5.2 Implications of the inherited architecture in the mountain building

The structural analysis presented here shows a structural model with a predominant thick-skinned style, where the basement is involved in the deformation through either the inversion of previous normal faults or new reverse faults. This model is consistent with the structural style characterizing the Malargüe fold-and-thrust belt between 34°30'S and 36°S (Mescua and Ramos, 2009; Mescua et al., 2014; Orts et al., 2012; Rojas Vera et al., 2014, Turienzo, 2010). Thin-skinned folding and thrusting south of 34°30'S in the eastern Principal Cordillera is observed exclusively in zones bounded by basement-involved structures in the Malargüe fold-and-thrust belt (Fig. 13). In turn, the Aconcagua fold-and-thrust belt between 33°30'S and 34°30'S is characterized by a predominant thin-skinned structural style that take advantage the low competence of some sedimentary layers (Giambiagi and Ramos, 2002; Ramos et al., 2004), and where thick-skinned style is just conspicuous and related to inversion of Mesozoic extensional depocenters or to the generation of by-pass thrusts (Giambiagi et al., 2003).

Structural style variations along the eastern Principal Cordillera have been associated with the degree of development of the Neuquén Basin due to changes on the crustal strength and inherited structural architecture (Giambiagi et al., 2012; Ramos et al., 1996). Respect to the latter, the thin-skinned Aconcagua fold-and-thrust belt developed across the narrowest and shallowest northern tip of the Neuquén Basin (Figure 2a). In turn, where the basin becomes wider, deeper and showing a high degree of depocenter development, inversion of older normal faults characterizes the deformation defining its thick-skinned structural style (c.f., Ramos et al., 1996).

Considering the contractional evolution within the Neuquén Basin, the differences between the north segment of the Principal Cordillera, in the Aconcagua fold-and-thrust belt, and the here studied segment, belonging to the Malargüe fold-and-thrust belt, can be resumed quantitatively by gradient of southward decrease in the amount of shortening accommodated across the eastern

Principal Cordillera (Fig. 16). This tendency is interrupted at nearly $34^{\circ}30'S$ where the amount of shortening of the eastern Principal Cordillera shows a notable break around the $34^{\circ}30'S$. North of this latitude the gradient is higher, despite the absolute value of shortening does not include the whole eastern Principal Cordillera (Fig. 16). Instead, south of $34^{\circ}30'S$, the gradient is lower than to the north, even though the shortening percentage continues decreasing southward (Fig. 16).

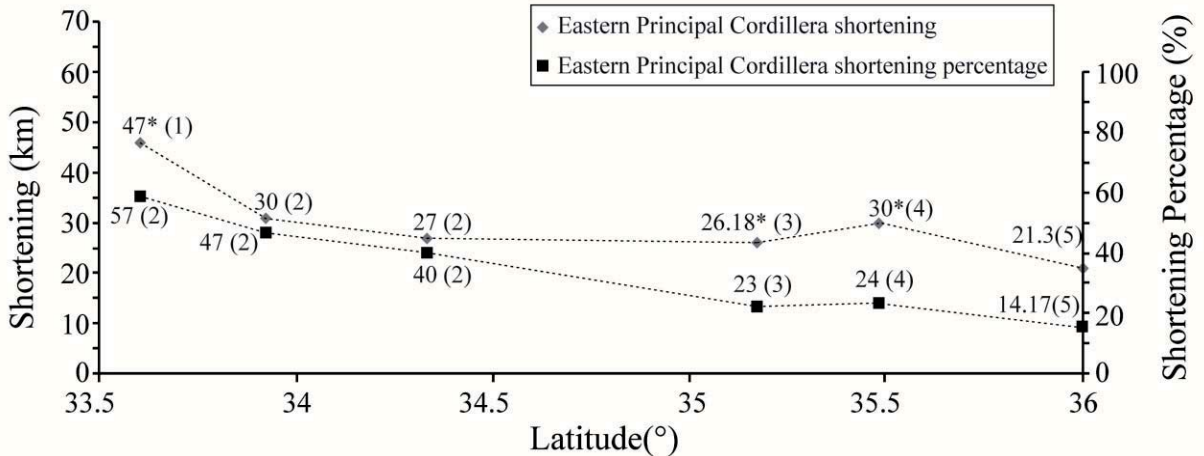


Figure 14. Latitudinal distribution of the upper-crustal horizontal shortening between $33^{\circ}30'$ and $36^{\circ}S$ based in: (1) Giambiagi and Ramos (2002), (2) Giambiagi et al. (2012), (3) Mescua et al. (2014), (4) This work and (5) Orts et al. (2012). The asterisk over values indicates shortening estimated across the whole eastern Principal Cordillera.

Southward decrease of shortening values is a tendency reported from the southern Bolivian orocline nearly $23^{\circ}S$ also inferred by a southward decrease on crustal thickening (e.g., Kley et al., 1999; Pose et al., 2005; Ramos et al., 2004). Beyond this value decrease tendency, the change on percentage shortening observed from the Aconcagua fold-and-thrust belt to the south to the Malargüe fold-and-thrust belt occurred along with an increase in the width of the fold and thrust belt. We propose that the southward decrease in percentage of shortening related to a higher width of the fold and thrust belt along the eastern Principal Cordillera is controlled by the structural styles. South of $34^{\circ}30'S$, inverted faults accommodates less shortening than the low-angle thrusts at the northern thin-skinned fold-and-thrust belt; in turn, where single inverted faults accommodate minor shortening, the zone affected by contraction is wider respect to the north region where shortening has been mostly accommodated by low-angle thrusts. Consequently, the mountain belt is lower and wider in the south respect to that observed north of $34^{\circ}30'S$ (Fig. 1). Despite the southward decreasing crustal thickening (Pose et al., 2005), this situation is reflected in deeper and narrower crustal roots in the thin-skinned segment respect to the wider thick-skinned inversion-related zone (Tassara and Echaurren, 2012).

Taking into account that eastward migration of deformation along the Malargüe fold-and-thrust belt resulted in an increase of the orogen width, previous works suggested that this has been primarily controlled by the slab shallowing occurred between 20 and 5 Ma (Folguera et al., 2006a, 2006b; Ramos and Folguera, 2009; Ramos et al., 2014). Nevertheless, the eastern limit of the Malargüe fold-and-thrust belt coincides spatially with the eastern extent of the Neuquén Basin,

which is also wider here than to the north in the Aconcagua fold-and-thrust belt and there is no shortening increase due to higher plate coupling as expected under slab-shallowing events (*cf.* Espurt et al., 2008; Gutscher et al., 2000) (Fig. 2). This situation suggests that the extent of deformation could be additionally, but not exclusively, controlled by the presence of the Neuquén Basin. In this regard, the southward widening of the Neuquén Basin would explain that south of 34°30'S the percentage decrease and the orogen is wider (Fig. 16).

The eastward advance of the deformation front in the Malargüe fold-and-thrust belt through a model with a basal detachment at depths of 8-12 km during the Neogene (Fig. 15) (Fariás et al., 2010; Giambiagi et al., 2012; Mescua et al., 2014; Turienzo et al., 2009) can be explained qualitatively using the critical wedge theory (Mescua et al., 2014). While the wedge was growing according to the parameters of this kinematic model (Dahlen et al., 1984; Davis et al., 1983), the preexisting normal fault structures would act as low shear zone concentrating the deformation as tectonic inversion, however, with minor displacement than in low-angle thrusts, thus favoring the migration. Therefore the major amount of previous normal faults south of 34°30'S (Fig. 2a) would favor both the thick-skinned structural style and the large eastward migration of the deformation in the Malargüe fold-and-thrust belt.

To sum up, the control of the Neuquén Basin in the southward decrease on percentage of shortening along the southern Central Andes, together with the structural style and the distribution of the shortening at the eastern Principal Cordillera, evidence that the previous architecture of the crust is critical for the understanding the latitudinal variations of the orogeny and its construction through time. This would indicate that the characteristics of the overriding plate have a very relevant control in mountain building processes. In this regard, variations in the dip of the subducting plate and its effects in the deformation of the overriding plate may be overestimated, simply because the quantitative effects of the overriding plate have been neglected, and near the study region there is no an increase of shortening value as expected for shallow subduction settings, but a wider fold and thrust belt with minor total shortening.

6 Conclusion

Based on structural and stratigraphic analysis we presented a deformational model for the eastern Principal Cordillera within the Malargüe fold-and-thrust belt at 35°30'S. This model is characterized by the involvement of the basement in the deformation through both the inversion of the previous normal fault and the generation of the new thrust mainly related to inversion tectonics. The development of the one or the other deformational mechanism would be controlled by either the dip or the orientation of normal faults respect to the compressional stress, thus explaining the variations in the basement-related deformational mechanism reported along the Malargüe fold-and-thrust belt.

Our balanced cross section of the Malargüe fold-and-thrust belt at 35°30'S consists in a hybrid structural model with basement-involved reverse faults rooted into a gently westward-dipping basal detachment transferring the deformation to sedimentary cover through thin-skinned folding and thrusting in restricted zones adjacent to basement blocks, accommodating approximately 30 km of tectonic shortening.

Despite the huge latitudinal contrast in the structural style along the eastern Principal Cordillera, the estimates of shortening is just slightly lower than the values in the northern thin-skinned region. We proposed that the larger development of the Neuquén Basin south of 34°30'S favored both the thick-skinned structural style and the large eastward migration of the deformation in the Malargüe fold-and-thrust belt, resulting in a large decrease of shortening percentages due to a wider distribution of deformation.

Finally, the previous architecture of the overriding plate crust is critical to understanding the Andean segmentation and to determining its influence on deformation patterns and its contrast to effects related to variation in the subducting plate during mountain building processes. In our study region, we propose an important control of a larger extensional development of the Neuquén Basin that explains plausibly a wider fold-and-thrust belt development, in contrast to the explanation related to changes in the subducting plate that has largely neglected the crustal inherited architecture that exhibits the Malargüe fold-and-thrust belt.

Acknowledgements

This work was supported by FONDECYT grants 1020272 and 11085022. F. Tapia's doctoral study at the University of Chile has been supported by Doctoral CONICYT scholarship. We thank Midland Valley, Ind. for providing an academic license for their software Move.

References

- Aguirre-Urreta, M.B., Tunik, M., Naipauer, M., Pazos, P., Ottone, E., Fanning, M., Ramos, V.A., 2011. Malargüe Group (Maastrichtian-Danian) deposits in the Neuquén Andes, Argentina: Implications for the onset of the first Atlantic transgression related to Western Gondwana break-up. *Gondwana Res.* 19, 482–494.
- Allmendinger, R.W., Ramos, V.A., Jordan, T.E., Palma, M., Isacks, B.L., 1983. Paleogeography and Andean structural geometry, northwest Argentina. *Tectonics* 2, 1–16.
- Alvarez Cerimedo, J., Orts, D., Rojas-Vera, E., Folguera, A., Bottesi, G., Ramos, V. 2013. Mecanismos y fases de construcción orogénicos del frente oriental andino (36°S, Argentina). *Andean Geology* 40 (3), 503-519.
- S.G.M., 1997. Mapa geológico de la República Argentina, escala 1:2.500.000, Buenos Aires, Argentina.
- Arregui, C.D., Carbone, O., Sattler, F., 2011. El Grupo Lotena (Jurásico Medio-Tardío) en la Cuenca Neuquina, in: Leanza, H.A., Arregui, C., Carbone, O., Danieli, J.C., Vallés, J.M. (Eds.), *Geología y Recursos Naturales de La Provincia de Neuquén. Relatorio XVIII Congreso Geológico Argentino*. Neuquén, pp. 91–98.
- Arriagada, C., Ferrando, R., Córdova, L., Morata, D., Roperch, P., 2013. The Maipo Orocline : A first scale structural feature in the Miocene to Recent geodynamic evolution in the central Chilean Andes. *Andean Geol.* 40, 419–437.
- Burckhardt, C., 1900. Profils géologiques transversaux de la cordillere argentina-chilienne stratigraphie et tectonique.pdf. An. del Mus. la PLata 1.

- Charrier, R., Baeza, O., Elgueta, S., Flynn, J., Gans, P., Kay, S., Muñoz, N., Wyss, A., Zurita, E., 2002. Evidence for Cenozoic extensional basin development and tectonic inversion south of the flat-slab segment, southern Central Andes, Chile (33° – 36° S.L.). *J. South Am. Earth Sci.* 15, 117–139.
- Charrier, R., Bustamante, M., Comte, D., Elgueta, S., Flynn, J.J., Iturra, N., Muñoz, N., Pardo, M., Thiele, R., Wyss, A.R., 2005. The Abanico extensional basin: Regional extension, chronology of tectonic inversion and relation to shallow seismic activity and Andean uplift. *Neues Jahrb. für Geol. und Palaontologie-Abhandlungen* 236, 43–77.
- Charrier, R., Pinto, L., Rodríguez, M.P., 2007. Tectonostratigraphic evolution of the Andean Orogen in Chile, in: Moreno, T., Gibbons, W. (Eds.), *The Andes of Chile*. Geological Society, London, pp. 21–114.
- Charrier, R., Ramos, V.A., Tapia, F., Sagripanti, L., 2014. Tectono-stratigraphic evolution of the Andean Orogen between 31 and 37 S (Chile and Western Argentina). *Geol. Soc. London, Spec. Publ.* 399.
- Dahlen, F.A., Suppe, J., Davis, D., 1984. Mechanics of fold-and-thrust belts and accretionary wedges: Cohesive Coulomb Theory. *J. Geophys. Res.* 89, 10087.
- Davidson, J.K., Vicente, J.-C., 1973. Características paleogeográficas y estructurales del área fronteriza de las nacientes del Teno (Chile) y Santa Elena (Argentina) (Cordillera Principal, 35° a $35^{\circ}15'$ de latitud sur), in: *V Congreso Geológico Argentino*. pp. 11–55.
- Davis, D., Suppe, J., Dahlen, F.A., 1983. Mechanics of fold-and-thrust belts and accretionary wedges. *J. Geophys. Res. Solid Earth* 88, 1153–1172.
- Di Giulio, A., Ronchi, A., Sanfilippo, A., Tiepolo, M., Pimentel, M., Ramos, V.A., 2012. Detrital zircon provenance from the Neuquén Basin (south-central Andes): Cretaceous geodynamic evolution and sedimentary response in a retroarc-foreland basin. *Geology* 40, 559–562.
- Espurt, N., Funiciello, F., Martinod, J., Guillaume, B., Regard, V., Faccenna, C., Brusset, S., 2008. Flat subduction dynamics and deformation of the South American plate: Insights from analog modeling. *Tectonics* 27.
- Farías, M., Charrier, R., Carretier, S., Martinod, J., Fock, A., Campbell, D., Cáceres, J., Comte, D., 2008. Late Miocene high and rapid surface uplift and its erosional response in the Andes of central Chile (33° – 35° S). *Tectonics* 27.
- Farías, M., Comte, D., Charrier, R., Martinod, J., David, C., Tassara, A., Tapia, F., Fock, A., 2010. Crustal-scale structural architecture in central Chile based on seismicity and surface geology: Implications for Andean mountain building. *Tectonics* 29.
- Fock, A., Charrier, R., Farías, M., Muñoz, M.A., 2006. Fallas de vergencia oeste en la Cordillera Principal de Chile Central: Inversión de la cuenca de Abanico. *Asoc. Geológica Argentina, Ser. Publicación Espec.* 6.

- Folguera, A., Orts, D., Spagnuolo, M.G., Vera, E.R., Litvak, V., Sagripanti, L., Ramos, M.E., Ramos, V.A., 2011. A review of Late Cretaceous to Quaternary palaeogeography of the southern Andes. *Biol. J. Linn. Soc.* 103, 250–268.
- Folguera, A., Ramos, V.A., 2011. Repeated eastward shifts of arc magmatism in the Southern Andes: A revision to the long-term pattern of Andean uplift and magmatism. *J. South Am. Earth Sci.* 32, 531–546.
- Folguera, A., Ramos, V.A., González Díaz, E.F., Hermanns, R., 2006a. Miocene to Quaternary deformation of the Guañacos fold-and-thrust belt in the Neuquén Andes between 37°S and 37°30'S, in: Kay, S.M., Ramos, V.A. (Eds.), *Evolution of an Andean Margin: A Tectonic and Magmatic View from the Andes to the Neuquén Basin (35°–39°S Lat)*. Geological Society of America, Special Papers 407, pp. 247–266.
- Folguera, A., Zapata, T., Ramos, V.A., 2006b. Late Cenozoic extension and the evolution of the Neuquén Andes, in: Kay, S.M., Ramos, V.A. (Eds.), *Evolution of an Andean Margin: A Tectonic and Magmatic View from the Andes to the Neuquén Basin (35°–39°S Lat)*. Geological Society of America, Special Papers 407, pp. 267–285.
- Franzese, J., Spalletti, L., Perez, I.G., Macdonald, D., 2003. Tectonic and paleoenvironmental evolution of Mesozoic sedimentary basins along the Andean foothills of Argentina (32 degrees-54 degrees S). *J. South Am. Earth Sci.* 16, 81–90.
- Franzese, J.R., Spalletti, L.A., 2001. Late Triassic-early Jurassic continental extension in southwestern Gondwana: tectonic segmentation and pre-break-up rifting. *J. South Am. Earth Sci.* 14, 257–270.
- Giambiagi, L.B., Alvarez, P.P., Godoy, E., Ramos, V.A., 2003a. The control of pre-existing extensional structures on the evolution of the southern sector of the Aconcagua fold and thrust belt, southern Andes. *Tectonophysics* 369, 1–19.
- Giambiagi, L.B., Bechis, F., Garcia, V.H., Clark, A.H., 2008. Temporal and spatial relationships of thick- and thin-skinned deformation: A case study from the Malargüe fold-and-thrust belt, southern Central Andes. *Tectonophysics* 459, 123–139.
- Giambiagi, L.B., Ghiglione, M., Cristallini, E., Bottesi, G., 2009a. Kinematic models of basement/cover interaction: Insights from the Malargüe fold and thrust belt, Mendoza, Argentina. *J. Struct. Geol.* 31, 1443–1457.
- Giambiagi, L.B., Mescua, J., Bechis, F., Tassara, A., Hoke, G.D., 2012. Thrust belts of the southern Central Andes: Along-strike variations in shortening, topography, crustal geometry, and denudation. *Geol. Soc. Am. Bull.* 124, 1339–1351.
- Giambiagi, L.B., Ramos, V.A., 2002. Structural evolution of the Andes in a transitional zone between flat and normal subduction (33°30'–33°45'S), Argentina and Chile. *J. South Am. Earth Sci.* 15, 101–116.

- Giambiagi, L.B., Ramos, V.A., Godoy, E., Álvarez, P.P., Orts, S., 2003b. Cenozoic deformation and tectonic style of the Andes, between 33 degrees and 34 degrees south latitude. *Tectonics* 22, 1041.
- Giambiagi, L.B., Tunik, M., Barredo, S., Bechis, F., Ghiglione, M., Alvarez, P.P., Drosina, M., 2009b. Cinemática de apertura del sector norte de la Cuenca Neuquina. *Rev. Asoc. Geológica Argentina* 65, 278–292.
- Godoy, E., Yáñez, G., Vera, E., 1999. Inversion of an Oligocene volcano-tectonic basin and uplifting of its superimposed Miocene magmatic arc in the Chilean Central Andes: First seismic and gravity evidences. *Tectonophysics* 306, 217–236.
- González, O., Vergara, M., 1962. Reconocimiento geológico de la Cordillera de los Andes entre los paralelos 35° y 38° S. *Inst. Investig. Geológicas* 1.
- Groeber, P., 1947. Observaciones geológicas a lo largo del meridiano 70°. I. Hojas Bardas Blancas y Los Molles. *Rev. Asoc. Geológica Argentina* 2, 409–433.
- Gulisano, C., 1981. El ciclo cuyano en el norte de Neuquén y sur de Mendoza, in: VIII Congreso Geológico Argentino. San Luis, Argentina, pp. 579–592.
- Gulisano, C., Gutiérrez Pleimling, A.R., 1995. The Jurassic of the Neuquén Basin: Mendoza Province. Guía de Campo, in: Asociación Geológica Argentina, Special Publication, Vol. 159. Argentina. p. 103.
- Gulisano, C., Gutiérrez Pleimling, A.R., Digregorio, R.E., 1984. Esquema estratigráfico de la secuencia Jurásica del oeste de la provincia de Neuquén, in: IX Congreso Geológico Argentino. pp. 236–259.
- Gutscher, M.-A., Spakman, W., Bijwaard, H., 2000. Geodynamic of flat slab subduction: Seismicity and tomographic constraints from the Andean margin. *Tectonics* 19, 814–833.
- Hervé, F. 1988. Late Paleozoic subduction and accretion in southern chile. *Episodes* 11, 183–188.
- Howell, J., Schwarz, E., Spalletti, L., Veiga, G.D., 2005. The Neuquén Basin: an overview, in: Howell, J., Schwarz, E., Spalletti, L., Veiga, G.D. (Eds.), *The Neuquén Basin, Argentina: A Case Study in Sequence Stratigraphy and Basin Dynamics*. Geological Society of London, Special Publications, 252, Londres, pp. 1–14.
- Jordan, T.E., Isacks, B.L., Allmendinger, R.W., Brewer, J.A., Ramos, V.A., Ando, C.J., 1983. Andean tectonics related to geometry of subducted Nazca plate. *Geol. Soc. Am. Bull.* 94, 341–361.
- Kay, S.M., Burns, M.W., Copeland, P., Mancilla, O. 2006. Uppero Cretaceous to Holocene magmatism and evidence for transient Miocene shallowing of the Andean subduction zone under the northern Neuquén Basin, in: Kay, S.M. and Ramos, V.A. (Eds), *Evolution of an Andean margin: A tectonic and magmatic view from the Andes to the Neuquén Basin (35°-39°S lat)*. *Geol. Soc. Am. Special Papers*, 407, pp. 19-60.
- Kay, S.M., Ramos, V.A., 2006. Overview of the tectonic evolution of the southern Central Andes of Mendoza and Neuquén (35°–39°S latitude), in: Kay, S.M. and Ramos, V.A. (Eds), *Evolution of an*

- Andean margin: A tectonic and magmatic view from the Andes to the Neuquén Basin (35° - 39° S lat). Geol. Soc. Am, Special Papers, 407, pp. 1–17.
- Kleiman, L.E., Japas, M.S., 2009. The Choiyoi volcanic province at 34° S– 36° S (San Rafael, Mendoza, Argentina): Implications for the Late Palaeozoic evolution of the southwestern margin of Gondwana. *Tectonophysics* 473, 283–299.
- Kley, J., Monaldi, C.R., Salfity, J.A., 1999. Along-strike segmentation of the Andean foreland: causes and consequences. *Tectonophysics* 301, 75–94.
- Kozlowsky, E., Manceda, R., Ramos, V.A., 1993. Estructura, in: Ramos, V.A. (Ed.), *Geología Y Recursos Naturales de La Provincia de Mendoza. XII Congreso Geológico Argentino*. Mendoza, pp. 235–256.
- Lanés, S., 2005. Late Triassic to Early Jurassic sedimentation in northern Neuquén Basin, Argentina: Tectosedimentary Evolution of the first transgression. *Geol. Acta* 3, 81–106.
- Lanés, S., Giambiagi, L.B., Bechis, F., Tunik, M., 2008. Late Triassic - Early Jurassic successions of the Atuel depocenter: sequence stratigraphy and tectonic controls. *Rev. Asoc. Geológica Argentina* 63, 534–548.
- Lanés, S., Palma, R.M., 1998. Environmental implications of oncoids and associated sediments from the Remoredó Formation (Lower Jurassic) Mendoza, Argentina. *Palaeogeogr. Palaeoclimatol. Palaeoecol.* 140, 357–366.
- Lanés, S., Salani, F.M., 1998. Petrografía, origen y paleoambiente sedimentario de las piroclastitas de la Formación Remoredó (Jurásico Temprano), Argentina ($35^{\circ}30'$ S- $70^{\circ}15'$ W). *Rev. Geológica Chile* 25, 141–152.
- Leanza, H. a., Mazzini, a., Corfu, F., Llambías, E.J., Svensen, H., Planke, S., Galland, O., 2013. The Chachil Limestone (Pliensbachian–earliest Toarcian) Neuquén Basin, Argentina: U–Pb age calibration and its significance on the Early Jurassic evolution of southwestern Gondwana. *J. South Am. Earth Sci.* 42, 171–185.
- Leanza, H.A., 1990. Estratigrafía del Paleozoico y Mesozoico anterior a los movimientos intermálmicos en la comarca del cerro Chachil, provincia del Neuquén. *Rev. Asoc. Geológica Argentina* 45, 272–299.
- Leanza, H.A., 1993. Estratigrafía del Mesozoico posterior a los movimientos intermálmicos en la comarca del cerro Chachil, provincia del Neuquén. *Rev. Asoc. Geológica Argentina* 48, 71–84.
- Leanza, H.A., 2009. Las principales discordancias del Mesozoico de la Cuenca Neuquina según observaciones de superficie Rev. Mus. Argentino Ciencias Nat. 11, 145–184.
- Legarreta, L., Kozlowsky, E., 1984. Secciones condensadas del Jurásico-Cretácico de los Andes del Sur de Mendoza: Estratigrafía y significado tectonosedimentario, in: IX Congreso Geológico Argentino. pp. 286–297.

- Legarreta, L., Uliana, M.A., 1991. Jurassic—Marine Oscillations and Geometry of Back-Arc Basin Fill, Central Argentine Andes, in: Sedimentation, Tectonics and Eustasy. Blackwell Publishing Ltd., pp. 429–450.
- Legarreta, L., Uliana, M.A., 1996. The Jurassic succession in west-central Argentina: stratal patterns, sequences and paleogeographic evolution. *Palaeogeogr. Palaeoclimatol. Palaeoecol.* 120, 303–330.
- Legarreta, L., Uliana, M.A., 1999. El Jurásico y Cretácico de la Cordillera Principal y la Cuenca Neuquina. Facies Sedimentarias., in: Caminos, R. (Ed.), Geología Argentina. Servicio Geológico Minero Argentino: Instituto de Geología y Recursos Minerales, Anales, pp. 399–416.
- Manceda, R., Figueroa, D., 1995. Inversion of the Mesozoic Neuquén Rift in the Malargüe Fold and Thrust Belt, Mendoza, Argentina, in: Tankard, A.J., Suárez S., R., Welsink, H.J. (Eds.), Petroleum Basin of South America. AAPG Memoir 62, pp. 369–382.
- Mazzini, A., Svensen, H., Leanza, H. a., Corfu, F., Planke, S., 2010. Early Jurassic shale chemostratigraphy and U–Pb ages from the Neuquén Basin (Argentina): Implications for the Toarcian Oceanic Anoxic Event. *Earth Planet. Sci. Lett.* 297, 633–645.
- Mescua, J.F., Giambiagi, L.B., 2012. Fault inversion vs. new thrust generation: A case study in the Malargüe fold-and-thrust belt, Andes of Argentina. *J. Struct. Geol.* 35, 51–63.
- Mescua, J.F., Giambiagi, L.B., Bechis, F. 2008. Evidencias de tectónica extensional en el Jurásico Tardío (Kimmeridgiano) del suroeste de la provincia de Mendoza. *Rev. Asoc. Geológica Argentina*.
- Mescua, J.F., Giambiagi, L.B., Bechis, F., 2012. Reply to L.V. Dimieri and M.M. Turienzo, 2012 comment on: “Fault inversion vs. new thrust generation: A case study in the Malargüe fold-and-thrust belt, Andes of Argentina” by J. F. Mescua and L. B. Giambiagi, *Journal of structural geology* 35 (2012) 51–63. *J. Struct. Geol.* 42, 283–287.
- Mescua, J.F., Giambiagi, L.B., Ramos, V.A., 2013. Late Cretaceous Uplift in the Malargüe fold-and-thrust belt (35° S), southern Central Andes of Argentina and Chile. *Andean Geol.* 40, 102–116.
- Mescua, J.F., Giambiagi, L.B., Tassara, A., Gimenez, M., Ramos, V.A., 2014. Influence of pre-Andean history over Cenozoic foreland deformation: Structural styles in the Malargüe fold-and-thrust belt at 35 S, Andes of Argentina. *Geosphere* 1–25.
- Mescua, J.F., Ramos, V.A., 2009. Estratigrafía y estructura de las nacientes del río Borbollón, alto río Diamante, provincia de Mendoza. *Rev. Asoc. Geológica Argentina* 65, 111–122.
- Muñoz-Saéz, C., Pinto, L., Charrier, R., Nalpas, T. 2014. Influence of depositional load on the development of a shortcut fault system during the inversion of an extensional basin: The Eocene-Oligocene Abanico Basin case, central Chile Andes (33° - 35° S). *Andean Geology* 41(1), 1-28.
- Orts, D.L., Folguera, A., Giménez, M., Ramos, V.A., 2012. Variable structural controls through time in the Southern Central Andes ($\sim 36^{\circ}$ S). *Andean Geol.* 39, 220–241.

- Parada, M.A., Féraud, G., Fuentes, F., Aguirre, L., Morata, D., Larrondo, P., 2005. Ages and cooling history of the Early Cretaceous Caleu pluton: testimony of a switch from a rifted to a compressional continental margin in central Chile. *J. Geol. Soc. London.* 162, 273–287.
- Pose, F.A., Spagnuolo, M.G., Folguera, A., 2005. Modelo para la variación del volumen orogénico andino y acortamientos en el sector 20°-46°S. *Rev. Asoc. Geológica Argentina* 60, 724–730.
- Ramos, V.A., 2000. The Southern Central Andes.pdf, in: Cordani, U.G., Milani, E.J., Thomas Philo, A., Campos, A. (Eds.), *Tectonic Evolution of South America. 31° International Geological Congress, Rio de Janeiro, Río de Janeiro*, pp. 561–604.
- Ramos, V.A., Cegarra, M., Cristallini, E., 1996. Cenozoic tectonics of the High Andes of west-central Argentina (30–36°S latitude). *Tectonophysics* 259, 185–200.
- Ramos, V.A., Folguera, A., 2005. Tectonic evolution of the Andes of Neuquén: constraints derived from the magmatic arc and foreland deformation, in: Veiga, G.D., Spalletti, L.A., Howell, J., Schwarz, E. (Eds.), *The Neuquén Basin: A Case Study in Sequence Stratigraphy and Basin Dinamics*. Geological Society of America, Special Papers 252, pp. 15–35.
- Ramos, V.A., Folguera, A., 2009. Andean flat-slab subduction through time, in: Murphy, J.B., Keppie, J.D., Hynes, A.J. (Eds.), *Ancient Orogens and Modern Analogues*. Geological Soc Publishing House, Bath, pp. 31–54.
- Ramos, V.A., Litvak, V.D., Folguera, A., Spagnuolo, M.G., 2014. An Andean tectonic cycle: From crustal thickening to extension in a thin crust (34°–37°SL). *Geosci. Front.* 1–17.
- Ramos, V.A., Zapata, T., Cristallini, E.O., Introcaso, A., 2004. The Andean thrust system—Latitudinal variations in structural styles and orogenic shortening, in: McClay, K.. (Ed.), *Thrust Tectonics and Hydrocarbon System*. AAPG Memoir, pp. 30–50.
- Rojas Vera, E. a., Folguera, A., Zamora Valcarce, G., Bottesi, G., Ramos, V.A., 2014. Structure and development of the Andean system between 36° and 39°S. *J. Geodyn.* 73, 34–52.
- Rosendahl, B.R., Reynolds, D.J., Lorber, P.M., Burgess, C.F., McGill, J., Scott, D., Lambiase, J.J., Derksen, S.J., 1986. Structural expressions of rifting: lessons from Lake Tanganyika, Africa. *Geol. Soc. London, Spec. Publ.* 25, 29–43.
- Schellart, W.P., 2008. Overriding plate shortening and extension above subduction zones: A parametric study to explain formation of the Andes Mountains. *Geol. Soc. Am. Bull.* 120, 1441–1454.
- Servicio Geológico Minero Argentino, 1997. Mapa geológico de la República Argentina, escala 1:2.500.000, Buenos Aires, Argentina.
- Servicio Nacional de Geología y Minería, 2002. Mapa geológico de Chile, escala 1:1.000.000, Mapa M61.
- Silvestro, J., Atencio, M., 2009. La cuenca cenozoica del río Grande y Palauco: edad, evolución y control estructural, faja plegada de Malargüe. *Rev. Asoc. Geológica Argentina* 65, 154–169.

- Silvestro, J., Kraemer, P., 2005. Evolución de las cuencas sinorogénicas de la Cordillera Principal entre 35°-36° S, Malargüe. Rev. Asoc. Geológica Argentina 60, 627–643.
- Sobolev, S. V., Babeyko, A.Y., Koulakov, I., Oncken, O., 2006. Mechanism of the Andean Orogeny: Insight from Numerical Modeling, in: Oncken, O., Chong, G., Franz, G., Giese, P., Götze, H.-J., Ramos, V.A., Strecker, M.R., Wigger, P. (Eds.), *The Andes, Active Subduction Orogeny*, Frontiers in Earth Sciences. Springer, pp. 513–535.
- Somoza, R., Ghidella, M.E., 2012. Late Cretaceous to recent plate motions in western South America revisited. *Earth Planet. Sci. Lett.* 331-332, 152–163.
- Spagnuolo, M.G., Litvak, V.D., Folguera, A., Bottesi, G., Ramos, V.A., 2012. Neogene magmatic expansion and mountain building processes in the southern Central Andes, 36–37°S, Argentina. *J. Geodyn.* 53, 81–94.
- Suppe, J., Medwedeff, D.A., 1990. Geometry and kinematics of fault-propagation folding. *Eclogae Geol. Helv.* 83, 409–454.
- Tassara, A., Echaurren, A., 2012. Anatomy of the Andean subduction zone: three-dimensional density model upgraded and compared against global-scale models. *Geophys. J. Int.* 189, 161–168.
- Tunik, M., Folguera, A., Naipauer, M., Pimentel, M., Ramos, V.A., 2010. Early uplift and orogenic deformation in the Neuquén Basin: Constraints on the Andean uplift from U–Pb and Hf isotopic data of detrital zircons. *Tectonophysics* 489, 258–273.
- Turienzo, M.M., 2010. Structural style of the Malargüe fold-and-thrust belt at the Diamante River area (34°30'–34°50'S) and its linkage with the Cordillera Frontal, Andes of central Argentina. *J. South Am. Earth Sci.* 29, 537–556.
- Turienzo, M.M., Dimieri, L. V., Frisicale, C., Araujo, V., Sánchez, N., 2009. Cenozoic structural evolution of the Argentinean Andes at 34°40'S: A close relationship between thick and thin-skinned deformation. *Andean Geol.* 65, 123–139.
- Valcarce, G.Z., Zapata, T., 2009. Evolución tectónica del frente andino en Neuquén. Rev. Asoc. Geológica Argentina 65, 192–203.
- Vergani, G.D., Tankard, J., Belotti, J., Welsink, J., 1995. Tectonic evolution and paleogeography of the Neuquén Basin, Argentina, in: Tankard, J., Suarez, R., Welsink, J. (Eds.), *Petroleum Basin of South America*. AAPG, pp. 383–402.
- Westermann, G., Riccardi, A., 1982. Ammonoid fauna from the early Middle Jurassic of Mendoza province, Argentina. *J. Paleontol.* 56, 11–41.
- Williams, G.D., Powell, C.M., Cooper, M.A., 1989. Geometry and kinematics of inversion tectonics. *Geol. Soc. London, Spec. Publ.* 44, 3–15.
- Yagupsky, D.L., Cristallini, E.O., Fantín, J., Valcarce, G.Z., Bottesi, G., Varadé, R., 2008. Oblique half-graben inversion of the Mesozoic Neuquén Rift in the Malargüe Fold and Thrust Belt, Mendoza, Argentina: New insights from analogue models. *J. Struct. Geol.* 30, 839–853.

- Yáñez, G., Cembrano, J., 2004. Role of viscous plate coupling in the late Tertiary Andean tectonics. *J. Geophys. Res.* 109, B02407.
- Yáñez, G., Ranero, C.R., Von Huene, R., Díaz, J., 2001. Magnetic anomaly interpretation across the southern central Andes (32°–34°S): The role of the Juan Fernández Ridge in the late Tertiary evolution of the margin. *J. Geophys. Res. B Solid Earth* 106, 6325–6345.
- Zamora Valcarce, G., Zapata, T., del Pino, D., Ansa, A., 2006. Structural evolution and magmatic characteristics of the Agrio fold-and-thrust belt, in: Kay, S.M., Ramos, V.A. (Eds.), *Evolution of an Andean Margin: A Tectonic and Magmatic View from the Andes to the Neuquén Basin*. Geological Soc Amer Inc, Boulder, pp. 125–145.
- Zamora Valcarce, G., Zapata, T., Pino, D., 2006. Structural evolution and magmatic characteristics of the Agrio fold-and-thrust belt, in: Kay, S.M., Ramos, V.A. (Eds.), *Evolution of an Andean Margin: A Tectonic and Magmatic View from the Andes to the Neuquén Basin*. Geological Society of America, Special Papers 407, pp. 125–145.
- Zapata, T., Folguera, A., 2005. Tectonic evolution of the Andean Fold and Thrust Belt of the southern Neuquén Basin, Argentina. *Geol. Soc. London, Spec. Publ.* 252, 37–56.

CAPÍTULO IV.

EVOLUCIÓN DE LA REGIÓN AXIAL DE LA CORDILLERA PRINCIPAL

IV.1 Introducción

En los capítulos anteriores se presentó la estructura y evolución de los dos mayores dominios estructurales cenozoicos de la Cordillera Principal, la Cuenca de Abanico y la faja plegada y corrida de Malargüe. En este capítulo, se analiza la evolución estructural de la región axial de la Cordillera Principal durante la inversión de la Cuenca de Abanico y la estructuración de la faja plegada y corrida de Malargüe. La particularidad de esta región reside en que corresponde a la zona de interacción directa entre ambos dominios estructurales por lo que su estudio permite entender cómo se propagó la deformación durante la fase neógena de deformación. Además, el estudio de esta región se vuelve necesario debido a que ha sido propuesto como el límite norte y oeste de la deformación extensional que afectó el retro-arco y arco durante el Plioceno tardío-Pleistoceno (Ramos et al., 2014 y referencias ahí).

Este capítulo consta sólo de una sección (artículo aceptado) donde se analiza la evolución del eje de la Cordillera Principal durante el Neógeno y Cuaternario a través de la caracterización de depósitos sinorogénicos miocenos asociados a la construcción orogénica. Así también se discute acerca de la deformación extensional propuesta para esta región y como se relaciona con los resultados obtenidos en este estudio.

IV.2 Artículo: "Late Cenozoic contractional evolution of the current arc region along the southern Central Andes (35°20'S)³

Late Cenozoic contractional evolution of the current arc-volcanic region along the southern Central Andes (35°20'S)

Felipe Tapia¹, Marcelo Fariás¹, Maximiliano Naipauer² and Jacqueline Puratich¹

¹*Departamento de Geología, Universidad de Chile, Santiago, Chile.*

²*Instituto de Estudios Andinos “Don Pablo Groeber”, Departamento de Ciencias Geológicas, FCEN, Universidad de Buenos Aires-CONICET, Buenos Aires, Argentina*

Abstract

The Andean internal zone records deformation, uplift and erosion that serve as proxies of variations on mountain building dynamics. Hence, the study of this region would give keys to understand the factors controlling the orogenic evolution. Structural, stratigraphic and geochronological data in the Andean internal zone at 35°20'S evidence that this region has only underwent contractional deformation since the late Miocene up to present, differing from coeval Pleistocene extensional tectonics affecting the retro-arc. Contractional deformation was characterized by the development of a piggy-back basin in the latest Miocene filled by synorogenic deposits. Afterward, an out-of-sequence thrusting event affected the region since at least the Pliocene until the Present. Shortening in the inner part of the Andean orogen would be favored by both the high orthogonality of the out-sequence structures with respect to the plate convergence vector and by the minor resistance to shortening produced by the southward decrease of the orogen height and by the removal of material via erosion of the uplifted mountain belt. In contrast, oblique structures, as those described farther north, accommodate strike-slip displacement. Likewise, we propose that erosion from the inner orogen favored the prolongation of the out-of-sequence thrusting event until the Present, differing from the situation north of the 34°S where this event ended by the Pliocene.

Keywords

Out-of-sequence thrusting, synorogenic deposits, Andean Cenozoic evolution.

1. Introduction

The current volcanic arc region along the southern Central Andes corresponds to the internal part of an orogen formed in an oceanic-continent subduction regime, developed near the present-day Pacific-Atlantic drainage divide (Fig. 1a). Subduction of the oceanic Nazca plate beneath the South American plate has resulted in almost continuous magmatism during the system's evolution, in addition to the involved stress transfer to the overriding plate. This process

³ Manuscrito aceptado 6 de Enero del 2015 en Journal of Geodynamics

has led to crustal shortening and thickening and the consequent uplift in the overriding South American plate mainly during the late Cenozoic (Charrier et al., 2007, 2014; Farías et al., 2008, 2010; Folguera et al., 2011; Giambiagi and Ramos, 2002; Giambiagi et al., 2003, 2008; Ramos et al., 2014; Ramos and Folguera, 2005; Ramos and Kay, 2006).

Despite the along-strike continuity of the mountain belt in the southern Central Andes, the orogenic volume and maximal crustal thickness gradually decreases to the south without exhibiting relevant changes in the decrease gradient (e.g., Pose et al., 2005; Tassara et al., 2005; Tassara and Echaurren, 2012). However, it has been proposed that the internal zone of the orogen evolved differently north and south of 35°S since the late Miocene (see Charrier et al., 2014 and references therein). In fact, the contractional stage north of 35°S ended by the Pliocene (Giambiagi et al., 2003), which was followed by strike-slip deformation until today (Farías et al., 2010), whereas south of 35°S, shortening would have been interrupted by an extensional episode in the early Pleistocene, which affected the retro-arc region and spread to the arc region (Folguera et al., 2006b, 2008, 2011, 2012; Ramos and Folguera, 2011; Spagnuolo et al., 2012). This event was preceded by a late Miocene eastward magmatic expansion and shortening migration to the foreland that produced the uplift of the San Rafael Block (see Ramos and Kay, 2006, and reference therein).

The extensional episode was characterized by the early Pleistocene-Holocene development of several NW-trending depressions with a concomitant development of intraplate volcanism in the retro-arc region between 35° and 40°S (cf. Ramos et al., 2014 and reference therein). This evolution is supported by several structural (Folguera et al., 2004, 2006b, 2008, 2010; Garcia Morabito and Folguera, 2005; Ramos and Kay, 2006; Rojas-Vera et al., 2010, 2014), geophysical (Folguera et al., 2007a, 2012), and petrological studies (Folguera et al., 2009; Kay et al., 2006; Ramos and Folguera, 2011). According to Folguera et al. (2006b; 2008), the northernmost depression extended up to the arc region slightly south of 35°S. There, they infer that the high volume of silicic volcanic material extruded by the Calabozos caldera since the early Pleistocene (cf., Hildreth et al., 1984) was controlled by extensional tectonics related to the development of the Las Loicas Trough, the northernmost extensional depression in Argentina. Nevertheless, there is no reported evidence for extension in this area, exposing the lack of appropriate structural studies and the poor knowledge of the Quaternary evolution of the internal zone of the Andean orogen at the latitudes of this study.

The proposed extensional evolution for the current arc region south of 35°S contrasts with those reported to the north and farther south at 36°30'S. In both regions, contractional deformation has dominated the internal part of the Andean range since the late Miocene as an out-of-sequence thrusting event, even though it evolved to transcurrent deformation by the Pliocene in the north (Folguera and Ramos, 2009, Folguera et al., 2004, 2006a, 2007b; Giambiagi and Ramos, 2002; Giambiagi et al., 2003; 2014; Godoy et al., 1999; Rojas-Vera et al., 2014).

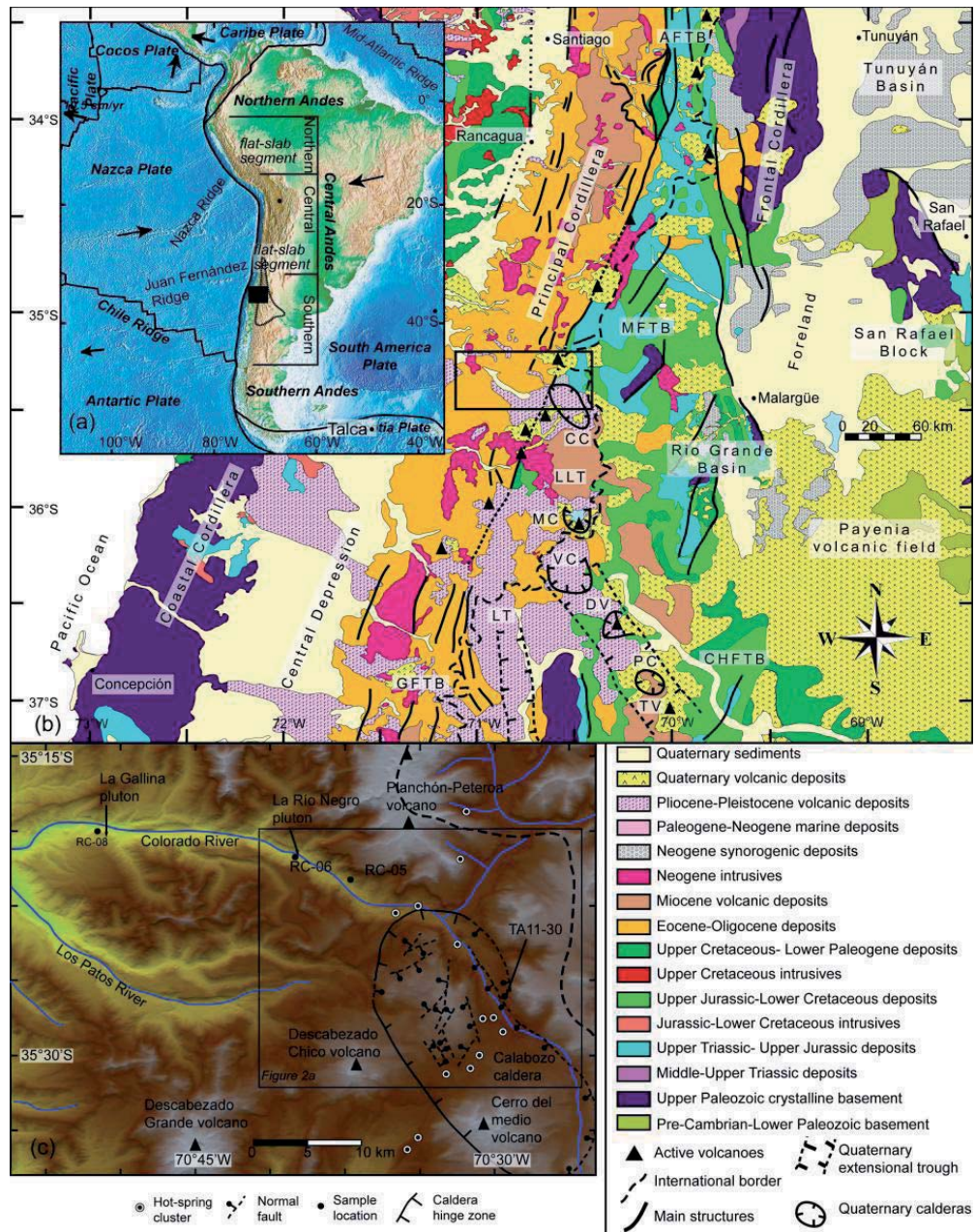


Figure 1: (a) Tectonic framework of the Andean margin. The arrows indicate the absolute plate motion; the dashed line delineates the Neuquén Basin margin; the filled black rectangle shows the location of Figure 1b. (b) Simplified geologic map of the Chilean-Argentinean Andean margin between 33° and 37°S showing major structures and main lithological units (Taken from Farías et al., 2010; Folguera et al., 2006b; Giambiagi et al., 2003, 2008, 2009, 2012; Servicio Geológico Minero Argentino, 1997; Servicio Nacional de Geología y Minería, 2002). The black rectangle shows the location of the Figure 2a. AFTB: Aconcagua fold-and-thrust belt; CC: Calabozos caldera; CHFTB: Chos Malal fold-and-thrust belt; DV: Domuyo volcano; GFTB: Guañacos fold-and-thrust belt; LLT: Las Loicas Trough; LT: Loncopue trough; MFTB: Malargüe fold-and-thrust belt; MC: Maule caldera; PC: Palao caldera; TV: Tromen volcano; VC: Varvarco caldera. (c) Digital elevation model (DEM) of the study area showing the location of the samples and the Calabozos caldera. Morphology and location of the normal fault of the caldera was taken from Hildreth et al., 1984. The black rectangle indicates the location of the Fig. 2a.

The eastward migration of shortening and expansion of the volcanic arc at these latitudes during the late Miocene has been interpreted as a consequence of a shallowing of the subducting slab, whereas the subsequent extension and intraplate volcanism has been explained by the steepening of the slab (see Ramos and Kay, 2006 and reference therein).

Nevertheless, extensional deformation has not been directly reported along the arc-region, but contractional deformation has been proposed for this area at a similar time (e.g., Farías et al., 2009). This is evidencing a decoupling between the deformation of the retro-arc and arc region during the event of slab shallowing and deepening, thus highlighting some concerns about the actual extent of the effects produced by the slab dynamics in the Andean evolution at these latitudes. In this context, this contribution addresses the question about the kinematic evolution of the arc-region in the scope of the actual extent of the extensional development reported in the retro-arc with respect to the contractional evolution that has characterized the late Cenozoic growth of the Andes.

In this context, this study focuses on determining the deformation that controls the Neogene to Quaternary evolution of the axial region of the Andes at 35°20'S. Our contribution mainly consists of new detailed field mapping and stratigraphic, structural, U/Pb age and apatite (U-Th)/He data. We focused particularly on a sedimentary unit corresponding to Neogene synorogenic deposits that record not only the erosional processes of the mountain belt but also constrain the timing of deformational events that affected this area and the source region related to the uplifted areas that supplied sediment to this basin. Our results show that the inner region of the mountain belt has been subjected to a continuous contractional regime from the middle Miocene to the Present, rather than the extensional setting inferred by previous studies. Furthermore, we discuss the deformation kinematics of the internal region of the Andean orogen and its differences with respect to the retro-arc region.

2 Tectonic setting of the southern Central Andes

The central Chile and Argentina region lies within the southern Central Andes, which are limited to north at ca. 33°S by the Pampean flat-slab segment (Fig. 1a). The Andean margin at these latitudes is characterized by the subduction of the oceanic Nazca plate beneath the South American continent (Fig. 1a) with a slab dip of ~30°E, corresponding to the typical example of the “Chilean-type subduction” in the sense of Uyeda and Kanamori (1979).

The southern Central Andes at the latitude of this work are segmented into four trench-parallel continental morphostructural units (Fig. 1b). From west to east, these are as follows: (1) the Coastal Cordillera, composed of Paleozoic metamorphic/crystalline basement and Jurassic-Cretaceous intrusive and volcanic rocks (Charrier et al., 2007); (2) the Central Depression, with a Quaternary volcano-sedimentary cover and a Mesozoic and Cenozoic basement (Farías et al., 2008); (3) the Principal Cordillera, consisting of Mesozoic and Cenozoic rocks (Charrier et al., 2007, Ramos, 2000a); and (4) the Foreland, composed of Neogene to Quaternary deposits that originated mainly by the erosion of the eastern Principal Cordillera and covering Mesozoic rift-related sedimentary rocks (Charrier et al., 2014). To the east, the Foreland is broken by the

uplifted Paleozoic-Triassic metamorphic/crystalline basement of the San Rafael Block (Fig. 1b) (González Díaz, 1972; Ramos et al., 2014 and references therein).

In this study, we subdivide the Principal Cordillera into a western and an eastern Principal Cordillera according to their geological and structural features. The western Principal Cordillera consists mostly of Cenozoic sequences (Fig. 1b) (Charrier et al., 2007). In contrast, the eastern Principal Cordillera is characterized by the exposure of Mesozoic sedimentary rocks covered by Cenozoic volcanic and sedimentary synorogenic deposits (Fig. 1b) (Ramos, 2000a and references therein). The boundary between the western and eastern Principal Cordillera is close to the axis of the Principal Cordillera and coincides with the current active volcanic arc and the Pacific-Atlantic watershed. This is the location of the study region (Fig. 1b).

The evolution of the southern Central Andes between 35° and 36°S comprises successive episodes of contractional, extensional and transcurrent deformation (e.g., Charrier et al., 2007, 2014; Ramos, 2000b). The last extensional event occurred between the Eocene and the late Oligocene along the western Principal Cordillera (Fig. 1b), forming the north-trending intra-arc extensional Abanico basin (Charrier et al., 1996, 2002; Godoy et al., 1999). This basin was filled with up to approximately 2,500 m of volcanic and volcanoclastic rocks with some fluvial and lacustrine deposits (Charrier et al., 2002). The basin-related deposits have been grouped into the Abanico Formation near Santiago and south of 35°S, the Coya-Machalí Formation between 34° and 35°S, and the Cura-Mallín Formation south of 36°S. Hereafter, these deposits will be referred as the Abanico Formation and the related basin as Abanico Basin. During the early Miocene, the basin began to be inverted in a process that concentrated most of shortening at its edges (Fock et al., 2006; Farías et al., 2010).

Following the initial stages of basin inversion, after ~18 Ma, deformation migrated eastwards, affecting the Mesozoic deposits that had accumulated in the Neuquén Basin (Fig. 1a), a back-arc basin formed during a widespread extensional tectonic event in South America (Charrier, 1979; Charrier et al., 2007; Mpodozis and Ramos, 1989; Uliana et al., 1989). The eastward migration of the deformation was characterized by the development of the hybrid thick- and thin-skinned Malargüe fold-and-thrust belt (Malargüe FTB) (Kozlowsky et al., 1993; Manceda and Figueroa, 1995) and subsequently by the uplift of the San Rafael Block (González Díaz, 1972). Simultaneously, the related-arc magmatism also expanded and migrated to the east up to 600 km from the current Pacific trench, reaching the San Rafael Block during the late Pliocene (Charrier et al., 2007; Kay et al., 2005; Litvak and Folguera, 2008; Ramos et al., 2014). During this Neogene contractional evolution, synorogenic deposits accumulated in the Río Grande foreland basin starting at ca. 18 Ma (Fig. 1b), which was cannibalized due to the progressive eastward migration of shortening (Silvestro and Atencio, 2009). The expansion of the magmatic arc and the eastward migration of the deformation front have been explained by crustal erosion caused by subduction (Kay et al., 2005) along with a shallowing of the subducted slab during the late Cenozoic (Ramos and Kay, 2006; Ramos et al., 2014; Spagnuolo et al., 2012).

In the Quaternary, the retro-arc region experienced an extensional event evidenced by normal faulting of the late Miocene uplifted peneplain that developed over the San Rafael Block (Folguera et al., 2008, 2007a, 2007b). This period was accompanied by basaltic volcanism

(Ramos and Folguera, 2011) and the development of huge calderas of rhyolitic to dacitic composition and subordinate basalts that were emplaced near the axis of the Cordillera during the last one million years (Grunder and Mahood, 1988; Grunder, 1987; Hildreth et al., 1984). The flood basalts of the retro-arc region have been interpreted as direct melts of the asthenosphere associated with the steepening of the subducted slab during the Quaternary (Kay et al., 2006). Likewise, the origin of rhyodacitic volcanic deposits near the axis of the Cordillera has been proposed to be the result of crustal delamination produced by the injection of asthenosphere during the steepening of the subducted slab (Ramos et al., 2014).

3 Geology of the study region

3.1 Generalities

The study region involves the eastern limit of the Abanico Formation and the westernmost outcrops of the Mesozoic series of the eastern Principal Cordillera (Fig. 1b). This zone coincides with a structural transition between the deformation that characterizes the domain of the Abanico Basin to the west and the Malargüe FTB to the east (Fig. 1b). Furthermore, the landscape of this zone is marked by the presence of Quaternary arc-related volcanic rocks forming a large plateau and edifices shaped by fluvial and glacial erosion and that discordantly overlie older geological units and structures.

To characterize the geology of this area, we performed geological mapping of outcropping rocks and structures, complemented with previously published and unpublished geological maps (Gonzalez and Vergara, 1962; Grunder, 1987; Grunder and Mahood, 1988; Grunder et al., 1987; Hildreth et al., 1984; Naranjo et al., 1999). This allowed the construction of a schematic cross section constrained by new chronological data (Fig. 6).

In relation to previous works, the regional map made by González and Vergara (1962) is the sole study of this type performed in the study region, even though certain local geothermal and volcanic studies have also been conducted in this region (Grunder, 1987; Hildreth et al., 1984; Naranjo et al., 1999; Naranjo and Haller, 2002). González and Vergara (1962) characterized the structure and described the stratigraphic units of the region at a 1:250,000 scale. When describing the Mesozoic series, the authors defined and named them with local names that differed from those used in the Argentinean and Chilean stratigraphic nomenclature. To avoid misunderstandings, we use the Argentinean nomenclature to compare and correlate the geology of both countries in this work.

3.2 Geological Units

The geology of the study region is displayed in the geologic map of Fig. 2a. The major stratigraphic units present in this area can be divided into four main associations: (1) the Mesozoic sediments of the Neuquén basin, which are subdivided into three main units, the Cuyo, Lotena and Mendoza groups; (2) the Abanico Formation; (3) the synorogenic deposits, here grouped into the Colorado Strata Unit; and (4) the Plio-Quaternary volcanic deposits. In addition, the zone features two main intrusive bodies of granodioritic to granitic composition of late

Miocene age. The nomenclature, lithology, age and tectonic setting of all these units are briefly described below, except for the synorogenic deposits, which are described later in Section 3.3.

The eastern area of the study region is mostly dominated by Mesozoic sedimentary series (Fig. 2a), which are associated with cycles of marine transgression and regression that occurred before the uplift of the Andean Cordillera. The oldest outcropping unit corresponds to the Cuyo Group (Sinemurian-Bajocian), which consists of off-shore shelf black shales grouped into the Tres Esquinas Formation and sandy fluvio-estuarine facies of the prograding Lajas Formation (Gulisano and Gutiérrez Pleimling, 1995). These two formations are separated by an erosional unconformity. The Cuyo Group is overlain by deltaic to shallow-marine clastic deposits belonging to the Lotena and the La Manga formations of Bajocian and Callovian ages, respectively. The gypsum layers of the Auquilco Formation (Oxfordian) overlie both formations. These formations make up the Lotena Group. The youngest Mesozoic unit is the Mendoza Group, composed of the red continental sandstones of the Tordillo Formation, the organic-rich deep-marine shaly marls of the Vaca Muerta Formation, and the shallow-marine limestones of the Chachao Formation.

In the western part of the study region, the Abanico Formation crops out (Fig. 2a) and is composed of a series of basic to intermediate volcanic-volcanoclastic rocks with intercalations of limestones, siltstones and very coarse- to fine-grained sandstones, as well as conglomerates with a significant volcanic component. Based on mammal fossil fauna and radiometric dating, the age of this formation north of the study region has been determined to be between the Eocene and the late Oligocene (Charrier et al., 2007, 2002, 1996; Godoy et al., 1999). This unit is discordantly covered by the volcanic Cola de Zorro Formation and a clastic synorogenic unit referred to here as the Colorado Strata Unit because of its excellent exposure along the homonymous valley.

The previous units are unconformably overlain by Plio-Quaternary arc-related volcanic rocks. We separated these volcanic rocks into three groups according to their age. In the western area, the Abanico Formation and the synorogenic deposits are covered by the almost undeformed basaltic-andesitic lava series of the Cola de Zorro Formation, which forms a large volcanic plateau emplaced over a low-relief surface now dissected by fluvial and glacial valleys. These rocks are distributed along the Colorado river valley and reach a maximum preserved thickness of 150 m. At 35.7°S, Drake (1976) reported an age span for this formation between 2.47 and 0.96 Ma. In the study region, an age obtained using the K-Ar method (whole-rock) is 2.02 ± 0.10 Ma near the base of the sequence (Fig. 2a) (Hildreth et al., 1984).

The second group of volcanic rocks corresponds to the deposits associated with the Peteroa-Azufre Volcano unit (Naranjo et al., 1999). This is the oldest unit of the Planchón Peteroa Volcanic Complex and consists of a series of basalts, basaltic-andesites, andesites and dacites cropping out along the northern slope of the Colorado river valley and farther north of the study area (Naranjo et al., 1999). The oldest and youngest reported K-Ar ages for this complex are 1.20 ± 0.03 Ma (Naranjo et al., 1999) and 0.55 ± 0.05 Ma (Hildreth et al., 1984), respectively, even though this complex records a series of historical eruptive events (Naranjo et al., 1999).

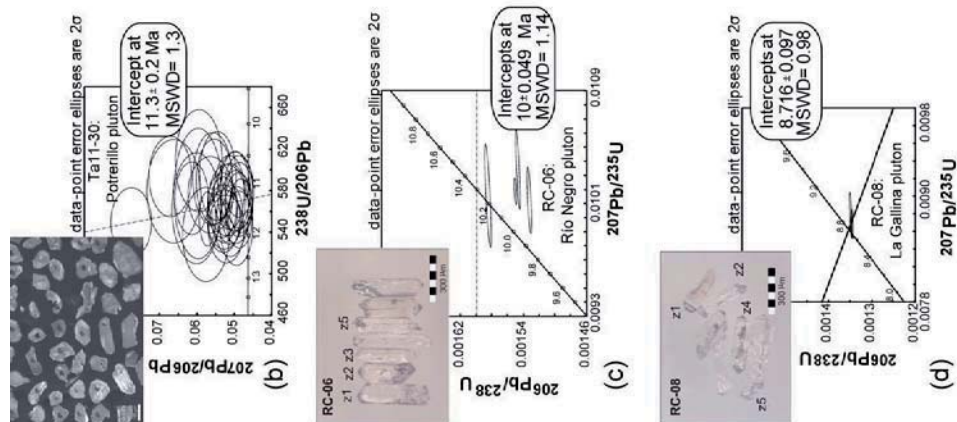
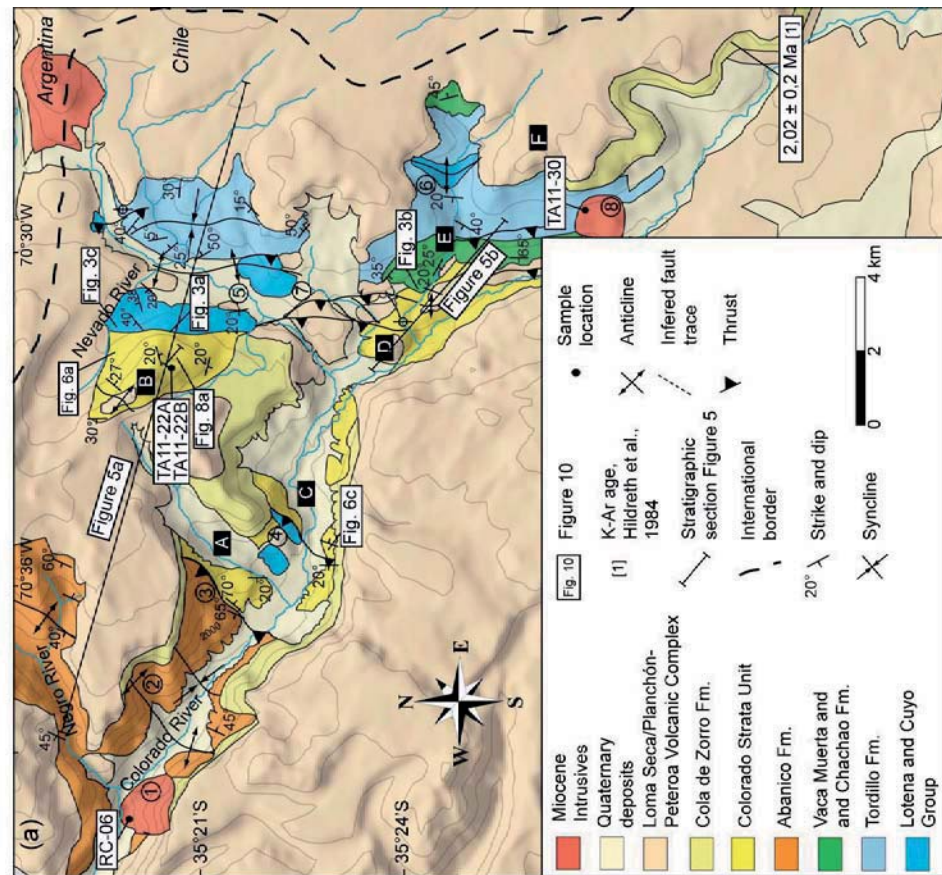


Figure 2: (a) Geological map of the study area. Circled numbers correspond to the following lithological and structural units: (1) Río Negro pluton; (2) Colorado anticline; (3) Novillo thrust; (4) Llollei thrust; (5) Valle Grande anticline; (6) Debia anticline; (7) Calabozos thrusts system; (8) Potrerillos pluton. Letters within black rectangles correspond to the following locations: (A) Novillo stream; (B) Cerro Las Yeguas; (C) Llollei; (D) Cerro El Pellejo; (E) Debia creek; (F) Cerro Negro. (b) Concordia diagrams for U-Pb determinations by LA-MC-ICP-MS for the Potrerillos pluton. (c) and (d) Concordia diagrams for U-Pb determinations by CA-TIMS for the Río Negro and La Gallina plutons. Ellipses for U-Pb data at $\pm 2\sigma$ error level.

The third volcanic group corresponds to the Loma Seca Formation (Grunder et al., 1987; Hildreth et al., 1984), which is distributed across almost the entire study region (Fig. 2a). The deposits are emplaced in deep paleovalleys excavated in the Mesozoic series and synorogenic deposits and form several volcanic plateau due to the high volume of erupted material. The formation consists of dacitic to rhyo-dacitic volcanic deposits derived from the eruption of 150 to 300 km³ of magma from the Calabozos caldera (Hildreth et al., 1984), which lies in the southeast sector of the study region (Fig. 2). The age of the Loma Seca Formation is constrained by K-Ar dating, yielding ages between 0.79 ± 0.15 and 0.14 ± 0.04 Ma (Hildreth et al., 1984), even though certain deposits were clearly emplaced after the last glacial event 4,400 years before the present (Espizua, 2005; Naranjo and Haller, 2002).

Two intrusive units that intruded Mesozoic and Cenozoic deformed rocks crop out in the area. In the eastern sector, the late Miocene Potrerillos pluton intrudes a Mesozoic series (Fig. 2a) and yields a zircon U/Pb age of 11.3 ± 0.20 Ma (error level at 2σ for all the ages reported in this study) obtained in this work (Fig. 2b; see Appendix A for the complete data set and analytical details). Given its petrological features and location, this pluton correlates with an intrusive body cropping out in the northeastern edge of the study region, near the international border (Fig. 2a). In the western sector, the Río Negro pluton intrudes the Abanico Formation (Fig. 2a) and yields a zircon U/Pb age of 10 ± 0.05 Ma, also determined in this study (zircon U-Pb age, Fig. 2c). Outside the study region, approximately 13 km west of the Río Negro pluton along the Colorado river valley, the La Gallina granodioritic pluton also intrudes the Abanico Formation, (Fig. 1c) and was also dated by this study, yielding a zircon U-Pb age of 8.688 ± 0.071 Ma (Fig. 2d). These plutons belong to the late Miocene intrusive belt (e.g., Farías et al., 2008; 2010) and evidence the magmatic activity in the western Principal Cordillera during the late Miocene.

3.3 The Colorado Strata Unit

The sedimentary strata grouped in the Colorado Strata Unit were deposited unconformably over the Mesozoic series (Fig. 3a). This unit crops out mostly in the central part of the study region (Fig. 2a). These sediments are unconformably overlain by Plio-Quaternary volcanic rocks (Fig. 3c), and the unit is limited to the west by the El Novillo thrust and to the east by the Valle Grande and Debia anticlines (Fig. 2a).

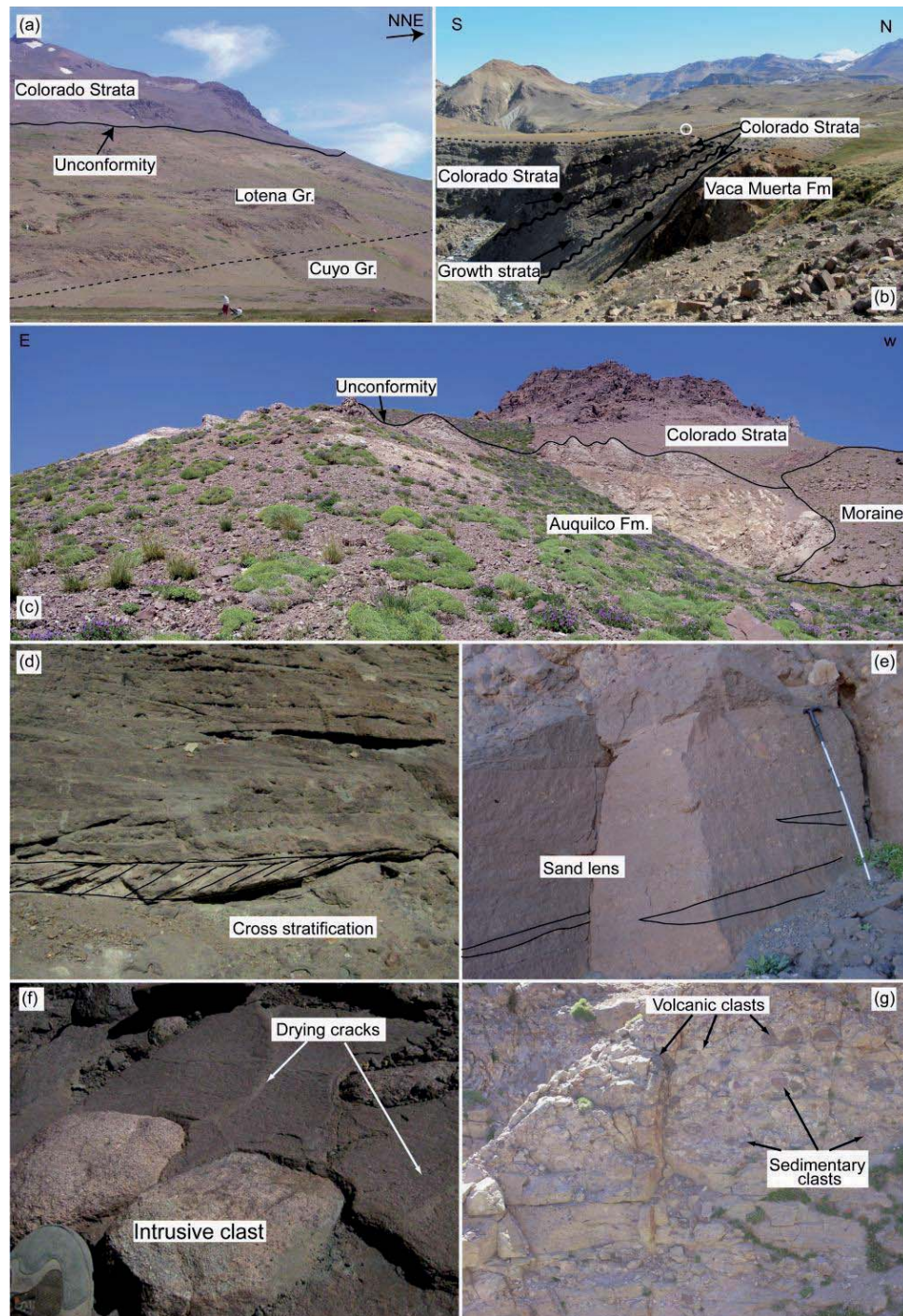


Figure 3: Features of the Colorado Strata Unit. (a) Unconformity between Mesozoic rocks and the synorogenic deposits of the Colorado Strata in the western slope of the Valle Grande valley. (b) Contact between the Colorado Strata and Vaca Muerta Formation in the Debia creek. The synorogenic deposits show growth strata. The white circle shows the scale. (c) Contact relationship between Auquilco Formation and Colorado Strata Unit in the northern slope of the Cerro Las Yeguas. (d) Cross stratification in sandstone. (e) Sand lens in a clast-supported conglomerate. (f) Intrusive clast and drying cracks in red siltstone of the synorogenic deposits. (g) Conglomerates with volcanic and sedimentary clasts. (See Figure 2a for location of the photographs).

The Colorado Strata Unit reaches up to 400 m in thickness. The conglomerates and sandstones that comprise this unit are moderate-to-poorly sorted, very coarse to medium grained and texturally and mineralogically immature. The conglomerate beds are 50 cm to 2 m thick and distributed in coalescent lenses, whereas sandstone beds are less than 1 m thick. The sandstones exhibit mostly planar stratification, even though they also show sedimentary structures such as cross stratification (Fig. 3d). The sandstones are also present as decametric lenses interbedded in the conglomerates, particularly between the conglomeratic coalescent lenses, and often exhibit lateral accretion (Fig. 3e).

Conglomerates are massively bedded, both clast and matrix supported, with some imbricated clasts levels, oligomictic, and with a predominance of volcanic and subordinate granitoid rock clasts (Figs. 3f and g). Paleocurrent measurements obtained from the eastern outcrops indicate a transport direction from the east (Fig. 3b).

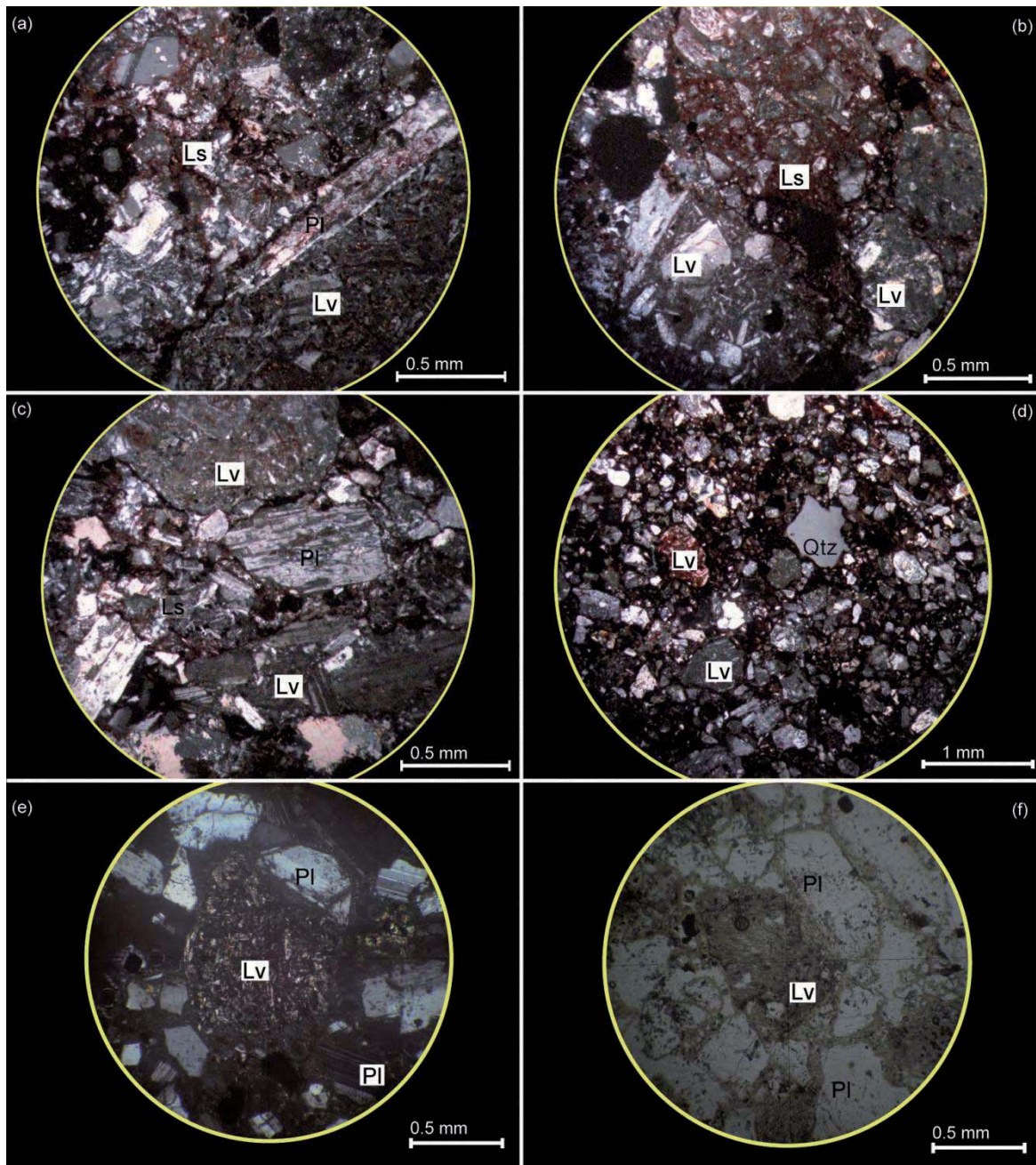


Figure 4. Photomicrographs of sandstones from different stratigraphic units of the study area. (a-c) Samples from the Colorado Strata Unit at the Cerro Las Yeguas of red sandstones with plagioclase feldspars and lithic fragments. (d) Red sandstone of the Tordillo Formation from the eastern limb of the Valle Grande anticline. (e-f) Sandstone of the Colorado Strata Unit in the Debia creek. Pl: plagioclase feldspars; Qtz: quartz; Lv: volcanic lithic; Ls: sedimentary lithic.

The conglomerate clasts are 10-40 cm in size, subangular to subrounded, and poorly sorted. The matrix features angular to subangular and poorly sorted grains and is mainly composed of feldspars and lithic fragments. The sandstones are lithic to feldspathic arenites composed of poorly sorted, immature, and coarse- to medium-grained sands. The major

constituents of the sandstones are lithic fragments and plagioclase feldspar (Fig. 4a). These lithic fragments are primarily volcanic fragments with porphyritic andesite and red sedimentary rock fragments (Figs. 4a, b, c, and e). The sedimentary fragments contain subrounded to rounded plagioclases and quartz in a red iron-oxide-rich matrix (Figs. 4a and b), very similar to the Tordillo Formation sandstones (Fig. 4d). The plagioclase feldspar components are coarse-grained, twined, and subhedral to euhedral altered crystals (Figs. 4a, c and e). The matrix of the sandstones corresponds to unidentifiable fragments altered to cryptocrystalline white mica and clay minerals (Figs. 4b and c).

The Colorado Strata Unit exhibits rotational onlaps, offlaps and apical wedges on the western flank of the Debia anticline (Fig. 2a and 3b). Because the sequence exhibits continuous cycles, without relevant vertical changes in bed thickness or facies, the change in dip is indicative of progressive unconformities in the growth strata. Based on the described features, this unit corresponds to synorogenic deposits.

According the described features of this unit, we interpret the depositional environment to have been an alluvial environment characterized by the successive deposition of debris flows and sandy sheet flows, with the ephemeral development of braided rivers in a proximal zone and lateral sand accretion on the conglomeratic bars. These features can be interpreted as the development of proximal alluvial fans with successive cyclic changes in transport energy. Given the observations made on this sequence in relation to the structures present in the area (Fig. 3b), the changes in transport energy may be a result of slope changes due to the activity of contractional structures.

3.4 Structure

To track the late Cenozoic evolution of the region, two WNW-ESE cross sections compile the structural features in the northern and central areas of the study region (Fig. 5). These sections are constrained only by surface geology for the shallow levels because of the absence of seismic and well data in the area. We describe the structures according to their relative timing with respect to the Colorado Strata Unit given the synorogenic nature of this unit.

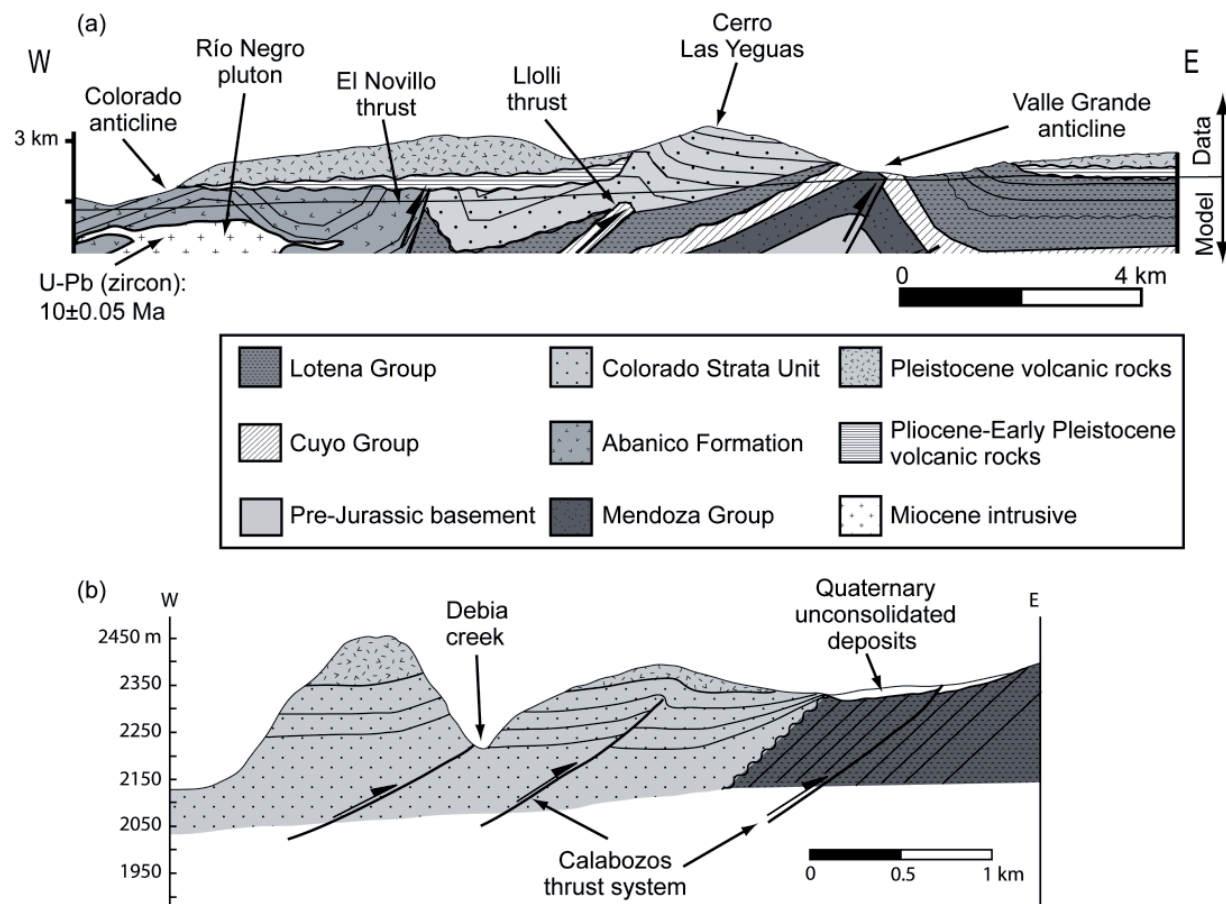


Figure 5. (a) Schematic structural cross-sections of the study area showing the main structural features described in the text (see Fig. 2a for location). (b) Structural cross-section along the Debía creek showing the details of the deformation associated with the Calabozos thrusts system

3.2.1 Pre- and syn-depositional structures

The western sector of the study region along the Colorado river is dominated by the development of the Colorado anticline, a high-amplitude east-vergent anticline involving the Abanico Formation (Fig. 5a). This structure has a half-wavelength of 5 km and front- and backlimb dips of 40°–50°E and 20°W, respectively. The core of the Colorado anticline hosts the Río Negro pluton (Fig. 5a). Although there is no direct evidence to determine the timing of activity of this structure, we infer that the Colorado anticline was formed during the inversion of the Abanico Basin after 20 Ma, given the age of deformation farther north (Charrier et al., 2002; Farías et al., 2010; Fock et al., 2006). This structure was likely active at 10 Ma due to the emplacement of the Río Negro pluton at its core, and ceased activity before the emplacement of the Cola de Zorro Formation at ca. 2.5 Ma.

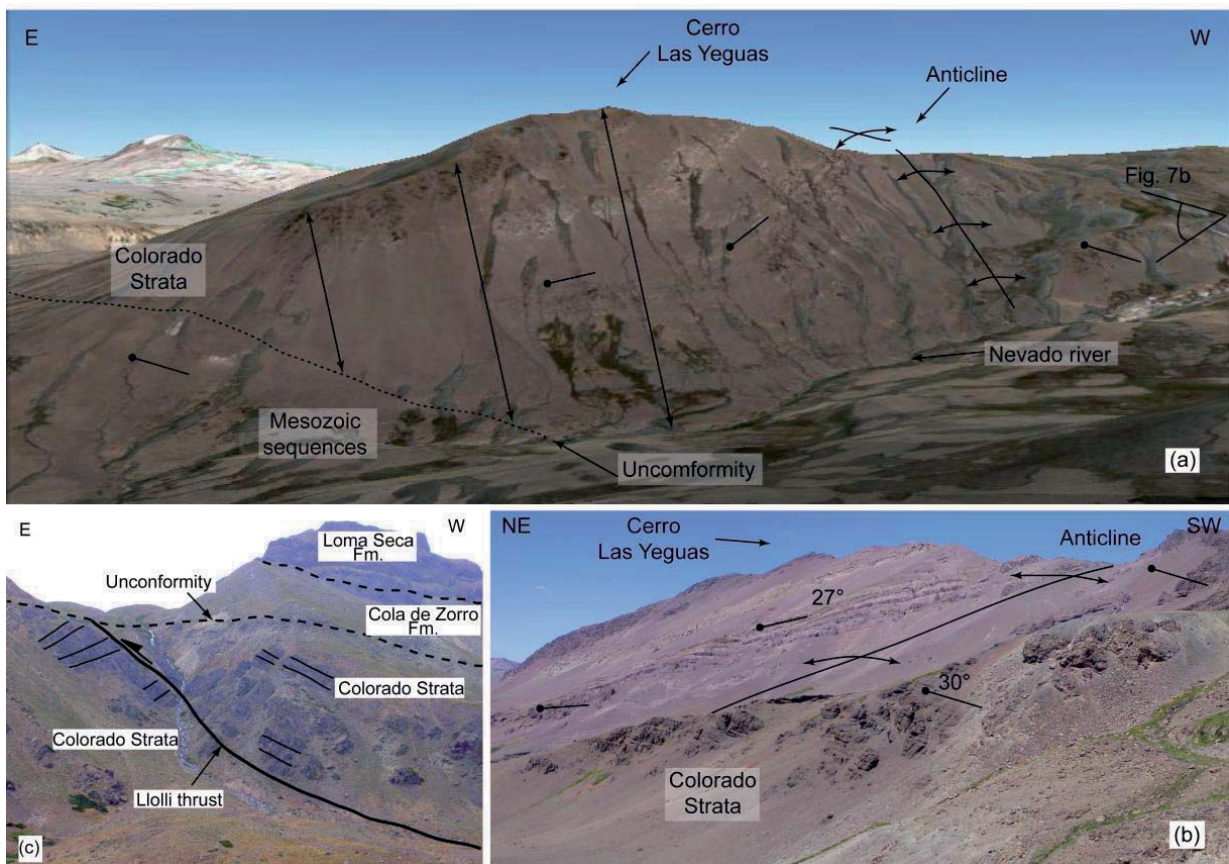


Figure 6. Geology of the Cerro Las Yeguas area. (a) Southward view of the disposition of the Colorado Strata Unit over the Mesozoic sequences. The double-head arrows show the western thickness growth of the synorogenic deposits. The image was taken from the Google Earth software. (b) Detailed view to west of the anticline along the Nevado river involving the synorogenic deposits. This fold is associated to the Llolli thrust deformation. (c) View to the southern slope of the Colorado river valley where the synorogenic deposits are repeated by the Llolli thrust. Unconformity over this thrust separates these deposits from the Neogene sedimentary rocks of the Cola de Zorro Formation.

Two N-S-trending anticlines, the Valle Grande and the Debia anticlines, control the contractional deformation in the eastern part of the region (Fig. 2a). The Valle Grande anticline is an east-vergent and asymmetric fold plunging to the north and south. This anticline involves the Cuyo and Lotena groups in its western limb and the Tordillo Formation in its eastern limb. It runs along the Valle Grande river valley, with a gently dipping backlimb (20° - 30° W) and a very steeply dipping forelimb (50° - 60° E), which is indicative of its east vergence (Fig. 5a). In the Cerro Las Yeguas area, the Colorado Strata Unit exhibits increasing thicknesses to the west (Figs. 6a and b), indicating that the accumulation zone was to the west, likely near the eastern front of the Colorado anticline. The angular unconformity between the synorogenic deposits and the back-limb of the Valle Grande anticline (Figs. 6a and b) indicates that the anticline began to develop before the synorogenic deposition. However, the lack of exposures of the base of the Colorado Strata Unit prohibits inferences of their relationship at the beginning of deposition. The

accumulation of the synorogenic deposits continued after the development of the angular unconformity observed in the Cerro Las Yeguas (Fig. 6a), as evidenced by progressive unconformities related to the westward growth strata.

Along Debia creek, the most important structural feature is the Debia anticline. It is a broad and symmetric structure plunging to the north, with a N-S strike and a 5 km-wide half-wavelength (Fig. 2a). It deforms Mesozoic strata with the gypsum layer of the Auquilco Formation in its core and the Tordillo, Vaca Muerta and Chachao Formations toward the limbs. Growth strata in the Colorado Strata Unit developed on the western flank of this anticline, indicating that deposition was simultaneous with the growth of the Debia anticline.

3.4.2 Post-depositional structures

Three main thrusts that continued to be active after the deposition of the Colorado Strata Unit characterize the study region. From west to east, they are named the El Novillo, Llolli and Calabozos thrust systems.

The El Novillo thrust corresponds to a NE-SW-trending structure that limits the Colorado Strata Unit to the east and the Abanico Formation to the west (Fig. 2a), putting the Abanico Formation over the synorogenic deposits (Fig. 5a). In the hanging wall of the El Novillo thrust, the Abanico Formation dips $\sim 60^{\circ}\text{W}$, whereas the Colorado Strata Unit in the footwall forms a tight syncline (Fig. 5a). In this area, the Colorado Strata Unit does not exhibit either growth strata or progressive unconformities. Thus, the deformation linked to this structure indicates that the El Novillo thrust was active after the deposition of the synorogenic deposits and before the deposition of the Pleistocene Cola de Zorro Formation.

The Llolli thrust is located immediately to the east of the El Novillo thrust (Figs. 2a and 5a). This structure cuts the synorogenic deposits, repeating the Colorado strata in the southern slope of the Colorado river (Fig. 6c). In the Cerro Las Yeguas locality, the Llolli thrust only folds the synorogenic deposits (Figs. 6a and b). This structure ends below undeformed Pleistocene volcanic rocks (Fig. 6c); thus, its activity is constrained between the deposition of the Colorado Strata Unit and the Pleistocene.

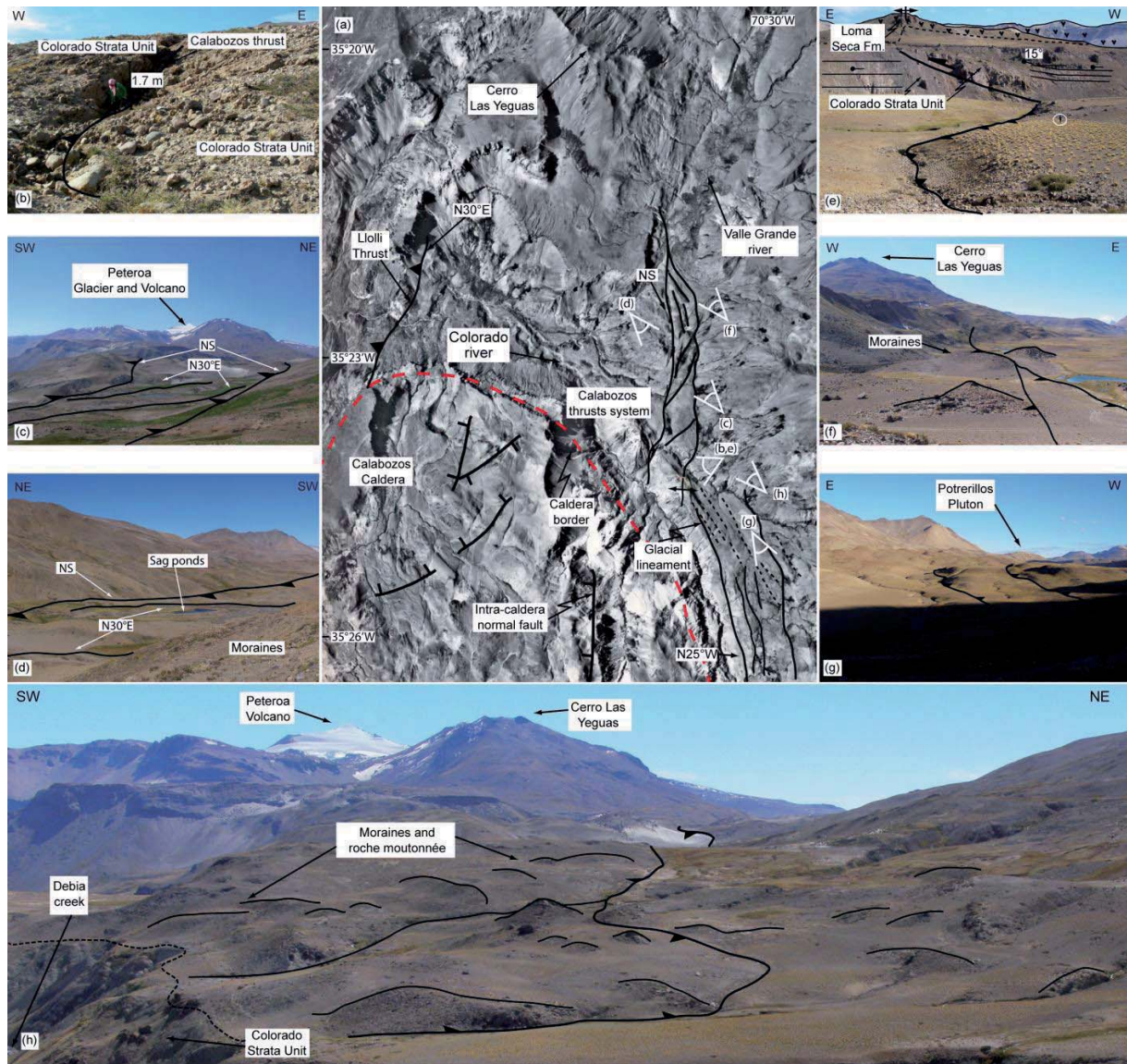


Figure 7. Main deformational features in the synorogenic deposits. (a) Aerial photograph showing the main traces of the Calabozos thrusts system, the eastern border of the Calabozos Caldera and location of the pictures in Figures 8b-8h. (b) Scarp associated with the Calabozos thrusts system in the Debia creek area. (c) NS trending main faults and related on echelon faults of the Calabozos thrusts system. (d) South view of the structural arrangement of the Calabozos thrusts along the sag pond developed between the N30°E trending echelon faults. (e) Deformation along the Debia creek showing the anticline formed by the Calabozos thrusts system. The white circle shows the scale. (f) Northern segment of the Calabozos thrusts system where only one branch can be recognized. (g) Quaternary unconsolidated deposits with reverse offset produced by the southern segment of the Calabozos thrusts system. (h) North view of the reverse main fault of the Calabozos thrusts system affecting moraines and *roches moutonnées* in the northern slope of the Debia creek.

The third post-depositional structure is the Calabozos thrust system (Fig. 2a). This structural system corresponds to east-vergent, low-angle reverse faults with three main branches striking approximately N-S dipping ca. 30°W (Fig. 5b and 7a), with a central branch extending

along 9 km long from the toe of the Cerro Las Yeguas in the Valle Grande area to near the Potrerillos pluton to the south (Fig. 7a). The thrust is best exposed in the Debia Creek. In this zone, the western branch ends to the south and a new branch appears to the east extending to the south (Fig. 7a). Here, the system presents its maximal surface separation of about 1.2 km. north and south of this area, the separation diminish to 300-500 m. The central branch at this creek develops a ~200 m width tectonic breccia that includes rocks of the Loma Seca Formation (Fig. 7b and e). Between central and eastern branches, the Colorado Strata Unit developed growth strata during deposition in a syncline (Fig. 3b). North of the Debia Creek to Valle Grande, the thrust consists of two well-developed branches offsetting the Loma Seca Formation, hillslope-related deposits, and glacier-related deposits and landforms (Figs. 7b, c, d, e, f and h). Here, the thrust produces a ~20 m scarp in both moraines and “roches moutonnées” (Fig. 7h), and has led to the development of sag ponds and disturbances in the river network (Figs. 7c and d). To the north, the offset decreases and disappears in the Valle Grande valley, where several relict scarps and breccias are observed (Fig. 7f). Here, only western branch of the thrust can be recognized. This branch can be observed up to the western slope of Valle Grande valley, where a fault breccia aligned with the trace of the fault described to the south is evidence of its northern extent. Considering the units deformed by the Calabozos thrusts system, it can be concluded that this fault has been active at least since the deposition of the Colorado Strata Unit.

4 Analytical constraints on the deformational and erosional evolution

4.1 U/Pb ages of the Colorado Strata Unit

Two samples located at the top of the Colorado Strata were collected (Fig. 8a) and dated via the zircon U-Pb method (LA-MC-ICP-MS). The analyzed samples correspond to a boulder-sized granite fragment from a conglomerate level (Fig. 8d) (sample TA11-22A) and the sandy levels surrounding the granitic boulder from the upper section of the Colorado Strata in Cerro Las Yeguas (Figs. 5a and b) (TA11-22B sample). The sample location appears in Fig. 2b, and the complete description of analytical methods and the results of the U-Pb geochronological determinations are provided in Appendix B.

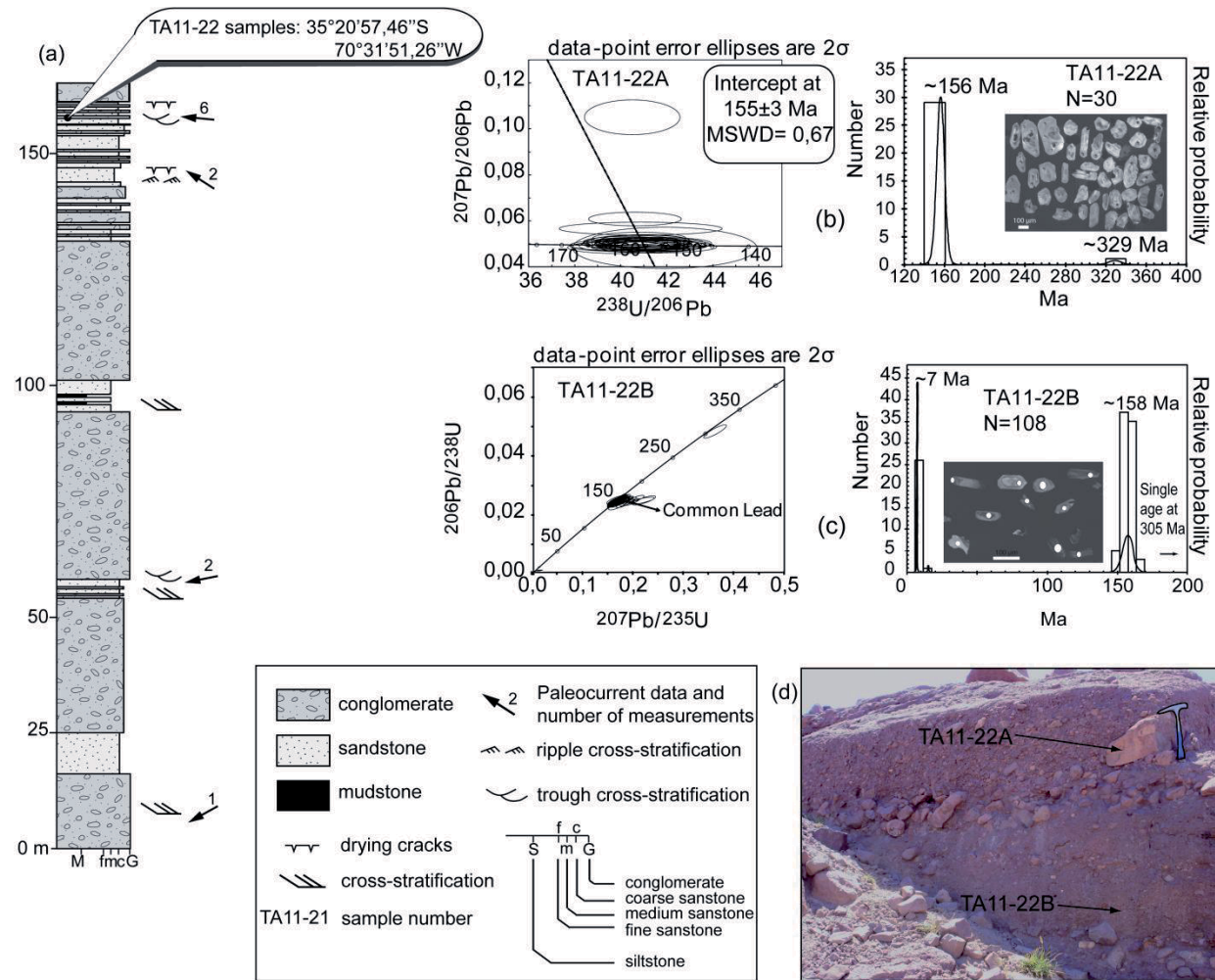


Figure 8. (a) Partial stratigraphic section of the Colorado Strata Unit at the Cerro Las Yeguas showing the main stratigraphic and sedimentary characteristics (See Figure 2a for location). Diagrams of Concordia (left) and frequency histogram and relative probability (right) for the zircon U-Pb age determinations of samples TA11-22A (b) and TA11-22B (c). Cathodoluminescence images of representative zircons are also shown as inset in the right diagrams. (d) Field photograph of the conglomerate and sandstone layers where the TA11-22A and TA11-22B samples were collected.

For the sandstone sample TA11-22B, 108 detrital zircons provide a pattern of detrital zircon U/Pb ages that constrain the maximum depositional age. The results show a spectra of concordant ages between ca. 6.8 Ma and ca. 305 Ma (Fig. 8c), bimodal maximum peaks at ca. 158 Ma (74%; ages between ca. 149.9 Ma and 166.6 Ma) and ca. 7 Ma (24%; ages between ca. 6.8 Ma and 7.9 Ma); and two single ages at ca. 305 Ma (Middle Pennsylvanian) and ca. 15 Ma (early Miocene). The maximum peak at ca. 7 Ma is the youngest and therefore corresponds the maximum depositional age of the upper section of the Colorado Strata (Fig. 8c).

For the sample TA11-22A, 30 analyzed zircon grains were used to determine the crystallization age of the granitic intrusive clast (Fig. 8b). The sample's results show a concordia age at 155.3 ± 3 Ma for 29 zircons (Fig. 8b) and a single age at 329.3 ± 6 Ma (Fig. 8b).

4.2 Apatite (U/Th/He) ages

Additionally, we obtained three apatite (U/Th)-He ages from rocks situated west of the Colorado Strata Unit to test the effects of exhumation of the western region during the evolution of the synorogenic unit as well as to better constrain its depositional age. Samples were taken along the Colorado river valley bottom from the Abanico Formation, the Río Negro pluton and the La Gallina pluton at approximately 1, 6 and 21 km west of the El Novillo thrust, respectively (Table 1, see Fig. 1c for location and Appendix C for details of the (U/Th)-He analytical methods and data).

Table 1. Apatite U/Th-He from rocks west of the El Novillo thrust along the valley bottom of the Colorado river

Sample	Unit	Latitude (°S)	Longitude (°W)		Corrected apatite U/Th-He Age [Ma] ± 2σ
RC05	Abanico Fm. tuff	35.36	70.62°	Mean weight age	1.18 ± 0.71
					0.26 ± 1.21
					1.70 ± 0.41
					1.47 ± 0.12
RC06	Río Negro pluton	35.33	70.68°	Mean weight age	3.96 ± 0.13
					3.74 ± 0.10
					3.83 ± 0.01
RC08	La Gallina pluton	35.31	70.83	Mean weight age	3.82 ± 0.12
					3.81 ± 0.70
					3.82 ± 0.01

The results show that the plutons west of the El Novillo thrust were exhumed at ca. 3.8 Ma, whereas the Abanico Formation immediately west of this thrust were exhumed at ca. 1.5 Ma. The apatite (U/Th)-He ages obtained from the plutonic rocks indicate the cooling of plutonic rocks produced by exhumation because their crystallization ages are approximately 8 million years older. These exhumation ages are slightly older than the beginning of the deposition of the Cola de Zorro Formation, which was deposited unconformably over the Colorado Strata Unit and older units, sealing the activity related to the El Novillo thrust. Therefore, the thermochronologic ages of the plutonic rocks record the erosion in response to the uplift of the Colorado anticline and structures farther west. Because the deposition of the Cola de Zorro Formation sealed the end of activity of the El Novillo thrust, the youngest age in the Abanico Formation should be related to the valley development that preceded the deposition of the Loma Seca Formation in paleovalleys starting at 0.9 Ma.

5 Discussion

5.1 Sedimentary source of the synorogenic deposits

The boulder-sized granite fragment dated to ca. 155 Ma (sample TA11-22A) and the Upper Jurassic zircon age population in the sandy sample (TA11-22B) suggest a derivation from Upper Jurassic granites extensively exposed along the present-day Coastal Cordillera (Fig. 1b).

However, the western flank of the Principal Cordillera, to the west of the study area, uplifted during the early Miocene and reactivated during the late Miocene (Fariás et al., 2010, 2008). This would have prevented sedimentary input from the Coastal Cordillera, even though the eastern domains of the Abanico Formation, particularly from the Colorado anticline to the El Novillo thrust, could have corresponded to a clastic source of the Colorado Strata Unit.

We propose that the main source for this age population is the Upper Jurassic Tordillo Formation (Río Damas Formation in Chile), which is widely exposed throughout the study region (see Fig. 1b). In fact, the petrographic descriptions of the sandstones and conglomerates of the Colorado Strata Unit reveal red sedimentary clasts and lithics similar to the petrography of the Tordillo Formation (Fig. 4d). These observations suggest that the Tordillo Formation was proximal to the basin and constituted the main source of the Upper Jurassic zircon population in the Colorado Strata.

Another possibility for the source of the analyzed granitic boulder could be recycling of either the Abanico Formation or the Neuquén Group (and their equivalents in Chile). The latter was deposited during the Late Cretaceous contractional deformation that led to the evolution of the back-arc Neuquén Basin into a foreland basin (Cobbold and Rossello, 2003; Di Giulio et al., 2012; Ramos and Folguera, 2005; Tunik et al., 2010). However, the Neuquén Group usually exhibits U/Pb zircon ages from the Upper Cretaceous (Di Giulio et al., 2012; Tunik et al., 2010; Willner et al., 2005), which are not observed in the analyzed sandy sample from the Colorado Strata Unit.

Likewise, the absence of U/Pb zircon ages in the synorogenic unit corresponding to the age of the Abanico Formation suggests discarding this unit as a source. Nevertheless, the clastic composition of the synorogenic deposits is very similar to the volcanic composition of the Abanico Formation. Moreover, the Abanico Formation usually lacks of zircon grains given its predominantly tholeiitic composition. Furthermore, based on studies performed farther north (Charrier et al., 2009 and references therein) and the crystallization and cooling ages of the La Gallina and Río Negro plutons, the deformation in the Abanico Formation is constrained between approximately 20 and 3 Ma, i.e., younger than the maximum depositional age of the Colorado Strata Unit. Therefore, the Abanico Formation was likely a clastic source to the synorogenic deposits despite the lack of zircon U/Pb ages belonging to the range of ages of this unit.

The provenance of the minor Miocene zircon population (ca. 7 Ma) of the upper section of the synorogenic deposits could be derived from volcanic rocks such as those identified in the eastern part of the study region and farther east, with ages spanning between ca. 17 and 5 Ma (Combina and Nullo, 2011; Silvestro and Kraemer, 2005). The westward growth strata observed in the Colorado Strata Unit also support a source from the east. Nevertheless, the Río Negro pluton, situated in the core of the Colorado Anticline a few kilometers west of the El Novillo thrust (Fig. 5a) is likely a source because its U/Pb zircon ages approximate this Miocene population despite the younger apatite U/Th-He ages obtained (ca. 3.8 Ma). The exhumation of these plutons may have begun earlier than the timing indicated by their apatite U/Th-He ages due to the low temperatures recorded by this thermochronometer.

Therefore, the Colorado Strata Unit was sourced mainly from the east and likely sourced from the Abanico Formation and the Río Negro pluton due to the activity of the Colorado Anticline and El Novillo thrust. There is no evidence for a relevant sedimentary input from either the western Principal Cordillera or farther west from the Coastal Cordillera. It is unlikely that incipient rivers west of the Colorado Anticline drained from the west to the basin. In contrast, it is likely that incipient rivers passed through the western Principal Cordillera draining to the west, as occurs at the present. In this scenario, the watershed could have been located farther to the east of the Debia and Valley Grande Anticlines, most likely east of the present-day drainage divide.

To summarize, the structural configuration in relation to the Colorado Strata Unit and the temporal relationship of deformation and deposition reveal that the synorogenic deposits developed in a basin enclosed by the Colorado anticline to the west and the Debia anticline to the east, forming a piggy-back basin system.

5.2 Synthesis of the Cenozoic evolution of the axial region and regional comparisons

Our results allow us to reconstruct the local evolution from the Miocene to the Present, which can be expanded to the north up to 35°S, where deposits with similar ages to the Colorado Strata Unit have been reported (González, 2008, Mosolf et al., 2011).

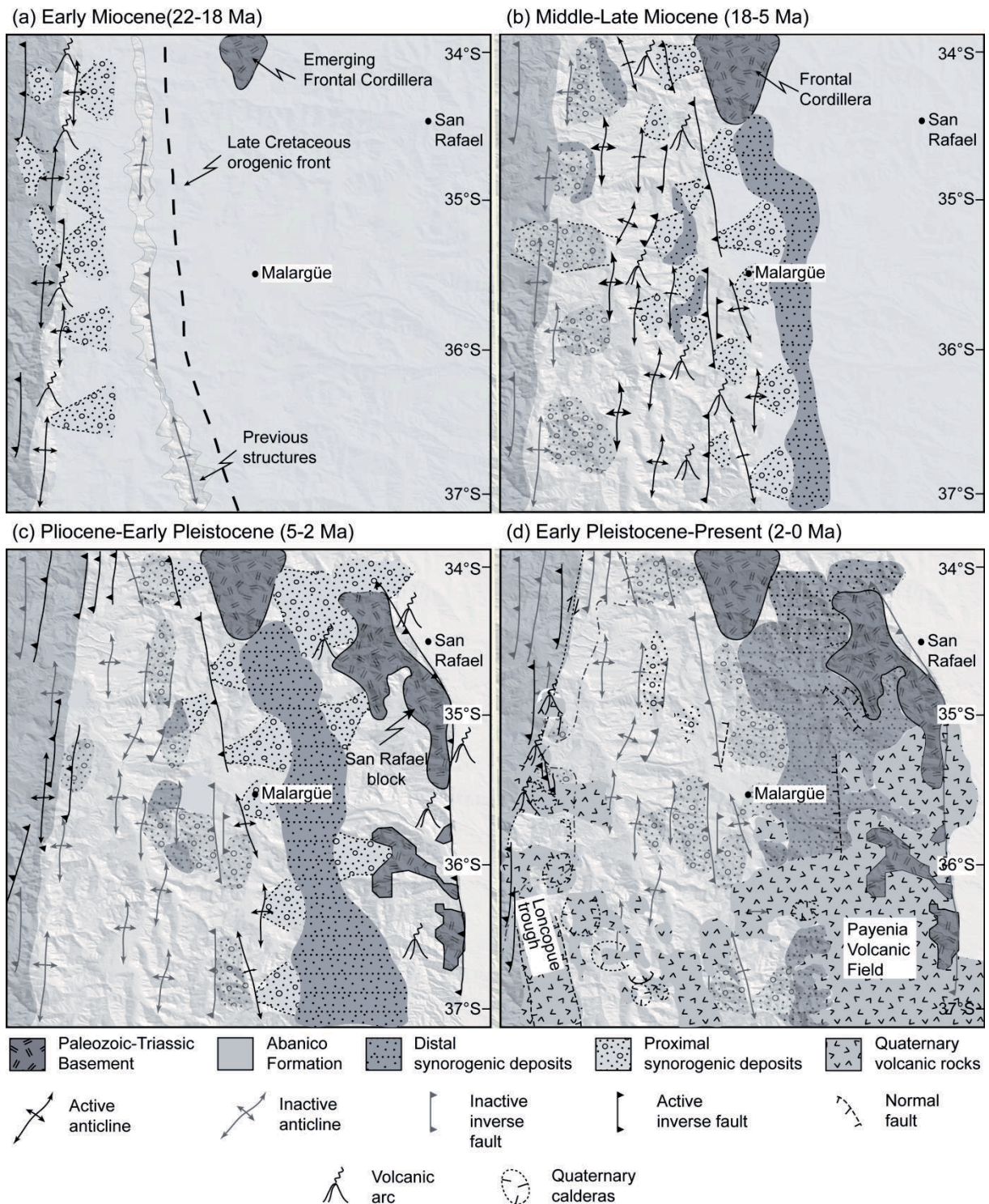


Figure 9. Interpretative maps summarizing the evolution across the Andean region between 34° and 37° S. The evolution between 34° and 35° S is based in Giambiagi et al., (2003) and Godoy et al., (1999). The cities of Malargüe and San Rafael are given for references. (a) Deformation and erosion of the western Principal Cordillera and western portion of Malargüe FTB. The synorogenic deposits were accumulated in front or between the growing structures. The previous Late Cretaceous orogenic front

would have acted as an eastern barrier for the sediments. The volcanic arc was located in the western Principal Cordillera. (b) Complete development of the Malargüe FTB due to the eastern migration of the deformation. The volcanism also migrated and expended toward the eastern Principal Cordillera. During this period the Frontal Cordillera was uplifted. (c) Maximum eastern expansion of the deformation and volcanism. . The deformation was located around of the Malargüe and San Rafael cities area along with the axial region of the Cordillera. This stage corresponds to the main uplift episode of both western Principal Cordillera and San Rafael block. The arc volcanic was around the San Rafael block. (d) Return of the related-arc volcanism to western Principal Cordillera. Moreover, extensional tectonic dominated the foreland along with the eruption of greater basalt flow which built the Payenia Volcanic Field. Toward the west a serie of calderas were formed while the shortening continued in the region.

Contractional deformation started in the western Principal Cordillera during the early Miocene with the inversion of the Abanico Basin and the onset of deformation along the western edge of the Malargüe FTB, represented by the Colorado, Valle Grande and Debia anticlines in the study region (Fig. 9a). Along with this evolution, the Colorado Strata Unit basin likely began to be filled during the first contractional event in the early Miocene, as evidenced by the growth strata that developed at the base of the sequence associated with the growth of the Debia anticline (Fig. 9a).

Following the in-sequence contractional deformation evolution proposed for this Andean region (Kozlowsky et al., 1993; Manceda and Figueroa, 1995; Silvestro and Kraemer, 2005), shortening has occurred in the Malargüe FTB since ca. 18-16 Ma (Fig. 9b) (cf. Mescua et al., 2014). Subsequently, several depocenters accumulated synorogenic sediments that were progressively deformed as shortening migrated to the east (Silvestro and Atencio, 2009; Silvestro and Kraemer, 2005). Although we do not have analytical evidence supporting this hypothesis during this stage, deposition continued in the Colorado Basin, and it is very likely that the erosion of the uplifting eastern zones supplied the sediments to this depocenter.

Between the late Miocene and the early Pleistocene, deformation was characterized by the development of both out-of-sequence and in-sequence thrusting that occurred simultaneously in the internal and external regions of the Andean orogen, respectively (Fig. 9c). In the axial region of the Principal Cordillera, thrusting and folding were associated with structures such as the El Novillo and Llolli thrusts, as well as the Calabozos thrust system, which deformed the synorogenic deposits and tilted the Abanico Formation to the west (Fig. 9c). This evolution, with the exception of the Calabozos thrust system, ended with the deposition of the Cola de Zorro Formation, which sealed the deformed sequences. However, the in-sequence thrusting is associated with the maximum expansion of the deformation toward the foreland, producing the uplift of the San Rafael Block and the broken foreland (Fig. 9c) (see Ramos et al., 2014). The origin of the out-of-sequence deformation and its implications are discussed in the next section.

The out-of-sequence thrusting episode was followed by the emplacement of the volcanic arc and the construction of the Peteroa-Azufre stratovolcano and Calabozos caldera (Fig. 9d), indicating the beginning of the current volcanic arc along the southern Central Andes. Thereafter, the shortening became concentrated in the internal zone to the south of the study region, as

evidenced by faults such as the Calabozos thrusts system and the development of the Guañacos fold-and-thrust belt farther south (Folguera et al., 2006a). In contrast, the retro-arc region has experienced extensional tectonics since the Early Pleistocene, and extension controlled the structural array and location of the volcanic centers that erupted the large basaltic flows of the Payenia volcanic field (Fig. 9d).

5.3 Kinematics context of the inner mountain belt.

The study area, particularly the Calabozos caldera, has been described as the northernmost tip of the NNW-trending extensional Las Loicas Trough, which has been proposed to have developed during the steepening of the subducting slab in the Quaternary after a period of slab shallowing during the Miocene (Folguera et al., 2008; Ramos et al., 2014). However, field observations made in our study area show that there is no evidence of normal faulting in the area, with the exception of several minor, local-scale normal faults in the core of volcanic edifices belonging to the Calabozos caldera (Fig. 1c) (Grunder and Mahood, 1988; Grunder, 1987; Grunder et al., 1987; Hildreth et al., 1984). Therefore, the region does not exhibit evidence for extending the extensional Las Loicas Trough to the current arc region.

In contrast, we observe an almost continuous contractional setting from the late Miocene to the present in this zone. Therefore, extensional tectonics did not affect the arc region during the Quaternary, but the area was affected by across-strike shortening. Several studies have noted that the tectonic regime of the axial zone of this part of the Southern Central Andes has been mainly transcurrent based on seismological focal mechanisms aligned with the regional El Fierro Thrust System (Fig. 1b) (e.g., Farías et al., 2010; Spagnuotto et al., 2014, Giamabiagi et al., 2014). In contrast, finite deformation estimates based on kinematic modeling of GPS data indicate shortening parallel to the plate convergence vector (~N78°E, see Fig. 1a and b) for the Southern Central Andes (cf., Métois et al., 2012; and reference therein).

The apparent disagreement between GPS-based kinematic models and seismological focal mechanisms can be explained by the high obliquity (45-50°) between the plate convergence vector and the El Fierro Thrust System with recorded strike-slip earthquakes (Fig. 1b). In contrast, structures more orthogonal to the plate convergence vector will favor shortening rather than strike-slip.

Nevertheless, shortening in the axis of the belt can only be achieved when vertical stress related to the height and weight of the mountain belt is less than the horizontal stress, as proposed for other zones of the Andes (e.g., Dalmayrac and Molnar, 1981; Farías et al., 2005; 2010). In this way, shortening related to the out-of-sequence thrusting in the study region is likely related to both the high orthogonality of the structural systems with respect to the plate convergence vector and to the minor resistance to shortening produced by the minor height of the mountain belt and the removal of material via erosion of the uplifted mountain belt. The former suggests strain partitioning in the axial zone in this part of the Andean Cordillera.

Likewise, the tectonic setting proposed here for the current axial region differs from the extensional setting that the retro-arc experienced during the subduction slab steepening stage (Ramos et al., 2014 and references therein). This observation also suggests strain partitioning between the axial zone with respect to the eastern mountain belt and foreland. In this way, shortening, strike-slip and extension could coexist in this part of the Andes.

Beyond the objective of this study, the origin of the strain partitioning between strike-slip/shortening in the axial region and the extensional setting in the retro-arc can be addressed to the effects of the shallowing and steepening of the subducting plate proposed for this Andean region during the latest Cenozoic (Kay et al., 2006; Ramos and Kay 2006). This type of process would produce changes in the thermal structure of the lithosphere, thus affecting the deformation behavior of the overriding plate (Gutscher, 2002). Along this line, we infer that these thermal changes during slab steepening produced different effects in the arc and retro-arc regions due to the differences in the rheology, lithospheric thickness, crustal structure, etc. However, further work is necessary to demonstrate this hypothesis. At a minimum, the extensional deformation did not affect the current axial/arc region at 35°30'S, as previously extrapolated to this region.

5.4 Out-of-sequence thrusting in the Southern Central Andes

Out-of-sequence thrusting in the inner parts of mountain belts has been widely documented in orogenic systems worldwide, including the southern Central Andes. In fact, north of the study region, out-of-sequence thrusting in the mountain belt ended by the Pliocene in the Aconcagua fold-and-thrust belt (33°-34°S) (Giambiagi and Ramos, 2002; Giambiagi et al., 2003). Only transcurrent deformation has occurred since then in the axial zone (Fariás et al., 2010, Giambiagi et al., 2014). In contrast, south of the study region, the Guañacos fold-and-thrust belt (37°S) experienced contractional deformation that began in the late Miocene and has continued until the Present (Folguera et al., 2006a). Thus, a regional-scale out-of-sequence event began during the late Miocene in the southern Central Andes. This event ended first north of the study region and has continued to the Present south of 35°S.

The origin of out-of-sequence events can be approached from the Coulomb wedge model (Davis et al., 1983), where out-of-sequence thrusting is an integral part of the formation of thrust belts because it maintains the critical wedge taper (Morley, 1988). Out-of-sequence thrusting in the wedge model can be triggered by the loss of the taper, which can be caused by either erosion, the elongation of the wedge through foreland propagation of the thrust belt or local obstacles that impede the propagation of in-sequence thrusts (Morley, 1988). Additionally, an increase in the friction along the taper may also produce out-of-sequence thrusting (Dahlen et al., 1984; Davis et al., 1983).

The late Miocene out-of-sequence thrusting event that affected the southern Central Andes was concurrent with large-magnitude rates of surface uplift between, at least, 33° and 35°S, which can be directly related to a coeval increase in shortening rates (cf. Giambiagi et al., 2003; 2014; Fariás et al., 2008; 2010). Furthermore, an increase in the regional slope of the mountain range produced by surface uplift would enhance material discharge from the orogen by

increasing erosional rates, a process that will also favor the development of out-of-sequence thrusts. Thus, the triggering of out-of-sequence thrusting in the southern Central Andes can be ascribed to the increasing shortening rates, but this process was undoubtedly also favored by mass transfer out from the mountain belt by erosion.

An increase in shortening rates may be a result of an increase in friction along the interplate contact due to the subduction of a more buoyant heterogeneity on the subducting slab. Along this line, Folguera and Ramos (2009) proposed the subduction of an oceanic rise related to the Mocha Fracture Zone beginning in the late Pliocene to explain a Pliocene-Pleistocene out-of-sequence thrusting event between 36 and 38°S. However, the beginning of the out-of-sequence thrusting event reported in our study began at least in the late Miocene, that is, approximately coeval with thrusting to the north to 33° (e.g., Giambiagi et al., 2003; Farías et al., 2010) and farther south in the Guañacos fold-and-thrust belt between 37°S and 37°30'S (Folguera et al., 2006a; Rojas Vera et al., 2014). Hence, the out-of-sequence thrusting event was a regional event in the southern Central Andes, extending along more than 500 km between 33° and 37°30'S. In addition, it began in the late Miocene, preceding the collision of the oceanic high proposed by Folguera and Ramos (2009). Therefore, it is unlikely that this oceanic feature controlled this thrusting event, even though it could have affected the thrusting in the Guañacos fold-and-thrust belt until the early Pleistocene. Therefore, another mechanism must be responsible for this event.

Therefore, considering the likely role of erosion on the development of out-of-sequence thrusting, such a mechanism indirectly implies a control exerted by climate. In fact, this would be the case when considering the fact that the out-of-sequence thrusting lasted longer in the south of the mountain belt than in the north. South of 33°S, precipitation rates increase significantly, the effects of mountain glaciations in the range become progressively larger, and there is a southward increase in long-term erosion rates (Carretier et al., 2014, 2012; Farías et al., 2008; 2012). To the south, the more intense erosion is a more efficient mechanism for sustaining the development of out-of-sequence thrusts through time.

6 Summary and Conclusions

The structural, sedimentological and geochronological studies in this portion of the arc in the southern Central Andes allow us to demonstrate that this region has experienced contractional deformation from at least the late Miocene to the Present. This deformation was characterized by the development of a piggy-back basin in the latest Miocene. Afterward, the region experienced shortening associated with an out-of-sequence thrusting event that affected the inner part of the Malargüe FTB from the Pliocene until the Present.

The southward increases in the rates of precipitation and erosion are a likely, efficient mechanism for material removal from the steepest zone of the orogen, which triggered the out-of-sequence thrusting in the internal region of the Andes Cordillera. More intense erosion and subsequent out-of-sequence thrusting illustrate the feedback between the surface processes and tectonics present along the southern Central Andes.

Acknowledgements

This research was supported by the FONDECYT grants 1120272 and 11085022. F. Tapia's doctoral study at the Universidad de Chile has been supported by Doctoral CONICYT Scholarship. This study was also supported by the Institute de Recherche pour le Développement (IRD-France). We thank R. Charrier, S. Calderón, J. Valenzuela and J. Cortés for field support. M. P. Rodríguez and S. Brichau are thanked for the numerous useful discussions regarding the geology of the Andes. The authors kindly thank M. Muñoz for detailed review and constructive comments.

References

- Carretier, S., Regard, V., Vassallo, R., Aguilar, G., Martinod, J., Riquelme, R., Pepin, E., Charrier, R., Herala, G., Farías, M., Guyot, J.-L., Vargas, G., Lagane, C., 2012. Slope and climate variability control of erosion in the Andes of central Chile. *Geology* 41, 195–198.
- Carretier, S., Tolorza, V., Rodríguez, M.P., Pepin, E., Aguilar, G., Regard, V., Martinod, J., Riquelme, R., Bonnet, S., Brichau, S., Herala, G., Pinto, L., Farías, M., Charrier, R., Guyot, J.L., 2014. Erosion in the Chilean Andes between 27 S and 39 S: tectonic, climatic and geomorphic control. *Geol. Soc. London, Spec. Publ.* 399. doi: 10.1144/SP399.16
- Charrier, R., 1979. El Triásico de Chile y regiones adyacentes en Argentina: Una reconstrucción paleogeográfica y paleoclimática. *Comunicaciones* 26, 1–47.
- Charrier, R., Wyss, A.R., Flynn, J.J., Swisher III, C.C., Norell, M.A., Zapatta, F., Mckenna, M.C., Novacek, M.J., 1996. New evidence for Late Mesozoic-Early Cenozoic evolution of the Central Chile. *J. South Am. Earth Sci.* 9, 393–422.
- Charrier, R., Baeza, O., Elgueta, S., Flynn, J., Gans, P., Kay, S., Muñoz, N., Wyss, A., Zurita, E., 2002. Evidence for Cenozoic extensional basin development and tectonic inversion south of the flat-slab segment, southern Central Andes, Chile (33°–36°S.L.). *J. South Am. Earth Sci.* 15, 117–139.
- Charrier, R., Pinto, L., Rodríguez, M.P., 2007. Tectonostratigraphic evolution of the Andean Orogen in Chile, in: Moreno, T., Gibbons, W. (Eds.), *The Andes of Chile*. Geological Society of London, pp. 21–114.
- Charrier, R., Farías, M., Maksaev, V., 2009. Evolución tectónica, paleogeográfica y metalogénica durante el Cenozoico en los Andes de Chile norte y central e implicaciones para las regiones adyacentes de Bolivia y Argentina. *Rev. Asoc. Geológica Argentina* 65, 5–35.
- Charrier, R., Ramos, V. A., Tapia, F., Sagripanti, L., 2014. Tectono-stratigraphic evolution of the Andean Orogen between 31 and 37 S (Chile and Western Argentina). *Geol. Soc. London, Spec. Publ* 399, doi: 10.1144/SP399.20

- Cobbold, P., Rossello, E., 2003. Aptian to recent compressional deformation, foothills of the Neuquén Basin, Argentina. *Mar. Pet. Geol.* 20, 429–443.
- Combina, A.M., Nullo, F., 2011. Ciclos tectónicos, volcánicos y sedimentarios del Cenozoico del sur de Mendoza-Argentina (35°-37°S y 69°30'W). *Andean Geol.* 38, 198–218.
- Dahlen, F. A., Suppe, J., Davis, D., 1984. Mechanics of fold-and-thrust belts and accretionary wedges: Cohesive Coulomb Theory. *J. Geophys. Res.* 89, 10087.
- Dalmayrac, B., Molnar, P., 1981. Parallel thrust and normal faulting in Peru and constraints on the state of stress. *Earth Planet. Sci. Lett.* 55, 473–481.
- Davis, D., Suppe, J., Dahlen, F.A., 1983. Mechanics of fold-and-thrust belts and accretionary wedges. *J. Geophys. Res. Solid Earth* 88, 1153–1172.
- Di Giulio, A., Ronchi, A., Sanfilippo, A., Tiepolo, M., Pimentel, M., Ramos, V. A., 2012. Detrital zircon provenance from the Neuquén Basin (south-central Andes): Cretaceous geodynamic evolution and sedimentary response in a retroarc-foreland basin. *Geology* 40, 559–562.
- Drake, R.E., 1976. Chronology of cenozoic igneous and tectonic events in the central Chilean Andes — latitudes 35° 30' to 36°S. *J. Volcanol. Geotherm. Res.* 1, 265–284.
- Espizúa, L.E., 2005. Holocene glacier chronology of Valenzuela Valley, Mendoza Andes, Argentina. *The Holocene* 15, 1079–1085.
- Farías, M., Charrier, R., Comte, D., Martinod, J., Héral, G., 2005. Late Cenozoic deformation and uplift of the western flank of the Altiplano: Evidence from the depositional, tectonic, and geomorphologic evolution and shallow seismic activity (northern Chile at 19°30'S). *Tectonics* 24, TC4001.
- Farías, M., Charrier, R., Carretier, S., Martinod, J., Fock, A., Campbell, D., Cáceres, J., Comte, D., 2008. Late Miocene high and rapid surface uplift and its erosional response in the Andes of central Chile (33°-35°S). *Tectonics* 27, doi:10.1029/2006TC002046.
- Farías, M., Tapia, F., Comte, D., 2009. La Falla Calabozos: Un cabalgamiento activo en la alta cordillera de Curicó, in: XII Congreso Geológico Chileno. Santiago, Chile, electronic abstract.
- Farías, M., Comte, D., Charrier, R., Martinod, J., David, C., Tassara, A., Tapia, F., Fock, A., 2010. Crustal-scale structural architecture in central Chile based on seismicity and surface geology: Implications for Andean mountain building. *Tectonics* 29. doi:10.1029/2009TC002480.
- Farías, M., Charrier, R., Carretier, S., Tapia, F., Astaburuaga, D., Puratich, J., Rodríguez, M.P., Urresty, C., Garrido, G., 2012. Contribución de largo-plazo de la segmentación climática en

Chile Central a la construcción Andina, in: XIII Congreso Geológico Chileno. Antofagasta, Chile, pp. 191–193.

Fock, A., Charrier, R., Farías, M., Muñoz, M.A., 2006. Fallas de vergencia oeste en la Cordillera Principal de Chile Central: Inversión de la cuenca de Abanico (33° - 34° S), in: Hongn, F., Becchio, R., Seggiario, R (Eds), XII Reunión sobre microtectónica y geología estructural. Rev. Asoc. Geológica Argentina, Serie D, Publicación Especial 6, 48-55.

Folguera, A., Ramos, V. A., 2009. Collision of the Mocha fracture zone and a <4 Ma old wave of orogenic uplift in the Andes (36 -38 S). *Lithosphere* 1, 364–369.

Folguera, A., Ramos, V. A., Hermanns, R.L., Naranjo, J., 2004. Neotectonics in the foothills of the southernmost central Andes (37° - 38° S): Evidence of strike-slip displacement along the Antiñir-Copahue fault zone. *Tectonics* 23, doi: 10.1029/2003TC001533.

Folguera, A., Ramos, V.A., González Díaz, E.F., Hermanns, R., 2006a. Miocene to Quaternary deformation of the Guañacos fold-and-thrust belt in the Neuquén Andes between 37° S and $37^{\circ}30'$ S. in: Kay, S.M., Ramos, V.A. (Eds.), Evolution of an Andean Margin: A Tectonic and Magmatic View from the Andes to the Neuquén Basin (35° - 39° S Lat). *Geol. Soc. Am. Spec. Pap.* 407, 247–266.

Folguera, A., Zapata, T., Ramos, V.A., 2006b. Late Cenozoic extension and the evolution of the Neuquén Andes, in: Kay, S.M., Ramos, V.A. (Eds.), Evolution of an Andean Margin: A Tectonic and Magmatic View from the Andes to the Neuquén Basin (35° - 39° S Lat). *Geological Society of America, Special Papers* 407, pp. 267–285.

Folguera, A., Introcaso, A., Giménez, M., Ruiz, F., Martínez, P., Tunstall, C., García Morabito, E., Ramos, V. A., 2007a. Crustal attenuation in the Southern Andean retroarc (38° - $39^{\circ}30'$ S) determined from tectonic and gravimetric studies: The Lonco-Luán asthenospheric anomaly. *Tectonophysics* 439, 129–147.

Folguera, A., Ramos, V. A., Zapata, T., Spagnuolo, M.G., 2007b. Andean evolution at the Guañacos and Chos Malal fold and thrust belts ($36^{\circ}30'$ - 37° S). *J. Geodyn.* 44, 129–148.

Folguera, A., Bottesi, G., Zapata, T., Ramos, V. A., 2008. Crustal collapse in the Andean backarc since 2 Ma: Tromen volcanic plateau, Southern Central Andes ($36^{\circ}40'$ - $37^{\circ}30'$ S). *Tectonophysics* 459, 140–160.

Folguera, A., Naranjo, J.A., Orihashi, Y., Sumino, H., Nagao, K., Polanco, E., Ramos, V.A., 2009. Retroarc volcanism in the northern San Rafael Block (34 degrees-35 degrees 30' S), southern Central Andes: Occurrence, age, and tectonic setting. *J. Volcanol. Geotherm. Res.* 186, 169–185.

- Folguera, A., Rojas Vera, E., Bottesi, G., Zamora Valcarce, G., Ramos, V. A., 2010. The Loncopué Trough: A Cenozoic basin produced by extension in the southern Central Andes. *J. Geodyn.* 49, 287–295.
- Folguera, A., Orts, D., Spagnuolo, M., Vera, E.R., Litvak, V., Sagripanti, L., Ramos, M.E., Ramos, V.A., 2011. A review of Late Cretaceous to Quaternary palaeogeography of the southern Andes. *Biol. J. Linn. Soc.* 103, 250–268.
- Folguera, A., Alasonati Tašárová, Z., Götze, H.-J., Rojas Vera, E., Giménez, M., Ramos, V. A., 2012. Retroarc extension in the last 6 Ma in the South-Central Andes (36°S–40°S) evaluated through a 3-D gravity modelling. *J. South Am. Earth Sci.* 40, 23–37.
- García Morabito, E., Folguera, A., 2005. El alto de Copahue-Pino Hachado y la fosa de Loncopué: un comportamiento tectónico episódico, Andes neuquinos (37°-39°S). *Rev. Asoc. Geológica Argentina* 60, 742–761.
- Giambiagi, L., Ramos, V.A., 2002. Structural evolution of the Andes in a transitional zone between flat and normal subduction (33°30'–33°45'S), Argentina and Chile. *J. South Am. Earth Sci.* 15, 101–116.
- Giambiagi, L., Ramos, V.A., Godoy, E., Alvarez, P.P., Orts, S., 2003. Cenozoic deformation and tectonic style of the Andes, between 33 degrees and 34 degrees south latitude. *Tectonics* 22, 1041.
- Giambiagi, L.B., Bechis, F., Garcia, V., Clark, A.H., 2008. Temporal and spatial relationships of thick- and thin-skinned deformation: A case study from the Malargüe fold-and-thrust belt, southern Central Andes. *Tectonophysics* 459, 123–139.
- Giambiagi, L., Ghiglione, M., Cristallini, E., Bottesi, G., 2009. Kinematic models of basement/cover interaction: Insights from the Malargüe fold and thrust belt, Mendoza, Argentina. *J. Struct. Geol.* 31, 1443–1457.
- Giambiagi, L.B., Tassara, A., Mescua, J., Tunik, M., Alvarez, P.P., Godoy, E., Hoke, G.D., Pinto, L., Spagnotto, S., Porras, H., Tapia, F., Jara, P., Bechis, F., Garcia, V.H., Suriano, J., Moreiras, S.M., Pagano, S.D., 2014. Evolution of shallow and deep structures along the Maipo-Tunuyán transect (33°–40°S): from the Pacific coast to the Andean foreland, in: Sepúlveda, S. A., Giambiagi, L. B., Moreiras, S. M., Pinto, L., Tunik, M., Hoke, G. D., Farías, M. (Eds), *Geodynamic Processes in the Andes of Central Chile and Argentina*. Geol. Soc. London, Spec. Publ. 399.
- Godoy, E., Yáñez, G., Vera, E., 1999. Inversion of an Oligocene volcano-tectonic basin and uplifting of its superimposed Miocene magmatic arc in the Chilean Central Andes: First seismic and gravity evidences. *Tectonophysics* 306, 217–236.

- González, A., 2008. Análisis estructural entre los valles del río Tinguiririca y Teno, Cordillera Principal de Chile Central: Microsismosidad y Geología Superficial. Unpublished thesis. Universidad de Chile.
- González Díaz, E.F., 1972. Descripción Geológica de la Hoja 27d, San Rafael, Provincia de Mendoza. Serv. Geológico Min. Argentino. Boletín 132, 1–127.
- González, O., Vergara, M., 1962. Reconocimiento geológico de la Cordillera de los Andes entre los paralelos 35° y 38° S. Inst. Investig. Geológicas 1.
- Grunder, A.L., 1987. Low $\delta^{18}\text{O}$ silicic volcanic rocks at the Calabozos caldera complex, southern Andes. Contrib. to Mineral. Petrol. 95, 71–81.
- Grunder, A.L., Thompson, J.M., Hildreth, W., 1987. The hydrothermal system of the Calabozos caldera, central Chilean Andes. J. Volcanol. Geotherm. Res. 32, 287–298.
- Grunder, A.L., Mahood, G.A., 1988. Physical and chemical models of zoned silicic magmas. The Loma Seca Tuff and Calabozos Caldera, southern Andes. J. Petrol. 29, 831–867.
- Gulisano, C., Gutiérrez Pleimling, A.R., 1995. The Jurassic of the Neuquén Basin: Mendoza Province. Guía de Campo, in: Asociación Geológica Argentina, Special Publication, Vol. 159. Argentina. p. 103.
- Gutscher, M.-A., 2002. Andean subduction styles and their effect on thermal structure and interplate coupling. J. South Am. Earth Sci. 15, 3–10.
- Hildreth, W., Grunder, A., Drake, R., 1984. The Loma Seca Tuff and the Calabozos caldera: A major ash-flow and caldera complex in the southern Andes of central Chile. Geol. Soc. Am. Bull. 95, 45–54.
- Kay, S.M., Godoy, E., Kurtz, A., 2005. Episodic arc migration, crustal thickening, subduction erosion, and magmatism in the south-central Andes. Geol. Soc. Am. Bull. 117, 67.
- Kay, S. M., Burns, M., Copeland, P., 2006. Upper Cretaceous to Holocene Magmatism over the Neuquén basin: evidence for transient shallowing of the subduction zone under the Neuquén Andes (36°S to 38°S latitude), in: Kay, S. M., and Ramos, V. A. (Eds.), Evolution of an Andean margin: A tectonic and magmatic view from the Andes to the Neuquén Basin (35°S-39°S lat): Geological Society of America Special Papers 407. pp.19-60.
- Kozlowsky, E., Manceda, R., Ramos, V.A., 1993. Estructura, in: Ramos, V.A. (Ed.), Geología y Recursos Naturales de La Provincia de Mendoza. Relatorio del XII Congreso Geológico Argentino. Mendoza, pp. 235–256.
- Litvak, V.D., Folguera, A., 2008. Determination of an arc-related signature in Late Miocene volcanism over the San Rafael Block, Southern Central Andes (34°30'–37°S) Argentina: the

Payenia shallow subducting zone, in: 7° International Symposium on Andean Geodynamics. Niza, pp. 289–291.

Manceda, R., Figueroa, D., 1995. Inversion of the Mesozoic Neuquén Rift in the Malargüe Fold and Thrust Belt, Mendoza, Argentina, in: Tankard, A.J., Suárez S., R., Welsink, H.J. (Eds.), Petroleum Basin of South America. AAPG Memoir 62, pp. 369–382.

Mescua, J.F., Giambiagi, L.B., Tassara, A., Gimenez, M., Ramos, V.A., 2014. Influence of pre-Andean history over Cenozoic foreland deformation: Structural styles in the Malargüe fold-and-thrust belt at 35 S, Andes of Argentina. *Geosphere* 1–25.

Métois, M., Socquet, a., Vigny, C., 2012. Interseismic coupling, segmentation and mechanical behavior of the central Chile subduction zone. *J. Geophys. Res. Solid Earth* 117.

Morley, C.K., 1988. Out-of-Sequence Thrusts. *Tectonics* 7, 539–561.

Mosolf, J.G., Gans, P.B., Wyss, A.R., Cottle, J.M., 2011. Detailed geologic field mapping and radiometric dating of the Abanico Formation in the Principal Cordillera, central Chile: Evidence of protracted volcanism and implications for Cenozoic tectonics, in: AGU Fall Meeting Abstracts. p. abstract #V13C–2623.

Mpodozis, C., Ramos, V.A., 1989. The Andes of Chile and Argentina, in: Erickson, G.E. (Ed.), *Geology of the Andes and Its Relation to Hydrocarbon and Mineral Resources*. Earth Sci. Ser, pp. 59–90.

Naranjo, J., Haller, M., 2002. Erupciones holocenas principalmente explosivas del volcán Planchón, Andes del sur (35°15'S). *Rev. geológica Chile* 29, 93–113.

Naranjo, J., Haller, M., Osteria, H., Pesce, A.H., Sruoga, P., 1999. Geología y peligros del Complejo Volcánico Planchón-Peteroa, Andes del Sur (35°15'S), Región del Maule, Chile-Provincia de Mendoza, Argentina. *Serv. Nac. Geol. y Minería, Bol.* 52, 55p.

Pose, F.A., Spagnuolo, M.G., Folguera, A., 2005. Modelo para la variación del volumen orogénico andino y acortamientos en el sector 20°–46°S. *Rev. Asoc. Geológica Argentina* 60, 724–730.

Ramos, V.A., 2000a. Las Provincias Geológicas del Territorio Argentino, in: Caminos, R. (Ed.), *Geología Argentina*. Instituto de Geología y Recursos Minerales, *Anales* 29(3), pp. 41–96.

Ramos, V.A., 2000b. The Southern Central Andes, in: Cordani, U.G., Milani, E.J., Thomas Philo, A., Campos, A. (Eds.), *Tectonic Evolution of South America*. 31° International Geological Congress, Rio de Janeiro, Río de Janeiro, pp. 561–604.

Ramos, V.A., Folguera, A., 2005. Tectonic evolution of the Andes of Neuquén: constraints derived from the magmatic arc and foreland deformation, in: Veiga, G., Spalletti, J., Howell, J.,

Schwarz, E., (Eds), The Neuquén Basin: A case study in sequence stratigraphy and basin dynamics. Geol. Soc. London, Spec. Publ. 252, 15–35.

Ramos, V.A., Kay, S.M., 2006. Overview of the tectonic evolution of the southern Central Andes of Mendoza and Neuquén (35°–39°S latitude), in: Kay, S.M., Ramos, V.A. (Eds.), Evolution of an Andean Margin: A Tectonic and Magmatic View from the Andes to the Neuquén Basin (35°–39°S Lat). Geological Society of America Special Papers 407. pp. 1–17.

Ramos, V.A., Folguera, A., 2011. Payenia volcanic province in the Southern Andes: An appraisal of an exceptional Quaternary tectonic setting. J. Volcanol. Geotherm. Res. 201, 53–64.

Ramos, V. A., Litvak, V.D., Folguera, A., Spagnuolo, M., 2014. An Andean tectonic cycle: From crustal thickening to extension in a thin crust (34°–37°SL). Geosci. Front. 1–17. Rojas Vera, E. a., Folguera, A., Zamora Valcarce, G., Bottesi, G., Ramos, V. a., 2014. Structure and development of the Andean system between 36° and 39°S. J. Geodyn. 73, 34–52.

Rojas Vera, E.A., Folguera, A., Valcarce, G.Z., Giménez, M., Ruiz, F., Martínez, P., Bottesi, G., Ramos, V.A., 2010. Neogene to Quaternary extensional reactivation of a fold and thrust belt: The Agrio belt in the Southern Central Andes and its relation to the Loncopué trough (38°–39°S). Tectonophysics 492, 279–294.

Servicio Geológico Minero Argentino, 1997. Mapa geológico de la República Argentina, escala 1:2.500.000, Buenos Aires, Argentina.

Servicio Nacional de Geología y Minería, 2002. Mapa geológico de Chile, escala 1:1.000.000, Mapa M61.

Silvestro, J., Kraemer, P., 2005. Evolución de las cuencas sinorogénicas de la Cordillera Principal entre 35°-36° S, Malargüe. Rev. Asoc. Geológica Argentina 60, 627–643.

Silvestro, J., Atencio, M., 2009. La cuenca cenozoica del río Grande y Palauco: edad, evolución y control estructural, faja plegada de Malargüe. Rev. Asoc. Geológica Argentina 65, 154–169.

Spagnuolo, M.G., Litvak, V.D., Folguera, A., Bottesi, G., Ramos, V.A., 2012. Neogene magmatic expansion and mountain building processes in the southern Central Andes, 36–37°S, Argentina. J. Geodyn. 53, 81–94.

Spagnotto, S., Nacif, S., Yacante, G., Giambiagi, L.B., 2014. Sismo Mw=6.0 del 7 de Junio del 2012 y aftershocks en las inmediaciones del Complejo Volcánico San Pedro-Pellado, Linares, Chile, in: XIX Congreso Geológico Argentino. Córdoba.

Tassara, A., 2005. Interaction between the Nazca and South American plates and formation of the Altiplano–Puna plateau: Review of a flexural analysis along the Andean margin (15°–34°S). Tectonophysics 399, 39–57.

- Tassara, A., Echaurren, A., 2012. Anatomy of the Andean subduction zone: three-dimensional density model upgraded and compared against global-scale models. *Geophys. J. Int.* 189, 161–168.
- Tunik, M., Folguera, A., Naipauer, M., Pimentel, M., Ramos, V.A., 2010. Early uplift and orogenic deformation in the Neuquén Basin: Constraints on the Andean uplift from U–Pb and Hf isotopic data of detrital zircons. *Tectonophysics* 489, 258–273.
- Uliana, M.A., Biddle, J., Cerdan, J.J., 1989. Mesozoic Extension and the Formation of Argentine Sedimentary Basins, in: Tankard, A.J., Balkwill, H.R. (Eds.), *Extensional Tectonics and Stratigraphy of the North Atlantic Margins*, vol.46. AAPG Memoir 46, pp. 599–614.
- Uyeda, S., Kanamori, H., 1979. Back-arc opening and the mode of subduction. *J. Geophys. Res.* 84, 1049.
- Willner, A.P., Thomson, S.N., Kröner, A., Wartho, J.-A., Wijbrans, J.A., Hervé, F., 2005. Time Markers for the Evolution and Exhumation History of a Late Palaeozoic Paired Metamorphic Belt in North–Central Chile (34° – $35^{\circ}30'S$). *J. Petrol.* 46, 1835–1858.

CAPÍTULO V.

LA CONSTRUCCIÓN DEL ORÓGENO ANDINO: SÍNTESIS Y DISCUSIÓN

V.1 Evolución estructural de los Andes a 35°S

Los resultados mostrados en este trabajo indican que la construcción de los Andes entre 34°45' y 35°S habría ocurrido fundamentalmente durante el Neógeno, consistente con lo reportado para la región inmediatamente al norte (Farías et al., 2010, 2008; Fock, 2005; Fock et al., 2006). La evolución neógena de este segmento andino estuvo altamente controlada por las estructuras y evolución mesozoica y paleógena de la corteza continental, tal como se detalló en los capítulos anteriores. Cabe mencionar que la evolución paleozoica, e incluso anterior, también pudo haber ejercido algún control sobre los períodos de deformación posteriores. Sin embargo, los escasos afloramientos de rocas paleozoicas impiden una detallada caracterización de la evolución pre-mesozoica a lo largo del área de estudio, impidiendo determinar cualitativa y cuantitativamente el control que pudo haber ejercido.

La deformación habría comenzado en torno a 20 Ma (Fig. V. 1a) en la parte este de la Cordillera Principal occidental (Fig. V. 1b y c) y continuado hasta al menos los 11 Ma, de acuerdo con la edad de los estratos sinorogénicos reconocidos en este estudio. En este sentido, de acuerdo a las edades, ubicación y características entre los depósitos del miembro inferior de la Formación Farellones en el área del cerro Alto del Padre y de la Unidad Estratos del Colorado en el sector de Valle Grande se puede establecer la correlación entre ellos, aún cuando ambas unidades se habrían depositado en depocentros distintos.

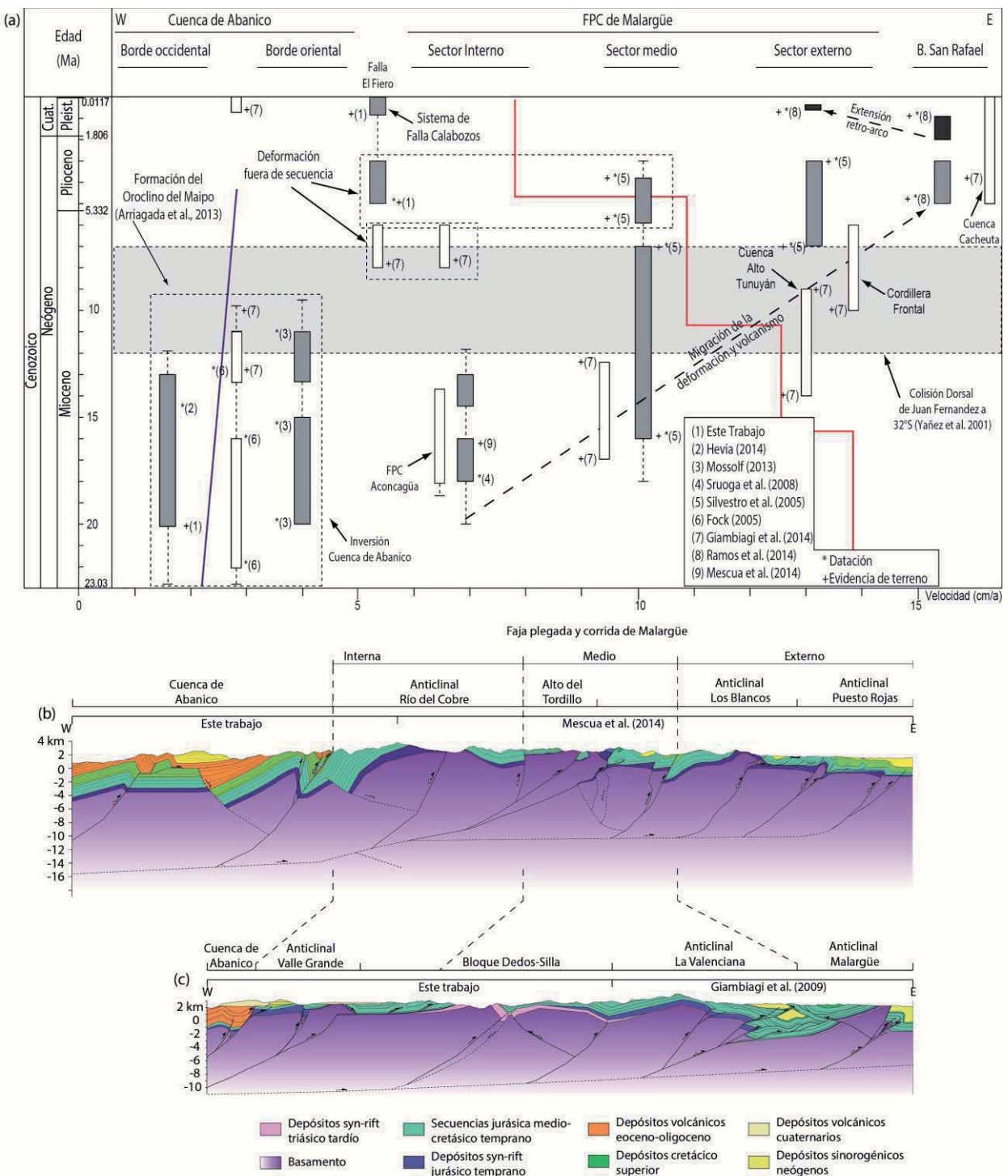


Fig. V.1. (a) Cuadro comparativo de la evolución neógena de los Andes de Chile central y el oeste de Argentina. Los rectángulos grises indican el periodo de inicio y término de la deformación de la zona del orógeno a 35°S. Los rectángulos blancos marcan los mismo pero a 33°30'S. La línea azul corresponde a la velocidad absoluta de la placa Sudamericana de acuerdo con Silver (1998); mientras que la línea roja muestra la tasa de convergencia entre las placas de Nazca y Sudamericana según Somoza y Ghidella (2012). (b) y (c) Perfiles estructurales de la corteza superior mostrando las principales estructuras a 35° y 35°30'S. Ver traza en Figura V. 2a

Este periodo de deformación contraccional se caracterizó por la inversión de las fallas normales que controlaron el depósito de la Fm. Abanico, conformando así anticlinales >10 km de longitud y un estilo de deformación de piel gruesa relacionada tanto a la inversión tectónica de fallas previas como a fallas nuevas formadas durante este periodo (Fig. V.1b y c). Si bien no existen dataciones en el lado oeste de la cuenca que indiquen el inicio de la deformación en esa área, se infiere que debería haber comenzado relativamente simultáneamente con la zona este de la cuenca, ya que a la latitud de Santiago depósitos sinorogénicos de 22 Ma acotan el inicio de la inversión de los bordes occidental y oriental de la cuenca (Fock, 2005). Las evidencias de inversión del borde occidental de la cuenca a la latitud de esta Tesis se remontan a 16 Ma (Fig. V. 1) como evidencian tanto los estratos de crecimiento en la unidad Corona del Fraile, en la ladera sur del río Teno (Hevia, 2014) así como los depósitos de la Formación Farellones de la misma edad en la ladera sur del río Tinguiririca, frente al estero La Gloria (Fig. II. 1). El principal periodo de deformación de la Cuenca de Abanico habría finalizado a 11 Ma (Fig. V. 1) de acuerdo con la edad más joven del miembro inferior de la Fm. Farellones en el área del cerro Alto del Padre.

El inicio de la deformación en la parte interna de la faja plegada y corrida de Malargüe habría comenzado simultáneamente con la inversión de la Cuenca de Abanico entre 20 y 18 (Fig. V. 1a) (Mescua et al., 2014). Durante este periodo, la deformación se focalizó en el depocentro Río del Cobre (Mescua et al., 2014) y en los altos de basamento del Tordillo y Dedos-Silla (Fig. V.1b y c). Fue durante este periodo que se desarrollaron los anticlinales Río del Cobre, Valle Grande y Debia, producto de la inversión de fallas normales mesozoicas. La deformación en este sector continuó hasta *ca.* 13 Ma (Fig. V. 1b y c), de acuerdo con la edad de niveles volcánicos no deformados que cubren las secuencias mesozoicas (Mescua et al., 2014).

A partir de 16 Ma y hasta 7 Ma (Fig. V. 1a), el frente de deformación migró al este, afectando a lo que actualmente se puede considerar como la parte central de la faja plegada y corrida de Malargüe. En ese momento fue cuando comenzó la inversión de las fallas normales asociadas al desarrollo de los anticlinales La Valenciana y Los Blancos (Fig. V.1b y c) (Mescua et al., 2014) junto con todas las estructuras asociadas al proceso de inversión, como el retrocorrimiento de La Brea, al oeste del anticlinal de La Valenciana (Silvestro y Kraemer, 2005). Durante este periodo, se habría producido la actividad fuera de secuencia del corrimiento Las Leñas que afectó a los altos de basamento del Tordillo y Dedos de Silla (Mescua et al., 2014). Cabe destacar que los estratos de crecimiento en la parte de arriba del miembro inferior de la Fm. Farellones tienen una edad de 11 Ma indicando que la deformación el lado oeste aún presentaba pulsos de deformación sincrónicamente con la parte media de la faja plegada y corrida de Malargüe (Fig. V.1a).

Desde 7 Ma (Fig. V. 1a), el frente deformación migró nuevamente al este, lo que marca el inicio del último periodo de estructuración de la faja plegada y corrida de Malargüe. En esta etapa se produjo el desarrollo de los anticlinales de Malargüe, Puesto Rojas y Chacay (Fig. V. 1b y c) (Mescua et al., 2014; Silvestro y Kraemer, 2005). Simultáneamente al desarrollo de la parte externa de la faja plegada, se produjo la deformación fuera de secuencia de la parte interna del orógeno (Fig. V. 1a) que afectó tanto a las secuencias mesozoicas como cenozoicas. Este periodo estuvo asociado con la actividad de las fallas el Baule, el Fierro, El Novillo y Llolli y deformación

del miembro superior de la Fm. Farellones (*s.s.* esta Tesis) y Estratos del Colorado, en el sector de los ríos Tinguiririca y Valle Grande, respectivamente.

La última fase de deformación corresponde al alzamiento del bloque San Rafael entre 5 y 2 Ma (Fig. V. 1a) (Ramos et al., 2014). Posteriormente, la región del retro-arco comprendida entre el bloque de San Rafael y el sector externo de la faja plegada y corrida de Malargüe, experimentó un periodo de extensión caracterizada por el desarrollo de fallas normales, no obstante, algunas estructuras compresivas continuaron su actividad incluso hasta el presente en el eje de la cordillera como el Cabalgamiento Calabozos.

V.2 Análisis comparativo a lo largo de los Andes de Chile central y el oeste de Argentina

V.2.1 La arquitectura cortical y modo de deformación

La integración de las secciones estructurales presentadas en los capítulos anteriores muestra un dominio de estructuras de vergencia este y manteo al oeste (Fig. V.2c). Estas estructuras, en su mayoría, se caracterizan por corresponder a fallas normales mesozoicas y paleógenas que se invirtieron (*s.s.* Williams et al., 1989) durante la fase de deformación neógena.

Lo anterior es consistente con los modelos propuestos anteriormente tanto al norte (*e.g.* Farías et al., 2010; Giambiagi et al., 2012; Turienzo et al., 2012) como al sur (*e.g.* Giambiagi et al., 2012; Rojas Vera et al., 2014) de 35°S donde las estructuras se encontrarían conectadas a través de un nivel de despegue profundo que se conectaría mecánicamente con la interfase de placas hacia el oeste, específicamente en el límite inferior del contacto sismogénico (Farías et al., 2010). Estos modelos plantean que a través de esta discontinuidad cortical los esfuerzos son transferidos desde la zona de subducción hacia la placa Sudamericana implicando un transporte tectónico en un sentido oeste-este.

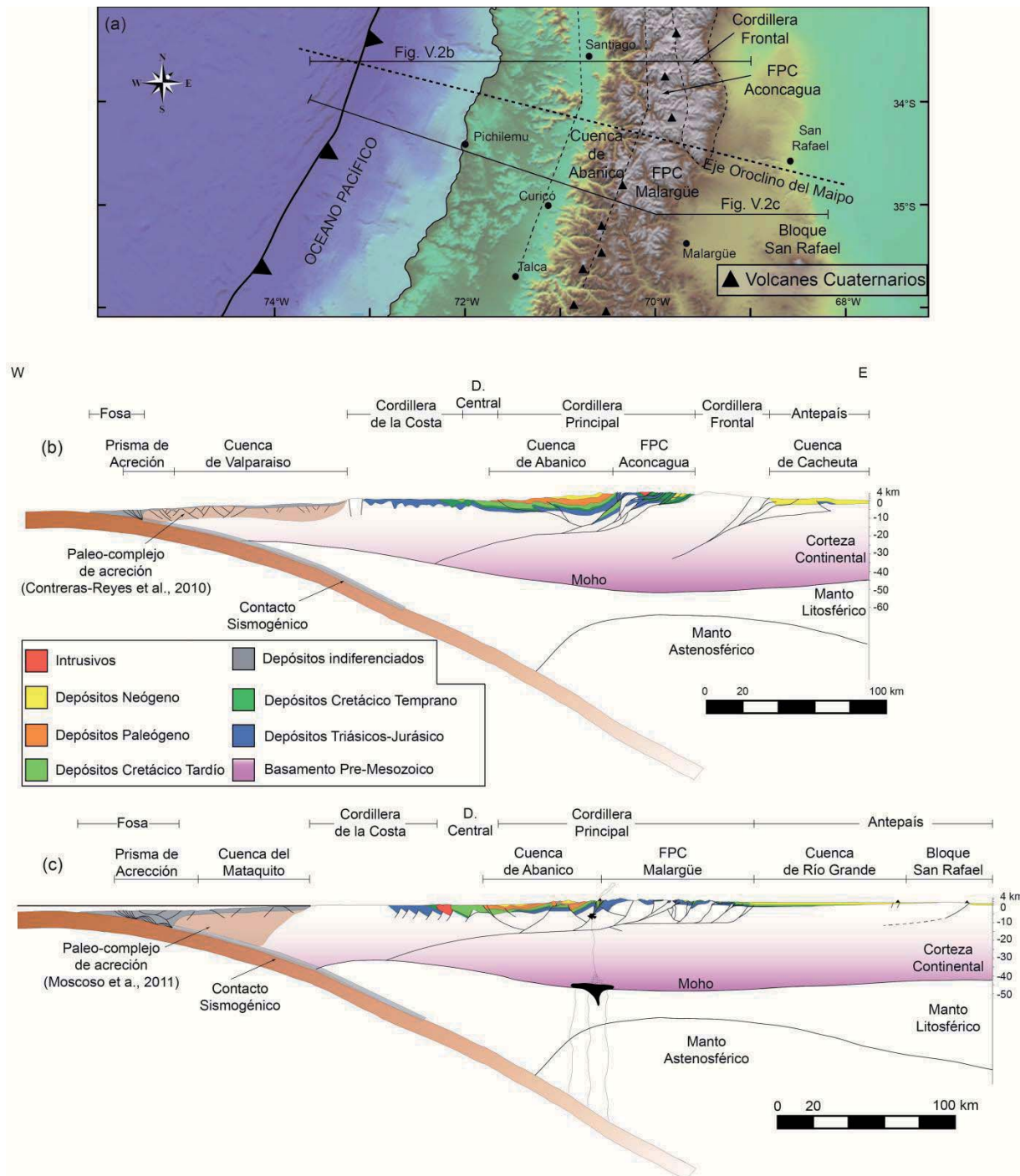


Fig. V.2. Arquitectura cortical de los Andes Centrales del sur. (a) Modelo de elevación digital (DEM) de los Andes Centrales del sur entre 33° y 36°S. En el DEM se muestran la ubicación de la Cuenca de Abanico, las fajas plegadas y corridas (FPC) de Aconcagua y Malargüe, junto con la Cordillera Frontal y el Bloque San Rafael. Arquitectura estructural de los Andes Centrales del sur a 33°30'S (a) y 35°S (b). Perfil del norte (a) modificado de Giambiagi et al. (2014). Límite Astenósfera-Litósfera, Moho y geometría de la losa basados en Tassara y Echaurren (2012). Morfología y características del antearco y y fosa tomados de Contreras-Reyes et al. (2010) y Moscoso et al. (2011). Estructura de la corteza superior del perfil (b) basada en este trabajo y Mescua et al. (2014). Ver traza de los perfiles en Fig. V.2a.

Por otra parte, la geometría y vergencia de las fallas, junto con la evolución propuesta, no pueden ser explicadas a través de una modelo de vergencia y transporte tectónico hacia el oeste, como lo propuesto por Armijo et al. (2010). En ese modelo, la Cordillera Frontal actuaría de *bulldozer* y motor principal durante la construcción de la cordillera, no obstante, al sur de 34°40'S no se desarrolla esta morfoestructura, lo que invalida aún más su aplicabilidad para esta porción de los Andes. Si bien el bloque San Rafael presenta características litológicas parecidas a la Cordillera Frontal, el acortamiento estimado para la Cordillera Principal es mucho mayor que el absorbido por este bloque de basamento de acuerdo con el desnivel vertical y dimensiones que presenta (e.g. González Díaz, 1972). De igual manera, el último periodo de deformación y alzamiento del bloque San Rafael se produjo entre 5 y 2 Ma (Fig. V.1) (ver Ramos et al., 2014), cuando ya la fase de deformación principal de la cordillera había terminado (Fig. V.1).

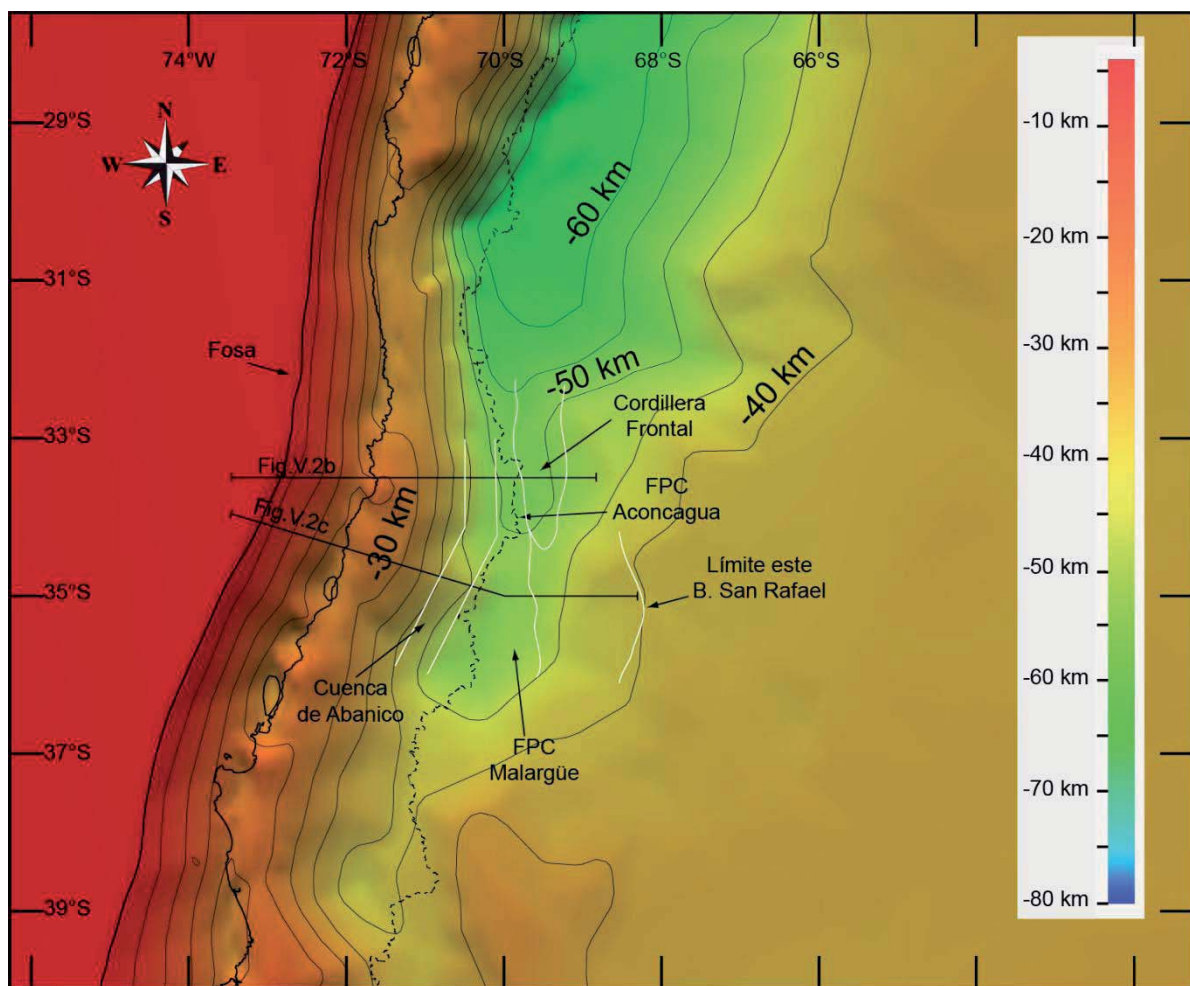


Fig. V.3. Espesor cortical de los Andes Centrales del Sur entre 30° y 40°S a partir de un modelo de inversión térmica (tomado de Tassara y Echaurren, 2012). Líneas negras delgadas corresponden a isópacas cada 5 km. Línea punteada corresponde a la frontera Chile-Argentina

Tal como se mencionó anteriormente, el modelo geométrico-estructural presentado para la latitud de 35°S es consistente con lo propuesto por Giambiagi et al. (2012) para 35°40'S y por Farías et al. (2010) para 33°30'-34°30'S. Además, en ambos trabajos se propone que el modelo cortical con un nivel de despegue regional que conecta la losa con la parte este de la placa

Sudamericana favorece un modo de deformación de cizalle simple, según la definición de Allmendinger y Gubbels (1996). En particular, al norte de 35°S, este modo de deformación fue sugerido para explicar los 10 km de diferencia en el espesor cortical entre el borde este y oeste de la Cuenca de Abanico (Fig. V.3), sin que existan diferencias en la cantidad de acortamiento a través de la cuenca (Fariás et al., 2010). Asimismo, la isotopía en circones de las rocas volcánicas del Neógeno mostró un abrupto cambio en la fuente litosférica del magma, lo cual habría sido producido por el avance hacia el oeste de corteza más antigua (Terreno Cuyania) bajo la Cordillera Principal producto de la deformación por cizalle simple del orógeno (Muñoz et al., 2013).

Contrariamente a lo anterior, al sur de 34°40' S, y de acuerdo con los modelos de Tassara y Echaurren (2012), el espesor cortical en la vertiente occidental, presenta valores de espesor cortical de 40-45 km (Fig. V.3), sin grandes diferencias a lo ancho de la Cuenca de Abanico, mientras que, el mayor espesor cortical (45-49 km) en esta región se ubica en la vertiente oriental en lo que corresponde a la faja plegada y corrida de Malargüe (Fig. V.3), coincidente con el mayor acortamiento cortical medido en superficie (ver Capítulo III y Tabla V-1). Esto hace suponer un modo de deformación distinto que el cizalle simple ya que hay una relación directa entre la región con mayor acortamiento acomodado y el engrosamiento de la corteza.

Al realizar un análisis en 2 dimensiones, el engrosamiento cortical (ΔT) producido por un acortamiento tectónico de la corteza continental (ΔL) se puede representar por la expresión:

$$(L + \Delta L) \cdot (T - \Delta T) = L \cdot T \Leftrightarrow \Delta T = T \left(1 - \frac{L}{L + \Delta L}\right); \text{(V-1)}$$

donde L y T son el largo y espesor final de la corteza, respectivamente. Este análisis supone que el acortamiento ejercerá un engrosamiento cortical en el cual el volumen del material se conserve. Esto solo será válido si no existen desplazamientos laterales de material, es decir, bajo un estado de cizalle puro en un modelo de *strain* plano.

En la Tabla V-1 se presentan los valores ocupados para la estimación del engrosamiento cortical. Los valores de acortamiento tectónico para la Cuenca de Abanico y la faja plegada y corrida de Malargüe corresponden a lo estimado en este trabajo (Capítulo II y III) y lo estimado por Mescua et al. (2014). Cabe destacar que la sección estructural de la faja plegada y corrida de Malargüe construida en este Tesis (Capítulo III) y por Mescua et al. (2014) fueron restauradas a un estadío previo al Cretácico Tardío, por lo que el acortamiento estimado por ambas no sólo corresponde al acomodado durante el Neógeno sino que también está contemplado el de la fase de deformación compresiva cretácica tardío-paleocena temprana.

Tabla V-1. Calculo del engrosamiento y el espesor inicial de los dominios estructurales de la Cordillera Principal a partir de los valores de acortamiento estimados.

Dominio Estructural	Largo final acortado <i>L</i> (km)	Acortamiento ΔL (km)	Espesor cortical actual <i>T</i> ⁴ (km)	Engrosamiento ΔT (km)	Espesor inicial calculado <i>T</i> - ΔT (km)	Alzamiento Δh (km)
Cuenca de Abanico	64 ³	20±2 ³	45	9,87-11,51	33,48-35,12	1,7-2,1
FPC Malargüe (35°S)	90 ²	27±3 ⁵	49	10,31-12,25	36,75-38,68	1,8-2
FPC Malargüe (35°30'S)	96,6 ³	30±3 ⁶	49	10,70-12,47	36,52-38,29	1,9-2,1

El engrosamiento cortical estimado en base al acortamiento *in-situ* para la Cuenca de Abanico variaría entre 9,87-11,51 km (Tabla V-1) lo que hace que el espesor cortical inicial de este sector varíe entre 33,48-35,12 km. En particular, el límite inferior de 33,48 km, asociado a un acortamiento de 18 km, es muy bajo respecto al espesor inferido para la cuenca durante el periodo de extensión, estimado a través del análisis petrogenético de los depósitos volcánicos de la Fm. Abanico (Kay et al., 2005; Muñoz et al., 2006; Nyström et al., 2003). Sin embargo, el borde occidental de la cuenca, el cual presenta los valores más bajos de espesor cortical, habría acumulado una menor cantidad de acortamiento que el oriental, evidenciado al comparar los depósitos sinorogénicos del Mioceno que afloran en uno y otro lugar. Los depósitos sinorogénicos de la unidad Corona del Fraile de 15 Ma, con estratos de crecimiento y acumulados sobre la Fm. Abanico en la confluencia de los ríos Teno y Claro (70°45'W/35°00'S) (Hevia, 2014) se encuentran a una altitud de 1.600 m, mientras que en el sector del Cerro Alto del Padre, depósitos sinorogénicos del miembro inferior de la Fm. Farellones, de la misma edad (Capítulo II), están a 2.700 m, sugiriendo que el sector oeste tendría un alzamiento menor que el lado este debido a que habría acomodado menos acortamiento. Lo anterior es válido solo si la tasa de erosión de ambos lugares es la misma o si el lado oriental de la Cuenca presentase tasas más altas, lo cual es una situación altamente probable si se considera que esas regiones estuvieron sometidas a la acción erosiva de glaciares durante el Pleistoceno y Holoceno (Espizúa, 2005, 2002; Puratich, 2010). En síntesis, se puede establecer que la diferencia de espesor cortical en la Cuenca de Abanico se

⁴ Tassara y Echaurren (2012)

⁵ Mescua et al. (2014)

⁶ Este trabajo

puede explicar por diferencias en el acortamiento medido en superficie a lo ancho de la cuenca. Así mismo, se puede establecer que el espesor cortical estimado bajo la vertiente occidental de la Cordillera Principal puede ser explicado por el acortamiento acomodado por la corteza superior observado y cuantificado en superficie.

Farías et al. (2008) estimaron que al sur de 34°30'S el alzamiento de superficie por acortamiento tectónico, luego de una compensación isostática y sin considerar la erosión, debería ser menor de lo que estimaron para la región de 33°30'S, llegando a un valor promedio de 1,5 y 1,8 km, pero el cual no pudo ser corroborado por la falta de estimaciones de la magnitud del acortamiento. Sin embargo, las estimaciones realizadas en esta tesis permitirían establecer valores de alzamiento al sur de 34°30'S.

Considerando la misma ecuación ocupada por Farías et al. (2008), el alzamiento de superficie (Δh) después de un engrosamiento (ΔT) y compensación isostática según un modelo de Airy, viene dado por:

$$\Delta h = \Delta T \left(1 - \frac{\rho_c}{\rho_m}\right); \text{(V-2)}$$

Si se considera una densidad de la corteza y el manto de $2.7 \cdot 10^3$ y $3.3 \cdot 10^3 \text{ kgm}^{-3}$, luego combinando (V-1) y (V-2) se obtiene:

$$\Delta h = \frac{T}{5,6} \left(1 - \frac{L}{(L+\Delta L)}\right); \text{(V-3)}$$

De acuerdo con los valores de la Tabla V-1 y a la Ecuación V-3, el alzamiento de la vertiente occidental de la Cordillera Principal correspondería a 1,7-2,1 km, un poco más altos que los valores inferidos por Farías et al. (2008), pero conteniendo los 1,8 km correspondientes a la altura promedio de la Cordillera Principal occidental. Dada la baja diferencia ($\pm 200 \text{ m}$) entre los valores de alzamiento estimados en este estudio y por Farías et al. (2008), y el valor de la altura promedio de la cordillera, se concluye que todo el alzamiento en esta región se puede explicar por el acortamiento tectónico observable en superficie. Esto, junto con la correspondencia entre el acortamiento y engrosamiento cortical discutido anteriormente, sugieren que la Cordillera Principal occidental se habría deformado bajo un modo de cizalle puro en el sentido de Allmendinger y Gubbels (1996) (Fig. V.4b). Adicionalmente, Farías et al. (2008) establecieron que lo más probable es que el alzamiento y deformación de la Cordillera Principal haya ocurrido simultáneamente, lo cual sería una directa consecuencia de este modo de deformación. Asimismo, se podría considerar que la parte interna de la faja plegada y corrida de Malargüe también fue deformada bajo cizalle puro ya que comenzó a deformarse junto con la Cuenca de Abanico (Fig. V.1), para luego no experimentar deformación salvo por la actividad fuera de secuencia que experimentó esa región durante el Mioceno tardío-Plioceno (Capítulo IV) (Mescua et al., 2014).

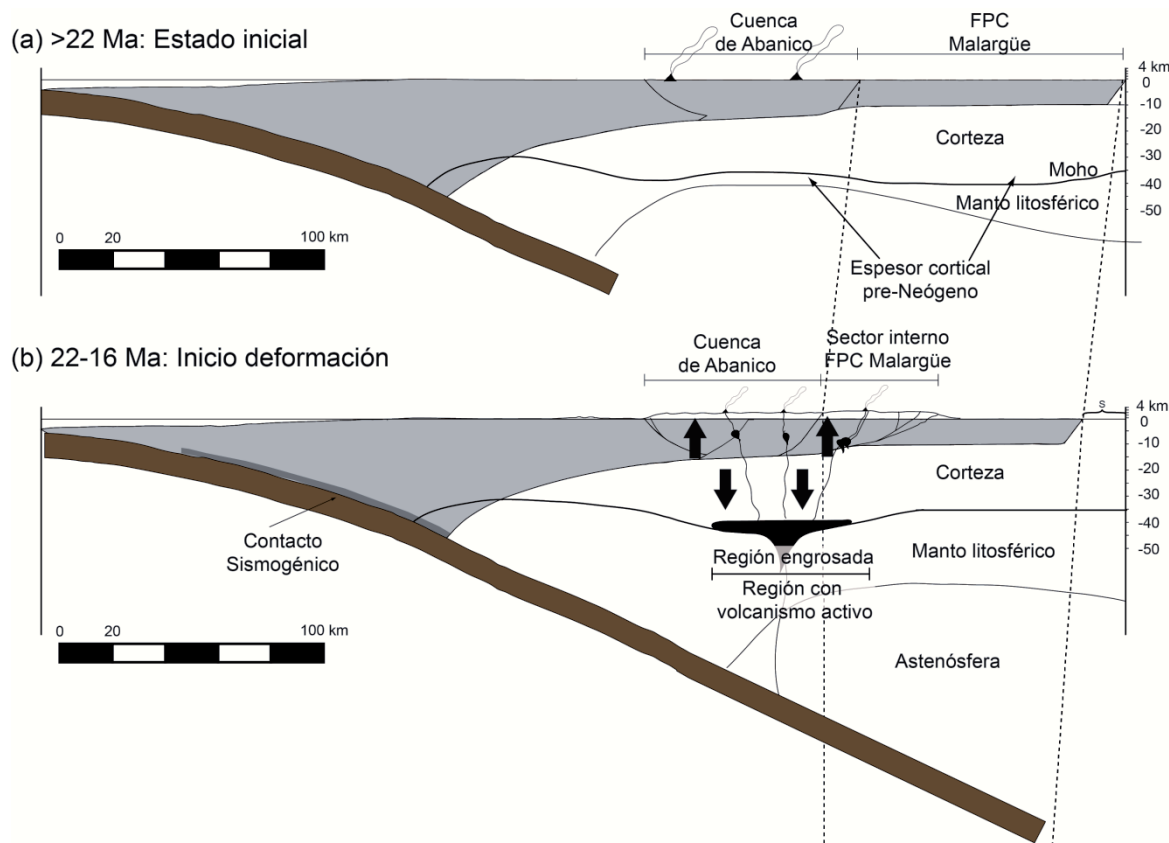
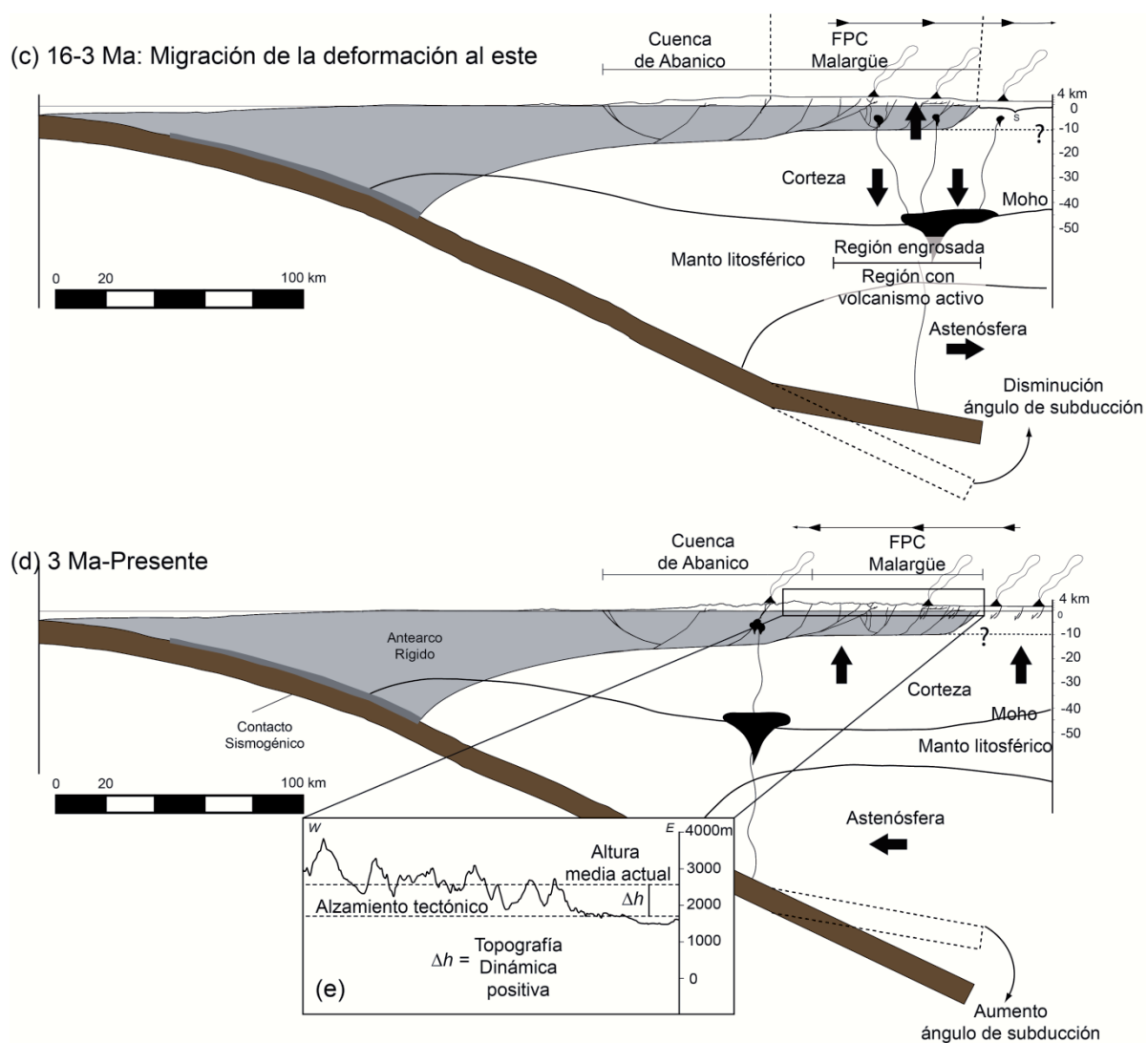


Fig. V. 4. Modelo evolutivo del engrosamiento cortical de los Andes Centrales del sur a 35°S. (a) Estado inicial >22 Ma previo al acortamiento. El espesor cortical inicial promedio para la corteza bajo la Cuenca de Abanico y Cuenca Neuquina es de 35 km. (b) Primer periodo de engrosamiento bajo la Cuenca de Abanico y la parte interna de la faja plegada y corrida de Malargüe bajo cizalle puro de acuerdo con el modelo de Allmendinger y Gubbels (1996). (c) Periodo de engrosamiento por cizalle puro bajo la faja plegada y corrida de Malargüe. Durante este periodo se produjo la somerización de la losa oceánica. (d) Estadio desde 3 Ma cuando se habría comenzado a empinar la losa oceánica, la astenósfera fluyó hacia el oeste. (e) Perfil topográfico de la vertiente oriental de la Cordillera Principal mostrando la diferencia entre la altura promedio y el alzamiento tectónico esperado para esta región. Ver discusión en el texto.

Las estimaciones del engrosamiento cortical a partir del acortamiento tectónico para la faja plegada y corrida de Malargüe entre 35° y 35°30'S (Ecuación V-1) entregan valores de 10,3-12,5 km, lo cual implica un espesor cortical de 36,52-38,29 km previo a 100 Ma. Estos valores se encuentran por encima de 35 km, estimación máxima para el espesor cortical de cuencas marinas desarrolladas sobre corteza continental (Mooney et al., 1998).



Continuación Fig. V. 4.

Mescua et al. (2014) estimaron también el espesor cortical previo a la deformación neógena a 35°S, encontrando un valor de 40 km, mayor a los máximos 35 km para una cuenca marina. Estos autores proponen que esta diferencia se debería a que el espesor cortical presentaba variaciones antes del engrosamiento neógeno, producto de la orogenia San Rafael (Pérmico). Esta fase de deformación habría engrosado la corteza, entre la fosa y el bloque San Rafael, y posteriormente se habría adelgazado durante la extensión mesozoica, pero sólo las regiones al oeste de la actual Depresión Central y la Cordillera Principal oriental, estableciéndose un bloque con mayor espesor cortical (>40 km) en la actual Cordillera Principal occidental. De esta forma, ellos proponen que el orógeno previo a 100 Ma tendría un espesor variable: el sector oeste 45 km y 32 km el este, lo que representaría una corteza promedio de 38-39 km consistente con los 40-45 km de acortamiento que estiman ellos para la Cordillera Principal a 35°S (Mescua et al., 2014).

Sin embargo, considerando que a través de análisis petrogenéticos se ha estimado que el espesor bajo la Cuenca de Abanico previo a 20 Ma habría sido de 35 km (Fuentes, 2004; Kay et

al., 2005; Montecinos et al., 2008; Muñoz et al., 2006), es posible calcular un factor de estiramiento (β) de acuerdo con la ecuación:

$$T_f = \frac{T_i}{\beta} (V-4)$$

donde T_f y T_i corresponden al espesor de la corteza después y antes de la extensión, respectivamente (Allen y Allen, 2005). Tomando $T_i=45$ km, como el valor mínimo del espesor cortical previo a la extensión eocena y sin considerar la contribución del acortamiento de las fases de deformación del Cretácico Tardío, y $T_f=35$ km se obtiene un valor de $\beta=1.29$. Este factor parece ser excesivamente alto si consideramos que recientes trabajos han determinado un valor de $\beta=1.28-1.49$ para en la Cuenca Neuquina (Sigismundi, 2011), en la cual hubo transgresiones marinas y un alto desarrollo de depocentros, características que la Cuenca de Abanico no tiene. En consecuencia, lo anterior hace improbable la existencia de un bloque de 45 km de espesor producto de la orogenia San Rafael.

Por otro lado, el valor estimado y teórico para el espesor de la corteza previo a 100 Ma, presentan una diferencia de 2-3 km, la cual es inferior al error de 5 km que tiene el modelo 3-D de densidad a través del cual fue estimado el espesor cortical (Tassara y Echaurren, 2012). Este error se debe a las incertezas propias de los datos y modelación geofísica (gravimetría y datos sísmicos) usada para acotar la profundidad del límite corteza-manto (Tassara y Echaurren, 2012). Además de lo anterior, tampoco fue realizada la corrección por topografía a los datos de la anomalía de Bouger, la cual en regiones con relieves altos como los Andes contribuye con valores de 10-25 mGal (Tassara y Echaurren, 2012). De acuerdo con esto, se puede establecer que el espesor cortical bajo la vertiente oriental de la Cordillera Principal es consecuencia del acortamiento acomodado por la corteza superior a través de la faja plegada y corrida de Malargüe. Esto indicaría que esta región, y en consecuencia toda la cordillera a 35°S (Fig. V.4c), se habría deformado bajo cizalle puro, contrastando con la región a 33°40'S, donde prevalece el modo de cizalle simple como mecanismo principal en la construcción del orógeno, y consistente con lo propuesto para 36°S (Astaburuaga, 2014).

Comparando la evolución estructural al norte y sur de 35°S (Fig. V.1), se puede observar que la deformación neógena comenzó en el sector de la Cuenca de Abanico entre 20 y 22 Ma, respectivamente (Fig. V.1). De la misma manera, el término del periodo principal de deformación en ambos lugares es distinto: 16 y 11 Ma (Fig. V.1), para el norte y sur, respectivamente. A pesar de lo anterior, ambas regiones muestran patrones similares en su evolución (Fig. V.1) que podría indicar que la parte occidental de la Cordillera Principal entre 33°30' y 35°S se deformó bajo cizalle puro, pero luego la región al norte de 35°S cambió a un modo de cizalle simple, cuando la deformación alcanzó la vertiente oriental, mientras al sur de esa latitud continuó el cizalle puro (Fig. V.4c). Gerbault et al. (2009) a través de modelos numéricos, reconoció que las regiones que se encuentran termalmente debilitadas se deformarían bajo cizalle puro. Esto concuerda con las características de la evolución de la cordillera a 35°S donde el volcanismo se expandió al este conforme el frente de deformación migraba, lo que debilitó termalmente la corteza y favoreció la deformación bajo cizalle puro (Fig. V.4c).

Ahora bien, el alzamiento tectónico producido por el acortamiento estimado para esta región corresponde a 1,8-2,1 km, de acuerdo con la Ecuación V-3. Sin embargo, estos valores son inferiores a la altura promedio actual de la cordillera de 2,67 km, lo que implicaría que el acortamiento ha sido subestimado o que el orógeno se encuentra isostáticamente descompensado y que existen factores externos que controlan la configuración actual de la cordillera a esta latitud.

En particular, para esta región ha sido propuesto un periodo de somerización de la placa oceánica entre 14-3 Ma asociado a la expansión del magmatismo con signatura de arco y la migración de la deformación hacia el este (Fig. V.4c) (Ramos et al., 2014 y referencias ahí). La principal implicancia de este proceso corresponde a la variación en la estructura termal de la zona de subducción debido a que la losa oceánica, más fría, se ubica bajo la litosfera continental, en una posición donde antes se encontraba la cuña astenosférica, más caliente (Gutscher, 2002). Lo anterior tiene consecuencias en la reología de la placa continental: en particular, el manto litosférico aumenta su espesor y por lo tanto se vuelve más denso, pudiendo implicar una disminución en la elevación de la superficie de la corteza (*cf.* Faccenna et al., 2014). Posterior a la disminución del ángulo de subducción se habría producido el empinamiento de la losa oceánica desde 3 Ma, lo que habría producido la migración de la cuña astenosférica hacia el oeste hasta su posición actual (Fig. V.4d) (Ramos y Folguera, 2011). La reubicación de la cuña astenosférica a su posición original implica un cambio en la dinámica del manto lo cual tiene una respuesta instantánea en la señal topográfica (Bertelloni y Gurnis, 1997; Dávila y Lithgow-Bertelloni, 2013). Durante la migración de la astenosfera habría ocurrido un progresivo reemplazo del manto litosférico, denso, por astenosfera más liviana lo que produjo una surgencia (*upwelling*) del manto litosférico induciendo, entonces, un alzamiento dinámico de la corteza o topografía dinámica (*e.g.* Dávila y Lithgow-Bertelloni, 2013; Faccenna et al., 2014; Guillaume et al., 2013, 2010). En este sentido, la topografía dinámica corresponde a la componente de la topografía que no se puede explicar por el alzamiento tectónico y que puede estar asociada con la convección del manto, lo cual también produce un movimiento vertical, de rocas hacia la superficie.

En resumen, el empinamiento de la losa durante el Plioceno tardío habría producido un *upwelling* del manto litosférico, produciendo un alzamiento dinámico del retro-arco y la vertiente oriental de la Cordillera Principal, lo que explicaría los 0.6-0.7 km de diferencia entre el alzamiento esperado por los ~30 km de acortamiento y la altura promedio actual de esa región de la cordillera (Fig. V.4e). Además, los 260 km que cubre el área que experimentó un alzamiento dinámico concuerda con los cientos de kilómetros de amplitud que puede alcanzar la topografía dinámica (*e.g.* Guillaume et al., 2013; Gurnis, 1993; Husson, 2006; Mitrovica et al., 1989; Ricard, 1993; Zhong y Gurnis, 1994). El aumento del ángulo de subducción y la migración de la cuña astenosférica también habrían originado el volcanismo basáltico que caracteriza la región del retro-arco al sur de 35°S y que está asociado al desarrollo de fallas normales formadas durante el Pleistoceno-Holoceno (Folguera et al., 2008, 2006; Ramos y Folguera, 2011; Ramos et al., 2014). Estas estructuras estarían relacionadas a un colapso y disminución del espesor de la corteza, observado al sur de 36°S (Folguera et al., 2012). Sin embargo, el adelgazamiento y colapso cortical no se evidencian a 35°S, ni tampoco el desarrollo de fosas extensionales que contengan el volcanismo cuaternario (Folguera et al., 2010; Ramos et al., 2014; Rojas Vera et al., 2010). En

cambio, en esta región dominan las fallas normales aisladas en las proximidades de los volcanes monogenéticos, las cuales se habrían formado por la flexura de alta longitud de onda que habría experimentado la corteza producto del alzamiento dinámico.

Contrario a lo anterior, la vertiente occidental de la cordillera no tendría una componente dinámica en su topografía, tal como lo muestran las estimaciones de alzamiento realizadas (Tabla V-1) y la continua deformación contraccional que experimentó esta región (Capítulo IV), sugiriendo que la losa oceánica bajo la parte interna del orógeno no habría variado el ángulo de subducción, consistente con lo que se observa en el actual segmento de subducción plana entre 27° y 33°S (Gans et al., 2011; Mulcahy et al., 2014).

De acuerdo con lo presentado anteriormente, una de las principales interrogantes corresponde al origen de la somerización y posterior empinamiento de la losa oceánica durante el Mioceno tardío. En particular, diversos trabajos han mostrado a través de modelos numéricos que el ángulo de subducción es inversamente proporcional a la velocidad de retroceso de la fosa (Heuret et al., 2007), por lo que una disminución o aumento de este parámetro en algún segmento de la subducción podría haber producido la somerización de la losa oceánica durante el Mioceno tardío. De la evolución propuesta en esta Tesis se desprende que la somerización de la losa oceánica habría comenzado *ca* 14 Ma (Ramos et al., 2014 y referencias ahí), de acuerdo con la edad en que la deformación alcanzó la vertiente oriental de la Cordillera Principal, gatillando la diferenciación en la evolución de las regiones al norte y sur de 35°S. Es a partir de 16 Ma que la tasa de deformación (Vd) en el sector norte aumentó respecto al sur, produciendo un diferencial en la velocidad de la trinchera (Vt) entre ambas regiones, dado que $Vt=Vup+Vd$, donde Vup es la velocidad de la placa superior y se puede considerar la misma para ambas regiones durante todo el Cenozoico. De acuerdo con lo anterior, la velocidad de la trinchera en el sector sur habría sido mayor (Fig. 4e), produciendo el avance de la placa Sudamericana sobre la placa oceánica, relativo a la región del norte, y en consecuencia la disminución del ángulo de subducción. Adicionalmente, esta hipótesis implicaría que fue durante este periodo (post- 16 Ma) que se habría comenzado a formar la curvatura que muestra actualmente el continente al sur de 33°S.

Ahora bien, la pregunta sería ¿por qué migró la deformación hacia el este antes de la disminución del ángulo de la subducción? Diversos modelos numéricos han observado que durante un periodo de deformación compresiva, la cuña mantélica es comprimida debido al engrosamiento cortical, produciendo que migre tanto la cuña mantélica como el magmatismo en dirección contraria de la fosa (Karlstrom et al., 2014). Lo anterior podría corresponder al inicio de la migración de la deformación ya que el volcanismo produce el debilitamiento termal y por ende una disminución de la resistencia a la deformación. De esta manera, se habría producido el inicio de la deformación de la vertiente oriental de la cordillera, durante la cual se produjo el aumento en la tasa de deformación, pero a un valor menor que la región al norte de 35°S, lo que favoreció el contraste de la velocidad de la fosa y, por ende, el inicio de la somerización de la losa oceánica.

El regreso de la subducción a su ángulo normal (30°) coincide con el fin de las rotaciones en sentido horario que experimentaron las rocas producto de la formación del oroclino (Arriagada et al., 2013), sugiriendo que las velocidades de la fosa al norte y sur de 35°S se igualaron o disminuyó su diferencia, produciendo el empinamiento de la losa oceánica, el flujo al oeste de la

astenosfera desplazada, el alzamiento del retro-arco y Cordillera Principal oriental, junto con el desarrollo de estructuras extensionales en el antepaís. La variación en la velocidad de la trinchera queda en evidencia al observar que a partir de 12 Ma, la tasa de deformación en el sector norte disminuyó (Giambiagi et al., 2014) y que actualmente no existen diferencias longitudinalmente en las velocidades de GPS de antearco entre 33°40'S y 36°S en el periodo inter-sísmico (Métois et al., 2012). Lo anterior implica que la velocidad de la fosa aumentó al norte de 35°S produciendo, a la vez, la disminución de la diferencia con la velocidad del sector sur. Si bien la evolución anterior explicaría la somerización y empinamiento de la losa oceánica, el origen de por qué disminuyó la tasa de deformación queda incierto. Una posibilidad podría corresponder a una disminución del acoplamiento en el contacto sismogénico producto de la mayor cantidad de sedimentos en la fosa desde la colisión de la dorsal de Juan Fernández, la cual impidió el flujo paralelo a la costa del material proveniente del continente lubricando el canal de subducción y disminuyendo el acople entre las placas. La colisión de la dorsal a 12 Ma coincide con la disminución en las tasas de acortamiento de la corteza superior a 33°40'S, evidenciando el control que ejerce la subducción sobre la deformación de la placa Sudamericana.

V.2.2 Diferencias latitudinales en la cantidad de deformación y el acortamiento

Una de las principales características que presentan los Andes al sur del oroclino boliviano es que el acortamiento disminuye continuamente hacia el sur. En la sección anterior se discutieron las diferencias en el modo de deformación y engrosamiento cortical que presentaría el orógeno, de acuerdo con la cantidad de acortamiento acomodado a lo largo de cada transecta. Al respecto, surge la interrogante: ¿Qué produce la disminución de acortamiento en el segmento comprendido entre 33°40'S y 36°S?

Tabla V-2. Comparación del acortamiento tectónico entre 33°30'S y 35°S

	CA	FPC	CF		Total			33°30'S	35°S
	33°30'S	35°S	33°30'S	35°S	33°30'S	35°S	33°30'S		
Ancho de la región acortada (km)	64	64	32	90	40	-	136	154	
Acortamiento (km)	16 ⁷	18-20	33 ⁸	27-30	23 ²	-	72	47	
Acortamiento (%)	20	23,81	50,77	23,08	36,51	-	34,62	23,38	

Al contrastar las 2 transectas mencionadas anteriormente, se puede establecer lo siguiente (Tabla V-II):

⁷ Farías et al. (2010)

⁸ Giambiagi et al. (2012)

- El acortamiento de la Cuenca de Abanico entre $33^{\circ}30'$ y 35° S se mantiene constante, de acuerdo con los valores estimados en este trabajo y por otros autores a lo largo del segmento de los Andes analizado (Fariñas et al., 2010) pudiendo incluso ser extendido hasta 36° S, donde estudios han mostrado un porcentaje de acortamiento similar que las regiones al norte (Astaburuaga, 2014)
- Coincidentemente, la Cuenca de Abanico muestra una tasa de acortamiento promedio constante de 2 mm a^{-1} a lo largo de este segmento de los Andes, a pesar de que el inicio y término de la deformación de ambas regiones se encuentre desfasada, concluyendo con cantidades y porcentajes de acortamiento similares.
- Los sectores correspondientes a las fajas plegadas y corridas de Aconcagua y Malargüe presentan un acortamiento promedio de 30 km; sin embargo, el porcentaje disminuye hacia el sur, producto de que en el segmento a la latitud de Malargüe la deformación se distribuye en una región más amplia (para un análisis más completo ver sección IV.3, Capítulo IV).
- La faja plegada y corrida de Aconcagua presenta una tasa de acortamiento promedio de 3 mm a^{-1} mientras que la de Malargüe 1.9 mm a^{-1} . Esto se debe principalmente a que la faja de deformación del norte se estructuró en menor tiempo que la del sur (Fig. V.1), no obstante, las diferencias finales en cantidad no son tan notorias.

En primer lugar se puede establecer que la diferencia de acortamiento total en superficie entre las dos regiones (Tabla VI-2) se manifiesta en el desarrollo de la Cordillera Frontal al norte de $34^{\circ}40'$ S. La Cordillera Frontal corresponde a un bloque de basamento que habría estado exhumado inicialmente durante el periodo de extensión mesozoica, como se mostró en el análisis de proveniencia en las secuencias sedimentarias Jurásicas de la Cuenca Neuquina (Fig. III.5), indicando que desde su primer alzamiento durante el Pérmico (Gregori y Benedini, 2013; Heredia et al., 2012; Mpodozis y Ramos, 1989) no ha experimentado ningún periodo importante de enterramiento (Hoke et al., 2014). Así mismo antes de su último periodo de alzamiento a los 10 Ma ya se establecía como un área de aporte para los depósitos sinorogénicos del Mioceno (Porras, 2013). Lo anterior indicaría que el basamento de la Cordillera Frontal se encontraba a niveles someros de la corteza al momento de la compresión neógena, lo que podría haber favorecido su deformación y alzamiento. Adicionalmente, Giambiagi et al. (2012) sugieren que la formación de la Cordillera Frontal al norte de $34^{\circ}30'$ S habría estado condicionado por el menor desarrollo de la Cuenca Neuquina en ese sector. Estos autores proponen que al norte de 35° S, la reología de la corteza inferior no fue modificada sustancialmente por los procesos de *rifting*, mientras que al sur de esta latitud, donde la cuenca tuvo un mayor desarrollo, el adelgazamiento y *underplating* de material máfico en la base de la corteza durante la extensión (Kay et al., 1989) podrían haber aumentado la resistencia e impedido el flujo de la corteza inferior durante periodos posteriores de compresión y entonces inhibiendo el alzamiento de basamento. Lo anterior indicaría que el basamento de la Cordillera Frontal se encontraba a niveles someros de la corteza al momento de la compresión neógena, lo que habría favorecido su deformación y alzamiento. Cabe mencionar que el control de la evolución previa en el alzamiento de la Cordillera Frontal también se ha propuesto a $27^{\circ}\text{-}28^{\circ}$ S donde la posición actual del basamento paleozoico respondería a su arquitectura heredada durante la extensión mesozoica (Martínez et al., 2014). Aún cuando lo anterior explicaría

el desarrollo de la Cordillera Frontal, la configuración previa de la corteza superior solo va a controlar el estilo estructural presente en una región, pero no la cantidad de acortamiento que experimentaría esa región.

Por otro lado, la presencia de un gradiente de acortamiento y la diferencia en las tasas de acortamiento que se observan al sur del segmento de subducción plana son consistentes con el desarrollo del oroclino del Maipo, evidenciado por las rotaciones de eje vertical de 24° en sentido horario que presentan las rocas más antiguas a 5 Ma, al sur de 34°30'S (Arriagada et al., 2013). Arriagada et al. (2013) propusieron que el origen de la disminución del acortamiento, y en consecuencia, del oroclino del Maipo, se debe a un mayor acople en el contacto sismogénico al norte de 33°30'S debido a la colisión de la dorsal oceánica de Juan Fernández y el desarrollo del segmento de subducción plana a partir de 12 Ma. Si bien, el mayor acople explicaría las diferencias en las tasas de deformación del sector norte respecto al sector sur, la variación se establece desde 18-16 Ma cuando la deformación migró al este y comenzó la estructuración de las fajas plegadas y corridas. Esto descartaría la llegada de la dorsal oceánica como la causa principal de la disminución del acortamiento al sur del segmento de subducción plana, aunque su llegada pudo haber acentuado aún más el gradiente de deformación.

Una variable a considerar corresponde al desfase en el inicio de la deformación entre las regiones a 33°30'S y 35°S, ya que ha sido propuesto como una causa de la diferencia de acortamiento para este segmento de los Andes (Spikings et al., 2008). De acuerdo con los datos obtenidos en esta tesis, el sector sur habría comenzado y terminado su periodo de deformación principal después (10-7 Ma, Spikings et al., 2008, Farías et al., 2012) que el segmento a la latitud de Santiago (13-10 Ma, Farías et al., 2008, 2010, 2012) (Fig. V.1), sugiriendo entonces que la diferencia de acortamiento se debe a una disminución de la edad de la deformación hacia el sur. Sin embargo, si se considera el tiempo de diferencia entre las regiones junto con la tasa promedio de acortamiento en la zona sur, solo se obtienen 8,8 km, lo cual sumado a los 47 km de la Cuenca de Abanico y faja plegada corrida de Malargüe, no igualan los 72 km de acortamiento que presenta el segmento norte (Tabla V-II), descartando un control temporal en la diferencia del acortamiento.

Por otra parte, variados han sido los estudios en los Andes, así como en otras zonas de subducción, que han propuestos diferentes parámetros que controlarían el acople entre las placas y, en consecuencia, el tipo y la cantidad de deformación en la placa superior (*e.g.* Doglioni et al., 2009, 2007; Heuret y Lallemand, 2005; Jarrard, 1986; Lallemand et al., 2008; Lamb y Davis, 2003; Pardo-Casas y Molnar, 1987; Pilger, 1984; Ramos, 2010; Ramos et al., 2004; Schellart, 2008; Silver, 1998; Sobolev et al., 2006; Somoza y Ghidella, 2005; Somoza y Zaffarana, 2008; Somoza, 1998; Tassara, 2005; Yáñez y Cembrano, 2004). De estos estudios se desprende que los parámetros de primer orden, a una escala global, corresponderían a la velocidad absoluta de la placa superior (V_{up}), la velocidad de convergencia y la edad de la losa. Cabe mencionar que Lamb y Davis (2003) propusieron un modelo donde el grado de acople presentaba una relación positiva a la cantidad de sedimentos en la fosa, lo que evidenciaría el control climático sobre la tectónica. Este modelo se aplica muy bien a la situación actual de los Andes ya que donde la cordillera presenta más deformación, la fosa tiene menos sedimentos, mientras que donde la fosa es más

ancha y está llena de sedimentos, la deformación sobre la placa continental es menor. Sin embargo, no han sido reportados datos para establecer la cantidad de sedimentos que podría haber tenido la fosa *ca.* 20 Ma, por lo que un control directo del clima en el gradiente de deformación en este sector de los Andes es muy difícil de cuantificar. A pesar de esto, sí se puede establecer que a partir de 12 Ma la llegada de la dorsal de Juan Fernández a su posición actual favoreció la diferencia en el grado de acople a lo largo de la cordillera, actuando como barrera en el flujo de sedimentos a lo largo de la fosa, lo que habría producido una segmentación del grado de acople entre las placas al norte y sur de la zona de colisión y en consecuencia una segmentación en la cantidad de deformación en el orógeno.

De acuerdo con los estudios llevados a cabo en los Andes, se ha propuesto una relación directa entre el aumento de la velocidad absoluta de Sudamérica y el comienzo de deformación compresiva durante el Neógeno (Fig. V.1) (Pardo-Casas y Molnar, 1987; Pilger, 1984; Somoza y Ghidella, 2005). De la misma manera, se ha relacionado el aumento de la velocidad de convergencia con el periodo de extensión oligocena y a la disminución del mismo parámetro con el inicio de la deformación en el Neógeno (Fig.V.1) (Somoza y Ghidella, 2005). En el caso del segmento de los Andes Centrales del sur analizado hasta ahora, estos parámetros no serán considerados como posibles causas ya que no varían latitudinalmente y se puede establecer que la región de 33°30'S y 35°S experimentaron la misma velocidad de convergencia y velocidad absoluta de Sudamérica durante su evolución dada la lejanía del polo de rotación tanto de la placa Sudamericana como de Nazca (e.g. DeMets et al., 2010).

El estudio de la relación entre acoplamiento y edad de la losa oceánica ha sido más controversial ya que hay autores que proponen que las regiones donde la losa es más vieja, el canal de subducción es más viscoso lo que generaría mayor acople (Yáñez y Cembrano, 2004). En el lado opuesto, se ha propuesto que una losa con menor edad tiene mayor flotabilidad por lo que al momento de intervenir en el canal de subducción tendería a empujar hacia la superficie, generando mayor acople, mientras que la subducción de una losa más vieja produce una mayor fuerza de *slab-pull* por su mayor densidad, y por lo tanto un menor acople (Heuret y Lallemand, 2005). Para el segmento de subducción al sur de la subducción plana y hasta 36°S no existe una variación mayor en la edad de la losa subductada (< 3 Ma Yáñez y Cembrano, 2004), ni tampoco un gran cambio en el grado de oblicuidad de la convergencia después de 20 Ma (Pardo-Casas y Molnar, 1987) que haga suponer alguna situación distinta a la observada en la actualidad. Por lo tanto, se desecha que la edad de la losa ejerza algún control de primer orden sobre la diferencia de acoplamiento en este sector de los Andes.

Otra arista para explicar diferencias en la deformación y acortamiento a lo largo de los Andes corresponde a variaciones en la resistencia a la deformación que pueda presentar la corteza continental (Giambiagi et al., 2012). De acuerdo con la evolución de este segmento de los Andes, la vertiente occidental no presenta marcadas diferencias en su evolución desde el Mesozoico hasta el Presente, al menos entre 33°30'S y 36°S (Charrier et al., 2014) sugiriendo que las características reológicas a lo largo de ese sector son uniformes. Esto último es consistente con lo expuesto en esta tesis en relación que la Cuenca de Abanico, a pesar de mostrar un desfase en el periodo de deformación entre el sector norte y sur, presenta las mismas tasas y cantidad de acortamiento

además de estilos estructurales similares a lo largo del segmento analizado. Por el contrario, la diferencia en los estilos estructurales, tasas y cantidad de acortamiento entre la región norte y sur hacen suponer que la vertiente oriental de los Andes podría presentar variaciones latitudinales en los parámetros reológicos de la corteza. Esto es consistente con el hecho que esa parte de la corteza continental no ha experimentado sustanciales períodos de deformación desde la extensión mesozoica, si se considera que durante el Cretácico Tardío el proto-orógeno andino se desarrolló mayormente en lo que hoy corresponde a la Cordillera de la Costa y parte de la Cordillera Principal occidental (ver Capítulo II) (Charrier et al., 2014). Estas diferencias reológicas podrían corresponder a la mayor rigidez que tendría la corteza inferior del lado oriental de la cordillera, al sur de 35°S, cuya composición sería comparativamente más máfica (Tassara y Yáñez, 2003), lo que habría sido heredado desde el Mesozoico (Giambiagi et al., 2012). Por último, las diferencias en las tasas de deformación entre las fajas plegadas y corridas desarrolladas en Argentina indicarían que las diferencias en la evolución del orógeno se manifiestan cuando la deformación arriba a ese sector de la corteza, consistente con la hipótesis de la diferencia reológica como principal control en la cantidad de deformación que puede absorber la corteza.

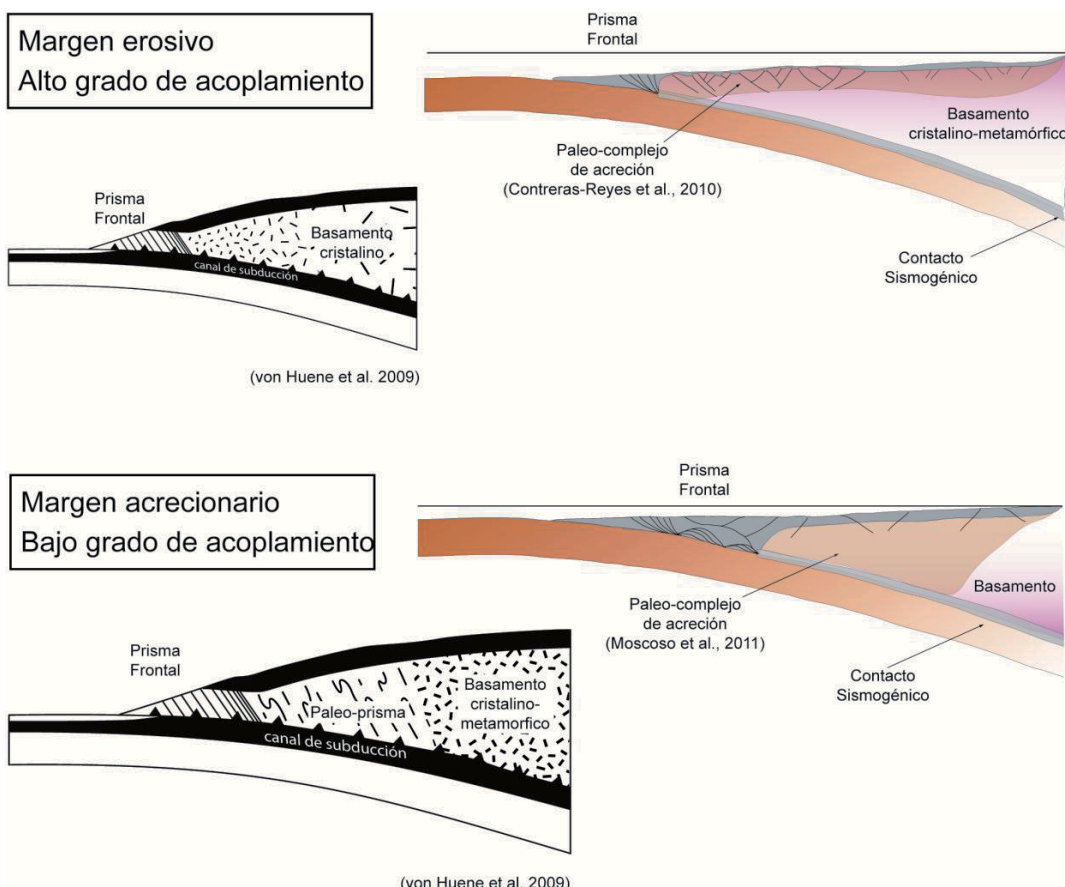


Fig. V.5. Sección esquemática del margen occidental de Sudamérica a 33°40'S (arriba) y 35°S (abajo) mostrando las diferencias entre ambas regiones. Se puede ver como varia las características litológicas de la corteza continental a lo largo y ancho del contacto sismogénico que condiciona el acople y la cantidad de *stress* transferidos hacia el continente. Nótese también como las características de ambas zonas coinciden con los modelos teóricos presentados por von Huene et al. (2009) para márgenes erosivos y convergentes.

De forma complementaria a lo anterior, un escenario posible que contribuya a explicar las variaciones en la cantidad de deformación podría estar relacionado a la segmentación litológica a lo largo del borde occidental de la placa Sudamericana. Estudios en la región del antearco y *trench-outer rise* muestran que la corteza superior de la placa continental (*backstop*) al norte de la zona de colisión de la dorsal de Juan Fernández está estructurado por un basamento metamórfico-cristalino (Contreras-Reyes et al., 2010 y referencias ahí) compuesto por rocas del Paleozoico-Jurásico Temprano que aflora en el lado occidental de la Cordillera de la Costa (Charrier et al., 2014). Mientras tanto, al sur de la dorsal asísmica, el *backstop* estaría formado no sólo por el basamento metamórfico-cristalino sino además por un paleo-complejo de acreción de edad Jurásica-Cretácica (Fig. V.5) (Contreras-Reyes et al., 2008), el cual aumenta su área de contacto con la placa oceánica desde 33°S hacia el sur (Fig. V.5) (Contreras-Reyes et al., 2010; Moscoso et al., 2011). De acuerdo con estas características, el contacto sismogénico a 35°S correspondería a un ante-arco débil (de acuerdo con la definición de Gerbault et al., 2009) el cual según modelos numéricos se caracteriza por deslizar más fácilmente sobre la placa oceánica (Gerbault et al., 2009). En otras palabras, la cantidad de *stress* de cizalle, o máximo, que puede acumular este material antes de deslizar es bajo comparado con un ante-arco fuerte formado solo por basamento cristalino (según definición de Gerbault et al., 2009), como al norte de 33°40'S (Fig. V.5). Lo anterior implica que la cantidad de *stress* que puede ser traspasada al continente es menor. La caracterización de un ante-arco débil y fuerte también implicaría la constitución de un margen acrecionario o erosivo, respectivamente (von Huene et al., 2009), lo que tiene directa relación a un menor o mayor grado de acople en el contacto sismogénico y por lo tanto en la cantidad de *stress* que se transmite al continente (Fig. V.5). De esta manera, se puede establecer que al sur de 33°S, el margen de subducción se transforma paulatinamente de un margen erosivo-altamente acoplado a un margen acrecionario-levemente acoplado (Contreras-Reyes et al., 2010). De este modo, se puede establecer que la variación en la reología del borde occidental de la placa Sudamericana podría contribuir a la diferencia en la cantidad de deformación que muestran los segmentos al norte y al sur de 35°S. En resumen, las diferencias reológicas presentes a lo largo de la corteza controlarían la cantidad de deformación y, en consecuencia, la disminución del acortamiento al sur de 33°S, evidenciando el fuerte control que tiene la evolución previa de corteza continental en la segmentación de los Andes.

CAPÍTULO VI.

CONCLUSIONES GENERALES

La construcción de un orógeno es el resultado de la interacción de diferentes procesos superficiales y profundos que varían espacial y temporalmente, originando una segmentación en la arquitectura y evolución de la cadena montañosa. En particular, la evolución neógena de los Andes Centrales del sur entre 34°45' y 35°30'S se encuentra fuertemente controlada por la arquitectura de la corteza, heredada de la evolución previa.

Durante el Jurásico Temprano y hasta el Cretácico Temprano, la región se caracterizó por el desarrollo de dos depocentros controlados por fallas normales y donde se acumularon los depósitos sedimentarios y volcánicos que conforman el relleno de la Cuenca Neuquina. Estos depocentros se encontraban separados por un alto topográfico compuesto por el basamento paleozoico, el cual fue una de las principales fuentes de sedimentos.

Para el Cretácico Tardío-Paleógeno, la región de estudio experimentó un periodo de deformación contraccional caracterizado por la acumulación de depósitos sinorogénicos con una marcada proveniencia desde el oeste, principalmente desde el arco magmático jurásico-cretácico inferior. Este periodo de deformación comprendió el primer periodo de estructuración de la faja plegada y corrida de Malargüe, generando la compartmentalización del sistema de antepaís y el desarrollo de depocentros aislados donde fueron acumulados los depósitos del Cretácico Tardío que afloran a lo largo del eje de la cordillera a la latitud de este estudio, diferenciándose de los ubicados más al este ,en territorio argentino.

La presencia de rocas volcánicas deformadas del Cretácico Tardío-Paleoceno en la vertiente occidental de la Cordillera Principal muestra una migración del arco magmático y cambios en la tectónica durante este periodo. Asimismo, su disposición discordante bajo los depósitos volcánicos eocenos de la Fm. Abanico, evidencian un nuevo pulso de deformación contraccional previo a la extensión que dio origen a la Cuenca de Abanico.

El desarrollo de la cuenca de intra-arco de Abanico se caracterizó por dos periodos de subsidencia tectónica durante el Eoceno-Oligoceno. El primero afectó la región más occidental de la Cordillera Principal, cercano a la Depresión Central, entre 45 y 37 Ma. Subsecuentemente, la acumulación los depósitos volcánicos ocurrió en la parte más oriental de la cordillera, en lo que actualmente corresponde al área fronteriza entre Chile y Argentina, entre los 37 y 22 Ma.

La deformación contraccional de la Cordillera Principal en este segmento de los Andes comenzó a los 20 Ma con la inversión de la Cuenca de Abanico y la acumulación de depósitos sinorogénicos de la misma edad, en la parte interna de la cordillera, donde aún se mantiene. Esta región experimentó deformación contraccional hasta los 11 Ma, reactivándose durante una fase de deformación fuera de secuencia a los 5 Ma.

La evolución estructural neógena de la cordillera a la latitud de 35°S se caracteriza tanto por la reactivación de estructuras previas como la formación de nuevas fallas que involucraron al basamento en la deformación, desarrollando así un estilo estructural de piel gruesa que domina la región, favorecido por la presencia de cuencas extensionales originadas durante el Mesozoico y Cenozoico temprano. Mientras que en el lado oeste de la cordillera el estilo de piel gruesa se mantiene invariante al sur del segmento de subducción plana hasta 35°S, en la vertiente oriental se produce una variación latitudinal caracterizada por un gradual predominio hacia el sur del estilo de deformación de escama gruesa, coincidentemente con el mayor desarrollo de depocentros mesozoicos extensionales, sugiriendo así el control de la arquitectura y evolución previa en la manera en que se acomoda la deformación durante las fases compresivas posteriores.

Durante la deformación de la vertiente occidental de la cordillera (20-11 Ma), cerca de 18 km de acortamiento fueron acomodados en la corteza superior. Por otro lado, la faja plegada y corrida de Malargüe acomodó 30 km de acortamiento, implicando una variación mínima con el acortamiento acomodado por la Cordillera Principal oriental a los 33°30'S. No obstante, el porcentaje de acortamiento disminuye hacia el sur debido a que la deformación se distribuyó en una región más amplia. De esta forma, se establece que la disminución hacia el sur del acortamiento medido en superficie se origina por la ausencia de la Cordillera Frontal al sur de 34°40'S, lo cual sería consecuencia directa de la menor cantidad de deformación que experimentó la corteza.

Esta menor cantidad de deformación y acortamiento es consistente con la disminución del espesor cortical y la altura de la cordillera hacia el sur del segmento de subducción plana y tiene implicancias directas en la forma en cómo se deforma la corteza. Es así como el acortamiento acomodado por la corteza superior ha sido transformado en engrosamiento cortical *in-situ* implicando un modo de deformación en cizalle puro, contrastando con el modo de cizalle simple que dominaría al norte de 35°S.

De esta forma se establece que la segmentación y variaciones de los Andes al sur del segmento de subducción plana son controladas por variaciones en la cantidad, y en consecuencia, en la forma de deformarse que presentaría la corteza. Esta última condicionada por la evolución y estructura previa del continente al momento de la construcción del orógeno. Finalmente, si bien, la evolución y arquitectura previa influye sobre el estilo de deformación de la corteza, la cantidad de deformación que experimenta el continente es la responsable de que la segmentación de los Andes, quedando aún por dilucidar si esto depende de la cantidad de deformación que puede acomodar la placa superior o a variaciones a lo largo de la placa subductada.

BIBLIOGRAFÍA

- Aguirre, L. 1960. Geología de los Andes de Chile Central, Provincia de Aconcagua. Boletín, Inst. Investig. Geológicas 9, 70.
- Aguirre, L., Calderón, S., Vergara, M., Oliveros, V., Morata, D., Belmar, M. 2009. Edades isotópicas de rocas de los valles Volcán y Tinguiririca, Chile central, en: XII Congreso Geológico Chileno. Santiago.
- Allen, P.A., Allen, J.R. 2005. Basin Analysis. Principles and Applications, 2º ed. 562 p.
- Allmendinger, R.W., Gubbels, T. 1996. Pure and simple shear plateau uplift, Altiplano-Puna, Argentina and Bolivia. *Tectonophysics* 259, 1–13.
- Armijo, R., Rauld, R., Thiele, R., Vargas, G., Campos, J., Lacassin, R., Kausel, E. 2010. The West Andean Thrust, the San Ramón Fault, and the seismic hazard for Santiago, Chile. *Tectonics* 29, TC2007.
- Arriagada, C., Ferrando, R., Córdova, L., Morata, D., Roperch, P. 2013. The Maipo Orocline : A first scale structural feature in the Miocene to Recent geodynamic evolution in the central Chilean Andes. *Andean Geol.* 40, 419–437.
- Astaburuaga, D. 2014. Evolución estructural del límite Mesozoico-Cenozoico de la Cordillera Principal entre 35°30' y 36°S, región del Maule, Chile. Tesis de Magister. Universidad de Chile. 140 p.
- Azcuy, C.L., Carrizo, H.A., Caminos, R. 1999. Carbonífero y Pérmico de las Sierras Pampeanas, Famatina, Precordillera, Cordillera Frontal y Bloque San Rafael, en: Caminos, R. (Ed.), Geología Argentina, *Anales* 29 (20). Instituto de Geología y Recursos Minerales, Buenos Aires, Argentina, pp. 261–319.
- Baldis, B., Peralta, S.H. 1999. Silúrico -Devónico de la Precordillera de Cuyo y Bloque San Rafael, en: Caminos, R. (Ed.), Geología Argentina, *Anales* 29 (20). Instituto de Geología y Recursos Minerales, Buenos Aires, Argentina, pp. 215–239.
- Bechis, F., Cristallini, E.O., Giambiagi, L.B., Yagupsky, D.L., Guzmán, C.G., García, V.H. 2014. Transtensional tectonics induced by oblique reactivation of previous lithospheric anisotropies during the Late Triassic to Early Jurassic rifting in the Neuquén basin: Insights from analog models. *J. Geodyn.* 79, 1–17.

Bibliografía

- Bechis, F., Giambiagi, L.B., García, V., Lanés, S., Cristallini, E., Tunik, M. 2010. Kinematic analysis of a transtensional fault system: The Atuel depocenter of the Neuquén basin, southern Central Andes, Argentina. *J. Struct. Geol.* 32, 886–899.
- Bertelloni, C.L., Gurnis, M. 1997. Cenozoic subsidence and uplift of continents from time-varying dynamic topography. *Geology* 25, 735.
- Bordonaro, O. 1999. Cámbrico y Ordovícico de la Precordillera y Bloque San Rafael, en: Caminos, R. (Ed.), *Geología Argentina, Anales* 29 (20). Instituto de Geología y Recursos Minerales, Buenos Aires, Argentina, pp. 189–205.
- Boyce, D., Charrier, R., Tapia, F., Farías, M. 2014. Mid-Cretaceous compressional deformation in Central Chile: The beginning of the Andean building, en: AGU Fall Meeting Abstracts.
- Busby, C.J., Bassett, K.N. 2007. Volcanic facies architecture of an intra-arc strike-slip basin, Santa Rita Mountains, Southern Arizona. *Bull. Volcanol.* 70, 85–103.
- Busby, C.J., Koerner, A.K., Melosh, B.L. 2013. Sierra Crest graben-vent system: A Walker Lane pull apart within the ancestral Cascades arc. *Geosphere* 9, 736–780.
- Centeno-García, E., Busby, C.J., Busby, M., Gehrels, G. 2011. Evolution of the Guerrero composite terrane along the Mexican margin, from extensional fringing arc to contractional continental arc. *Geol. Soc. Am. Bull.* 123, 1776–1797.
- Charrier, R. 1973. Geología de las Provincias O'Higgins y Colchagua. *Boletín, Inst. Investig. Geológicas* 7, 69 p.
- Charrier, R. 1979. El Triásico de Chile y regiones adyacentes en Argentina: Una reconstrucción paleogeográfica y paleoclimática. *Comunicaciones* 26, 1–47.
- Charrier, R., Baeza, O., Elgueta, S., Flynn, J., Gans, P., Kay, S., Muñoz, N., Wyss, A., Zurita, E. 2002. Evidence for Cenozoic extensional basin development and tectonic inversion south of the flat-slab segment, southern Central Andes, Chile (33°–36°S.L.). *J. South Am. Earth Sci.* 15, 117–139.
- Charrier, R., Bustamante, M., Comte, D., Elgueta, S., Flynn, J.J., Iturra, N., Muñoz, N., Pardo, M., Thiele, R., Wyss, A.R. 2005. The Abanico extensional basin: Regional extension, chronology of tectonic inversion and relation to shallow seismic activity and Andean uplift. *Neues Jahrb. Fur Geol. Und Palaontologie-Abhandlungen* 236, 43–77.
- Charrier, R., Croft, D.A., Flynn, J.J., Pinto, L., Wyss, A.R. 2012. Mamíferos fósiles cenozoicos en Chile: Implicancias paleontológicas y tectónicas. Continuación de investigaciones iniciadas por Darwin en América del Sur, en: Veloso, A., Spotorno, A. (Eds.), *Darwin Y La Evolución: Avances En La Universidad de Chile*. Editorial Universitaria, Santiago, Chile, pp. 281–316.
- Charrier, R., Farías, M., Maksaev, V. 2009. Evolución tectónica, paleogeográfica y metalogénica durante el Cenozoico en los Andes de Chile norte y central e implicaciones para las regiones adyacentes de Bolivia y Argentina. *Rev. la Asoc. Geológica Argentina* 65, 5–35.

Bibliografía

- Charrier, R., Pinto, L., Rodríguez, M.P. 2007. Tectonostratigraphic evolution of the Andean Orogen in Chile, en: Moreno, T., Gibbons, W. (Eds.), *The Andes of Chile*. Geological Society, London, pp. 21–114.
- Charrier, R., Ramos, V.A., Tapia, F., Sagripanti, L. 2014. Tectono-stratigraphic evolution of the Andean Orogen between 31 and 37 S (Chile and Western Argentina), en: Sepúlveda, S.A., Giambiagi, L.B., Moreiras, S.M., Pinto, L., Tunik, M., Hoke, G.D. y Farías, M. (Eds.), *Geodynamics Processes in the Andes of Central Chile y Argentina*. Geol. Soc. London, Spec. Publ. 399, doi 10.1144/SP399.20.
- Charrier, R., Wyss, A.R., Flynn, J.J., Swisher III, C.C., Norell, M.A., Zapatta, F., McKenna, M.C., Novacek, M.J. 1996. New evidence for Late Mesozoic-Early Cenozoic evolution of the Central Chile. *J. South Am. Earth Sci.* 9, 393–422.
- Contreras-Reyes, E., Flueh, E.R., Grevemeyer, I. 2010. Tectonic control on sediment accretion and subduction off south central Chile: Implications for coseismic rupture processes of the 1960 and 2010 megathrust earthquakes. *Tectonics* 29.
- Contreras-Reyes, E., Grevemeyer, I., Flueh, E.R., Reichert, C. 2008. Upper lithospheric structure of the subduction zone offshore of southern Arauco peninsula, Chile, at 38°S. *J. Geophys. Res.* 113, B07303.
- Dahlen, F.A., Suppe, J., Davis, D. 1984. Mechanics of fold-and-thrust belts and accretionary wedges: Cohesive Coulomb Theory. *J. Geophys. Res.* 89, 10087.
- Davidson, J. 1971. Tectónica y paleogeografía de la Cordillera Principal en el área de las Nacientes del Teno Curicó, Chile. Memoria de Título. Universidad de Chile. 160 p.
- Davidson, J., Vicente, J.-C. 1973. Características paleogeográficas y estructurales del área fronteriza de las nacientes del Teno (Chile) y Santa Elena (Argentina) (Cordillera Principal, 35° a 35°15' de latitud sur), en: V Congreso Geológico Argentino. pp. 11–55.
- Dávila, F.M., Lithgow-Bertelloni, C. 2013. Dynamic topography in South America. *J. South Am. Earth Sci.* 43, 127–144.
- Davis, D., Suppe, J., Dahlen, F.A. 1983. Mechanics of fold-and-thrust belts and accretionary wedges. *J. Geophys. Res. Solid Earth* 88, 1153–1172.
- DeCelles, P.G., Giles, K.A. 1996. Foreland basin systems. *Basin Res.* 8, 105–123.
- Deckart, K., Hervé, F., Fanning, M., Ramírez, V., Calderón, M., Godoy, E. 2014. U-Pb Geochronology and Hf-O Isotopes of zircons from the Pennsylvanian Coastal Batholith, South-Central Chile. *Andean Geol.* 41, 49–82.
- DeMets, C., Gordon, R.G., Argus, D.F. 2010. Geologically current plate motions. *Geophys. J. Int.* 181, 1–80.

Bibliografía

- Di Giulio, A., Ronchi, A. Sanfilippo, A., Tiepolo, M., Pimentel, M., Ramos, V.A., 2012. Detrital zircon provenance from the Neuquén Basin (south-central Andes): Cretaceous geodynamic evolution and sedimentary response in a retroarc-foreland basin. *Geology* 40, 559–562.
- Dickinson, W.R., Gehrels, G.E. 2009. Use of U–Pb ages of detrital zircons to infer maximum depositional ages of strata: A test against a Colorado Plateau Mesozoic database. *Earth Planet. Sci. Lett.* 288, 115–125.
- Dimieri, L.V. 1997. Tectonic wedge geometry at Bardas Blancas, southern Andes (36 °S), Argentina. *J. Struct. Geol.* 19, 1419–1422.
- Doglioni, C., Carminati, E., Cuffaro, M., Scrocca, D. 2007. Subduction kinematics and dynamic constraints. *Earth-Science Rev.* 83, 125–175.
- Doglioni, C., Tonarini, S., Innocenti, F. 2009. Mantle wedge asymmetries and geochemical signatures along W- and E–NE-directed subduction zones. *Lithos* 113, 179–189.
- Espizúa, L.E. 2002. Late Pleistocene and Holocene glacier fluctuations in the Mendoza Andes, Argentina, en: Casassa, G., Sepúlveda, F., Sinclair, R.M. (Eds.), *The Patagonian Icefields: A Unique Natural Laboratory for Environmental and Climate Change Studies*. Springer Berlin Heidelberg, pp. 55–65.
- Espizúa, L.E. 2005. Holocene glacier chronology of Valenzuela Valley, Mendoza Andes, Argentina. *The Holocene* 15, 1079–1085.
- Faccenna, C., Becker, T.W., Miller, M.S., Serpelloni, E., Willett, S.D. 2014. Isostasy, dynamic topography, and the elevation of the Apennines of Italy. *Earth Planet. Sci. Lett.* 407, 163–174.
- Farías, M., Charrier, R., Carretier, S., Martinod, J., Fock, A., Campbell, D., Cáceres, J., Comte, D. 2008. Late Miocene high and rapid surface uplift and its erosional response in the Andes of central Chile (33°–35°S). *Tectonics* 27.
- Farías, M., Comte, D., Charrier, R., Martinod, J., David, C., Tassara, A., Tapia, F., Fock, A. 2010. Crustal-scale structural architecture in central Chile based on seismicity and surface geology: Implications for Andean mountain building. *Tectonics* 29.
- Farías, M., Charrier, R., Carretier, S., Tapia, F., Astaburuaga, D., Puratic, J., Rodríguez, M., Urresty, C., Garrido, G. 2012. Contribución de largo-plazo de la segmentación climática en Chile Central a la construcción Andina, en: XIII Congreso Geológico Chileno, pp. 191-193.
- Fennell, L., Chiachiarelli, F., Orts, D., Echaurren, A., Kietzmann, D., Rojas Vera, E., Folguera, A. 2014. Levantamiento cretácico superior de la faja plegada y corrida de Malargüe: Evidencias de crecimiento en el Gr. Neuquén, en XIX Congreso Geológico Argentino. Actas electrónicas.
- Flynn, J.J., Charrier, R., Croft, D.A., Wyss, A.R. 2012. Cenozoic Andean faunas: shedding new light on South American mammal evolution, biogeography, environments and tectónics, en: Patterson, B.D., Costa, L.P. (Eds.), *Bones, Clones, and Biomes*. The University of Chicago Press, Chicago & London, pp. 51–75.

Bibliografía

- Flynn, J.J., Wyss, A.R., Croft, D.A., Charrier, R. 2003. The Tinguiririca Fauna, Chile: biochronology, paleoecology, biogeography, and a new earliest Oligocene South American Land Mammal "Age". *Palaeogeogr. Palaeoclimatol. Palaeoecol.* 195, 229–259.
- Fock, A. 2005. Cronología y Tectónica de la Exhumación en el Neógeno de los Andes de Chile Central entre los 33° y los 34°S. Tesis de Magister. Universidad de Chile. 235 p.
- Fock, A., Charrier, R., Farías, M., Muñoz, M.A. 2006. Fallas de vergencia oeste en la Cordillera Principal de Chile Central: Inversión de la cuenca de Abanico. Asoc. Geológica Argentina, Ser. Publicación Espec. 6.
- Folguera, A., Alasonati Tašárová, Z., Götze, H.-J., Rojas Vera, E., Giménez, M., Ramos, V.A. 2012. Retroarc extension in the last 6 Ma in the South-Central Andes (36°S–40°S) evaluated through a 3-D gravity modelling. *J. South Am. Earth Sci.* 40, 23–37.
- Folguera, A., Bottesi, G., Zapata, T., Ramos, V.A. 2008. Crustal collapse in the Andean backarc since 2 Ma: Tromen volcanic plateau, Southern Central Andes (36°40'–37°30'S). *Tectonophysics* 459, 140–160.
- Folguera, A., Orts, D., Spagnuolo, M.G., Vera, E.R., Litvak, V., Sagripanti, L., Ramos, M.E., Ramos, V.A. 2011. A review of Late Cretaceous to Quaternary palaeogeography of the southern Andes. *Biol. J. Linn. Soc.* 103, 250–268.
- Folguera, A., Rojas Vera, E., Bottesi, G., Zamora Valcarce, G., Ramos, V.A. 2010. The Loncopué Trough: A Cenozoic basin produced by extension in the southern Central Andes. *J. Geodyn.* 49, 287–295.
- Folguera, A., Zapata, T., Ramos, V.A. 2006. Late Cenozoic extension and the evolution of the Neuquén Andes, en: Kay, S.M., Ramos, V.A. (Eds.), *Evolution of an Andean Margin: A Tectonic and Magmatic View from the Andes to the Neuquén Basin (35°-39°S Lat)*. Geological Society of America, Special Papers 407, pp. 267–285.
- Fuentes, F. 2004. Petrología y metamorfismo de muy bajo grado de unidades volcánicas Oligoceno-Miocenas en la ladera occidental de los Andes de Chile central (33°S). Tesis de Doctorado. Universidad de Chile. 407 p.
- Gansser, A. 1973. Facts and theories on the Andes. *Journal Geological Society of London* 129: 93–131.
- Gans, C.R., Beck, S.L., Zandt, G., Gilbert, H., Alvarado, P., Anderson, M., Linkimer, L. 2011. Continental and oceanic crustal structure of the Pampean flat slab region, western Argentina, using receiver function analysis: new high-resolution results. *Geophys. J. Int.* 186, 45–58.
- Gerbault, M., Cembrano, J., Mpodozis, C., Farías, M., Pardo, M. 2009. Continental margin deformation along the Andean subduction zone: Thermo-mechanical models. *Phys. Earth Planet. Inter.* 177, 180–205.

Bibliografía

- Giambiagi, L.B., Bechis, F., Garcia, V.H., Clark, A.H. 2008. Temporal and spatial relationships of thick- and thin-skinned deformation: A case study from the Malargüe fold-and-thrust belt, southern Central Andes. *Tectonophysics* 459, 123–139.
- Giambiagi, L.B., Ghiglione, M., Cristallini, E., Bottesi, G. 2009. Kinematic models of basement/cover interaction: Insights from the Malargüe fold and thrust belt, Mendoza, Argentina. *J. Struct. Geol.* 31, 1443–1457.
- Giambiagi, L.B., Mescua, J., Bechis, F., Tassara, A., Hoke, G.D. 2012. Thrust belts of the southern Central Andes: Along-strike variations in shortening, topography, crustal geometry, and denudation. *Geol. Soc. Am. Bull.* 124, 1339–1351.
- Giambiagi, L.B., Ramos, V.A. 2002. Structural evolution of the Andes in a transitional zone between flat and normal subduction ($33^{\circ}30'$ – $33^{\circ}45'$ S), Argentina and Chile. *J. South Am. Earth Sci.* 15, 101–116.
- Giambiagi, L.B., Suriano, J., Mescua, J.F. 2005. Extensión multiepisódica durante el Jurásico temprano en el depocentro Atuel de la cuenca neuquina. *Rev. la Asoc. Geológica Argentina* 60, 524–534.
- Giambiagi, L.B., Tassara, A., Mescua, J., Tunik, M., Alvarez, P.P., Godoy, E., Hoke, G.D., Pinto, L., Spagnotto, S., Porras, H., Tapia, F., Jara, P., Bechis, F., Garcia, V.H., Suriano, J., Moreiras, S.M., Pagano, S.D. 2014. Evolution of shallow and deep structures along the Maipo-Tunuyan transect (33° – 40° S): from the Pacific coast to the Andean foreland, en: Sepúlveda, S.A., Giambiagi, L.B., Moreiras, S.M., Pinto, L., Tunik, M., Hoke, G.D. y Farías, M. (Eds), *Geodynamics Processes in the Andes of Central Chile y Argentina*. Geol. Soc. London, Spec. Publ. 399, doi 10.1144/SP399.14.
- González, A. 2008. Análisis estructural entre los valles del río Tinguiririca y Teno, Cordillera Principal de Chile Central: Microsismosidad y Geología Superficial. Memoria de Título. Universidad de Chile. 90 p.
- González Díaz, E.F. 1972. Descripción Geológica de la Hoja 27d, San Rafael, Provincia de Mendoza. Serv. Geológico Min. Argentino. Boletín 132, 1–127.
- González, O., Vergara, M. 1962. Reconocimiento geológico de la Cordillera de los Andes entre los paralelos 35° y 38° S. Inst. Investig. Geológicas 1.
- Gregori, D., Benedini, L. 2013. The Cordon del Portillo Permian magmatism, Mendoza, Argentina, plutonic and volcanic sequences at the western margin of Gondwana. *J. South Am. Earth Sci.* 42, 61–73.
- Guillaume, B., Gautheron, C., Simon-Labréteau, T., Martinod, J., Roddaz, M., Douville, E. 2013. Dynamic topography control on Patagonian relief evolution as inferred from low temperature thermochronology. *Earth Planet. Sci. Lett.* 364, 157–167.

Bibliografía

- Guillaume, B., Moroni, M., Funiciello, F., Martinod, J., Faccenna, C. 2010. Mantle flow and dynamic topography associated with slab window opening: Insights from laboratory models. *Tectonophysics* 496, 83–98.
- Gurnis, M. 1993. Phanerozoic marine inundation of continents driven by dynamic topography above subducting slabs. *Nature* 364, 589–593.
- Gutscher, M.-A. 2002. Andean subduction styles and their effect on thermal structure and interplate coupling. *J. South Am. Earth Sci.* 15, 3–10.
- Heredia, N., Farias, P., García-sansegundo, J., Giambiagi, L.B. 2012. The Basement of the Andean Frontal Cordillera in the Cordón del Plata. *Andean Geol.* 39, 242–257.
- Hervé, F., Calderón, M., Fanning, C.M., Pankhurst, R.J., Godoy, E. 2013. Provenance variations in the Late Paleozoic accretionary complex of central Chile as indicated by detrital zircons. *Gondwana Res.* 23, 1122–1135.
- Heuret, A., Funiciello, F., Faccenna, C., Lallemand, S. 2007. Plate kinematics, slab shape and back-arc stress: A comparison between laboratory models and current subduction zones. *Earth Planet. Sci. Lett.* 256, 473–483.
- Heuret, A., Lallemand, S. 2005. Plate motions, slab dynamics and back-arc deformation. *Phys. Earth Planet. Inter.* 149, 31–51.
- Hevia, A. 2014. Evolución tectono-estratigráfica de depósitos cenozoicos en la cuenca del río Teno, vertiente occidental de la Cordillera Principal. Memoria de Título. Universidad de Chile. 63 p.
- Hoke, G.D., Gruber, N.R., Mescua, J.F., Giambiagi, L.B., Fitzgerald, P.G., Metcalf, J.R. 2014. Near pure surface uplift of the Argentine Frontal Cordillera: insights from (U-Th)/He thermochronometry and geomorphic analysis, en: Sepúlveda, S.A., Giambiagi, L.B., Moreiras, S.M., Pinto, L., Tunik, M., Hoke, G:D. y Farías, M. (Eds), *Geodynamics Processes in the Andes of Central Chile y Argentina*. Geol. Soc. London, Spec. Publ. 399, doi 10.1144/SP399.4.
- Husson, L. 2006. Dynamic topography above retreating subduction zones. *Geology* 34, 741–744.
- Japas, M.S., Salvarredi, J.A., Kleiman, L.E. 2008. Control estructural en la distribución de las mineralizaciones de uranio del ciclo Choiyoi, bloque de San Rafael, Mendoza . *Rev. la Asoc. Geológica Argentina* 63 , 204–212.
- Jarrard, R.D. 1986. Relations among subduction parameters. *Rev. Geophys.* 24, 217.
- Jordan, T.E., Burns, W.M., Veiga, R., Pangaro, F., Copeland, P., Kelley, S., Mpodozis, C. 2001. Extension and basin formation in the southern Andes caused by increased convergence rate: A mid-Cenozoic trigger for the Andes. *Tectonics* 20, 308–324.
- Karlstrom, L., Lee, C.-T.A., Manga, M. 2014. The role of magmatically driven lithospheric thickening on arc front migration. *Geochemistry, Geophys. Geosystems* 15.

Bibliografía

- Kay., S.M., Burns, W.M., Copeland, P., Mancilla, O. 2006. Upper Cretaceous to Holocene magmatism and evidence for transient Miocene shallowing of the Andean subduction zone under the Northern Neuquén Basin. en: Kay, S.M. y Ramos, V. (eds) Evolution of an Andean margin: A tectonic and magmatic view from the Andes to the Neuquén Basin (35°S-39°S lat). Geological Society of America Special Papers 407, 19-60.
- Kay, S.M., Godoy, E., Kurtz, A. 2005. Episodic arc migration, crustal thickening, subduction erosion, and magmatism in the south-central Andes. *Geol. Soc. Am. Bull.* 117, 67-88.
- Kay, S.M., Ramos, V.A., Mpodozis, C., Sruoga, P. 1989. Late Paleozoic to Jurassic silicic magmatism at the Gondwana margin: Analogy to the Middle Proterozoic in North America? *Geology* 17, 324-328.
- Kley, J., Monaldi, C.R., Salfity, J.A. 1999. Along-strike segmentation of the Andean foreland: causes and consequences. *Tectonophysics* 301, 75-94.
- Klohn, C. 1960. Geología de la Cordillera de los Andes de Chile Central, Provincia de Santiago, Colchagua y Curicó. *Boletín, Inst. Investig. Geológicas* 8, 95 p.
- Kozlowsky, E., Manceda, R., Ramos, V.A. 1993. Estructura, en: Ramos, V.A. (Ed.), Geología Y Recursos Naturales de La Provincia de Mendoza. XII Congreso Geológico Argentino. Mendoza, pp. 235-256.
- Lallemand, S., Heuret, A., Faccenna, C., Funiciello, F. 2008. Subduction dynamics as revealed by trench migration. *Tectonics* 27.
- Lamb, S., Davis, P. 2003. Cenozoic climate change as a possible cause for the rise of the Andes. *Nature* 425, 792-797.
- Legarreta, L., Kozlowsky, E. 1984. Secciones condensadas del Jurásico-Cretácico de los Andes del Sur de Mendoza: Estratigrafía y significado tectonosedimentario, en: IX Congreso Geológico Argentino. pp. 286-297.
- Malbran, F. 1986. Estudio Geológico-Estructural del Área del río Clarillo con énfasis en la Formación Coya-Machalí, Hoya del río Tinguiririca, Chile. Memoria de Título. Universidad de Chile. 221 p.
- Manceda, R., Figueroa, D. 1995. Inversion of the Mesozoic Neuquén Rift in the Malargüe Fold and Thrust Belt, Mendoza, Argentina, en: Tankard, A.J., Suárez S., R., Welsink, H.J. (Eds.), Petroleum Basin of South America. AAPG Memoir 62, pp. 369-382.
- Martínez, F., Arriagada, C., Valdivia, R., Peña, M. 2014. El rol del basamento pre-rift durante la deformación andina: nuevas ideas extraídas del estilo “thick-skinned” en la Cordillera Frontal del norte de Chile (27°-28°S), en: XIX Congreso Geológico Argentino. Córdoba, Argentina.
- Martinod, J., Husson, L., Roperch, P., Guillaume, B., Espurt, N. 2010. Horizontal subduction zones, convergence velocity and the building of the Andes. *Earth Planet. Sci. Lett.* 299, 299-309.

Bibliografía

- Mescua, J.F., Giambiagi, L.B., Ramos, V.A. 2013. Late Cretaceous Uplift in the Malargüe fold-and-thrust belt (35° S), southern Central Andes of Argentina and Chile. *Andean Geol.* 40, 102–116.
- Mescua, J.F., Giambiagi, L.B., Tassara, A., Gimenez, M., Ramos, V.A. 2014. Influence of pre-Andean history over Cenozoic foreland deformation: Structural styles in the Malargüe fold-and-thrust belt at 35° S, Andes of Argentina. *Geosphere* 1–25.
- Métois, M., Socquet, a., Vigny, C. 2012. Interseismic coupling, segmentation and mechanical behavior of the central Chile subduction zone. *J. Geophys. Res. Solid Earth* 117.
- Mitrovica, J., Beaumont, C., Jarvis, G. 1989. Tilting of continental interiors by the dynamical effects of subduction. *Tectonics* 8, 1079–1094.
- Montecinos, P., Scharer, U., Vergara, M., Aguirre, L. 2008. Lithospheric Origin of Oligocene-Miocene Magmatism in Central Chile: U-Pb Ages and Sr-Pb-Hf Isotope Composition of Minerals. *J. Petrol.* 49, 555–580.
- Mooney, W.D., Laske, G., Masters, T.G. 1998. CRUST 5.1: A global crustal model at $5^{\circ} \times 5^{\circ}$. *J. Geophys. Res.* 103, 727–747.
- Moscoso, E., Greve, I., Contreras-Reyes, E., Flueh, E.R., Dzierma, Y., Rabbel, W., Thorwart, M. 2011. Revealing the deep structure and rupture plane of the 2010 Maule, Chile earthquake (Mw=8.8) using wide angle seismic data. *Earth Planet. Sci. Lett.* 307, 147–155.
- Mosolf, J.G. 2013. Stratigraphy, structure, and geochronology of the Abanico Formation in the Principal Cordillera, central Chile: Evidence of protracted volcanism and implications for Andean tectonics. Ph.D Thesis. University of California.
- Mosolf, J.G., Gans, P.B., Wyss, A.R., Cottle, J.M., 2011. Detailed geologic field mapping and radiometric dating of the Abanico Formation in the Principal Cordillera, central Chile: Evidence of protracted volcanism and implications for Cenozoic tectonics, en: AGU Fall Meeting Abstracts. abstract #V13C–2623.
- Mpodozis, C., Ramos, V.A. 1989. The Andes of Chile and Argentina, en: Erickson, G.E. (Ed.), *Geology of the Andes and Its Relation to Hydrocarbon and Mineral Resources*. Earth Sci. Ser, pp. 59–90.
- Mulcahy, P., Chen, C., Kay, S.M., Brown, L.D., Isacks, B.L., Sandvol, E., Heit, B., Yuan, X., Coira, B.L. 2014. Central Andean mantle and crustal seismicity beneath the Southern Puna plateau and the northern margin of the Chilean-Pampean flat slab. *Tectonics* 33, 1636–1658.
- Muñoz, M., Farías, M., Charrier, R., Fanning, C.M., Polve, M., Deckart, K. 2013. Isotopic shifts in the Cenozoic Andean arc of central Chile: Records of an evolving basement throughout cordilleran arc mountain building. *Geology* 41, 931–934.
- Muñoz, M., Fuentes, F., Vergara, M., Aguirre, L., Olov Nyström, J., Féraud, G., Demant, A. 2006. Abanico East Formation: petrology and geochemistry of volcanic rocks behind the Cenozoic arc

- front in the Andean Cordillera, central Chile ($33^{\circ}50'S$). *Rev. geológica Chilena* Chile 33, 109–140.
- Naipauer, M., Tapia, F., Farías, M., Pimentel, M., Ramos, V.A. 2014. Evolución Mesozoica de las áreas de aporte sedimentario en el sur de los Andes Centrales: El registro de las Edades U-Pb en circones, en: XIX Congreso Geológico Argentino. Córdoba, Argentina.
- Nyström, J.O., Vergara, M., Morata, D., Levi, B. 2003. Tertiary volcanism during extension in the Andean foothills of central Chile ($33^{\circ}15'-33^{\circ}45'S$). *Geol. Soc. Am. Bull.* 115, 1523–1537.
- Oliveros, V., Labbé, M., Rossel, P., Charrier, R., Encinas, A. 2012. Late Jurassic paleogeographic evolution of the Andean back-arc basin: New constraints from the Lagunillas Formation, northern Chile ($27^{\circ}30'-28^{\circ}30'S$). *J. South Am. Earth Sci.* 37, 25–40.
- Orts, D.L., Folguera, A., Giménez, M., Ramos, V.A. 2012. Variable structural controls through time in the Southern Central Andes ($\sim 36^{\circ}\text{S}$). *Andean Geol.* 39, 220–241.
- Orts, S., Ramos, V.A. 2006. Evidence of Middle to Late Cretaceous compressive deformation en the High Andes of Mendoza, Argentina. *Backbone of the Americas Meeting, Abstracts with Programs* 5: p. 65. Mendoza.
- Pardo-Casas, F., Molnar, P. 1987. Relative motion of the Nazca (Farallon) and South American plates since Late Cretaceous time. *Tectonics* 6, 233–248.
- Pilger, R.H. 1984. Cenozoic plate kinematics, subduction and magmatism: South American Andes. *J. Geol. Soc.* 141, 793–802.
- Piquer, J., Castelli, J.C., Charrier, R., Yáñez, G. 2010. El Cenozoico del alto río Teno, Cordillera Principal, Chile central: estratigrafía, plutonismo y su relación con estructuras profundas. *Andean Geol.* 37, 32–53.
- Porras, H. 2013. Registro del levantamiento de la Cordillera de los Andes durante el Mioceno basado en las características geoquímicas y mineralógicas de los depósitos sintectónicos de la Cuenca del Alto Tunuyán ($33^{\circ}30'S$, Argentina). Tesis de Magíster. Universidad de Chile. 257 p.
- Puratich, J. 2010. Influencia del desarrollo glaciar en la evolución morfológica de la alta Cordillera de los Andes en la parte norte de la región del Maule ($35^{\circ}15'S$ - $35^{\circ}50'S$). Memoria de Título. Universidad de Chile. 122 p.
- Radic, J.P. 2010. Las cuencas cenozoicas y su control en el volcanismo de los Complejos Nevados de Chillán y Copahue-Callaqui (Andes del Sur, $36\text{-}39^{\circ}\text{S}$) . *Andean Geol.* 37 , 220–246.
- Ramos, V.A. 2010. The tectonic regime along the Andes: Present-day and Mesozoic regimes. *Geol. J.* 45, 2–25.
- Ramos, V.A., Cegarra, M., Cristallini, E. 1996. Cenozoic tectonics of the High Andes of west-central Argentina ($30\text{-}36^{\circ}\text{S}$ latitude). *Tectonophysics* 259, 185–200.

- Ramos, V.A., Folguera, A. 2005. Tectonic evolution of the Andes of Neuquén: constraints derived from the magmatic arc and foreland deformation, en: Veiga, G.D., Spalletti, L.A., Howell, J., Schwarz, E. (Eds.), *The Neuquén Basin: A Case Study in Sequence Stratigraphy and Basin Dinamics*. Geological Society of America, Special Papers 252, pp. 15–35.
- Ramos, V.A., Folguera, A. 2011. Payenia volcanic province in the Southern Andes: An appraisal of an exceptional Quaternary tectonic setting. *J. Volcanol. Geotherm. Res.* 201, 53–64.
- Ramos, V.A., Kay, S.M. 2006. Overview of the tectonic evolution of the southern Central Andes of Mendoza and Neuquén (35°–39°S latitude), en: Kay, S.M., Ramos, V.A. (Eds.), *Evolution of an Andean Margin: A Tectonic and Magmatic View from the Andes to the Neuquén Basin (35°–39°S)*. Geological Society of America Special Papers 407, pp. 1–17.
- Ramos, V.A., Litvak, V.D., Folguera, A., Spagnuolo, M.G. 2014. An Andean tectonic cycle: From crustal thickening to extension in a thin crust (34°–37°SL). *Geosci. Front* 5 (3). 351–357.
- Ramos, V.A., Zapata, T., Cristallini, E.O., Introcaso, A. 2004. The Andean thrust system—Latitudinal variations in structural styles and orogenic shortening, en: McClay, K. (Ed.), *Thrust Tectonics and Hydrocarbon System*. AAPG Memoir, pp. 30–50.
- Ricard, Y., Richards, M., Lithgow-Bertelloni, C., Le Stunff, Y. 1993. A geodynamic model of mantle density heterogeneity. *J. Geophys. Res.* 98, 21895–21909.
- Rojas Vera, E.A., Folguera, A., Zamora Valcarce, G., Bottesi, G., Ramos, V.A. 2014. Structure and development of the Andean system between 36° and 39°S. *J. Geodyn.* 73, 34–52.
- Rojas Vera, E.A., Folguera, A., Valcarce, G.Z., Giménez, M., Ruiz, F., Martínez, P., Bottesi, G., Ramos, V.A. 2010. Neogene to Quaternary extensional reactivation of a fold and thrust belt: The Agrio belt in the Southern Central Andes and its relation to the Loncopué trough (38°–39°S). *Tectonophysics* 492, 279–294.
- Rossel, P., Oliveros, V., Mescua, J., Tapia, F., Ducea, M.N., Calderón, S., Charrier, R., Hoffman, D. 2014. The Upper Jurassic volcanism of the Río Damas-Tordillo Formation (33°–35,5°S): Insights on petrogenesis, chronology, provenance and tectonic implications. *Andean Geol.* 41, 529–557.
- Schellart, W.P. 2008. Overriding plate shortening and extension above subduction zones: A parametric study to explain formation of the Andes Mountains. *Geol. Soc. Am. Bull.* 120, 1441–1454.
- Schiuma, M., Llambías, E.J. 2008. New ages and chemical analysis on lower Jurassic volcanism close to the Dorsal de Huincul, Neuquén. *Rev. la Asoc. Geológica Argentina* 63, 644–652.
- Scisciani, V., Calamita, F., Tavarnelli, E., Rusciadelli, G., Ori, G.G., Paltrinieri, W. 2001. Foreland-dipping normal faults in the inner edges of syn-orogenic basins: a case from the Central Apennines, Italy. *Tectonophysics* 330, 211–224.

Bibliografía

- Sellés, D., Gana, P. 2001. Geología del área de Talagante-San Francisco de Mostazal. Escala 1:100.000. Servicio Nacional de Geología y Minería, Serie Geológica Básica, v. 4.
- Sernageomin, 2003. Carta Geológica de Chile (escala 1:1.000.000). Servicio Nacional de Geología y Minería, Publicación Geológica Digital 4.
- Sigismondi, M.E. 2011. El estiramiento cortical de la Cuenca Neuquina: Modelo de cizalla simple, en: XVIII Congreso Geológico Argentino. Neuquén, pp. 858–859.
- Silver, P.G. 1998. Coupling of South American and African Plate Motion and Plate Deformation. *Science* 279, 60–63.
- Silvestro, J., Kraemer, P. 2005. Evolución de las cuencas sinorogénicas de la Cordillera Principal entre 35°-36° S, Malargüe. *Rev. la Asoc. Geológica Argentina* 60, 627–643.
- Sobolev, S. V, Babeyko, A.Y., Koulakov, I., Oncken, O. 2006. Mechanism of the Andean Orogeny: Insight from Numerical Modeling, en: Oncken, O., Chong, G., Franz, G., Giese, P., Götze, H.-J., Ramos, V., Strecker, M., Wigger, P. (Eds.), *The Andes, Active Subduction Orogeny*, Frontiers in Earth Sciences. Springer, pp. 513–535.
- Somoza, R. 1998. Update Nazca (Farallon)-South America relative motions during the last 40 My: implication for mountain building in the central Andean region. *J. South Am. Earth Sci.* 11, 211–215.
- Somoza, R., Ghidella, M.E. 2005. Convergencia en el margen occidental de América del Sur durante el Cenozoico: subducción de las placas de Nazca, Farallón y Aluk. *Rev. la Asoc. Geológica Argentina* 60, 797–809.
- Somoza, R., Ghidella, M.E. 2012. Late Cretaceous to recent plate motions in western South America revisited. *Earth Planet. Sci. Lett.* 331-332, 152–163.
- Somoza, R., Zaffarana, C.B. 2008. Mid-Cretaceous polar standstill of South America, motion of the Atlantic hotspots and the birth of the Andean cordillera. *Earth Planet. Sci. Lett.* 271, 267–277.
- Spagnuolo, M.G., Folguera, A., Litvak, V., Vera, E. a. R., Ramos, V.A. 2012a. Late Cretaceous arc rocks in the Andean retroarc region at 36.5°S: Evidence supporting a Late Cretaceous slab shallowing. *J. South Am. Earth Sci.* 38, 44–56.
- Spagnuolo, M.G., Litvak, V.D., Folguera, A., Bottesi, G., Ramos, V.A. 2012b. Neogene magmatic expansion and mountain building processes in the southern Central Andes, 36–37°S, Argentina. *J. Geodyn.* 53, 81–94.
- Spikings, R. Dungan, M., Foeken, J., Carter, A., Page, L., Stuart, F., 2008. Tectonic response of the central Chilean margin (35-38° S) to the collision and subduction of heterogeneous oceanic crust: a thermochronological study. *J. Geol. Soc. London.* 165, 941–953.
- Suppe, J. 1983. Geometry and kinematics of fault-bend folding. *Am J Sci* 283, 684–721.

Bibliografía

- Tapia, F. 2010. Análisis estructural del sector occidental de la faja plegada y corrida de Malargüe en el curso superior del Río Colorado de Lontué ($35^{\circ}18'$ y $35^{\circ}23'S$), Región del Maule, Chile. Memoria de Título. Universidad de Chile. 102 p.
- Tassara, A. 2005. Interaction between the Nazca and South American plates and formation of the Altiplano–Puna plateau: Review of a flexural analysis along the Andean margin (15° – 34° S). *Tectonophysics* 399, 39–57.
- Tassara, A., Echaurren, A. 2012. Anatomy of the Andean subduction zone: three-dimensional density model upgraded and compared against global-scale models. *Geophys. J. Int.* 189, 161–168.
- Tassara, A., Yáñez, G.A. 2003. Relación entre el espesor elástico de la litosfera y la segmentación tectónica del margen andino (15–47 S). *Rev. geológica Chile* 30, 159–186.
- Thiele, R. 1980. Hoja Santiago, Región Metropolitana. Serv. Nac. Geol. a y Minería, Cart. Geológica Chile 29, 21 p.
- Thomas, H. 1958. Geología de la Cordillera de la Costa entre el valle de La Ligua y la cuesta de Barriga. *Boletín, Inst. Investig. Geológicas* 86.
- Tunik, M., Folguera, A., Naipauer, M., Pimentel, M., Ramos, V.A. 2010. Early uplift and orogenic deformation in the Neuquén Basin: Constraints on the Andean uplift from U–Pb and Hf isotopic data of detrital zircons. *Tectonophysics* 489, 258–273.
- Turienzo, M.M. 2010. Structural style of the Malargüe fold-and-thrust belt at the Diamante River area ($34^{\circ}30'$ – $34^{\circ}50'S$) and its linkage with the Cordillera Frontal, Andes of central Argentina. *J. South Am. Earth Sci.* 29, 537–556.
- Turienzo, M.M., Dimieri, L.L. V., Frisicale, C., Araujo, V., Sánchez, N., Sánchez, N. 2012. Cenozoic structural evolution of the Argentinean Andes at $34^{\circ}40'S$: A close relationship between thick and thin-skinned deformation. *Andean Geol.* 39, 123–139.
- Vennari, V., Lescano, M., Naipauer, M., Aguirre-Urreta, B., Concheyro, A., Schaltegger, U., Armstrong, R., Pimentel, M., Ramos, V. 2014. Jurassic-Cretaceous boundary in the High Andes using high-precision U-Pb data.
- Von Huene, R., Ranero, C.R., Scholl, D.W. 2009. Convergent Margin Structure in High-Quality Geophysical Images and Current Kinematic and Dynamic Models, en: Lallemand, S., Funiciello, F. (Eds.), *Subduction Zone Geodynamics, Frontiers in Earth Sciences*. Springer Berlin Heidelberg, pp. 137–157.
- Wall, R., Sellés, D., Gana, P. 1999. Geología de la Hoja Santiago, área de Tiltil-Santiago, Región Metropolitana. Servicio Nacional de Geología y Minería, Mapa Geológico, v.11.
- Williams, G.D., Powell, C.M., Cooper, M.A. 1989. Geometry and kinematics of inversion tectonics. *Geol. Soc. London, Spec. Publ.* 44, 3–15.

Bibliografía

- Willner, A.P., Thomson, S.N., Kröner, A., Wartho, J.-A., Wijbrans, J., Hervé, F. 2005. Time Markers for the Evolution and Exhumation History of a Late Palaeozoic Paired Metamorphic Belt in North-Central Chile (34° – $35^{\circ}30'S$). *J. Petrol.* 46, 1835–1858.
- Wyss, A.R., Charrier, R., Flynn, J.J. 1996. Fossil mammals as a tool in Andean stratigraphy : dwindling evidence of Late Cretaceous volcanism in the South Central Main Range. *PaleoBios* 17, 13–27.
- Wyss, A.R., Flynn, J.J., Norell, M.A., Swisher III, C.C., Novacek, M.J., McKenna, M.C., Charrier, R. 1994. Paleogene Mammals from the Andes of Central Chile : A Preliminary Taxonomic , Biostratigraphic , and Geochronologic Assessment. *Novitates* 31.
- Yagupsky, D.L., Cristallini, E.O., Fantín, J., Valcarce, G.Z., Bottesi, G., Varadé, R. 2008. Oblique half-graben inversion of the Mesozoic Neuquén Rift in the Malargüe Fold and Thrust Belt, Mendoza, Argentina: New insights from analogue models. *J. Struct. Geol.* 30, 839–853.
- Yáñez, G., Cembrano, J. 2004. Role of viscous plate coupling in the late Tertiary Andean tectonics. *J. Geophys. Res.* 109 (B2).
- Zamora Valcarce, G., Zapata, T. 2005. Estilo estructural del frente de la faja plegada Neuquina a los $37^{\circ}S$. en: VI Congreso de Exploración Y desarrollo de Hidrocarburos. Actas electrónicas
- Zamora Valcarce, G., Zapata, T., del Pino, D., Ansa, A., Pino, D. 2006. Structural evolution and magmatic characteristics of the Agrio fold-and-thrust belt, en: Kay, S.M., Ramos, V.A. (Eds.), Evolution of an Andean Margin: A Tectonic and Magmatic View from the Andes to the Neuquén Basin. Geological Society of America, Special Papers 407, pp. 125–145.
- Zamora Valcarce, G., Zapata, T. 2009. Evolución tectónica del frente andino en Neuquén. *Rev. la Asoc. Geológica Argentina* 65, 192–203.
- Zapata, T., Folguera, A., 2005. Tectonic evolution of the Andean Fold and Thrust Belt of the southern Neuquén Basin, Argentina, en: Veiga, G.D., Spalletti, L.A., Howell, J., Schwarz, E. (Eds.), The Neuquén Basin: Argentina: A Case Study in Sequence Stratigraphy and Basin Dynamics. Geological Society, London, Special Publications 252, pp. 37–56.
- Zapatta, F. 1995. Nuevos antecedentes estratigráficos y estructura del área de Termas del Flaco, valle del río Tinguiririca, VI región, Chile. Universidad de Chile, 122 p.
- Zhong, S., Gurnis, M. 1994. Controls on trench topography from dynamic models of subducted slabs. *J. Geophys. Res. Solid Earth* 99, 15683–15695.

Anexo I

Publicaciones de coautor

Geological Society, London, Special Publications Online First

Tectono-stratigraphic evolution of the Andean Orogen between 31 and 37°S (Chile and Western Argentina)

Reynaldo Charrier, Victor A. Ramos, Felipe Tapia and Lucía Sagripanti

Geological Society, London, Special Publications, first published August 27, 2014; doi 10.1144/SP399.20

Email alerting service	click here to receive free e-mail alerts when new articles cite this article
Permission request	click here to seek permission to re-use all or part of this article
Subscribe	click here to subscribe to Geological Society, London, Special Publications or the Lyell Collection
How to cite	click here for further information about Online First and how to cite articles

Notes

Tectono-stratigraphic evolution of the Andean Orogen between 31 and 37°S (Chile and Western Argentina)

REYNALDO CHARRIER^{1,2*}, VICTOR A. RAMOS³, FELIPE TAPIA¹ & LUCÍA SAGRIPANTI³

¹*Departamento de Geología, Universidad de Chile, Plaza Ercilla 803, Santiago, Chile*

²*Escuela de Ciencias de la Tierra, Universidad Andres Bello, Campus República, Salvador Sanfuentes 2357, Santiago, Chile*

³*Laboratorio de Tectónica Andina, Instituto de Estudios Andinos Don Pablo Groeber, Universidad de Buenos Aires-CONICET, Intendente Güirales 2160, Ciudad Universitaria, C1428EGA, Capital Federal, Buenos Aires, Argentina*

*Corresponding author (e-mail: rcharrie@ing.uchile.cl)

Abstract: In this classic segment, many tectonic processes, like flat-subduction, terrane accretion and steepening of the subduction, among others, provide a robust framework for their understanding. Five orogenic cycles, with variations in location and type of magmatism, tectonic regimes and development of different accretionary prisms, show a complex evolution. Accretion of a continental terrane in the Pampean cycle exhumed lower to middle crust in Early Cambrian. The Ordovician magmatic arc, associated metamorphism and foreland basin formation characterized the Famatinian cycle. In Late Devonian, the collision of Chilenia and associated high-pressure/low-temperature metamorphism contrasts with the late Palaeozoic accretionary prisms. Contractual deformation in Early to Middle Permian was followed by extension and rhyolitic (Choiyoi) magmatism. Triassic to earliest Jurassic rifting was followed by subduction and extension, dominated by Pacific marine ingresses, during Jurassic and Early Cretaceous. The Late Cretaceous was characterized by uplift and exhumation of the Andean Cordillera. An Atlantic ingress occurred in latest Cretaceous. Cenozoic contraction and uplift pulses alternate with Oligocene extension. Late Cenozoic subduction was characterized by the Pampean flat-subduction, the clockwise block tectonic rotations in the normal subduction segments and the magmatism in Payenia. These processes provide evidence that the Andean tectonic model is far from a straightforward geological evolution.

This chapter will focus on the general framework of the Andes along this segment of the orogen, as an introduction to the different specific contributions of the following chapters. This part of the southern Central Andes of Argentina and Chile has received the attention of numerous overviews and syntheses in recent years, such as the publications of Mpodozis & Ramos (1989), Ramos *et al.* (1996b), Ramos (1988b, 1999) and Charrier *et al.* (2007, 2009). However, several articles have been published in recent years that complement and modify the tectonic and palaeogeographic reconstructions and interpretations presented in previous syntheses. Therefore, the objective of this introductory chapter will be to present a brief updated summary, taking into consideration the most recent advances in the geological knowledge of the region.

Tectonic cycles

The continental margin of southern South America was an active plate margin during most of its history. The Neoproterozoic to late Palaeozoic evolution is punctuated by a succession of tectonic regimes in which extension and compression alternate through time. As a result, terrane accretion and westward arc migration alternate with periods of rifting and extensional basin formation. Although accretion of some terranes has been documented until Jurassic time, as in Patagonia (Madre de Dios terrane; Thompson & Hervé 2002), the post-Triassic history is characterized by the eastward retreat of the continental margin and eastward arc migration, attributed to a combination of shallowing of the subducting plate and subduction erosion. The period between the latest Permian and earliest Jurassic

corresponds to an episode of arrested continental drift, which, however, does not mean that subduction along the continental margin ceased. Different palaeogeographic organizations were developed at that time, and a widely distributed magmatism with essentially different affinities occurred. It is therefore possible to differentiate major stages in the

tectonostratigraphic evolution of the Chilean-Argentine Andes, which can be related to the following episodes of supercontinent evolution: (a) breakup of Rodinia; (b) Gondwanaland assembly; and (c) post-Pangaea breakup (Fig. 1).

These stages can in turn be subdivided into shorter tectonic cycles separated from each other

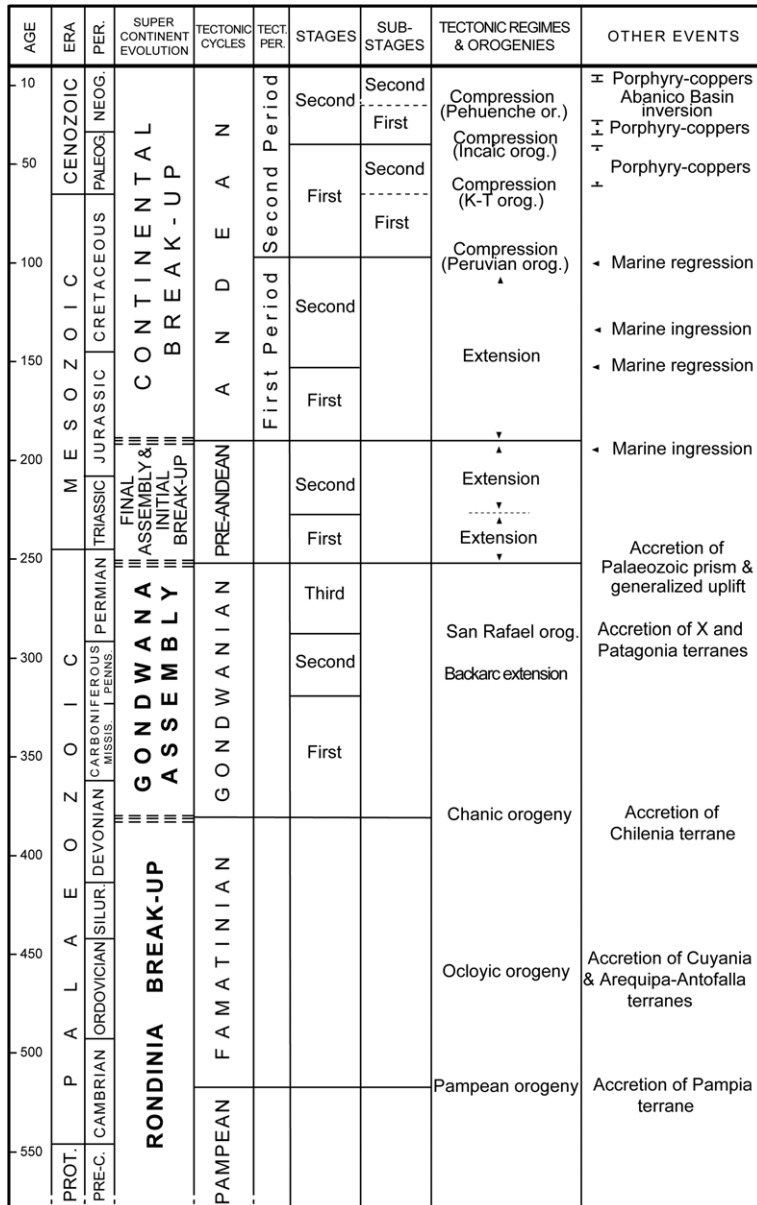


Fig. 1. Tectonic cycles, orogenies and events in the evolution of the continental margin of southern South America compared with the supercontinent evolution.

ANDES OF CENTRAL CHILE AND WESTERN ARGENTINA

by regional unconformities or by significant palaeogeographic changes that indicate the occurrence of drastic tectonic events in the continental margin. These tectonic events have been related to modifications in the dynamics of the lithospheric plates (see James 1971; Rutland 1971; Charrier 1973; Aguirre *et al.* 1974; Frutos 1981; Jordan *et al.* 1983a, 1997; Malumián & Ramos 1984; Ramos *et al.* 1986; Isacks 1988; Ramos 1988a; Mpodozis & Ramos 1989). As a result of that, tectonic cycles have been identified along the western southern South America, which according to Mpodozis & Ramos (1989) and Charrier *et al.* (2007) are (Fig. 1): *Pampean* (Neoproterozoic–Early Cambrian), *Famatinian* (latest Cambrian–Early Devonian), *Gondwanian* (Late Devonian–early Late Permian), *pre-Andean* (latest Permian–earliest Jurassic) and *Andean* (Early Jurassic–Present).

Morphostructural units

The northern part of the analysed segment (31–33°S) is located in the flat-slab subduction segment developed between *c.* 27 and *c.* 33°S. There the passive Juan Fernández Ridge has been subducting the continental margin since *c.* 12 Ma with an eastward dip of *c.* 20° to the east beneath the forearc to almost horizontal beneath the retroarc (Jordan *et al.* 1983a; Yáñez *et al.* 2001; Pardo *et al.* 2002). This Andean segment, known as the Pampean flat-slab segment, is characterized by the absence of recent volcanic activity and of a Central Depression, existing further south in the normal subduction segment (south of 33°S). Therefore, in this segment no differentiation can be made easily between a Coastal and a Principal Cordillera, and the Coastal Cordillera has been extended further east (Rodríguez 2013; Rodríguez *et al.* 2013, 2014). East of this extended Coastal Cordillera, other morphostructural units are developed, which gradually disappear southwards or are not developed further south in the normal subduction segment. These are, from west to east: the Frontal Cordillera, the PreCORDILLERA and the Sierras Pampeanas (Fig. 2). The alignment of the crustal earthquake epicentres parallel to the projection of the subducted Juan Fernández Ridge shows the strong control that this subduction exerted in the more recent morphologic, magmatic and tectonic features of the Andean cordillera in the flat-slab segment (Alvarado *et al.* 2009).

South of the flat-slab subduction segment (south of *c.* 33°S), the Wadati–Benioff zone dips *c.* 30°E (Cahill & Isacks 1992). As indicated, in this segment, a Central Depression is well developed separating the Coastal Cordillera, to the west, from the Principal Cordillera, to the east, with the edifices

of the volcanic arc (Fig. 2). The western flank of the Principal Cordillera is located in Chile, while the eastern flank is located in Argentina.

Pampean tectonic cycle (Neoproterozoic–Early Cambrian)

The Pampean tectonic cycle as proposed by Aceñolaza & Tosselli (1976) includes sedimentation, magmatism and important deformation that took place in Early to Middle Cambrian in northwestern Argentina (Coira *et al.* 1982). The orogenic deformation at that time, in the central segment analysed here (31–37°S), was located along the Eastern Pampean Ranges, and its extension to the south (Fig. 2) (Ramos 1988a; Rapela *et al.* 1998; Chernicoff *et al.* 2012).

The Eastern Sierras Pampeanas comprises an orogenic belt characterized by metamorphic rocks of middle-to-high amphibolite facies, low-grade metapelites and granulite facies meta-basic rocks (Gordillo 1984; Kraemer *et al.* 1995; Rapela *et al.* 1998). Medium-grade para- and ortho-gneisses and schists constitute the dominant lithology; large massifs composed of garnet-cordierite pelitic migmatites are also characteristic (Rapela *et al.* 1998). Geochemical and isotopic studies show a typical calc-alkaline magmatic arc related to subduction (Lira *et al.* 1996; Rapela *et al.* 1998). Ultrabasic rocks dominated by harzburgites, chromitites and serpentinites have been interpreted as a disrupted ophiolitic sequence (Escayola *et al.* 1996; Ramos *et al.* 2000).

This orogenic belt has been interpreted as (a) the result of a collision between a Pampean block against the Río de La Plata Craton (Ramos 1988a; Ramos & Vujovich 1993; Rapela *et al.* 1998); (b) in the context of a subduction of a mid-ocean ridge beneath the palaeo-Pacific Gondwana margin (e.g. Gromet & Simpson 2000; Simpson *et al.* 2003; Piñán-Llamas & Simpson 2006; Schwartz *et al.* 2008); or (c) the result of complex strike-slip tectonics between Kalahari and Río de la Plata craton (Rapela *et al.* 2007; Casquet *et al.* 2012; Spagnuolo *et al.* 2012a).

In recent years more precise studies of the pre- and post-collisional suites seem to indicate that the main episode of deformation is bracketed between 537 and 530 Ma (Iannizzotto *et al.* 2013), and the tectonic evolution comprises a complex geological history to fit all of the observations (Escayola *et al.* 2007; Ramos *et al.* 2010). This model implies a primitive island arc that under western subduction collided against the Río de la Plata Craton by the end of the Ediacaran (Escayola *et al.* 2007). This oceanic terrane of the Eastern Sierras Pampeanas known as the Córdoba terrane

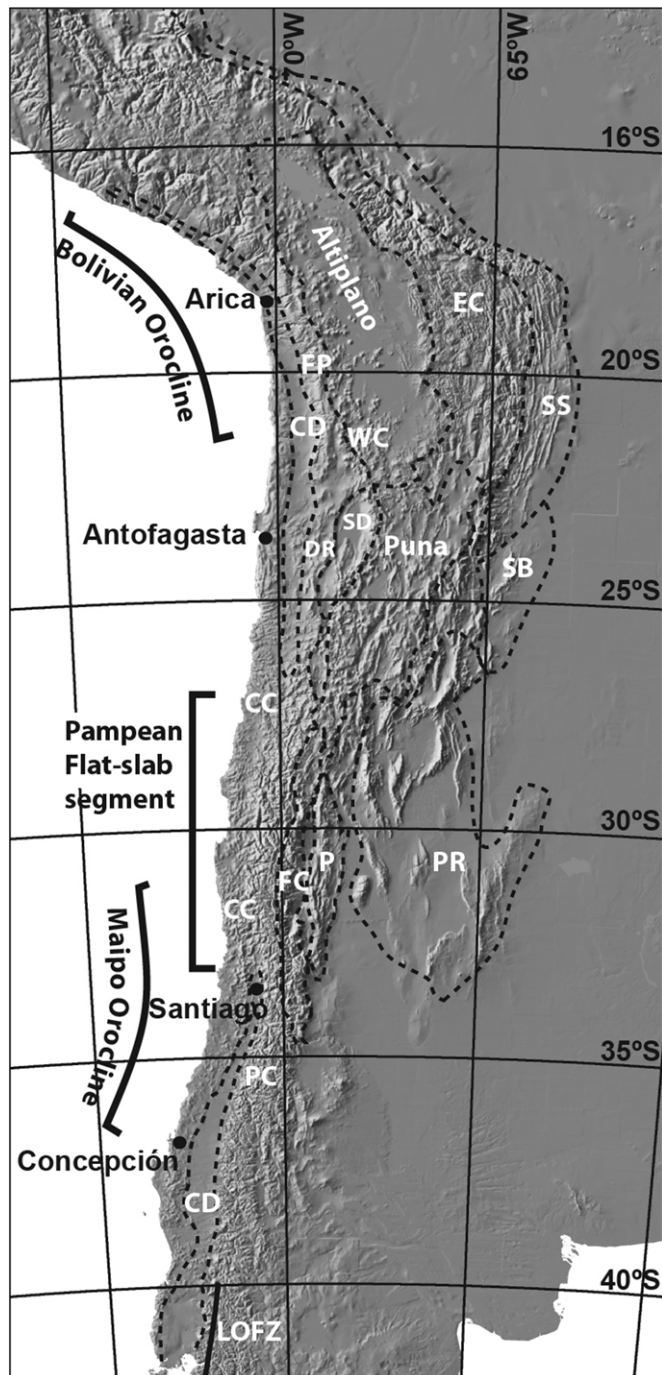


Fig. 2. Digital elevation model of the Andes between 16 and 40°S with indication of the main geographical, tectonic and morphostructural features. Abbreviations: CC, Coastal Cordillera; CD, Central Depression; DR, Domeyko Range; EC, Eastern Cordillera; FC, Frontal Cordillera; FP, Forearc Precordillera (western flank of the Altiplano); LOFZ, Liquiñe–Ofqui Fault Zone; P, Precordillera in Argentina; PC, Principal Cordillera; PR, Pampean Ranges; SB, Santa Barbara System; SD, Salar Depressions; SS, Subandean System; WC, Western Cordillera. Rectangle: Andean region considered in this chapter.

ANDES OF CENTRAL CHILE AND WESTERN ARGENTINA

is composed of several belts of ophiolites (Mutti 1997; Ramos *et al.* 2000, 2010). This collision was followed by the final collision of Pampia through an east-dipping subduction against the Río de la Plata craton as proposed by Kraemer *et al.* (1995), Escayola *et al.* (2007) and Ramos *et al.* (2010). Among the post-collisional effects, the emplacement of mafic bodies of Ocean-Island Basalts (OIB) signature emplaced at about 520 Ma could be interpreted as evidence of slab breakoff (Tibaldi *et al.* 2008), associated with general anatexis and crustal delamination as indicated by extensive rhyolitic plateaux preserved in the northern sector of Eastern Sierras Pampeanas, such as the Oncán Rhyolites and Los Burros Rhyodacites of 532–512 Ma (Leal *et al.* 2004). These regions have been affected by ductile shear deformation along some weakness zones during the early Palaeozoic (Martino 2003).

Famatinian tectonic cycle (Cambrian to Late Devonian)

The Famatinian orogenic cycle as proposed by Aceñolaza & Tosselli (1976) comprises the evolution of two important sedimentary sequences, separated by an important angular unconformity. The basal sequence comprises Early Cambrian to Middle Ordovician carbonatic and clastic platform deposits of the Cuyo Precordillera deformed during the Ocloyic diastrophism at about 460 Ma (Astini *et al.* 1996; Ramos 2004, and references therein). Both sequences were deformed during the Middle to Late Devonian, developing the Chanic unconformity that separates these deposits from the late Palaeozoic sequences. The different sedimentary, magmatic and metamorphic rocks of these two sequences will be described from west to east.

Frontal Cordillera

In Cordón del Carrizalito region, in the southern Frontal Cordillera, north of the Río Diamante valley, is exposed a sequence of turbidites of the Las Lagunitas Formation (Fig. 3) (Volkheimer 1978). Graptolites of Ordovician age have been found in these turbidites, previously interpreted as Carboniferous deposits (Tickyj *et al.* 2009a). These rocks are characterized by low-grade metamorphism, and are intruded by pre-tectonic to syntectonic granitoids such as the Carrizalito Tonalite and Pampa de Los Avestruces Granite deformed during the Chanic orogeny (Tickyj *et al.* 2009b; Tickyj 2011). The studies of García-Sansegundo *et al.* (2014a) described the Chanic structures as west-vergent, in contrast with the east-vergent late Palaeozoic structures.

North of 34°S at Cordón del Plata region, in northern Frontal Cordillera (Fig. 3), Heredia *et al.* (2002, 2012) described the Vallecitos beds, low-grade metamorphic rocks correlated with Devonian turbidites of western Precordillera. These rocks as well as the Las Lagunitas Formation were deformed during the Middle to Late Devonian Chanic deformation.

Exposures of metamorphic basement rocks that include ultrabasic rocks occur within the Frontal Cordillera as a medium-grade unit further south (Polanski 1964, 1972; Bjerg *et al.* 1990; López & Gregori 2004), known as the Guaruaraz Complex (Willner *et al.* 2011). This complex consists of garnet–micaschist and quartzitic schist, metasediments with intercalated lenses of garnet bearing amphibolite with a N- or E-MORB (normal or enriched mid-ocean ridge basalt) geochemical signature, serpentinite with tremolite-/talc-bearing wall rocks and marbles and calc-silicates. Willner *et al.* (2011) interpreted this sequence as related to a high-pressure–low-temperature metamorphism, with a metamorphic peak dated in 385 Ma, followed by decompression and retrograde metamorphism between 348 and 337 Ma, associated with the new stage of subduction along the Pacific margin. These high pressure–low temperature conditions (12–14 kbar–550 °C) are interpreted as a collisional metamorphism, distinctive from the subduction complexes of the western series (basal accretion) younger than 307 Ma and the eastern series (frontal accretion) younger than 330–345 Ma (Hervé *et al.* 2013).

Cuyo Precordillera

This region comprises a series of platform sedimentary rocks, which are unconformably deposited on scarce syn-rift deposits, mainly preserved in the northern Precordillera. The Cerro de la Totora Formation includes some evaporites and red-beds of Early Cambrian age (515 Ma), which fill the half-graben system developed on the Grenvillian age basement (Rapalini & Astini 1998; Rapalini 2012).

The platform deposits comprise mainly an Early Cambrian to Early Ordovician carbonate sequence bearing typical *Olenellus* trilobites of Laurentia derivation (Bordonaro 1980, 1992). Various studies have characterized the complex third-order sequences of these carbonates (Cañas 1999; Keller 1999), the palaeogeographic connections of their fauna (Benedetto *et al.* 1999) and their tectonosequences (Astini *et al.* 1995; Thomas & Astini 1996).

These platform deposits are bounded to the west by slope deposits (Alonso *et al.* 2008; Voldman *et al.* 2010) and the Famatinian ophiolites (Haller & Ramos 1984, 1993). This sequence of mafic, ultramafic and granulitic rocks of Middle to Late

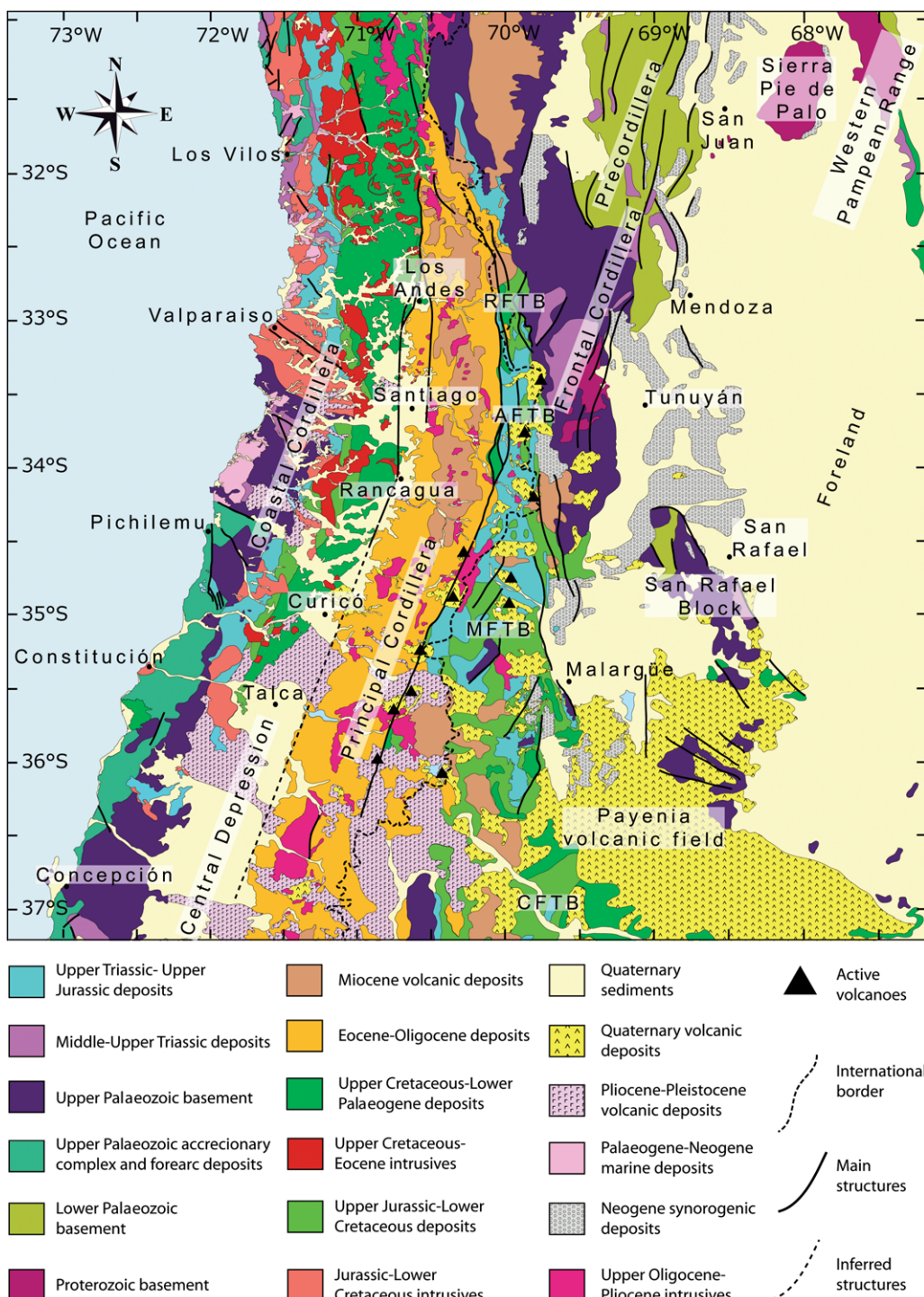


Fig. 3. Geological map of the Andean region between 31 and 37°S. Abbreviations: RFTB, Ramada fold-and-thrust belt; AFTB, Aconcagua fold-and-thrust belt; MFTB, Malargüe fold-and-thrust belt; CFTB, Chos-Malal fold-and-thrust belt.

ANDES OF CENTRAL CHILE AND WESTERN ARGENTINA

Ordovician age extends for more than 1000 km along the eastern slope of the Andes near the boundary between the Precordillera and the Frontal Cordillera (Fig. 3) (Ramos *et al.* 2000). These rocks show a dominant E-MORB composition, as well as the Silurian and Devonian mafic rocks and pillow lavas further to the west (Cortés & Kay 1994). The time of emplacement of these ophiolites is constrained by the Middle to Late Devonian age of the low-grade metamorphism of these rocks (Buggish *et al.* 1994; Davis *et al.* 1999; Robinson *et al.* 2005).

The subsequent clastic deposits above the platform successions were characterized by two syn-orogenic sequences; the older comprises the sandstones, conglomerates, glacial deposits and turbidites with olistostromes and olistoliths of Late Ordovician to Silurian age, represented by numerous formations (Astini *et al.* 1996). A second syn-orogenic sequence is represented by the turbidites and clastic deposits of Early to Middle Devonian age. Both sequences are separated by an angular unconformity seen in the Cuesta del Tambolar region between the eroded tilted carbonates and the Silurian deposits, interpreted there as the expression of a peripheral bulge associated with the deformation of the Sierra de Pie de Palo (Fig. 3) (Astini *et al.* 1995). Both sequences are affected by the Chanuc unconformity, associated with an important period of uplift, stacking and deformation of the Frontal Cordillera and western Precordillera with a characteristic west-vergence (Von Gosen 1992; García-Sansegundo *et al.* 2014a).

Western Sierras Pampeanas

The western Sierras Pampeanas as defined by Caminos (1979) encompasses the Sierra de Pie de Palo and the belt of westernmost Sierras Pampeanas, such as the Valle Fértil, La Huerta and other basement uplifts further to the east. This region is the locus of the Famatinian orogeny, which has been preserved in metamorphic facies that, based on their characteristics, can be divided into several belts.

The western slope of Sierra de Pie de Palo pre-served a belt of limestones and quartzites, known as the Caucete Group (Vujovich & Ramos 1994), heavily deformed and overridden by the Pie de Palo Complex, an ophiolite sequence of Grenville age (Vujovich & Kay 1998). Based on detrital zircons and geochemistry, the Caucete Group has been correlated with the sedimentary Cambrian and Ordovician sequences of Precordillera (Naipauer *et al.* 2010a, b). The metamorphic conditions of the Caucete Group indicate high pressures and modest temperatures in amphibolite facies. These conditions occurred during subduction of a cold sedimentary slab in an A-subduction zone setting (Van Staal *et al.* 2011) around 460 Ma (Ramos 2004). The

data indicate a clockwise pressure–temperature ($P-T$) trajectory reaching a peak pressure of roughly 13 kbar at 450 °C, and then heating as pressure declined, reaching a maximum temperature of roughly 500–560 °C at pressures of 8–10 kbar. This fact has been explained by these authors as continuous subduction of a cold sedimentary slab (Caucete Group) after amalgamation with the Pie de Palo Complex in the subduction channel, followed by underthrusting of progressively more buoyant Precordillera crust.

Further to the east the remaining western Sierras Pampeanas have been extensively studied. Two dominant rock types characterized this region, a western magmatic belt that consists of latest Cambrian, Early to Middle Ordovician calc-alkaline granitoids and metamorphic rocks produced in the same interval (Ramos 1988a, 2004). After the pioneering work of Pankhurst & Rapela (1998) and Quenardelle & Ramos (1999), several new studies have characterized the geological evolution of the Ordovician magmatic arc. The petrological conditions of these granitoids have been studied by Otamendi *et al.* (2008, 2009a, b, 2010a, b, and references therein) complemented by the analyses of Verdecchia *et al.* (2007) and Casquet *et al.* (2012, and references therein). The wall rocks of these granitoids were characterized by Verdecchia *et al.* (2007), who found fossil shelly faunas preserved in the metamorphic rocks of Ordovician age. Further north, the Ordovician rocks are preserved in sedimentary facies and sedimentological studies show that sedimentation took place in an extensional environment (Mángano & Buatois 1996). Similar conclusions were obtained for the Ordovician age of the metamorphism (Collo *et al.* 2008), and the extensional regime of the magmatic rocks (Collo *et al.* 2009).

Tectonic evolution of the Famatinian cycle

Although several tectonic models have been proposed to explain the early Palaeozoic history of central Chile and western Argentina, sometimes with contrasting interpretations, such as accretions of allochthonous terranes (Ramos 1988a; Astini *et al.* 1995) or by continent–continent collisions involving Laurentia and Gondwana (Dalla Salda *et al.* 1992a, b), in recent years some consensus has been obtained for the evolution of that region (see Ramos & Dalla Salda 2011).

Most of the authors agree that the main deformation that affected the early Palaeozoic the Precordillera platform and slope deposits occurred at about 460 Ma almost in the upper part of the Darriwillian (Thomas & Astini 2003; Ramos 2004). This deformation explains the stacking of different thrust sheets of the eastern Precordillera and the

development of olistoliths in the foreland basin during Late Ordovician as part of the Ocloyic deformation (Thomas & Astini 2007). These authors explain the deformation by a collision of the Cuyania (or a larger Precordillera) terrane, an allochthonous terrane derived from the Ouachita embayment of Laurentia that collided against the proto-margin of Gondwana (Astini *et al.* 1995; Thomas & Astini 1996). The first palaeomagnetic data obtained from Cerro Totora syn-rift deposits confirmed this origin for Cuyania (Rapalini & Astini 1998), and, although the new data from the polar apparent curve of Gondwana poses some uncertainties in the location of Cuyania in the Early Cambrian, the recent palaeomagnetic analysis of Rapalini (2012) shows that the origin in the Ouachita embayment is still the best alternative to explain most of the existing data.

The western margin of Sierras Pampeanas shows that the Cambrian–Ordovician calc-alkaline magmatic arc lasted between the Furongian (497–485 Ma) and the Darriwilian (457–458 Ma), reaching the maximum activity in the Early Ordovician (Pankhurst & Rapela 1998; Quenardelle & Ramos 1999; Rapela *et al.* 2010; Dahlquist *et al.* 2013, and references therein). The metamorphic peak was around 460 Ma (Ramos 2004; Van Staal *et al.* 2011; and references therein). This peak was associated with the collision of the Cuyania terrane (Von Gosen *et al.* 2002; Chernicoff & Ramos 2003) by the end of Middle Ordovician.

The consensus that has been obtained for the Ocloyic deformation is greater than that for the various alternatives still discussed for the Silurian and Devonian evolution, which ends with the Chanic deformation at Middle to Late Devonian times. There is agreement to relate that deformation with the collision of the Chilenia terrane, but is not clear where the magmatic arc was located. Most authors have agreed with the proposal of Cucchi (1972), who dated by K–Ar the deformation and low-grade metamorphism of western Precordillera as Late Devonian. New Ar–Ar ages and metamorphic studies confirm the age and the low-grade metamorphism related to the collision (Bugdish *et al.* 1994; Robinson *et al.* 2005; Voldman *et al.* 2009).

The main problem that has persisted since the early proposal of Ramos *et al.* (1984, 1986) is the polarity of subduction. These authors proposed an eastern subduction, a criterion that was followed by subsequent studies (see Willner *et al.* 2011, and references therein). On the other hand, the hypothesis of a western subduction beneath the Chilenia terrane proposed by Astini *et al.* (1995) was followed by Davis *et al.* (1999), Gerbi *et al.* (2002), Heredia *et al.* (2012) and González-Menéndez *et al.* (2013), among others. The uncertainty about

the location and age of the magmatic arc make these two alternatives difficult to reconcile. Heredia *et al.* (2012) interpreted a Devonian arc developed in the Frontal Cordillera based on the clasts found in the Devonian (?) Vallecitos beds, but the ages of this arc and these beds are not well constrained. Since the peak of high-pressure metamorphism occurred at 385–390 Ma (Willner *et al.* 2011) in Middle Devonian times, and is related to the collision of Chilenia and Cuyania, the arc inferred from the Vallecitos clasts could be Late Devonian and associated with east-dipping subduction from the Pacific side. The other criterion to establish the polarity of subduction is the dominant Chanic vergence of deformation. García-Sansegundo *et al.* (2014a) describe a dominant west-vergence for the early Palaeozoic rocks of the Frontal Cordillera in the Cordón del Carrizalito region. Until the age and location of the magmatic arc are established, it will not be possible to address the polarity of the subduction. Moreover, the propagation of the uplift and deformation of the Frontal Cordillera produced the syn-orogenic deposits of the Angualasto Group in the Precordillera at the Early Carboniferous (Limarino *et al.* 2006).

Gondwanian tectonic cycle (Mississippian–Lopingian)

The Gondwanan units north of c. 33°S differ considerably from those exposed south of this latitude and will be described in two different segments.

Northern segment

North of c. 33°S the following Gondwanan units were recognized from west to east on both sides of the Andean Cordillera.

Accretionary prism rocks. Polyphase deformed metamorphic rocks of the Choapa Metamorphic Complex are exposed along or next to the coast line, northwards of Los Vilos (Fig. 3). This complex consists mostly of grey-coloured phyllites, schists, fine-grained gneisses and metabasites (Muñoz-Cristi 1942; Thiele & Hervé 1984; Hervé 1988; Hervé *et al.* 1988; Irwin *et al.* 1988; Godoy & Charrier 1991; Rivano & Sepúlveda 1991; Rebollo & Charrier 1994; Charrier *et al.* 2007; Hervé *et al.* 2007; Richter *et al.* 2007; Willner *et al.* 2008, 2012; García-Sansegundo *et al.* 2014b), with protoliths of fine- to coarse-grained sedimentary deposits for the phyllites, quartz-mica schists and gneisses, and basic to ultrabasic volcanic rocks, with occasional pillow structures, for the green-coloured, amphibole schists. The Choapa Metamorphic Complex resulted from basal and frontal

ANDES OF CENTRAL CHILE AND WESTERN ARGENTINA

accretion in a subduction complex and has been subjected to different $P-T$ metamorphic conditions. The presence of phengite-rich muscovite and garnet relics indicates the first stage of very high pressures, probably in the subduction channel, followed by retrogression to greenschist facies conditions. This occurred between 308 and 274 Ma (from Late Pennsylvanian to the end of Cisuralian, in the Early Permian) with a high-pressure–low-temperature peak at c. 279 Ma (Willner *et al.* 2008, 2012). Exhumation and deformation, like broken formation-type breccias (mélange-type 1 of Cowan 1985), of the metamorphic complex continued during Mesozoic times and resetting events on minerals have ages that correspond to known extensional or compressional Mesozoic events in this region of the Andes (Willner *et al.* 2012). Recent U–Pb Sensitive High Resolution Ion Micro Probe (SHRIMP) age determinations on detritic zircons from the Choapa Complex immediately north of the region considered here indicate that sedimentation occurred until at least Early Triassic and, thus, that metamorphic processes affected the accretionary prism until at least early Mesozoic times (Empanar & Calderón 2014).

Forearc basin deposits. Two sedimentary stages have been recognized in the forearc region. In the first one, the meta-sedimentary unit Agua Dulce Metaturbidites, and the not metamorphic, strongly folded turbiditic Arrayán Formation, were deposited in a forearc basin (Rivano & Sepúlveda 1991; Rebolledo & Charrier 1994). These units have maximum depositional ages of 337 and 343 Ma, respectively (Willner *et al.* 2008). Supply of the Arrayán Formation is from the NW and the deposits accumulated on the western side of the basin in Carboniferous time (Rebolledo & Charrier 1994; Willner *et al.* 2008, 2012). Platformal deposits of the forearc Arrayán basin are exposed on the eastern side of the basin in the present day western Frontal Cordillera, intruded by granitoids of Cisuralian age (Elqui plutonic complex). These slightly contact-metamorphosed deposits consist of a rhythmic alternation of slates and sandstones of at least 1500 m thick, which have been included in the Hurtado Formation (Mpodozis & Cornejo 1988). These deposits are considered to be the prolongation of a series of similar outcrops representing a transgressive–regressive event, some of which further north contain fossil remains indicating a Middle Devonian to Mississippian age, and a provenance of sediments from a volcanic source located to the east and SE (Charrier *et al.* 2007 and references therein). The continuous Devonian to Mississippian sedimentation in the retrowedge Arrayán basin (Charrier *et al.* 2007; García-Sansegundo *et al.* 2014b) demonstrates that the Late Devonian

Chanic deformation did not affect the western margin of the Chilenia terrane.

The second sedimentary stage occurred in third stage of the Gondwanian cycle (Charrier *et al.* 2007) and is characterized by coarse- to fine-grained, fossiliferous marine deposits with turbiditic and calcareous intercalations exposed close to the coast, north of Los Vilos. The Quebrada Mal Paso Beds and Huéntelauquén Formation (Muñoz-Cristi 1973; Charrier 1977; Mundaca *et al.* 1979; Rivano & Sepúlveda 1983, 1985, 1991; Irwin *et al.* 1988; Méndez-Bedia *et al.* 2009) unconformably overlie the Arrayán Formation, and mark a major palaeogeographic change at the moment of deposition. A maximum depositional age of 303 Ma was obtained by Willner *et al.* (2008). Although Rivano & Sepúlveda (1983, 1985, 1991) favour a Late Pennsylvanian to Cisuralian (Early Permian) age, other authors consider that its fossil content indicates a Permian (Fuenzalida 1940; Muñoz-Cristi 1942, 1968; Minato & Tazawa 1977; Thiele & Hervé 1984; Mundaca *et al.* 1979) or a mid-Permian age (Díaz-Martínez *et al.* 2000). A Guadalupian age would be consistent with its maximum depositional age of 303 Ma (Willner *et al.* 2008) and its unconformable superposition on the Arrayán Formation.

Main magmatic arc rocks. The magmatic arc is not exposed in the study region, although it is well represented further north in the Frontal Cordillera, between 29 and 31°S, where it forms the Elqui–Limarí and Chollay batholiths, and still further north the Montosa–El Potro batholith (Nasi *et al.* 1985; Mpodozis & Kay 1990, 1992). The Elqui plutonic complex includes series of plutons that range in age from the Mississippian to the Late Triassic (Hervé *et al.* 2014), indicating a protracted magmatic history in this region of the Frontal Cordillera. New U–Pb ages obtained by Hervé *et al.* (2014) plus those obtained by previous authors (Pankhurst *et al.* 1996; Pineda & Calderón 2008; Coloma *et al.* 2012) form four groups, falling into the Late Mississippian, Late Pennsylvanian to Cisuralian, Late Lopingian to Middle Triassic, and Late Triassic, respectively. The second group with ages between 301 and 284 Ma predates the San Rafael orogeny, coincides in time with the evolution of the Choapa metamorphic complex and corresponds to the next Gondwanan unit to the east. Geochemical features indicate development in a magmatic arc associated with a subduction zone on a gradually thickening crust.

The rhyolitic welded ash-tuffs and flows of the Guanaco Sonso Formation (lower portion of the Pastos Blancos Group) exposed in the Elqui drainage basin (c. 30°S) are related to this plutonic activity. They yielded K–Ar biotite ages of 281 ± 6 , 262 ± 6 and 260 ± 6 Ma, and a U–Pb

zircon age of 265.8 ± 5.6 Ma, which except for the first one correspond to the Guadalupian (Martin *et al.* 1999). Based on these ages, the Guanaco Sonso Formation should instead be included in the post-tectonic Guadalupian to early Lopingian third stage of Gondwanian evolution of Charrier *et al.* (2007) and thus be related to the Colangüil plutonic activity, which yielded ages between *c.* 279 and *c.* 252 Ma (Sato *et al.* 1990; Sato & Llambías 1993, 2014), rather than to the pre-tectonic second group of Hervé *et al.* (2014).

In the Elqui valley, immediately north of the region considered here, K–Ar hornblende and biotite age determinations in this batholith yielded Permian ages of 297 ± 9 and 258 ± 4 Ma, respectively (Nasi *et al.* 1985, 1990), which coincide within errors with the age of the second group of Hervé *et al.* (2014). These ages also coincide fairly well with a recent U–Pb age determination of 282.7 ± 5.8 Ma for a rhyolitic volcanic sequence that still further north overlies the western El Tránsito Metamorphic Complex (Salazar *et al.* 2009). The felsic character of these units makes it difficult to differentiate them from each other and the wide age range covered by them suggests that there existed a long lasting felsic volcanic activity from at least Pennsylvanian to Triassic times. Late Pennsylvanian to Cisuralian activity corresponds to the second group of Hervé *et al.* (2014) and is pre-tectonic relative to the San Rafael orogeny, whereas the Guadalupian to early Lopingian activity is post-tectonic. The latter, according to its age, would correspond to a volcanic activity coeval with intrusion of the Colangüil plutonic activity, deposition of the Huettelauquén Formation and the subduction-related lower portion of the Choiyoi Group (Kay *et al.* 1989; Kleiman & Japas 2009). A third stage of activity would include the felsic upper portion of the Choiyoi Group in Argentina and the Matahuaiaco Formation, exposed further west in Chile in the Elqui river drainage, which has been assigned to the early stage of the next tectonic Pre-Andean cycle (Charrier *et al.* 2007).

Retroarc magmatic rocks. The Colangüil batholith and associated volcanic rocks are exposed north of 31°S to east of the previous arc rocks in the Cordillera Frontal along the Argentine slope in the province of San Juan. The batholith is composed of several granitoids varying from granodiorites to granites as the Los Puentes, Los Lavaderos, Las Opeñas, Agua Blanca and Chita plutons (Sato *et al.* 1990), with K–Ar ages varying between 272 and 247 Ma (Sato & Llambías 1993). The coarse-grained granodiorites have an Early to Middle Permian age, and they are typically calc-alkaline with magmatic arc affinities, associated with the final stage of subduction in a retroarc setting, and

as early post-orogenic products respect to the orogenic San Rafael deformation (Sato & Llambías 1993). The granites are commonly fine grained and characterized by granophytic textures consistent with intrusions at shallow levels, and have a transitional signature from calc-alkaline to alkali (A-type). They were interpreted as reflecting an evolution to an extensional post-orogenic setting during Late Permian times. These granitoids are associated with lava flows, ignimbrites and tuffs of andesitic and rhyolitic composition, which follow the same trend as the plutonic rocks. Based on the geochemical characteristics, the calc-alkaline series was assigned to a pre-Choiyoi field, typical of an arc setting, while the younger transitional series was assigned to a Choiyoi field of within-plate affinities in an extensional regime (Kay *et al.* 1989).

Retroarc basin deposits. Several authors have described the sedimentation in the retroarc region of this segment of the Andes as part of the Calingasta and Uspallata basins developed in the Fron-
tal Cordillera and the Precordillera, as well as an intraplate basin known as the Paganzo basin developed between the Precordillera and the Sierras Pampeanas (Fig. 3) (Ramos *et al.* 1986; López Gamundi *et al.* 1994, among others). These authors recognized two different stages separated by the San Rafael orogenic deformation in the Middle Permian. The first stage is unconformably overlying the Devonian deposits and comprises mainly Late Carboniferous to Early Permian sequences, where a complete record of different glacial stages has been recognized. The Early Carboniferous is only preserved in the eastern Precordillera (Fig. 3) where the Angualasto Group of mainly Visean age recorded the first infills of the retroarc marine basin with an early glacial stage (Fernández-Seveso & Tankard 1995; Limarino *et al.* 2013). The upper part of the first stage comprises widely developed marine deposits in the Precordillera, and recorded the glacial diamictites, overlain by transgressive postglacial shales (Pazos 2002; Limarino & Spalletti 2006). These transgressive facies were succeeded by deltaic and fluvial sequences bearing coal beds where recent U–Pb ages indicate a late Bashkirian age (Gulbranson *et al.* 2010; Spalletti *et al.* 2012; Limarino *et al.* 2013).

The sequences above the San Rafael unconfor-
mity of Early–Middle Permian age are mainly volcaniclastic, pyroclastic and volcanic rocks associated with the lower and upper parts of the Choiyoi Group (Kay *et al.* 1989; Kleiman & Japas 2009). The lower part of the Choiyoi volcanic rocks is subduction related, while the upper part cor-
responds to an extensional regime that controlled the extensive rhyolitic plateaux in the foreland

ANDES OF CENTRAL CHILE AND WESTERN ARGENTINA

area (Mpodozis & Ramos 1989; Mpodozis & Kay 1992; Llambías 1999).

There is no agreement on the dominant tectonic regime after the Late Devonian Chaníe compressive deformation. Fernández-Seveso & Tankard (1995) interpreted that the described sequences reflect changes from transtensional to extensional regimes. A similar extensional regime was proposed by Astini (1996), Astini *et al.* (2011), and Martínez *et al.* (2011) for the Mississippian (348–342 Ma) based on the occurrence of rhyolites at about 28°S in the southern Puna, coeval with the well-known occurrence of A-type granites in the Sierras Pampeanas (Grosjean *et al.* 2009). On the other hand, after the Chaníe deformation during Middle to Late Devonian times (Ramos *et al.* 1986) compressional deformation and flexural loading produced the foreland basin where the Mississippian deposits of the Angualasto Group and El Ratón Formation have accumulated (Heredia *et al.* 2012). As a result of this deformation, the Protoprecordillera was uplifted and remained as a positive area until the end of the Carboniferous, when it collapsed by extensional faulting (Limarino *et al.* 2013).

Southern segment

South of 33°S and further south of the considered region, four Gondwanan units are exposed continuously paralleling the coast from west to east (see Fig. 3): a metamorphic complex; a north–south elongated Coastal Batholith that intrudes the former; an extensive batholith emplaced in the Frontal Cordillera; and an extensive volcanic episode in the Frontal Cordillera and further east in the San Rafael Block (Fig. 3) represented by the Choiyoi Group.

Metamorphic complex. In this segment the metamorphic complex includes the eastern and a western series that form a paired metamorphic belt (González-Bonorino 1970, 1971; González-Bonorino & Aguirre 1970; Aguirre *et al.* 1972; Hervé *et al.* 1974, 1984, 2003, 2013; Hervé 1977; Kato & Godoy 1995; Willner 2005; Willner *et al.* 2004, 2005, 2008; Glodny *et al.* 2005, 2006, 2008), interpreted recently as the result of frontal and basal accretion in a subduction system, respectively (Richter *et al.* 2007; Willner *et al.* 2008).

The western series, which was deposited shortly after the eastern series (Hervé *et al.* 2013), consists of polyphase deformed and metamorphosed sandstones and pelites, metacherts, metabasites, occasionally with pillow structures and scarce serpentine bodies, formed by basal accretion under a higher $P-T$ metamorphic gradient, while the eastern series consists mainly of polyphase deformed metaturbidites, with recognizable primary

structures and lenses of calc-silicate rocks, deposited in a retrograde or forearc basin, metamorphosed by a low $P-T$ gradient (Glodny *et al.* 2006; Richter *et al.* 2007; Hervé *et al.* 2013). All SHRIMP U–Pb age determinations on igneous detrital zircons from the accretionary complex yielded peaks older than Mesozoic. The youngest peak obtained from the eastern series was dated at 330–345 Ma, while the youngest peak in the western series was dated at 307 Ma (Hervé *et al.* 2013). All these ages are older or coeval with the Coastal Batholith, and coincide with ages determined for the Agua Dulce metaturbidites and the non-metamorphic Arrayán Formation north of c. 33°S, respectively. Moreover, ages of detrital zircons in both series indicate a major input from the Famatinian orogenic belt and subordinately from Pampean and Grenvillian sources (Hervé *et al.* 2013).

Ar–Ar dating of white mica in the metamorphic series indicates for the western series a peak of high- $P-T$ metamorphism between 320 and 288 Ma and for the eastern series a peak of high-temperature metamorphism between 302 and 294 Ma (Willner *et al.* 2005). According to the age and the contact metamorphism affecting the eastern series, the sedimentation, at least in the western series, began before emplacement of the Coastal Batholith (see below).

South of the Lanalhue lineament (c. 38°S) conditions seem to have been different from those to north of this latitude. Here the metamorphic complex bends to the east and consists mainly of the western series, which is here much younger than further north (Hervé *et al.* 2013).

Deposits in the Coastal Cordillera close to Concepción, in the southern part of the considered region, form the newly proposed Patagual–El Venario unit (Mardonez *et al.* 2012). These deposits overlie unconformably the eastern series and are unconformably covered in the Bio Bio valley by the marine, Carnian Santa Juana Formation (Nielsen 2005). This unit consists of a tightly folded and slightly metamorphosed (epizone close to the anchizone) alternation of pelitic and thick psammitic layers, which differentiates them from the eastern series and the overlying early Late Triassic deposits. Its loosely constrained age, between the Early Permian (age of the thermal metamorphism in the eastern series of the metamorphic complex, south of 33°S) and the early Late Triassic Santa Juana Formation makes its age assignment difficult. Considering that this unit overlies the eastern series, which was affected by thermal metamorphism between 302 and 294 Ma (Willner *et al.* 2005), its maximum age is early Sakmarian, in the Early Permian. According to the lithologic description, strong deformation and low-grade metamorphism, which are reminiscent of the Agua Dulce

metaturbidites and the Arrayán Formation, we suggest that the tectonic setting for this unit is the late Palaeozoic forearc or retrowedge basin. Another possibility is that these deposits accumulated in a rift basin during the first stage of the Pre-Andean cycle.

Its strong deformation and low metamorphic grade suggest that the Lopingian to Early Triassic deposits close to the continental margin would at that time still have been affected by processes related to subduction activity, as has been shown by the presence of Triassic detritic zircons in rocks of the Choapa Metamorphic Complex (Emparan & Calderón 2014).

Coastal batholith. This batholith consists of a series of plutons of calc-alkaline character, meta- to peraluminous composition, and granitic to quartz-dioritic lithologies exposed along the Coastal Cordillera, between 33 and 38°20'S, intruding to the east the metamorphic complex (Fig. 3). Further south (38°S), the batholith curves to the east and can be followed southwards along the Principal Cordillera. This shift is probably controlled by the NW-orientated Lanalhue lineament (Glodny *et al.* 2008; Hervé *et al.* 2013). According to the recent SHRIMP U–Pb age determinations, the Coastal Batholith was emplaced in a c. 19 Ma period, between 319.6 ± 3.3 and 300.8 ± 2.4 Ma, in Pennsylvanian time, according to Deckart *et al.* (2014). This age differs considerably from the ages recently obtained by Hervé *et al.* (2014) for the Elqui plutonic complex, which fall into the Early Permian (Cisuralian; 301–284 Ma). Ages for the metamorphic peaks on the western series indicate that metamorphism overlapped with emplacement of plutons of the Coastal Batholith (Hervé *et al.* 2013).

Frontal Cordillera batholith

Further east, along the Frontal Cordillera, there are several granitoid stocks and batholiths, exposed south of 33°S latitude (Fig. 3). These granitoids outcrop from the Cordón del Plata to the Cordón del Portillo region, and continuous further south until the Río Diamante valley. They have been described by Polanski (1964, 1972) and Caminos (1965) as typical calc-alkaline metaluminous granitoids emplaced in the Carboniferous deposits. Petford & Gregori (1994) and Gregori *et al.* (1996) compared this belt of Frontal Cordillera granitoids with the Coastal Batholith of Peru and concluded that they share similar La/Yb ratios, Al₂O₃ contents and several petrographic characteristics that show a typical subduction setting. These authors interpreted these granitoids as emplaced in a several thousand metres-thick sedimentary sequence formed in an extensional regime. The first U–Pb ages of the

Frontal Cordillera of this segment were presented by Orme & Atherton (1999), ranging in age between 276 and 262 Ma and with ϵ Nd between –2.5 and –3.5. These posttectonic granitoids were also recognized in the Frontal Cordillera by Gregori & Benedini (2013), who interpreted these Cisuralian and Guadalupian granodiorites, tonalites and monzogranites of I-type as emplaced subsequent to the San Rafael orogeny that closed the Carboniferous basin between 284 and 276 Ma. The new ages seem to discard the presence of Carboniferous granitoids in this sector of Frontal Cordillera assumed by Caminos (1979).

Choiyoi volcanic rocks. These volcanic rocks, recognized in this segment of the Andes by Groeber (1953), are widely represented in the Frontal Cordillera and further east in the San Rafael Block as well as in the foothills of western Sierras Pampeanas. The volcanic rocks of the Choiyoi Group formed after the San Rafael tectonic phase. This group is subdivided into two essentially different units. A lower unit consisting of volcanic rocks of basic to intermediate composition and calc-alkaline signature (Poma & Ramos 1994) developed in late Cisuralian and Guadalupian times in an arc setting in association with subduction of oceanic lithosphere, an upper volcanic unit consisting of silicic volcanic and volcaniclastic deposits and sub-volcanic intrusives derived from crustal melting under extensional tectonic conditions deposited in Lopingian to Anisian times (Kay *et al.* 1989; Mpodozis & Kay 1990; Llambías *et al.* 1993, 2003; Llambías & Sato 1995; Spalletti 1999; Martínez 2005; Martínez *et al.* 2006; Giambiagi & Martínez 2008). New U–Pb ages have been presented by Rocha Campos *et al.* (2011), which confirm a Guadalupian age for this section of the older Choiyoi volcanic rocks. The partly coeval age of this older Choiyoi unit with deposition of the Huéntelauquén deposits, its location further east of the retrowedge or foreland basin, and its calc-alkaline signature indicate that it corresponds to a subduction related magmatic arc developed during closure of the retrowedge basin and uplift of the continental margin at the final stage of Gondwanan evolution (third stage of Charrier *et al.* 2007). The younger Choiyoi unit has, in turn, been assigned to the next pre-Andean tectonic cycle.

Gondwanan tectonic evolution

Based on the marked difference between the regions north and south of 33°S, it is difficult to reconcile the late Palaeozoic tectonic evolution of the two regions in one single coherent model, which is evidence that more information is necessary to solve this problem. However, some general conclusions

ANDES OF CENTRAL CHILE AND WESTERN ARGENTINA

can be drawn on the basis of the available information. The post-Devonian age of the units described from the western slope of the Andes suggests that these developed on the rear side of Chilenia. The recent chronologic data for the metamorphic complexes and plutonic belts north and south of 33°S indicate that:

- (1) Maximum depositional ages for the deposits accreted by basal and frontal accretion in both regions are approximately the same; however, the peaks of high $P-T$ metamorphism in the paired belt, south of 33°S, are older than in the Choapa Metamorphic Complex, to the north of this latitude.
- (2) Emplacement of the Coastal Batholith, south of 33°S, is older (Pennsylvanian) than the Elqui plutonic complex (Cisuralian), in the Frontal Cordillera, north of 33°S. This evidence indicates that the Choapa Complex and the paired metamorphic complex south of 33°S probably belong to two different accretionary complexes, and that the plutonic belts correspond to two different subduction-related magmatic arcs.
- (3) The late stage of emplacement of the Elqui plutonic complex in late Cisuralian and Guadalupian times is coeval with sedimentation of the Huinetlauquén Formation, in the retro-wedge basin, and the lower Choiyoi Group would thus correspond to the extrusive products of the magmatic arc.

Additionally, two features – the narrow width of the outcrops of the western series north of the NW-orientated Lanalhue lineament (*c.* 38°S) and the considerably wider outcrops of this series to the south of the lineament that interrupts the southward prolongation of the Coastal Batholith and apparently caused its bend towards the Principal Cordillera (Hervé *et al.* 2013), and the much younger depositional age of the western series to the south of the lineament containing abundant Permian detrital zircons (Hervé *et al.* 2013) – suggest that: (a) the accretionary complex was considerably wider than the present day outcrops; (b) its age is younger towards the SW; and (c) the probable orientation of the accretionary complex and the Gondwana coast was NNW–SSE.

Although there is no consensus on the tectonic regime during the Carboniferous, there is agreement that the San Rafael orogeny caused in Early to Middle Permian (late Cisuralian to early Guadalupian) generalized uplift of the region (Ramos 1988b; Mpodozis & Kay 1992; López Gamundi *et al.* 1994; Limarino *et al.* 2006, 2013; Giambiagi *et al.* 2011; Willner *et al.* 2008, 2012; García-Sansegundo *et al.* 2014a, among others). This tectonic event was responsible for deformation of the

Arrayán Formation in the forearc (Charrier *et al.* 2007) and the cataclastic fabric in the El Volcán plutonic unit of the Elqui plutonic complex (Mpodozis & Kay 1990).

It has been proposed that the late Palaeozoic evolution of this sector of the Andes can be explained by a period of subduction in the Carboniferous times associated with extension after the Chaní compressive orogenic episode in the Middle to Late Devonian, with an active subduction-related magmatic arc. This arc expanded and migrated towards the foreland, reaching the Central Precordillera and the western side of the Sierras Pampeanas during Early Permian times, associated with the San Rafael orogenic deformation. Subsequent extension and formation of extensive rhyolitic plateaux were associated with delamination of the lower crust owing to injection of hot anhydrous asthenosphere. These processes were previously interpreted as produced by orogenic collapse and slab break-off by Mpodozis & Ramos (1989), Kay *et al.* (1989) and Mpodozis & Kay (1992). However, this evidence together with the new available U–Pb ages favour the interpretation advanced by Ramos & Folguera (2009), where these episodes can easily be explained by a period of slab shallowing followed by steepening of the subduction zone, as proposed by Martínez *et al.* (2006).

Pre-Andean tectonic cycle (Lopingian–late Early Jurassic)

The term Pre-Andean is used for a period of arrested or very slow subduction during which extensional tectonic conditions prevailed following deformation of the Late Permian deposits, closure of the retro-wedge or forearc basin, exhumation of the continental margin and intense erosion on the Palaeozoic units. Groeber (1922) presented the first description of these deposits along the continental margin. Extensional conditions on the thickened crust of the continental margin determined the reactivation of pre-existent weakness zones like the sutures of the Palaeozoic terranes accreted to western Gondwana (Ramos & Kay 1991; Ramos 1994). The weakness zone defined a different palaeogeographic organization compared with those that prevailed earlier and later, that is, in the Gondwanan and Andean tectonic cycles, consisting of NW-trending rift basins (Charrier 1979; Uliana & Biddle 1988; Suárez & Bell 1992) (Fig. 4). Additionally, extension favoured the development of a widely distributed felsic magmatism that resulted predominantly from intense crustal melting (upper Choiyoi magmatic province; Rapela & Kay 1988; Kay *et al.* 1989; Llambías 1999; Spallati 1999). End of this

cycle is marked by resumption or more intense subduction activity along the continental margin and development of the Early Jurassic magmatic arc. The pre-Andean cycle reflects the tectonic conditions determined by the assembly of Gondwana, but also the initial processes that later resulted in its breakup.

Generalized extension and the existence of weakness zones (sutures) on the continental margin resulted in the development of the following

basins and successions of associated basins (Fig. 4): (a) El Quereo–Los Molles, next to the coast, at c. 32°S; (b) La Ramada, further east in the high Andes; (c) Cuyo, in the Precordillera and Andean foreland, in the San Juan–Mendoza region; (d) Bermejo, SW of La Rioja, in the northeastern San Juan province; and (e) Curepto–Bio Bío–Temuco, further south, which extends south-southeastwards from the coast up to the high Andes, at 40°S. Deposits in these basins are generally marine next

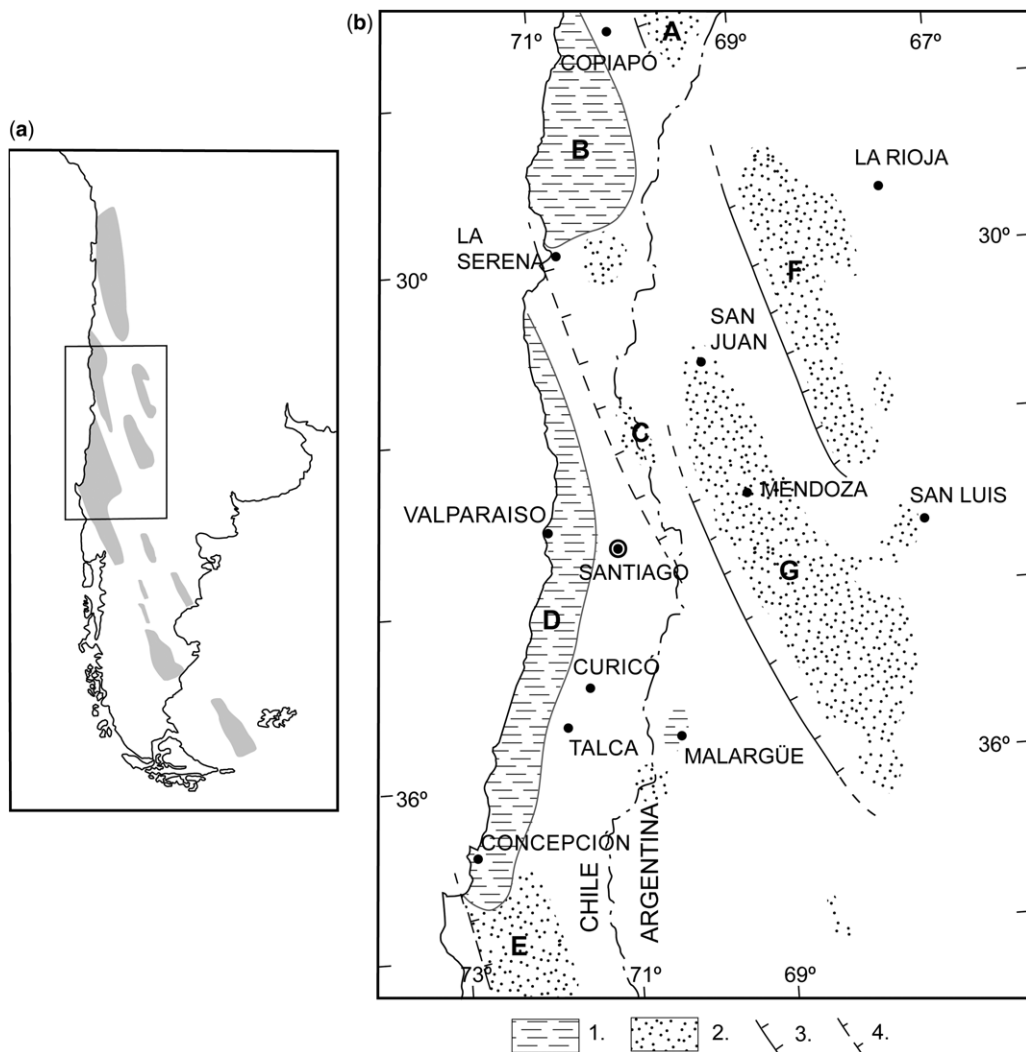


Fig. 4. Generalized palaeogeographic sketch for the Triassic in the Andean region of Argentina and Chile. (a) Southern part of South America showing in grey the approximate distribution of the basins, based on Uliana & Biddle (1988). Rectangle corresponds to the area represented in (b). (b) Distribution of the marine and continental deposits in the Triassic basins. 1. Marine deposits; 2. continental deposits; 3. observed basin bounding faults; 4. inferred faults. A, Profeta–La Ternera basin; B, San Félix–Rivadavia basin; C, La Ramada basin; D, El Quereo–Los Molles basin; E, Curepto–Bio Bío–Temuco basin; F, Bermejo basin; and G, Cuyo basin; based on Charrier *et al.* (2007).

ANDES OF CENTRAL CHILE AND WESTERN ARGENTINA

to the coast and continental towards their south-southeastern prolongation. The extensional faults that control the basins in Chile have not been clearly identified and the structural pattern is certainly more complicated than represented here. In Argentina, sedimentary polarity, seismic data and structural analyses indicate that some of the basins consist of hemigrabens (Milana & Alcober 1994; López Gamundi 1994).

Two rift stages have been detected in the evolution of the Pre-Andean cycle, each one consisting of a phase of tectonic subsidence followed by a phase of thermal subsidence (Charrier *et al.* 2007), a model that coincides with the one developed by Milana & Alcober (1994) and Milana (1998) for the Bermejo basin, in Argentina (Fig. 4). According to Charrier *et al.* (2007), in Chile, the first stage would have begun in Lopingian times (Late Permian) and ended by Ladinian to Carnian times (Middle Triassic to early Late Triassic), while the second one would have lasted from Late Triassic (post-Carnian) to Pliensbachian, in Early Jurassic times. Each phase of tectonic subsidence would have been accompanied by a pulse of felsic volcanism followed by marine or continental deposits, depending on the distance from the Triassic coast.

Sedimentary deposits of the first stage are known in the Coastal Cordillera north of 32°S in the El Quereo–Los Molles basin. These consist of a series of marine outcrops that can be grouped into the El Quereo Formation (Muñoz-Cristi 1942, 1973; Cecioni & Westermann 1968; Mundaca *et al.* 1979; Irwin *et al.* 1988; García 1991; Rivano & Sepúlveda 1991). These deposits reveal an Early? to Middle Triassic transgression–regression sedimentary cycle beginning with breccias and separated from the deposits of the second stage by the thick felsic volcanic and volcanioclastic Pichidangui Formation, associated with initiation of the second tectonic subsidence phase of the pre-Andean cycle.

Second-stage deposits have a latest Triassic to Early Jurassic age and therefore correspond to the late portion of the second stage, probably to the thermal subsidence phase occurring after the felsic volcanic event (Charrier *et al.* 2007). In the high Andes, at 31°S, Early Jurassic transgressive marine deposits of the Tres Cruces Formation are exposed overlying conformably the Late Triassic, continental, sedimentary and volcanic Las Breas Formation. This formation contains rests of *Dicroidium* flora and was recently dated at 219.5 ± 1.7 Ma (Norian) (U–Pb SHRIMP zircon crystallization age) on a dacitic volcanic breccia from the base of the formation (Hervé *et al.* 2014). The Las Cruces Formation is in turn covered by backarc volcanic and volcanioclastic deposits of the Late Jurassic Algarrobal Formation (Dedios 1967; Letelier 1977;

Mpodozis & Cornejo 1988; Pineda & Emparan 2006). At the coast, at 32°S, overlying the Pichidangui Formation, is the transgressive–regressive Los Molles Formation (Cecioni & Westermann 1968; Bell & Suárez 1995). The mostly marine deposits of the second stage, exposed along the Coastal Cordillera, south of 35°S, overlie, between 35 and 36°15'S, silicic volcanic deposits assigned to the bimodal volcanic Pichidangui Formation (Vicente 1974; Vergara *et al.* 1995) (La Totora–Pichidangui volcanic pulse) related to the upper Choiyoi magmatic province (Charrier *et al.* 2007). Further south of 36°15'S, they rest on Palaeozoic intrusive and metamorphic rocks (Fig. 3). The presence of a rather continuous series of marine deposits assigned to the second stage along the Coastal Cordillera, between 35 and 37°S (Curepto–Bio Bío–Temuco basin; see Charrier *et al.* 2007, Fig. 3.11, p. 39), suggests that the region covered by marine deposits during the thermal subsidence phase of the second stage was considerable and that the sea extended beyond the faults that controlled subsidence of the basin. We assign the marine Retian Malargüe rift deposits on the eastern versant of the Principal Cordillera, in Argentina, at c. 36°S (Riccardi & Iglesia Llanos 1999) (Fig. 4) to the earliest rift stages of the Jurassic backarc basin rather than to the second stage of the Pre-Andean cycle as previously proposed by Charrier *et al.* (2007). These deposits belong to one of the depocentres related to the Neuquén basin (Fig. 5).

Continental Triassic to Early Jurassic deposits were accumulated in the south-southeastward prolongation of the basins or in smaller isolated basins. These contain generally abundant volcanic and volcanioclastic deposits, like the Carnian–Norian Los Tilos sequence in the high Andes, at c. 30°S, somewhat north of the considered region (Martin *et al.* 1999), probably deposited in the prolongation of the San Félix basin (see Charrier *et al.* 2007, Fig. 3.11, p. 39). Other deposits apparently filled separated basins, like the La Ramada, in the high Andes, at 32°S (Álvarez 1996; Álvarez & Ramos 1999), the various depocentres of Cuyo basin located in the Frontal Cordillera, Precordillera and Andean foreland, between 31 and 36°S (Legarreta *et al.* 1992; Kokogián *et al.* 1993, 1999; Manceda & Figueroa 1995; Barredo *et al.* 2012), and the depocentres in the Sierras Pampeanas (Milana & Alcober 1994; Milana 1998), between 29 and 33°S (Fig. 4).

The best dated deposits are in the Cuyo basin in the Potrerillos depocentre, and were included in the Uspallata Group. These are separated from Devonian turbiditic deposits (Villavicencio Formation) and volcanic rocks of the Choiyoi Group by a normal fault and unconformably overlain by Miocene foreland deposits of the Mariño Formation.

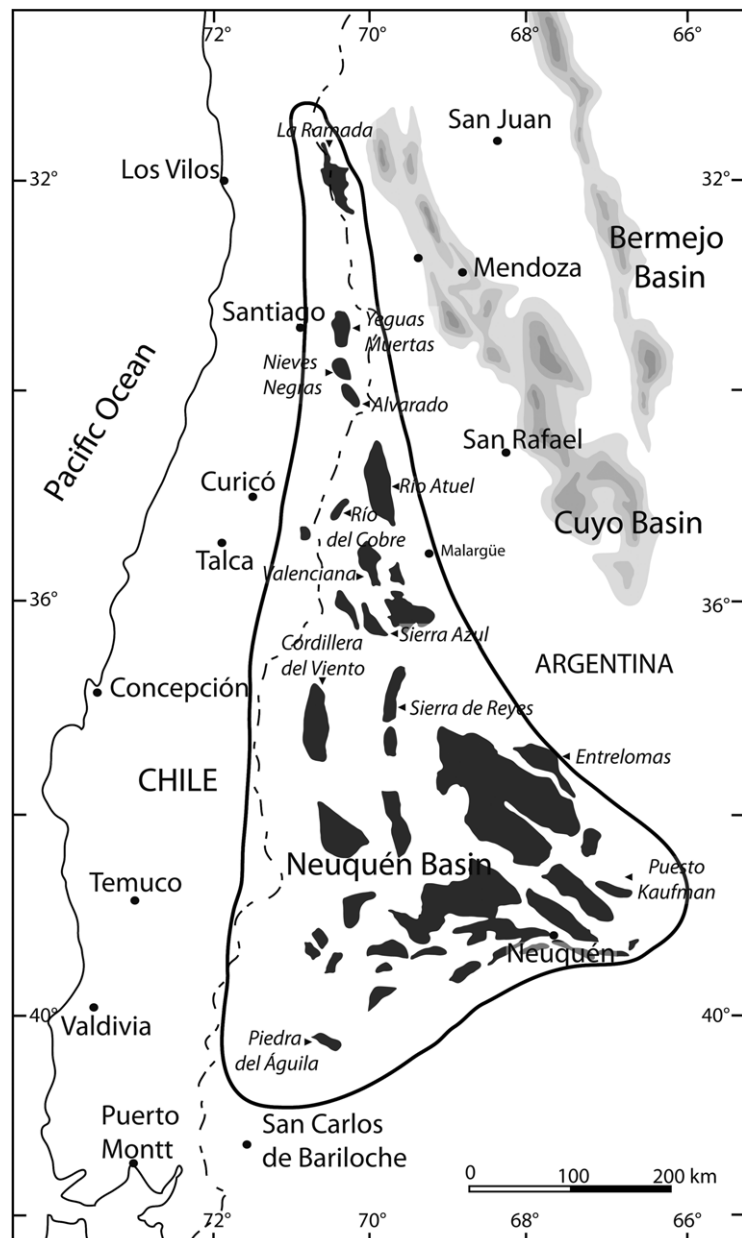


Fig. 5. Main depocentres of the Triassic–Early Jurassic rifts with the location of Alto del Tigre High (after Giambiagi *et al.* 2003b).

The Uspallata Group forms a 1385 m-thick continental sedimentary succession rich in fossil plants consisting of the following formations, from bottom to top (Spalletti *et al.* 1999, 2005, 2008): Río Mendoza (314 m; Anisian; 243 ± 4.7 Ma; Ávila *et al.* 2006), Cerro de las Cabras (190 m), Potrerillos (735 m; late Middle to early Late

Triassic; 239.2 ± 4.5 , 239.7 ± 2.2 and 230.3 ± 2.3 Ma), Cacheuta (44 m; early Late Triassic) and Río Blanco (102 m). The succession consists at the bottom and top of alluvial conglomerates and in the middle part of fluvial medium- to fine-grained deposits with tuff intercalations. The Río Mendoza, Cerro de las Cabras and Potrerillos formations

ANDES OF CENTRAL CHILE AND WESTERN ARGENTINA

correspond to the syn-rift phase of the basin, while the two upper units correspond to the sag phase. A rich fossil flora recovered in the Potrerillos and Cacheuta formations was used to propose a biozonation of the whole Triassic (Spalletti *et al.* 1999, 2005).

However, recent precise U–Pb dating in zircons from the Rincón Blanco, one of the northern depocentres of the Cuyo basin, has presented new ages from the base to the top of the sequence (Barredo *et al.* 2012). The SHRIMP age obtained for the base is 246.4 ± 1.1 Ma; the middle sequences yielded a SHRIMP age of 239.5 ± 1.9 Ma and Laser Ablation age of 238.0 ± 5.4 Ma; and the top, for both methods yielded 230.3 ± 1.5 and 230.3 ± 3.4 Ma (Barredo *et al.* 2012). These geochronological data, which are similar to those for the Potrerillos depocentre, indicate that almost the whole sedimentation is circumscribed to the Middle Triassic and the base of the Late Triassic, reaching neither the Norian nor the Rhaetian. The age differences observed between the Pre-Andean evolution in Chile and Argentina possibly indicate that extension began earlier in Chile than in Argentina. However, more precise chronological support is needed to make this decision.

Deposits in the Coastal Cordillera close to Concepción, in the southern part of the considered region, form the newly proposed Patagual–El Venado unit (Mardonez *et al.* 2012). These deposits overlay unconformably the eastern series and are unconformably covered in the Bio Bío valley by the marine, Carnian Santa Juana Formation (Nielsen 2005). This unit consists of a tightly folded and slightly metamorphosed (epizone close to the anchizone) alternation of pelitic and thick psammitic layers, which differentiates them from the eastern series and the overlying early Late Triassic deposits. Its loosely constrained age, which must be younger than the Early Permian, which is the age of the thermal metamorphism on the eastern series of the metamorphic complex, south of 33°S (between 302 and 294 Ma; Willner *et al.* 2005), and older than the early Late Triassic Santa Juana Formation, makes its age assignment difficult. According to these considerations, these deposits could correspond to (a) Permian forearc basin accumulations equivalent to the Huentelauquén Formation (third stage of the Gondwanan cycle) or (b) Latest Permian to Early Triassic deposits, which in this case would have accumulated during the first stage of the Pre-Andean cycle and, therefore, represent evidence for rifting in the first stage of the Pre-Andean cycle in this region.

In the Elqui plutonic complex, in the Frontal Cordillera north of 33°S , the plutonic and subvolcanic units included in the Late Lopingian to Middle Triassic age group (264–242 Ma) of Hervé

et al. (2014) (Ingaguás superunit of Mpodozis & Kay 1990, 1992) represent the intrusive equivalents of the felsic upper Choiyoi Group (Nasi *et al.* 1985; Mpodozis & Kay 1990) and possibly of the Mathuaico Formation. These plutons, along with the Laguna gabbro, form an epizonal association of intrusive rocks derived from deep, garnet-bearing levels in a thickened crust, and hypersilicic, calc-alkaline to transitional A-type granites (Nasi *et al.* 1985, 1990; Mpodozis & Cornejo 1988; Mpodozis & Kay 1990, 1992). These units consist predominantly of biotite–hornblende granodiorites and monzogranites, and syenogranites; graphic granites are known from the youngest El Colorado units. The given age range comprises a 22 Ma time lapse that goes from the Capitanian (late Middle Permian) to the Anisian/Ladinian boundary (Middle Triassic), and therefore coincides with the first stage of the Pre-Andean cycle.

Norian and somewhat younger Triassic ages have been also obtained along the coast: (a) in the northern part of the considered region in the A-type to transitional Altos de Talinay Plutonic Complex (Gana 1991; Emparan & Pineda 2006; Emparan & Calderón 2014), and further south in the Tranquilla and Millahue units (Parada *et al.* 1988, 1991, 1999, 2007; Rivano & Sepúlveda 1991); (b) in the Norian ‘Dioritas Gnésicas de Cartagena’ (Gana & Tosdal 1996), next to San Antonio, at $33^{\circ}30'\text{S}$, and (c) in the Norian fayalite, anorogenic A-type Cobquecura pluton (Vásquez & Franz 2008). All these widely distributed plutonic units demonstrate the great regional extension of the Choiyoi Magmatic Province.

Andean tectonic cycle (late Early Jurassic–present)

The beginning of this long-lasting cycle was determined in Chile by the initiation of subduction-related volcanism in the late Early Jurassic (Pliensbachian) (Charrier *et al.* 2007, and references therein). However, on the eastern versant of the Andes in central Argentina, a post-Choiyoi extensional event occurred in the Late Triassic that formed new depocentres in the region where later the backarc basin developed during Jurassic times. This extensional event and the initiation of sedimentation in the backarc region are considered in Argentina to mark the beginning of the Andean cycle. Thus, the age of the beginning of this cycle remains a question that needs further investigation: (a) do the Late Triassic deposits in Argentina belong to the second stage of the Pre-Andean cycle; or (b) did the new geodynamic conditions at this moment cause extension of the continental margin already in the Late Triassic, whereas subduction

magmas reached the surface of the crust somewhat later in Pliensbachian time?

The Pre-Andean cycle, which began with renewal or intensification of subduction underneath the central Argentine–Chilean continental margin, reflects evolution of the continental margin during continental breakup and continental drift (Fig. 1). Subduction created conditions for arc magmatism, active almost uninterruptedly right through to the present day, and extensional tectonic conditions along the continental margin. During early evolution of this cycle (Pliensbachian to late Early or early Late Cretaceous), in northern and central Chile, the arc was located along the present day Coastal Cordillera, parallel to the western margin of Gondwana with a backarc basin on its eastern side. In contrast, the later evolution (Late Cretaceous and Cenozoic) is characterized by gradual eastward shift of the magmatic arc and by the development of retroarc foreland basins on the eastern side of the arc. These two major periods correspond to the Early and Late periods, respectively, described by Coira *et al.* (1982) for this tectonic cycle. However, each of these periods can be subdivided into shorter stages, which can be differentiated from each other by major palaeogeographic changes (Fig. 1). These changes are a consequence of major modifications of the convergence and subduction pattern in this region.

Early period (Pliensbachian–late Early Cretaceous)

The early period of the Andean tectonic cycle ended in late Early or early Late Cretaceous with the Peruvian tectonic phase (Fig. 1) that caused a considerable crustal thickening, major palaeogeographic reorganization and modification of the tectonic regime in this Andean region (Coira *et al.* 1982; Mpodozis & Ramos 1989). Evolution of this early period in central Chile and Argentina is characterized by a dominating extensional tectonic regime, a rather thin crust, the development of a magmatic arc slightly oblique to the present day Pacific coast and a backarc basin on its eastern side (Mpodozis & Ramos 1989, 2008; Ramos 2010). This orientation of the arc–backarc basin palaeogeographic pair suggests that the late Proterozoic and Palaeozoic sutures and other major structures along the western margin of Gondwana still exerted a control on the tectonic evolution of this region. The tectonic evolution was further controlled by a rather loose plate coupling (negative trench roll-back) caused by the subduction of a considerably old and dense oceanic plate that had remained practically quiet during the pre-Andean cycle.

The two stages in which this Early period has been subdivided are reflected in the late Early to Late Jurassic and latest Jurassic to late Early Cretaceous by two magmatic episodes along the arc and two transgression–regression cycles in the backarc. This separation is clear for the backarc basin deposits, although it is less evident for the arc deposits and plutonic units. However, the plutonic units of the second stage are slightly shifted to the east of the plutonic units of the first stage (Sernageomin 2002). In the arc region, the beginning of this cycle is defined by the first appearance of subduction related lavas covering and interrupting sedimentation of the westernmost marine deposits of the second stage of the pre-Andean cycle (i.e. Pan de Azúcar, Profeta and Los Molles formations; see Charrier *et al.* 2007), whereas in the eastern flank of the Andes it seems to have begun before. In fact, structuration of the backarc basins of the Early Period began there in the latest Triassic–earliest Jurassic (Pre-Cuyano sedimentary cycle), suggesting that the tectonic conditions (tectonic subsidence) had changed before the subduction-related magmas could reach the surface. The first stage (late Sinemurian–Pliensbachian to Kimmeridgian) is characterized by intense activity in the arc and development of a transgressive–regressive marine cycle in the backarc basin. At the end of this stage a second phase of tectonic subsidence followed by thermal subsidence began. This second stage (Kimmeridgian to Aptian–Albian) is characterized by apparently less activity in the arc, and by a second transgression–regression marine cycle in the backarc basin.

Palaeogeography during this Early Period was apparently controlled by NNW-orientated structures, somehow like in the Pre-Andean cycle. This is demonstrated by the reduction in the width of the presently remaining arc towards the north, and its almost complete absence in the Arica region, in northernmost Chile. This plus the eastward shift of the magmatic arc in the second stage, allows identification in the second stage and south of c. 30°S (latitude of La Serena) of another depocentre, the Lo Prado basin, located west of the arc (i.e. in the Coastal Cordillera) and therefore in a forearc position (Charrier 1984; Charrier *et al.* 2007). Additionally, in this region, the backarc basin, which is known as the Mendoza–Neuquén basin, gradually bends southeastwards, and becomes considerably wider than further north. This basin, which extends eastwards into Argentina, represents the southernmost part of the Jurassic–Early Cretaceous backarc basin, which is traceable without interruption along the eastern side of the magmatic arc from at least southern Ecuador to southern Argentina, at c. 40°S, and, possibly, still further south (Vicente 2005).

ANDES OF CENTRAL CHILE AND WESTERN ARGENTINA

First stage (Pliensbachian–Kimmeridgian)

Magmatic arc. Along the coast a wide swath consisting mostly of Middle–Late Jurassic and Early Cretaceous plutons and associated volcanic units represents the arc activity (Fig. 3). In the northern part of the study region, Jurassic plutonic units can be continuously followed up to 34°S (Fig. 3). Further south, exposures are patchy, up to 38°S, where they begin to occur further east, in the high Andes, following the bend formed by the Palaeozoic units (south of the region included in Fig. 3; see Sernageomin 2002, for more detail). North of 33°S, they consist of monzodiorites and granodiorites of Late Jurassic age assigned to the Puerto Oscuro and Cavilolén units, with Sr initial ratios of 0.7034 and 0.7035 (Parada *et al.* 1988; Rivano & Sepúlveda 1991). These initial ratios, being lower than those obtained in the Late Triassic Tranquilla and Millahue units (0.7063 and 0.7050), indicate a different magma source directly derived from the upper mantle and associated with the recently renewed subduction activity. South of 33°S, they consist of several units (Laguna Verde, El Sauce, Peñuelas, Limache and Lluu-Lliu) comprising I-type, calc-alkaline diorites, tonalities, granodiorites and granites (Gana & Tosdal 1996). According to these authors, intrusion of these units occurred in only 6 myr, between 162 and 156 Ma (Oxfordian to Kimmeridgian times), implying a very rapid pulse of ascent of large amounts of magma. This magmatic pulse can be related to the event of rift-associated subsidence that facilitated extrusion of magmas in the backarc at this time (see Oliveros *et al.* 2012; Rossel *et al.* 2013) and permitted the marine ingressions in the backarc basin.

Volcanic deposits associated with the Jurassic arc are well exposed in the Coastal Cordillera south of 31°S (Fig. 3). These are the Middle–Late Jurassic Ajial Formation (Thomas 1958; Piracés 1977; Vergara *et al.* 1995) and the Late Jurassic Horqueta Formation (Piracés 1977), separated from each other by the Middle Jurassic marine Cerro Calera Formation (Piracés 1976; Nasi & Thiele 1982) that represents a westward advance of the backarc deposits into the arc domain. Further south, at 35°S, the Jurassic arc volcanic activity is represented by the Middle Jurassic Altos de Huamapu Formation (Morel 1981). The mentioned arc deposits conformably overlie Sinemurian marine deposits assigned to the late stage of the pre-Andean cycle in the Curepto region (Thiele 1965). The Horqueta volcanic activity coincides with the rapid plutonic pulse detected by Gana & Tosdal (1996) in the Coastal Cordillera west of Santiago (see above). The Jurassic arc formed a rather low relief, which probably indicates high rates of subsidence (Oliveros *et al.* 2007; Charrier *et al.* 2007).

Backarc deposits. The first transgression–regression cycle (*first stage*) in the backarc basin in this region is represented on the western side of the cordillera by the following marine deposits, from north to south: (a) lower member of the Lagunilla Formation (Aguirre 1960); (b) Río Colina Formation (Thiele 1980); (c) Nieves Negras Formation (Álvarez *et al.* 1997; Charrier *et al.* 2002) formerly Leñas–Espinoza Formation of Klohn (1960) and Charrier (1982); (d) Nacientes del Teno Formation, at 35°S (Klohn 1960) and 36°S (Muñoz & Niemeyer 1984); (e) Valle Grande Formation (González & Vergara 1962), at 35°30'S; and (f) Nacientes del Bio Bío Formation (De la Cruz & Suárez 1997; Suárez & Emparan 1997), at 38°30'S. The base of these formations is not exposed, except for the Nacientes del Teno, which unconformably overlies rhyolitic rocks of possible Triassic age at 35°S (Davidson 1971; Davidson & Vicente 1973), and of confirmed Triassic age (Cajón de Troncoso Beds), between 36 and 37°S (Muñoz & Niemeyer 1984). These formations consist of thick successions of sandstones (some of them turbiditic), marls and limestones, and represent a transgression–regression cycle that ends with thick Oxfordian evaporitic deposits, generally named ‘Yeso Principal’ (Schiller 1912) or more formally Auquilco Formation (Groober 1946), in Argentina, and the Santa Elena Member of the Nacientes del Teno Formation in Chile (Klohn 1960; Davidson 1971; Davidson & Vicente 1973). This gypsum unit, which is the middle member of the Lagunilla Formation, at 33°S (Aguirre 1960), is overlain by the upper member of the Lagunilla Formation (Aguirre 1960) and its southern equivalent, the Río Damas Formation (Klohn 1960), which consists of breccias and alluvial fan deposits that grade towards the east into the red, finer-grained and thinner fluvial sandstones of the Tordillo Formation (Klohn 1960; Arcos 1987). At its type locality (Río de las Damas, next to Termas del Flaco, at 35°S), the Río Damas Formation consists of a c. 3000 m-thick red continental, detrital succession, with coarse and fine intercalations, which includes at the top a member comprising >1000 m of andesitic lavas culminating in breccias containing enormous angular blocks, some over 4 m in diameter (Arcos 1987). Close to its contact with the Baños del Flaco Formation, dinosaur tracks are well exposed (Casamiquela & Fasola 1968; Moreno & Pino 2002; Moreno & Benton 2005). Thus, the Río Damas Formation and northern equivalents represent the final deposits of the first transgression–regression cycle in the backarc basin. Because of the thick backarc volcanic intercalation at the upper part of this formation (Rossel *et al.* 2014), which is overlain by coarse breccias, it has been considered to also represent the initial deposits of

the Second stage of the Early Period, associated with the tectonic subsidence phase (Charrier *et al.* 2007). These deposits are conformably overlain by Late Jurassic to Early Cretaceous marine sediments that form the bulk of the second transgression–regression cycle of the second stage.

Along the eastern slope of the Principal Cordillera the depocentres of the first transgression are represented by a series of alternate sub-basins. The Ramada depocentre in the northern section ($31^{\circ}30' - 32^{\circ}30'S$) has a complete section of continental and volcanic deposits of the Triassic Rancho de Lata Formation, unconformably overlain by the Los Patillos Formation of Early Jurasssic age. This last unit has a rich fauna of ammonites studied by Alvarez (1996) that includes from the Aalenian until the Callovian. The Alto del Tigre High is located in the central segment at the latitude of the Mount Aconcagua ($32^{\circ}30' - 33^{\circ}30'S$) (Fig. 5). It is a positive area where there is no deposition of the Triassic–Early Jurassic deposits known since the early work of Groeber (1918).

Further south, the Yeguas Muertas, Nieves Negras, Alvarado, Río del Cobre, Río Atuel–La Valenciana, Palauco, Sierra Azul, Sierra de Reyes and Cordillera del Viento are some of the depocentres of the Neuquén basin located south of $33^{\circ}S$ (Fig. 5). In particular, the Rio Atuel–La Valenciana is an important subsidence zone west of Malargüe ($34^{\circ} - 35^{\circ}30'S$) with a thick sequence of Triassic rift deposits that continue with the different units of the Cuyo Group represented by Arroyo Malo, El Freno, Puesto Araya and Tres Esquina Formations (Fig. 6) (Legarreta *et al.* 1993). The marine sequence dated by ammonites goes from Rhaetian to Toarcian in a complex fluvio-deltaic array (Lanés 2005).

It is interesting to remark that the Cuyo Group is overlain by the Callovian transgression of the La Manga Formation of the Lotena Group (Fig. 6). This unit includes a thin sequence of limestones between 50 and 100 m thick that covers all the depocentres from La Ramada towards the south, including the Alto del Tigre High (Giambiagi *et al.* 2003a, b). This carbonate platform is followed by a generalized regression that ended with the Auquilco Formation, a thick gypsum deposit up to 200 m thick widely distributed in the Principal Cordillera (Legarreta *et al.* 1993).

Second stage (Kimmeridgian–Albian)

From $30^{\circ}S$ southwards the distribution of the marine deposits accumulated during the second stage forms two clearly separated depositional areas: one in the Coastal Cordillera, and the other in the Principal Cordillera, and mostly on its eastern side (Charrier 1984; Mpodozis & Ramos 1989;

Charrier & Muñoz 1994; Charrier *et al.* 2007). The two basins are separated from each other by a volcanic domain that we propose to name the Lo Prado volcanic arc. Therefore, it is possible to identify three palaeogeographic domains at this moment, from west to east: (a) the Lo Prado forearc basin, bounded to the west by a relief formed on older units; (b) the Lo Prado volcanic arc; and (c) the Mendoza–Neuquén backarc basin, the latter including volcanic activity.

Forearc (Lo Prado forearc basin). Immediately north of the here considered region, in the Elqui river valley transect, at $30^{\circ}S$, on top of the Jurassic arc deposits, the forearc or rather the transitional deposits between the arc and a marine basin to the west are represented by the >4000 m-thick, volcanic, principally basaltic andesites and marine sedimentary Arqueros Formation (Berriasian–Albian) and the >2000 m-thick, continental, mostly red and volcanic Quebrada Marquesa Formation (Hauterivian–early Albian) (Aguirre & Egert 1965, 1970; Thomas 1967; Emparan & Pineda 2006; Rivano & Sepúlveda 1991). The Quebrada Marquesa Formation interfingers with and covers gradually the Arqueros Formation; in its lower portion it contains abundant marine intercalations, some of which are fossiliferous, and consists in its upper portion of a thick succession of pyroxene–olivine bearing basaltic andesites and pyroxene–amphibole bearing andesites (Aguirre & Egert 1965; Emparan & Pineda 1999, 2006; Emparan & Calderón 2014). In this region, the Early Cretaceous backarc deposits (Río Tascadero Formation) are exposed over 60 km to the east in the high cordillera (Mpodozis & Cornejo 1988), where, like the Arqueros Formation, they interfinger with and grade upwards to red continental, volcanic and volcanioclastic facies (Pucalume Formation). In our palaeogeographic reconstruction the Marquesa Formation represents the late Early Cretaceous western facies associated with the magmatic arc, and the Pucalume Formation represents either the easternmost deposits of the magmatic arc or volcanic deposits that resulted from volcanic activity in the backarc.

Southern deposits with similar facies and the same stratigraphic position that the Arqueros Formation are the Lo Prado (Berriasian to Valanginian) and the La Lajuela (Early Cretaceous) formations. Both formations are constrained to the Coastal Cordillera south of c. $34^{\circ}S$ and correspond to the oldest forearc basin deposits, which contain abundant lavas derived from the volcanic arc flanking the basin to the east. These units overlie, from north to south, the Late Jurassic arc-related Agua Salada Volcanic Complex (Emparan & Pineda 2006; Emparan & Calderón 2014), the Horqueta (Thomas 1958; Piracés 1977; Nasi & Thiele 1982;

ANDES OF CENTRAL CHILE AND WESTERN ARGENTINA

Period	Stage	Western flank	Eastern flank
Cretaceous	Maastrichtian		Malargüe Gr.
	Campanian		
	Santonian		
	Coniacian	B.R.C.U.	Neuquén Gr.
	Turonian		
	Cenomanian		
	Albian	Cristo Redentor or Colimapu Fm.	Rayoso Gr.
	Aptian		Rayoso Fm.
	Barremian		Huitrín Fm.
	Hauterivian	San José, Lo Valdés or Baños del Flaco Fm.	Agrio Fm.
	Valanginian		Mulichinco Fm.
	Berriasian		Quintuco Fm.
	Tithonian		Vaca Muerta Fm.
Jurassic	Kimmeridgian	Río Damas Fm.	Tordillo Fm.
	Oxfordian	Lagunilla or Nacientes del Teno Fm.	Gypsum Mber.
	Callovian		Lower Member
	Bathonian		
	Bajocian		
	Aalenian		
	Toarcian		
	Pliensbachian		
	Sinemurian		
	Hettangian		
	Triassic		
			Lotena Gr.
			Auquilco Fm. "Yeso Principal"
			La Manga Fm. Lotena Fm.
			Cuyo Group
			Tábanos Fm.
			Lajas Fm.
			Los Molles Fm.

Fig. 6. Stratigraphic succession of the Jurassic to Cretaceous deposits in the Principal Cordillera in central Chile and Argentina, between 32 and 37°S. Based on Aguirre (1960), Klohn (1960), González & Vergara (1962), González (1963), Davidson (1971), Davidson & Vicente (1973), Thiele (1980), Charrier (1981a) and Charrier *et al.* (2002).

Rivano & Sepúlveda 1991; Rivano 1996; Vergara *et al.* 1995) and Altos de Hualmapu formations (Bravo 2001). The Arqueros, Lo Prado and La Lajuela formations are conformably overlain by thick continental volcanic and volcanioclastic deposits of the Quebrada Marquesa (Rivano & Sepúlveda 1991; Emparan & Calderón 2014), Veta Negra Formation (Piracés 1977; Nasi &

Thiele 1982; Vergara *et al.* 1995) and El Culener Beds (Bravo 2001), respectively. These extremely thick successions form a narrow band of almost continuous outcrops up to almost 36°S (Fig. 3). The stratigraphic position of the Veta Negra Formation and the age of the oldest granitoids that intrude this unit bracket its age to the Berriasian–Albian (Vergara *et al.* 1995). Notwithstanding the

stratigraphic position of the Veta Negra Formation, radioisotopic age determinations in this unit indicate that it is slightly older (*c.* 119 Ma; Aguirre *et al.* 1999; Fuentes *et al.* 2001, 2005) than the older lavas of the northern equivalent Arqueros Formation (117–115 Ma) (Morata & Aguirre 2003), suggesting a northward progression of volcanism and tectonic extension (Morata & Aguirre 2003; Morata *et al.* 2008).

The rather deep depositional conditions detected for the lower Lo Prado marine deposits and the several thousand metres-thick pile encompassed by the Lo Prado and Veta Negra formations indicate intense subsidence in the forearc basin (Vergara *et al.* 1995). Additionally, the rather primitive geochemical composition of the Lo Prado rocks with low MgO and high K content, that fall in the classification of high-K and shoshonitic porphyric basaltic andesites and andesites, and their low initial Sr ratios (*c.* 0.7036) are indicative of intense crustal extension in the basin during Early Cretaceous time (Morata & Aguirre 2003; Parada *et al.* 2005). Similarly, the flood-basalt-type flows of the overlying Veta Negra lavas (Åberg *et al.* 1984), the presence in this formation of approximately north–south-orientated dyke swarms suggestive of fissural eruptions parallel to the strike of the basin (Vergara *et al.* 1995), and its geochemical features (low La/Yb ratios, low $^{87}\text{Sr}/^{86}\text{Sr}$ ratio of 0.70374 and more primitive Sr–Nd ratios than those of the Jurassic lavas), indicating an attenuated crust (Vergara *et al.* 1995; Morata & Aguirre 2003), are additional evidence for extensional tectonic conditions during Early Cretaceous times in the Lo Prado forearc basin. This basin corresponds to the aborted marginal basin of Åberg *et al.* (1984) and the intra-arc basin of Charrier (1984).

On the eastern flank of the Coastal Cordillera, the 3000 m-thick Las Chilcas Formation overlies with an apparently conformable contact the Veta Negra Formation (Wall *et al.* 1999). The lower volcanic portion of this formation has been dated (U–Pb) at 109.6 ± 0.1 and 106.5 ± 0.2 Ma (Wall *et al.* 1999), while lavas from its upper portion yielded K–Ar ages in plagioclase of 95 ± 3 Ma (Gallego 1994). Based on these ages, we suggest that the Las Chilcas Formation formed during the transition from the Early to the Late period of Andean evolution. The lower portion, consisting of basaltic and andesitic lavas and dacitic and rhyolithic pyroclastics, developed in apparent conformity with the underlying Veta Negra Formation, would be the continuation of the volcanic activity developed in the Lo Prado forearc basin, whereas the coarse conglomerates of its upper part would correspond to syn-orogenic deposits associated with the Peruvian orogeny. We discuss this point below.

Lo Prado magmatic arc. Early Cretaceous plutonic rocks form an almost continuous swath of hypabyssal dioritic to granitic plutons, which mostly intrude the Early Cretaceous deposits mentioned above (Rivano & Sepúlveda 1991; Gana & Tosdal 1996; Rivano *et al.* 1993; Emparan & Calderón 2014). K–Ar age determinations on these plutons yielded ages 134–86 Ma (Parada *et al.* 1988; Bravo 2001). Recent $^{40}\text{Ar}/^{39}\text{Ar}$ dates in the northward prolongation of this swath, immediately north of the here considered region, yielded ages between 139 and 100 Ma (Valanginian–Albian) (Emparan & Calderón 2014). Low Sr initial ratios obtained on Early Cretaceous granitoids in the northern part of the region (31° – 32°S) indicate an upper mantle origin, with virtually no continental crust involvement for these magmas (Parada *et al.* 1988; Creixell *et al.* 2011). This conclusion confirms the idea that the crust was thin and the tectonic conditions were extensional during development of the forearc basin, as well as in the Principal Cordillera, where thermal subsidence dominated the retroarc basins.

Arc volcanic rocks are also exposed further east and only in the northern part of the region (north of 32°S). These have been assigned to the Pucalume Formation, unless they correspond to backarc volcanic activity (Charrier *et al.* 2007). In the Aconcagua area the Late Jurassic–Early Cretaceous successions are interbedded with backarc basalts and pyroclastic deposits (Cristallini & Ramos 1996).

Backarc basin (Mendoza–Neuquén basin). Backarc basin deposits in this region are exposed in Chile in the High Andes close to the international boundary and extend eastwards into western Argentina (Fig. 3). These generally consist mostly of sedimentary marine facies; however, at some localities they interfinger with volcanic deposits that, depending on their location, are interpreted as the easternmost arc deposits or to products of backarc volcanic activity.

In the high cordillera, in northern part of the region, between 31 and 32°S , volcanic deposits of the Late Jurassic Algarrobal Formation are exposed. These deposits interfinger and are covered by the conglomeratic Mostazal Formation (Mpodozis & Cornejo 1988; Oliveros *et al.* 2012), which is a western lateral facies of the Kimmeridgian, finer-grained, continental Tordillo Formation exposed next to the international border, between 31 and 33°S (Rivano & Sepúlveda 1991; Rivano *et al.* 1993; Lo Forte *et al.* 1996; Aguirre-Urreta & Lo Forte 1996). The great distance (>80 km) that separates these volcanic deposits from those of the arc in this region suggests that they correspond to backarc volcanism, as has been observed in some regions along the central Argentina–Chilean Andes (Charrier *et al.* 2007; Mescua *et al.* 2008;

ANDES OF CENTRAL CHILE AND WESTERN ARGENTINA

Mpodozis & Ramos 2008; Oliveros *et al.* 2012, among others).

Second-stage backarc marine sedimentary deposits in the northern part of the region consist of the Early Cretaceous Río Tascadero Formation (Mpodozis & Cornejo 1988; Rivano & Sepúlveda 1991). This unit forms a NNW-orientated swath that extends south-southeastwards into Argentina. Southwards, on the western flank of the cordillera, at 31°30'S, there is another similarly orientated swath, extending also into Argentina and consisting predominantly of volcanic and volcaniclastic deposits with mostly coarse detritic intercalations (breccias, conglomerates, and sandstones), and minor and finer marine fossiliferous calcareous sandstones, assigned to the Los Pelambres Formation (Rivano & Sepúlveda 1991).

Similar deposits exposed along the international border and next to it on the eastern flank of the cordillera at 33°S have been assigned to the Juncal Formation (Ramos *et al.* 1990; Aguirre-Urreta & Lo Forte 1996; Cristallini & Ramos 1996). Further east, the volcanic intercalations rapidly disappear eastwards, indicating that the source of the lavas and coarse volcaniclastic sediments was located to the west. Their source can either be the volcanic Lo Prado arc or volcanic edifices developed in the backarc basin to the east of the main magmatic arc. Because of the considerable distance separating the volcanic arc in the Coastal Cordillera and the volcanic deposits exposed along the axis of the Principal Cordillera, we favour the existence of volcanic activity in the backarc at this time coexisting with marine sedimentation. If this interpretation is correct it would emphasize the importance of volcanism in the backarc during the early period of the Andean Cycle (Ramos 1999; Charrier *et al.* 2007; Oliveros *et al.* 2012; Rossel *et al.* 2013).

Further south, between 33 and 36°15'S, along the western side of the Principal Cordillera (Fig. 3), but with a more external position than the previously mentioned units, Late Jurassic (Kimmeridgian) to late Early Cretaceous (Aptian–Albian), red continental and marine backarc deposits have been assigned to the upper member of the Lagunillas (Aguirre 1960) and Río Damas (Klohn 1960) formations, and the overlying marine San José (Aguirre 1960), Lo Valdés (González 1963; Hallam *et al.* 1986) and Baños del Flaco (Klohn 1960; González & Vergara 1962; Covacevich *et al.* 1976; Charrier 1981a; Arcos 1987) formations, and the red, detritic, continental Colimapu Formation (Klohn 1960) (see Fig. 6). These form a continuous, although considerably thrusted and folded, swath of outcrops that extends further east into Argentina. The marine rocks consist of thick, richly fossiliferous successions of predominantly calcareous neritic to shallow (external platform) sediments. Lavas in the

Lo Valdés Formation form a thin intercalation in its lower portion (Biró-Bagóczky 1964), and volcanic intercalations in the Baños del Flaco Formation, a few kilometres to the south of the previous locality (*c.* 34°S), form a 440 m-thick succession of volcanic breccias and silicic lavas between marine fossiliferous sediments of Tithonian–Neocomian age (Charrier 1981b). In these formations the volcanic intercalations and volcanic components in the detritic deposits rapidly disappear eastwards, indicating again that the source of the lavas and coarse volcaniclastic sediments was located towards the west. At Termas del Flaco, in the Tinguiririca river valley, at 35°S, only the lowest portion of the Baños del Flaco is exposed. Its upper portion, and probably also the overlying Colimapu Formation, have been eroded in this place (Charrier *et al.* 1996). The final regressive episode led to the deposition of a second, generally thin band of gypsum ('Yeso Secundario' or 'Yeso Barremiano') at the base of the 1500 m-thick, red detrital Colimapu Formation (Klohn 1960; González & Vergara 1962; González 1963; Charrier 1981b), which corresponds to the generally fine-grained continental deposits with thin calcareous intercalations containing ostracodes that followed the regression in Aptian–Albian times. In the Maule river valley (36°S), a recent dating with detritic zircons yielded an Aptian maximum age for deposition of these deposits (Astaburuaga 2014). This formation is a lateral equivalent of the Huitrín–Rayoso Formation in western Argentina (Fig. 6).

At the end of the first Andean stage, a major plate reorganization associated with a great increase in generation of oceanic crust in the proto-Pacific (Larson 1991) and rapid westward drift of South America modified the tectonic conditions in the continental margin of South America. This geo-dynamic event, known as the Peruvian orogeny (Steinmann 1929; see also Groeber 1951; Charrier & Vicente 1972; Vicente *et al.* 1973; Ramos 1988b, 2010; Reutter 2001; Tunik *et al.* 2010), caused along western South America uplift of the continental margin, the marine regression referred above and definite emersion in the backarc basin, compressive deformation of the existing units, and crustal thickening. As a result of this phase, the first Andean mountain range was formed.

Late period (early Late Cretaceous: Present)

The Peruvian orogeny separates the Early and Late periods into which Coira *et al.* (1982) subdivided the evolution of the Andean tectonic cycle. After this episode the palaeogeographic organization in this region of the Andes changed

completely: the backarc basin was inverted, the magmatic arc shifted considerably eastwards, a new mountain range was developed, a continental retroarc foreland basin was formed to the east of the arc instead of a backarc basin, and a rather wide forearc region west of the arc was produced as a result of eastward arc migration. Oblique subduction also prevailed at this time, although the movement of the oceanic plates towards the continent was mostly northeastward orientated, producing dextral displacement along trench-parallel faults. Moreover, some authors suggest from plan view reconstructions an orthogonal subduction for this moment, thus, dextral displacement could be less important (Arriagada *et al.* 2008; Martinod *et al.* 2010). The Late Period has been subdivided into two stages separated from each other by a major orogenic phase that occurred in middle Eocene, the Incaic orogeny (Fig. 1). Each one of these stages can be, in turn, subdivided into two substages by orogenic episodes that occurred at approximately the Cretaceous–Cenozoic boundary ('K–T' orogeny; Cornejo *et al.* 2003) and the Oligocene–Miocene boundary (Pehuenche orogeny; Fig. 1), respectively.

First stage (early Late Cretaceous–middle Eocene)

During the first stage, in the region between 31 and 37°S, a high sea-level stand in latest Cretaceous–earliest Cenozoic times caused a slight marine ingressions along the western border of the present day Coastal Cordillera, and an extended marine incursion of Atlantic origin, on the eastern side of the mountain range that reached the axis of the present-day Principal Cordillera. This marine ingressions from the Atlantic side was favoured by the tectonic loading and subsequent subsidence that developed a long foredeep along the eastern foothills of the Andes (Aguirre-Urreta *et al.* 2011).

For a better understanding of the following description of geological units, we will describe them separately in two different segments: a northern (31°–34°S) and a southern segment (34°–37°S).

Northern segment. The arc is represented by two parallel, close to each other, series of small and medium-sized plutonic outcrops located along the eastern flank of the Coastal Cordillera, immediately to the east of the previous arc representatives (Fig. 3). These outcrops can be followed up to 34°S, where they disappear or have not been identified. They consist of monzodiorites and subordinated granodiorites, gabbros, diorites and hypabissal andesitic and dioritic bodies (Rivano & Sepúlveda 1991; Rivano *et al.* 1993; Sellés & Gana 2001), and have been included by these

authors in the Cogotí superunit, and more recently in the Illapel Plutonic Complex by Morata *et al.* (2010) and Ferrando *et al.* (2014).

Stratified deposits corresponding to this stage are represented, between 31 and 33°S, by the following Late Cretaceous volcanic, volcanioclastic and sedimentary stratigraphic units: (a) upper part of the Las Chilcas; (b) the Viñita and its equivalent the Salamanca; and (c) the Lo Valle formations, with ages ranging from 95.3 to 64.6 ± 5 Ma (Drake *et al.* 1976; Rivano & Sepúlveda 1991; Rivano *et al.* 1993; Gallego 1994; Mpodozis *et al.* 2009; Jara & Charrier 2014). The coarse and thick conglomeratic deposits of the upper Las Chilcas Formation, with a marine calcareous intercalation and some basaltic and andesitic–basaltic lavas at the top, would correspond to syn-orogenic deposits accumulated in a retroarc foreland basin developed with the Peruvian orogeny, which was deep enough to be invaded by the sea, and volcanic-arc deposits in its eastern and western border, respectively.

In fact, in this region, apatite fission track ages indicate for the western Coastal Cordillera the existence of a cooling event that began at 106–98 Ma (Gana & Zentilli 2000). This age is complemented by studies in the Caleu pluton on the eastern Coastal Cordillera indicating that crystallization occurred in the interval 94.2–97.3 Ma and that cooling occurred until about 90 Ma (Parada *et al.* 2005; Ferrando *et al.* 2014). These data have been confirmed by Willner *et al.* (2005), who reported for the eastern and western series of the metamorphic complex a cooling event between 113 and 80 Ma. This event is probably related to an exhumation process associated with uplift that can be associated with the Peruvian orogeny. Considering that it coincides with the age of the Las Chilcas Formation, we propose that the Las Chilcas Formation formed during the end of the Early period of Andean evolution and the beginning of the Late period, and represents the transition from an extensional to a compressional tectonic regime. A similar view has been proposed for the Caleu pluton (Parada *et al.* 2005). The calc-alkaline, silicic pyroclastic deposits, intermediate lavas and continental sediments of the Lo Valle Formation (Thomas 1958; Godoy 1982; Moscoso *et al.* 1982; Rivano 1996; Gana & Wall 1997) cover unconformably the Las Chilcas Formation. The Lo Valle Formation represents the deposits of the Late Cretaceous volcanic arc. K–Ar and Ar–Ar age determinations from samples collected at 33°S yielded 70.5 ± 2.5, 64.6 ± 5, 72.4 ± 1.4 and 71.4 ± 1.4 Ma (Vergara & Drake 1978; Drake *et al.* 1976; Gana & Wall 1997). According to these ages the unconformity that separates the Las Chilcas Formation from the overlying Lo Valle Formation represents a 20 Ma hiatus (Gana & Wall 1997).

ANDES OF CENTRAL CHILE AND WESTERN ARGENTINA

Southern segment. Further south, between 33 and 37°S, Late Cretaceous to Palaeogene deposits are exposed on the western and eastern flanks of the Coastal Cordillera, and in the Principal Cordillera. On the western flank of the Coastal Cordillera to south of Santiago, deposits of both Late Cretaceous to early Paleocene age and of late Paleocene (?) to Eocene age have been reported. The Late Cretaceous to Paleocene outcrops consist of fossiliferous marine platformational deposits related to the eustatic high stand developed at this time, and are exposed in the following localities, from north to south: Algarrobo (Levi & Aguirre 1960; Tavera 1980; Wall *et al.* 1996; Yury-Yáñez *et al.* 2012), Topocalma (Charrier 1973; Cecioni 1978; Tavera 1979), Faro Carranza, south of Constitución (Chanco Formation; Cecioni 1983), and in the Arauco region, at the latitude of Concepción (*c.* 37°S) (Quiriquina Formation; Steinmann *et al.* 1895; Wetzel 1930; Muñoz-Cristi 1946, 1956; Biró-Bagóczky 1982; Stinnesbeck 1986; Finger *et al.* 2007; Salazar *et al.* 2010; Buatois & Encinas 2011). The Quiriquina Formation overlies the late Palaeozoic metamorphic complex and is unconformably overlain by the late Paleocene (?) to Eocene Concepción Group.

In the coastal region at the latitude of Concepción, late Paleocene (?)–Eocene deposits of the Concepción Group comprise alternations of continental and marine deposits accumulated in extensional basins formed along the coast in late Paleocene (?) to Eocene times. This outstanding succession containing hydrocarbon and important coal reserves is characterized by an alternation of transgressive and regressive episodes, controlled by eustatic changes, local subsidence and uplift of tectonic blocks (Wenzel *et al.* 1975; Pineda 1983a, b), and general uplift of the Andean range. It consists of the following formations, some of which interfinger with each other: Pilpilco (early Eocene, littoral marine sequence, partly continental), Curanilahue (early Eocene, a mainly continental sequence, coal-bearing strata), Boca Lebu (early Eocene, marine transgressive sequence), Trihueco (middle Eocene, a mainly continental sequence, coal-bearing strata) and Millongue (middle to late Eocene, marine sequence) (Tavera 1942; Muñoz-Cristi 1946, 1973; Pineda 1983a, b; Arévalo 1984; Finger *et al.* 2007). Along the eastern flank of the Coastal Cordillera up 35°15'S, the Late Cretaceous Lo Valle Formation is further exposed (Bravo 2001).

In the Principal Cordillera at 35°S, upward fining and thinning red-coloured fluvial deposits that unconformably rest on Jurassic terms of the Baños del Flaco Formation and unconformably underlie early Oligocene mammal bearing levels of the Abanico Formation have been informally named

Brownish-red Clastic Unit by Charrier *et al.* (1996). Similar deposits crop out next to the water divide at 36°S overlying Middle to Late Jurassic rocks of the Nacientes del Teno Formation and underlying the Late Cenozoic volcanic deposits assigned to the Campanario Formation (Drake 1976; Hildreth *et al.* 1998). These have been included in the Estero Cristales Beds by Muñoz & Niemeyer (1984). According to their stratigraphic position, these deposits can be assigned a Late Cretaceous age and correlated with the Late Cretaceous Neuquén Group on the eastern side of the cordillera (Charrier *et al.* 1996; Mescua 2011). On the western side of the cordillera, these units can be correlated with the upper Las Chilcas and the Viñita formations, further north. In westernmost Argentina, between 33 and 38°S on the eastern side of the Principal Cordillera, marine deposits of the Saldeño Formation (Tunik 2003) and the Malargüe Group (Bertels 1969, 1970; Aguirre-Ureta *et al.* 2011) testify to the far-reaching nature of the Late Cretaceous to early Cenozoic Atlantic transgression. The absence of these deposits in Chile suggests the existence of a relief that stopped the advance of the sea further west.

Along the western flank of the Andes, in Argentina between 35 and 38°S, the Late Cretaceous, 1500 m-thick red fluvial detritic deposits of the Neuquén Group, and the overlying Bajada del Agrio Group correspond to the retroarc foreland deposits related to the Peruvian orogeny (Ramos 1981; Ramos & Folguera 2005; Tunik *et al.* 2010; Di Giulio *et al.* 2012) (Fig. 1). New U–Pb detrital zircons age determinations indicate an early phase of westward-sourced deposits followed by deposition of sediments originated to the east of the retroarc foreland basin associated with uplift of the peripheral bulge as a consequence of the Late Cretaceous thrust front migration (Di Giulio *et al.* 2012).

In middle Eocene, the Incaic orogeny put an end to this stage. This event coincides with the peak of high convergence rate associated with a considerable reduction of the obliquity of convergence after 45 Ma (Pardo-Casas & Molnar 1987).

Second stage (middle Eocene–Present)

The northern part of the considered region, between 31 and 33°S, is located in the southern part of the flat-slab segment, where the Central Depression and the volcanic arc are not developed. This is the region where the Frontal Cordillera, the Pre-cordillera and the Pampean ranges are developed (Fig. 2). The southern part, instead, between 33 and 37°S, is located in the transition to and in the normal subduction segment, where the Central Depression and the volcanic arc (along the axis of

the Principal Cordillera) have developed. In this stage, the Maipo orocline occurred in close relationship with the Pampean flat-slab. Palaeomagnetic rotations are observed within the normal subduction segment (Arriagada *et al.* 2013). In the considered region, second-stage deposits are located in all morphostructural units. We will describe the deposits from west to east.

Western Coastal Cordillera. No Oligocene deposits exist along the coastal region in Chile, probably because of the eustatic low stand at this time. Between $33^{\circ}40'$ and $34^{\circ}15'S$, exposures of Miocene marine sediments are known as the Navidad Formation *sensu* Darwin (1846) and Tavera (1979). Recent work subdivided these deposits into the Navidad, Licancheo and Rapel formations (Encinas *et al.* 2006a). The Navidad Formation has been assigned a late Miocene age and the Licancheo and Rapel formations a Pliocene age by Finger *et al.* (2003) and Encinas *et al.* (2006a), whereas Gutiérrez *et al.* (2013) assigned an early to middle Miocene age to the Navidad Formation and a late Miocene age to the Licancheo and Rapel formations. The latter is overlain by the late Miocene to Pliocene, transitional marine to continental, richly tuffaceous La Cueva Formation (Tavera 1979), which interfingers and is overlain to the east by continental deposits of the Potrero Alto Beds of uncertain Miocene–Pliocene to Pleistocene age (Wall *et al.* 1996). According to Encinas *et al.* (2006a), the Navidad Formation was deposited on a rapidly subsiding basin, which reached depths of 1500 m; in contrast, Gutiérrez *et al.* (2013) favour a shallow coastal to outer shelf environment for this formation. The Navidad Formation can be correlated with the Ranquil Formation, to the south at $37^{\circ}S$.

The source of sediments in the Navidad basin based on the analysis of heavy mineral assemblages is the nearshore basement rocks (metamorphic and intrusive units) in the Coastal Cordillera and the central Chilean forearc (Rodríguez *et al.* 2012). Sediment supply from the latter began with erosion at the present-day eastern Central Depression (western Abanico Formation), later at the eastern Central Depression–western Principal Cordillera border (Miocene plutons), and finally in the western Principal Cordillera (Farellones Formation) (Rodríguez *et al.* 2012). The eastwards shift of the sediment source indicates the slow and gradual retreat experienced by the nick-points, which, according to Farías *et al.* (2008), arrived in the western Principal Cordillera between 2 and 6 myr after onset of surface uplift, at $c. 7.6$ Ma, and >2 myr later in the eastern Principal Cordillera.

Along the coast of central Chile, Plio-Pleistocene events are widely documented by: (a) marine deposits of the upper Coquimbo Formation (at $30^{\circ}S$)

and correlatives, like the Pliocene upper La Cueva formations (at $34^{\circ}S$) and further south the Tubul Formation (at $37^{\circ}S$) in the Arauco region; (b) fluvial deposits exposed in coastal–near river drainages, like the Confluencia and Caleta Horcón formations (Rivano 1996), and the Potrero Alto Beds; and (c) shoreline and fluvial geomorphic features that testify to a considerable uplift of the forearc. Five well-preserved marine terraces (wave-cut platforms) (Darwin 1846; Paskoff 1970, 1977; Fuenzalida *et al.* 1965; Ota *et al.* 1995; Saillard *et al.* 2009, 2012) and pedimentary surfaces developed in fluvial drainages connected with the marine terraces (Rodríguez *et al.* 2013) have been reported. Cosmogenic datings on these features yielded 6, 122, 232, 321 and 690 ka, and allow reconstruction of a non-steady history of uplift to $c. 100$ – 150 m during interglacial periods after 400 ± 100 ka (Saillard *et al.* 2009; Regard *et al.* 2010; Rodríguez *et al.* 2013).

Central Depression. Until recently, this morphostructural feature, which is developed south of $33^{\circ}S$, has been considered to be of tectonic origin (i.e. Carter & Aguirre 1965) and related to the subduction of the Juan Fernández Ridge (i.e. Jordan *et al.* 1983b). However, based on analyses of uplift markers and nick-point progression supported by geochronological and thermochronological dating, it has been recently interpreted as an erosional feature (Farías *et al.* 2008). However, the Quaternary alluvial and fluvial deposits derived from the Principal Cordillera that build up the $c. 400$ m thick infill, as well as new tectonic evidence, show that the Central Depression is tectonically controlled (see Giambiagi *et al.* 2014). Explosive volcanic activity in the volcanic arc produced abundant lahar and volcanic avalanche deposits such as La Cueva Formation in the coastal region (Encinas *et al.* 2006b). Between $33^{\circ}30'$ and $37^{\circ}S$, tuff and ash-flow deposits covered the Central Depression, that is, the Pudahuel–Machalí Ignimbrite (Stern *et al.* 1984), Teno (MacPhail & Saa 1967; Marangunic *et al.* 1979), Tinguiririca (Abele 1982) and Laja (MacPhail 1966) lahars.

The origin of the Pudahuel–Machalí Ignimbrite (Stern *et al.* 1984) has been associated with the Maipo Caldera, in the high Andes, at $34^{\circ}S$. The ignimbrite flow was channelized along the main river valleys towards the coastal region, and into Argentina, along the Yaucha and Papagayos valleys. The tuff deposits in Pudahuel, next to Santiago, and Machalí, east of Rancagua, yielded apatite fission track ages of 0.44 ± 0.08 and 0.47 ± 0.007 Ma, respectively (Stern *et al.* 1984).

Principal and Frontal Cordillera. In the northernmost part of the region (31° – $32^{\circ}S$), Oligocene

ANDES OF CENTRAL CHILE AND WESTERN ARGENTINA

plutonic rocks (El Maitén–Junquillar and Bocatoma units) form extensive outcrops that intrude Permo-Triassic volcanics of the Choiyoi Group and younger Mesozoic units (Fig. 3) (Mpodozis & Cornejo 1988; Martin *et al.* 1997; Bissig *et al.* 2001). Further south, these outcrops disappear and two alignments of scattered intrusives of early and middle to late Miocene age (the latter to the east of the former) are exposed along the western flank of the Principal Cordillera. The La Obra and the San Gabriel plutons in the Maipo river valley next to Santiago belong to this group of intrusives. Some of these plutonic bodies are associated with super-giant late Miocene to Pliocene porphyry Cu–Mo ore bodies such as Los Pelambres, Río Blanco–Los Bronces and El Teniente. These ore deposits developed within hydrothermal alteration zones linked to multiphase stocks, breccia pipes and diatreme structures in rocks of Oligocene to Miocene age (Cuadra 1986; Serrano *et al.* 1996; Vivallo *et al.* 1999; Camus 2002, 2003; Skewes *et al.* 2002; Maksaev *et al.* 2004; Charrier *et al.* 2009; Mpodozis & Cornejo 2012).

Some of the stratified units of this stage exposed between 31 and 33°S have been previously considered to represent much older ages. Recent studies have shown that they formed essentially during Oligocene to Miocene times (Mpodozis *et al.* 2009; Jara & Charrier 2014; Jara *et al.* 2014). According to this age and their volcanic and volcaniclastic nature with only subordinated sedimentary intercalations, they can be correlated with similar deposits exposed between 29 and 30°S on the eastern flank of the cordillera in the Valle del Cura region (Winocur *et al.* 2014), and with the Abanico and Farellones formations well exposed 33°S along the western flank of the Principal Cordillera and to the north (Fig. 3).

The dominantly volcanic, middle–late Eocene to Oligocene Abanico Formation, and the Miocene Farellones Formation make up the pre-Pliocene Cenozoic deposits in the Principal Cordillera of Central Chile (31°–36°S) (Aguirre 1960; Klohn 1960; González & Vergara 1962; Charrier 1973, 1981*a, b*; Thiele 1980; Charrier *et al.* 2002; Godoy 2011). The Abanico Formation consists of a locally strongly folded, c. 3000 m-thick succession of volcanic, pyroclastic volcaniclastic and sedimentary deposits including abundant subvolcanic intrusions of the same age (Vergara *et al.* 2004), with a well-developed paragenesis of low-grade metamorphic minerals (Padilla & Vergara 1985; Levi *et al.* 1989; Aguirre *et al.* 2000; Fuentes *et al.* 2001, 2005; Bevins *et al.* 2003; Fuentes 2004; Muñoz *et al.* 2006, 2010). The outcrops of this formation form two north–south orientated swaths separated by the Farellones Formation (Fig. 3) (Sernageomin 2002). This formation contains abundant

mammalian rests (Flynn *et al.* 2007; Charrier *et al.* 2012). At the western side of the Abanico outcrops, 34.3 ± 2.2 Ma old basal Abanico deposits unconformably overlie the 72.4 ± 1.4 and 71.4 ± 1.4 Ma old Lo Valle Formation (Gana & Wall 1997). At the eastern side of the Abanico exposures, the oldest age obtained for the base of the Abanico Formation is 37.67 ± 0.31 Ma (Charrier *et al.* 1996). The Abanico Formation was deposited in an extensional basin formed while the crust was relatively thin, persisting throughout the Oligocene epoch, and underwent subsequent tectonic inversion in late Oligocene to early Miocene time (Pehuenche orogeny, see Fig. 1). This diachronic extensional event has not been recognized in northern Chile (Charrier *et al.* 2009, 2013) and seems to have been concentrated between 28 and 39°S, and probably extended further south, up to 43°S (Godoy 2011).

The younger Farellones Formation is a 2400 m thick, gently folded, almost entirely volcanic unit forming a continuous north–south trending swath between approximately 32 and 35°S (Fig. 3) (Thiele 1980; Charrier 1981*a, b*; Vergara *et al.* 1988). The deposits of the Farellones Formation typically cover the Abanico Formation, up to 35°S, where this formation is not exposed any more. The views about the contact are controversial (Charrier *et al.* 2002; 2007). It has generally been reported as unconformable (Aguirre 1960; Klohn 1960; Jaros & Zelman 1967; Charrier 1973, 1981*a, b*; Thiele 1980; Quiroga 2013). Growth strata have been observed at several localities between the upper Abanico and the lower Farellones deposits (Fock *et al.* 2006; Quiroga 2013). The contractional event evidenced by the growth strata has been associated with the inversion of pre-existing normal faults that participated in the development of the Abanico basin (Charrier *et al.* 2002; Fock *et al.* 2006; Farías *et al.* 2010). Inversion along the eastern side of the basin linked to El Diablo fault triggered the development of the east-vergent thrust–fold belt systems during middle Miocene on the eastern flank of the Principal Cordillera (Ramos *et al.* 1996*b*; Giambiagi *et al.* 2003*a*; Mescua 2011; Muñoz-Saez *et al.* 2014; Giambiagi *et al.* 2014). Furthermore, inversion along the San Ramón Fault on the western side of the Abanico basin caused west-vergent thrusting of the Abanico Formation deposits over the Central Depression (Rauld 2002; Armijo *et al.* 2010). Recent activity has been detected on the San Ramón Fault (Vargas & Rebolledo 2012).

South of 36°S, the prolongation of the younger part of Abanico Formation is the Cura–Mallín Formation (Niemeyer & Muñoz 1983; Muñoz & Niemeyer 1984; Charrier *et al.* 2002; Radic *et al.* 2002; Flynn *et al.* 2008). This formation

accumulated in the southern prolongation of the Abanico Extensional basin (Elgueta 1990; Vergara *et al.* 1997; Jordan *et al.* 2001; Charrier *et al.* 2002; Radic *et al.* 2002; Croft *et al.* 2003; Flynn *et al.* 2008) that in this region was inverted during late Miocene times (Burns & Jordan 1999; Radic *et al.* 2002).

The Cura–Mallín Formation is conformably overlain by the andesitic and conglomeratic Trapa–Trapa Formation, which in turn is unconformably overlain by the late Miocene Campanario Formation, which is a southern equivalent of the upper Farellones Formation and the Pliocene Cola de Zorro Formation (González & Vergara 1962; Muñoz & Niemeyer 1984; Astaburuaga 2014). A nearly coeval stratigraphic series has been recognized in the Andacollo region on the Argentine side of the Andes at 37°S (Jordan *et al.* 2001), where these authors applied the same formation names as used in Chile. These Argentine deposits unconformably overlie the early Cenozoic Serie Andesítica, and are overlain by the late Miocene sedimentary and volcaniclastic Pichi Neuquén Formation.

Scattered Plio-Pleistocene volcanic activity on the western Principal Cordillera has been reported for areas located next to the El Teniente ore deposit at 34°S (Camus 1977; Charrier & Munizaga 1979; Charrier 1981*b*; Cuadra 1986; Godoy & Lara 1994; Gómez 2001) and Sierras de Bellavista at 34°45'S (Klohn 1960; Vergara 1969; Charrier 1973; Malbran 1986; Eyquem 2009). These volcanic centres form a north–south alignment suggesting a tectonic control for this activity. Finally, the volcanoes of the present-day magmatic arc lie east of the eastern outcrops of the Abanico Formation, covering Mesozoic units and forming the northern part of the Southern Volcanic Zone (Stern *et al.* 2007). From north to south the most important of these volcanoes are named Tupungato, San José, Maipo and Maipo caldera, Tinguiririca, Planchón–Peteroa, Descabezado Grande, Cerro Azul, Descabezado Chico, San Pedro, Longaví and Chillán, some of which are aligned with the El Diablo fault (see Fig. 3). Isotopic studies on late Neogene magmatic rocks from the Chilean Principal Cordillera reveal a source contamination probably resulting from the deep westwards underthrusting of the basement beneath the orogen, a process that is coeval with thickening and uplifting events in the Andes (Muñoz *et al.* 2013).

Thermochronometric studies oriented to constrain the tectonic-related exhumation history in central Chile, between 28.5° and 32°S, reveal that uplift of the Coastal Cordillera occurred mostly in Palaeogene times (apatite fission track (AFT) ages between *c.* 60 and 40 Ma and apatite He (AHe) ages around 30 Ma) and that little exhumation occurred during the rest of the Neogene in

that region, while exhumation ages from the Fron-
tal Cordillera are younger AFT ages between *c.* 40 and 8 Ma and AHe ages from *c.* 20 to 6 Ma). Thermal modelling of AFT and AHe data allows recognition of three main episodes of accelerated cooling affecting different areas of the Frontal Cordillera: *c.* 30, *c.* 22–17 and *c.* 7 Ma. The first of them coincides with the early stages of development of a late Oligocene extensional intra-arc basin along the eastern Frontal Cordillera, between 29 and 30°S, and is interpreted as a consequence of tectonic exhumation. The early and late Miocene periods of accelerated cooling along the Frontal Cordillera correlate with periods of contractional deformation widely recognized throughout the Central Andes and, thus, interpreted as a consequence of surface-uplift (Rodríguez 2013; Rodríguez *et al.* 2014).

¹⁰Be content in bed-load from different rivers and across a major climatic gradient on the western flank of the mountain range in central Chile has been analysed in order to determine erosion rates associated with uplift (Carretier *et al.* 2013). This study confirms the primary role of slope as a control of erosion even under contrasting climates and supports the view that the influence of runoff variability on millennial erosion rates increases with aridity. However, even if current erosion rates are decoupled from precipitation rates, climate still plays a fundamental role by accelerating the erosion response to uplift (Carretier *et al.* 2014).

Foreland. In Neogene times in the Andean foreland some processes related to shallowing and steepening of the subducting slab occurred, which are described next.

Pampean flat-slab subduction. The magmatic arc that was developed during previous stages of the Andean cycle along the western slope of the Andes expanded and shifted during late Miocene to the Quaternary to the Argentine side between 31 and 33°30'S latitude (Fig. 7) associated with a period of shallowing of the subduction zone (Jordan *et al.* 1983*a, b*).

Magmatic activity ended in the Principal Cordillera at about 8.6 Ma and in Sierras Pampeanas at 1.9 Ma with the last subduction-related volcanism more than 750 km away from the trench (Ramos *et al.* 2002). The first migration of the volcanic arc at these latitudes is recorded in the Aconcagua volcanic rocks. Huge amounts of andesitic and dacitic rocks were erupted at about 15.8 ± 0.4 and 8.9 ± 0.5 Ma in the Aconcagua massif on the eastern side of the Principal Cordillera, at 33°S (see Fig. 3). This area constitutes the new volcanic front 50 km east of the Farellones arc in the western slope. The retroarc magmatism of Paramillos,

ANDES OF CENTRAL CHILE AND WESTERN ARGENTINA

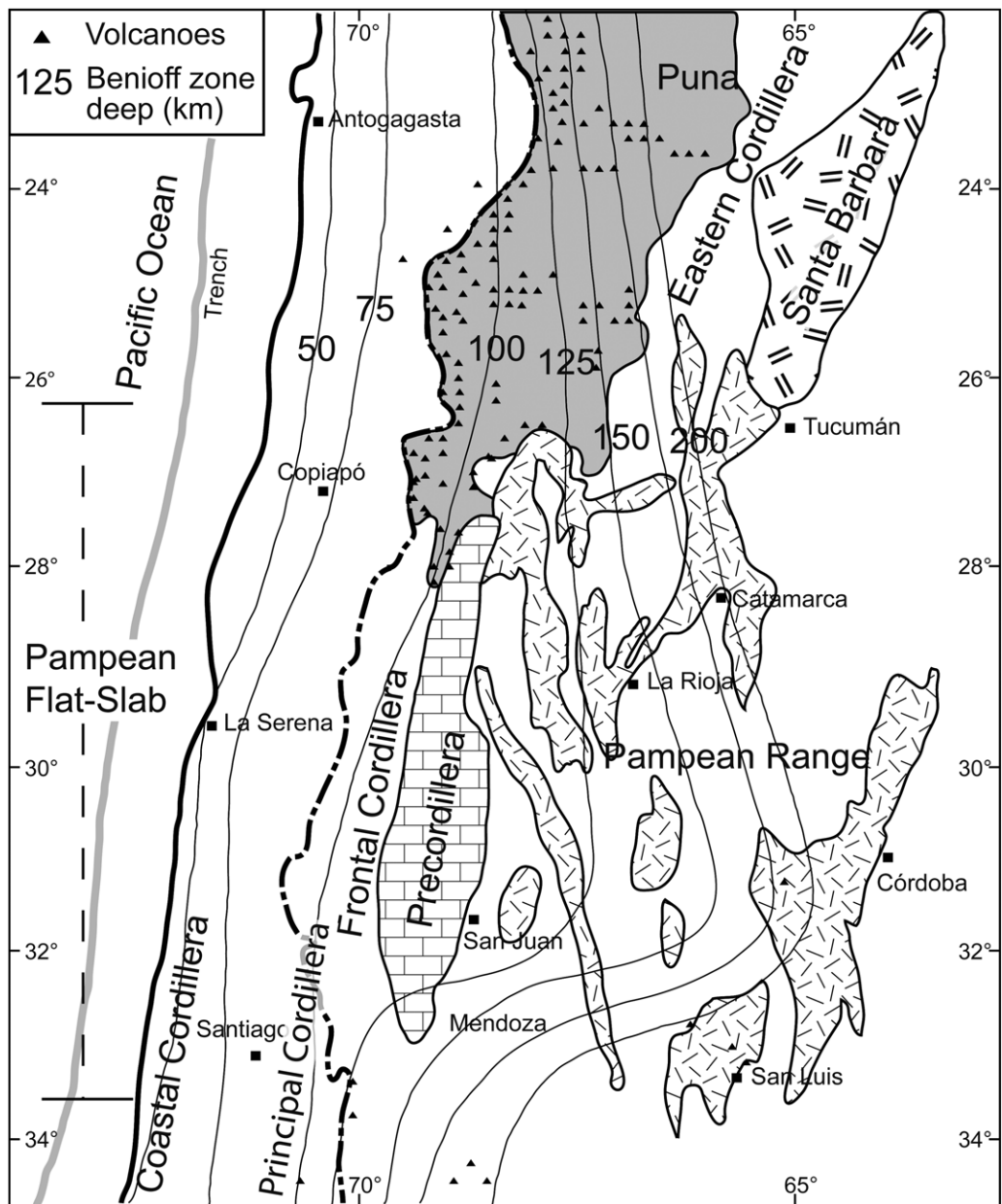


Fig. 7. The Pampean flat-slab segment with the different geological provinces in the foreland, the Quaternary volcanic arc and the isobath to the subducted oceanic slab (after Ramos *et al.* 2002).

west of the city of Mendoza, was shut off at 15.2 Ma, almost at the same time that the migration took place (Ramos *et al.* 1996b). Geochemical studies show a typical calc-alkaline signature of these volcanic rocks (Kay & Abbruzzi 1996).

The shifting of the magmatic arc was preceded by an important deformation in the western half

of the Aconcagua fold-and-thrust belt (Fig. 3) (Ramos *et al.* 1996a). At about 8.6 Ma, the thin-skinned Aconcagua fold-and-thrust belt detached in Jurassic evaporites ceased. As a result of that, the orogenic front migrated about 25 km from Las Cuevas to Río de Las Vacas (Ramos *et al.* 1996b). Syn-orogenic deposits were preserved in

isolated exposures between Principal and Frontal Cordilleras, in the Uspallata–Calingasta depression and in the present foreland basin in the foothills around Mendoza (Fig. 3). Magnetostratigraphic

studies performed in the foothills show that sedimentation started at 15.7 Ma in the Mariño Formation with distal fluvial and eolian deposits with a low sedimentation rate. This unit was followed

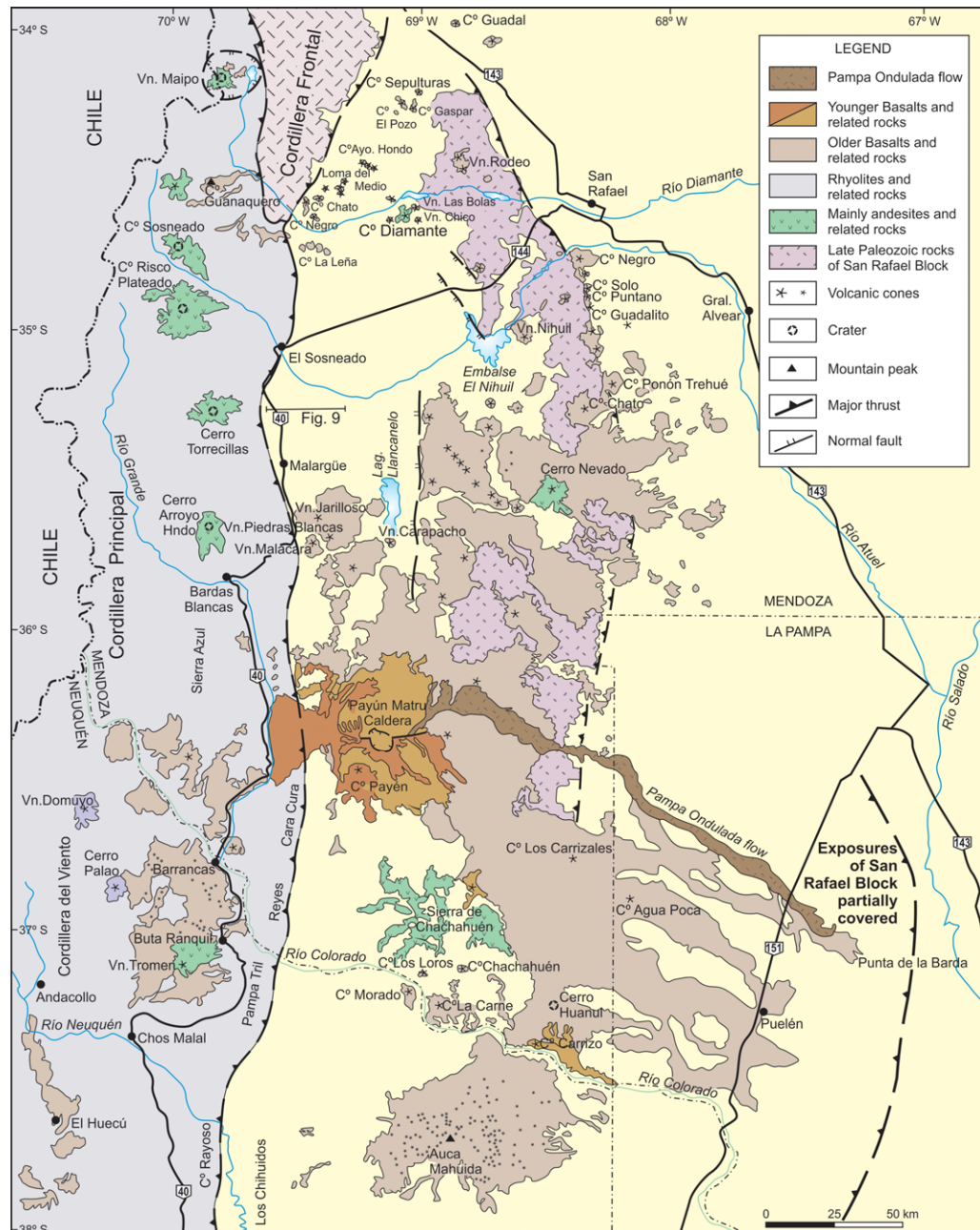


Fig. 8. The Miocene magmatic arc rocks, the Quaternary Payenia basaltic province and the Present thrust front (after Ramos & Folguera 2011).

ANDES OF CENTRAL CHILE AND WESTERN ARGENTINA

by the conglomerates and sandstones of La Pilon Formation at 11.7 Ma, which exhibit a marked increase in accumulation rate with time (Irigoyen *et al.* 2000).

There is no magmatic activity in the Principal and Frontal Cordilleras. Magmatic arc rocks are concentrated in the Sierras Pampeanas between 8 and 6 Ma. Volcanic arc rocks are widespread in the Sierra de San Luis (Urbina & Sruoga 2009) and consist of high-K andesites and dacites with typical shoshonites in the Sierra del Morro, which recorded the latest eruption at 1.9 Ma along the flat-slab subduction segment (Ramos *et al.* 1991, 2002; Kay *et al.* 1991).

The magmatic expansion was accompanied by the development of a broken foreland where several late Cenozoic basins were formed related to tectonic loading and dynamic subsidence (Dávila *et al.* 2005).

The neotectonic activity is presently concentrated between Precordillera and Sierras Pampeanas, where large intracrustal earthquakes have occurred (Alvarado *et al.* 2009). Surface fault ruptures and other neotectonic features indicate important Quaternary deformation (Schmidt *et al.* 2011).

Payenia palaeoflat-slab subduction. South of 33°30'S latitude a different geological setting is observed (Fig. 8). The Principal Cordillera is flanked by the Frontal Cordillera up to 34°30'S, where south of this latitude the foothills of the Andes are in contact with an extensive basaltic plateau of Quaternary age between 34 and 37°S (Ramos & Folguera 2011). This basaltic plateau is known as the Payenia volcanic province.

The Principal Cordillera between 35 and 37.5°S latitudes recorded in the Miocene an important expansion of the magmatic arc from the Chilean slope to the foreland eastern foothills (Spagnuolo *et al.* 2012b; Folguera & Ramos 2011). After a period of extension during the Oligocene, where the within-plate alkaline basaltic rocks of Palauco Formation erupted, a series of granitic stocks were emplaced in the eastern slope of the Principal Cordillera. Subvolcanic bodies of calc-alkaline andesites with ages ranging from middle to late Miocene are found in the foreland extra-andean plains. The eruption of these rocks is also linked to another phase of contraction and deformation (Spagnuolo *et al.* 2012b). The within-plate basalts of the Payenia volcanic province are unconformably overlying previous deposits and extend over an area larger than 40 000 km² between 33°30' and 38°S latitudes. The huge Payún Matru caldera is the main feature related to the Payenia retroarc basalts (Bertotto *et al.* 2009; Llambías *et al.* 2010). The basalts have an estimated volcanic

volume of about 8387 km³ erupted through more than 800 volcanic centres in the last c. 2 Ma (Ramos & Folguera 2011; Gudnason *et al.* 2012; Søager *et al.* 2013).

The sedimentary basin evolution at these latitudes during the Cenozoic shows the transit from a single foreland basin to a broken foreland basin associated with the uplift and exhumation of the San Rafael Block (Silvestro & Atencio 2009; Ramos *et al.* 2014). Geophysical studies have demonstrated that the steepening of a subducted slab is the more appropriate process to explain the extension and characteristics of the Payenia basaltic retroarc province (Burd *et al.* 2008).

Concluding remarks

The analysis of the geology of this sector of the southern Central Andes shows continuous subduction along the proto-Pacific margin of Gondwana and the present margin of South America during most of the Cenozoic. However, it is possible to identify an accretionary orogen during the Palaeozoic, with docking of different terranes, and a Meso-Cenozoic subduction with different tectonic regimes. These variations defined tectonic cycles with different processes, where extensional and compressive regimes alternate through time. The accretion of continental basement terranes produced the obduction of slices of oceanic crust, high-pressure–low-temperature metamorphism, and important shifting to the trench of the magmatic arcs. Periods of shallow subduction, partially combined in late Palaeozoic times with the processes of accretionary orogenesis, produced broken forelands under extreme contraction and subsequent extension and widespread rhyolitic volcanism. The Mesozoic was characterized by subduction with generalized extension until late Early Cretaceous, when evidence of contraction and orogeny led to the present Andean tectonic setting with dominant contraction. The development of segments with flat-slab subduction with no arc-magmatism alternates with segments where, after periods of flat subduction, the steepening of the subduction zone produced generalized extension and backarc basaltic magmatism.

All these processes indicate the complexities of the classic Andean tectonic setting, where the simple subduction of oceanic crust under continental crust controls the orogenesis. The analysed segment, one of the classical sectors of the Central Andes, with excellent exposures and where many of these processes have been first recognized, enhanced the importance of understanding the relationship among magmatism, metamorphism, sedimentation and deformation.

The authors thank the participants of the IGCP 586-Y 'Geodynamic Processes in the Andes, 32–34°S' for their invitation to prepare this introductory chapter to this book. They thank two anonymous reviewers for their valuable suggestions that considerably improved the manuscript and several colleagues who provided in-press manuscripts on subjects related to the considered region. The authors acknowledge: FONDECYT Project no. 1120272, 'Extension, inversion and propagation: key tectonic styles on the development of the Andean Cordillera of central Chile-Argentina (32–36°S)'.

References

- ABELE, G. 1982. El lahar Tinguiririca: su significado entre los lahares chilenos. *Informaciones Geográficas*, **29**, 21–34.
- ÄBERG, G., AGUIRRE, L., LEVI, B. & NYSTRÖM, J. O. 1984. Spreading subsidence and generation of ensialic marginal basin: an example from the Early Cretaceous of Central Chile. In: KOKELAAR, B. P. & HOWELLS, M. F. (eds) *Marginal Basin Geology*. Geological Society, London, Special Publications, **16**, 185–193.
- ACEÑOLAZA, G. & TOSSELLI, A. C. 1976. Consideraciones estratigráficas y tectónicas sobre el Paleozoico inferior del Noroeste Argentino. In: *II Congreso Latinoamericano de Geología*, Caracas, 1973, **2**, 755–764.
- AGUIRRE, L. 1960. Geología de los Andes de Chile Central, provincia de Aconcagua. *Boletín del Instituto de Investigaciones Geológicas*, **9**, 1–70.
- AGUIRRE, L. & EGERT, E. 1965. *Cuadrángulo Quebrada Marquesa, Provincia de Coquimbo*. Instituto de Investigaciones Geológicas, Santiago, Carta Geológica de Chile, escala 1:50.000, Carta 15.
- AGUIRRE, L. & EGERT, E. 1970. *Cuadrángulo Lambert (La Serena), Provincia de Coquimbo*. Instituto de Investigaciones Geológicas, Santiago, Carta Geológica de Chile, escala 1:50.000, Carta 23.
- AGUIRRE, L., HERVÉ, F. & GODOY, E. 1972. Distribution of metamorphic facies in Chile, an outline. *Kristallinkum*, **9**, 7–19.
- AGUIRRE, L., CHARRIER, R. ET AL. 1974. Andean Magmatism: its paleogeographical and structural setting in the central part (30–35°S) of the Southern Andes. *Pacific Geology*, **8**, 1–38.
- AGUIRRE, L., FÉRAUD, G., MORATA, D., VERGARA, M. & ROBINSON, D. 1999. Time interval between volcanism and burial metamorphism and rate of basin subsidence in a Cretaceous Andean extensional setting. *Tectonophysics*, **313**, 433–447.
- AGUIRRE, L., ROBINSON, D., BEVINS, R. E., MORATA, D., VERGARA, M., FONSECA, E. & CARRASCO, J. 2000. A low-grade metamorphic model for the Miocene volcanic sequences in the Andes of central Chile. *New Zealand Journal of Geology and Geophysics*, **43**, 83–93.
- AGUIRRE-URRETA, B., TUNIK, M., NAIPAUER, M., PAZOS, P., OTTONE, E., FANNING, M. & RAMOS, V. A. 2011. Malargüe Group (Maastrichtian–Danian) deposits in the Neuquén Andes, Argentina: implications for the onset of the first Atlantic transgression related to Western Gondwana break-up. *Gondwana Research*, **19**, 482–494.
- AGUIRRE-URRETA, M. B. & LO FORTE, G. L. 1996. Los depósitos tithoneocomianos. In: RAMOS, V. A. (ed.) *Geología de la región del Aconcagua, provincias de San Juan y Mendoza, República Argentina*. Dirección Nacional del Servicio Geológico, Buenos Aires, Anales, **24**, 179–230.
- ALONSO, J. L., GALLATEGUI, J., GARCÍA-SANSEGUNDO, J., FARIAS, P., RODRÍGUEZ FERNÁNDEZ, L. R. & RAMOS, V. A. 2008. Extensional tectonics and gravitational collapse in an Ordovician passive margin: the Western Argentine Precordillera. *Gondwana Research*, **13**, 204–215.
- ALVARADO, P., PARDO, M., GILBERT, H., MIRANDA, F., ANDERSON, M., SAEZ, M. & BECK, S. 2009. Flat-slab subduction and crustal models for the seismically active Sierras Pampeanas región of Argentina. In: KAY, S. M., RAMOS, V. A. & DICKINSON, W. R. (eds) *Backbone of the Americas: Shallow Subduction, Plateau Uplift, and Ridge and Terrane Collision*. Geological Society of America, Boulder, CO, Memoirs, **204**, 261–278.
- ÁLVAREZ, P. P. 1996. Los depósitos triásicos y jurásicos de la Alta Cordillera de San Juan. In: RAMOS, V. (ed.) *Geología de la Región del Aconcagua, provincias de San Juan y Mendoza*. Subsecretaría de Minería de la Nación, Dirección Nacional del Servicio Geológico, Buenos Aires, Anales, **24**, 59–137.
- ÁLVAREZ, P. P. & RAMOS, V. A. 1999. The Mercedario Rift System in the Principal Cordillera of Argentina and Chile (32°SL). *Journal of South American Earth Sciences*, **12**, 17–31.
- ÁLVAREZ, P. P., AGUIRRE-URRETA, M. B., GODOY, E. & RAMOS, V. A. 1997. Estratigrafía del Jurásico de la Cordillera Principal de Argentina y Chile (33°45'–34°00'LS). In: *VIII Congreso Geológico Chileno Antofagasta*. Antofagasta, **1**, 425–429.
- ARÉVALO, A. 1984. *Geología de subsuperficie del área al sur del río Lebu, VIII Región*. Thesis, Departamento de Geología, Universidad de Chile, Santiago.
- ARCOS, R. 1987. *Geología del Cuadrángulo Termas del Flaco, provincia de Colchagua, VI Región, Chile*. Thesis, Departamento de Geología, Universidad de Chile.
- ARMIJOS, R., RAULD, R., THIELE, R., VARGAS, G., CAMPOS, J., LACASSIN, R. & KAUSEL, E. 2010. The West Andean Thrust, the San Ramón Fault, and the seismic hazard for Santiago, Chile. *Tectonics*, **29**, TC2007, <http://dx.doi.org/10.1029/2008TC002427>
- ARRIAGADA, C., ROPERCH, P., MPODOZIS, C. & COBBOLD, P. R. 2008. Paleogene building of the Bolivian Orocline: tectonic restoration of the Central Andes in 2-D map view. *Tectonics*, **27**, TC6014, <http://dx.doi.org/10.1029/2008TC002269>
- ARRIAGADA, C., FERRANDO, R., CÓRDOVA, L., MORATA, D. & ROPERCH, P. 2013. The Maipo Orocline: a first scale structural feature in the Miocene to recent geodynamic evolution in the Central Andes. *Andean Geology*, **40**, 419–137.
- ASTABURUAGA, D. 2014. *Geología estructural y configuración del límite Mesozoico-Cenozoico de la Cordillera Principal entre 35°30' y 36°S, Región del Maule, Chile*. Master's thesis, Departamento de Geología, Universidad de Chile.

ANDES OF CENTRAL CHILE AND WESTERN ARGENTINA

- ASTINI, R. A. 1996. Las fases diastróficas del Paleozoico Medio en la Precordillera del oeste argentino. In: *Evidencias estratigráficas. XIII Congreso Geológico Argentino y III Congreso de Exploración de Hidrocarburos*, Buenos Aires, **5**, 509–526.
- ASTINI, R. A., BENEDETTO, J. L. & VACCARI, N. E. 1995. The early Paleozoic evolution of the Argentine Precordillera as a Laurentian rifted, drifted, and collided terrane: a geodynamic model. *Geological Society of America, Bulletin*, **107**, 253–273.
- ASTINI, R., RAMOS, V. A., BENEDETTO, J. L., VACCARI, N. E. & CAÑAS, F. L. 1996. La Precordillera: un terreno exótico a Gondwana. In: *XIII Congreso Geológico Argentino y III Congreso Exploración de Hidrocarburos*, Buenos Aires, **5**, 293–324.
- ASTINI, R. A., MARTINA, F. & DÁVILA, F. M. 2011. La Formación Los Llantenes en la Precordillera de Jagüé (La Rioja) y la identificación de un episodio de extensión en la evolución temprana de las cuencas del Paleozoico superior en el oeste argentino. *Andean Geology*, **38**, 245–267.
- ÁVILA, J. N., CHEMALLE, F., JR, MALLMANN, G., KAWASHITA, K. & ARMSTRONG, R. 2006. Combined stratigraphic and isotopic studies of Triassic strata, Cuyo Basin, Argentine Precordillera. *Geological Society of America Bulletin*, **118**, 1088–1098.
- BARREDO, S., CHEMALLE, F., MARSICANO, C., ÁVILA, J. N., OTTONE, E. G. & RAMOS, V. A. 2012. Tectono-sequence stratigraphy and U–Pb zircon ages of the Rincón Blanco depocenter, northern Cuyo Rift, Argentina. *Gondwana Research*, **21**, 624–636.
- BELL, M. & SUÁREZ, M. 1995. Slope apron deposits of the Lower Jurassic Los Molles Formation, Central Chile. *Revista Geológica de Chile*, **22**, 103–114.
- BENEDETTO, J. L., SÁNCHEZ, T. M., CARRERA, M. G., BRUSSA, E. D. & SALAS, M. J. 1999. Paleontological constraints in successive paleogeographic positions of Precordillera terrane during the Early Paleozoic. In: RAMOS, V. A. & KEPPIE, D. (eds) *Laurentia-Gondwana Connections Before Pangea*. Geological Society of America, Boulder, CO, Special Papers, **336**, 21–42.
- BERTELS, A. 1969. Estratigrafía del límite Cretácico-Terciario en Patagonia septentrional. *Revista Asociación Geológica Argentina*, **24**, 41–54.
- BERTELS, A. 1970. Micropaleontología y estratigrafía del límite Cretácico-Terciario en Huantraico (Provincia del Neuquén, Parte II). *Ameghiniana*, **4**, 253–298.
- BERTOTTO, G. W., CINGOLANI, C. & BERG, E. 2009. Geochemical variations in Cenozoic back-arc basalts at the border of La Pampa and Mendoza provinces, Argentina. *Journal of South American Earth Sciences*, **28**, 360–373.
- BEVINS, R. E., ROBINSON, D., AGUIRRE, L. & VERGARA, M. 2003. Episodic burial metamorphism in the Andes – a viable model? *Geology*, **31**, 705–708.
- BIRÓ-BAGÓCZKY, L. 1964. *Estudio sobre el límite Titoniano y el Neocomiano en la Formación Lo Valdés, Provincia de Santiago, principalmente en base a ammonoideos*, Región Metropolitana, Chile. Thesis, Departamento de Geología, Universidad de Chile.
- BIRÓ-BAGÓCZKY, L. 1982. Revisión y redefinición de los “Estratos de Quiriquina”, Campaniano-Maastrichtiano, en su localidad tipo en la Isla Quiriquina, 36° 35' Lat. S, Chile, Sudamérica, con un perfil complementario en Cocholgue. In: *III Congreso Geológico Chileno*, Concepción, **1**, A 29–64.
- BISSIG, T., LEE, J. K. W., CLARK, A. H. & HEATHER, K. B. 2001. The Cenozoic history of magmatic activity and hydrothermal alteration in the central Andean flat-slab region: new $^{40}\text{Ar}/^{39}\text{Ar}$ constraints from the El Indio–Pascua Au (-Ag, Cu) belt, 29°20'–30°30'S. *International Geology Review*, **43**, 312–340.
- BJERG, E. A., GREGORI, D. A., LOSADA CALDERON, A. & LABUDIA, C. H. 1990. Las metamorfitas del faldeo oriental de la Cuchilla de Guaraparaz, Cordillera Frontal, Provincia de Mendoza. *Revista de la Asociación Geológica Argentina*, **45**, 234–245.
- BORDONARO, O. 1980. El Cámbrico de la quebrada de Zonda, Provincia de San Juan. *Revista de la Asociación Geológica Argentina*, **35**, 26–40.
- BORDONARO, O. 1992. El Cámbrico de Sudamérica. In: GUTIÉRREZ MARCO, J. C., SAAVEDRA, J. & RÁBANO, I. (eds) *Paleozoico inferior de Ibero América*. Universidad de Extremadura, Mérida, 69–84.
- BRAVO, P. 2001. *Geología del borde oriental de la Cordillera de la Costa entre los ríos Mataquito y Maule, VII Región*. Thesis, Departamento de Geología, Universidad de Chile.
- BUATOIS, L. A. & ENCINAS, A. 2011. Ichnology, sequence stratigraphy and depositional evolution of an Upper Cretaceous rocky shoreline in central Chile: Bioerosion structures in a transgressed metamorphic basement. *Cretaceous Resource*, **32**, 203–212.
- BUGGISH, W., von GOSEN, W., HENJES-KUNST, F. & KRUMM, S. 1994. The age of Early Paleozoic deformation and metamorphism in the Argentine Precordillera – evidence from K–Ar data. *Zentralblatt für Geologie und Paläontologie, Teil 1*, **1**, 275–286.
- BURD, A. I., BOOKER, J. R., POMPOSIELLO, M. C., FAVENTO, A., LARSEN, J., GIORDANENG, G. & OROZCO BERNAL, L. 2008. Electrical conductivity beneath the Payún Matrú volcanic field in the Andean back-arc of Argentina near 36.5°S: insights into the magma source. In: *VII International Symposium on Andean Geodynamics*, Nice, Extended Abstract, 90–93.
- BURNS, W. M. & JORDAN, T. E. 1999. Extension in the Southern Andes as evidenced by an Oligo-Miocene intra-arc basin. In: *IV International Symposium on Andean Geodynamics (ISAG)*, Göttingen, 115–118.
- CAHILL, T. & ISACKS, B. 1992. Seismicity and shape of the subducted Nazca Plate. *Journal of Geophysical Research*, **97**, 17 503–17 529.
- CAMINOS, R. 1965. Geología de la vertiente oriental del Cordón del Plata, Cordillera Frontal de Mendoza. *Revista de la Asociación Geológica Argentina*, **20**, 351–392.
- CAMINOS, R. 1979. Cordillera Frontal. In: TURNER, J. C. M. (ed.) *Geología Regional Argentina*. Academia Nacional de Ciencias, Córdoba, Argentina, **1**, 397–453.
- CAMUS, F. 1977. Geología del área de emplazamiento de los depósitos de cuarzo Olla Blanca, provincia de Cachapoal. *Revista Geológica de Chile*, **4**, 43–54.
- CAMUS, F. 2002. The Andean porphyry systems. In: COOKE, D. R. & PONGRATZ, J. (eds) *Giant Ore Deposits: Characteristics, Genesis and Exploration*. CODES, Australia, Special Publications, **4**, 5–21.

- CAMUS, F. 2003. *Geología de los sistemas porfíricos en los Andes de Chile*. Servicio Nacional de Geología y Minería, Santiago.
- CAÑAS, F. L. 1999. Facies and sequences of the Late Cambrian-Early Ordovician carbonates of the Argentine Precordillera: a stratigraphic comparison with Laurentian platforms. In: RAMOS, V. A. & KEPPIE, J. D. (eds) *Laurentia-Gondwana Connections before Pangea*. Geological Society of America, Boulder, CO, Special Papers, **336**, 43–62.
- CARRETIER, S., REGARD, V. ET AL. 2013. Slope and climate variability control of erosion in the Andes of central Chile. *Geology*, **41**, 195–198.
- CARRETIER, S., TOLORZA, V. ET AL. 2014. Erosion in the Chilean Andes between 27°S and 39°S: tectonics, climatic and geomorphic control. In: SEPÚLVEDA, S. A., GIAMBIAGI, L. B., MOREIRAS, S. M., PINTO, L., TUNIK, M., HOKE, G. D. & FARÍAS, M. (eds) *Geodynamic Processes in the Andes of Central Chile and Argentina*. Geological Society, London, Special Publications, **399**. First published online April 9, 2014, <http://dx.doi.org/10.1144/SP399.16>
- CARTER, W. & AGUIRRE, L. 1965. Structural Geology of Aconcagua province and its relationship to the central Valley Graben, Chile. *Geological Society of America Bulletin*, **76**, 651–664.
- CASAMIQUELA, R. M. & FASOLA, A. 1968. Sobre pisadas de dinosaurios del Cretácico Inferior de Colchagua (Chile). *Boletín Departamento de Geología, Universidad de Chile*, **30**, 1–24.
- CASQUET, C., RAPELA, C. ET AL. 2012. A history of Proterozoic terranes in southern South America: from Rodinia to Gondwana. *Geoscience Frontiers*, **3**, 137–145.
- CECIONI, G. 1978. Petroleum possibilities of the Darwin's Navidad Formation near Santiago, Chile. *Publicación Ocasional del Museo Nacional de Historia Natural, Chile*, **25**, 3–28.
- CECIONI, G. 1983. Chanco Formation, a potential Cretaceous reservoir, central Chile. *Journal of Petroleum Geology*, **6**, 89–93.
- CECIONI, G. & WESTERMANN, G. E. G. 1968. The Triassic–Jurassic marine transition of coastal central Chile. *Pacific Geology*, **1**, 41–75.
- CHARRIER, R. 1973. Geología de las Provincias O'Higgins y Colchagua. *Instituto de Investigación de Recursos Naturales, Santiago*, **7**, 11–69.
- CHARRIER, R. 1977. Geology of region of Huentelauquén, Coquimbo Province, Chile. In: ISHIKAWA, T. & AGUIRRE, L. (eds) *Comparative Studies on the Geology of the Circum-Pacific Orogenic Belt in Japan and Chile*. First Report. Japanese Society for Promotion of Science, Tokyo, 81–94.
- CHARRIER, R. 1979. El Triásico de Chile y regiones adyacentes de Argentina: una reconstrucción paleogeográfica y paleoclimática. *Comunicaciones*, **26**, 1–37.
- CHARRIER, R. 1981a. Mesozoic and Cenozoic stratigraphy of the Central Argentinian Chilean Andes (32°–35°S) and chronology of their tectonic evolution. *Zentralblatt für Geologie und Paläontologie*, Teil **1**, 344–355.
- CHARRIER, R. 1981b. *Geologie der chilenischen Hauptkordillere zwischen 34°30' südlicher Breite und ihre tektonische, magmatische und paleogeographische Entwicklung*. Berliner Geowissenschaftliche Abhandlungen (A), Berlin, **36**.
- CHARRIER, R. 1982. La Formación Leñas-Espinoza: redifinición, petrografía y ambiente de sedimentación. *Revista Geológica de Chile*, **17**, 71–82.
- CHARRIER, R. 1984. Areas subsidentes en el borde occidental de la cuenca de tras arco jurásico cretácico, Cordillera Principal Chilena entre 34° y 34°30'S. In: *IX Congreso Geológico Argentino*. Bariloche, Argentina, Actas, **2**, 107–124.
- CHARRIER, R. & VICENTE, J. C. 1972. Liminary and Geosyncline Andes: major orogenic phases and synchronical evolution of the Central and Austral sectors of the Southern Andes. *Conferencia sobre Problemas de la Tierra Sólida, Buenos Aires*, **2**, 451–470.
- CHARRIER, R. & MUNIZAGA, F. 1979. Edades K–Ar de volcanitas cenozoicas del sector cordillerano del río Cachapoal, Chile (34° 15' de latitud Sur). *Revista Geológica de Chile*, **7**, 41–51.
- CHARRIER, R. & MUÑOZ, N. 1994. Jurassic–Cretaceous paleogeographic evolution of the Chilean Andes at 23°–24°S and 34°–35°S latitude: a comparative analysis. In: REUTTER, K. J., SCHEUBER, E. & WIGGER, P. (eds) *Tectonics of the Southern Central Andes*. Springer, Heidelberg, 233–242.
- CHARRIER, R., WYSS, A. R. ET AL. 1996. New evidence for late Mesozoic–Early Cenozoic evolution of the Chilean Andes in the Upper Tinguiririca valley (35°S), Central Chile. *Journal of South American Earth Sciences*, **9**, 393–422.
- CHARRIER, R., BAEZA, O. ET AL. 2002. Evidence for Cenozoic extensional basin development and tectonic inversion south of the flat-slab segment, southern Central Andes, Chile, (33°–36° S.L.). *Journal of South American Earth Sciences*, **15**, 17–139.
- CHARRIER, R., PINTO, L. & RODRÍGUEZ, M. P. 2007. Tectonostratigraphic evolution of the Andean Orogen in Chile. In: MORENO, T. & GIBBONS, W. (eds) *The Geology of Chile*. Geological Society, London, 21–114.
- CHARRIER, R., FARÍAS, M. & MAKSAEV, V. 2009. Evolución tectónica, paleogeográfica y metalógénica durante el Cenozoico en los Andes de Chile norte y central e implicaciones para las regiones adyacentes de Bolivia y Argentina. *Revista de la Asociación Geológica Argentina*, **65**, 5–35.
- CHARRIER, R., CROFT, D. A., FLYNN, J. J., PINTO, L. & WYSS, A. R. 2012. Mamíferos fósiles cenozoicos en Chile: implicancias paleontológicas y tectónicas. Continuación de investigaciones iniciadas por Darwin en América del Sur. In: VELOSO, A. & SPOTORNO, A. (eds) *Darwin y la evolución: avances en la Universidad de Chile*. Editorial Universitaria, Santiago de Chile, 281–316.
- CHARRIER, R., HÉRAIL, G., PINTO, L., GARCÍA, M., RIQUELME, R., FARÍAS, M. & MUÑOZ, N. 2013. Cenozoic tectonic evolution in the Central Andes in northern Chile and west-central Bolivia. Implications for paleogeographic, magmatic and mountain building evolution. *International Journal of Earth Sciences*, **102**, 235–264, <http://dx.doi.org/10.1007/s00531-012-0801-4>
- CHERNICOFF, J. & RAMOS, V. A. 2003. El basamento de la Sierra de San Luis: nuevas evidencias magnéticas y sus

ANDES OF CENTRAL CHILE AND WESTERN ARGENTINA

- implicancias tectónicas. *Revista de la Asociación Geológica Argentina*, **58**, 511–524.
- CHERNICOFF, C. J., ZAPPETTINI, E. O., SANTOS, J. O. S., GODEAS, M. C., BELOUZOVA, E. & MCNAUGHTON, N. K. 2012. Identification and isotopic studies of early Cambrian magmatism (El Carancho Igneous Complex) at the boundary between Pampia terrane and the Río de la Plata craton, La Pampa province, Argentina. *Gondwana Research*, **21**, 378–393.
- COIRA, B. L., DAVIDSON, J. D., MIODOZIS, C. & RAMOS, V. A. 1982. Tectonic and magmatic evolution of the Andes of Northern Argentina and Chile. *Earth Science Reviews*, **18**, 303–332.
- COLLO, G., ASTINI, R. A., CARDONA, A., DO CAMPO, M. D. & CORDANI, U. 2008. Edad del metamorfismo de las unidades con bajo grado de la región central del Famatina: La impronta del ciclo orogénico oclóblico. *Revista Geológica de Chile*, **35**, 191–213.
- COLLO, G., ASTINI, R. A., CAWOOD, P. A., BUCHAN, C. & PIMENTEL, M. 2009. U–Pb detrital zircon ages and Sm–Nd isotopic features in low-grade metasedimentary rocks of the Famatina belt: implications for late Neoproterozoic–early Palaeozoic evolution of the proto-Andean margin of Gondwana. *Journal of the Geological Society*, **166**, 303–319.
- COLOMA, F., SALAZAR, E. & CREIXELL, C. 2012. Nuevos antecedentes acerca de la construcción de los plutones Pérmicos y Permo-Triásicos en el valle del río Tránsito, región de Atacama, Chile. In: *XIII Congreso Geológico Chileno*, Antofagasta, Temática Session 3: Magmatism and Metamorphism, 324–326, digital abstract.
- CORNEJO, P., MATTHEWS, S. & PÉREZ, C. 2003. The ‘K–T’ compressive deformation event in northern Chile (24°–27°S). In: *X Congreso Geológico Chileno*, Concepción, Temática Session 1: Tectonics, 13 p., digital.
- CORTÉS, J. M. & KAY, S. M. 1994. Una dorsal oceánica como origen de las lavas almohadilladas del Grupo Ciénaga del Medio (Silúrico-Devónico) de la Precordillera de Mendoza. In: *VII Congreso Geológico Chileno*, Concepción, Actas, **1**, 1005–1009.
- COVACEVICH, V., VARELA, J. & VERGARA, M. 1976. Estratigrafía y sedimentación de la Formación Baños del Flaco al sur del río Tinguiririca, Cordillera de los Andes, provincia de Curicó, Chile. In: *I Congreso Geológico Chileno*, Santiago, **1**, A191–A211.
- COWAN, D. S. 1985. Structural styles in Mesozoic and Cenozoic melanges in the western Cordillera of North America. *Geological Society of America Bulletin*, **96**, 451–462.
- CREIXELL, C., PARADA, M. A., MORATA, D., VÁSQUEZ, P., PÉREZ DE ARCE, C. & ARRIAGADA, C. 2011. Middle–Late Jurassic to Early Cretaceous transtension and transpression during arc building in central Chile: evidence from mafic dike swarms. *Andean Geology*, **38**, 16–42.
- CRISTALLINI, E. O. & RAMOS, V. A. 1996. Los depósitos continentales cretácicos y volcanitas asociadas. In: RAMOS, V. A. (ed.) *Geología de la Región del Aconcagua, Provincias de San Juan y Mendoza*. Dirección Nacional del Servicio Geológico, Buenos Aires, Argentina, Anales, **24**, 231–274.
- CROFT, D. A., RADIC, J. P., ZURITA, E., CHARRIER, R., FLYNN, J. & WYSS, A. R. 2003. A Miocene toxodontid (Mammalia: notoungulata) from the sedimentary series of the Cura-Mallín Formation, Lonquimay, Chile. *Revista Geológica de Chile*, **30**, 285–298.
- CUADRA, P. 1986. Geocronología K–Ar del yacimiento El Teniente y áreas adyacentes. *Revista Geológica de Chile*, **27**, 3–26.
- CUCCHI, R. J. 1972. Edades radimétricas y correlación de metamorfitas de la Precordillera, San Juan–Mendoza, Rep. Argentina. *Revista de la Asociación Geológica Argentina*, **26**, 503–515.
- DALLA SALDA, L. H., CINGOLANI, C. & VARELA, R. 1992a. Early Palaeozoic Orogenic belt of the Andes in south-western South America – result of Laurentia–Gondwana collision. *Geology*, **20**, 617–620.
- DALLA SALDA, L., DALZIEL, I. W. D., CINGOLANI, C. A. & VARELA, R. 1992b. Did the Taconic Appalachians continue into southern South America? *Geology*, **20**, 1059–1062.
- DAHLQUIST, J. A., PANKHURST, R. J. ET AL. 2013. Hf and Nd isotopes in Early Ordovician to Early Carboniferous granites as monitors of crustal growth in the Proto-Andean margin of Gondwana. *Gondwana Research*, **23**, 1617–1630.
- DARWIN, C. 1846. *Geological Observations on South America; Part III, The Geology of the Voyage of the Beagle*. Smith Elder, London.
- DAVIDSON, J. 1971. *Tectónica y paleogeografía de la Cordillera Principal en el área de las Nacientes del Teno, Curicó, Chile*. Thesis, Departamento de Geología, Universidad de Chile.
- DAVIDSON, J. & VICENTE, J. C. 1973. Características paleogeográficas y estructurales del área fronteriza de las nacientes del Teno (Chile) y Santa Elena (Argentina), (Cordillera Principal, 35° a 35°15' de Latitud Sur). In: *V Congreso Geológico Argentino*. Carlos Paz, Argentina, Actas, **5**, 11–55.
- DÁVILA, F. M., ASTINI, R. A. & JORDAN, T. E. 2005. Cargas subcorticales en el antepaís andino y la planicie pampeana: evidencias estratigráficas, topográficas y geofísicas. *Revista de la Asociación Geológica Argentina*, **60**, 775–786.
- DAVIS, J. S., ROESKE, S. M., MCCLELLAND, W. C. & SNEE, L. W. 1999. Closing the ocean between the Precordillera terrane and Chilenia: early Devonian ophiolite emplacement and deformation in the southwest Precordillera. In: RAMOS, V. A. & KEPPIE, J. D. (eds) *Laurentia–Gondwana Connections before Pangea*. Geological Society of America, Boulder, CO, Special Papers, **336**, 115–138.
- DECKART, K., HERVÉ, F., FANNING, C. M., RAMÍREZ, V., CALDERÓN, M. & GÓDOY, E. 2014. U–Pb geochronology and Hf–O isotopes of zircons from the Pennsylvanian Coastal Batholith, south-central Chile. *Andean Geology*, **41**, 49–82.
- DEDIOS, P. 1967. *Cuadrángulo Vicuña, Provincia de Coquimbo*. Instituto de Investigaciones Geológicas, Santiago, Carta, **16**.
- DE LA CRUZ, R. & SUÁREZ, M. 1997. El Jurásico de la cuenca de Neuquén en Lonquimay, Chile: formación Nacientes del Biobio (38°–39°S). *Revista Geológica de Chile*, **24**, 3–24.
- DÍAZ-MARTÍNEZ, E., MAMET, B., ISAACSON, P. E. & GRADER, G. W. 2000. Permian marine sedimentation

- in northern Chile: new paleontological evidence from the Juan de Morales Formation, and regional paleogeographic implications. *Journal of South American Earth Sciences*, **13**, 511–525.
- DI GIULIO, A., RONCHI, A., SANFILIPPO, A., TIEPOLO, M., PIMENTEL, M. & RAMOS, V. A. 2012. Detrital zircon provenance from the Neuquén Basin (south-central Andes): Cretaceous geodynamic evolution and sedimentary response in a retroarc-foreland basin. *Geology*, **40**, 559–562.
- DRAKE, R. E. 1976. Chronology of Cenozoic igneous and tectonic events in the Central Chilean Andes-latitudes 35°30'–36°00'S. *Journal of Volcanology and Geothermal Research*, **1**, 265–284.
- DRAKE, R. E., CURTIS, G. & VERGARA, M. 1976. Potassium–argon dating of igneous activity in the central Chilean Andes – latitude 33°S. *Journal of Volcanology and Geothermal Research*, **1**, 285–295.
- ELGUETA, S. 1990. Sedimentación marina y paleogeografía del Terciario Superior de la Cuenca de Temuco, Chile. In: *II Simposio sobre el Terciario en Chile*. Concepción, Chile, Actas, **1**, 85–96.
- EMPARAN, C. & CALDERÓN, G. 2014. *Geología del Área Ovalle-Peña Blanca, Región de Coquimbo*. Servicio Nacional de Geología y Minería, Santiago.
- EMPARAN, C. & PINEDA, G. 1999. *Área Condoriaco-Rivadavia, Región de Coquimbo*. Servicio Nacional de Geología y Minería, Santiago, Mapas Geológicos, **12**.
- EMPARAN, C. & PINEDA, G. 2006. *Geología del Área Andacollo-Puerto Aldea, Región de Coquimbo*. Servicio Nacional de Geología y Minería, Santiago, Carta Geológica de Chile, Serie Geología Básica, **96**.
- ENCINAS, A., LE ROUX, J., BUATOIS, L. A., NIELSEN, S. N., FINGER, K. L., FOURTANIER, E. & LAVENU, A. 2006a. Nuevo esquema estratigráfico para los depósitos marinos mio-pliocenos del área de Navidad (33°00'–34°30'S), Chile central. *Revista Geológica de Chile*, **33**, 221–246.
- ENCINAS, A., MAKSAEV, V., PINTO, L., LE ROUX, J., MUNIZAGA, F. & ZENTILLI, M. 2006b. Pliocene lahar deposits in the Coastal Cordillera of central Chile: implications for uplift, avalanche deposits, and porphyry copper systems in the Main Andean Cordillera. *Journal of South American Earth Sciences*, **20**, 369–381.
- ESCAYOLA, M. P., RAMÉ, G. A. & KRAEMER, P. E. 1996. Caracterización y significado geotectónico de las fajas ultramárficas de las Sierras Pampeanas de Córdoba. In: *XIII Congreso Geológico Argentino y III Congreso de Exploración de Hidrocarburos*. Mendoza, Argentina, **3**, 421–438.
- ESCAYOLA, M. P., PIMENTEL, M. & ARMSTRONG, R. 2007. Neoproterozoic backarc basin: sensitive high-resolution ion microprobe U–Pb and Sm–Nd isotopic evidence from the Eastern Pampean Ranges, Argentina. *Geology*, **35**, 495–498.
- EYQUEM, D. 2009. *Volcanismo cuaternario de Sierras de Bellavista. Comparación geoquímica con el magmatismo contemporáneo del arco comprendido entre los 34°30' y los 35°30'S*. Thesis, Departamento de Geología, Universidad de Chile, Santiago.
- FARÍAS, M., CHARRIER, R. ET AL. 2008. Late Miocene high and rapid surface uplift and its erosional response in the Andes of central Chile (33°–35°S). *Tectonics*, **27**, TC1005, <http://dx.doi.org/10.1029/2006TC002046>
- FARÍAS, M., COMTE, D. ET AL. 2010. Crustal scale architecture in central Chile based on seismicity and surface geology: implications for Andean mountain building. *Tectonics*, **29**, TC3006, <http://dx.doi.org/10.1029/2009TC002480>
- FERNÁNDEZ-SEVESO, F. & TANKARD, A. J. 1995. Tectonics and stratigraphy of the Late Paleozoic Paganzo basin of western Argentina and its regional implications. In: TANKARD, A. J., SUÁREZ SORUCO, R. & WELSINK, H. J. (eds) *Petroleum Basins of South America*. American Association of Petroleum Geologists, Tulsa, OK, Memoirs, **62**, 285–301.
- FERRANDO, R., ROPERCH, P., MORATA, D., ARRIAGADA, C., RUFFET, G. & CÓRDOBA, M. L. 2014. A paleomagnetic and magnetic fabric study of the Illapel Plutonic complex, Coastal Range, central Chile: implications for emplacement mechanism and regional tectonic evolution during the mid-Cretaceous. *Journal of South American Earth Science*, **50**, 12–26.
- FINGER, K., ENCINAS, A., NIELSEN, S. & PETERSON, D. 2003. Microfaunal indications of late Miocene deep-water basins off the central coast of Chile. In: *X Congreso Geológico Chileno*. Concepción, Tematic Session 3, 8 p., digital abstract.
- FINGER, K. L., NIELSEN, S. N., DEVRIES, T. J., ENCINAS, A. & PETERSON, D. E. 2007. Paleontologic evidence for sedimentary displacement in Neogene forearc basins of Central Chile. *Palaios*, **22**, 3–16, <http://dx.doi.org/10.2110/palo.2005.p05-081r>
- FLYNN, J. J., WYSS, A. R. & CHARRIER, R. 2007. South America's missing mammals. *Scientific American*, **296**, 68–75.
- FLYNN, J. J., CHARRIER, R., CROFT, D. A., GANS, P. B., HERIOTT, T. M., WERTHEIM, J. A. & WYSS, A. R. 2008. Chronologic implications of new Miocene mammals from the Cura–Mallín and Trapa–Trapa Formations, Laguna del Laja area, south Central Chile. *Journal of South American Earth Sciences*, **26**, 412–423.
- FOCK, A., CHARRIER, R., FARÍAS, M. & MUÑOZ, M. 2006. Fallas de vergencia Oeste en la Cordillera Principal de Chile Central: inversión de la cuenca de Abanico (33°–34°S). In: HONGN, F., BECCIO, R. & SEGGIARIO, R. (eds) *XII Reunión sobre microtectónica y geología estructural*. Revista de la Asociación Geológica Argentina, Serie D, Publicación Especial, Buenos Aires, Argentina, **9**, 48–55.
- FOLGUERA, A. & RAMOS, V. A. 2011. Repeated eastward shifts of arc magmatism in the Southern Andes: a revision to the long-term pattern of Andean uplift and magmatism. *Journal of South American Earth Sciences*, **32**, 531–546, <http://dx.doi.org/10.1016/j.jsames.2011.04.003>
- FRUTOS, J. 1981. Andean tectonic as consequence of sea-floor spreading. *Tectonophysics*, **72**, 21–32.
- FUENTES, F. 2004. *Petrología y metamorfismo de muy bajo grado de unidades volcánicas oligo-miocenas en la ladera occidental de los Andes de Chile Central (33°S)*. PhD thesis, Universidad de Chile.
- FUENTES, F., FÉRAUD, G., AGUIRRE, L. & MORATA, D. 2001. Convergent strategy to date metamorphic minerals in subgreenschist facies metabasites by the $^{40}\text{Ar}/^{39}\text{Ar}$ method. In: *III South American Symposium on Isotope Geology*. Pucón, Chile, electronic abstracts, 34–36.

ANDES OF CENTRAL CHILE AND WESTERN ARGENTINA

- FUENTES, F., FÉRAUD, G., AGUIRRE, L. & MORATA, D. 2005. $^{40}\text{Ar}/^{39}\text{Ar}$ dating of volcanism and subsequent very low-grade metamorphism in a subsiding basin: example of the Cretaceous lava series from central Chile. *Chemical Geology*, **214**, 157–177.
- FUENZALIDA, H. 1940. Algunos afloramientos Paleozoicos de la desembocadura del Choapa. *Boletín del Museo Nacional de Historia Natural*, **28**, 37–64.
- FUENZALIDA, H., COOKE, R., PASKOFF, R., SEGERSTROM, K. & WEISCHET, W. 1965. High stands of Quaternary sea level along the Chilean coast. In: WRIGHT, H. E. & FREY, D. (eds) *International Studies on the Quaternary. Papers Prepared on the Occasion of the VII Congress of the International Association for Quaternary Research* Boulder, Colorado. Geological Society of America, Boulder, CO, Special Papers, **84**, 473–496.
- GALLEGOS, A. 1994. *Paleoambiente y mecanismo de deposición de la secuencia sedimentaria que aflora en el sector de Polpaico, Región Metropolitana, Chile*. Thesis, Departamento de Geología, Universidad de Chile, Santiago.
- GANAS, P. 1991. Magmatismo bimodal del Triásico Superior – Jurásico Inferior, en la Cordillera de la Costa, Provincias de Elqui y Limarí, Chile. *Revista Geológica de Chile*, **18**, 55–67.
- GANAS, P. & TOSDAL, R. M. 1996. Geocronología U–Pb y K–Ar en intrusivos del Paleozoico y Mesozoico de la Cordillera de la Costa, región de Valparaíso, Chile. *Revista Geológica de Chile*, **23**, 151–164.
- GANAS, P. & WALL, R. 1997. Evidencias geocronológicas $^{40}\text{Ar}/^{39}\text{Ar}$ y K–Ar de un hiato Cretácico Superior-Eoceno en Chile Central (33° – $33^{\circ}30'$ S). *Revista Geológica de Chile*, **24**, 145–163.
- GANAS, P. & ZENTILLI, M. 2000. Historia tectónica y exhumación de intrusivos de la Cordillera de la Costa de Chile central. In: *IX Congreso Geológico Chileno*. Puerto Varas, Actas, **2**, 664–668.
- GARCÍA, C. 1991. *Geología del sector de quebrada El Teniente, Región de Coquimbo*. Thesis, Departamento de Geología, Universidad de Chile.
- GARCÍA-SANSEGUNDO, J., FARÍAS, P., RUBIO-ORDÓÑEZ, A. & HEREDIA, N. 2014a. The Palaeozoic basement of the Andean Frontal Cordillera at 34° S (Cordón del Carrizalito, Mendoza Province, Argentina): geotectonic implications. *Journal of Iberian Geology*, **40**, 321–330. http://dx.doi.org/10.5209/rev_JIGE.2014.v40.n2.45299.
- GARCÍA-SANSEGUNDO, J., FARÍAS, P., HEREDIA, N., GALLASTEGUIL, G., CHARRIER, R., RUBIO-ORDÓÑEZ, A. & CUESTA, A. 2014b. Structure of the Andean Paleozoic basement in the Chilean coast at 31° – $30'$ S: geodynamic evolution of a subduction margin. *Journal of Iberian Geology*, **40**, 293–308. http://dx.doi.org/10.5209/rev_JIGE.2014.v40.n2.45300.
- GERBI, C., ROESKE, S. M. & DAVIS, J. S. 2002. Geology and structural history of the southwest Precordillera margin, northern Mendoza Province, Argentina. *Journal of South American Earth Sciences*, **14**, 821–835.
- GIAMBIAGI, L. & MARTÍNEZ, A. N. 2008. Permo-Triassic oblique extension in the Uspallata–Potrerillos area, western Argentina. *Journal of South American Earth Sciences*, **26**, 252–260.
- GIAMBIAGI, L., MESCÚA, J., BECHIS, F., MARTÍNEZ, A. & FOLGUERA, A. 2011. Pre-Andean deformation of the Precordillera southern sector, Southern Central Andes. *Geosphere*, **7**, 219–239.
- GIAMBIAGI, L., TASSARA, A. ET AL. 2014. Evolution of shallow and deep structures along the Maipo – Tunuyán transect (33° – 40° S): from the Pacific coast to the Andean foreland. In: SEPÚLVEDA, S. A., GIAMBIAGI, L. B., MOREIRAS, S. M., PINTO, L., TUNIK, M., HOKE, G. D. & FARÍAS, M. (eds) *Geodynamic Processes in the Andes of Central Chile and Argentina*. Geological Society, London, Special Publications, **399**. First published online February 27, 2014, <http://dx.doi.org/10.1144/SP399.14>
- GIAMBIAGI, L. B., RAMOS, V. A., GODOY, E., ÁLVAREZ, P. P. & ORTS, S. 2003a. Cenozoic deformation and tectonic style of the Andes, between 33° and 34° South Latitude. *Tectonics*, **22**, 1041–1051.
- GIAMBIAGI, L. B., ÁLVAREZ, P. P., GODOY, E. & RAMOS, V. A. 2003b. The control of pre-existing extensional structures on the evolution of the southern sector of the Aconcagua fold and thrust belt, Southern Andes. *Tectonophysics*, **369**, 1–19.
- GLODNY, J., LOHRMANN, J., ECHTLER, H., GRÄFE, K., SEIFERT, W., COLLAO, S. & FIGUEROA, O. 2005. Internal dynamics of a paleoaccretionary wedge: insights from combined isotope tectonochronology and sandbox modelling of the south-central Chilean fore-arc. *Earth and Planetary Science Letters*, **231**, 23–39.
- GLODNY, J., ECHTLER, H. ET AL. 2006. Long-term geological evolution and mass flow balance of the South-Central Andes. In: ONCKEN, O., CHONG, G., FRANZ, G., GIESE, P., GÖTZE, H. J., RAMOS, V., STRECKER, M. & WIGGER, P. (eds) *The Andes – Active Subduction Orogeny*. Frontiers in Earth Sciences, Springer, Berlin, **1**, 401–442.
- GLODNY, J., ECHTLER, H., COLLAO, S., ARDILES, M., BURÓN, P. & FIGUEROA, O. 2008. Differential Late Paleozoic active margin evolution in South-Central Chile (37° – 40° S) – the Lanalhue Fault Zone. *Journal of South American Earth Sciences*, **26**, 397–411.
- GODOY, E. 1982. Geología del área de Montenegro, Cuesta de Chacabuco, Región Metropolitana. El problema de la Formación Lo Valle. In: *II Congreso Geológico Chileno*, Concepción, **1**, A124–A146.
- GODOY, E. 2011. Structural setting and diachronism in the Central Andean Eocene to Miocene volcano-tectonic basins. In: SALFITY, J. A. & MARQUILLAS, R. A. (eds) *Cenozoic Geology of the Central Andes of Argentina*. SCS, Salta, Argentina, 155–167.
- GODOY, E. & CHARRIER, R. 1991. Antecedentes mineralógicos para el origen de las metabasitas y metacherts del Complejo Metamórfico del Choapa (Región de Coquimbo, Chile): un prisma de acreción Paleozoico Inferior. In: *VI Congreso Geológico Chileno*, Viña del Mar, Actas, 410–414.
- GODOY, E. & LARA, L. 1994. Segmentación estructural andina a los 33° – 34° : nuevos datos en la Cordillera Principal. In: *VII Congreso Geológico Chileno*, Concepción, **2**, 1344–1348.
- GÓMEZ, R. 2001. *Geología de las unidades volcanogénicas cenozoicas del área industrial de la Mina El Teniente, entre Colón y Coya, Cordillera Principal*

- de Rancagua, VI Región.* Thesis, Departamento de Geología, Universidad de Chile.
- GONZÁLEZ, O. 1963. Observaciones geológicas en el valle del Río Volcán. *Revista Minerales*, **17**, 20–61.
- GONZÁLEZ, O. & VERGARA, M. 1962. Reconocimiento geológico de la Cordillera de los Andes entre los paralelos 35° y 38° latitud S. Instituto de Geología, Universidad de Chile, Santiago, Publicación, **24**.
- GONZÁLEZ-BONORINO, F. 1970. Series metamórficas del basamento cristalino de la Cordillera de la Costa de Chile Central. Departamento de Geología, Universidad de Chile. *Publicaciones*, **37**, 1–68.
- GONZÁLEZ-BONORINO, F. 1971. Metamorphism of the crystalline basement of Central Chile. *Journal of Petrology*, **12**, 149–175.
- GONZÁLEZ-BONORINO, F. & AGUIRRE, L. 1970. Metamorphic facies series of the crystalline basement of Chile. *Geologische Rundschau*, **59**, 979–993.
- GONZÁLEZ-MENÉNDEZ, L., GALLASTEGUI, G., CUESTA, A., HEREDIA, N. & RUBIO-ORDÓÑEZ, A. 2013. Petrogenesis of Early Paleozoic basalts and gabbros in the western Cuyania terrane: constraints on the tectonic setting of the southwestern Gondwana margin (Sierra del Tigre, Andean Argentine Precordillera). *Gondwana Research*, **24**, 359–376.
- GORDILLO, C. E. 1984. Migmatitas cordieríticas de la Sierra de Córdoba, condiciones físicas de la migmatización. Academia Nacional de Ciencias. *Misclánea*, **68**, 1–40.
- GREGORI, D. & BENEDINI, L. 2013. The Cordon del Portillo Permian magmatism, Mendoza, Argentina, plutonic and volcanic sequences at the western margin of Gondwana. *Journal of South American Earth Sciences*, **42**, 61–73.
- GREGORI, D. A., FERNÁNDEZ-TURIEL, J. L., LÓPEZ-SOLER, A. & PETFORD, N. 1996. Geochemistry of Upper Palaeozoic–Lower Triassic granitoids of the Central Frontal Cordillera ($33^{\circ}10'$ – $33^{\circ}45'$), Argentina. *Journal of South American Earth Sciences*, **9**, 141–151.
- GROEBER, P. 1918. Estratigrafía del Dogger en la República Argentina. Estudio sintético comparativo. *Dirección General de Minas, Geología e Hidrogeología, Boletín*, **18**, Serie B (Geología), 1–81.
- GROEBER, P. 1922. Pérmico y Triásico en la costa de Chile. *Revista de la Sociedad Argentina de Ciencias Naturales*, **5**, 979–994.
- GROEBER, P. 1946. Observaciones geológicas a lo largo del meridiano 70° . 1, Hoja Chos Malal. *Revista de la Asociación Geológica Argentina*, **1**, 117–208. Reprint in Asociación Geológica Argentina, Serie C, Reimpresiones (1980) 1, 1–174.
- GROEBER, P. 1951. La Alta Cordillera entre las latitudes 34° y $29^{\circ}30'$. Instituto Investigaciones de las Ciencias Naturales. *Revista del Museo Argentino de Ciencias Naturales Bernardino Rivadavia (Ciencias Geológicas)*, **1**, 1–352.
- GROEBER, P. 1953. Mesozoico. *Geografía de la República Argentina, Sociedad Argentina de Estudios Geográficos GAEA, Buenos Aires*, **2**, 9–541.
- GROMET, L. P. & SIMPSON, C. 2000. Cambrian orogeny in the Sierras Pampeanas, Argentina: ridge subduction or continental collision? *Geological Society of America Abstracts with Programs*, **32**, A-505.
- GROSSE, P., SÖLLNER, F., BÁEZ, M. A., TOSSETTI, A. J., ROSSI, J. N. & ROSA, J. D. 2009. Lower Carboniferous post-orogenic granites in central-eastern Sierra de Velasco, Sierras Pampeanas, Argentina: U–Pb monazite geochronology, geochemistry and Sr–Nd isotopes. *International Journal of Earth Sciences*, **98**, 1001–1025.
- GUDNASON, J., HOLM, P. M., SØAGER, N. & LLAMBÍAS, E. J. 2012. Geochronology of the late Pliocene to recent volcanic activity in the Payenia back-arc volcanic province, Mendoza, Argentina. *Journal of South American Earth Sciences*, **37**, 191–201.
- GULBRANSON, E. L., MONTAÑEZ, I. P., SCHMITZ, M. D., LIMARINO, C. O., ISBELL, J. L., MARENSSI, S. A. & CROWLEY, J. L. 2010. High-precision U–Pb calibration of Carboniferous glaciation and climate history, Paganzo Group, NW Argentina. *Geological Society of America Bulletin*, **122**, 1480–1498.
- GUTIÉRREZ, N. M., HINOJOSA, L. F., LE ROUX, J. P. & PEDROZA, V. 2013. Evidence for an Early–Middle Miocene age of the Navidad Formation (central Chile): paleontological, paleoclimatic and tectonic implications. *Andean Geology*, **40**, 66–78.
- HALLAM, A., BIRÓ-BAGÓCZKY, L. & PÉREZ, E. 1986. Facies analysis of the Valdés Formation (Tithonian–Hauterivian) of the High Cordillera of Central Chile, and the Paleogeographic evolution of the Andean Basin. *Geological Magazine*, **123**, 425–435.
- HALLER, M. J. & RAMOS, V. A. 1984. Las ofiolitas famatinianas (Eopaleozoico) de las provincias de San Juan y Mendoza. In: *IX Congreso Geológico Argentino, Bariloche*, 66–83.
- HALLER, M. J. & RAMOS, V. A. 1993. Las ofiolitas y otras rocas afines. In: RAMOS, V. A. (ed.) *Geología y Recursos Naturales de Mendoza. Relatorio XII Congreso Geológico Argentino y II Congreso de Exploración de Hidrocarburos*. Buenos Aires, 31–40.
- HEREDIA, N., FERNÁNDEZ, L. R. R., GALLASTEGUI, G., BUSQUETS, P. & COLOMBO, F. 2002. Geological setting of the Argentine Frontal Cordillera in the flat-slab segment ($30^{\circ} 00'$ – $31^{\circ} 30'$ S latitude). *Journal of South American Earth Sciences*, **15**, 79–99.
- HEREDIA, N., FARIAS, P., GARCÍA-SANSEGUNDO, J. & GIAMBAGI, L. 2012. The Basement of the Andean Frontal Cordillera in the Cordón del Plata (Mendoza, Argentina): geodynamic evolution. *Andean Geology*, **39**, 242–257.
- HERVÉ, F. 1977. Petrology of the Crystalline Basement of the Nahuelbuta Mountains, Southcentral Chile. In: ISHIKAWA, T. & AGUIRRE, L. (eds) *Comparative Studies on the Geology of the Circum Pacific Orogenic Belt in Japan and Chile*. Japan Society for the Promotion of Science, Tokyo, 1–51.
- HERVÉ, F. 1988. Late Palaeozoic subduction and accretion in Southern Chile. *Episodes*, **11**, 183–188.
- HERVÉ, F., MUNIZAGA, F., GODOY, E. & AGUIRRE, L. 1974. Late Paleozoic K/Ar ages of blueschists from Pichilemu, Central Chile. *Earth and Planetary Science Letters*, **23**, 261–264.
- HERVÉ, F., KAWASHITA, K., MUNIZAGA, F. & BASEI, M. 1984. Rb–Sr isotopic ages from late Paleozoic metamorphic rocks of Central Chile. *Journal of the Geological Society London*, **141**, 877–884.

ANDES OF CENTRAL CHILE AND WESTERN ARGENTINA

- HERVÉ, F., MUNIZAGA, F., PARADA, M. A., BROOK, M., PANKHURST, R. J., SNELLING, N. J. & DRAKE, R. 1988. Granitoids of the Coast Range of central Chile: geochronology and geologic setting. *Journal of South American Earth Sciences*, **1**, 185–194.
- HERVÉ, F., FANNING, C. M. & PANKHURST, R. J. 2003. Detrital zircon age patterns and provenance of the metamorphic complexes of southern Chile. *Journal of South American Earth Sciences*, **16**, 107–123.
- HERVÉ, F., FAÚNDEZ, V., CALDERÓN, M., MASSONNE, H.-J. & WILLNER, A. P. 2007. Metamorphic and plutonic basement complexes. In: MORENO, T. & GIBBONS, W. (eds) *The Geology of Chile*. Geological Society, London, 5–20.
- HERVÉ, F., CALDERÓN, M., FANNING, C. M., PANKHURST, R. J. & GODOY, E. 2013. Provenance variations in the Late Paleozoic accretionary complex of central Chile as indicated by detrital zircons. *Gondwana Research*, **23**, 1122–1135.
- HERVÉ, F., FANNING, C. M., CALDERÓN, M. & MPODOZIS, C. 2014. Early Permian to Late Triassic batholiths of the Chilean Frontal Cordillera (28° – 31° S): SHRIMP U–Pb zircon ages and Lu–Hf and O isotope systematics. *Lithos*, **184**–**187**, 436–446.
- HILDRETH, W., SINGER, B., GODOY, E. & MUNIZAGA, F. 1998. The age and constitution of Cerro Campanario, a mafic stratovolcano in the Andes of Central Chile. *Revista Geológica de Chile*, **25**, 17–28.
- IANNIZZOTTO, N. F., RAPELA, C. W., BALDO, E. G. A., GALINDO, C., FANNING, C. M. & PANKHURST, R. J. 2013. The Sierra Norte–Ambargasta batholith: Late Ediacaran–Early Cambrian magmatism associated with Pampean transpressional tectonics. *Journal of South American Earth Sciences*, **42**, 127–143.
- IRIGOYEN, M. V., BUCHAN, K. L. & BROWN, R. L. 2000. Magnetostratigraphy of Neogene Andean foreland-basin strata, lat 33° S, Mendoza Province, Argentina. *Geological Society of America Bulletin*, **112**, 803–816.
- IRWIN, J. J., GARCÍA, C., HERVÉ, F. & BROOK, M. 1988. Geology of part of a long-lived dynamic plate margin – the Coastal Cordillera of north-central Chile, latitude $30^{\circ}51'$ – 31° S. *Canadian Journal of Earth Sciences*, **25**, 603–624.
- ISACKS, B. L. 1988. Uplift of the Central Andean Plateau and bending of the Bolivian Orocline. *Journal of Geophysical Research*, **93**, 3211–3231.
- JAMES, D. E. 1971. Plate tectonic model for the evolution of the Central Andes. *Geological Society of America Bulletin*, **82**, 3325–3346.
- JARA, P. & CHARRIER, R. 2014. Nuevos antecedentes geocronológicos y estratigráficos para la Alta Cordillera de Chile central a $\sim 32^{\circ}10'$ S. Implicancias paleogeográficas y estructurales. *Andean Geology*, **41**, 174–209, <http://dx.doi.org/10.5027/andgeoV41n1-a07>
- JARA, P., LIKEMAN, J., WINOCUR, D., GUIGLIONE, M. C., CRISTALLINI, E. O., PINTO, L. & CHARRIER, R. 2014. Role of basin width variation in tectonic inversion: insight from analogue modelling and implications for the tectonic inversion of the Abanico Basin, 32° – 34° S, Central Andes. In: SEPÚLVEDA, S. A., GIAMBIAGI, L. B., MOREIRAS, S. M., PINTO, L., TUNIK, M., HOKE, G. D. & FARÍAS, M. (eds) *Geodynamic Processes in the Andes of Central Chile and Argentina*. Geological Society, London, Special Publications, **399**. First published online February 27, 2014, <http://dx.doi.org/10.1144/SP399.7>
- JAROS, J. & ZELMAN, J. 1967. *La relación estructural entre las formaciones Abanico y Farellones en la Cordillera del Mesón, Provincia de Aconcagua, Chile*. Departamento de Geología, Universidad de Chile, Santiago de Chile, **34**.
- JORDAN, T., ISACKS, B., RAMOS, V. A. & ALLMENDINGER, R. W. 1983a. Mountain building model: the Central Andes. *Episodes*, **1983**, 20–26.
- JORDAN, T. E., ISACKS, B. L., ALLMENDINGER, R. W., BREWER, J. A., RAMOS, V. A. & ANDO, C. J. 1983b. Andean tectonics related to geometry of subducted Nazca plate. *Geological Society of America Bulletin*, **94**, 341–361.
- JORDAN, T. E., REYNOLDS III, J. H. & ENKSON, J. P. 1997. Variability in age of initial shortening and uplift in the central Andes, 16 – $33^{\circ}30'$ S. In: RUDDIMAN, W. (ed.) *Tectonic Uplift and Climate Change*. Plenum, New York, 41–61.
- JORDAN, T. E., BURNS, W. M., VEIGA, R., PANGARO, F., COPELAND, P., KELLEY, S. & MPODOZIS, C. 2001. Extension and basin formation in the southern Andes caused by increased convergence rate: a Mid-Cenozoic trigger for the Andes. *Tectonics*, **20**, 308–324.
- KATO, T. & GODOY, E. 1995. Petrogenesis and tectonic significance of late Paleozoic coarse-crystalline blueschist and amphibolite boulders in the Coastal Range of Chile. *International Geology Review*, **37**, 992–1006.
- KAY, S. M. & ABBRUZZI, J. M. 1996. Magmatic evidence for Neogene lithospheric evolution of the Central Andean flat-slab between 30 and 32° S. *Tectonophysics*, **259**, 15–28.
- KAY, S. M., RAMOS, V., MPODOZIS, C. & SRUOGA, P. 1989. Late Paleozoic to Jurasic silicic magmatism at the Gondwana margin: analogy to the Middle Proterozoic in North America. *Geology*, **17**, 324–328.
- KAY, S. M., MPODOZIS, C., RAMOS, V. A. & MUNIZAGA, F. 1991. Magma source variations for mid to late Tertiary volcanic rocks erupted over a shallowing subduction zone and through a thickening crust in the Main Andean Cordillera (28 – 33° S). In: HARMON, R. S. & RAPELA, C. W. (eds) *Andean Magmatism and its Tectonic Setting*. Geological Society of America, Boulder, CO, Special Papers, **265**, 113–137.
- KELLER, M. 1999. *Argentine Precordillera, sedimentary and plate tectonic history of a Laurentian crustal fragment in South America*. Geological Society of America, Boulder, CO, Special Papers, **341**, 1–131.
- KLEIMAN, L. E. & JAPAS, M. S. 2009. The Choioyi volcanic province at 34° S– 36° S (San Rafael, Mendoza, Argentina): implications for the Late Palaeozoic evolution of the southwestern margin of Gondwana. *Tectonophysics*, **473**, 283–299.
- KLOHN, C. 1960. Geología de la Cordillera de los Andes de Chile Central, provincia de Santiago, O'Higgins, Colchagua y Curicó. *Instituto Investigaciones Geológicas Boletín*, **8**, 1–95.
- KOKOGIÁN, D. A., FERNÁNDEZ-SEVESO, F. & MOSQUERA, A. 1993. Las secuencias sedimentarias triásicas. In: *9º Congreso Geológico Argentino*. Mendoza, Relatorio, 65–78.

- KOKOGIÁN, D. A., SPALLETTI, L. ET AL. 1999. Depósitos continentales triásicos. In: CAMINOS, R. (ed.) *Geología Argentina*. Servicio Geológico Minero Argentino, Buenos Aires, Argentina, Anales, **29**, 377–397.
- KRAEMER, P., ESCAYOLA, M. & MARTINO, R. 1995. Hipótesis sobre la evolución tectónica neoproterozoica de las Sierras Pampeanas de Córdoba ($30^{\circ}40' - 32^{\circ}40'S$), Argentina. *Revista de la Asociación Geológica Argentina*, **50**, 47–59.
- LANÉS, L. 2005. Late Triassic to Early Jurassic sedimentation in northern Neuquén Basin, Argentina: tectono sedimentary evolution of the first transgression. *Geológica Acta*, **3**, 81–106.
- LARSON, R. L. 1991. Geological consequences of superplumes. *Geology*, **19**, 963–966.
- LEAL, P. R., HARTMANN, L. A., SANTOS, O., MIRÓ, R. & RAMOS, V. A. 2004. Volcanismo postorogénico en el extremo norte de las Sierras Pampeanas Orientales: nuevos datos geocronológicos y sus implicancias tectónicas. *Revista de la Asociación Geológica Argentina*, **58**, 593–607.
- LEGARRETA, L., KOKOGIAN, D. A. & DELLAPE, D. A. 1992. Estructuración terciaria de la cuenca Cuyana: ¿Cuánto de inversión tectónica? *Revista Asociación Geología Argentina*, **47**, 83–86.
- LEGARRETA, L., GULISANO, C. A. & ULIANA, M. A. 1993. Las secuencias sedimentarias jurásico-cretácicas. In: RAMOS, V. A. (ed.) *Relatorio Geología y Recursos Naturales de Mendoza. XII Congreso Geológico Argentino y II Congreso de Exploración de Hidrocarburos*, Buenos Aires, 87–114.
- LETELIER, M. 1977. *Petrología y ambiente de deposición y estructura de las Formaciones Matahuaiaco, Las Breas, Tres Cruces sensu lato e intrusivos permotriásicos en el área de Rivadavia-Alcohuás, valle de Elqui, IV Región, Chile*. Thesis, Departamento de Geología, Universidad de Chile.
- LEVI, B. & AGUIRRE, L. 1960. El Conglomerado de Algarrobo y su relación con las formaciones de Cretácico Superior de Chile central. *I Jornadas Geológicas Argentinas*, **2**, 417–431.
- LEVI, B., AGUIRRE, L., NYSTRÖM, J., PADILLA, H. & VÉGARA, M. 1989. Low-grade regional metamorphism in the Mesozoic-Cenozoic volcanic sequences of the Central Andes. *Journal of Metamorphic Petrology*, **7**, 487–495.
- LIMARINO, C. O. & SPALLETTI, L. A. 2006. Paleogeography of the upper Paleozoic basins of southern South America: an overview. *Journal of South American Earth Sciences*, **22**, 134–155.
- LIMARINO, C. O., TRIPALDI, A., MARENSSI, S. & FAUQUÉ, L. 2006. Tectonic, sea-level, and climatic controls on Late Paleozoic sedimentation in the western basins of Argentina. *Journal of South American Earth Sciences*, **22**, 205–226.
- LIMARINO, C. O., CÉSARI, S. N., SPALLETTI, L. A., TABOADA, A. C., ISBELL, J. L., GEUNA, S. & GULBRANSON, E. L. 2013. A paleoclimatic review of southern South America during the late Paleozoic: a record from icehouse to extreme greenhouse conditions. *Gondwana Research*, **25**, 1396–1421.
- LIRA, R., MILLONE, H. A., KIRSCHBAUM, A. M. & MORENO, R. S. 1996. Calc-alkaline arc granitoid activity in the Sierra Norte-Ambargasta Ranges, central Argentina. *Journal of South American Earth Sciences*, **10**, 157–177.
- LLAMBÍAS, E. J. 1999. Las rocas ígneas gondwánicas. El magmatismo gondwánico durante el Paleozoico Superior-Triásico. In: CAMINOS, R. (ed.) *Geología Argentina*. Instituto de Geología y Recursos Minerales, Buenos Aires, Argentina, Anales, **29**, 349–363.
- LLAMBÍAS, E. J. & SATO, A. M. 1995. El Batolito de Colanguil: transición entre orogénesis y anorogénesis. *Revista de la Asociación Geológica Argentina*, **50**, 111–131.
- LLAMBÍAS, E. J., KLEIMAN, L. E. & SALVARREDI, J. A. 1993. El magmatismo gondwánico. In: RAMOS, V. A. (ed.) *Geología y Recursos Naturales de Mendoza. Relatorio XIII Congreso Geológico Argentino and II Congreso de Exploración de Hidrocarburos*, Mendoza, **1**, 53–64.
- LLAMBÍAS, E. J., QUENARDELLE, S. & MONTENEGRO, T. 2003. The Choiyoi Group from central Argentina: a subalkaline transitional to alkaline association in the craton adjacent to the active margin of the Gondwana continent. *Journal of South American Earth Sciences*, **16**, 243–257.
- LLAMBÍAS, E. J., BERTOTTO, G. W., RISSO, C. & HERNANDO, I. 2010. El volcanismo cuaternario en el retroarco de Payenia: una revisión. *Revista de la Asociación Geológica Argentina*. Zurich, **67**, 278–300.
- LO FORTE, G. L., ANSELMI, G. & AGUIRRE-URRETA, M. B. 1996. Tithonian Paleogeography of the Aconcagua Basin, West-Central Andes of Argentina. In: RICCARDI, A. C. (ed.) *Advances in Jurassic Research, Geo-Research Forum*, Transtec Publications, Zurich, **1–2**, 369–376.
- LÓPEZ, V. & GREGORI, D. A. 2004. Provenance and evolution of the Guaruaraz Complex, Cordillera Frontal, Argentina. *Gondwana Research*, **7**, 1197–1208.
- LÓPEZ GAMUNDÍ, O. 1994. Facies distribution in an asymmetric half graben: the northern Cuyo Basin (Triassic), western Argentina. In: *XIV International Sedimentological Congress*, Recife, Abstract, 6–7.
- LÓPEZ GAMUNDÍ, O. R., ESPEJO, I., CONAGHAN, P. J. & POWELL, C. McA. 1994. Southern South America. In: VEEVERS, J. J. & POWELL, C. McA. (eds) *Permian Triassic Pangean Basins and Foldbelts Along the Panthalassan Margin of Gondwanaland*. Geological Society of America, Boulder, CO, Memoirs, **184**, 281–329.
- MACPHAIL, D. D. 1966. El gran lahar del Laja. *Estudios Geográficos*. Departamento de Geografía, Universidad de Chile, Santiago, 133–155.
- MACPHAIL, D. D. & SAA, R. 1967. Los Cerrillos de Teno: a laharic landscape of Central Chile. *Annals of the Association of American Geographers*, **59**, 171.
- MAKSAEV, V., MUNIZAGA, F., MCWILLIAMS, M., FANNING, M., MATHUR, R., RUIZ, J. & ZENTILLI, M. 2004. New chronology for El Teniente, Chilean Andes, from U/Pb, $^{40}\text{Ar}/^{39}\text{Ar}$, Re/Os and fission-track dating: implications for the evolution of a supergiant porphyry Cu-Mo deposit. In: SILLITOE, R. H., PERELLÓ, J. & VIDAL, C. E. (eds) *Andean Metallogeny: New Discoveries, Concepts, Update*. Society of Economic Geologists, Littleton, CO, Special Publications, **11**, 15–54.
- MALBRAN, F. 1986. *Estudio geológico-estructural del área de río Clarillo, con énfasis en la Formación Coya-Machalí, hoyo del río Tinguiririca, Chile*. Thesis,

ANDES OF CENTRAL CHILE AND WESTERN ARGENTINA

- Departamento de Geología, Universidad de Chile, Santiago.
- MALUMIÁN, N. & RAMOS, V. A. 1984. Magmatic intervals, transgression-regression cycles and oceanic events in the Cetraceous and Tertiary of southern South America. *Earth and Planetary Science Letters*, **67**, 228–237.
- MANCEDA, R. & FIGUEROA, D. 1995. Inversion of the Mesozoic Neuquén rift in the Malargüe fold-thrust belt, Mendoza, Argentina. In: TANKARD, A. J., SUAREZ, R. & WELSINK, H. J. (eds) *Petroleum Basins of South America*. American Association of Petroleum Geologists, Tulsa, OK, Memoirs, **62**, 369–382.
- MÁNGANO, M. G. & BUATOIS, L. A. 1996. Shallow marine event sedimentation in a volcanic arc-related setting: the Ordovician Suri Formation, Famatina Range, northwest Argentina (Famatina System). *Sedimentary Geology*, **105**, 63–90.
- MARANGUNIC, C., MORENO, H. & VARELA, J. 1979. Observaciones sobre los depósitos de relleno de la Depresión Longitudinal de Chile entre los ríos Tinguiririca y Maule. In: *II Congreso Geológico Chileno*, Arica, **3**, J129–J139.
- MARDONEZ, D., VELÁSQUEZ, R., MERINO, R. & BONILLA, R. 2012. Caracterización y condiciones de metamorfismo de una nueva unidad dentro del paleozoico de la Cordillera de la Costa (Unidad Patagual – El Venado), Región de Biobío, Chile. In: *XIII Congreso Geológico Chileno*, Antofagasta, 365–367.
- MARTIN, M., CLAVERO, J. & MPODOZIS, C. 1997. Eocene to Late Miocene magmatic development of the El Indio Belt, ~30°S, north central Chile. In: *VIII Congreso Geológico Chileno*, Antofagasta, **1**, 149–153.
- MARTIN, M. W., CLAVERO, J. & MPODOZIS, C. 1999. Late Paleozoic to Early Jurassic tectonic development of the high Andean Principal Cordillera, El Indio region, Chile (29°–30°S). *Journal of South American Earth Sciences*, **12**, 33–49.
- MARTINA, F., VIRAMONTE, J. M., ASTINI, R. A., PIMENTEL, M. M. & DANTAS, E. 2011. Mississippian volcanism in the southern Central Andes: new U–Pb SHRIMP zircon geochronology and whole-rock geochemistry. *Gondwana Research*, **19**, 524–544.
- MARTÍNEZ, A. N. 2005. *Secuencias volcánicas Permo-Triásicas de los cordones del Portillo y del Plata, Cordillera Frontal, Mendoza: su interpretación tectónica*. PhD thesis, Universidad de Buenos Aires.
- MARTÍNEZ, A. N., RODRÍGUEZ BLANCO, L. & RAMOS, V. A. 2006. Permo-Triassic magmatism of the Choiyoi Group in the Cordillera Frontal of Mendoza, Argentina: geological variations associated with changes in Paleo-Benioff zone. In: *Backbone of the Americas*. Asociación Geológica Argentina and Geological Society of America, Mendoza, Argentina, Abstracts with Programs, **77**.
- MARTINO, R. D. 2003. Las fajas de deformación dúctil de las Sierras Pampeanas de Córdoba: Una reseña general. *Revista de la Asociación Geológica Argentina*, **58**, 549–571.
- MARTINOD, J., HUSSON, L., ROSPERCH, P., GUILLAUME, B. & ESPURT, N. 2010. Horizontal subduction zones, convergence velocity and the building of the Andes. *Earth and Planetary Science Letters*, **299**, 299–309.
- MÉNDEZ-BEDIA, I., CHARRIER, R., BUSQUETS, P. & COLOMBO, F. 2009. Barras litorales carbonatadas en el Paleozoico Superior Andino (Formación Huentelauquén, Norte Chico, Chile). In: *XII Congreso Geológico Chileno*, Santiago, Actas, 1–4.
- MESCUA, J. F. 2011. *Evolución estructural de la Cordillera Principal entre Las Choicas y Santa Elena (35° S), Provincia de Mendoza, Argentina*. PhD thesis, Departamento de Ciencias Geológicas, Universidad de Buenos Aires.
- MESCUA, J. F., GIAMBIAGI, L. B. & BECHIS, F. 2008. Evidencias de tectónica extensional en el Jurásico Tardío (Kimeridgiano) del suroeste de la provincia de Mendoza. *Revista de la Asociación Geológica Argentina*, **63**, 512–519.
- MILANA, J. P. 1998. Anatomía de parasecuencias en un lago de rift y su relación con la generación de hidrocarburos, cuenca triásica de Ischigualasto, San Juan. *Revista de la Asociación Geológica Argentina*, **53**, 365–387.
- MILANA, J. P. & ALCOBER, O. 1994. Modelo tectosedimentario de la cuenca triásica de Ischigualasto (San Juan, Argentina). *Revista de la Asociación Geológica Argentina*, **49**, 217–235.
- MINATO, M. & TAZAWA, J. 1977. Fossils of the Huéntelauquén Formation at the locality F, Coquimbo Province, Chile. In: ISHIKAWA, T. & AGUIRRE, L. (eds) *Comparative Studies of the Circum-Pacific Orogenic Belt in Japan and Chile*. First Report. Japan Society for the Promotion of Science, Tokyo, 95–117.
- MORATA, D. & AGUIRRE, L. 2003. Extensional Lower Cretaceous volcanism in the Coastal Range (29°20'–30°S), Chile: geochemistry and petrogenesis. *Journal of South American Earth Sciences*, **16**, 459–476.
- MORATA, D., FÉRAUD, G., AGUIRRE, L., ARANCIBIA, G., BELMAR, M., MORALES, S. & CARRILLO, J. 2008. Geochronology of the Lower Cretaceous volcanism from the Coastal Range (29°20'–30°S), Chile. *Revista Geológica de Chile*, **35**, 123–145.
- MORATA, D., VARAS, M. J., HIGGINS, M., VALENCIA, V. & VÉRHOORT, J. 2010. Episodic emplacement of the Illapel Plutonic Complex (Coastal Cordillera, central Chile): Sr and Nd isotopic, and zircon U–Pb geochronological constraints. In: *South American Symposium on Isotope Geology*, 7, Brasilia, [http://refhub.elsevier.com/S0895-9811\(1300169-7/sref26\)](http://refhub.elsevier.com/S0895-9811(1300169-7/sref26))
- MOREL, R. 1981. *Geología del sector Norte de la hoja Gualleco, entre los 35° 00' y 35° 10' lat. Sur, Provincia de Talca, VII Región, Chile*. Thesis, Departamento de Geología, Universidad de Chile.
- MORENO, K. & BENTON, M. J. 2005. Occurrence of sauropod dinosaur tracks in the Upper Jurassic of Chile (redescription of *Iguanodonichnus frenki*). *Journal of South American Earth Sciences*, **20**, 253–257.
- MORENO, K. & PINO, M. 2002. Huellas de dinosaurios en la Formación Baños del Flaco (Titoniano-Jurásico Superior), VI Región, Chile: paleoetología y paleoambiente. *Revista Geológica de Chile*, **29**, 191–206.
- MOSCOSO, R., PADILLA, H. & RIVANO, S. 1982. *Hoja Los Andes, Región de Valparaíso*. Servicio Nacional de Geología y Minería, Santiago, Carta Geológica de Chile, **52**.
- MPODOZIS, C. & CORNEJO, P. 1988. *Carta Geológica de Chile, hoja Pisco Elqui, IV Región de Coquimbo a*

- escala 1: 250.000. Servicio Nacional de Geología y Minería, Santiago de Chile, **68**.
- MPODOZIS, C. & CORNEJO, P. 2012. Cenozoic tectonics and porphyry copper systems of the Chilean Andes. In: HEDENQUIST, J. W., HARRIS, M. & CAMUS, F. (eds) *Geology and Genesis of Major Copper Deposits and Districts of the World: A tribute to Richard H. Sillitoe*. Society of Economic Geologists, Littleton, CO, Special Publications, **16**, 329–360.
- MPODOZIS, C. & KAY, S. M. 1990. Provincias magmáticas ácidas y evolución tectónica de Gondwana: Andes chilenos (28°–31°S). *Revista Geológica de Chile*, **17**, 153–180.
- MPODOZIS, C. & KAY, S. M. 1992. Late Paleozoic to Triassic evolution of the Gondwana margin: evidence from Chilean Frontal Cordilleran batholiths (28°S to 31°S). *Geological Society of America Bulletin*, **104**, 999–1014.
- MPODOZIS, C. & RAMOS, V. A. 1989. The Andes of Chile and Argentina. In: ERICKSEN, G. E., CAÑAS PINOCHE, M. T. & REINEMUD, J. A. (eds) *Geology of the Andes and its Relation to Hydrocarbon and Mineral Resources*. Circumpacific Council for Energy and Mineral Resources, Houston, Earth Sciences Series, **11**, 59–90.
- MPODOZIS, C. & RAMOS, V. A. 2008. Tectónica jurásica en Argentina y Chile: extensión, subducción oblicua, rifting, deriva y colisiones? *Revista de la Asociación Geológica Argentina*, **63**, 481–497.
- MPODOZIS, C., BROCKWAY, H., MARQUARDT, C. & PERELLÓ, J. 2009. Geocronología U/Pb y tectónica de la región Los Pelambres-Cerro Mercedario: implicancias para la evolución cenozoica de los Andes del centro de Chile y Argentina. In: *XII Congreso Geológico Chileno*, Santiago, electronic abstract.
- MUNDACA, P., PADILLA, H. & CHARRIER, R. 1979. Geología del área comprendida entre Quebrada Angostura, Cerro Talinai y Punta Claditas, Provincia de Choapa. In: *II Congreso Geológico Chileno*, Arica, Actas, **1**, A121–A161.
- MUÑOZ, J. & NIEMEYER, H. 1984. *Hoja Laguna del Maule, Regiones del Maule y del Bío-Bío*. Servicio Nacional de Geología y Minería, Santiago, Carta, **64**.
- MUÑOZ, M., FUENTES, F., VÉRGARA, M., AGUIRRE, L., NYSTRÖM, J. O., FÉRAUD, G. & DEMANT, A. 2006. Abanico East Formation: petrology and geochemistry of volcanic rocks behind the Cenozoic arc front in the Andean Cordillera, central Chile (33°50'S). *Revista Geológica de Chile*, **33**, 109–140.
- MUÑOZ, M., AGUIRRE, L., VÉRGARA, M., DEMANT, A., FUENTES, F. & FOCK, A. 2010. Prehnite- pumpellyite facies metamorphism in the eastern belt of the Abanico Formation, Andean Cordillera of central Chile (33° 50'S): chemical and scale controls on mineral assemblages, reaction progress and the equilibrium state. *Andean Geology*, **37**, 54–77.
- MUÑOZ, M., FARÍAS, M., CHARRIER, R., FANNING, C. M., POLVÉ, M. & DECKART, K. 2013. Isotopic shifts in the Cenozoic Andean arc of central Chile: records of an evolving basement throughout cordilleran arc mountain building. *Geology*, **41**, 931–934.
- MUÑOZ-CRISTI, J. 1942. Rasgos generales de la construcción geológica de la Cordillera de la Costa; especialmente en la Provincia de Coquimbo. In: *Congreso Panamericano de Ingeniería de Minas y Geología*. Santiago, Chile, Anales, **1**, 285–318.
- MUÑOZ-CRISTI, J. 1946. Estado actual del conocimiento sobre la geología de la provincia de Arauco. *Anales Facultad de Ciencias Físicas y Matemáticas, Universidad de Chile*, **3**, 30–63.
- MUÑOZ-CRISTI, J. 1956. Chile. In: YENKS, W. F. (ed.) *Handbook of South American Geology*. Geological Society of America, Boulder, CO, Memoirs, **65**, 187–214.
- MUÑOZ-CRISTI, J. 1968. Evolución geológica del territorio chileno. *Boletín de la Academia de Ciencias de Chile*, **1**, 18–26.
- MUÑOZ-CRISTI, J. 1973. *Geología de Chile: Pre-Paleozoico, Paleozoico y Mesozoico*. Editorial Andrés Bello, Santiago.
- MUÑOZ-SAEZ, C., PINTO, L., CHARRIER, R. & NALPAS, T. 2014. Importance of volcanic load and shortcut fault development during inversion of the Abanico basin, Central Chile (33°–35°S). *Andean Geology*, **41**, 1–28.
- MUTTI, D. I. 1997. La secuencia ofiolítica basal desmembrada de las sierras de Córdoba. *Revista de la Asociación Geológica Argentina*, **52**, 275–285.
- NAIPAUER, M., VUJOVICH, G. I., CINGOLANI, C. A. & MCCLELLAND, W. C. 2010a. Detrital zircon analysis from the Neoproterozoic–Cambrian sedimentary cover (Cuyania terrane), Sierra de Pie de Palo, Argentina: evidences of a rift and passive margin system. *Journal South American Earth Sciences*, **29**, 306–326.
- NAIPAUER, M., CINGOLANI, C. A., VUJOVICH, G. I. & CHEMALE, F. 2010b. Geochemistry and Nd isotopic signatures of metasedimentary rocks of the Caucete Group, Sierra de Pie de Palo, Argentina: implications for their provenance. *Journal South American Earth Sciences*, **30**, 84–96.
- NASI, C. & THIELE, R. 1982. Estratigrafía del Jurásico y Cretácico de la Cordillera de la Costa al sur del río Maipo, entre Melipilla y Laguna de aculeo (Chile Central). *Revista Geológica de Chile*, **16**, 81–99.
- NASI, C., MPODOZIS, C., CORNEJO, P., MOSCOSO, R. & MAKSAEV, V. 1985. El batolito Elqui-Limari (Paleozoico Superior-Triásico): características petrográficas, geoquímicas y significado tectónico. *Revista Geológica de Chile*, **25–26**, 77–111.
- NASI, C., MOSCOSO, R. & MAKSAEV, V. 1990. Hoja Guanta, *Regiones de Atacama y Coquimbo*. Servicio Nacional de Geología y Minería, Santiago.
- NIELSEN, S. 2005. The Triassic Santa Juana Formation at the lower Biobío River, south central Chile. *Journal of South American Earth Sciences*, **19**, 547–562.
- NIEMEYER, H. & MUÑOZ, J. 1983. *Geología de la Hoja Laguna de La Laja*. Servicio Nacional de Geología y Minería, Santiago, Serie Carta Geológica de Chile, **58**.
- OLIVEROS, V., MORATA, D., AGUIRRE, L., FÉRAUD, G. & FORNARI, G. 2007. Jurassic to Early Cretaceous subduction-related magmatism in the Coastal Cordillera of northern Chile (18°30'–24°S): geochemistry and petrogenesis. *Revista Geológica de Chile*, **34**, 209–232.
- OLIVEROS, V., LABBÉ, M., ROSEL, P., CHARRIER, R. & ENCINAS, A. 2012. Late Jurassic paleogeographic evolution of the Andean back-arc basin: new constraints

ANDES OF CENTRAL CHILE AND WESTERN ARGENTINA

- from the Lagunillas Formation, northern Chile ($27^{\circ}30' - 28^{\circ}30'S$). *Journal of South American Earth Sciences*, **37**, 25–40.
- ORME, H. M. & ATHERTON, M. P. 1999. New U–Pb and Sr–Nd Data from the Frontal Cordillera Composite Batholith, Mendoza: implications for Magma Source and Evolution. In: *IV International Symposium on Andean Geology*, Göttingen, 555–558.
- OTA, Y., MIYAUCHI, T., PASKOFF, R. & KOBA, M. 1995. Plio–Quaternary terraces and their deformation along the Altos de Talinay, North–Central Chile. *Revista Geológica de Chile*, **22**, 89–102.
- OTAMENDI, J. E., TIBALDI, A. M., VUJOVICH, G. I. & VIÑAO, G. A. 2008. Metamorphic evolution of migmatites from the deep Famatinian arc crust exposed in Sierras Valle Fértil e La Huerta, San Juan, Argentina. *Journal of South American Earth Sciences*, **25**, 313–335.
- OTAMENDI, J. E., VUJOVICH, G. I., DE LA ROSA, J. D., TIBALDI, A. M., CASTRO, A. & MARTINO, R. D. 2009a. Geology and petrology of a deep crustal zone from the Famatinian paleo-arc, Sierras Valle Fértil–la Huerta, San Juan, Argentina. *Journal of South American Earth Sciences*, **27**, 258–279.
- OTAMENDI, J. E., DUCEA, M. N., TIBALDI, A. M., BERGANTZ, G., DE LA ROSA, J. D. & VUJOVICH, G. I. 2009b. Generation of tonalitic and dioritic magmas by coupled partial melting of gabbroic and metasedimentary rocks within the deep crust of the Famatinian magmatic arc, Argentina. *Journal of Petrology*, **50**, 841–873.
- OTAMENDI, J. E., CRISTOFOLINI, E., TIBALDI, A. M., QUEVEDO, F. & BALIANI, I. 2010a. Petrology of mafic and ultramafic layered rocks from the Jaboncillo Valley, Sierra de Valle Fértil, Argentina: implications for the evolution of magmas in the lower crust of the Famatinian arc. *Journal of South American Earth Sciences*, **29**, 685–704.
- OTAMENDI, J. E., PINOTTI, L. P., BASEI, M. A. S. & TIBALDI, A. M. 2010b. Evaluation of petrogenetic models for intermediate and silicic plutonic rocks from the Sierra de Valle Fértil-La Huerta, Argentina: petrologic constraints on the origin of igneous rocks in the Ordovician Famatinian-Puna paleoarc. *Journal of South American Earth Sciences*, **30**, 29–45.
- PADILLA, H. & VERGARA, M. 1985. Control estructural y alteración de tipo campo geotérmico en los intrusivos subvolcánicos miocénicos del área de la Cuesta de Chacabuco-Baños del Corazón, Chile central. *Revista Geológica de Chile*, **24**, 3–17.
- PANKHURST, R. J. & RAPELA, C. W. 1998. The proto-Andean margin of Gondwana: an introduction. In: PANKHURST, R. J. & RAPELA, C. W. (eds) *The Proto-Andean Margin of Gondwana*. Geological Society, London, Special Publications, **142**, 1–9.
- PANKHURST, R. J., MILLAR, I. L. & HERVÉ, F. 1996. A Permo-Carboniferous U–Pb age for part of the Guanta Unit of the Elqui–Limari Batholith at Rio del Transito, Northern Chile. *Revista Geologica de Chile*, **23**, 35–42.
- PARADA, M. A., RIVANO, S. & SEPÚLVEDA, P. 1988. Mesozoic and Cainozoic plutonic development in the Andes of central Chile. *Journal of South American Earth Sciences*, **1**, 249–260.
- PARADA, M. A., LEVI, B. & NYSTRÖM, J. 1991. Geochemistry of the Triassic to Jurassic plutonism of central Chile (30° to 33° S): petrogenetic implications and a tectonic discussion. In: HARMON, R. S. & RAPELA, C. W. (eds) *Andean Magmatism and its Tectonic Setting*. Geological Society of America, Boulder, CO, Special Papers, **265**, 99–112.
- PARADA, M. A., NYSTROM, J. O. & LEVI, B. 1999. Multiple sources for the Coastal Batholith of central Chile (31° – 34° S): geochemical and Sr–Nd isotopic evidence and tectonic implications. *Lithos*, **46**, 505–521.
- PARADA, M. A., FÉRAUD, G., FUENTES, F., AGUIRRE, L., MORATA, D. & LARRONDO, P. 2005. Ages and cooling history of the Early Cretaceous Caleu pluton: testimony of a switch from a rifted to a compressional continental margin in central Chile. *Journal of the Geological Society of London*, **162**, 273–287.
- PARADA, M. A., LÓPEZ-ESCOBAR, L. ET AL. 2007. Andean magmatism. In: MORENO, T. & GIBBONS, W. (eds) *The Geology of Chile*. Geological Society, London, 115–146.
- PARDO, M., COMTE, D. & MONFRET, T. 2002. Seismotectonic and stress distribution in the central Chile subduction zone. *Journal of South American Earth Sciences*, **15**, 11–22.
- PARDO-CASAS, F. & MOLNAR, P. 1987. Relative motion of the Nazca (Farallon) and South American plates since Late Cretaceous time. *Tectonics*, **6**, 233–248.
- PASKOFF, R. 1970. *Recherches Géomorphologiques Dans le Chili Semi-Aride*. Biscaye Frères, Bordeaux.
- PASKOFF, R. 1977. The Quaternary of Chile: the state of research. *Quaternary Research*, **8**, 2–31.
- PAZOS, P. J. 2002. The Late Carboniferous glacial to post-glacial transition: facies and sequence stratigraphy, Western Paganzo Basin, Argentina. *Gondwana Research*, **5**, 467–487.
- PETFORD, N. & GREGORI, D. A. 1994. Geological and geochemical comparison between the coastal batholith (Perú) and the Frontal Cordillera composite batholith (Argentina). In: *VII Congreso Geológico Chileno*, Concepción, Actas, **2**, 1428–1432.
- PINEDA, V. 1983a. *Evolución paleogeográfica de la península de Arauco durante el Cretácico Superior-Terciario*. Thesis, Departamento de Geología, Universidad de Chile, Santiago.
- PINEDA, V. 1983b. Evolución Paleogeográfica de la Cuenca Sedimentaria Cretácico-Terciaria de Arauco. *Geología y Recursos Minerales de Chile*, Universidad Concepción, **1**, 375–390.
- PINEDA, G. & CALDERÓN, M. 2008. *Geología del área Monte Patria-El Maqui, Región de Coquimbo*. Servicio Nacional de Geología y Minería, Santiago.
- PINEDA, G. & EMPARAN, C. 2006. *Geología del área Vicuña-Pichasca, Región de Coquimbo*. Servicio Nacional de Geología y Minería, Santiago.
- PIÑÁN-LLAMAS, A. & SIMPSON, C. 2006. Deformation of Gondwana margin turbidites during the Pampean orogeny, north-central Argentina. *Bulletin Geological Society of America*, **118**, 1270–1279.
- PIRACÉS, R. 1976. Estratigrafía de la Cordillera de la Costa entre la cuesta El Melón y Limache, Provincia de Valparaíso, Chile. In: *I Congreso Geológico Chileno*, Santiago, Actas, **1**(A), 65–82.

- PIRACÉS, R. 1977. *Geología de la Cordillera de la Costa entre Catapilco y Limache, región de Aconcagua*. Thesis, Departamento de Geología, Universidad de Chile.
- POLANSKI, J. 1964. Descripción geológica de la Hoja 25a Volcán San José, provincia de Mendoza. *Dirección Nacional de Geología y Minería, Boletín*, **98**, 1–94.
- POLANSKI, J. 1972. Descripción geológica de la Hoja 24a-b Cerro Tupungato, provincia de Mendoza. *Dirección Nacional de Geología y Minería, Boletín*, **128**, 1–110.
- POMA, S. & RAMOS, V. A. 1994. Las secuencias básicas iniciales del Grupo Choioi. Cordon del Portillo, Mendoza: sus implicancias tectónicas. In: *VII Congreso Geológico Chileno*, Concepción, Actas, **2**, 1162–1166.
- QUENARDELLE, S. & RAMOS, V. A. 1999. The Ordovician western Sierras Pampeanas magmatic belt: record of Precordillera accretion in Argentina. In: RAMOS, V. A. & KEPPIE, D. (eds) *Laurentia Gondwana Connections before Pangea*. Geological Society of America, Boulder, CO, Special Papers, **336**, 63–86.
- QUIROGA, R. 2013. *Análisis estructural de los depósitos cenozoicos de la Cordillera Principal entre el cerro Provincia y el cordón El Quempo, Región Metropolitana, Chile (33°18' a 33°25'S)*. Thesis, Departamento de Geología, Universidad de Chile.
- RADIC, J. P., ROJAS, L., CARPINELLI, A. & ZURITA, E. 2002. Evolución tectónica de la Cuenca de Curamallín, región cordillerana chileno argentina (36°30'–39°00'S). In: *XV Congreso Geológico Argentino, El Calafate*, **3**, 233–237.
- RAMOS, V. A. 1981. *Descripción geológica de la hoja 33 c. Los Chihuidos Norte, provincia de Neuquén*. Servicio Geológico Nacional, Buenos Aires, **182**.
- RAMOS, V. A. 1988a. Tectonics of the Late Proterozoic–Early Paleozoic: a collisional history of southern South America. *Episodes*, **11**, 168–174.
- RAMOS, V. A. 1988b. The tectonics of the Central Andes; 30° to 33° S latitude. In: CLARK, S. & BURCHFIELD, D. (eds) *Processes in Continental Lithospheric Deformation*. Geological Society of America, Boulder, CO, Special Paper, **218**, 31–54.
- RAMOS, V. A. 1994. Terranes of southern Gondwanaland and their control in the Andean structure (30–33°S lat.). In: REUTTER, K. J., SCHEUBER, E. & WIGGER, P. J. (eds) *Tectonics of the Southern Central Andes, Structure and Evolution of an Active Continental Margin*. Springer, Berlin, 249–261.
- RAMOS, V. A. 1999. Rasgos estructurales del territorio argentino. I. Evolución tectónica de la Argentina. In: CAMINOS, R. (ed.) *Geología Argentina*. Instituto de Geología y Recursos Naturales, Buenos Aires, Argentina, Anales, **29**, 715–784.
- RAMOS, V. A. 2004. Cuyania, an exotic block to Gondwana: review of a historical success and the present problems. *Gondwana Research*, **7**, 1009–1026.
- RAMOS, V. A. 2010. The tectonic regime along the Andes: present settings as a key for the Mesozoic regimes. *Geological Journal*, **45**, 2–25.
- RAMOS, V. A. & DALLA SALDA, L. 2011. Occidentalalia: Un terreno acrecionado sobre el margen gondwánico? In: *XVIII Congreso Geológico Argentino*, Neuquén, Actas, 222–223.
- RAMOS, V. A. & FOLGUERA, A. 2005. Tectonic evolution of the Andes of Neuquén: constraints derived from the magmatic arc and foreland deformation. In: VEIGA, G. D., SPALLETTI, L. A., HOWELL, J. A. & SCHWARZ, E. (eds) *The Neuquén Basin, Argentina: A Case Study in Sequence Stratigraphy and Basin Dynamics*. Geological Society, London, Special Publications, **252**, 15–35.
- RAMOS, V. A. & FOLGUERA, A. 2009. Andean flat slab subduction through time. In: MURPHY, B. (ed.) *Ancient Orogens and Modern Analogues*. Geological Society, London, Special Publications, **327**, 31–54.
- RAMOS, V. A. & FOLGUERA, A. 2011. Payenia volcanic province in Southern Andes: an appraisal of an exceptional Quaternary tectonic setting. *Journal of Volcanology and Geothermal Research*, **201**, 53–64.
- RAMOS, V. A. & KAY, S. M. 1991. Triassic rifting and associated basalts in the Cuyo basin, central Argentina. In: HARMON, R. S. & RAPELA, C. W. (eds) *Andean Magmatism and its Tectonic Setting*. Geological Society of America, Boulder, CO, Special Papers, **265**, 79–91.
- RAMOS, V. A. & VUJOVICH, G. I. 1993. The Pampia Craton within Western Gondwanaland. In: ORTEGA-GUTIÉRREZ, F., CONEY, P., CENTENO-GARCÍA, E. & GÓMEZ-CABALLERO, A. (eds) *Proceedings of The First Circum-Pacific and Circum-Atlantic Terrane Conference*, México, 113–116.
- RAMOS, V. A., JORDAN, T. E., ALLMENDINGER, R. W., KAY, S. M., CORTÉS, J. M. & PALMA, M. A. 1984. Chilenia: un terreno alóctono en la evolución paleozoica de los Andes Centrales. In: *IX Congreso Geológico Argentino*, Bariloche, Actas, **2**, 84–106.
- RAMOS, V. A., JORDAN, T. E., ALLMENDINGER, R. W., MPODOZIS, C., KAY, S., CORTÉS, J. M. & PALMA, M. A. 1986. Paleozoic terranes of the Central Argentinean Andes. *Tectonics*, **5**, 855–880.
- RAMOS, V. A., RIVANO, S., AGUIRRE-URRETA, M. B., GODOY, E. & LO FORTE, G. L. 1990. El Mesozoico del cordón del Límite entre Portezuelo Navarro y Monos de Agua (Chile-Argentina). In: *XI Congreso Geológico Argentino*, San Juan, Actas, **2**, 43–46.
- RAMOS, V. A., MUNIZAGA, F. & KAY, S. M. 1991. El magmatismo cenozoico a los 33°S de latitud: geocronología y relaciones tectónicas. In: *VI Congreso Geológico Chileno*, Viña del Mar, Actas, **1**, 892–896.
- RAMOS, V. A., AGUIRRE-URRETA, M. B. & ÁLVAREZ, P. P. 1996a. *Geología de la Región del Aconcagua*. Dirección Nacional del Servicio Geológico, Buenos Aires, Subsecretaría de Minería de la Nación Anales, **24**.
- RAMOS, V. A., CEGARRA, M. & CRISTALLINI, E. 1996b. Cenozoic tectonics of the High Andes of west-central Argentina, (30°–36°S latitude). *Tectonophysics*, **259**, 185–200.
- RAMOS, V. A., ESCAYOLA, M., MUTTI, D. & VUJOVICH, G. I. 2000. Proterozoic–early Paleozoic ophiolites in the Andean basement of southern South America. In: DILEK, Y., MOORES, E. M., ELTHON, D. & NICOLAS, A. (eds) *Ophiolites and Oceanic Crust: New Insights from Field Studies and Ocean Drilling Program*. Geological Society of America, Boulder, CO, Special Papers, **349**, 331–349.

ANDES OF CENTRAL CHILE AND WESTERN ARGENTINA

- RAMOS, V. A., CRISTALLINI, E. O. & PÉREZ, D. J. 2002. The Pampean flat-slab of the Central Andes. *Journal of South America Earth Sciences*, **15**, 59–78.
- RAMOS, V. A., VUJOVICH, G., MARTINO, R. & OTAMENDI, J. 2010. Pampia: a large cratonic block missing in the Rodinia supercontinent. *Journal of Geodynamics*, **50**, 243–255.
- RAMOS, V. A., LITVAK, V., FOLGUERA, A. & SPAGNUOLO, M. 2014. An Andean tectonic cycle: from crustal thickening to extension in a thin crust (34° – 37° S). *Geoscience Frontiers*, **5**, 351–367. <http://dx.doi.org/10.1016/j.gsf.2013.12.009>
- RAPALINI, A. E. 2012. Paleomagnetic evidence for the origin of the Argentine Precordillera, fifteen years later: what is new, what has changed, what is still valid? *Latinmag Letters*, **2**, 1–20.
- RAPALINI, A. E. & ASTINI, R. A. 1998. Paleomagnetic confirmation of the Laurentian origin of the Argentine Precordillera. *Earth and Planetary Science Letters*, **155**, 1–14.
- RAPELA, C. & KAY, S. 1988. Late Paleozoic to Recent magmatic evolution of northern Patagonia. *Episodes*, **11**, 175–182.
- RAPELA, C. W., PANKHURST, R. J., CASQUET, C., BALDO, E., SAAVERDRA, J., GALINDO, C. & FANNING, C. M. 1998. The Pampean Orogeny of the southern Proto-Andean: Cambrian continental collision in the Sierras de Córdoba. In: PANKHURST, R. J. & RAPELA, C. W. (eds) *The Proto-Andean Margin of Gondwana*. Geological Society, London, Special Publications, **142**, 181–217.
- RAPELA, C. W., PANKHURST, R. J. ET AL. 2007. The Río de la Plata craton and the assembly of SW Gondwana. *Earth-Science Reviews*, **83**, 49–82.
- RAPELA, C. W., PANKHURST, R. J., CASQUET, C., BALDO, E., GALINDO, C., FANNING, C. M. & DAHLQUIST, J. A. 2010. The Western Sierras Pampeanas: protracted Grenville-age history (1330–1030 Ma) of intra-oceanic arcs, subduction–accretion at continental-edge and AMCG intraplate magmatism. *Journal of South American Earth Sciences*, **29**, 105–127.
- RAULD, R. A. 2002. *Análisis morfoestructural del frente cordillerano: Santiago oriente entre el río Mapocho y Quebrada de Macul*. Thesis, Departamento de Geología, Universidad de Chile, Santiago.
- REBOLLEDO, S. & CHARRIER, R. 1994. Evolución del basamento paleozoico en el área de Punta Claditas, Región de Coquimbo, Chile (31° – 32° S). *Revista Geológica de Chile*, **21**, 55–69.
- REGARD, V., SAILLARD, M. ET AL. 2010. Renewed uplift of the Central Andes Forearc revealed by coastal evolution during the Quaternary. *Earth and Planetary Science Letters*, **297**, 199–210.
- REUTTER, K. J. 2001. Le Ande centrali: elemento di un'origenesi di margine continentale attivo. *Acta Naturalia de l'Ateneo Parmense*, **37**, 5–37.
- RICCARDI, A. C. & IGLESIAS LLANOS, M. P. 1999. Primer hallazgo de ammonites en el Triásico de Argentina. *Revista de la Asociación Geológica Argentina*, **54**, 298–300.
- RICHTER, P., RING, U., WILLNER, A. P. & LEISS, B. 2007. Structural contacts in subduction complexes and their tectonic significance: the Late Palaeozoic coastal accretionary wedge of central Chile. *Journal of the Geological Society, London*, **164**, 203–214.
- RIVANO, S. 1996. *Geología de las Hojas Quillota y Portillo*. Servicio Nacional de Geología y Minería. Santiago.
- RIVANO, S. & SEPÚLVEDA, P. 1983. Hallazgo de foraminíferos del Carbonífero Superior en la Formación Huentelauquén. *Revista Geológica de Chile*, **19**–**20**, 25–35.
- RIVANO, S. & SEPÚLVEDA, P. 1985. Las calizas de la Formación Huentelauquén: depósitos de aguas templadas a frías en el Carbonífero Superior–Pérmitico Inferior. *Revista Geológica de Chile*, **25**–**26**, 29–38.
- RIVANO, S. & SEPÚLVEDA, P. 1991. *Hoja Illapel, Región de Coquimbo. Carta Geológica de Chile*. Servicio Nacional de Geología y Minería, Santiago.
- RIVANO, S., SEPÚLVEDA, P., BORIC, R. & ESPÍNEIRA, D. 1993. *Hoja Quillota y Portillo*. Servicio Nacional de Geología y Minería, Santiago, Carta Geológica de Chile, **73**.
- ROBINSON, D., BEVINS, R. E. & RUBINSTEIN, N. 2005. Subgreenschist facies metamorphism of metabasites from the Precordillera terrane of western Argentina: constraints on the latter stages of accretion to Gondwana. *European Journal of Mineralogy*, **17**, 441–452.
- ROCHA CAMPOS, A. C., BASEI, M. A. ET AL. 2011. 30 million years of Permian volcanism recorded in the Choiyoi igneous province (W Argentina) and their source for younger ash fall deposits in the Paraná Basin: SHRIMP U–Pb zircon geochronology evidence. *Gondwana Research*, **19**, 509–523.
- RODRÍGUEZ, M. P. 2013. Cenozoic uplift and exhumation above the southern part of the flat slab subduction segment of Chile (28.5 – 32° S). Thesis, Departamento de Geología, Universidad de Chile, Santiago.
- RODRÍGUEZ, M. P., PINTO, L. & ENCINAS, A. 2012. Cenozoic erosion in the Andean forearc in Central Chile (33° – 34° S): Sediment provenance inferred by heavy mineral studies. In: RASBURY, E. T., HEMMING, S. R. & RIGGS, N. (eds) *Mineralogical and Geochemical Approaches to Provenance*. Geological Society of America, Boulder, CO, Special Papers, **487**, 141–162.
- RODRÍGUEZ, M. P., CARRETIER, S. ET AL. 2013. Geochronology of pediments and marine terraces in north-central Chile and their implications for Quaternary uplift in the Western Andes. *Geomorphology*, **180**–**181**, 33–46.
- RODRÍGUEZ, M. P., AGUILAR, G., URRESTY, C. & CHARRIER, R. 2014. Neogene landscape evolution in the Andes of north-central Chile between 28 and 32° S: interplay between tectonic and erosional processes. In: SEPÚLVEDA, S. A., GIAMBIAGI, L. B., MOREIRAS, S. M., PINTO, L., TUNIK, M., HOKE, G. D. & FARÍAS, M. (eds) *Geodynamic Processes in the Andes of Central Chile and Argentina*. Geological Society, London, Special Publications, **399**. First published online April 2, 2014, <http://dx.doi.org/10.1144/SP399.15>
- ROSSEL, P., OLIVEROS, V., DUCEA, M. N., CHARRIER, R., SCAILLET, S., RETAMAL, L. & FIGUEROA, O. 2013. The Early Andean subduction system as an analogue to island arcs: evidence from across-arc geochemical variations in northern Chile. *Lithos*, **179**, 211–230, <http://dx.doi.org/10.1016/j.lithos.2013.08.014>
- ROSSEL, P., OLIVEROS, V. ET AL. 2014. La Formación Rio Damas-Tordillo (33° – 35.5° S): antecedentes

- sobre petrogénesis, proveniencia e implicancias tectónicas. *Andean Geology*, <http://www.scielo.cl/andgeol.htm>
- RUTLAND, R. W. R. 1971. Andean Orogeny and ocean floor spreading. *Nature*, **233**, 252–255.
- SAILLARD, M., HALL, S. R. ET AL. 2009. Non-steady long-term uplift rates and Pleistocene marine terrace development along the Andean margin of Chile (31°S) inferred from ^{10}Be dating. *Earth and Planetary Science Letters*, **277**, 50–63.
- SAILLARD, M., RIOTTE, J., REGARD, V., VIOLETTE, A., HÉRAIL, G., AUDIN, L. & RIQUELME, R. 2012. Beach ridges U-Th dating in Tongoy bay and tectonic implications for a peninsula–bay system, Chile. *Journal of South American Earth Sciences*, **40**, 77–84.
- SALAZAR, C., STINNESBECK, W. & QUINZIO-SINN, L. A. 2010. Ammonites from the Maastrichtian (Upper Cretaceous) Quiriquina Formation in central Chile. *Neues Jahrbuch für Geologie und Paläontologie, Abhandlungen*, **257**, 181–236.
- SALAZAR, E., ARRIAGADA, C., MPODOZIS, C., MARTÍNEZ, F., PEÑA, M. & ÁLVAREZ, J. 2009. Análisis Estructural del Oroclino de Vallenar: Primeros Resultados. In: *XII Congreso Geológico Chileno*, Santiago, electronic actas.
- SATO, A. M. & LLAMBÍAS, E. J. 1993. El Grupo Choiyoi, provincia de San Juan: equivalente efusivo del Batolito de Colangüil. In: BORDONARO, O. (ed.) *Geología y Recursos Naturales de la provincia de San Juan, Relatorio XI Congreso Geológico Argentino*, San Juan, 100–122.
- SATO, A. M., LLAMBÍAS, E. J., SHAW, S. E. & CASTRO, C. E. 1990. El Batolito de Colangüil: modelo del magmatismo neopaleozoico de la provincia de San Juan. In: BORDONARO, O. (ed.) *Geología y Recursos Naturales de la provincia de San Juan, Relatorio XI Congreso Geológico Argentino*, San Juan, 100–122.
- SATO, A. M., LLAMBÍAS, E. J., BASEI, M. A. S. & CASTRO, C. E. 2014. El magmatismo Choiyoi de la Cordillera Frontal de San Juan. In: *XIX Congreso Geológico Argentino*, Córdoba, Session 21: Pre-Andean tectonics, Presentation no. 52, Digital.
- SCHWARTZ, J. J., GROMET, L. P. & MIRÓ, R. 2008. Timing and duration of the calc-alkaline arc of the Pampean orogeny: implications for the late Neoproterozoic to Cambrian evolution of western Gondwana. *Journal of Geology*, **116**, 39–61.
- SCHILLER, W. 1912. La Alta Cordillera de San Juan y Mendoza y parte de la provincia de San Juan. *Anales del Ministerio de Agricultura, Sección Geología, Mineralogía y Minería*, **7**, 1–68.
- SCHMIDT, S., HETZEL, R., MINGORANCE, F. & RAMOS, V. A. 2011. Coseismic displacements and Holocene slip rates for two active thrust faults at the mountain front of the Andean Precordillera ($\sim 33^\circ\text{S}$). *Tectonics*, **30**, TC5011, <http://dx.doi.org/10.1029/2011TC002932>
- SELLÉS, D. & GANA, P. 2001. *Geología del área Talagante-San Francisco de Mostazal, Regiones metropolitana y del Libertador Bernardo O'Higgins*. Servicio Nacional de Geología y Minería, Santiago, Carta Geológica, Serie Geología Básica, **74**.
- SERRANO, L., VARGAS, R. & STAMBUK, V. 1996. The Late Miocene Río Blanco–Los Bronces copper deposit central Chilean Andes. In: CAMUS, F., SILLITOE, R. H. & PETERSEN, R. (eds) *Andean Copper Deposits: New Discoveries, Mineralization Styles and Metallogeny*. Society of Economic Geologists, Littleton, CO, Special Publications, **5**, 119–130.
- SILVESTRO, J. & ATENCIO, M. 2009. La cuenca cenozoica del Río Grande y Palauco: edad, evolución y control estructural. Faja plegada de Malargüe (36°S). *Revista de la Asociación Geológica Argentina*, **65**, 154–169.
- SIMPSON, C., LAW, R. D., GROMET, L. P., MIRO, R. & NORTHRUP, C. J. 2003. Paleozoic deformation in the Sierras de Córdoba and Sierra de La Minas, eastern Sierras Pampeanas, Argentina. *Journal of South American Earth Sciences*, **15**, 749–764.
- SERNAGEOMIN. 2002. *Mapa Geológico de Chile, escala 1: 1.000.000*. Servicio Nacional de Geología y Minería, Santiago, **75**.
- SKEWES, M. A., ARÉVALO, A., FLOODY, R., ZÚÑIGA, P. & STERN, C. R. 2002. The giant El Teniente breccia deposit: hypogene copper distribution and emplacement. In: GOLDFARB, R. J. & NIELSEN, R. L. (eds) *Integrated Methods for Discovery: Global Exploration in the Twenty-first Century*. Society of Economic Geologists, Littleton, CO, Special Publications, **9**, 299–332.
- SØAGER, N., HOLM, P. M. & LLAMBÍAS, E. J. 2013. Payenia volcanic province, southern Mendoza, Argentina: OIB mantle upwelling in a backarc environment. *Chemical Geology*, **349–350**, 36–53.
- SPAGNUOLO, C., RAPALINI, A. E. & ASTINI, R. A. 2012a. Assembly of Pampia to the SW Gondwana margin: a case of strike-slip docking? *Gondwana Research*, **21**, 406–421.
- SPAGNUOLO, M. G., LITVAK, V. D., FOLGUERA, A., BOTTESSI, G. & RAMOS, V. A. 2012b. Neogene magmatic expansion and mountain building processes in the southern Central Andes, 36 – 37°S , Argentina. *Journal of Geodynamics*, **53**, 81–94.
- SPALLETTI, L. 1999. Cuencas triásicas del oeste argentino: origen y evolución. *Acta Geológica Hispánica*, **32**, 29–50.
- SPALLETTI, L., ARTABE, A., MOREL, E. & BREA, M. 1999. Paleofloristic biozonation and chronostratigraphy of the Argentine Triassic. *Ameghiniana*, **36**, 419–451.
- SPALLETTI, L., MOREL, E., ARTABE, A., ZAVATTIERI, A. & GANUZA, D. 2005. Estratigrafía, facies y paleoflora de la sucesión triásica de Potrerillos, Mendoza, República Argentina. *Revista Geológica de Chile*, **32**, 249–272.
- SPALLETTI, L. A., FANNING, C. M. & RAPELA, C. W. 2008. Dating the Triassic continental rift in the southern Andes: the Potrerillos Formation, Cuyo Basin, Argentina. *Geologica Acta*, **6**, 267–283.
- SPALLETTI, L. A., LIMARINO, C. O. & COLOMBO PIÑOL, F. 2012. Petrology and geochemistry of Carboniferous siliciclastics from the Argentine Frontal Cordillera: a test of methods for interpreting provenance and tectonic setting. *Journal of South American Earth Sciences*, **36**, 32–54.
- STEINMANN, G. 1929. *Geologie von Perú*. Karl Winter, Heidelberg.
- STEINMANN, G., DEEKE, W. & MÖRICKE, W. 1895. Das Alter und die Fauna der Quiriquina Schichten in Chile. *Neues Jahrbuch Mineralogie und Palaeontologie*, **10**, 1–118.

ANDES OF CENTRAL CHILE AND WESTERN ARGENTINA

- STERN, C. R., AMINI, H., CHARRIER, R., GODOY, E., HERVÉ, F. & VARELA, J. 1984. Petrochemistry and age of rhyolitic pyroclastics flows which occur along the drainage valleys of the Río Maipo and Río Cachapoal (Chile) and the Río Chaucha and Río Papagayos (Argentina). *Revista Geológica de Chile*, **23**, 39–52.
- STERN, C. R., MORENO, H. ET AL. 2007. Chilean volcanoes. In: MORENO, T. & GIBBONS, W. (eds) *The Geology of Chile*. Geological Society, London, 147–178.
- STINNESBECK, W. 1986. Zu den faunistischen und paläoökologischen Verhältnissen in der Quriquina Formation (Maastrichtium) Zentral-Chiles. *Palaeontographica*, **194**, 99–237.
- SUÁREZ, M. & BELL, M. 1992. Triassic rift-related sedimentary basins in northern Chile (24° – 29° S). *Journal of South American Earth Sciences*, **6**, 109–121.
- SUÁREZ, M. & EMPARAN, C. 1997. Hoja Curacautín, *Regiones de Araucanía y Bío-Bío*. Carta geológica de Chile, Santiago, Servicio Nacional de Geología y Minería, **71**.
- TAVERA, J. 1942. Contribución al estudio de la estratigrafía y paleontología del Terciario de Arauco. In: *I Congreso Panamericano de Ingeniería de Minas y Geología*. Santiago, Chile, **2**, 580–632.
- TAVERA, J. 1979. Estratigrafía y paleontología de la Formación Navidad, Provincia de Colchagua, Chile ($30^{\circ}50'$ – 34° S). *Boletín del Museo Nacional de Historia Natural, Santiago*, **36**.
- TAVERA, J. 1980. *El Cretáceo y Terciario de Alagarrobo*. Imprentas Gráficas, Santiago.
- THIELE, R. 1965. *El Triásico-Jurásico del Departamento de Curepto en la Provincia de Talca*. Departamento de Geología, Universidad de Chile, Santiago, Chile, **28**.
- THIELE, R. 1980. Hoja Santiago. Región Metropolitana. Carta Geológica de Chile. *Instituto de Investigaciones Geológicas*, **39**, 1–51.
- THIELE, R. & HERVÉ, F. 1984. Sedimentación y Tectónica de antearco en los terrenos pre-andinos del Norte Chico. *Revista Geológica de Chile*, **22**, 61–75.
- THOMAS, H. 1958. Geología de la Cordillera de la Costa entre el valle de La Ligua y la cuesta de Barriga. *Instituto de Investigaciones Geológicas Boletín*, **2**, 1–80.
- THOMAS, H. 1967. *Geología de la Hoja Ovalle, Provincia de Coquimbo*. Instituto de Investigaciones Geológicas, Santiago, Boletín, **23**.
- THOMAS, W. A. & ASTINI, R. A. 1996. The Argentine Pre-cordillera: a traveller from the Ouachita embayment of North American Laurentia. *Science*, **273**, 752–757.
- THOMAS, W. A. & ASTINI, R. A. 2003. Ordovician accretion of the Argentine Precordillera terrane to Gondwana: a review. *Journal of South American Earth Sciences*, **16**, 67–79.
- THOMAS, W. A. & ASTINI, R. A. 2007. Vestiges of an Ordovician west-vergent thin-skinned Ocoyic thrust belt in the Argentine Pre-cordillera, southern Central Andes. *Journal of Structural Geology*, **29**, 1369–1385.
- THOMPSON, S. N. & HERVÉ, F. 2002. New time constraints for the age of metamorphism at the ancestral Pacific Gondwana margin of southern Chile. *Revista Geológica de Chile*, **29**, 255–271.
- TIBALDI, A. M., OTAMENDI, J. E., GROMET, L. P. & DEMICHELIS, A. H. 2008. Suya Taco and Sol de Mayo mafic complexes from eastern Sierras Pampeanas, Argentina: evidence for the emplacement of primitive OIB-like magmas into deep crustal levels at a late stage of the Pampean orogeny. *Journal of South American Earth Sciences*, **26**, 172–187.
- TICKYJ, H. 2011. Granitoides calcoalcalinos tardío-famatinianos en el Cordon del Carrizalito, Cordillera Frontal, Mendoza. In: *XVIII Congreso Geológico Argentino*, Neuquén, 1531–1532.
- TICKYJ, H., RODRÍGUEZ RAISING, M., CINGOLANI, C. A., ALFARO, M. & URIZ, N. 2009a. Graptolitos ordovícicos en el Sur de la Cordillera frontal de Mendoza. *Revista de la Asociación Geológica Argentina*, **64**, 295–302.
- TICKYJ, H., FERNÁNDEZ, M. A., CHEMALE, J. F. & CINGOLANI, C. A. 2009b. *Granodiorita Pampa de los Aves truces, Cordillera Frontal, Mendoza: Un intrusivo sintectónico de edad devónica inferior*. 14º Reunión de Tectónica y 3º Taller de Campo de Tectónica, p. 27, Córdoba.
- TUNIK, M. A. 2003. Interpretación paleoambiental de los depósitos de la Formación Saldeño (Cretácico Superior), en la alta cordillera de Mendoza. *Revista de la Asociación Geológica Argentina*, **58**, 417–433.
- TUNIK, M., FOLGUERA, A., NAIPAUER, M., PIMENTEL, M. & RAMOS, V. A. 2010. Early uplift and orogenic deformation in the Neuquén basin: constraints on the Andean uplift from U-Pb and Hf isotopic data of detrital zircons. *Tectonophysics*, **489**, 258–273.
- ULIANA, M. A. & BIDDLE, K. T. 1988. Mesozoic–Cenozoic paleogeographic and geodynamic evolution of southern South America. *Revista Brasileira de Geociências*, **18**, 172–190.
- URBINA, N. P. & SRUOGA, P. 2009. La faja metalogenética de San Luis, Sierras Pampeanas: mineralización y geocronología en el contexto metalogenético regional. *Revista de la Asociación Geológica Argentina*, **64**, 635–645.
- VAN STAAL, C. R., VUJOVICH, G. I. & NAIPAUER, M. 2011. An Alpine-style Ordovician collision complex in the Sierra de Pie de Palo, Argentina: record of subduction of Cuyania beneath the Famatina arc. *Journal of Structural Geology*, **33**, 343–361.
- VARGAS, G. & REBOLLEDO, S. 2012. Paleoseismología de la Falla San Ramón e implicancias para el peligro sismico de Santiago. In: *XIII Congreso Geológico Chileno*, Antofagasta, electronic abstract.
- VÁSQUEZ, P. & FRANZ, G. 2008. The Triassic Cobquecura Pluton (Central Chile): an example of a fayalite-bearing A-type intrusive massif at a continental margin. *Tectonophysics*, **459**, 66–84.
- VERDECCHIA, S. O., BALDO, E. G., BENEDETTO, J. L. & BORGHI, P. A. 2007. The first shelly faunas from metamorphic rocks of the Sierras Pampeanas (La Cébila Formation, Sierra de Ambato, Argentina): age and paleogeographic implications. *Ameghiniana*, **44**, 493–498.
- VERGARA, M. 1969. *Rocas volcánicas y sedimentario-volcánicas Mesozoicas y Cenozoicas en la latitud 34° 30'S, Chile*. Departamento de Geología, Universidad de Chile, Santiago, Chile, **32**.
- VERGARA, M. & DRAKE, R. 1978. *Edades K–Ar y su implicancia en la Geología Regional de Chile central*. Universidad de Chile, Departamento de Geología y Geofísica, Santiago, Comunicaciones, **23**.

- VERGARA, M., CHARRIER, R., MUNIZAGA, F., RIVANO, S., SEPÚLVEDA, P., THIELE, R. & DRAKE, R. 1988. Miocene volcanism in the central Chilean Andes ($31^{\circ}30'S$ – $34^{\circ}35'S$). *Journal of South American Earth Sciences*, **1**, 199–209.
- VERGARA, M., LEVI, B., NYSTROM, J. & CANCINO, A. 1995. Jurassic and Early Cretaceous island arc volcanism extension and subsidence in the Coastal Range of central Chile. *Geological Society of America Bulletin*, **107**, 1427–1440.
- VERGARA, M., LOPEZ ESCOBAR, L. & HICKEY-VARGAS, R. 1997. Geoquímica de las rocas volcánicas miocenas de la cuenca intermontana de Parral y Nuble. In: *VIII Congreso Geológico Chileno*. Antofagasta, Actas, **2**, 1570–1573.
- VERGARA, M., LÓPEZ-ESCOBAR, L., PALMA, J. L., HICKEY-VARGAS, R. & ROESCHMANN, C. 2004. Late Tertiary episodes in the area of the city of Santiago de Chile: new geochronological and geochemical data. *Journal of South American Earth Sciences*, **17**, 227–238.
- VICENTE, J. C. 1974. Geological cross section of the Andes between Santiago and Mendoza (33° Lat. S.) Guide Book, Excursion D-5, International Association of Volcanology and Chemistry of Earth's Interior. In: *Symposium Andean and Antarctic Problems*. Santiago, Chile, 1–10.
- VICENTE, J. C. 2005. Dynamic paleogeography of the Jurassic Andean Basin: pattern of transgression and localization of main straits through the magmatic arc. *Revista de la Asociación Geológica Argentina*, **60**, 221–250.
- VICENTE, J. C., CHARRIER, R., DAVIDSON, J., MPODOZIS, C. & RIVANO, S. 1973. La orogénesis subhercínica: fase mayor de la evolución paleogeográfica y estructural de los Andes argentino-chilenos centrales. In: *V Congreso Geológico Argentino*. Carlos Paz, Argentina, Actas, **5**, 81–98.
- VIVALLO, W., ZANETTINI, J. C. M., GARDEWEG, M., MÁRQUEZ, M. J., TASSARA, A. & GONZÁLEZ, R. A. 1999. *Mapa de recursos minerales del área fronteriza argentino-chilena entre los 34° y 56° S*. Servicio Nacional de Geología y Minería, Chile, Publicación Multinacional, **1**.
- VOLDMAN, G. G., ALBANESE, G. L. & RAMOS, V. A. 2009. Ordovician metamorphic event in the carbonate platform of the Argentine Precordillera: implications for the geotectonic evolution of the proto-Andean margin of Gondwana. *Geology*, **37**, 311–314.
- VOLDMAN, G. G., ALBANESE, G. L. & RAMOS, V. A. 2010. Conodont geothermometry of the lower Paleozoic from the Precordillera (Cuyania terrane), northwestern Argentina. *Journal of South American Earth Sciences*, **29**, 278–288.
- VOLKHEIMER, W. 1978. Descripción geológica de la Hoja 27b, Cerro Sosneado, Provincia de Mendoza. *Secretaría de Estado de Minería, Boletín*, **151**, 1–83, Buenos Aires.
- VON GOSEN, W. 1992. Structural evolution of the Argentine Precordillera: the Río San Juan Section. *Journal of Structural Geology*, **14**, 643–667.
- VON GOSEN, W., LOSKE, W. & PROZZI, C. 2002. New isotopic dating of intrusive rocks in the Sierra de San Luis (Argentina): implications for the geodynamic history of the Eastern Sierras Pampeanas. *Journal of South American Earth Sciences*, **15**, 237–250.
- VUJOVICH, G. & KAY, S. M. 1998. A Laurentian? Grenville-age oceanic arc/back-arc terrane in the Sierra de Pie de Palo, Western Sierras Pampeanas, Argentina. In: PANKHURST, R. & RAPELA, C. W. (eds) *Protomargin of Gondwana*. Geological Society, London, Special Publications, **142**, 159–180.
- VUJOVICH, G. & RAMOS, V. A. 1994. La Faja de Angaco y su relación con las Sierras Pampeanas Occidentales, Argentina. In: *VII Congreso Geológico Chileno*, Concepción, Actas, **1**, 215–219.
- WALL, R., GANA, P. & GUTIÉRREZ, A. 1996. *Mapa Geológico del área de San Antonio-Melipilla*. Regiones de Valparaíso, Metropolitana y del Libertador General Bernardo O'Higgins, Servicio Nacional de Geología y Minería, Mapa, Santiago, Chile, **2**.
- WALL, R., SELLES, D. & GANA, P. 1999. *Mapa área Tilttil–Santiago, región Metropolitana*. Servicio Nacional de Geología y Minería, Chile.
- WENZEL, O., WATHELET, J., CHÁVEZ, L. & BONILLA, R. 1975. La sedimentación cíclica Meso-Cenozoica en la región Carbonífera de Arauco–Concepción, Chile. In: *II Congreso Americano de Geología Económica*, Buenos Aires, 215–237.
- WETZEL, W. 1930. Die Quiriquina Schichten als Sediment und paläontologisches Archiv. *Palaeontographica*, **73**, 49–101.
- WILLNER, A. P. 2005. Pressure–temperature evolution of a Late Palaeozoic paired metamorphic belt in north-central Chile (34° – 35° $30'$ S). *Journal of Petrology*, **46**, 1805–1833.
- WILLNER, A. P., GLODNY, J., GERYA, T. V., GODOY, E. & MASSONNE, H. 2004. A counterclockwise PT path of high-pressure/low-temperature rocks from the Coastal Cordillera accretionary complex of south-central Chile: constraints for the earliest stage of subduction mass flow. *Lithos*, **75**, 283–310.
- WILLNER, A. P., THOMSON, S. N., KRÖNER, A., WARTHO, J.-A., WIJBRANS, J. R. & HERVÉ, F. 2005. Time markers for the evolution and exhumation history of a Late Palaeozoic paired metamorphic belt in North-Central Chile (34° – 35° $30'$ S). *Journal of Petrology*, **46**, 1835–1858.
- WILLNER, A. P., GERDES, A. & MASSONNE, H. J. 2008. History of crustal growth and recycling at the Pacific convergent margin of South America at latitudes 29 – 36° S revealed by a U–Pb and Lu–Hf isotope study of detrital zircon from late Paleozoic accretionary systems. *Chemical Geology*, **253**, 114–129.
- WILLNER, A. P., GERDES, A., MASSONNE, H.-J., SCHMIDT, A., SUDO, M., THOMSON, S. N. & VUJOVICH, G. 2011. The geodynamics of collision of a microplate (Chilenia) in Devonian times deduced by the pressure–temperature–time evolution within part of a collisional belt (Guarguaraz Complex, W-Argentina). *Contributions to Mineralogy and Petrology*, **162**, 303–327.
- WILLNER, A. P., MASSONNE, H.-J., RING, U., SUDO, M. & THOMSON, S. N. 2012. P-T evolution and timing of a late Palaeozoic fore-arc system and its heterogeneous Mesozoic overprint in north-central Chile (latitudes 31 – 32° S). *Geological Magazine*, **149**, 177–207.

ANDES OF CENTRAL CHILE AND WESTERN ARGENTINA

- WINOCUR, D. A., LITVAK, V. D. & RAMOS, V. A. 2014. Magmatic and tectonic evolution of the Oligocene Valle del Cura basin, main Andes of Argentina and Chile: evidence for generalized extension. In: SEPÚLVEDA, S. A., GIAMBIAGI, L. B., MOREIRAS, S. M., PINTO, L., TUNIK, M., HOKE, G. D. & FARÍAS, M. (eds) *Geodynamic Processes in the Andes of Central Chile and Argentina*. Geological Society, London, Special Publications, **399**. First published online February 17, 2014, <http://dx.doi.org/10.1144/SP399.2>
- YÁÑEZ, G., CEMBRANO, S., PARDO, M., RANERO, C. & SELLÉS, D. 2001. The Challenger–Juan Fernández–Maipo major tectonic transition of the Nazca–Andean subduction system at 33°–34°S: geodynamic evidence and implications. *Journal of South American Earth Sciences*, **15**, 23–38.
- YURY-YÁÑEZ, R. E., OTERO, R. A., SOTO-ACUÑA, S., SUÁREZ, M. E., RUBILAR-ROGERS, D. & SALLABERRY, M. 2012. First bird remains from the Eocene of Algarrobo, central Chile. *Andean Geology*, **39**, 548–557.

Geological Society, London, Special Publications Online First

Evolution of shallow and deep structures along the Maipo–Tunuyán transect (33°40'S): from the Pacific coast to the Andean foreland

Laura Giambiagi, Andrés Tassara, José Mescua, Maisa Tunik, Pamela P. Alvarez, Estanislao Godoy, Greg Hoke, Luisa Pinto, Silvana Spagnotto, Hernán Porras, Felipe Tapia, Pamela Jara, Florencia Bechis, Víctor H. García, Julieta Suriano, Stella Maris Moreiras and Sebastián D. Pagano

Geological Society, London, Special Publications, first published February 27, 2014; doi 10.1144/SP399.14

Email alerting service	click here to receive free e-mail alerts when new articles cite this article
Permission request	click here to seek permission to re-use all or part of this article
Subscribe	click here to subscribe to Geological Society, London, Special Publications or the Lyell Collection
How to cite	click here for further information about Online First and how to cite articles

Notes

Evolution of shallow and deep structures along the Maipo–Tunuyán transect ($33^{\circ}40'S$): from the Pacific coast to the Andean foreland

LAURA GIAMBIAGI^{1*}, ANDRÉS TASSARA², JOSÉ MESCUA¹, MAISA TUNIK³,
PAMELA P. ALVAREZ⁴, ESTANISLAO GODOY⁵, GREG HOKE⁶, LUISA PINTO⁷,
SILVANA SPAGNOTTO⁸, HERNÁN PORRAS⁶, FELIPE TAPIA⁶, PAMELA JARA⁹,
FLORENCIA BECHIS¹⁰, VÍCTOR H. GARCÍA³, JULIETA SURIANO¹¹, STELLA
MARIS MOREIRAS¹ & SEBASTIÁN D. PAGANO¹

¹*IANIGLA, CCT Mendoza, Centro Regional de Investigaciones Científicas y Tecnológicas,
Parque San Martín s/n, 5500 Mendoza, Argentina*

²*Departamento de Ciencias de la Tierra, Universidad de Concepción, Victor Lamas 1290,
Concepción, Chile*

³*CONICET, Universidad Nacional de Río Negro, Argentina*

⁴*Tehema S.A., Virginia Subercaseaux 4100, Pirque, Chile*

⁵*Consultant, Virginia Subercaseaux 4100, Pirque, Chile*

⁶*Department of Earth Sciences, Syracuse University, Syracuse, NY, 13244, USA*

⁷*Departamento de Ciencias Geológicas, Universidad de Chile, Chile*

⁸*Departamento de Ciencias Geológicas, Universidad Nacional de San Luis, Argentina*

⁹*Departamento de Ingeniería en Minas, Universidad de Santiago de Chile, Chile*

¹⁰*IIDyPCA, CONICET, Universidad Nacional de Río Negro, Argentina*

¹¹*Departamento de Ciencias Geológicas, Universidad de Buenos Aires, Argentina*

*Corresponding author (e-mail: lgambiagi@mendoza-conicet.gob.ar)

Abstract: We propose an integrated kinematic model with mechanical constraints of the Maipo–Tunuyán transect ($33^{\circ}40'S$) across the Andes. The model describes the relation between horizontal shortening, uplift, crustal thickening and activity of the magmatic arc, while accounting for the main deep processes that have shaped the Andes since Early Miocene time. We construct a conceptual model of the mechanical interplay between deep and shallow deformational processes, which considers a locked subduction interface cyclically released during megathrust earthquakes. During the coupling phase, long-term deformation is confined to the thermally and mechanically weakened Andean strip, where plastic deformation is achieved by movement along a main décollement located at the base of the upper brittle crust. The model proposes a passive surface uplift in the Coastal Range as the master décollement decreases its slip eastwards, transferring shortening to a broad area above a theoretical point S where the master detachment touches the Moho horizon. When the crustal root achieves its actual thickness of 50 km between 12 and 10 Ma, it resists further thickening and gravity-driven forces and thrusting shifts eastwards into the lowlands achieving a total Miocene–Holocene shortening of 71 km.

The Andes, the world's largest non-collisional orogen, is considered the paradigm for geodynamic processes associated with the convergence of an oceanic plate (Nazca) below a continental plate margin (South American western margin). Although these mountains have been described as a consequence of crustal shortening that leads to crustal thickening and surface uplift (Isacks 1988; Sheffels 1990; Allmendinger *et al.* 1997), the mechanisms by which this crustal shortening is achieved remain

controversial (e.g. Garzione *et al.* 2008; DeCelles *et al.* 2009; Ehlers & Poulsen 2009; Armijo *et al.* 2010; Farías *et al.* 2010).

Tectonic plates near subduction zones are displaced towards the trench by buoyancy forces, such as slab pull and ridge push. These driving forces are resisted by forces associated with mantle viscosity, slab bending around the outer-rise and interplate friction (Forsyth & Uyeda 1975; Heuret & Lallemand 2005; Lamb 2006; Iaffaldano & Bunge

2008; Schellart 2008). Part of the work done by the driving forces is stored as elastic strain energy associated with the deformation of the upper plate above the seismogenic portion of the locked subduction interface. The elastic deformation accumulated during the decades to centuries of the interseismic period is cyclically recovered by the coseismic slip of both plates along the megathrust during earthquakes and their post-seismic relaxation phases (Savage 1983; Wang *et al.* 2012). If the Earth were purely elastic, then no permanent deformation would accumulate at active continental margins at geological timescales, all the convergence would be absorbed by coseismic interplate slip and no Andean-type mountains would exist. The elastic behaviour is appropriated to describe the rheology of the cold and rigid forearc and foreland regions, whereas the hot and weak arc-back-arc region is dominated by brittle (plastic) deformation of the upper crust and ductile (viscous) deformation of the lower crust and lithospheric mantle (Hyndman *et al.* 2005). In this context, the long-term structure of the arc-back-arc region is the result of the imbalance between compressive strain accumulated during the interseismic period and extensional strain activated by the co- and post-seismic phases, but summed over thousands or millions of seismic cycles.

Andean-type margins are geodynamically controlled in the long term by a strong coupling between the forearc and the down-going slab (Lamb 2006) and a comparatively rapid advance of the foreland (and the entire upper plate) toward the forearc with respect to the ocean-wards rollback velocity of the subducted slab (Heuret & Lallemand 2005; Schellart 2008). The permanently deforming arc-back-arc region located between the colliding forearc and foreland regions accumulates shortening and thickening to construct the Andes and its crustal roots. However, the mechanisms and structures by which this process actually occurs are not well understood. Our study explores a possible solution. We focus on this problem by studying the Maipo-Tunuyán transect across the Southern Central Andes ($33^{\circ}40'S$) at the latitudes of the cities of Santiago and Mendoza, which has been the subject of a number of tectono-structural studies including the pioneering observations of Darwin (Giambiagi *et al.* 2009). Because of the amount of pre-existing data, this transect constitutes a key area for understanding the role of deep-seated structural and tectonic processes on the constitution of the central Chilean-Argentinean Orogen.

Several conceptual models of deep crustal deformation have been proposed for the Andes between 18° and 38°S . These models can be divided into two types: east-vergent and west-vergent models. Among the first to be proposed are the wedge model

(Allmendinger *et al.* 1990), the duplex model (Schmitz 1994) and the east-vergent décollement model (Allmendinger & Gubbels 1996; Giambiagi *et al.* 2003b, 2012; Ramos *et al.* 2004; Farías *et al.* 2010). The east-vergent models assume a shallow subhorizontal to gently west-dipping detachment located at different depths in the upper crust or at the transition between the upper and lower crust. This crustal-scale detachment has been identified within a shallow brittle-ductile transition (e.g. Tassara 2005; Farías *et al.* 2010) and it concentrates nearly all the horizontal crustal shortening between the forearc and foreland. The eastwards propagation of deformation into the foreland generates predominantly east-verging upper crustal thrusts and folds. These models propose an underthrusting of the rigid, cold South American craton under the mechanically and thermally weakened Andean sector (Allmendinger & Gubbels 1996). The diametrically opposed west-vergent model proposed by Armijo *et al.* (2010) argues for the existence of a ramp-flat décollement dipping to the east and the growth of the Andes mountain belt as a bivergent orogen. In this model, it is the forearc (coastal crustal-scale rigid block) that underthrusts beneath the Principal Cordillera.

The aim of this paper is to propose an integrated Miocene to present kinematic model with mechanical constraints for the Maipo-Tunuyán transect ($33^{\circ}40'S$) that correlates with the large volume of geological and geophysical studies carried out by numerous authors. For that purpose, we construct a conceptual model of mechanical interplay between deep and shallow deformational processes based on thermomechanical and kinematic modeling.

The Andes between 33° and 34°S latitudes: geological framework

The $33^{\circ}40'S$ transect (Fig. 1) is located in a transition zone between a subhorizontal subduction segment north of 33°S and a zone of normal subduction south of 34°S (Stauder 1975; Barazangi & Isacks 1976; Cahill & Isacks 1992; Tassara *et al.* 2006). The abrupt southwards disappearance of the Precordillera and Sierras Pampeanas has been related to variation in the slab geometry (Jordan *et al.* 1983; Charrier *et al.*, this volume, in review). At this latitude, the Andes of Argentina and Chile are composed from West to East by the Coastal Range, the Central Depression, the Principal Cordillera, the Frontal Cordillera and the Cerrilladas Pedemontanas range, where the pre-existing extensional structures of the Triassic Cuyo basin are partially inverted (Fig. 2a).

The Coastal Range can be divided into two sectors. The western sector with low topographic

STRUCTURE EVOLUTION ALONG MAIPO–TUNAYÁN TRANSECT

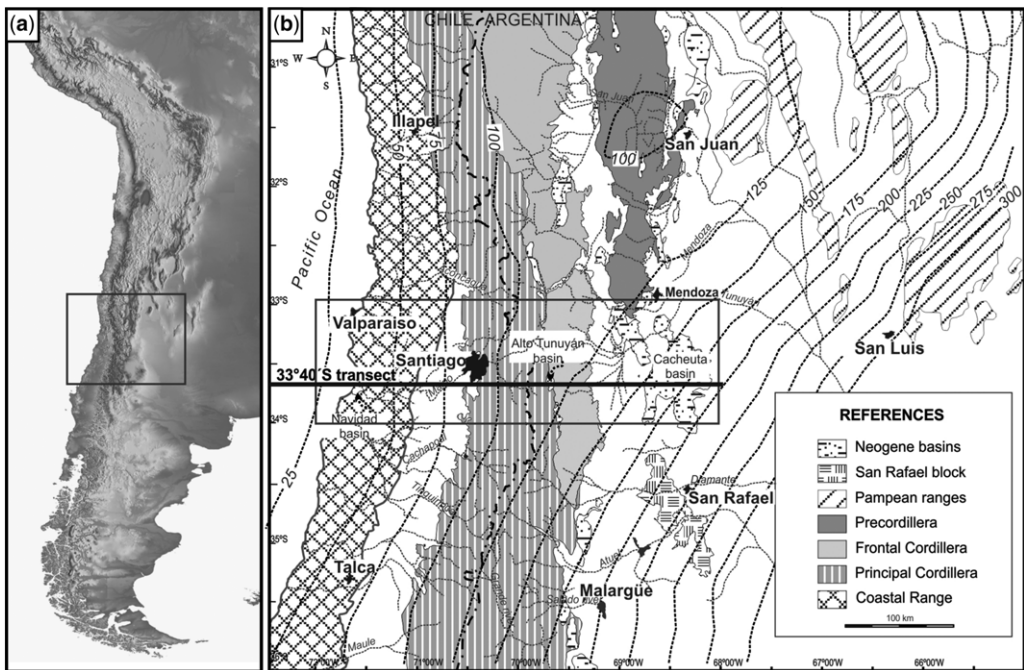


Fig. 1. (a) Shaded relief map of the Andes. Box indicates location of map in Figure 1b. (b) Regional map of the Andes at latitudet 31–36°S highlighting the present-day morphostructural units. The 33°40'S transect crosses the Coastal Range, the Central Depression, the Principal and Frontal cordilleras and the foreland. Dashed black lines represent depth of the subducted Nazca plate (from Tassara & Echaurren 2012). Notice the location of the transect above the transition segment between flat and normal subducted slab. Box indicates location of map in Figure 2.

altitude (<500 m) is composed of a series of Late Pliocene–Pleistocene marine ablation terraces (Wall *et al.* 1996; Rodríguez *et al.* 2012) carved on Late Palaeozoic–Middle Jurassic plutons (Sellés & Gana 2001). The eastern sector with altitudes up to 2000 m and relicts of high-elevated peneplains at different elevations (Brüggen 1950; Fariñas *et al.* 2008) is made up of Cretaceous plutons within a Late Jurassic–Early Cretaceous sedimentary and volcanic country rock.

The Central Depression at an elevation of 700–500 m.a.s.l separates the Coastal Range from the Principal Cordillera. It consists of a Quaternary sedimentary and ignimbritic cover of up to 500 m thickness beneath the Santiago valley (Araneda *et al.* 2000) and basement rocks cropping out in junction ridges and isolated hills reaching 1600 m a.s.l. (Rodríguez *et al.* 2012).

The Principal Cordillera is also subdivided into western and eastern sectors. The western sector consists of Eocene–Early Miocene volcaniclastic rocks of the Abanico extensional basin (Charrier *et al.* 2002), covered by the Miocene volcanic-arc rocks of the Farellones Formation (21.6–16.6 Ma; Aguirre *et al.* 2000) which young southwards (Godoy 2014). The eastern Principal Cordillera

consists of a thick sequence of Mesozoic sedimentary rocks, highly deformed into the Aconcagua fold-and-thrust belt (Giambiagi *et al.* 2003a).

The Frontal Cordillera at this latitude corresponds to the Cordon del Portillo range, where Proterozoic metamorphic rocks, Late Palaeozoic marine deposits, Carboniferous–Permian granitoids and Permo-Triassic volcanic rocks crop out (Polanski 1964). This range is uplifted by several east-vergent faults of the Portillo fault system.

The Cerrilladas Pedemontanas range is marked by the inversion of Triassic extensional faults of the Cuyo basin and moderately dipping basement faults (García & Casa 2014). Triassic continental rocks are covered by Neogene to Quaternary synorogenic deposits of the Cacheuta basin (Irigoyen *et al.* 2000). The Quaternary volcanic arc at this latitude is represented by the Marmolejo-Espíritu Santo-San José volcanic centre, located along the crest of the Andes 300 km east of the Chile trench.

Thermomechanical modelling

A necessary first-order constraint for the construction of a crustal-scale balanced cross-section is the

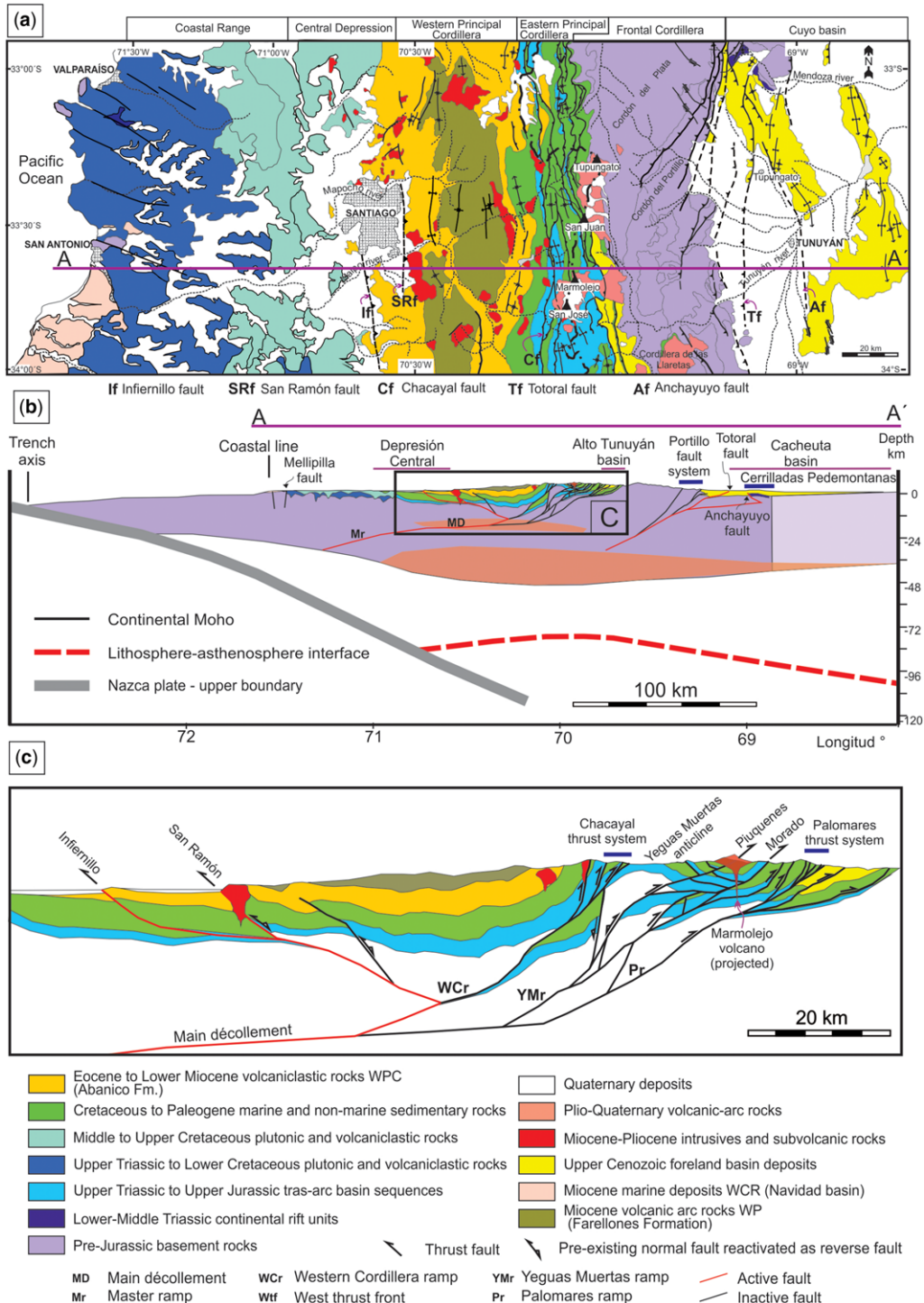


Fig. 2. (a) Simplified map of the Andean orogen between 33° and 34° S. Modified from Polanski (1964), Gana *et al.* (1996), Wall *et al.* (1996), Sellés & Gana (2001), Giambiagi & Ramos (2002) and Giambiagi *et al.* (2003a). (b) Balanced cross-section from coast to foreland, based on our own data and detailed compilation from Polanski (1964).

STRUCTURE EVOLUTION ALONG MAIPO–TUNAYÁN TRANSECT

expected mechanical structure of the lithosphere, particularly the identification of eventual ductile zones associated with brittle–ductile transitions that can serve as master detachments. The gravity-based and seismically constrained three-dimensional density model of the Andean margin developed by Tassara *et al.* (2006) and recently upgraded by Tassara & Echaurren (2012) contains the geometries for the subducted slab, the lithosphere–asthenosphere boundary of the South American plate (LAB), the continental Moho and the intra-crustal discontinuity, which separates the upper crust (density 2700 kg m^{-3}) from the lower crust (density 3100 kg m^{-3}). Based on these geometries and analytical formulations of the heat transfer equation (Turcotte & Schubert 2002) with appropriate boundary conditions, a 3D thermal model of the Andean margin has been developed (Morales & Tassara 2012; Tassara & Morales 2013). This model accounts for heat conduction from the LAB and subduction megathrust with radiogenic heat generation into the crust and thermal advection by the subducted plate, and predicts the distribution of temperature inside the Andean lithosphere.

The 3D thermal model and the original density model serve as the base to construct a 3D mechanical model based on the concept of the yield strength envelope (Goetze & Evans 1979; Burov & Diament 1995; Karato 2008). This envelope predicts the mechanical behaviour (brittle, elastic or thermally activated ductile creep) of a compositionally layered lithosphere with depth along a given 1D geotherm via the extrapolation of constitutive rheological laws for different Earth materials from experimental conditions to lithospheric space–temporal scales.

We use a preliminary version of the thermo-mechanical model (Tassara 2012) to extract an east–west cross-section along the Maipo–Tunuyán transect (Fig. 2b). This section shows that most of the upper-middle crust has a brittle-elastic behaviour, particularly for the cold and rigid forearc and foreland regions. However, a ductile behaviour is predicted by the model below the Principal Cordillera within a thin layer ($<5 \text{ km}$) at mid-crustal depths (15–20 km) and for the entire lower crust (i.e. deeper than 30 km).

Kinematic model of subduction orogeny

Our kinematic model with thermomechanical constraints (Fig. 3) accounts for the long-term

deformation of the Andean convergent margin between the cratonic interior of the South American plate and the forearc. It considers a coupled slab–forearc system with elastic loading and release associated with the megathrust seismic cycle. We kinematically model a velocity gradient ΔV_x between the continental lithospheric plate and the underlying asthenospheric mantle by fixing the slab–forearc interface and applying a westwards movement of the continental plate along an artificial line at the base of the Moho. This artificial line has no geological significance; it has been designed for the purpose of kinematical modelling and represents a broad area with dislocation creeping and a vertical velocity gradient ΔV_x constrained between the Moho and the lithosphere–asthenosphere boundary. Displacement is transmitted along this base using the *trishear* algorithm with p/s (propagation/displacement) ratio between 0 and 0.5 until the singularity point S below the Cordilleran axis (Fig. 3). At the singularity S, which is located above the downdip limit of the coupled seismogenic zone, shortening is transmitted to a ramp-flat master décollement, modelled with the fault parallel flow algorithm as a passive master fault. Above this décollement, crustal block B experiences brittle deformation. Below the décollement, the crust thickens by ductile deformation. Inside crustal block A, deformation diffuses westwards and upwards in a triangular zone of distributed shear. This deformation represents flexural permanent deformation above the S point.

The geometry of our proposed master décollement coincides with previous conceptual models for deep crustal deformation proposing an eastwards vergence of the orogen (Allmendinger *et al.* 1990; Allmendinger & Gubbels 1996; Ramos *et al.* 2004) and with the active ramp-flat structure dipping 10°W beneath the western Principal Cordillera and $25\text{--}30^\circ\text{W}$ beneath the Coastal Range proposed by Farías *et al.* (2010) based on seismological studies. In our model, the décollement ramps up beneath the easternmost sector of the Chilean slope of the Andes. The vertical component of slip in this ramp would be much greater than in the Argentinean slope, where low-angle thrusting develops. The abrupt rising of the international border sector may therefore be a consequence of localized rapid uplift on this segment of the transect.

The rationale follows Isacks' (1988) conceptual model in which brittle crustal horizontal shortening in the back-arc upper crust is compensated by

Fig. 2. (Continued) Gana & Tosdal (1996), Alvarez *et al.* (1999), Godoy *et al.* (1999), Giambiagi & Ramos (2002), Giambiagi *et al.* (2003a, b), Rauld *et al.* (2006), Godoy (2011). Red lines indicate faults with Quaternary activity. Geophysical data was extracted from the ACHISZS electronic database (www.achiszs.edu.cl/~achiszs/accessdb.html). (c) Detail of the cross-section in (b) for the sector of Principal Cordillera. Red lines indicate faults with Quaternary activity.

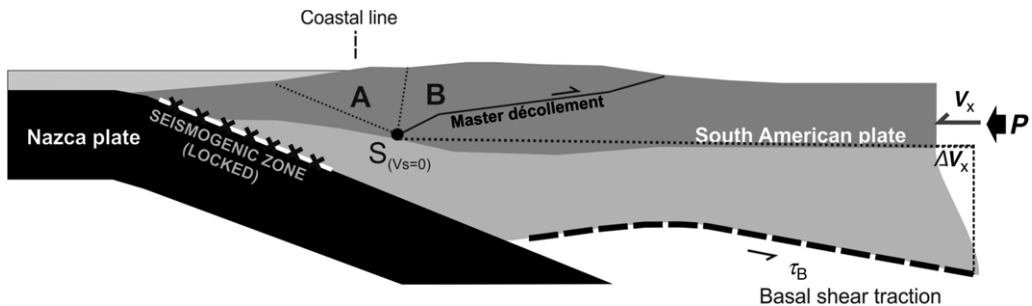


Fig. 3. Conceptual model for the 33°40'S transect. A velocity gradient ΔV_x is applied at the back of the foreland area during the 100% locked interseismic period. We kinematically model deformation by applying movement along an artificial basal line at the Moho, which transmits displacement westwards until the singularity point S. At this point S shortening is transmitted to a ramp-flat master décollement, modelled as a passive master fault. Above this décollement, crustal block B experiences brittle deformation. Below this line, the crust thickens by ductile deformation. Inside crustal block A, deformation diffuses westwards and upwards in a triangular zone of distributed shear.

ductile thickening in the arc and back-arc lower crust, and with the Andean microplate model of Brooks *et al.* (2003) in which a west-dipping décollement below the Andes mountain belt is viscously coupled to the South American craton and allows continuous creeping and stress transmission across the boundary.

We perform a forward model using the 2DMove academic license, taking into account the geological and geophysical constraints and the thermo-mechanical model. We assume plain strain along the transect, without magmatic additions or subduction erosion. Shortening estimates rely on upper crustal deformation measured all along the transect and the balanced cross-section, which provides a minimum estimate of horizontal shortening. First of all, we reconstruct the Late Cretaceous–Early Paleocene and Eocene–Early Miocene compressional and extensional events using the available geological and geochemical studies. For the Early Miocene–present shortening period, we carry out 36 steps each of 2 km shortening, constrained by the timing of movement along the main structures of previous studies (Godoy *et al.* 1999; Giambiagi & Ramos 2002; Giambiagi *et al.* 2003a), isotopic analysis (Ramos *et al.* 1996; Kay *et al.* 2005) and exhumation analysis (Kurtz *et al.* 1997; Maskaev *et al.* 2004, 2009; Hoke *et al.* 2014). With these data we calculate an average shortening rate for each period. Every 2–3 steps, we simulate erosion and sedimentation in accordance with sedimentological, palaeogeographic and provenance studies from the foreland and forearc basins (Irigoyen *et al.* 2000; Giambiagi *et al.* 2001; Rodríguez *et al.* 2012; Porras *et al.*, this volume, *in review*), and allow flexural-isostatic adjustments of the lithosphere due to local load changes assuming a default value for the Young's modulus $E = 7 \times 10^{10}$ Pa and the effective elastic thickness (T_e) calculated

in Tassara *et al.* (2007). Considering that we take into account the effects of erosion and sedimentation, topographic data presented here are purely qualitative.

Structure of the 33°40'S transect

The present-day structure of the 33°40'S transect is represented in Figure 2b, c. The crust below the Andes appears to reach its greatest thickness of 50 km at a longitude near 69°45'W. This longitude closely corresponds to the location of the highest peaks at this latitude that reach an altitude of 6000 m in the Marmolejo volcano. The Coastal Range (Fig. 4a) represents an east-dipping gentle homocline of Upper Palaeozoic–Cretaceous rocks (Wall *et al.* 1999). No major Andean thrust fault has been identified in this range, which is affected mainly by high-angle pre-Andean NNW–NW-trending faults such as the Melipilla fault (Yáñez *et al.* 2002), which may have been inherited from the Late Triassic continental-scale rifting.

The western Principal Cordillera comprises the Late Eocene–Miocene volcanic arc and is dominated by the inversion of the Abanico extensional basin (Fig. 4b). Fock *et al.* (2006) proposed that this inversion has a bivergent sense. According to Godoy *et al.* (1999) however, a double vergence for Abanico is developed only south of this latitude; at the transect latitude, the Abanico master faults are only inverted in its western edge.

The Front Range east of Santiago city represents the western thrust front of the Principal Cordillera. It was uplifted by inversion of the east-dipping Abanico master fault system, including the Infiernillo and San Ramón faults (Godoy *et al.* 1999; Fock *et al.* 2006; Rauld *et al.* 2006). The latter of which has been described by Rauld *et al.* (2006)

STRUCTURE EVOLUTION ALONG MAIPO–TUNAYÁN TRANSECT

and Armijo *et al.* (2010) as a feature active during the Holocene. The hanging wall of the San Ramón fault is folded into a tight syncline–anticline pair interpreted to be generated by an underlying basement ramp (Godoy *et al.* 1999). Toward the east, east-dipping faults with small throws are inferred to fold the Abanico and Farellones strata (Armijo *et al.* 2010).

The east-vergent Chacayal thrust system marks the border between western and eastern Principal Cordillera sectors (Giambiagi & Ramos 2002). This thrust system, which uplifts a thick sheet of Upper Jurassic sedimentary rocks (Fig. 4c), runs from the Las Cuevas river ($32^{\circ}50'S$) to the Maipo river ($34^{\circ}10'S$) for more than 150 km along-strike and corresponds to the most important structure in the western slope of the Principal Cordillera. The Aconcagua fold-and-thrust belt presents an overall geometry of a low-angle eastwards-tapering wedge, characterized by a dense array of east-vergent imbricate low-angle thrusts (Fig. 4d) with subordinate west-vergent out-of-sequence thrusts (Fig. 4d) (Giambiagi & Ramos 2002). The western sector of the belt is dominated by a broad anticline related to the inversion of the Triassic–Jurassic Yeguas Muertas extensional depocentre (Alvarez *et al.* 1999).

The Frontal Cordillera represents a rigid block uplifted by the Portillo fault system, located at its eastern margin (Fig. 4e). This system corresponds to a series of east-vergent deeply seated thrust faults (Fig. 4f), which uplift the pre-Jurassic basement rocks on top of the Middle Miocene–Quaternary sedimentary rocks deposited in the foreland basin (Polanski 1964; Giambiagi *et al.* 2003a). The foreland area comprises Neogene–Quaternary sedimentary deposits gently folded into open anticlines (Fig. 4g). The Triassic Cuyo basin is partially inverted in this sector by reactivation of pre-existing structures, such as the Anchayuyo fault, and generation of new thrusts (Fig. 4h).

Deformational periods

Even although the tectonic evolution of the transect can be regarded as a continuous deformational event from the Early Miocene to the present, with crustal thickening and widening and uplift of the Andean ranges, we can separate this evolution into several periods of deformation during which rock uplift and erosion shape the orogen.

The Late Cretaceous–Paleocene deformational event

The Andean orogeny started in several segments with contractional deformation during Late Cretaceous time when the back-arc basins began to be

tectonically inverted (Mpodozis & Ramos 1989). Deformation in the southern Central Andean thrust belts north and south of this transect started during the Upper Cretaceous–Palaeogene shortening event (Mpodozis & Ramos 1989; Tunik *et al.* 2010; Orts *et al.* 2012; Mescua *et al.* 2013). According to Tapia *et al.* (2012), in the studied transect this contractional event was localized in the Coastal Cordillera and the western sector of the Principal Cordillera. However, Godoy (2014) argues that the evidence for this event in the Main Range is dubious and interprets the area to represent a structural knot that resisted K–T (Cretaceous–Tertiary) deformation.

In the eastern Principal Cordillera on the other hand, continental sediments were deposited in the northern Neuquén foreland basin (Tunik *et al.* 2010) which culminated with an Atlantic marine ingress during Maastrichtian time (Tunik 2003; Aguirre-Urrreta *et al.* 2011). Further east, geothermocronological analysis indicates that the foreland area east of Frontal Cordillera was stable (not deformed nor uplifted) during the Jurassic–Palaeogene period (Ávila *et al.* 2005). Further structural studies are needed to understand the deformation during this stage, which is beyond the scope of this study.

Given the lack of precise constraints for the deformation during Cretaceous–Palaeogene time in the studied transect, we estimated the shortening based on the assumption of conservation of the crustal area along the section. We used the Tassara & Echaurren (2012) geophysical model to calculate the crustal area at present. Taking into account the shortening estimations based on structural studies (Godoy *et al.* 1999; Giambiagi & Ramos 2002; Giambiagi *et al.* 2003a; Fig. 2b), an initial crustal thickness of $T_0 = 40$ km is needed to accommodate Andean shortening along the transect. However, crustal thickness was not constant across-strike before the Neogene, since a Palaeogene extensional event led to a thin crust (of 30–35 km of thickness) in the western Principal Cordillera (see the following section). In order to preserve crustal area, this region of thin crust should be compensated with a thick region which we associate with the Cretaceous–Palaeogene contractional deformation developed to the west of the extended sector. A block of 42-km-thick crust in the present Coastal Cordillera and Central Depression can account for the missing crustal area. We modelled this block of thicker crust with 10 km of Late Cretaceous–Palaeogene shortening (Fig. 5a).

The Eocene–Early Miocene extensional event

During Eocene–Early Miocene time, a protracted extensional event took place with deformation concentrated in the western sector of the Principal

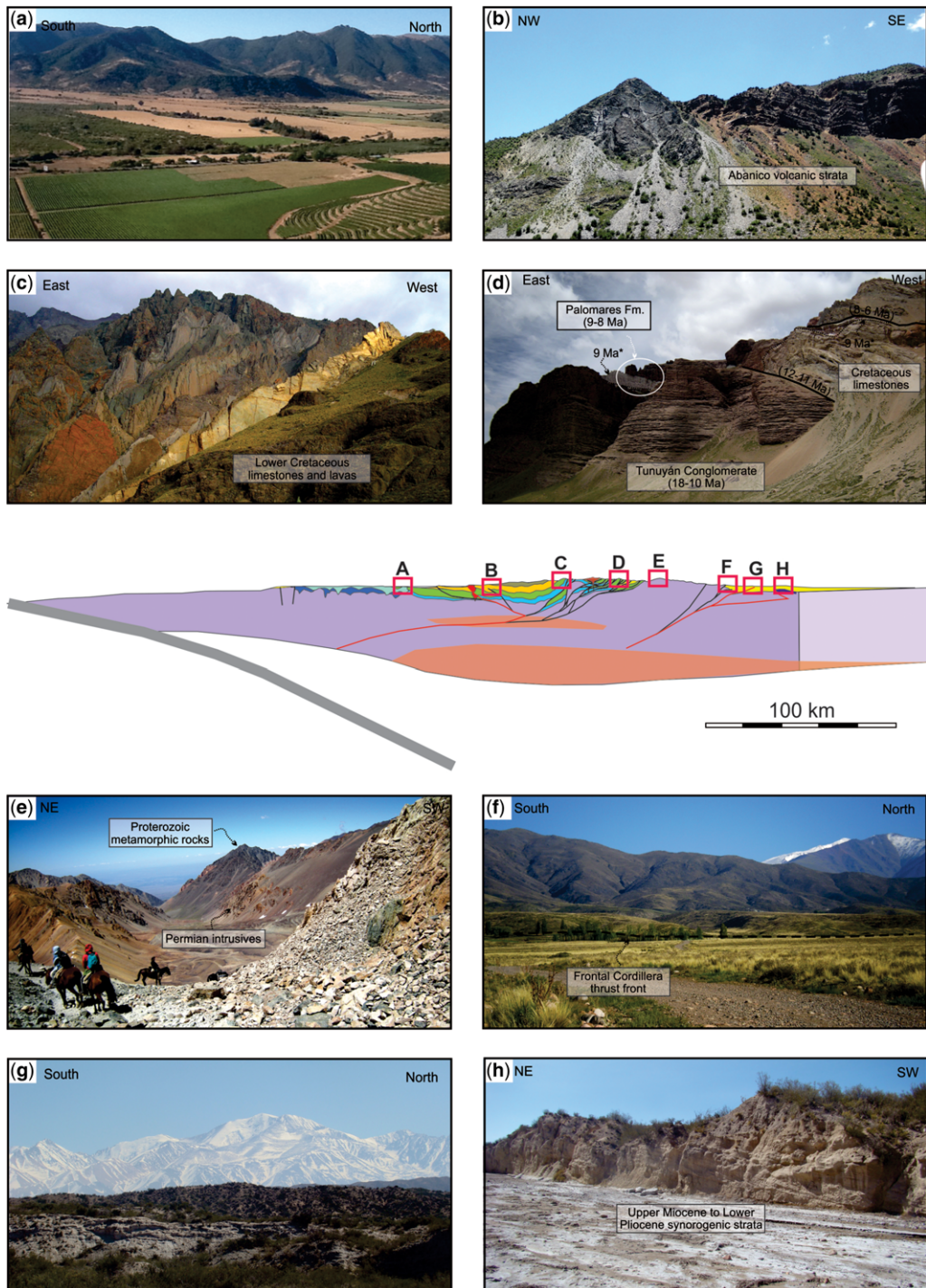


Fig. 4. Photographs of the 33°40'S transect. (a) Central Depression and Coastal Range (photograph P. Alvarez). (b) Abanico strata deformed into open west-vergent folds in the western Principal Cordillera (photograph J. Suriano). (c) Vertical mesozoic beds uplifted by the Chacayal fault and back-tilted by the Aconcagua FTB faults (photograph L. Pinto). (d) Palomares fault system in the Aconcagua FTB, uplifting Mesozoic strata over the Neogene synorogenic

STRUCTURE EVOLUTION ALONG MAIPO–TUNAYÁN TRANSECT

Cordillera (Charrier *et al.* 2002). This event has been linked to a segmented roll back subduction event (Mpodozis & Cornejo 2012) in contrast to the compressive deformation registered in the Andean margin north of 25°S (Carrapa *et al.* 2005; Hongn *et al.* 2007). Normal faulting was associated with crustal thinning and tholeiitic magmatism of the Abanico Formation (Nyström *et al.* 1993; Kay & Kurtz 1995; Zurita *et al.* 2000; Muñoz *et al.* 2006), whose $^{40}\text{Ar}/^{39}\text{Ar}$ ages at the latitude of Santiago (33°S) range from 35 to 21 Ma (Muñoz *et al.* 2006). The extensional basin was filled with up to 3000 m of volcaniclastic deposits, and acidic to intermediate lavas with sedimentary intercalations (Charrier *et al.* 2002). Even although geochemical analyses suggest it was formed upon a *c.* 30–35-km thick continental crust (Nyström *et al.* 2003; Kay *et al.* 2005; Muñoz *et al.* 2006), there is no evidence of marine sedimentation. Isotopic analysis and comparison between western and eastern outcrops of the Abanico Formation indicate higher crustal contamination, suggesting larger crustal thickness to the east (Fuentes 2004; Muñoz *et al.* 2006) and an asymmetric geometry of the extensional basin, due to the concentration of extensional deformation in the western master fault system.

During this period, the Coastal Range should have been elevated due to isostatic compensation of the Late Cretaceous–Paleocene crustal thickening event and locally by isostatic rebound close to the Abanico east-dipping master fault. Further east in the Neuquén basin, Paleocene continental distal sediments were deposited tapering towards the east.

The extensional structures of the Abanico basin have been obliterated by the later compressional faults. Inferred master faults have been suggested to be located beneath the Central Depression (Godoy *et al.* 1999; Fock *et al.* 2006). Much more speculative is the existence of eastern basin-border faults. Apatite and zircon fission track cooling ages from the eastern Coastal Cordillera constrain an exhumation period between 36 and 42 Ma (Fariñas *et al.* 2008), which could be related to uplift of the rift shoulder westwards of the master fault (Fock 2005; Charrier *et al.* 2007) at the beginning of the extensional period (since Late Eocene).

The Early Miocene (21–18 Ma)

The last major shortening event began during the Early Miocene with the inversion of the Abanico

basin (Godoy *et al.* 1999; Charrier *et al.* 2002; Fock *et al.* 2006). After that, chronological data suggest that deformation has accumulated during a single period of shortening between the Early Miocene and the present (Giambiagi *et al.* 2003a; Porras *et al.*, this volume, in review). The onset of deformation in the western slope is marked by the change from low-K Abanico Formation tholeiites to calc-alkaline dacites of the Teniente Volcanic Complex (Kay *et al.* 2005, 2006), between 21 and 19 Ma (Charrier *et al.* 2002, 2005). This inversion occurred coevally with the development of the Farellones volcanic arc of Early–Middle Miocene age (Vergara *et al.* 1999). A 22.5 Ma U–Pb zircon SHRIMP age of the base of the Farellones Formation along the Ramón–Damas Range anticline marks the beginning of the Farellones arc at this transect (Fock 2005).

In our model, the western Principal Cordillera is related to the generation of the Main décollement (MD) rooted in the singularly point S at the contact between the Moho and mantle sub-arc lithosphere, *c.* 40 km depth from the surface, and the Western Cordillera ramp (WCr) inferred to be located below the Western thrust front (WTF). We interpret this event as the generation of an important detachment connected to the Chilean ramp proposed by Fariñas *et al.* (2010) and located between 12 and 15 km depth beneath the Principal Cordillera. Eastwards movement of the upper crust relative to the stable and long-lived lower crust MASH (melting, assimilation, storage and homogenization) zone proposed by Muñoz *et al.* (2012) could explain the width of up to 40 km of the Farellones volcanic arc. The main uplifted sectors for this period are the eastern Coastal Range and the western Principal Cordillera, above the Western Cordillera ramp (the Front Range east of the city of Santiago). The passive uplift of both sectors is in agreement with provenance studies of heavy mineral assemblages for the lower Navidad Formation (Rodríguez *et al.* 2012), whose radiometric ages indicate deposition during 23–18 Ma (Gutiérrez *et al.* 2013) and apatite fission track (AFT) age (18.3 ± 2.6 Ma) for an Upper Cretaceous deposit (Fock 2005).

The passage of the pre-existing Abanico master normal faults over the WCr could have reactivated these structures as passive back-thrusts and favoured the intrusion of the La Obra pluton (19.6 Ma; Kurtz *et al.* 1997). In the foreland, retroarc volcanism of the Contreras Formation (18.3 Ma;

Fig. 4. (Continued) units (photograph M. Tunik). (e) Frontal Cordillera from the Portillo pass (photograph M. Tunik). (f) Frontal Cordillera active thrust front (photograph L. Giambiagi). (g) Looking westwards from the Cacheuta basin. Strata on front correspond to uplifted Neogene synorogenic deposits (photograph L. Giambiagi). (h) Neogene deposits uplifted and folded at the easternmost sector of the transect (photograph L. Giambiagi).

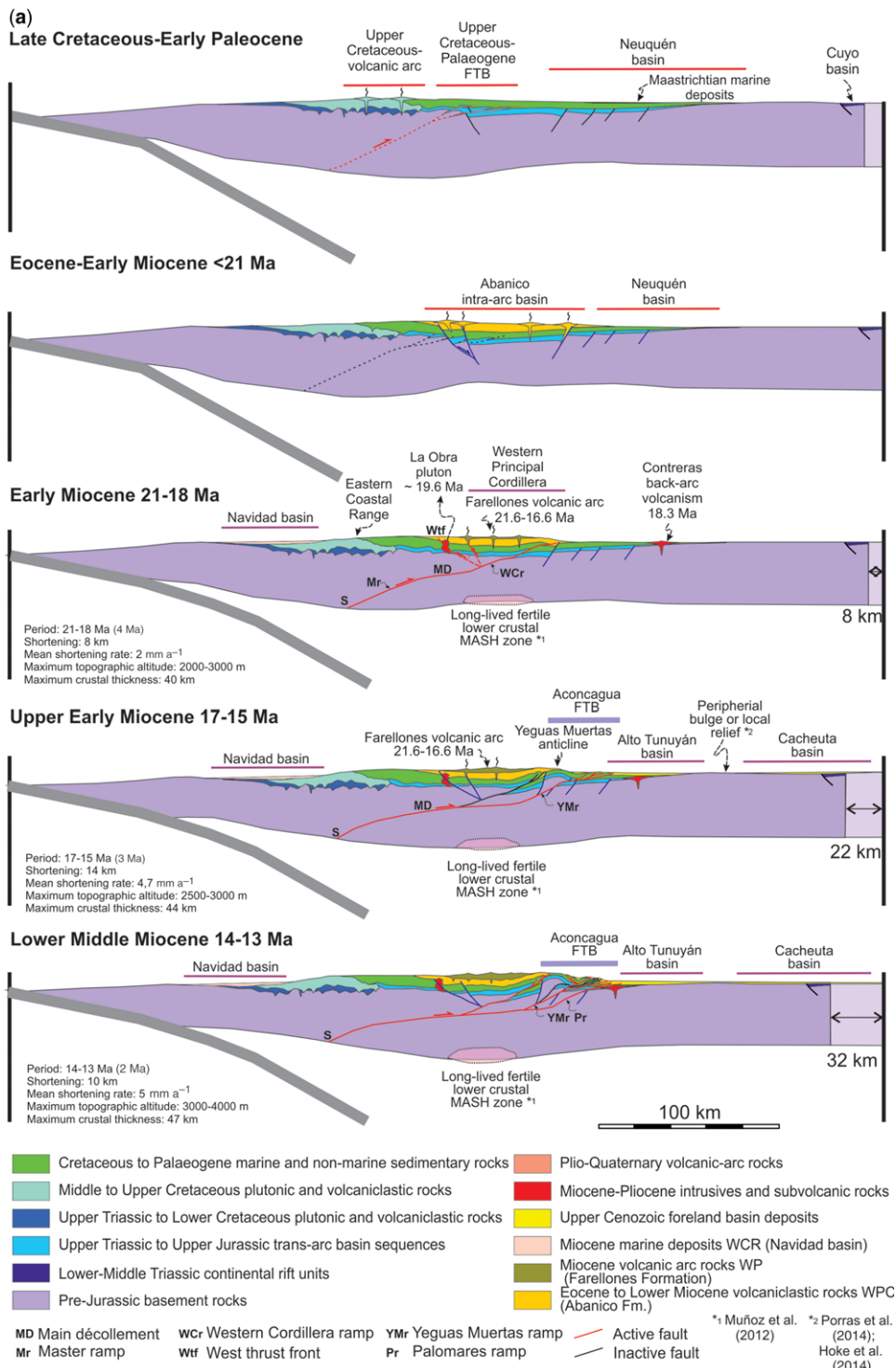


Fig. 5. Model for the evolution of the 33°40'S transect from the Late Cretaceous to the present. (a) Deformational periods from the Late Cretaceous–Early Paleocene compressional event to the early Middle Miocene phase.

STRUCTURE EVOLUTION ALONG MAIPO–TUNAYÁN TRANSECT

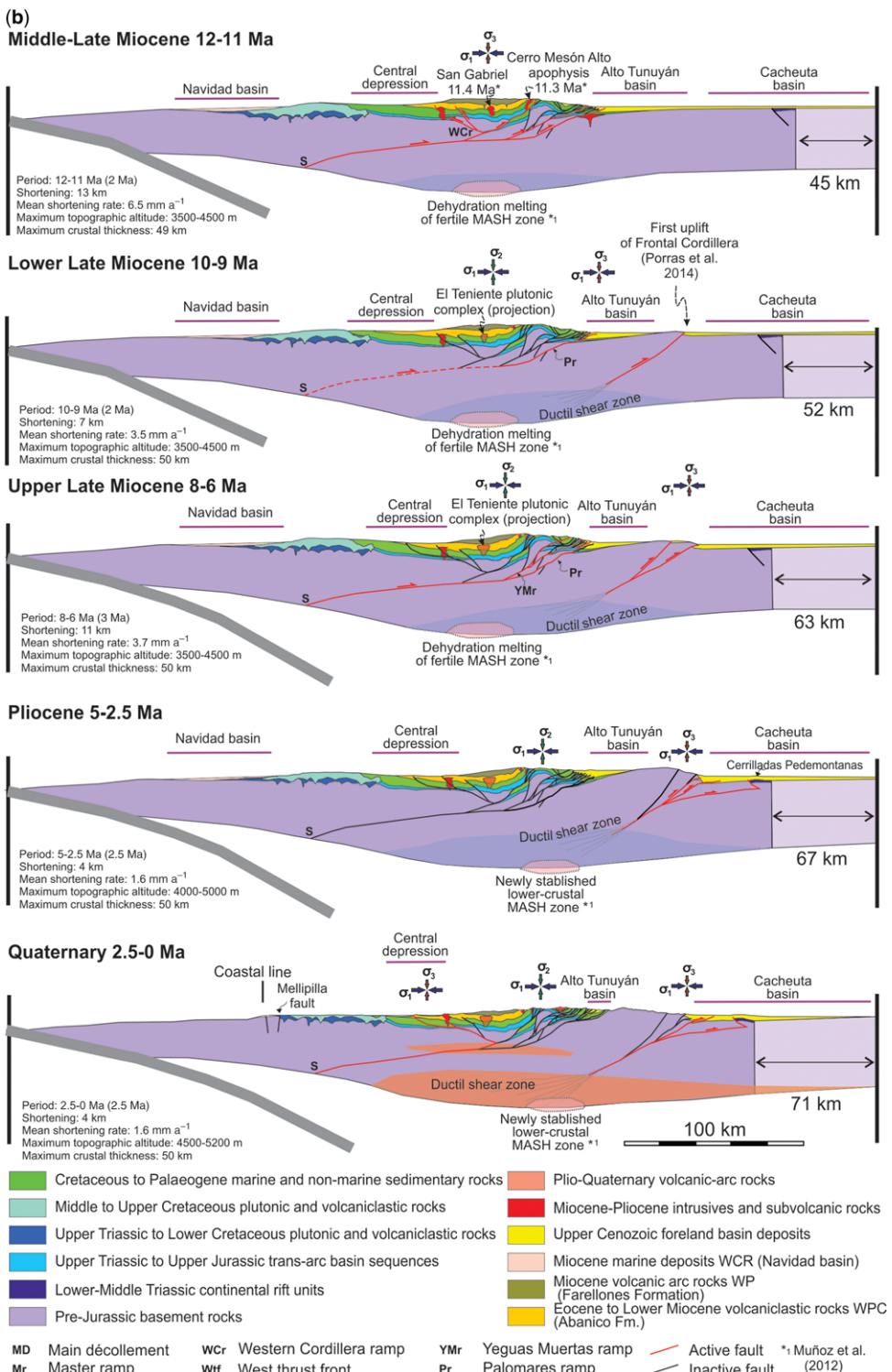


Fig. 5. (Continued) (b) Deformational periods from the Middle–Late Miocene to the present.

Giambiagi & Ramos 2002) with geochemical signatures of unthickened crust (Ramos *et al.* 1996) pre-dates the formation of the Alto Tunuyán foreland basin.

We calculated 8 km of shortening concentrated in the western Principal Cordillera (7 km) and the Coastal Range (1 km), with a mean shortening rate of 2 mm a^{-1} for this period. Beneath the western Principal Cordillera, the crust achieved its maximum thickness (40 km) and maximum topographic elevation ranges between 2000 and 3000 m a.s.l.

The Late Early Miocene (17–15 Ma)

This period marks the beginning of deformation along the Aconcagua FTB (fold-and-thrust belt), linked to the prolongation of the Main décollement eastwards and the formation of the Yeguas Muertas ramp beneath the homonymous anticline (Giambiagi *et al.* 2003a, b). By this time, driving forces cannot supply the energy needed to elevate the western Principal Cordillera by movement along the WCr (supercritical wedge stage), and the orogen begins to grow in width to lower the taper by propagating forwards towards the foreland. According to Muñoz *et al.* (2012), this shift in the locus of deformation should be related to the rapid ascent of subduction-related mantle-derived magmas that had little interaction with the upper lithosphere, such as those analysed by these authors in the western Principal Cordillera.

The earliest Neogene synorogenic strata appear in the Alto Tunuyán basin at *c.* 17–16 Ma, with source region restricted to the volcanic rocks of the Principal Cordillera and to the Frontal Cordillera (Porras *et al.*, this volume, *in review*). For this last source region, Porras *et al.* (this volume, *in review*) propose the existence of a peripheral bulge located in what is now the Frontal Cordillera, while Hoke *et al.* (2014) suggest a significant pre-Middle Miocene local relief. Further studies are required in order to decide which option is the best. During this period, the Cacheuta basin, apparently disconnected from the Alto Tunuyán basin, only received aeolian deposits (Irigoyen *et al.* 2000).

The uplift of the western Principal Cordillera evidenced in the provenance of the Navidad basin (Rodríguez *et al.* 2012) is due to overriding of this sector of the range across the Yeguas Muertas ramp. Movement along the Main décollement and this ramp achieves 14 km of shortening in the Aconcagua FTB, with an average shortening rate of 4.7 mm a^{-1} . Maximum topographic elevation is between 2500 and 3000 m in the western Principal Cordillera, and the crust thickens to 44 km below the westernmost Principal Cordillera as suggested by geochemical data (Kay *et al.* 2005). Flexural-isostatic compensation of this sector of the orogen

could explain the exhumation rates of the La Obra pluton ($0.5\text{--}0.6 \text{ mm a}^{-1}$) during this period (Kurtz *et al.* 1997).

The coeval uplift of the eastern Coastal Cordillera and the Principal Cordillera leads to the formation of a depocentre filled by up to 3000 m of arc-related volcanics of the Farellones Formation (Vergara *et al.* 1988; Elgueta *et al.* 1999; Godoy *et al.* 1999). Magma migration within the arc may have been enhanced by active movement along the Western Cordillera ramp and the associated back-thrusts.

The Middle Miocene (15–11 Ma)

During this phase, upper crust deformation is localized in the eastern Principal Cordillera with the development of the east-vergent in-sequence Aconcagua FTB faults and associated back-thrusts close to the international border. Cross-cutting relationships between thrust faults suggest the cyclic activation–deactivation of the Western, Yeguas Muertas and Palomares ramps with important shortening (17 km) in the Principal Cordillera. The period between 12 and 11 Ma corresponds to one of quiescence in deformation along the Aconcagua FTB, when the thrust front became inactive and erosion of the previously uplifted area was responsible for the generation of an important unconformity between the Cretaceous strata and the Middle Miocene synorogenic deposits (Giambiagi *et al.* 2001). Instead, deformation is concentrated in the Chilean slope of the Principal Cordillera with the reactivation of the Western Cordillera ramp and movement along the pre-existing San Ramón and Infiernillo faults (Fock *et al.* 2006). After this short quiescence period, the reactivation of the Yeguas Muertas and Palomares ramps leads to generation of out-of-sequence thrusts in the Aconcagua FTB.

This is a period of high crustal shortening (23 km) concentrated along the international border and the eastern Principal Cordillera, with the mean shortening rates of 5 mm a^{-1} and 6.5 mm a^{-1} for the 15–13 and 12–11 Ma periods, respectively. The crust almost achieves a thickness of 49 km, with an eastwards shift in the crustal keel. Important space creation due to flexural compensation of the tectonic load, immediately to the east of the Aconcagua FTB, is registered both in the Alto Tunuyán and Cacheuta basins (Irigoyen *et al.* 2000; Giambiagi *et al.* 2001).

At the end of this phase, the volcanic activity practically wanes and only very localized activity is recorded during late Middle Miocene–Late Pliocene time, in agreement with a highly compressive stress regime in the arc region. The present volcanic arc develops in the latest Pliocene along the watershed. Instead, barren and

STRUCTURE EVOLUTION ALONG MAIPO–TUNAYÁN TRANSECT

mineralization-hosting intrusives, such as La Gloria and San Gabriel plutons and Cerro Mesón Alto porphyry (Deckart *et al.* 2010), intrude the Miocene Farellones Formation or the Upper Cretaceous sedimentary rocks.

The Late Miocene (10–6 Ma)

At the beginning of this phase around 10–9 Ma, the crust achieves its present maximum thickness of 50 km in accordance with isotopic analysis (Kay *et al.* 2005). At this point, driving forces can no longer supply the energy needed to thicken the crust and uplift the range and the crustal root is likely to grow laterally in width instead of increasing its depth, with a reduction in shortening rates. This is in accordance with the proposition of Muñoz *et al.* (2012) for the existence of deep crustal hot zones. According to these authors, the repeated basalt intrusion into the lower crust induces a significant thermal perturbation, with the amphibolitic lower crust reaching temperatures up to 750–870°C and increased melt component. This promotes the ductile behaviour of the lowermost crust and the widening of the crustal root.

Overall, no volcanic activity is registered during this period. Instead, the Teniente Plutonic Complex intrudes the Abanico and Farellones formations between 12 and 7 Ma (Kay & Kurtz 1995; Kurtz *et al.* 1997; Kay *et al.* 2005).

During the early Late Miocene (10–9 Ma), reactivation of the Palomares ramp leads to out-of-sequence thrusting in the Aconcagua thrust front and the cannibalization of the Alto Tunuyán foreland basin deposits. Seven kilometres of shortening are achieved during this phase at the thrust front. Provenance analysis of the synorogenic fill of the Alto Tunuyán foreland basin indicates the beginning of uplift of the Frontal Cordillera (Porras *et al.*, this volume, in review), thrusts of which have been inferred to be deeply seated in a ductile shear zone of the lower crust (Giambiagi *et al.* 2012).

During the latest Late Miocene (8–6 Ma), the sedimentary record indicates important uplift of the Frontal Cordillera between 33°30' and 34°30'S (Irigoyen *et al.*, 2000; Giambiagi *et al.* 2003a; Porras *et al.*, this volume, in review). Thermochronological studies in Argentina both bordering and within the study area show that very little exhumation has occurred in this area during Cenozoic time. An apatite (U–Th)/He study in the Frontal Cordillera between 32°50' and 33°40' yields pre-Miocene exhumation rates of c. 12 m Ma⁻¹, with an increase to 40 m Ma⁻¹ at 25 Ma and an inferred onset of rapid river incision between 10 and 7 Ma, roughly within geological constraints (Hoke *et al.* 2014).

A couple of million years after the onset of uplift in the Frontal Cordillera, the Principal

Cordillera experiences important reactivation of the Yeguas Muertas and Palomares ramps with generation of out-of-sequence thrusts (e.g. Piuquenes and Morado) and the reactivation of the Palomares thrust system (Giambiagi & Ramos 2002).

At this time, movement along the Yeguas Muertas ramp would cause the Western Cordillera ramp to ramp up with a vertical component of slip much greater than the eastern Principal Cordillera and a localized rapid uplift. This is in agreement with fission track data from the Miocene plutons exposed in the western Principal Cordillera, compatible with <3 km of denudation of the El Teniente district since Late Miocene time (Maskaev *et al.* 2004), and the identification of a main stage of surface uplift in the Chilean slope during Late Miocene–Early Pliocene time with maximum vertical throw 0.7–1.1 km (Fariñas *et al.* 2008).

During Early Miocene–Early Pliocene time, the western sector of the Coastal Cordillera is submerged as evidenced by the marine deposits of the Navidad Formation and younger units (Encinas *et al.* 2008; Gutiérrez *et al.* 2013), and is subjected to local extensional stress field (Lavenu & Encinas 2005). Flexural elasticity of the rigid cold forearc region causes the western Coastal Range to subside while the eastern sector of the range is uplifted. This is in agreement with geologic evidence for subsidence between 10 and 4 Ma in this sector of the transect (Encinas *et al.* 2006).

The Pliocene (5–2.5 Ma)

During Pliocene time, the magmatic activity reassumes its current locus along the High Andean drainage divide. Around this time, the Main décollement becomes inactive and there is a lull in deformation in the Principal Cordillera, concomitant with the mineralization of the El Teniente porphyry whose magmatic-hydrothermal centre records 6 Ma of continuous activity during 9–3 Ma (Mpodozis & Cornejo 2012). Compressional deformation occurs only in the eastern Frontal Cordillera with generation of thrusts affecting the Miocene–Early Pliocene synorogenic deposits of the Cacheuta basin, and in the Cerrilladas Pedemontanas with the generation of an angular unconformity in the synorogenic units (Yrigoyen 1993; Irigoyen *et al.* 2000) and the inversion of the Anchayuyo fault (Giambiagi *et al.* submitted to Tectonics).

The compressional deformation in the Frontal Cordillera is coeval with movement along NE dextral and WNW sinistral strike-slip faults reported to affect the El Teniente porphyry copper deposits in western Principal Cordillera (Garrido *et al.* 1994). According to these authors, the strike-slip faults were active before, during and after the

formation of the giant porphyry Cu–Mo deposit (6.3–4.3 Ma, Maksaev *et al.* 2004), indicating a strike-slip regime during Early Pliocene time.

The widening of the crustal root during this stage favours the Coastal Cordillera uplifts by isostatic rebound, evidenced by the emergence of marine deposits between 4.4 and 2.7 Ma (Encinas *et al.* 2006) and the onset of knickpoint retreat in the western Coastal Range around 4.6 Ma (Fariás *et al.* 2008). This process would have partially blocked the drainage, inducing sedimentation in the Central depression (Fariás *et al.* 2008). The widening of the crustal root could in turn be responsible for the increase in topographic elevation by isostatic compensation. The enhanced erosion related to increased relief during 6–3 Ma suggested by Maksaev *et al.* (2009) could be attributed to this phenomenon.

The Quaternary (2.5 Ma–present)

The distribution of shallow earthquake epicentres in the Andes between 33° and 34°S gives important clues for the Quaternary deformation along the transect. In the Chilean slope of the Andes, shallow seismic activity is distributed mainly along the western flank of the Principal Cordillera at depths of 12 and 15 km (Barrientos *et al.* 2004), and beneath the Central depression at depths shallower than 20 km (Fariás *et al.* 2010). This suggests that at least the western portion of the Main décollement is active today. Beneath the Western Principal Cordillera, seismicity is concentrated on the steeper portion of the main décollement. We suspect that slip occurs aseismically on the gently dipping segments of this detachment zone. This is in agreement with minor Quaternary movement along the San Ramón fault, whose scarp has been linked to the vertical offsets (0.7–1.1 km) of the peneplains present in the western Principal Cordillera before 2.3 Ma (Fariás *et al.* 2008).

In the High Andes close to the Chilean–Argentine border, most shallow earthquakes of $M > 5$ show focal mechanisms related to strike-slip kinematics (Barrientos *et al.* 2004), such as the M_w 6.9 Las Melosas earthquake (Alvarado *et al.* 2005). Beneath the eastern part of the Frontal Cordillera and the Cuyo basin shallow focal mechanisms are related to compressional kinematics (Alvarado *et al.* 2007). The neotectonics of the Andean retrowedge at this latitude is characterized by movement along buried faults that fold the Quaternary deposits (García & Casa 2014).

During this phase, the backward tilting of the Principal and Frontal cordilleras by movement along the Portillo thrust system and the isostatic readjustment of the thickened crust could be responsible for the tilting to the west (1–3°) of several

flat erosional surfaces located between 2600 and 3200 m a.s.l. in the western Principal Cordillera (Fariás *et al.* 2008). We propose that the increase in gravitational potential energy due to crustal roots formation and mountain uplift prevents the main décollement from propagating eastwards. Instead, reactivation of the WPC back-thrusts should have implied less work against resisting stresses.

Discussion: implications of the model

The kinematic model presented in this work integrates structural, sedimentological, petrological, geochronological and geophysical data for the studied transect. The geological constraints available for the area allowed us to build a complete model that describes the relation between horizontal shortening, uplift, crustal thickening and activity of the magmatic arc, accounting for the main deep processes that have shaped the Andes since Early Miocene times. These geological and geochemical constraints reinforce previous hypotheses of a west-dipping detachment at the transition from brittle-elastic to ductile rheology in the crust below the Andean strip (Allmendinger & Gubbels 1996; Ramos *et al.* 2004; Fariás *et al.* 2010; Giambiagi *et al.* 2012), and are consistent with the east-vergent models. Furthermore, the model allows us to discuss some aspects of Andean history in light of our results.

Our model proposes passive surface uplift in the Coastal Range as the master décollement decreases its slip downwards transferring shortening to a broad area above the singularity point S, where the master detachment touches the Moho horizon (Figs 3 & 5). During the 18–5 Ma period, the main phase of deformation is located in the Aconcagua FTB. As the crust thickens from 40 to 50 km and the upper crust shortens to 52 km, the S point slowly migrates westwards (Fig. 5b). This migration generates a slowly propagating wave of surface uplift in the Coastal Range, from its eastern part at c. 18 Ma to its western part at the beginning of Pliocene time, in agreement with provenance studies from the Navidad basin (Rodríguez *et al.* 2012). Coeval uplift of the Coastal Range and Principal Cordillera creates the Central Depression, inducing thick sedimentary filling as suggested by Fariás *et al.* (2008). This explains why no important coastal-parallel faults have been observed in the Coastal Range, even although it experienced significant topographic uplift during Cenozoic time suggested by the exposure of the Miocene marine deposits (Encinas *et al.* 2008; Gutiérrez *et al.* 2013). Moreover, the presence of relict continental erosion surfaces with different elevations developed close to sea level and uplifted

STRUCTURE EVOLUTION ALONG MAIPO–TUNAYÁN TRANSECT

up to 2.1 km a.s.l. (Fariñas *et al.* 2008) indicates several pulses of Coastal Range uplift.

The eastward migration of the volcanic arc during Late Miocene–Quaternary time could be related to an eastwards migration of the trench due to tectonic erosion of the continental margin, as proposed by Stern (1989, 2011) and Kay *et al.* (2005); the delamination of an eclogitic root in the lower crust and mantle lithosphere (Kay & Kay 1993; DeCelles *et al.* 2009); and to shortening of the brittle crust above the major décollement. Migration of the volcanic arc can be explained by our model without invoking the decrease in the angle of subduction of the oceanic slab for this period of time, consistent with the proposal of Godoy (2005). Instead, the overall decrease in the volume of the asthenospheric wedge due to the construction of the crustal root could inhibit the influx of hot asthenosphere into the region and be responsible for the cooling of the subarc mantle and the eastward migration of the arc, as proposed by Stern (1989).

Underthrusting of the mechanically strong South American craton beneath the Andean strip leads to thickening of the crust. Kay *et al.* (1999) and Kay & Mpodozis (2001) argued that the transformation of hydrous lower-crustal amphibolite to garnet-bearing eclogite during crustal thickening can be responsible for the exsolution of fluids. These fluids can substantially decrease the strength of the lower crust. In this way, crustal thickening before Middle Miocene time may have favoured increased deformation during the Middle–Late Miocene (12–10 Ma) period, enhancing horizontal shortening in the Principal Cordillera and widening of the crustal roots. The forces that support the Andes provide an upper limit to the height of the mountain range and also to crustal thickness (Molnar & Lyon-Caen 1988). In our study area, the critical value seems to be of the order 50 km. Once this thickness is achieved, gravitational potential forces created by the buoyant crustal root are higher than unbalanced driving tectonic forces and therefore thrusting shifts eastwards into the lowlands. Even although convergence was steady, faults in the Principal Cordillera become inactive, the main décollement is deactivated and a new décollement is formed in the east to uplift the Frontal Cordillera.

Conclusions

In this paper we propose a kinematic model with thermomechanical constraints for the Miocene–present evolution of the Southern Central Andes at the latitude of the city of Santiago. Our model assumes a main décollement located at the base

of the upper crust (15–12 km in depth), which produces the underthrusting of the South American craton beneath the Andean strip. The total amount of horizontal shortening calculated with our master-detachment is 71 km, distributed between the western and eastern slopes of the Principal Cordillera (17 and 35 km, respectively), the Frontal Cordillera and foreland area (16 km). On the other hand, the Coastal Range undergoes passive surface uplift with only 3 km of shortening.

During the 18–5 Ma period, the main phase of deformation is located in the Aconcagua FTB. As the crust thickens from 40 to 50 km and the upper crust shortens by 52 km, the thrust front migrates from the Principal Cordillera to the Frontal Cordillera with a peak of deformation at c. 12–10 Ma. After the Andean crust achieves its present thickness of 50 km beneath the western Principal Cordillera, gravitational stresses drive the lateral expansion of the crustal root westwards and eastwards, driving surface uplift of the Central Depression and both slopes of the Principal Cordillera by isostatic response. Afterwards, during Pliocene time (5–2.5 Ma), there was a lull in deformation both in the eastern and western slope of the Andes with a deactivation of the master décollement. Uplift at this time is concentrated in the easternmost sector of the Frontal Cordillera and the Cachete basin. During Quaternary time, there is a reactivation of contractional deformation in the actual thrust front and in the Frontal range close to the city of Santiago as evidenced by seismological studies, suggesting the reactivation of the western sector of the main décollement.

This research was supported by grants from CONICET (PIP 638 and PIP 112-201102-00484), the Agencia de Promoción Científica y Tecnológica (PICT-2011-1079) and UNESCO (IGCP-586Y). Bárbara Carrapa and Andrés Folguera are sincerely thanked for their critical and helpful comments and suggestions. We thank Midland Valley Ltd. for the Academic Licence of the Move[©] Software. We would like to acknowledge the IGCP 586 Y group for fruitful discussions and suggestions.

References

- AGUIRRE, L., FERAUD, G., VERGARA, M., CARRASCO, J. & MORATA, D. 2000. $^{40}\text{Ar}/^{39}\text{Ar}$ ages of basic flows from the Valle Nevado stratigraphic sequence (Farellones Formation), Andes of Central Chile. *IX Congreso Geológico Chileno*, 1, Puerto Varas, Chile, 583–585.
- AGUIRRE-URRETA, B., TUNIK, M., NAIPAUE, M., PAZOS, P., OTTONE, E., FANNING, M. & RAMOS, V. A. 2011. Malargüe Group (Maastrichtian–Danian) deposits in the Neuquén Andes, Argentina: implications for the onset of the first Atlantic transgression related to Western Gondwana break-up. *Gondwana Research*, 19, 482–494.

- ALLMENDINGER, R. W. & GUBBELS, T. 1996. Pure and simple shear plateau uplift, Altiplano-Puna, Argentina and Bolivia. *Tectonophysics*, **259**, 1–13.
- ALLMENDINGER, R. W., FIGUEROA, D., SNYDER, D., BEER, J., MPODOZIS, C. & ISACKS, B. L. 1990. Foreland shortening and crustal balancing in the Andes at 30°S Latitude. *Tectonics*, **9**, 789–809.
- ALLMENDINGER, R. W., ISACKS, B. L., JORDAN, T. E. & KAY, S. M. 1997. The evolution of the Altiplano-Puna plateau of the Central Andes. *Annual Reviews of Earth Science*, **25**, 139–174.
- ALVARADO, P., BECK, S., ZANDT, G., ARAUJO, M. & TRIEP, E. 2005. Crustal deformation in the south-central Andes backarc terranes as viewed from regional broadband seismic waveform modeling. *Geophysical Journal International*, **163**, 580–598.
- ALVARADO, P., BECK, S. & ZANDT, G. 2007. Crustal structure of the south-central Andes Cordillera and backarc region from regional waveform modeling. *Geophysical Journal International*, **170**, 858–875.
- ALVAREZ, P. P., GODOY, E. & GIAMBIAGI, L. 1999. Estratigrafía de la Alta Cordillera de Chile Central a la latitud del paso Piuquenes (33°35' LS). In: *Proceedings of the XIV Congreso Geológico Argentino*, Salta, Argentina, **1**, 55.
- ARANEDA, M., AVENDAÑO, M. S. & MERLO, C. 2000. Modelo gravimétrico de la cuenca de Santiago, etapa II final. In: *Proceedings of the IX Congreso Geológico Chileno*, Puerto Varas, Chile.
- ARMIJOS, R., RAULD, R., THIELE, G., VARGAS, J., CAMPOS, R., LACASSIN, R. & KAUSEL, E. 2010. The West Andean Thrust, the San Ramón Fault, and the seismogenic hazard for Santiago, Chile. *Tectonics*, **29**, TC2007, <http://dx.doi.org/10.1029/2008tc002427>
- ÁVILA, J. N., CHEMALLE, F., MALLMANN, G., BORBA, A. W. & LUFT, F. F. 2005. Thermal evolution of inverted basins: constraints from apatite fission track thermochronology in the Cuyo Basin, Argentinean Precordillera. *Radiation Measurements*, **39**, 603–611.
- BARAZANGI, B. A. & ISACKS, B. L. 1976. Spatial distribution of earthquakes and subduction of the Nazca Plate beneath South America. *Geology*, **4**, 686–692.
- BARRIENTOS, S., VERA, E., ALVARADO, P. & MONFRET, T. 2004. Crustal Seismicity in Central Chile. *Journal of South American Earth Sciences*, **16**, 759–768.
- BROOKS, B. A., BEVIS, M. ET AL. 2003. Crustal motion in the Southern Andes (26°–36°S): do the Andes behave like a microplate? *Geochemistry, Geophysics, Geosystems*, **4**, 1085, <http://dx.doi.org/10.1029/2003GC000505>
- BRÜEGGEN, J. 1950. *Fundamentos de la Geología de Chile*. Instituto Geográfico Militar, Santiago, Chile.
- BUROV, E. & DIAMENT, M. 1995. The effective elastic thickness (T_e) of continental lithosphere: what does it really mean? *Journal of Geophysical Research*, **100**, 3905–3927.
- CAHILL, T. & ISACKS, B. L. 1992. Seismicity and shape of the subducted Nazca Plate. *Journal of Geophysical Research*, **97**, 17503–17529.
- CARRAPA, B., ADELmann, D., HILLEY, G. E., MORTIMER, E., SOBEL, E. R. & STRECKER, M. R. 2005. Oligocene uplift and development of plateau morphology in the southern central Andes. *Tectonics*, **24**, TC4011, <http://dx.doi.org/10.1029/2004TC001762>
- CHARRIER, R., BAEZA, O. ET AL. 2002. Evidence for Cenozoic extensional basin development and tectonic inversion south of the flat-slab segment, southern Central Andes, Chile (33°–36°S.L.). *Journal of South American Earth Sciences*, **15**, 117–139.
- CHARRIER, R., BUSTAMANTE, M. ET AL. 2005. The Abanico extensional basin: regional extension, chronology of tectonic inversion, and relation to shallow seismic activity and Andean uplift. *Neues Jahrbuch für Geologie und Paläontologie*, **236**, 43–77.
- CHARRIER, R., PINTO, L. & RODRÍGUEZ, M. P. 2007. Tectonostratigraphic evolution of the Andean Orogen in Chile. In: MORENO, T. & GIBBONS, W. (eds) *The Geology of Chile*. Geological Society, London, 21–113.
- CHARRIER, R., RAMOS, V. A., SAGRIPANTI, L. & TAPIA, F. In review. Tectono-stratigraphic evolution of the Andean Orogen between 31° and 37°S (Chile and Western Argentina). In: SEPÚLVEDA, S. A., GIAMBIAGI, L. B., MOREIRAS, S. M., PINTO, L., TUNIK, M., HOKE, G. D. & FARÍAS, M. (eds) *Geodynamic Processes in the Andes of Central Chile and Argentina*. Geological Society, London, Special Publications, **399**.
- DECELLES, P. G., DUCEA, M. N., KAPP, P. & ZANDT, G. 2009. Cyclicity in Cordilleran orogenic systems. *Nature Geoscience*, **2**, 251–257, <http://dx.doi.org/10.1038/Ngeo469>.
- DECKART, K., GODOY, E., BERTENS, A., JEREZ, D. & SAEED, A. 2010. Barren Miocene granitoids in the Central Andean metallogenetic belt, Chile: geochemistry and Nd–Hf and U–Pb isotope systematic. *Andean Geology*, **37**, 1–31.
- EHLERS, T. A. & POULSEN, C. J. 2009. Influence of Andean uplift on climate and paleoaltimetry estimates. *Earth and Planetary Science Letters*, **281**, 238–248.
- ELGUETA, S., CHARRIER, R., AGUIRRE, R., KIEFFER, G. & VATIN-PERIGNON, N. 1999. Volcanogenic sedimentation model for the Miocene Farellones Formation, Andean Cordillera, central Chile. In: *Proceedings of the IV International Symposium on Andean Geodynamics*, Göttingen.
- ENCINAS, A., LE ROUX, J. P., BUATOIS, L. A., NIELSEN, S. N., FINGER, K. L., FOURTANIER, E. & LAVENU, A. 2006. Nuevo esquema estratigráfico para los depósitos marinos mioceno-pliocenos del área de Navidad (33°00'–34°30'S), Chile central. *Revista Geológica de Chile*, **33**, 221–246.
- ENCINAS, A., FINGER, K., NIELSEN, S., LAVENU, A., BUATOIS, L., PETERSON, D. & LE ROUX, J. P. 2008. Rapid and major coastal subsidence during the late Miocene in south-central Chile. *Journal of South American Earth Sciences*, **25**, 157–175.
- FARIAS, M., CHARRIER, R. ET AL. 2008. Late Miocene high and rapid surface uplift and its erosional response in the Andes of central Chile (33°–35°S). *Tectonics*, **27**, TC1005, <http://dx.doi.org/10.1029/2006TC002046>
- FARIAS, M., COMTE, D. ET AL. 2010. Crustal-scale structural architecture in central Chile based on seismicity and surface geology: implications for Andean mountain building. *Tectonics*, **29**, TC3006, <http://dx.doi.org/10.1029/2009TC002480>
- FOCK, A. 2005. *Cronología y tectónica de la exhumación en el Neógeno de los Andes de Chile central entre los 33° y los 34°S*. MSc thesis, Universidad de Chile, Chile.

STRUCTURE EVOLUTION ALONG MAIPO–TUNAYÁN TRANSECT

- FOCK, A., CHARRIER, R., MARSAEV, V., FARÍAS, M. & ALVAREZ, P. 2006. Evolución cenozoica de los Andes de Chile Central (33° – 34° S). In: *Proceedings of the IX Congreso Geológico Chileno*, Antofagasta, Chile, **2**, 205–208.
- FORSYTH, D. & UYEDA, S. 1975. On the relative importance of the driving forces of plate motion. *Geophysical Journal Royal Astronomic Society*, **43**, 163–200.
- FUENTES, F. 2004. *Petrología y metamorfismo de muy bajo grado de unidades volcánicas oligoceno-miocenas en la ladera occidental de los Andes de Chile central (33°S)*. PhD thesis, Universidad de Chile, Chile.
- GANÀ, P. & TOSDAL, R. 1996. Geocronología U–Pb y k–Ar en intrusivos del Paleozoico y mesozoico de la Cordillera de la Costa, Región de Valparaíso, Chile. *Revista Geológica de Chile*, **23**, 151–164.
- GANÀ, P., WALL, R. & GUTIÉRREZ, A. 1996. Mapa geológico del área Valparaíso-Curacaví, Regiones de Valparaíso y Metropolitana. Servicio Nacional de Geología y Minería, map scale 1:100 000.
- GARCÍA, V. H. & CASA, A. 2014. Quaternary tectonics and seismic potential of the Andean retrowedge at 33° – 34° S. In: SEPÚLVEDA, S. A., GIAMBIAGI, L. B., MOREIRAS, S. M., PINTO, L., TUNIK, M., HOKE, G. D. & FARÍAS, M. (eds) *Geodynamic Processes in the Andes of Central Chile and Argentina*. Geological Society, London, Special Publications, **399**. First published online February 27, 2014, <http://dx.doi.org/10.1144/SP399.11>
- GARRIDO, I., RIVEROS, M., CLADOUHOS, T., ESPÍÑEIRA, D. & ALLMENDINGER, R. 1994. Modelo geológico estructural de El Teniente. In: *Proceedings of the VII Congreso Geológico Chileno*, Concepción, Chile. Actas 2: 1553–1558.
- GARZIONE, C., HOKE, G. ET AL. 2008. The rise of the Andes. *Science*, **320**, 1304–1307.
- GIAMBIAGI, L. & RAMOS, V. A. 2002. Structural evolution of the Andes between $33^{\circ}30'$ and $33^{\circ}45'$ S, above the transition zone between the flat and normal subduction segment, Argentina and Chile. *Journal of South American Earth Sciences*, **15**, 99–114.
- GIAMBIAGI, L., TUNIK, M. & GHIGLIONE, M. 2001. Cenozoic tectonic evolution of the Alto Tunuyán foreland basin above the transition zone between the flat and normal subduction segment ($33^{\circ}30'$ – 34° S), western Argentina. *Journal of South American Earth Sciences*, **14**, 707–724.
- GIAMBIAGI, L., RAMOS, V. A., GODOY, E., ALVAREZ, P. P. & ORTS, S. 2003a. Cenozoic deformation and tectonic style of the Andes, between 33° and 34° South Latitude. *Tectonics*, **22**, 1041, <http://dx.doi.org/10.1029/2001TC001354>
- GIAMBIAGI, L., ALVAREZ, P., GODOY, E. & RAMOS, V. 2003b. The control of pre-existing extensional structures on the evolution of the southern sector of the Aconcagua fold and thrust belt, southern Andes. *Tectonophysics*, **369**, 1–19.
- GIAMBIAGI, L., TUNIK, M., RAMOS, V. & GODOY, E. 2009. The High Andean Cordillera of central Argentina and Chile along the Piuquenes pass – Cordón del Portillo transect: Darwin's pioneering observations compared with modern geology. *Revista Asociación Geológica Argentina*, **64**, 43–54.
- GIAMBIAGI, L., MESCÚA, J., BECHIS, F., TASSARA, A. & HOKE, G. 2012. Thrust belts of the Southern Central Andes: along-strike variations in shortening, topography, crustal geometry, and denudation. *Geological Society of America Bulletin*, **124**, 1339–1351.
- GODOY, E. 2005. Tectonic erosion in the Central Andes: use and abuse. In: *Proceedings of the VI International Symposium on Andean Geodynamics*, Barcelona, Spain, 330–332.
- GODOY, E. 2011. Structural setting and diachronism in the Central Andean Eocene to Miocene volcano-tectonic basins. In: SALFITY, J. A. & MARQUILLA, R. (eds) *Cenozoic Geology of the Central Andes of Argentina*. SCR Publisher, Salta, Argentina, 155–167.
- GODOY, E. 2014. The north-western margin of the Neuquén Basin in the headwater regions of the Maipo drainage, Chile. In: SEPÚLVEDA, S. A., GIAMBIAGI, L. B., MOREIRAS, S. M., PINTO, L., TUNIK, M., HOKE, G. D. & FARÍAS, M. (eds) *Geodynamic Processes in the Andes of Central Chile and Argentina*. Geological Society, London, Special Publications, **399**. First published online February 27, 2014, <http://dx.doi.org/10.1144/SP399.13>
- GODOY, E., YAÑEZ, G. & VERA, E. 1999. Inversion of an Oligocene volcano-tectonic basin and uplift of its superimposed Miocene magmatic arc, Chilean Central Andes: first seismic and gravity evidence. *Tectonophysics*, **306**, 217–326.
- GOETZE, C. & EVANS, B. 1979. Stress and temperature in the bending lithosphere as constrained by experimental rock mechanics. *Geophysical Journal of the Royal Astronomical Society*, **59**, 463–478.
- GUTIÉRREZ, N., HINOJOSA, L., LE ROUX, J. P. & PEDROZA, V. 2013. Evidence for an Early-Middle Miocene age of the Navidad Formation (central Chile): paleontological, paleoclimatic and tectonic implications. *Andean Geology*, **40**, 66–78.
- HEURET, A. & LALLEMAND, S. 2005. Plate motions, slab dynamics and back-arc deformation. *Physics of the Earth and Planetary Interiors*, **149**, 31–51.
- HOKE, G. D., GRABER, N. R., MESCÚA, J. F., GIAMBIAGI, L. B., FITZGERALD, P. G. & METCALF, J. R. 2014. Near pure surface uplift of the Argentine Frontal Cordillera: insights from (U–Th)/He thermochronology and geomorphic analysis. In: SEPÚLVEDA, S. A., GIAMBIAGI, L. B., MOREIRAS, S. M., PINTO, L., TUNIK, M., HOKE, G. D. & FARÍAS, M. (eds) *Geodynamic Processes in the Andes of Central Chile and Argentina*. Geological Society, London, Special Publications, **399**. First published online February 5, 2014, <http://dx.doi.org/10.1144/SP399.4>
- HONGN, F., DEL PAPA, C., POWELL, J., PETRINOVIC, I., MON, R. & DERACO, V. 2007. Middle Eocene deformation and sedimentation in the Puna-Eastern Cordillera transition (23° – 26° S): control by preexisting heterogeneities on the pattern of initial Andean shortening. *Geology*, **35**, 271–274.
- HYNDMAN, R. D., CURRIE, C. A. & MAZZOTTI, S. P. 2005. Subduction zone backarcs, mobile belts, and orogenic heat. *GSA Today*, **15**, 4–10.
- IAFFALDANO, G. & BUNGE, H. P. 2008. Strong plate coupling along the Nazca-South American convergent margin. *Geology*, **36**, 443–446.

- IRIGOYEN, M. V., BUCHAN, K. L. & BROWN, R. L. 2000. Magnetostratigraphy of Neogene Andean foreland-basin strata, lat 33°S, Mendoza Province, Argentina. *Geological Society of America, Bulletin*, **112**, 803–816.
- ISACKS, B. 1988. Uplift of the Central Andean plateau and bending of the Bolivian Orocline. *Journal of Geophysical Research*, **93**, 3211–3231.
- JORDAN, T. E., ISACKS, B. L., ALLMENDINGER, R. W., BREWER, J. A., RAMOS, V. A. & ANDO, C. J. 1983. Andean tectonics related to geometry of subducted Nazca plate. *Geological Society of America, Bulletin*, **94**, 341–361.
- KARATO, S. 2008. *Deformation of Earth Materials: An Introduction to the Rheology of Solid Earth*. Cambridge University Press, Cambridge.
- KAY, R. W. & KAY, S. 1993. Delamination and delamination magmatism. *Tectonophysics*, **219**, 177–189.
- KAY, S. & KURTZ, A. 1995. *Magmatic and tectonic characterization of the El Teniente region. Internal report, Superintendencia de Geología, El Teniente, CODELCO*.
- KAY, S. M. & MPODOZIS, C. 2001. Central Andean ore deposits linked to evolving shallow subduction systems and thickening crust. *GSA Today*, **11**, 4–11.
- KAY, S. M., MPODOZIS, C. & COIRA, B. 1999. Neogene magmatism, tectonism and mineral deposits of the Central Andes (22°–33°S Latitude). In: SKINNER, B. J. (ed.) *Geology and Ore Deposits of the Central Andes*. Society of Economic Geologists, Lancaster, USA, Special Publications, **7**, 27–59.
- KAY, S. M., GODOY, E. & KURTZ, A. 2005. Episodic arc migration, crustal thickening, subduction erosion, and magmatism in the south-central Andes. *Geological Society of America, Bulletin*, **117**, 67–88.
- KAY, S. M., BURNS, M., COPELAND, P. & MANCILLA, O. 2006. Upper Cretaceous to Holocene magmatism and evidence for transient Miocene shallowing of the Andean subduction zone under the northern Neuquén Basin. In: KAY, S. M. & RAMOS, V. A. (eds) *Evolution of an Andean margin: A Tectonic and Magmatic view from the Andes to the Neuquén basin (35°–39°S lat)*. Geological Society of America, Boulder, Colorado, Special Paper, **407**, 19–60.
- KURTZ, A., KAY, S. M., CHARRIER, R. & FARRAR, E. 1997. Geochronology of Miocene plutons and exhumation history of the El Teniente region, Central Chile (34°–35°S). *Revista Geológica de Chile*, **24**, 73–90.
- LAMB, S. 2006. Shear stresses on megathrusts: implications for mountain building behind subduction zones. *Journal of Geophysical Research*, **111**, B07401, <http://dx.doi.org/10.1029/2005JB003916>
- LAVENU, A. & ENCINAS, A. 2005. Brittle deformation of the Neogene deposits of the Navidad Basin (Coastal Cordillera, 34°S, central Chile). *Revista Geológica de Chile*, **32**, 229–248.
- MAKSAEV, V., MUNIZAG, V. F., MACWILLIAMS, M., FANNING, M., MATHUR, R., RUIZ, J. & ZENTILLI, M. 2004. New chronology for El Teniente, Chilean Andes, from U–Pb, 40Ar/39Ar, Re–Os and fission-track dating. In: ?? (eds) *Implications for the Evolution of a Supergiant Porphyry Cu–Mo deposit*. Society of Economic Geologists, Lancaster, USA, Special Publication, **11**, 15–54.
- MAKSAEV, V., MUNIZAGA, F., ZENTILLI, M. & CHARRIER, R. 2009. Fission track thermochronology of Neogene plutons in the Principal Andean Cordillera of central Chile (33°–35°S): implications for tectonic evolution and porphyry Cu–Mo mineralization. *Andean Geology*, **36**, 153–171.
- MESCUA, J., GIAMBIAGI, L. & RAMOS, V. A. 2013. Late Cretaceous uplift in the Malargüe fold-and-thrust belt (35°S), Southern Central Andes of Argentina and Chile. *Andean Geology*, **40**, 102–116.
- MOLNAR, P. & LYON-CÄN, H. 1988. Some simple physical aspects of the support, structure, and evolution of mountain belts. *Geological Society of America, Special Paper*, **218**, 179–207.
- MORALES, D. & TASSARA, A. 2012. Avances hacia un modelo termal 3D del margen Andino. In: *Proceedings of the XII Congreso Geológico Chileno, Antofagasta, Chile*, 498–499.
- MPODOZIS, C. & CORNEJO, P. 2012. Cenozoic tectonics and porphyry copper systems of the Chilean Andes. In: HEDENQUIST, J. W., HARRIS, M. & CAMUS, F. (eds) *Geology and Genesis of Major Copper Deposits and Districts of the World: A Tribute to Richard H. Sillitoe*. Society of Economic Geologists, Lancaster, USA, Special Publication, **16**, 329–360.
- MPODOZIS, C. & RAMOS, V. A. 1989. The Andes of Chile and Argentina. In: ERICKSEN, G. E., CAÑAS, M. T. & REINEMUND, J. A. (eds) *Geology of the Andes and its Relation to Hydrocarbon and Mineral Resources*. Circum-Pacific Council for Energy and Mineral Resources, Lancaster, USA, Earth Science Series, **11**, 59–90.
- MUÑOZ, M., FUENTES, F., VERGARA, M., AGUIRRE, L., NYSTRÖM, J. O. & FÉRAUD, G. 2006. Abanico East Formation: petrology and geochemistry of volcanic rocks behind the Cenozoic arc front in the Andean Cordillera, central Chile (33°50'S). *Revista Geológica de Chile*, **33**, 109–140.
- MUÑOZ, M., CHARRIER, R., FANNING, C. M., MAKSAEV, V. & DECKART, K. 2012. Zircon trace element and O–Hf isotope analyses of mineralized intrusions from El Teniente Ore Deposit, Chilean Andes: constraints on the source and magmatic evolution of porphyry Cu–Mo related magmas. *Journal of Petrology*, **53**, 1091–1122.
- NYSTRÖM, J., PARADA, M. & VERGARA, M. 1993. *Sr–Nd Isotope Compositions of Cretaceous to Miocene Volcanic Rocks in Central Chile: A Trend Towards a MORB Signature and a Reversal with Time*. II International Symposium on Andean Geodynamics (ISAG), Oxford, UK, IRD (eds), 411–414.
- NYSTRÖM, J. O., VERGARA, M., MORATA, D. & LEVI, B. 2003. Tertiary volcanism in central Chile (33°15'–33°45'S): a case of Andean Magmatism. *Geological Society of America, Bulletin*, **115**, 1523–1537.
- ORTS, D., FOLGUERA, A., GIMÉNEZ, M. & RAMOS, V. A. 2012. Variable structural controls through time in the Southern Central Andes (36°S). *Andean Geology*, **39**, 220–241.
- POLANSKI, J. 1964. Descripción geológica de la Hoja 25 a–b – Volcán de San José, provincia de Mendoza, Dirección Nacional de Geología y Minería, Boletín 98, 1–92, Buenos Aires, Argentina.

STRUCTURE EVOLUTION ALONG MAIPO–TUNAYÁN TRANSECT

- PORRAS, H., PINTO, L., TUNIK, M. & GIAMBIAGI, L. In review. Provenance analysis using whole-rock geochemistry and U–Pb dating of the Alto Tunuyán basin: implications for its palaeogeographic evolution. In: SEPÚLVEDA, S. A., GIAMBIAGI, L. B., MOREIRAS, S. M., PINTO, L., TUNIK, M., HOKE, G. D. & FARIAS, M. (eds) *Geodynamic Processes in the Andes of Central Chile and Argentina*. Geological Society, London, Special Publications, **399**.
- RAMOS, V. A., GODOY, E., GODOY, V. & PÁNGARO, F. 1996. Evolución tectónica de la Cordillera Principal argentina-chilena a la latitud del Paso de Piuquenes ($33^{\circ}30'S$). In: *Proceeding of the XIII Congreso Geológico Argentino*, Buenos Aires, Argentina, 337–352.
- RAMOS, V. A., ZAPATA, T., CRISTALLINI, E. & INTROCASO, A. 2004. The Andean thrust system: latitudinal variations in structural styles and orogenic shortening. In: MCCLAY, K. R. (ed.) *Thrust Tectonics and Hydrocarbon Systems*. American Association of Petroleum Geology, Boulder, USA, Memoir, **82**, 30–50.
- RAULD, R., VARGAS, G., ARMijo, R., ORMEÑO, A., VALDERAS, C. & CAMPOS, J. 2006. Cuantificación de escarpes de falla y deformación reciente en el frente cordillerano de Santiago. In: *Proceedings of the XI Congreso Geológico Chileno*, Antofagasta, Chile, 447–450.
- RODRÍGUEZ, M. P., PINTO LINCOÑIR, L. & ENCINAS, A. 2012. Cenozoic erosion in the Andean forearc in Central Chile (33° – 34° S): sediment provenance inferred by heavy mineral studies. In: RASBURY, E. T., HEMMING, S. R. & RIGGS, N. R. (eds) *Mineralogical and Geochemical Approaches to Provenance*. Geological Society of America, Boulder, Special Paper, **487**, 141–162.
- SAVAGE, J. C. 1983. A dislocation model of strain accumulation and release at a subduction zone. *Journal of Geophysical Research*, **88**, 4984–4996.
- SCHELLART, W. P. 2008. Overriding plate shortening and extension above subduction zones: a parametric study to explain formation of the Andes Mountains. *Geological Society of America Bulletin*, **120**, 1441–1454.
- SCHMITZ, M. 1994. A balanced model of the southern Central Andes. *Tectonics*, **13**, 484–492.
- SELLÉS, D. & GANA, P. 2001. *Geología del área Talagante-San Francisco de Mostazal: Regiones Metropolitana y del Libertador General Bernardo O'Higgins. I: 100 000*. SERNAGEOMIN, Carga Geológica de Chile, Serie Geológica Básica.
- SHEFFELS, B. 1990. Lower bound on the amount of crustal shortening in the Central Bolivian Andes. *Geology*, **18**, 812–815.
- STAUDER, W. 1975. Subduction of the Nazca Plate under Peru as evidenced by focal mechanism and by seismicity. *Journal of Geophysical Research*, **80**, 1053–1064.
- STERN, C. R. 1989. Pliocene to present migration of the volcanic front, Andean Southern Volcanic Zone. *Revista Geológica de Chile*, **16**, 145–162.
- STERN, C. R. 2011. Subduction erosion: rates, mechanisms, and its role in arc magmatism and the evolution of the continental crust and mantle. *Gondwana Research*, **20**, 284–338.
- TAPIA, F., FARIAS, M. & ASTABURUAGA, D. 2012. Deforación cretácica-paleocena y sus evidencias en la cordillera de los Andes de Chile Central (33.7° – 36° S). *XI Congreso Geológico Chileno*, Antofagasta, Chile, 232–234.
- TASSARA, A. 2005. Interaction between the Nazca and South American plates and formation of the Altiplano–Puna plateau: review of a flexural analysis along the Andean margin (15° – 34° S). *Tectonophysics*, **399**, 39–57.
- TASSARA, A. 2012. Thermomechanical support of high topography: a review of hypothesis, observations and models on the Altiplano-Puna Plateau. In: *Proceedings of the American Geophysical Union Annual Meeting*, San Francisco.
- TASSARA, A. & ECHAURREN, A. 2012. Anatomy of the Andean subduction zone: three-dimensional density model upgraded and compared against global-scale models. *Geophysical Journal International*, **189**, 161–168.
- TASSARA, A. & MORALES, D. 2013. 3D temperature model of south-western South America. *Annual Meeting of the European Geosciences Union*, Vienna, Austria. *Geophysical Research Abstracts*, V15, EGU2013–945.
- TASSARA, A., GÖTZE, H.-J., SCHMIDT, S. & HACKNEY, R. 2006. Three-dimensional density model of the Nazca plate and the Andean continental margin. *Journal of Geophysical Research*, **111**, B09404, <http://dx.doi.org/10.1029/2005JB003976>
- TASSARA, A., SWAIN, C., HACKNEY, R. & KIRBY, J. 2007. Elastic thickness structure of South America estimated using wavelets and satellite-derived gravity data. *Earth and Planetary Science Letters*, **253**, 17–36.
- TUNIK, M. 2003. Interpretación paleoambiental de la Formación Saldeño (Cretácico superior), en la Alta Cordillera de Mendoza, Argentina. *Revista de la Asociación Geológica Argentina*, **58**, 417–433.
- TUNIK, M., FOLGUERA, A., NAIPAUER, M., PIMENTEL, M. & RAMOS, V. A. 2010. Early uplift and orogenic deformation in the Neuquén basin: constraints on the Andean uplift from U–Pb and Hf isotopic data of detrital zircons. *Tectonophysics*, **489**, 258–273.
- TURCOTTE, D. L. & SCHUBERT, G. 2002. *Geodynamics*. Cambridge University Press, Cambridge, New York.
- VERGARA, M., CHARRIER, F., MUNIZAGA, F., RIVANO, S., SEPÚLVEDA, P., THIELE, R. & DRAKE, M. 1988. Miocene vulcanism in the central Chilean Andes ($31^{\circ}30'S$ – $34^{\circ}35'S$). *Journal of South American Earth Sciences*, **1**, 199–209.
- VERGARA, M., MORATA, D., VILLARROEL, R., NYSTRÖM, J. & AGUIRRE, L. 1999. Ar/Ar ages, very low-grade metamorphism and geochemistry of the volcanic rocks from 'Cerro El Abanico', Santiago Andean Cordillera ($33^{\circ}30'S$ – $70^{\circ}30'$ – $70^{\circ}25'W$). In: *Proceedings of the IV International Symposium on Andean Geodynamics*, Göttingen, Germany, 785–788.
- WALL, R., GANA, P. & GUTIÉRREZ, A. 1996. Mapa Geológico del área de San Antonio-Melipilla. Regiones de Valparaíso y Metropolitana. Sernageomin, Santiago, Mapas Geológicos N°1, 1:100.000.
- WALL, R., SELLÉS, D. & GANA, P. 1999. Hoja Tilit-Santiago, Área Metropolitana. 1: 100 000. Sernageomin.
- WANG, L., SHUM, C. K. ET AL. 2012. Coseismic slip of the 2010 Mw 8.8 Great Maule, Chile, earthquake quantified by the inversion of GRACE observation. *Earth and Planetary Science Letters*, **335**, 167–179.

- YAÑEZ, G., CEMBRANO, J., PARDO, M., RANERO, C. & SELLES, D. 2002. The Challenger-Juan Fernández-Maipo major tectonic transition of the Nazca – Andean subduction system at 33–34°S: geodynamic evidence and implications. *Journal of South American Earth Sciences*, **15**, 23–38.
- YRIGOYEN, M. R. 1993. Los depósitos sinorogénicos terciarios. In: RAMOS, V. A. (ed.) *Geología y recursos naturales de la Provincia de Mendoza*, Mendoza, Argentina, 123–148.
- ZURITA, E., MUÑOZ, N., CHARRIER, R., HARAMBOUR, S. & ELGUETA, S. 2000. Madurez termal de la materia orgánica de la Formación Abanico = Coya Machalí, Cordillera Principal, Chile Central: resultados e interpretación. In: *Proceedings of the IX Congreso Geológico Chileno*, Puerto Varas, Chile, 726–730.

The Upper Jurassic volcanism of the Río Damas-Tordillo Formation (33°-35.5°S): Insights on petrogenesis, chronology, provenance and tectonic implications

Pablo Rossel^{1,8}, *Verónica Oliveros¹, José Mescua², Felipe Tapia³, Mihai N. Ducea^{4,5}, Sergio Calderón^{3,6}, Reynaldo Charrier^{3,7}, Derek Hoffman⁴

¹ Departamento Ciencias de la Tierra, Universidad de Concepción, Casilla 160-C, Concepción, Chile.

pabrossel@udec.cl; voliveros@udec.cl

² Instituto Argentino de Nivología, Glaciología y Ciencias Ambientales (IANIGLA), CCT Mendoza, CONICET. Avda. Ruiz Leal s/n, Parque General San Martín, Mendoza (5500), Argentina.

jmescua@mendoza-conicet.gob.ar

³ Departamento de Geología, Universidad de Chile, Plaza Ercilla # 803, Santiago, Chile.

ftapiasilva@gmail.com; rcharrie@ing.uchile.cl

⁴ Department of Geosciences, University of Arizona, Tucson, AZ 85721, USA.

ducea@email.arizona.edu; mantis@email.arizona.edu

⁵ Universitatea Bucuresti, Facultatea de Geologie Geofizica, Strada N. Balcescu Nr 1, Bucuresti, Romania.

⁶ Escuela de Ciencias de la Tierra, Universidad Andrés Bello, Quillota 980, Viña del Mar, Chile.

sergio.calderon@unab.cl

⁷ Escuela Ciencias de la Tierra, Universidad Andrés Bello, Campus Repùblica, Avenida Repùblica 237, Santiago, Chile.

rcharrier@unab.cl

⁸ Present address: Facultad de Ingeniería, Geología, Universidad Andrés Bello, Autopista Concepción-Talcahuano 7100, Concepción, Chile.

pablo.rossel@unab.cl

* Corresponding author: voliveros@udec.cl

ABSTRACT. The uppermost Jurassic continental and volcanic deposits of the Río Damas-Tordillo Formation represent an interval of intense continental deposition within the Jurassic to Early Cretaceous dominantly marine environment of the Mendoza-Neuquén back-arc basin. Stratigraphic and geochronological data indicate that progressive emersion of the arc and forearc domain, disconnecting the back-arc region from the Pacific Ocean, occurred during the Late Jurassic and probably the Early Cretaceous (~160-140 Ma). This change in the margin configuration induced a marine regression and the subsequent deposition of continental material in the back-arc basin. The most likely source of the sediments would have been the Jurassic arc, located west of the back-arc basin. The maximum depositional age of 146.4±4.4 Ma obtained from a red sandstone immediately below volcanic rocks confirms recent Tithonian maximum depositional ages assigned to the Río Damas-Tordillo Formation, and suggests that the volcanic rocks, overlain by marine fossiliferous Tithonian-Hauterivian sequences, should have erupted within a short time span during the Late Jurassic. Volcanism was probably facilitated by the presence of extensional structures related to the formation of the back-arc basin. Elemental and isotopic data, along with forward AFC models, suggest a depleted sub-arc asthenospheric mantle source for the volcanic rocks and the fractionation of olivine and plagioclase, along with small volumes of lower crust assimilation, as the main processes involved in the magmatic evolution. It is not possible to establish a different source and petrogenetic conditions for the Río Damas-Tordillo Formation and the magmatism in the arc domain located further west, at the present-day Coastal Cordillera.

Keywords: Jurassic, Volcanism, Central Chile, Detrital zircons, Isotopes.

RESUMEN. El volcanismo jurásico superior de la Formación Río Damas-Tordillo (33°-35,5°S): antecedentes sobre petrogénesis, cronología, proveniencia e implicancias tectónicas. Los depósitos continentales y volcánicos del Jurásico tardío, pertenecientes a la Formación Río Damas-Tordillo, representan un período de intensa sedimentación continental dentro del registro mayormente marino observado en la Cuenca Neuquina, durante el Jurásico y Cretácico Inferior. Datos estratigráficos y geocronológicos indican una progresiva emersión del dominio de arco y antearco, desconectando finalmente a la cuenca de trasarco del Océano Pacífico durante el Jurásico Superior. Este cambio en la configuración del margen tuvo como resultado el desarrollo de una regresión marina y posterior sedimentación continental en la cuenca de trasarco. La fuente de sedimentos más probable habría sido el arco jurásico, ubicado hacia el oeste de la cuenca. La edad máxima de $146,4 \pm 4,4$ Ma, obtenida en una arenisca roja inmediatamente por debajo de las rocas volcánicas, confirma las edades máximas de depósito titoniana, asignadas recientemente a la Formación Río Damas-Tordillo, y sugiere que las rocas volcánicas cubiertas por secuencias marinas fosilíferas del Titoniano-Hauteriviano fueron emplazadas en un período muy restringido hacia fines del Jurásico. Este volcanismo probablemente fue facilitado por la presencia de estructuras extensionales relacionadas con el desarrollo de la cuenca de trasarco. Datos geoquímicos elementales e isotópicos, junto con modelamientos de ACF, sugieren un manto astenosférico deprimido como fuente del material ígneo, y el fraccionamiento de olivino y plagioclasa, combinado con pequeños volúmenes de asimilación de corteza inferior, como los principales procesos involucrados en la evolución de los magmas. No es posible diferenciar, en términos geoquímicos, la fuente y los procesos petrogenéticos del volcanismo jurásico reconocido en la cordillera de la Costa y el de la Formación Río Damas-Tordillo.

Palabras clave: Jurásico, Volcanismo, Chile central, Circones detríticos, Isótopos.

1. Introduction

The voluminous magmatism developed during the Jurassic and Early Cretaceous in the Coastal Cordillera from southern Perú to central Chile, was mainly produced during a period of active subduction and extensional/trans-tensional tectonics (Creixell *et al.*, 2006, 2009, 2011; Grocott and Taylor, 2002; Oliveros *et al.*, 2006, 2007; Schueber and González, 1999). Subduction of the cold and dense Phoenix plate under the South American continent resulted in roll-back of the oceanic plate, constant outboard migration of the trench, thinning of the continental crust and the development of a N-S trending paleogeography (Charrier *et al.*, 2007; Mpodozis and Ramos, 2008). This period was characterized by a magmatic arc emplaced in the present-day Coastal Cordillera and extensive back-arc basins to the east (Charrier *et al.*, 2007; Martínez *et al.*, 2012; Vicente, 2006), where much more restricted volcanic activity took place (Rossel *et al.*, 2013).

The main arc domain has been widely studied in the past decades (Creixell *et al.*, 2006, 2009, 2011; Kramer *et al.*, 2004; Lucassen *et al.*, 2006; Oliveros *et al.*, 2006, 2007; Parada *et al.*, 1999; Vergara *et al.*, 1995) in order to constrain the genesis and sources of this important magmatic province. Recently Rossel *et al.* (2013) have studied the genesis of back-arc volcanism in northern Chile and Oliveros *et al.* (2012) the features of the non-marine back-arc deposits in the same region.

In Central Chile, the Jurassic arc domain is represented by the Lower Jurassic Ajial Formation and the Upper Jurassic Horqueta Formation. The first is predominantly composed by acidic volcanic lavas and pyroclastic rocks, deposited under alternate marine and continental conditions, while on the other hand the Horqueta Formation is a sedimentary-volcanic unit deposited under continental conditions, with mostly acidic lavas and pyroclastic rocks at the base that grade to intermediate to basaltic lavas to the top of the unit (Vergara *et al.*, 1995).

The sedimentary beds of the Río Damas and Tordillo Formations represent the Upper Jurassic continental back-arc deposits, cropping out in the Principal Cordillera of central Chile and Argentina, respectively. These sequences have been studied in detail in terms of their depositional and tectonic environment (Davidson and Vicente, 1973; Legarreta, 1976; López-Gómez *et al.*, 2009; Mescua *et al.*, 2008; Naipauer *et al.*, 2012, 2014; Spalletti *et al.*, 2008; Thiele, 1980; Yrigoyen, 1979; Zavala *et al.*, 2008). In contrast, the volcanic deposits within these units are relatively unexplored and their petrogenesis remains undetermined. In particular, it is not clear whether the volcanism represents an eastern part of the main volcanic arc or a retro-arc belt within the back-arc basin.

Below, we present a new set of whole-rock elemental and isotopic data for the volcanic rocks as well as new geochronological results for the sedimentary rocks of the Río Damas-Tordillo Formation, which

allow to better understand the stratigraphic position, sources, evolution and tectonic setting of the volcanism developed close to the Jurassic-Cretaceous boundary in the Principal Cordillera of Chile and Argentina, between 33° and 35.5° S. The Upper Jurassic units were sampled at two localities close to the Chile-Argentina border, the Río Volcán and the Termas del Flaco-Las Leñas areas (Fig. 1) where the volcanic and sedimentary rocks of the Río Damas-Tordillo Formation crop out in continuous sections.

2. Geological Setting

Within the context of the mainly extensional/transtensional tectonics recognized for the arc and back-arc domains in northern and central Chile and

Argentina during the Jurassic (Creixell *et al.*, 2006, 2009, 2011; Grocott and Taylor, 2002; Legarreta and Uliana, 1999; Scheuber and González, 1999) it is possible to identify two transgression-regression cycles during Jurassic and Early Cretaceous times. The red continental clastic deposits of the Kimmeridgian-Tithonian Río Damas-Tordillo Formation (33 to 35.5° S; Figs. 1, 2 and 3) reflect the transition between: (a) the culmination of the first Jurassic transgression-regression event, and (b) the initiation of the second one, which began in the Tithonian with the reactivation of normal faults that participated in the early development of the backarc basin extension (tectonic subsidence) associated with volcanism and very coarse breccia deposits (Charrier *et al.*, 2007). Thus, the lavas contained in the Río Damas-Tordillo Formation represent

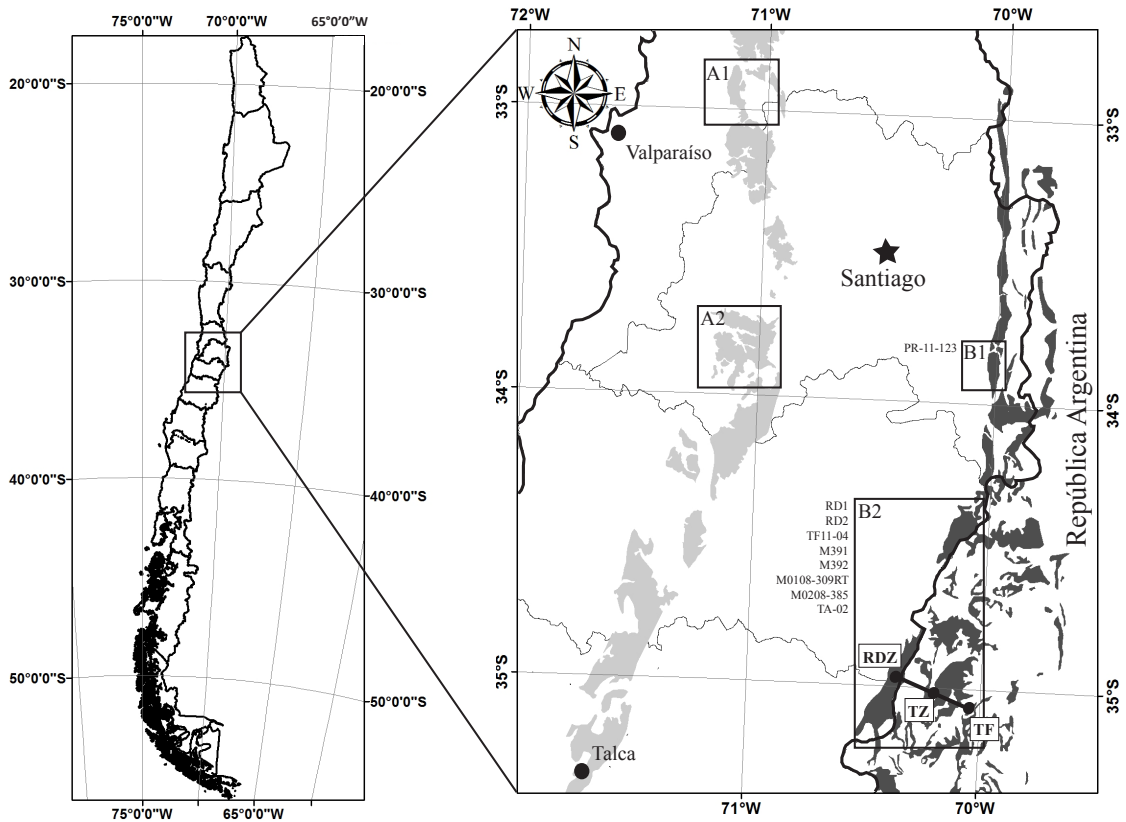


FIG. 1. Simplified geological map of the studied area, showing the location of the relevant units. The gray areas represent the outcrops of the Jurassic volcanic rocks assigned to the arc domain (Ajial and Horqueta formations) and the dark gray areas represent the outcrops of Río Damas and Tordillo Formations. **A1.** Ajial and Horqueta formations and **A2.** Horqueta Formation sampling zones of Vergara *et al.*, 1995; **B1.** Río Volcán area; **B2.** Termas del Flaco and Paso Vergara-Cordón del Burrero area. **RDZ:** Río Damas Zone; **TZ:** Transition Zone; **TF:** Tordillo Formation Zone. Modified after SERNAGEOMIN (2003) and Caminos *et al.* (1993).

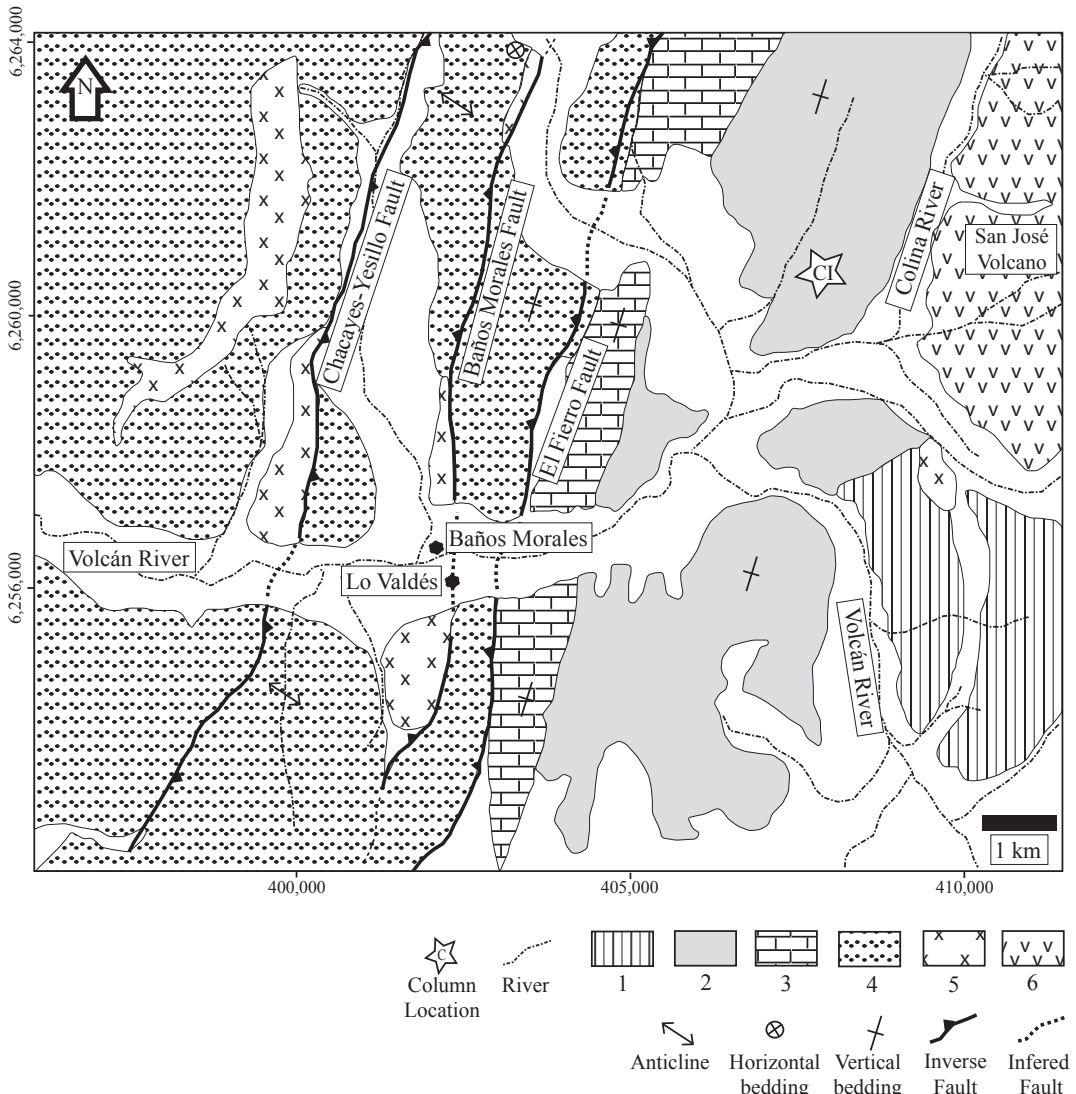


FIG. 2. Simplified geological map of the Rio Volcán area (B1 in Fig. 1). Stars show the location of sections in figure 5. **1.** Río Colina Formation; **2.** Río Damas-Tordillo Formation; **3.** Lo Valdés Formation; **4.** Cenozoic volcano-sedimentary deposits; **5.** Miocene intrusives; **6.** Quaternary volcanism. Modified after Calderón (2008).

a particular event of volcanic activity, accompanied by continental sedimentation, that took place during the latest Jurassic-earliest Cretaceous in the western border of the Mendoza-Neuquén Basin (Mescua, 2011; Fig. 4). The volcanic deposits are interpreted as either the distal components of the main volcanic arc developed to the west in the present-day Coastal Cordillera (Davidson, 1971; Davidson and Vicente; 1973), or back-arc volcanism emplaced through the normal faults that accommodated the extension in

the back-arc basin (Charrier *et al.*, 2007). The back-arc volcanism would have occurred also during the Early Cretaceous, since volcanic intercalations have been found within the marine Tithonian-Hauterivian Lo Valdés and Baños del Flaco formations, which overlie the Río Damas Formation in this same region (González, 1963; Biro-Bagoczky, 1964), between 33°30'S and 34°15'S.

In the Rio Volcán area, close to La Valdés village, the Río Damas Formation (Klohn, 1960; Figs. 2 and 5)

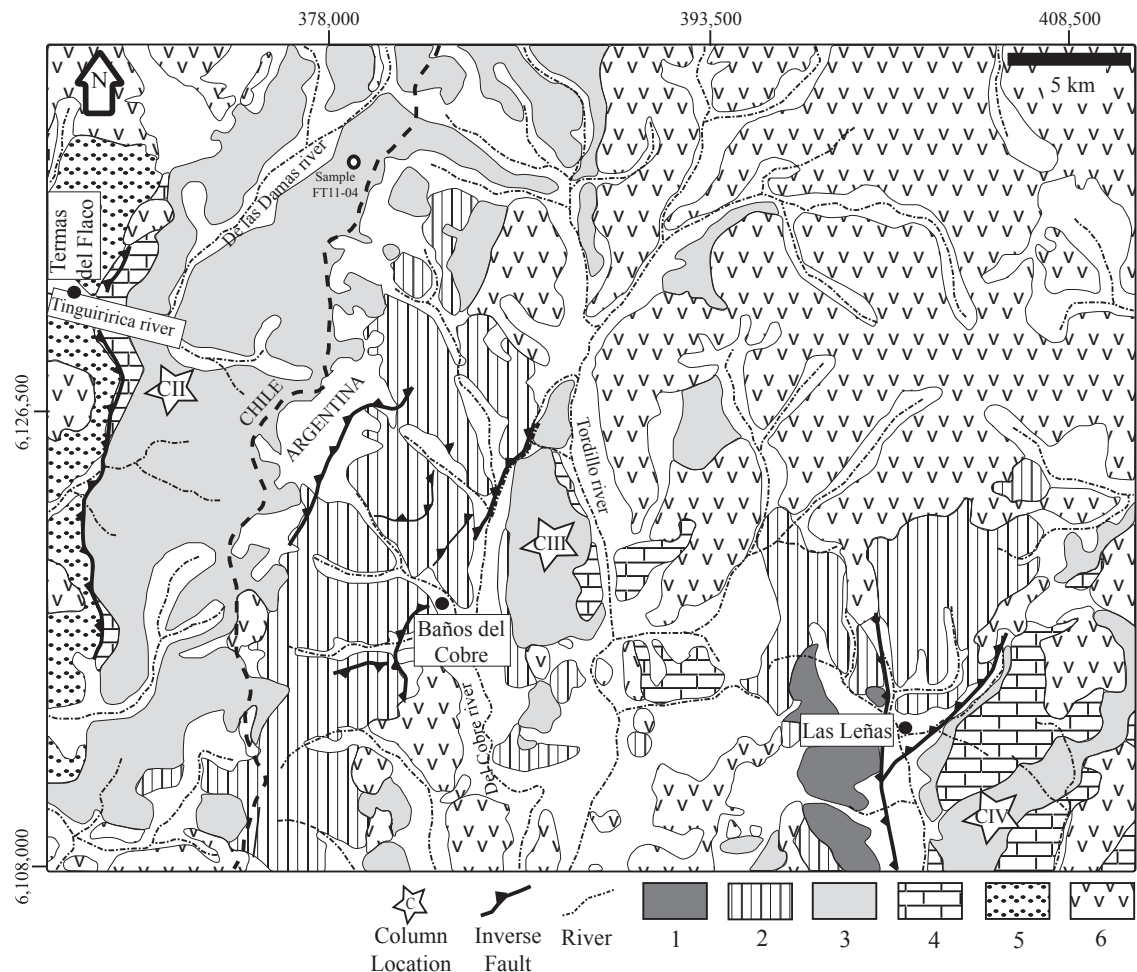


FIG. 3. Simplified geological map of the Termas del Flaco-Las Leñas area (B2 in Fig. 2). Stars show the location of sections in figure 5. 1. Choiyoi rocks; 2. Jurassic marine sediments; 3. Río Damas-Tordillo Formation; 4. Post-Tithonian marine deposits; 5. Cenozoic volcano-sedimentary deposits; 6. Quaternary volcanism. Modified after Mescua (2011).

concordantly overlies Callovian-Oxfordian marine and evaporitic deposits of the Río Colina Formation (González, 1963), composed mainly by limestones, calcareous shales, sandstones and conglomerates with minor intercalations of lavas, and important levels of gypsum, and underlies the marine deposits of the Lo Valdés Formation (González, 1963), which comprises by over 1,000 m of marine fossiliferous deposits of Tithonian-Hauterivian age, with intercalated hialoclastic andesites (Hallam *et al.*, 1986; Thiele, 1980). In this area the Río Damas Formation is represented by a basal level (3 to 10 m) of massive coarse sandstones that underlie a series of andesitic lava flows with a maximum thickness of 500 m. To the top the lavas

become more brecciated and are overlaid by a series of clastic continental conglomerates and breccias that contain abundant volcanic clasts of the andesitic lava flows (Fig. 5).

At its type locality, close to Termas del Flaco area (Fig. 3), the Río Damas Formation consists of a *ca.* 3,000-m-thick continental succession of red beds, with intercalations of coarse- and fine-grained rocks, that includes at the top >1,000 m of andesitic lavas and volcanic breccias with large angular blocks, some over 4 m in diameter (Charrier *et al.*, 1996), and underlies the marine deposits of the Termas del Flaco Formation of Tithonian age (Klohn, 1960; Fig. 5). To the east, the Río Damas

Formation interingers the clastic continental rocks of the Tordillo Formation (Stipanicic, 1969; Fig. 5), mainly red sandstones with conglomerates and shales that are representative of fluvial, eolian, alluvial and playa lake environments (Legarreta *et al.*, 1993).

South of 35.5°S, the Río Damas Formation overlays the gypsum deposits of Santa Elena Formation located on top of Nacientes del Teno Formation (Davidson, 1971; Davidson and Vicente, 1973).

The Tordillo Formation, which is the Argentinean equivalent to the Río Damas Formation, concordantly overlies in concordance the evaporitic deposits of the Auquilco Formation (Stipanicic, 1965), composed mainly by gypsum, anhydrite and minor limestones of Oxfordian age, with a maximum thickness of 400 m, and underlies in concordance the marine deposits of the Vaca Muerta Formation (Weaver, 1931), which

represent a new marine flooding in the back-arc basin, evidenced by deposits of black shales and fossiliferous limestones of Tithonian-Berriasian age.

As show in figure 4, the deposits of the Río Damas-Tordillo Formation represent a main event of emersion of the back-arc basin that took place during the Kimmeridgian. A decrease in the proportion of volcanic rocks from west to east suggests that the contribution of volcanic material is mainly from the west (Fig. 5). These units present abrupt changes in thickness in the studied area. A main depocenter was located in the western part of the basin, controlled by active extensional faults (Mescua, 2011; Mescua *et al.*, 2008), confirming the existence of very active tectonics during this period of the Jurassic.

The deposits of the Río Damas-Tordillo Formation are tilted and deformed as a consequence of

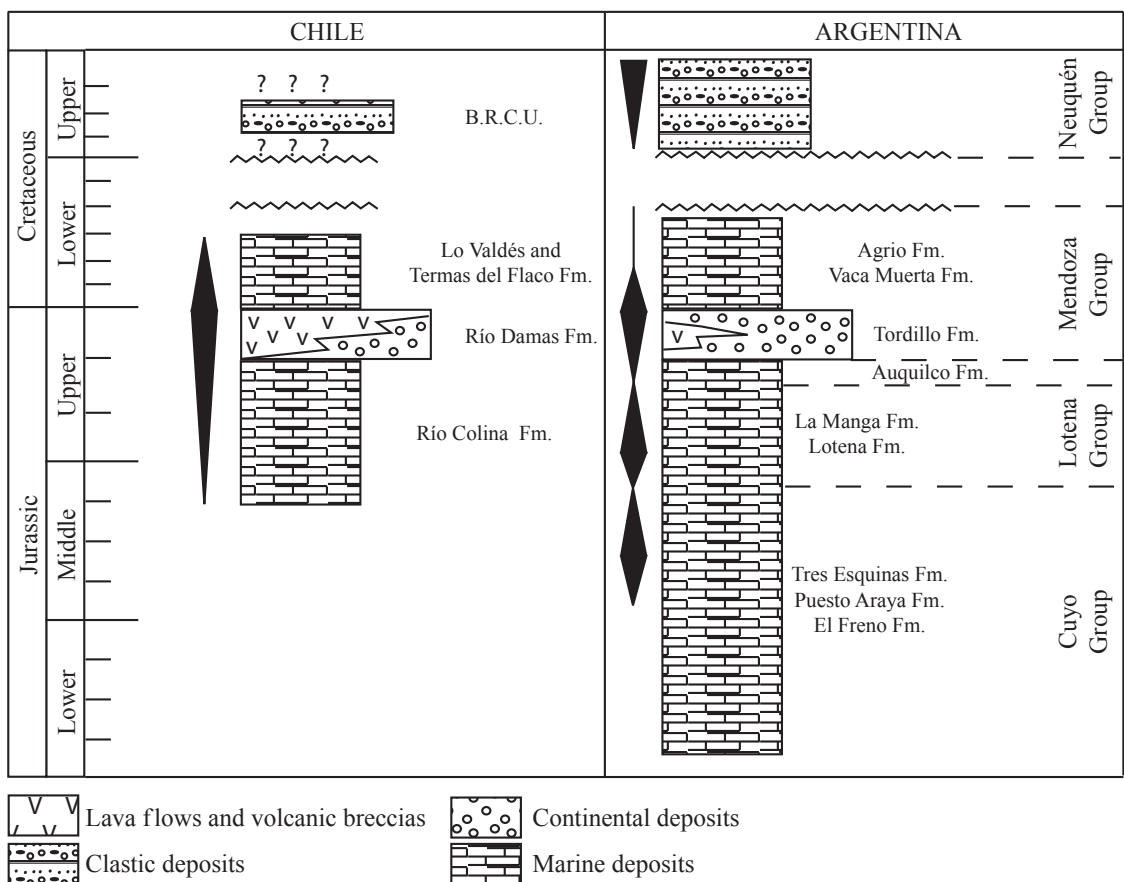


FIG. 4. Tectonostratigraphic chart of the Jurassic to Lower Cretaceous back-arc sequences cropping out in the studied areas in Chile (Río Volcán and Baños del Flaco) and Argentina (Loma de las Vegas and East of Valle de Las Leñas).

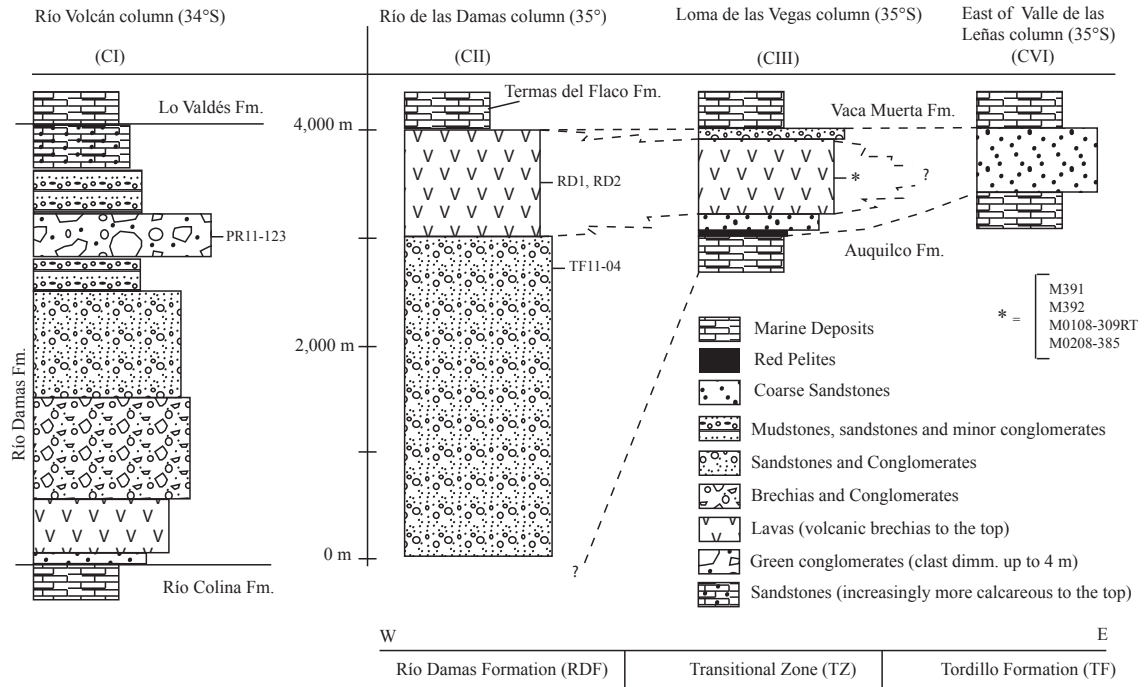


FIG. 5. Schematic sections of the Río Damas-Tordillo Formation at the sampling locations, showing the stratigraphic position of the continental deposits at 34° and 35°S, and their lateral variations at 35°S. Transitional zone is equivalent to the ‘lateral intercalation zone’ defined by Mescua (2011). Thickness of the restored sections are reported in the work of Calderón (2008) for the Río Volcán area, Charrier *et al.* (1996) for the Termas del Flaco area and Mescua (2011) for the Loma de las Vegas and east of Valle de Las Leñas areas. Note the thickness of the breccias and conglomerates beds at the top of Río Volcán section in contrast to the scarce clastic material in the Termas del Flaco section.

the development of the Andean fold and thrust belt. In the studied areas (Figs. 2 and 3), the Río Damas Formation crops out in the backlimb of great anticlines of 10 km of wavelength, and the beds have moderate to high dips, being locally subvertical. The Tordillo Formation crops out in smaller folds (5 to 1 km wavelength), with dips under 45°. A major unconformity separates Mesozoic units from the much less deformed Cenozoic deposits (Charrier *et al.*, 2007; Mescua *et al.*, 2012).

3. Petrography of the Río Damas-Tordillo Formation Volcanic Components

The volcanic rocks of the Río Damas-Tordillo Formation are mainly red brownish to dark purple porphyritic, sometimes vesicular, lava flows and sills. Intercalations of volcanic breccias bearing fragments of andesitic lavas of 1 to 4 m in size and more fine grained pyroclastic deposits can be found along the frontier of Chile and Argentina. The samples analyzed

in this work correspond mainly to basaltic andesites and minor andesites.

3.1. Petrography of the primary components

The studied lavas have a porphyritic texture, with up to 35% of phenocrysts content. Euhedral plagioclase phenocrysts up to 4 cm in size represent *ca.* 70% of the phenocrysts content of the rocks. Precise petrographic determination of their composition is difficult because of the alteration. However, the Michell-Levy method was applied to eight single crystals in one fresh sample (sample M391, figure 5), indicating that the plagioclases are andesine in composition (An_{38}). 25% of the phenocrysts correspond to eu- and sub-hedral clinopyroxene crystals; and the remaining 5% of the phenocrysts are Fe-Ti oxides, mostly magnetite with subordinate ilmenite. The groundmass has an intersertal texture and it is composed of plagioclase microlites, Fe-Ti oxides and alteration minerals.

3.2. Petrography of the alteration components

All the volcanic and sedimentary rocks of the Río Damas-Tordillo Formation are altered to some extent, as a consequence of burial and contact metamorphism (Calderón, 2008; Levi *et al.*, 1989; Oliveros *et al.*, 2008; Robinson *et al.*, 2004). The alteration in general is very penetrative, partly hiding the primary features of the rock, particularly at the contact between beds, vesicular portions or highly fractured zones of the lava flows and in the fine matrix of volcanic and sedimentary rocks. Central portion of lava flows or restricted domains within the sedimentary rocks are often less affected by the alteration processes. The observed alteration minerals are: prehnite, pumpeyllite, chlorite, epidote, titanite, actinolite, calcite, quartz, white mica (sericite), albite and K-feldspar, defining a typical mineralogy of prehnite-pumpeyllite facies in concordance with the reported by others authors for this Andean region (Calderón, 2008; Levi *et al.*, 1989; Oliveros *et al.*, 2008; Robinson *et al.*, 2004). The fine grained volcanic litharenites from the easternmost outcrops of the Río Damas Formation, in the head of the Maipo river valley at 34°15'S, bear scarce calcite and chlorite as secondary mineral phases, indicating that the alteration degree diminishes eastward (Charrier, 1981).

Plagioclase phenocrysts, microlites and fragments in the volcanic rocks are partial to completely replaced by a mixture of sericite, clays and minor albite and epidote. The clinopyroxenes are often completely replaced by chlorite and titanite, but fresh phenocrysts can be observed in the central part of the lava flows. The components of the matrix or groundmass are often replaced by chlorite, titanite and clays. Finally, the vesicles of the lavas are filled with calcite, quartz, prehnite, pumpeyllite, and it is possible to recognize multiple stages of mineral formation.

4. Samples and Methods

Seven slightly altered lava samples, one sample of sandstone and one sample of a granitic clast from a polymictic sedimentary breccia of the Río Damas-Tordillo Formation were collected for analysis (Fig. 1).

4.1. Whole rock analysis

Major and trace element concentrations were determined using standard XRF and ICP-MS

techniques at University of Arizona. Major elements were performed on a HORIBA XRF instrument on powdered pressed pellets; analytical precision is about 2% of the reported value. Whole-rock trace elements were measured in solution using a Thermo Element X-Series II single collector ICP-MS at the University of Arizona (Rossel *et al.*, 2013). Approximately 5 mg of sample were dissolved in about 7 ml of concentrated HF-HNO₃ mixtures, dried down and redissolved in a mild 1% nitric acid before being analyzed. Several 1-10 ppm internal standards were used for different elements. Columbia River Basalt material standard material was used as an external standard. Analysis routines involved 30 individual measurements of isotopes free of interferences. Typical analytical errors are 3-5% of the reported values.

Sr and Nd isotopic analyses were performed at the University of Arizona (following procedures outlined in Otamendi *et al.*, 2009) on a VG Sector 54 multicollector TIMS instrument, the Sr isotopic ratios were normalized to ⁸⁶Sr/⁸⁸Sr=0.1194, whereas the Nd isotopic ratios were normalized to ¹⁴⁶Nd/¹⁴⁴Nd=0.7219. Estimated analytical $\pm 2\sigma$ uncertainties are: ⁸⁷Sr/⁸⁶Sr=0.001% and ¹⁴³Nd/¹⁴⁴Nd=0.001%. Ten analyses of standard SRM 987 analyzed during the course of this study yielded mean ratios of ⁸⁷Sr/⁸⁶Sr=0.710264 \pm 7 and six analyses of Nd standard La Jolla Nd yielded a mean ratio of ¹⁴³Nd/¹⁴⁴Nd=0.511848 \pm 11. Procedural blanks averaged from five determinations were: Sr-150 pg, and Nd-5.5 pg.

The common isotopes of Pb were analyzed on the sample aliquots from which Rb-Sr and Sm-Nd isotopes were analyzed following the procedures described in Drew *et al.* (2009). Separate batches of dissolved samples were saved for lead chemistry. Pb was extracted on Sr-spec columns (Drew *et al.*, 2009). Lead isotope analysis was conducted on a GV Instruments multicollector inductively coupled plasma mass spectrometer (MC-ICP-MS) at the University of Arizona (Thibodeau *et al.*, 2007). Samples were introduced into the instrument by free aspiration with a low-flow concentric nebulizer into a water-cooled chamber. A blank, consisting of 2% HNO₃, was run before each sample. Before analysis, all samples were spiked with a Tl solution to achieve a Pb/Tl ratio of ~10. Throughout the experiment, the standard National Bureau of Standards(NBS)-981 was run to monitor the stability of the instrument.

4.2. U-Pb geochronology of igneous and detrital zircons

Zircons were extracted from a granitic clast in a sedimentary breccia (PR-11-123) and from a sandstone (TF11-04) by crushing, milling, gravitational separation and heavy liquids treatment. At least 50 crystals were randomly selected (regardless their size, form or color) using a stereomicroscope and then mounted in 25 mm epoxy and polished.

U-Pb geochronology of zircons was conducted by LA-MC-ICP-MS at the Arizona LaserChron Center (Gehrels *et al.*, 2008). The analyses involve ablation of zircon with a New Wave/Lambda Physik DUV193 Excimer laser (operating at a wavelength of 193 nm) using a spot diameter of 25 or 35 μm . The ablated material is carried with helium gas into the plasma source of a GV Instruments Isoprobe, which is equipped with a flight tube of sufficient width that U, Th, and Pb isotopes are measured simultaneously. All measurements were made in static mode, using Faraday detectors for ^{238}U and ^{232}Th , an ion-counting channel for ^{204}Pb , and either Faraday collectors or ion counting channels for $^{208-206}\text{Pb}$. Ion yields are $\sim 1 \text{ mV ppm}^{-1}$. Each analysis consists of one 20 s-integration on peaks with the laser off (for backgrounds), twenty 1 s-integrations with the laser firing, and a 30 s delay to purge the previous sample and to prepare for the next analysis. The ablation pit is $\sim 15 \mu\text{m}$ in depth.

For each analysis, the errors in determining $^{206}\text{Pb}/^{238}\text{U}$ and $^{206}\text{Pb}/^{204}\text{Pb}$ result in a measurement error of $\sim 1\%$ (at 2σ level) in the $^{206}\text{Pb}/^{238}\text{U}$ age. The errors in measurement of $^{206}\text{Pb}/^{207}\text{Pb}$ and $^{206}\text{Pb}/^{204}\text{Pb}$ also result in $\sim 1\%$ (2σ) uncertainty in age for grains that are $>1.0 \text{ Ga}$, but are substantially larger for younger grains due to low intensity of the ^{207}Pb signal. For most analyses, the crossover in precision of $^{206}\text{Pb}/^{238}\text{U}$ and $^{206}\text{Pb}/^{207}\text{Pb}$ ages occurs at $\sim 1.0 \text{ Ga}$. Common Pb correction is accomplished by using the measured ^{204}Pb and assuming an initial Pb composition from Stacey and Kramers (1975) (with uncertainties of 1.0 for $^{206}\text{Pb}/^{204}\text{Pb}$ and 0.3 for $^{207}\text{Pb}/^{204}\text{Pb}$). The measurement of ^{204}Pb is unaffected by the presence of ^{204}Hg because backgrounds are measured on peaks (thereby subtracting any background ^{204}Hg and ^{204}Pb), and because very little Hg is present in the argon gas. Interelement fractionation of Pb/U is generally $\sim 20\%$, whereas fractionation of Pb isotopes is generally $<2\%$. In-run analysis of fragments of a large Sri Lanka zircon

crystal (generally every fifth measurement) with known age of $564 \pm 4 \text{ Ma}$ (2σ error) is used to correct for this fractionation (see Gehrels *et al.*, 2008). The uncertainty resulting from the calibration correction is generally $\sim 1\%$ (2σ) for both $^{206}\text{Pb}/^{207}\text{Pb}$ and $^{206}\text{Pb}/^{238}\text{U}$ ages.

The reported ages are determined from the weighted mean of the $^{206}\text{Pb}/^{238}\text{U}$ ages of the concordant and overlapping analyses (Ludwig, 2003). The reported uncertainty (labeled ‘mean’) is based on the scatter and precision of the set of $^{206}\text{Pb}/^{238}\text{U}$ or $^{206}\text{Pb}/^{207}\text{Pb}$ ages, weighted according to their measurement errors (shown at 1σ). The systematic error, which includes contributions from the standard calibration, age of the calibration standard, composition of common Pb and U decay constants, is generally $\sim 1-2\%$ (2σ).

5. Results

5.1. Whole Rock Chemistry

The major and trace elements abundances for the studied volcanic rocks are listed in the Table 1.

5.1.1. Alteration

The alteration that affects the Mesozoic and Cenozoic volcano-sedimentary rocks cropping out in the Andes of Central Chile, which can be very pervasive, is the result of the combination of very low-grade burial metamorphism (Prenlite-Pumpellyite facies), and contact metamorphism and hydrothermal alteration related to the intrusion of numerous granitic stocks of Miocene age (Calderón, 2008; Levi *et al.*, 1989; Muñoz *et al.*, 2009; Oliveros *et al.*, 2008; Robinson *et al.*, 2004; Thiele, 1980).

Although the studied samples exhibited slight to moderate evidences of alteration, the afore mentioned processes were likely responsible for an increase in the amount of total alkalis as it is inferred from the comparison between the total alkalis *versus* silica classification plot (TAS) and the diagram for altered rocks which plots Zr/Ti *versus* Nb/Y (Fig. 6). In the first diagram, an important number of samples plot in the trachy-andesite and trachy-dacite fields, whereas in the diagram for altered rocks the samples plot in the basalts, basaltic andesites-andesites and dacites-ryolites fields. Therefore, the alkali enrichment of the rocks is likely due to the albitionization/sericitization of the plagioclase phenocrysts or

microlites and clinopyroxene chloritization, not to magmatic processes. The samples also show higher dispersion for large ion lithophile elements (LILE) than high field strength elements (HFSE) (Fig. 7), suggesting that HFSE are less mobile during alteration processes, and therefore more reliable for determining the petrogenesis of the rocks. The light REE (LREE) are enriched in comparison to the heavy REE (HREE), a pattern that is independent of the alteration degree of the sample (Fig. 7).

The most altered sample is MO208-385. The plagioclase and clinopyroxene phenocrysts are completely replaced by sericite and clays and chlorite, respectively, the matrix is chloritized and the numerous vesicles filled with calcite, chlorite, pumeyllite, prehnite and quartz. It has low abundances of Ba and Th, and high concentrations of Cs (Table 1). The patterns for the REE and HFSE, are similar to those of the less altered rocks, but in general the concentration of these elements is lower in MO208-385.

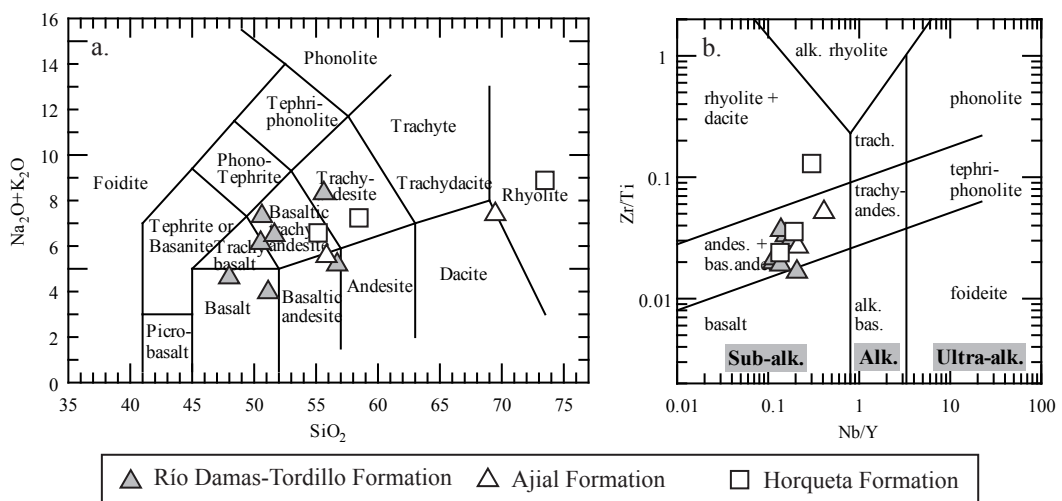


FIG. 6. **a.** Total alkali versus silica classification diagram (TAS, Le Maitre, 1989); **b.** Nb/Y versus Zr/Ti classification diagram for altered volcanic rocks (Pearce, 1996 after Winchester and Floyd, 1977). Data from Ajial and Horqueta Formations in the Coastal Cordillera of Central Chile are after Vergara *et al.* (1995).

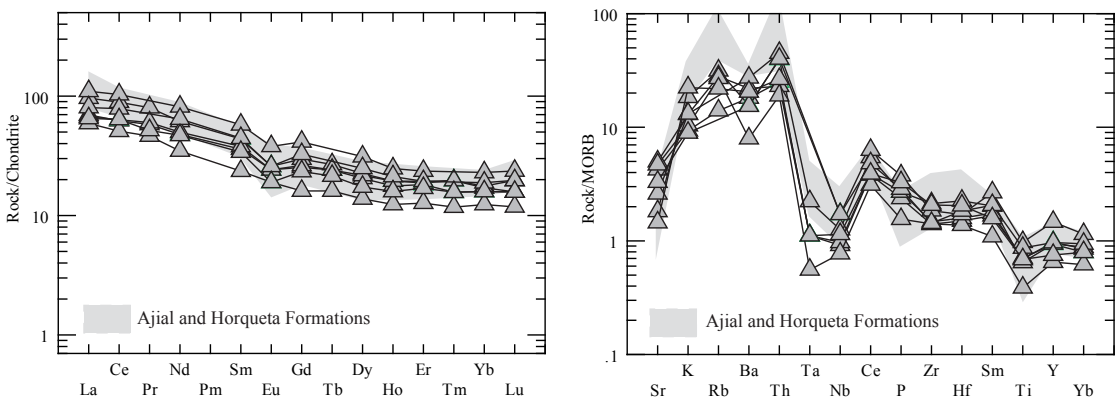


FIG. 7. Chondrite-normalized Rare Earth elements (REE) patterns and MORB-normalized trace elements patterns for volcanic rocks from the Río Damas Formation in the principal cordillera. Data from Ajial and Horqueta Formations in the Coastal Cordillera of Central Chile are after Vergara *et al.* (1995). Normalizing values are from Sun and McDonough (1989) (Chondrite) and Pearce (1983) (MORB).

TABLE 1. MAJOR AND TRACE ELEMENT CHEMISTRY OF UPPER JURASSIC BACK-ARC VOLCANIC ROCKS IN THE STUDIED UNITS.

Área	Cordón del Burrero				Termas del Flaco		Paso Vergara
Sample	M391	M392	M0108-309RT	M0208-385	RD-1	RD-2	TA-02
SiO ₂	48.77	55.63	50.58	56.78	51.53	51.11	50.78
TiO ₂	1.06	0.97	1.04	0.58	1.46	1.30	1.03
Al ₂ O ₃	17.56	16.60	16.90	17.69	15.91	17.35	15.50
FeO(t)	9.25	6.04	8.78	5.95	11.70	9.32	7.88
MnO	0.11	0.12	0.20	0.14	0.09	0.13	0.19
MgO	4.65	2.30	4.93	4.57	5.42	3.70	4.33
CaO	8.90	4.95	5.50	4.85	1.12	8.75	3.58
Na ₂ O	3.29	5.78	4.32	3.73	4.71	2.84	4.08
K ₂ O	1.40	2.76	1.95	1.55	1.97	1.34	3.35
P ₂ O ₅	0.29	0.33	0.33	0.19	0.46	0.35	0.40
LOI	2.88	1.82	3.91	2.40	4.41	2.83	8.78
Total	98.16	97.29	98.44	98.43	98.78	99.02	99.90
#Mg	47.26	40.45	50.02	57.80	45.23	41.44	49.46
Rb	28.0	63.0	56.0	54.0	-	-	43.7
Cs	0.3	0.2	-	3.7	-	-	2.4
Pb	12.0	6.0	11.0	-	-	-	3.4
Ba	362.0	312.0	440.0	159.0	546.0	307.0	410.2
Th	5.0	7.9	4.6	3.8	9.0	8.0	5.3
U	1.4	2.2	1.3	1.0	-	-	2.0
Nb	3.2	4.4	3.4	2.7	6.0	6.0	4.0
Ta	0.2	0.4	0.2	0.1	-	-	0.2
Sr	508.0	218.0	598.0	562.0	312.0	395.0	173.9
Zr	126.0	192.0	133.0	127.0	166.0	129.0	186.1
Hf	3.6	5.4	3.8	3.3	4.1	4.4	4.9
Sc	32.0	28.0	29.0	16.0	35.0	27.0	10.2
V	284.0	246.0	275.0	145.0	338.0	278.0	159.6
Cr	-	40.0	-	-	8.0	3.0	37.3
Ni	-	-	-	-	9.0	7.0	21.0
Zn	80.0	50.0	170.0	60.0	361.0	111.0	159.7
Y	28	28.2	29.2	19.5	44	29	22.5
La	16.5	22.8	15.9	14.0	26.0	19.0	15.4
Ce	38.1	54.4	38.8	31.1	63.0	48.0	39.0
Pr	5.5	7.6	5.7	4.4	-	-	4.9
Nd	22.3	28.7	23.3	16.2	38.0	30.0	21.9
Sm	5.5	6.7	5.8	3.6	8.8	6.8	5.2
Eu	1.4	1.5	1.4	1.1	2.2	1.5	1.1
Gd	5.2	6.1	5.4	3.3	8.5	6.7	4.8
Tb	0.9	1.0	0.9	0.6	-	-	0.8
Dy	5.2	5.7	5.5	3.5	7.9	6.3	4.4
Ho	1.0	1.1	1.1	0.7	1.4	1.2	0.9
Er	3.0	3.1	3.2	2.1	3.9	3.2	2.8
Tm	0.4	0.5	0.5	0.3	-	-	0.4
Yb	2.7	3.0	2.9	2.1	3.9	3.2	2.7
Lu	0.4	0.5	0.4	0.3	0.6	0.5	0.4
ΣREE	108.3	142.6	110.8	83.3	164.2	126.3	104.7

(oxides in wt.%, trace elements in ppm)

5.1.2. Major elements

The SiO₂ content (anhydrous base) in the rocks of the Río Damas-Tordillo Formation varies between 48.77% and 56.78%. The total alkalis vary between 4.28 and 8.54%, although partly due to alteration processes. In general, the lavas have low MgO (2.30-5.42%) and high Al₂O₃ (15.91-17.69%) contents. The #Mg¹ of the rocks varies between 40.45 and 57.80%, indicating differentiation processes in its evolution. The contents of MgO, TiO₂, Al₂O₃, CaO and FeO_t apparently decrease with increasing SiO₂, this is probably related to the fractionation of mineral phases such as magnetite, olivine, plagioclase and clinopyroxene, which are observed in the samples. On the contrary, the alkalis, K₂O and Na₂O, increase with increasing SiO₂, which is due to the incompatible behavior of these elements during the early stages of magma differentiation.

Considering the high dispersion of major elements including silica, oxides are not useful as petrogenetic tools in the studied rocks, and they will be only used for comparison purposes in this work.

5.1.3. Trace elements

MORB-normalized multielement spider diagrams exhibit similar patterns for all the studied samples of the Río Damas-Tordillo Formation (Fig. 7), with enrichment in LILE compared to HFSE. The LILE concentrations are quite variable since these elements are more mobile during alteration and incompatible during early stages of crystal fractionation. The lavas have marked negative Nb-Ta-Ti and positive Pb anomalies. Zr and Th have well defined positive correlations with SiO₂ content, but with higher dispersion for Zr. Sr has a high dispersion but apparent negative correlation

with SiO₂, probably because of the replacement of CaO during plagioclase fractionation. V has a well defined negative correlation with SiO₂, likely due to fractionation of mineral phases such as magnetite or ilmenite. A similar behavior should be expected for elements like Cr and Ni, although they were not measured in all samples.

Chondrite-normalized REE patterns exhibit a negative slope, with significant enrichment in light REE (LREE) compared to the heavy REE (HREE). Chondrite-normalized La/Yb ratios ([La/Yb]_n) range between 4 and 6. The HREE show a rather flat pattern and have abundances between 12 and 23 times the chondritic value. Incipient Eu negative anomalies are present in all the studied rocks, except for the sample MO208-385.

5.1.4. Isotopes

Three samples of the Río Damas-Tordillo Formation were analyzed for Nd, Sr and Pb isotopes; the results are listed in the Table 2.

Nd and Sr isotopic ratios normalized to 150 Ma (Fig. 8a) show values in a restricted range between 0.51282 and 0.51253 and 0.7040 and 0.7044 respectively. On the other hand, the isotopic ratios of Pb (²⁰⁶Pb/²⁰⁴Pb=18.57-18.96; ²⁰⁷Pb/²⁰⁴Pb=15.61-15.64; ²⁰⁸Pb/²⁰⁴Pb=38.52-39.04) show a wider range (Fig. 8b) of values but still in the range of rocks of the Jurassic volcanic arc of northern Chile (Kramer *et al.*, 2004; Lucassen *et al.*, 2006).

5.2. U-Pb Geochronology

The results of U-Pb dating of magmatic and detrital zircons in rocks from the Río Damas-Tordillo Formation are listed in Table 3.

TABLE 2. Sr, Nd AND Pb ISOTOPIC COMPOSITION OF RÍO DAMAS-TORDILLO FORMATION VOLCANIC ROCKS.

Sample	⁸⁷ Sr/ ⁸⁶ Sr	⁸⁷ Sr/ ⁸⁶ Sr(i)	¹⁴³ Nd/ ¹⁴⁴ Nd	¹⁴³ Nd/ ¹⁴⁴ Nd(i)	εNd	εNd(i)	²⁰⁶ Pb/ ²⁰⁴ Pb	²⁰⁷ Pb/ ²⁰⁴ Pb	²⁰⁸ Pb/ ²⁰⁴ Pb
M391	0.7044	0.7040	0.51318	0.51282	25.40	7.2	18.57	15.61	38.52
M392	0.7061	0.7044	0.51278	0.51253	6.73	1.7	18.77	15.64	38.79
TA-02	0.7057	0.7043	0.51273	0.51258	4.37	2.7	18.96	15.63	39.04

¹(MgOwt%/PM_{MgO})/((MgOwt%/PM_{MgO})+(FeOwt%/PM_{FeO}))*100

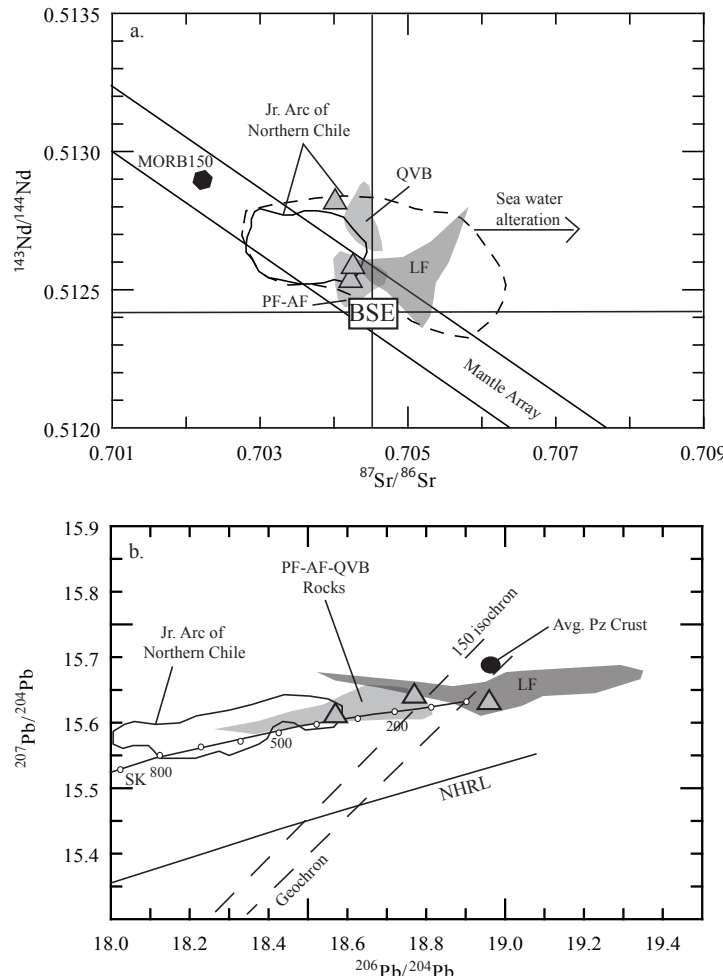


FIG. 8. a. $^{87}\text{Sr}/^{86}\text{Sr}$ versus $^{143}\text{Nd}/^{144}\text{Nd}$ diagram from samples of the Río Damas Formation. **BSE:** Bulk Silica Earth, ages corrected for in situ decay at 150 Ma. Dashed line shows isotopic composition of the Jurassic arc rocks in northern Chile and heavy line shows high density (>95%) of published data these rocks; MORB 150 is actual MORB corrected for *in situ* decay, gray fields are from Upper Jurassic back-arc rocks in northern Chile; b. Pb isotopic ratios for volcanic rocks of the Río Damas Formation. **SK:** The Stacey and Kramer (1975) curve of common Pb growth for the average Earth. **NHRL:** Northern Hemisphere Reference Line after Hart (1984); heavy line shows isotopic composition of the Jurassic arc rocks in northern Chile (>90% of published data), gray fields are from Upper Jurassic back-arc rocks in northern Chile. The 150-Ma isochron and the geochron were calculated following the procedures of Stacey and Kramer (1975) and Faure and Mesing (2005); **QVB:** Quebrada Vicuña Beds; **PF:** Picudo Formation; **AF:** Algarrobal Formation and **LF:** Lagunillas Formation. Arc isotopic data after Kramer *et al.* (2004), Lucassen and Franz (1994), Lucassen *et al.* (2006) and Rossel *et al.* (2013). Upper Jurassic back-arc isotopic data after Rossel *et al.* (2013). Average Paleozoic Crust (Av. Pz Crust) data after Lucassen *et al.* (2002).

Sample PR-11-123 is a granitic fragment extracted from the polymictic breccia in the top of the Río Volcán section (Fig. 5) that yielded a Carboniferous age of 333.1 ± 6.0 Ma (Fig. 9a). The younger analyzed zircons in this sample probably reflect a Pb loss or accidental crystals.

Sample TF11-04 is a red sandstone collected at the top of the sedimentary part in the Termas del Flaco section, but below the volcanic rocks of the sequence (Fig. 5). A total of the 92 zircons grains were analyzed (Table 3). The distribution of the ages is characterized as unimodal with a peaks *ca.* 158 Ma. There are two isolated ages at 415 Ma. The calculated mean age of the youngest five grains, that overlap in age at 2σ , yields a maximum depositional age of 146.4 ± 4.4 Ma (Fig. 9b), for the clastic sediments of the Río Damas-Tordillo Formation in this area.

6. Discussion

6.1. Age and provenance of the Río Damas-Tordillo Formation.

The age of the Río Damas-Tordillo Formation has been commonly assigned to the Kimmeridgian based on its stratigraphic position between Oxfordian and Tithonian-Huaterivian marine fossiliferous deposits (Klohn, 1960; Legarreta y Uliana, 1999; Thiele, 1980). However, the maximum Late Tithonian depositional age of 146.4 ± 4.4 Ma obtained on the base of the youngest group of zircons with concordant ages in sample TF11-04, which underlies the volcanic succession at the Río de las Damas area, is younger than the age constrained by the fossiliferous content of the lowest part of the overlying Lo Valdés, Baños

TABLE 3. SUMMARY OF U-Pb LA-MC-ICP-MS DATA FOR DETRITAL ZIRCON. PREFERRED AGE (GRAY COLUMN) IS EITHER THE $^{207}\text{Pb}/^{206}\text{Pb}$ OR THE $^{238}\text{U}/^{206}\text{Pb}$ AGE WITH THE LOWEST DEGREE OF DISCORDANCE RELATIVE TO THE CONCORDIA LINE (*i.e.*, 1σ error).

Sample and spot #	U	Th/U	$^{238}\text{U}/^{206}\text{Pb}$	$\pm 1\sigma$	$^{207}\text{Pb}/^{206}\text{Pb}$	$\pm 1\sigma$	$^{206}\text{Pb}/^{238}\text{U}$	$\pm 1\sigma$	$^{207}\text{Pb}/^{206}\text{Pb}$	$\pm 1\sigma$	Preferred	$\pm 1\sigma$
	[ppm]			[%]		[%]	Age	[Ma]		[Ma]	Age	[Ma]
PR-11-123-1	100	1.3	0.0525	2.1	18.8228	7.6	330.0	6.9	334.2	171.4	330.0	6.9
PR-11-123-1R	14	2.6	0.0552	8.8	22.7329	63.6	346.4	29.8	-111.3	1738.5	346.4	29.8
PR-11-123-2C	227	1.0	0.0544	1.1	18.9113	2.7	341.6	3.7	323.6	61.3	341.6	3.7
PR-11-123-3C	579	2.6	0.0548	1.6	18.6625	1.3	343.7	5.5	353.6	29.1	343.7	5.5
PR-11-123-3R	262	4.0	0.0550	2.2	18.4121	2.0	345.2	7.4	384.0	45.4	345.2	7.4
PR-11-123-4C	333	1.1	0.0502	1.6	19.8328	3.2	315.8	4.8	214.5	74.0	315.8	4.8
PR-11-123-4R	576	1.6	0.0499	2.2	19.0104	1.6	313.9	6.6	311.7	36.3	313.9	6.6
PR-11-123-5C	168	3.7	0.0523	1.3	19.5149	3.9	328.5	4.1	251.8	89.5	328.5	4.1
PR-11-123-5R	221	2.6	0.0533	2.0	19.0126	2.0	335.0	6.5	311.4	45.3	335.0	6.5
PR-11-123-6C	275	0.5	0.0094	3.4	20.9155	9.0	60.4	2.1	89.9	214.8	60.4	2.1
PR-11-123-6R	274	0.5	0.0100	5.9	18.8785	12.8	63.8	3.8	327.5	291.7	63.8	3.8
PR-11-123-7C	114	1.2	0.0540	2.1	19.3769	4.7	339.0	6.8	268.1	107.0	339.0	6.8
PR-11-123-7R	122	1.9	0.0575	3.3	19.4626	2.3	360.6	11.7	258.0	53.5	360.6	11.7
PR-11-123-8C	66	1.4	0.0565	3.5	19.2067	9.4	354.5	12.1	288.3	216.0	354.5	12.1
PR-11-123-8R	92	1.7	0.0546	4.3	19.4018	5.7	342.8	14.4	265.1	130.4	342.8	14.4
PR-11-123-9C	93	1.2	0.0480	1.6	19.4508	6.6	302.2	4.9	259.3	152.1	302.2	4.9
PR-11-123-9R	217	0.9	0.0486	1.5	19.3005	3.0	305.6	4.4	277.1	68.4	305.6	4.4
PR-11-123-10C	101	1.2	0.0540	1.8	18.8729	6.5	339.3	6.0	328.2	147.6	339.3	6.0
PR-11-123-10R	97	1.5	0.0544	1.6	19.6292	7.0	341.6	5.2	238.3	161.0	341.6	5.2
PR-11-123-11C	239	1.6	0.0536	1.8	18.9899	3.4	336.7	5.9	314.2	76.6	336.7	5.9
PR-11-123-11R	239	2.2	0.0543	1.7	18.7253	3.2	340.8	5.8	346.0	73.4	340.8	5.8
PR-11-123-12C	516	5.2	0.0529	2.1	18.9022	1.4	332.3	6.8	324.7	32.0	332.3	6.8
PR-11-123-12R	426	5.0	0.0550	1.6	19.0728	1.8	344.9	5.5	304.3	40.1	344.9	5.5
PR-11-123-13C	116	2.1	0.0480	2.1	18.3738	8.5	301.9	6.3	388.7	190.0	301.9	6.3
PR-11-123-13R	261	4.2	0.0483	4.2	19.1231	2.6	304.0	12.4	298.2	58.5	304.0	12.4
PR-11-123-14C	121	2.9	0.0538	2.2	19.0948	2.2	337.6	7.2	301.6	50.3	337.6	7.2
PR-11-123-14R	151	6.8	0.0521	6.6	18.7119	6.2	327.6	21.0	347.6	140.1	327.6	21.0
PR-11-123-15C	103	2.6	0.0536	4.5	20.1394	7.8	336.6	14.7	178.8	182.7	336.6	14.7

Table 3 continued.

Sample and spot #	U [ppm]	Th/U	$^{238}\text{U}/^{206}\text{Pb}$	$\pm 1\sigma$ [%]	$^{207}\text{Pb}/^{206}\text{Pb}$	$\pm 1\sigma$ [%]	$^{206}\text{Pb}/^{238}\text{U}$	$\pm 1\sigma$ [Ma]	$^{207}\text{Pb}/^{206}\text{Pb}$	$\pm 1\sigma$ [Ma]	Preferred Age	$\pm 1\sigma$ [Ma]
PR-11-123-15R	131	4.4	0.0554	6.2	18.6750	6.7	347.8	20.8	352.1	151.2	347.8	20.8
PR-11-123-16C	63	1.2	0.0481	2.7	19.1422	10.4	302.6	7.9	295.9	238.6	302.6	7.9
PR-11-123-16R	70	1.2	0.0471	3.7	19.3692	12.5	297.0	10.8	269.0	288.0	297.0	10.8
PR-11-123-17C	390	1.5	0.0093	3.7	24.3699	11.9	60.0	2.2	-285.4	303.3	60.0	2.2
PR-11-123-17R	406	2.6	0.0093	2.2	22.5507	17.8	59.4	1.3	-91.5	439.6	59.4	1.3
PR-11-123-18C	148	2.0	0.0533	2.1	19.3189	5.0	334.8	7.0	274.9	114.3	334.8	7.0
PR-11-123-18R	155	2.5	0.0526	2.2	18.3669	4.5	330.3	7.2	389.5	100.6	330.3	7.2
PR-11-123-19C	98	1.5	0.0539	1.6	19.3016	7.9	338.5	5.3	277.0	180.9	338.5	5.3
PR-11-123-19R	152	1.2	0.0544	1.2	19.0097	4.0	341.2	3.9	311.8	91.3	341.2	3.9
PR-11-123-20R	403	10.5	0.0266	4.2	18.6743	4.1	169.0	7.0	352.1	92.3	169.0	7.0
PR-11-123-21C	124	2.8	0.0522	3.9	19.4985	5.0	327.7	12.4	253.7	114.3	327.7	12.4
PR-11-123-21R	228	3.8	0.0483	3.7	19.0286	3.0	304.1	10.9	309.5	67.8	304.1	10.9
PR-11-123-22C	111	1.4	0.2683	15.1	9.9677	6.5	1,532.1	205.9	1,630.1	121.5	1,630.1	121.5
PR-11-123-22R	691	10.2	0.1654	5.8	12.6634	0.7	986.9	52.9	1,171.3	13.2	1,171.3	13.2
PR-11-123-23C	752	1.2	0.0535	1.0	18.8061	1.8	336.1	3.3	336.3	40.1	336.1	3.3
PR-11-123-23R	840	1.3	0.0531	1.4	18.4368	3.9	333.8	4.6	381.0	88.1	333.8	4.6
PR-11-123-24C	283	8.7	0.0549	1.0	18.6840	3.2	344.5	3.5	351.0	73.2	344.5	3.5
PR-11-123-24R	294	9.4	0.0544	3.8	18.6638	4.4	341.4	12.8	353.4	98.8	341.4	12.8
PR-11-123-25C	188	3.6	0.1518	7.8	13.5682	2.1	911.0	66.5	1,033.3	41.9	1,033.3	41.9
PR-11-123-25R	283	8.9	0.0585	3.7	18.2815	1.9	366.7	13.2	400.0	43.4	366.7	13.2
PR-11-123-26C	475	7.0	0.0552	1.6	18.9680	1.7	346.3	5.3	316.8	38.2	346.3	5.3
PR-11-123-26R	377	2.8	0.0544	1.3	18.9474	1.7	341.5	4.3	319.2	37.7	341.5	4.3
DRH-TF11-04-01	743	1.3	0.0264	1.9	19.9867	2.5	167.9	3.1	196.6	58.4	167.9	3.1
DRH-TF11-04-02	118	1.4	0.0251	7.5	26.0025	35.3	159.9	11.9	-453.5	954.2	159.9	11.9
DRH-TF11-04-03	231	0.9	0.0230	1.8	20.6445	11.0	146.4	2.6	120.7	260.8	146.4	2.6
DRH-TF11-04-04	120	1.3	0.0247	4.5	23.9583	15.7	157.4	7.0	-242.2	398.5	157.4	7.0
DRH-TF11-04-05	133	1.2	0.0253	5.7	24.0754	20.8	161.0	9.0	-254.6	531.7	161.0	9.0

Table 3 continued.

Sample and spot #	U	Th/U	$^{238}\text{U}/^{206}\text{Pb}$	$\pm 1\sigma$	$^{207}\text{Pb}/^{206}\text{Pb}$	$\pm 1\sigma$	$^{206}\text{Pb}/^{238}\text{U}$	$\pm 1\sigma$	$^{207}\text{Pb}/^{206}\text{Pb}$	$\pm 1\sigma$	Preferred	$\pm 1\sigma$
	[ppm]			[%]		[%]	Age	[Ma]		[Ma]	Age	[Ma]
DRH-TF11-04-06	107	1.2	0.0241	4.0	23.2492	43.5	153.7	6.1	-166.9	1130.7	153.7	6.1
DRH-TF11-04-07	74	1.5	0.0252	5.2	17.7545	19.0	160.5	8.2	465.1	424.9	160.5	8.2
DRH-TF11-04-08	35	1.6	0.0246	11.8	0.9092	4,319.9	156.4	18.2	0.0	887.6	156.4	18.2
DRH-TF11-04-09	25	2.2	0.0238	14.1	23.7811	73.6	151.4	21.0	-223.5	2,159.6	151.4	21.0
DRH-TF11-04-10	60	1.9	0.0240	6.5	20.2290	35.1	153.1	9.8	168.4	843.2	153.1	9.8
DRH-TF11-04-11	58	2.1	0.0234	9.1	22.6514	33.5	149.3	13.5	-102.4	844.2	149.3	13.5
DRH-TF11-04-12	582	1.0	0.0250	1.1	20.7168	4.0	159.4	1.8	112.5	95.0	159.4	1.8
DRH-TF11-04-13	81	1.3	0.0236	6.4	28.4484	32.3	150.5	9.5	-696.6	915.5	150.5	9.5
DRH-TF11-04-14	86	1.3	0.0240	5.9	17.5954	23.4	152.8	8.9	485.1	523.3	152.8	8.9
DRH-TF11-04-15	64	1.5	0.0238	7.7	24.9313	35.2	151.3	11.5	-343.8	932.5	151.3	11.5
DRH-TF11-04-16	42	2.1	0.0235	13.4	17.6725	84.0	150.0	19.9	475.4	2,402.4	150.0	19.9
DRH-TF11-04-17	53	2.0	0.0223	11.8	5.7286	811.3	142.1	16.6	2601.9	1,414.8	142.1	16.6
DRH-TF11-04-18	71	1.3	0.0242	6.4	28.7721	44.5	153.9	9.7	-728.1	1,296.9	153.9	9.7
DRH-TF11-04-19	113	1.1	0.0237	4.4	19.6255	19.1	151.0	6.6	238.7	443.2	151.0	6.6
DRH-TF11-04-20	109	1.1	0.0237	6.5	24.8673	35.5	151.1	9.7	-337.2	939.6	151.1	9.7
DRH-TF11-04-21	80	1.5	0.0241	5.3	25.8012	29.2	153.4	8.0	-433.1	781.5	153.4	8.0
DRH-TF11-04-22	50	1.7	0.0244	10.6	17.3503	40.2	155.2	16.3	515.9	919.0	155.2	16.3
DRH-TF11-04-23	64	2.3	0.0235	4.9	25.9946	50.2	149.6	7.3	-452.7	1,399.6	149.6	7.3
DRH-TF11-04-24	82	1.4	0.0259	7.4	21.2937	18.3	165.0	12.1	47.3	441.4	165.0	12.1
DRH-TF11-04-26	55	1.6	0.0238	7.6	20.9524	36.4	151.7	11.4	85.8	890.2	151.7	11.4
DRH-TF11-04-27	85	1.9	0.0241	4.9	25.1299	43.6	153.4	7.5	-364.3	1,176.5	153.4	7.5
DRH-TF11-04-28	57	1.9	0.0235	8.9	21.4463	85.2	149.9	13.2	30.2	2,641.5	149.9	13.2
DRH-TF11-04-30	93	1.5	0.0234	8.2	22.3183	29.5	149.4	12.2	-66.2	734.3	149.4	12.2
DRH-TF11-04-31	71	1.5	0.0243	5.2	19.3555	28.2	154.5	7.9	270.6	658.2	154.5	7.9
DRH-TF11-04-32	89	1.6	0.0234	5.6	34.4345	36.5	149.2	8.2	-1259.9	1,177.7	149.2	8.2
DRH-TF11-04-33	37	1.7	0.0244	11.5	7.3632	171.0	155.3	17.6	2,174.4	100.0	155.3	17.6
DRH-TF11-04-34	55	2.7	0.0234	8.2	19.1891	50.2	149.2	12.1	290.3	1,220.9	149.2	12.1
DRH-TF11-04-35	76	1.3	0.0249	4.4	20.6699	39.5	158.3	6.9	117.9	966.5	158.3	6.9
DRH-TF11-04-36	50	1.8	0.0239	8.2	-4.5169	610.1	152.4	12.4	0.0	72.2	152.4	12.4

Table 3 continued.

Sample and spot #	U [ppm]	Th/U	$^{238}\text{U}/^{206}\text{Pb}$	$\pm 1\sigma$ [%]	$^{207}\text{Pb}/^{206}\text{Pb}$	$\pm 1\sigma$ [%]	$^{206}\text{Pb}/^{238}\text{U}$	$\pm 1\sigma$ [Ma]	$^{207}\text{Pb}/^{206}\text{Pb}$	$\pm 1\sigma$ [Ma]	Preferred Age	$\pm 1\sigma$ [Ma]
DRH-TF11-04-37	45	1.6	0.0249	10.8	32.0652	143.0	158.4	16.9	-1041.3	0.0	158.4	16.9
DRH-TF11-04-38	34	2.0	0.0244	11.9	18.0705	56.6	155.6	18.3	425.9	1372.6	155.6	18.3
DRH-TF11-04-39	48	2.1	0.0241	12.2	-6.0070	639.7	153.3	18.5	0.0	537.0	153.3	18.5
DRH-TF11-04-40	89	1.2	0.0240	4.8	23.8860	22.9	152.8	7.2	-234.6	584.6	152.8	7.2
DRH-TF11-04-41	551	0.9	0.0258	1.0	19.9390	5.8	163.9	1.7	202.1	134.8	163.9	1.7
DRH-TF11-04-42	165	1.3	0.0236	4.5	23.4158	16.9	150.6	6.6	-184.7	425.4	150.6	6.6
DRH-TF11-04-43	142	1.3	0.0241	4.5	21.7155	24.4	153.7	6.9	0.3	595.0	153.7	6.9
DRH-TF11-04-44	96	1.3	0.0241	2.2	25.0870	29.9	153.3	3.3	-359.9	788.0	153.3	3.3
DRH-TF11-04-45	46	1.7	0.0239	6.4	9.4789	222.2	152.3	9.7	1723.0	448.9	152.3	9.7
DRH-TF11-04-46	148	1.2	0.0239	3.2	22.8034	20.3	152.1	4.8	-118.9	505.8	152.1	4.8
DRH-TF11-04-48	88	1.4	0.0243	4.5	22.8172	40.1	154.7	6.9	-120.4	1,024.8	154.7	6.9
DRH-TF11-04-50	66	1.9	0.0231	9.2	28.0171	162.0	147.3	13.4	-654.4	0.0	147.3	13.4
DRH-TF11-04-51	57	2.0	0.0237	8.8	18.4251	31.3	151.2	13.1	382.4	720.2	151.2	13.1
DRH-TF11-04-52	59	1.8	0.0247	11.3	24.6712	59.6	157.6	17.5	-316.9	1,668.5	157.6	17.5
DRH-TF11-04-53	593	1.9	0.0257	1.2	20.1049	3.2	163.5	1.9	182.8	75.0	163.5	1.9
DRH-TF11-04-54	77	1.2	0.0239	7.2	27.6237	41.7	152.3	10.9	-615.7	1,180.8	152.3	10.9
DRH-TF11-04-56	47	1.9	0.0229	11.5	20.7883	37.6	145.8	16.5	104.4	917.8	145.8	16.5
DRH-TF11-04-57	92	1.2	0.0232	10.1	37.8593	46.7	147.7	14.8	-1568.8	1,648.9	147.7	14.8
DRH-TF11-04-58	68	1.2	0.0235	8.8	28.5826	67.6	150.0	13.0	-709.7	2,107.7	150.0	13.0
DRH-TF11-04-59	47	1.7	0.0238	9.2	25.2388	55.1	151.6	13.7	-375.5	1,534.2	151.6	13.7
DRH-TF11-04-60	98	1.4	0.0230	5.7	23.0943	25.4	146.9	8.3	-150.3	639.8	146.9	8.3
DRH-TF11-04-61	754	1.4	0.0253	1.7	19.9679	2.8	161.2	2.7	198.7	66.1	161.2	2.7
DRH-TF11-04-62	54	1.3	0.0240	10.0	21.7219	42.0	153.1	15.1	-0.4	1,055.2	153.1	15.1
DRH-TF11-04-63	46	2.1	0.0233	12.1	35.4644	291.1	148.6	17.8	-1353.5	0.0	148.6	17.8
DRH-TF11-04-64	68	1.6	0.0248	5.6	19.9352	17.7	158.2	8.7	202.5	412.6	158.2	8.7
DRH-TF11-04-65	47	1.7	0.0233	11.8	24.8110	41.3	148.6	17.3	-331.4	1,103.4	148.6	17.3
DRH-TF11-04-66	116	1.3	0.0248	6.8	17.2881	18.9	158.1	10.6	523.8	418.5	158.1	10.6
DRH-TF11-04-67	79	1.8	0.0245	4.7	29.3404	39.1	156.1	7.2	-783.1	1,141.0	156.1	7.2
DRH-TF11-04-68	56	1.1	0.0236	9.3	22.8353	45.9	150.7	13.8	-122.4	1,188.8	150.7	13.8

Table 3 continued.

Sample and spot #	U [ppm]	Th/U	$^{238}\text{U}/^{206}\text{Pb}$	$\pm 1\sigma$ [%]	$^{207}\text{Pb}/^{206}\text{Pb}$	$\pm 1\sigma$ [%]	$^{206}\text{Pb}/^{238}\text{U}$	$\pm 1\sigma$ [Ma]	$^{207}\text{Pb}/^{206}\text{Pb}$	$\pm 1\sigma$ [Ma]	Preferred Age	$\pm 1\sigma$ [Ma]
DRH-TF11-04-69	73	1.2	0.0243	5.7	24.4583	38.0	154.7	8.7	-294.7	1001.3	154.7	8.7
DRH-TF11-04-70	74	1.1	0.0237	9.2	27.2725	38.9	150.8	13.8	-580.9	1086.2	150.8	13.8
DRH-TF11-04-71	49	2.2	0.0232	12.2	-1.4331	1957.6	148.1	17.9	0.0	258.0	148.1	17.9
DRH-TF11-04-72	174	1.7	0.0253	2.2	19.0882	20.5	161.1	3.5	302.4	472.5	161.1	3.5
DRH-TF11-04-73	86	1.3	0.0241	4.8	20.1474	26.5	153.5	7.3	177.9	627.7	153.5	7.3
DRH-TF11-04-74	98	1.2	0.0243	5.1	23.0649	21.4	154.5	7.7	-147.1	534.7	154.5	7.7
DRH-TF11-04-75	76	1.6	0.0236	5.3	26.0206	28.1	150.4	7.9	-455.4	752.1	150.4	7.9
DRH-TF11-04-76	62	1.7	0.0247	6.9	23.5920	35.5	157.1	10.7	-203.4	914.3	157.1	10.7
DRH-TF11-04-77	62	1.6	0.0244	8.9	16.4401	51.8	155.6	13.6	633.1	1,194.7	155.6	13.6
DRH-TF11-04-78	49	1.6	0.0244	5.9	31.1980	62.9	155.3	9.0	-960.0	2,025.8	155.3	9.0
DRH-TF11-04-79	67	1.6	0.0243	7.4	22.4175	52.3	154.8	11.3	-77.0	1,365.5	154.8	11.3
DRH-TF11-04-81	46	1.0	0.0241	11.7	17.5381	61.5	153.5	17.7	492.3	1,503.5	153.5	17.7
DRH-TF11-04-82	62	1.2	0.0285	9.2	23.4923	24.4	180.8	16.5	-192.8	617.9	180.8	16.5
DRH-TF11-04-83	86	0.9	0.0250	3.8	22.1112	23.7	159.2	5.9	-43.4	584.0	159.2	5.9
DRH-TF11-04-84	44	1.7	0.0241	7.5	24.8768	51.3	153.5	11.4	-338.2	1,405.0	153.5	11.4
DRH-TF11-04-85	57	1.4	0.0249	7.0	35.7139	42.0	158.6	11.0	-1,376.1	1,407.2	158.6	11.0
DRH-TF11-04-86	135	1.1	0.0238	2.1	22.3357	13.6	151.7	3.2	-68.1	334.5	151.7	3.2
DRH-TF11-04-88	141	1.3	0.0231	4.2	22.4801	13.5	147.2	6.1	-83.8	332.0	147.2	6.1
DRH-TF11-04-91	62	1.4	0.0244	6.6	27.6614	52.7	155.1	10.1	-619.4	1,531.2	155.1	10.1
DRH-TF11-04-92	40	1.5	0.0255	11.1	37.7432	68.2	162.2	17.7	-1,558.4	636.8	162.2	17.7
DRH-TF11-04-93	66	2.0	0.0244	6.9	38.2223	60.2	155.6	10.5	-1,601.1	398.0	155.6	10.5
DRH-TF11-04-94	97	1.7	0.0232	8.3	23.1940	30.4	147.6	12.1	-161.0	770.4	147.6	12.1
DRH-TF11-04-95	51	1.9	0.0239	6.3	26.0615	55.4	152.1	9.5	-459.5	1,570.3	152.1	9.5
DRH-TF11-04-96	29	1.8	0.0244	11.0	11.7195	50.4	155.1	16.9	1,323.0	1,048.4	155.1	16.9
DRH-TF11-04-97	84	1.6	0.0241	4.9	19.2723	24.5	153.4	7.5	280.5	567.6	153.4	7.5
DRH-TF11-04-98	68	1.6	0.0254	7.9	21.0165	26.4	161.9	12.6	78.5	635.6	161.9	12.6
DRH-TF11-04-100	38	2.0	0.0242	6.0	12.3622	30.2	154.0	9.1	1218.8	607.9	154.0	9.1
DRH-TF11-04-R33	82	2.3	0.0665	1.7	19.5027	9.3	414.9	7.0	253.2	214.5	414.9	7.0
DRH-TF11-04-R33	108	1.4	0.0666	1.9	17.8182	11.6	415.8	7.5	457.2	257.4	415.8	7.5

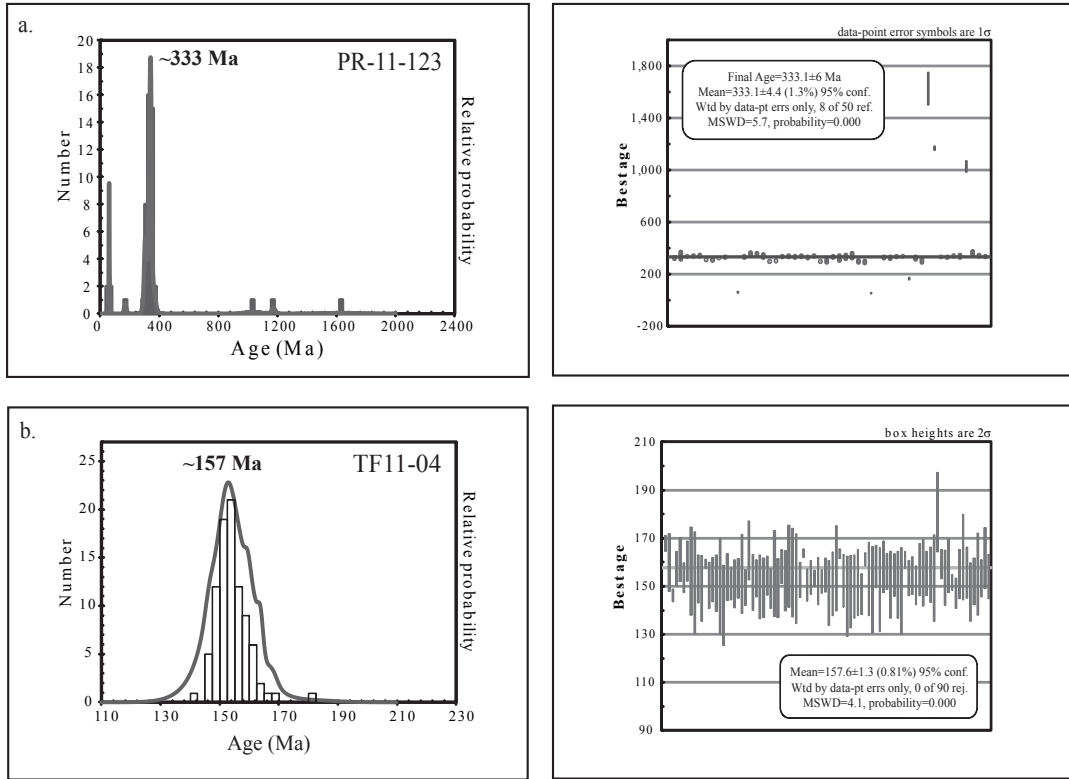


FIG. 9. Probability density plots for the preferred U-Pb ages of the two selected samples **a.** sample PR-11-123 is a granitic clast sampled from a breccia at the Río Volcán section; **b.** sample TF11-04 is a red sandstone from the top of the sedimentary sequence at the Termas del Flaco section.

del Flaco and Vaca Muerta formations. This would indicate that either the Tithonian age assigned to the fossiliferous content of the overlying units or the age assumed for the Kimmeridgian/Tithonian and Jurassic/Cretaceous boundaries are wrong. Whatever is the reason for the disagreement between the stratigraphic *versus* absolute ages of the Río Damas-Tordillo Formation, the results presented in this work are consistent with other maximum depositional ages obtained in sedimentary rocks of the same unit in the Río Volcán area, and in the southern part of the Neuquén basin, that have extended the age range of the Río Damas-Tordillo Formation into the Tithonian and, as in the study region, even into the earliest Cretaceous (Aguirre *et al.*, 2009; Cucchi *et al.*, 2005; Leanza and Hugo, 1997; Naipauer *et al.*, 2012, 2014). Therefore, the events of continental clastic deposition in the western and southern margin of the Neuquén basin would have been continuous beyond the Kimmeridgian/

Tithonian and even the Jurassic/Cretaceous boundary, practically overlapping the maximum age assigned to the overlaying marine deposits of the Vaca Muerta (early late Tithonian), and lower Lo Valdés (Tithonian) and Termas del Flaco (Late Tithonian) formations (Biro-Bagoczky, 1964, 1980; Charrier, 1981; Hallam *et al.*, 1986; Klohn, 1960; Leanza, 1981; Riccardi, 2008a, b; Thiele, 1980). The volcanic intercalation of basaltic andesitic lavas and breccias of the Río Damas-Tordillo Formation should have been emplaced in a restricted time span. Volcanic activity was probably facilitated by the presence of extensional structures related to the formation of the back-arc basin (Charrier *et al.*, 2007).

The main peak of 157.6 ± 1.3 Ma observed in the zircon population of sample TF11-04, with zircons as old as ~ 170 Ma, is consistent with the reported ages of plutonic bodies and dikes cropping out in the Coastal Cordillera of central Chile (Creixell *et al.*, 2006; Gana and Tosdal, 1996; Godoy and Loske, 1988;

Hervé *et al.*, 1988; Parada *et al.*, 1999) suggesting that this area would have been the main source of sediments feeding the back-arc basin during Upper Jurassic. This implies that an important part of the Jurassic arc domain was exhumed and eroded in Oxfordian and Tithonian times, exposing the epizonal intrusives of Middle Jurassic age, and probably the upper part of the Horqueta Formation.

The age of 333.1 ± 4.4 Ma obtained in the granitic fragment located at the top of the Río Volcán section; represents the first reported evidence for Carboniferous sources for sediments of the Río Damas-Tordillo Formation at this latitude. Recent studies of the Jurassic sequences in the southern end of the Neuquén basin have shown an important component of Paleozoic zircons in clastic sediments of Tordillo and Quebrada del Sapo formations, being interpreted as the result of erosion of the exposed basement in the Huincul High (Naipauer *et al.*, 2012). However, this topographic relief was located too far in the south (39° S) to be considered as a likely source of the sediments that accumulated at the present-day $33\text{--}35^{\circ}$ S latitudes. Sediments of late Paleozoic age have also been identified in red clastic sequences of Kimmeridgian/Tithonian age in northern Chile, and their likely sources attributed to numerous Carboniferous to Permian intrusions that crop out in the Principal Cordillera ($28\text{--}29^{\circ}$ S; Oliveros *et al.*, 2012). At the latitude of the present study, no Paleozoic plutonic rocks older than 320 Ma have been reported in the Chilean territory (Deckart *et al.*, 2014). Given the large size of the granitic clasts, their source must have been an unexposed extension of Carboniferous granitoid located near the Chile-Argentina border, rather than the present-day nearest outcrops of Paleozoic granitoids in the Coastal Cordillera between 33° and 38° S.

An important feature to take into account for the Río Damas-Tordillo Formation is the rough variations in the architecture of the stratigraphic sections in the different studied locations. As we show in figure 5, major variations in the thickness and disposition of the sedimentary and volcanic deposits can be observed in studied areas. In the Río Volcán section, the Río Damas-Tordillo Formation is composed of a basal level of mostly volcanic rocks, overlaid by a thick sequence of continental clastic sediments, while in the Termas del Flaco area the volcanic rocks overlie the clastic sedimentary deposits. Considering the important amount of large volcanic clasts of the same

composition observed in the base of the sequence, we interpret these variations as the result of a mayor tectonic cannibalism in the northern area, related to a more active faulting.

6.2. Constrains on the magma sources of the Río Damas-Tordillo volcanism

The volcanic rocks of the Río Damas-Tordillo Formation are characterized by an enrichment in LILE compared to HFSE, negative slopes in the REE diagrams, marked Nb-Ta negative and positive Ce anomalies. Such characteristics are considered as representative of subduction-related magmas (Pearce, 1982), and are typical of calc-alkaline magmatism globally (Fig. 10). In both the trace elements and REE diagrams, samples show sub-parallel trends, suggesting that they have a co-genetic origin and are the result of various degrees of differentiation from a common source.

The Mg# and the MgO contents of the analyzed samples (Table 1) indicate that no primitive magmas were analyzed and suggest previous olivine and clinopyroxene fractionation. Nb/Zr ratios (Fig. 11a) are indicative of mantle depletion as they are not influenced by fluid enrichment or fractional crystallization; Nb/Zr ratios and multielement diagrams of the analyzed samples have a narrow range similar

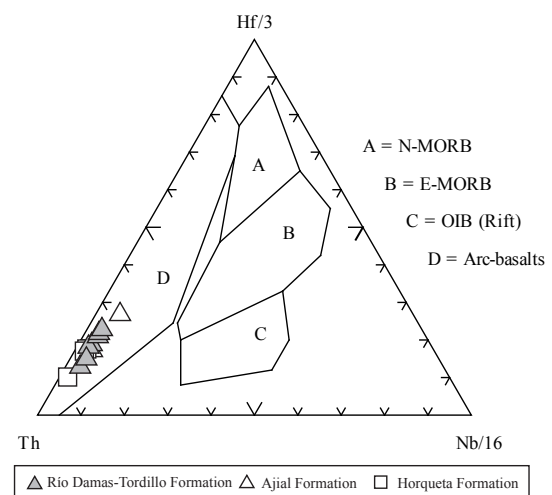


FIG. 10. Tectonic setting discrimination diagram (Cabanis and Lecolle, 1989) for volcanic (basic-intermediate) rocks in the studied area. Ajial and Horqueta Formation samples in the Coastal Cordillera in Central Chile after Vergara *et al.*, 1995.

to the normal mid-ocean ridge basalts (N-MORB) composition, and indicate either slight depletion or enrichment relative to N-MORB. Low ($\text{La}_{\text{N}}/\text{Yb}_{\text{N}}$) ratios (4-5.4) or flat REE patterns are interpreted as the result of partial melting of a depleted mantle source. $\text{Yb}_{\text{N}} > 10$ excludes the possibility of the garnet as a residual phase in the source of the Río Damas-Tordillo magmas.

The high abundances of Ba, K and Sr relative to HFSE, such as Nb and Ta, would favor the hypothesis of fluid enrichment in the slab/mantle boundary of a subduction zone (Peate *et al.*, 1997). The Th/La versus Sm/La diagram can be used to trace the addition of sediments to the mantle wedge beneath the arc (Plank, 2005), or contamination of the magmas by forearc subduction erosion or during interaction with the crust (Hildreth and Moorbath, 1988; Stern, 1991, 2011). In figure 11a, the rocks of the Río Damas-Tordillo Formation plot slightly aligned to the sediment/crust contamination vector, suggesting that this process would control the generation of the parental magmas, as it is in the case of the Jurassic Horqueta and Ajial Formations volcanism. However, given the small number of samples analyzed for this study the last observation should be taken with caution.

High variability in Ba and Sr contents probably reflects feldspar alteration, which is consistent with the pervasive sericite replacement observed in the plagioclase phenocrysts. Low abundances of Zr, V, Y and REE in sample MO208-385 could be the result of the intense alteration of the rock.

The Nd-Sr isotopic composition of the Río Damas-Tordillo Formation lavas is in the range of the Jurassic volcanic and plutonic rocks (arc magmatism) cropping out in the Coastal Cordillera in northern and central Chile (Kramer *et al.*, 2004; Lucassen *et al.*, 2006; Rossel *et al.*, 2013; Vergara *et al.*, 1995). Therefore, it is possible to infer a depleted mantle source for the magmas of the Río Damas-Tordillo Formation, similar to that of the Jurassic arc magmatism and some back-arc volcanics like the Quebrada Vicuña Beds, at 26-28°S, but different from the sources of the other back-arc units of northern Chile (Rossel *et al.*, 2013).

On the other hand, Pb isotopes show a large dispersion between the Jurassic Arc field and the average Paleozoic Crust composition (Fig. 8b). This suggests different degrees of crustal assimilation, which is more evident in this system because of the small amounts of radiogenic Pb in the mantle and

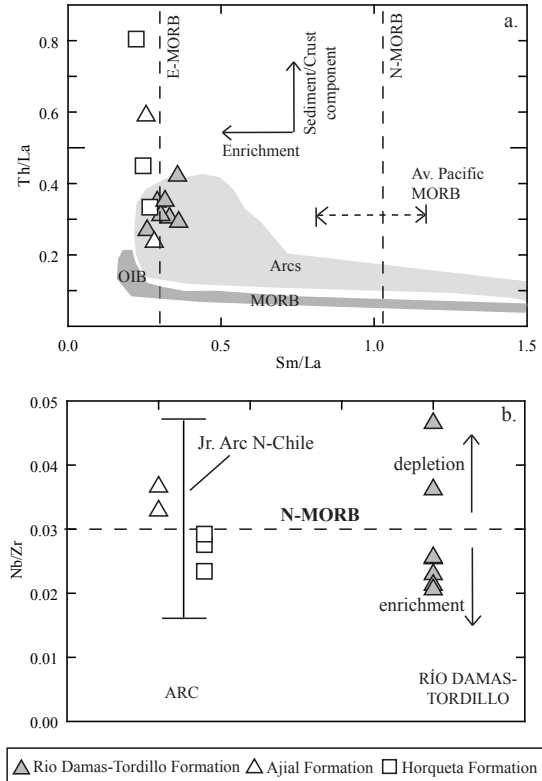


FIG. 11. **a.** Th/La versus Sm/La diagram. Arcs, OIB and MORB fields, enrichment and sediment component vectors and Average Sm/La values for normal, enriched and Pacific MORB (dotted lines: N.MORB, E.MORB, Pacific MORB) are after Plank (2005); **b.** Nb/Zr ratios, N-MORB value in dotted line is after Sun and McDonough (1989). Data from Ajial and Horqueta Formations in the Coastal Cordillera of Central Chile are after Vergara *et al.* (1995).

high Pb in the crust. The compositional variations in the Pb isotopes is in part also due to the pervasive alteration of the studied rocks as well.

In order to better constrain the source of the Río Damas-Tordillo lavas and the Jurassic arc rocks of central Chile, Equilibrated Melting, Assimilation and Fractional Crystallization (AFC) and mixing forward modeling were performed using our elemental data (Fig. 12). The results show that it is possible to achieve the compositional features of the most primitive samples of the arc and the Río Damas-Tordillo Formation by 15% melting of a mixture of 80% Depleted Mantle (DM) and 20% Primitive Mantle (PM), and subsequent fractionation of olivine with minor amounts (<10%) of assimilation of lower crust. To achieve the composition of the more evolved arc

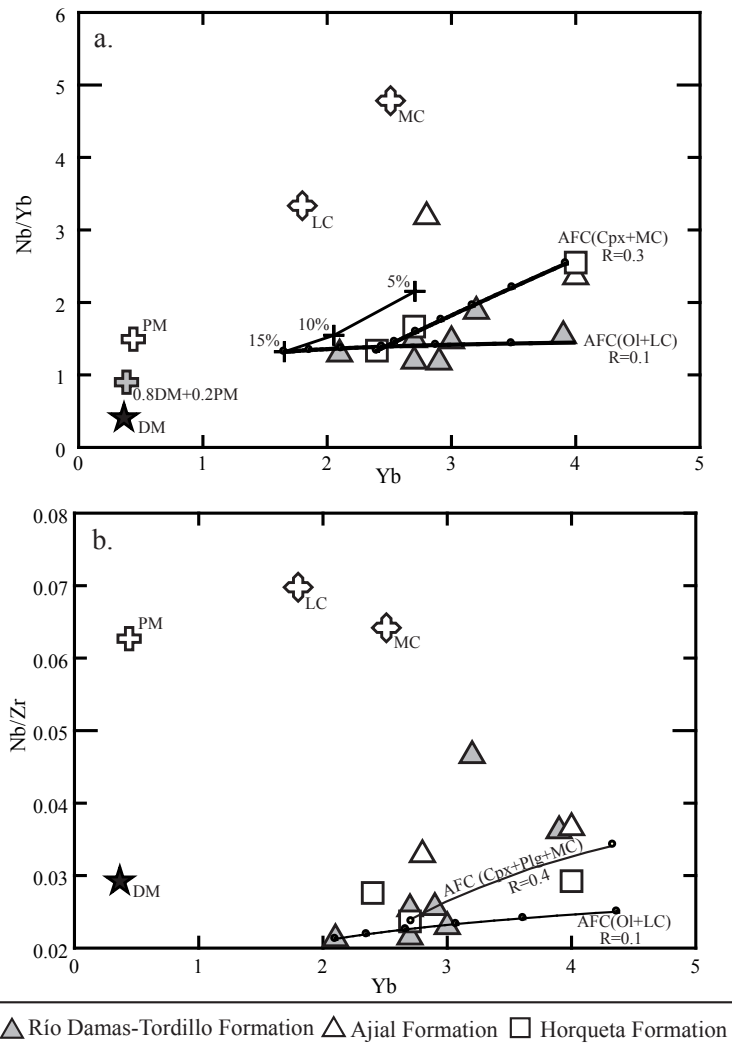


FIG. 12. **a.** Nb/Yb versus Yb and **b.** Nb/Zr versus Yb diagrams for Jurassic arc and back-arc volcanic rocks in central Chile. Trajectories with crosses represent Equilibrated Melting in steps of 5%. Lines with circles represent AFC process after DePaolo (1981), the 'r' factor in the AFC equation is shown. Steps in crystallization model are 10%. Starting values in a) is the modeled concentration of Nb, Zr and Yb after 15% of melting of a mixture of 80% of DM and 20% of PM. Starting values in b) are the measured concentrations of Nb, Zr and Yb in the less differentiated sample of the Río Damas Fm. (MO208-385) and in sample Mel22 of the Horqueta Fm. (Vergara *et al.*, 1995). LC: Lower Continental Crust and MC: Middle Continental Crust, after Rudnick and Gao (2003). Data from Ajial and Horqueta Formations in the Coastal Cordillera of central Chile after Vergara *et al.* (1995).

samples, the assimilation of significant amounts of middle continental crust, along with progressive fractionation of clinopyroxene and plagioclase is required. This is consistent with the observed Eu anomalies and the high Sr isotope ratios reported by Vergara *et al.* (1995).

Unlike in northern Chile (26°-30°S), where geochemical variations between the Jurassic arc and

back-arc magmatism are clearly observed (Rossel *et al.*, 2013), it is not possible to differentiate the sources and processes involved in the generation of the arc magmatism in central Chile and the lavas of the Río Damas-Tordillo Formation based only in the elemental and isotopic composition of these rocks. The volcanism of the Río Damas-Tordillo Formation could therefore represent arc activity.

6.3. A tectonic framework for the Río Damas-Tordillo Formation

Taking into account the geochemistry, petrology and probably age of the Río Damas-Tordillo lavas according to the new dates here supplied and its stratigraphic location, we propose the following evolutionary model for the latest Jurassic deposits in central Chile and Argentina between 32°S and 35°S (Fig. 13).

During the Lower and Middle Jurassic the trans-tensional/extensional regime of subduction in the Andean margin (Charrier *et al.*, 2007; Grocott and Taylor, 2002; Mpodozis and Ramos, 2008; Scheuber and González, 1999) resulted in a paleogeographic configuration characterized by the development of a voluminous volcanic arc that was mostly submerged considering the numerous intercalations of marine deposits between the lavas of the Ajial Formation in the Coastal Cordillera (Charrier *et al.*, 2007; Vergara *et al.*, 1995). The inferred paleogeography suggests that a connection existed between the Pacific Ocean and the Neuquén basin to the east (Legarreta and Uliana, 1999; Howell *et al.*, 2005).

Between the Middle and Upper Jurassic, the change to transpressional regime has been proposed in northern and central Chile, probably as the result of an increased coupling between the two plates (Creixell *et al.*, 2011; Ring *et al.*, 2012; Scheubert and González, 1999). This change, in addition to the accumulation of volcanic material, could be responsible of the progressive emersion of the arc and probably the forearc domain, and subsequent disconnection of the back-arc with the Pacific Ocean during Kimmeridgian and Tithonian times (Klohn, 1960; Legarreta *et al.*, 1999; Mescua, 2011; Thiele, 1980), leading to continental sedimentation in both domains, as recorded by Horqueta Formation (arc) and Río Damas-Tordillo Formation (back-arc).

During the Kimmeridgian and Tithonian, the back-arc at the studied latitudes show evidences for extensional conditions, with sedimentation controlled by normal faulting (Cegarra and Ramos, 1996; Charrier *et al.*, 2007; Giambiagi *et al.*, 2003; Mescua *et al.*, 2008; Pángaro *et al.*, 1996). The plate coupling probably concentrated the deformation in the arc domain due to thermal softening, avoiding the development of compressive or transpressive structures in back-arc domain.

The regional long-term extension since the beginning of the Mesozoic (Legarreta and Uliana, 1999)

led to a progressive thinning of crust (Charrier *et al.*, 2007; Mpodozis and Ramos, 2008), which together with the presence of active normal faults, likely favored the rapid ascent of important volumes of magma in the back-arc during Tithonian, as suggested by the >1,000 m-thick sequences of basaltic andesitic lavas of the Río Damas Formation recognized at the Jurassic-Cretaceous boundary in the High Andes of central Chile.

During late Tithonian a new transgression in the Neuquén basin is recorded by the Lo Valdés and Vaca Muerta formations (Klohn, 1960; Legarreta and Uliana, 1999), but no units of this age are observed in Coastal Cordillera, since the upper portion of the Horqueta Formation is eroded (Vergara *et al.*, 1995). A possible explanation for this configuration is that the uplift and erosion of the Mesozoic arc continued into the Tithonian, leading to the development of unconformity observed between the Horqueta and Lo Prado Formations (Vergara *et al.*, 1995) and Lower Cretaceous granitoids and Lo Prado (Gana and Tosdal, 1996). This is consistent with the presence of numerous zircons of Tithonian age in the Río Damas-Tordillo Formation rocks. The marine transgression originated in the Pacific ocean, since the Atlantic Ocean was not open by the end of the Jurassic, and was facilitated by the progressive ascent of the eustatic level since 160 Ma., which reached its maximum at *ca.* 140 Ma. (Haq *et al.*, 1987). The marine transgression occurred through narrow channels that crosscut the arc highlands and connected the ocean with the back-arc basin during Tithonian and Lower Cretaceous, as proposed for Early Jurassic by Vicente (2005).

7. Conclusions

A period of more transpressive conditions in the Andean margin during the Late Jurassic probably led to the emersion of the arc and fore arc domain, disconnecting the back-arc Mendoza-Neuquén basin from the ocean with a subsequent marine regression phase. The final stage of this regression is recorded by the red clastic deposits of the Río Damas-Tordillo Formation.

Provenance data indicate that an important source of sediments was the uplifted arc domain to the west, represented by Middle to Upper Jurassic granitoids and the Horqueta and Ajial Formations; these are located in the present-day Coastal Cordillera. The supply of sediments from the west continued at least until

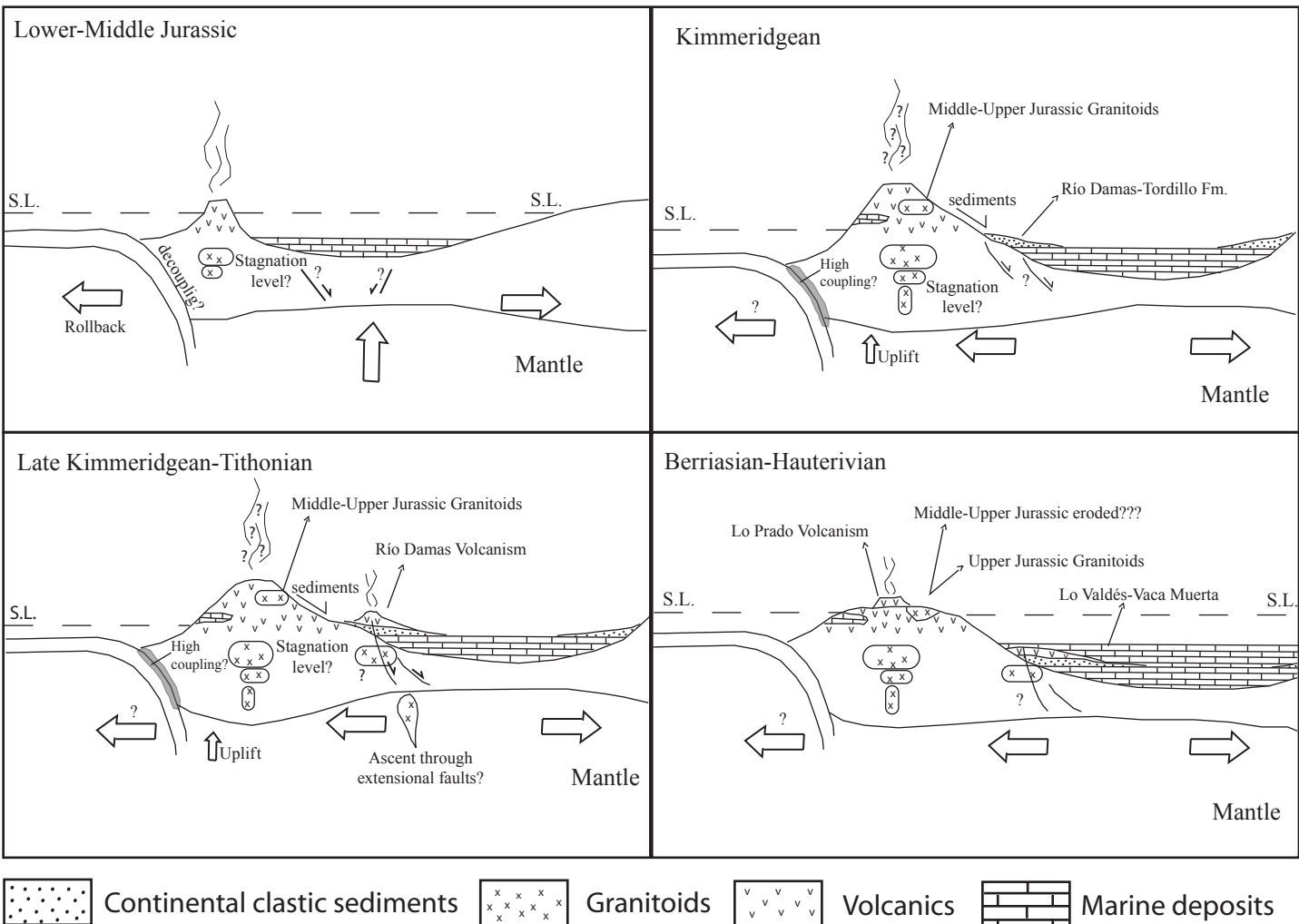


FIG. 13. Jurassic to Early Cretaceous evolution across the western margin of South America between 33° and 35.5° S. S.L.: Sea Level. White arrows show the direction of the main driving forces acting in the subduction margin.

~146 Ma. The protracted extension in the region since the beginning of the Mesozoic, led to a progressive thinning of the crust, which together with the presence of active normal faults, probably facilitated the rapid ascent of important volumes of lavas in the back-arc during the Kimmeridgian and Tithonian.

The geochemical and isotopic composition of volcanic rocks of the Río Damas-Tordillo Formation indicates a clear subduction-related affinity for the magmatism and points for a depleted sub-arc asthenospheric mantle as the source for the igneous materials. Major and trace elements contents and forward ACF models suggest olivine and plagioclase fractionation combined with small volumes of lower crust assimilation as the main processes controlling magma evolution. Future studies will aim to establish if the source and petrogenetic conditions of the volcanism represented by the Río Damas-Tordillo Formation lavas are different from those of the magmatism in the arc domain.

Acknowledgements

This study was funded by the Fondecyt N°11080040 and N°1120272 research grants. Mihai N. Ducea was also funded by grant PN-II-ID-PCE-2011-3-0217 from Romanian UEFISCDI. J. Mescua was founded by PICT-14144 (Agencia Nacional de Promoción Científica y Técnica) y PIP-5843 (CONICET). M. Labbé is thanked for assistance in the field work. S.M. Kay and an anonymous reviewer are thanked for their helpful comments that significantly improved the manuscript.

References

- Aguirre, L.; Calderón, S.; Vergara, M.; Oliveros, V.; Morata, D.; Belmar, M. 2009. Edades isotópicas de rocas de los valles Volcán y Tinguiririca, Chile central. *In Congreso Geológico Chileno*, No. 12, Actas S8-001 (digital): 4 p. Santiago.
- Biro-Bagoczky, L. 1964. Estudio sobre el límite Titoniano y el Neocomiano en la Formación Lo Valdés, Provincia de Santiago, principalmente en base a ammonoides, Región Metropolitana, Chile. Memoria de Título (Unpublished), Universidad de Chile, Departamento de Geología: 118 p.
- Biro-Bagoczky, L. 1980. Estudio sobre el límite entre el Titoniano y el Neocomiano en la Formación Lo Valdés, provincia de Santiago (33°50'lat. Sur), Chile; principalmente sobre la base de ammonoides. *In Congreso Argentino de Paleontología y Bioestratigrafía*, No. 2 y Congreso Latinoamericano Paleontología, No. 1, Actas 1: 137-152. Buenos Aires.
- Cabanis, B.; Lecolle, M. 1989. Le diagramme La/10-Y/15-Nb/8: un outil pour la discrimination des séries volcaniques et la mise en évidence des processus de mélange et/ou de contamination crustales. *Comptes Rendus de l'Academie de Sciences de Paris*, série II 309: 2023-2029.
- Calderón, S. 2008. Condiciones físicas y químicas del metamorfismo de muy bajo grado de las secuencias mesozoicas en el valle del Río Volcán (33°50'-34°00'S). Memoria de Título (Unpublished), Universidad de Chile, Departamento de Geología: 107 p.
- Caminos, R.; Nullo, F.E.; Panza, J.L.; Ramos, V.A. 1993. Mapa Geológico de la provincia de Mendoza. Secretaría de Minería, Dirección Nacional del Servicio Geológico, Buenos Aires, Argentina.
- Cegarra, M.I.; Ramos, V.A. 1996. La faja plegada y corrida del Aconcagua. *In Geología de la región del Aconcagua, provincias de San Juan y Mendoza* (Ramos, V.A.; editor). Subsecretaría de Minería de la Nación, Dirección Nacional del Servicio Geológico, Anales 24: 387-422.
- Charrier, R. 1981. Geologie der chilenischen Hauptkordillere zwischen 34° und 34°30' südlicher Breite und ihre tektonische, magmatische und paläogeographische Entwicklung. *Berliner Geowissenschaftliche Abhandlungen*, Reihe A 36: 370 p.
- Charrier, R.; Wyss, A.R.; Flynn, J.J.; Swisher, C.; Norell, M.A.; Zapata, F.; McKenna, M.C.; Novacek, M.J. 1996. New evidence for Late Mesozoic-Early Cenozoic evolution of the Chilean Andes in the Upper Tinguiririca Valley (35°S), Central Chile. *Journal of South American Earth Sciences* 9: 393-422.
- Charrier, R.; Pinto, L.; Rodríguez, M.P. 2007. Tectono-stratigraphic evolution of the Andean Orogen in Chile. *In The Geology of Chile* (Moreno, T.; Gibbons, W.; editors). The Geological Society: 21-144. London.
- Chen, J.H.; Wasserbarg, G.J. 1981. The isotopic composition of uranium and lead in Allende inclusions and meteoritic phosphates. *Earth and Planetary Science Letters* 52: 1-15.
- Creixell, C.; Parada, M.A.; Roperch, P.; Morata, D.; Arriagada, C.; Pérez de Arce, C. 2006. Syntectonic emplacement of the Middle Jurassic Concón Mafic Dike Swarm, Coastal Range, central Chile (33°S). *Tectonophysics* 425: 101-122.
- Creixell, C.; Parada, M.A.; Morata, D.; Roperch, P.; Arriagada, C. 2009. The genetic link between mafic dike swarms and plutonic reservoirs in the Mesozoic

- of central Chile (30°-33°45'S): insights from AMS and geochemistry. International Journal of Earth Sciences 98: 177-201.
- Creixell, C.; Parada, M.A.; Morata, D.; Vásquez, P.; Pérez de Arce, C.; Arriagada, C. 2011. Middle-Late Jurassic to Early Cretaceous transtension and transpression during arc building in central Chile: evidence from mafic dike swarms. Andean Geology 38 (1): 37-63. doi: 10.5027/andgeoV38n1-a04
- Cucchi, R.; Leanza, H.A.; Repol, D.; Escosteguy, L.; González, R.; Daniela, J.C. 2005. Hoja Geológica 3972-IV, Junín de los Andes. Provincia del Neuquén. Instituto de Geología y Recursos Minerales, Servicio Geológico Minero Argentino, Boletín 357: 102 p.
- Davidson, J. 1971. Geología del área de las Nacientes del Teno, provincia de Curicó, Chile. Memoria de Título (Unpublished), Universidad de Chile, Departamento de Geología: 160 p.
- Davidson, J.; Vicente, J.C. 1973. Características paleogeográficas y estructurales del área fronteriza de las nacientes del Teno (Chile) y Santa Elena (Argentina) (Cordillera Principal, 35° a 35°15' latitud sur). In Congreso Geológico Argentino, No. 5, Actas 5: 11-55. Buenos Aires.
- DePaolo, D.J. 1981. Trace element and isotopic effects of combined wallrock assimilation and fractional crystallization. Earth and Planetary Science Letters 53: 189-202.
- Deckart, K.; Hervé, F.; Fanning, C.M.; Ramírez, V.; Calderón, M.; Godoy, E. 2014. U-Pb geochronology and Hf-O isotopes of zircons from the Pennsylvanian Coastal Batholith, south-central Chile. Andean Geology 41 (1): 49-82. doi: 10.5027/andgeoV41n1-a03
- Drew, S.T.; Ducea, M.N.; Schoenbohm, L.M. 2009. Mafic volcanism on the Puna Plateau, NW Argentina: Implications for lithospheric composition and evolution with an emphasis on lithospheric foundering. Lithosphere 1: 305-318. doi: 10.1130/L54.1.
- Faure, G. 1986. Principles of Isotope Geochemistry. John Wiley: 464 p. New York.
- Faure, G.; Mensing, T.M. 2005. Isotopes: Principles and Applications. John Wiley: 928 p. New York.
- Gana, P.; Tosdal, R. 1996. Geocronología U-Pb y K-Ar en intrusivos del Paleozoico y Mesozoico de la Cordillera de la Costa, Región de Valparaíso, Chile. Revista Geológica de Chile 23 (2): 151-164. doi: 10.5027/andgeoV23n2-a04
- Gehrels, G.E.; Valencia, V.A.; Ruiz, J. 2008. Enhanced precision, accuracy, efficiency, and spatial resolution of U-Pb ages by laser ablation-multicollector-inductively coupled plasma-mass spectrometry. Geochemistry, Geophysics, Geosystems 9: Q03017. doi: 10.1029/2007GC001805.
- Giambiagi, L.B.; Álvarez, P.; Godoy, E.; Ramos, V.A. 2003. The control of preexisting extensional structures on the evolution of the southern sector of the Aconcagua fold and thrust belt, southern Andes. Tectonophysics 369: 1-19.
- Godoy, E.; Loske, W. 1988. Tectonismo sinplutónico de dioritas Jurásicas al sur de Valparaíso: datos U-Pb sobre la ‘fase Quintay’. Revista Geológica de Chile 15 (2): 119-127. doi: 10.5027/andgeoV15n2-a02
- González, O. 1963. Observaciones geológicas en el valle del Río Volcán. Revista Minerales 17 (81): 20-61. Santiago.
- Grocott, J.; Taylor, G.K. 2002. Magmatic arc fault systems, deformation partitioning and emplacement of granitic complexes in the Coastal Cordillera, north Chilean Andes (25°30'S to 27°00'S). Journal of the Geological Society 159 (4): 425-442.
- Hallam, A.; Biro-Bagoczky, L.; Pérez, E. 1986. Facies analysis of the Lo Valdés Formation of the High Cordillera of central Chile, and the paleogeographic evolution of the Andean basin. Geological Magazine 123 (4): 425-435.
- Haq, B.U.; Hardenbol, J.; Vail, P.R. 1987. Chronology of fluctuating sea levels since the Triassic (250 million years ago to present). Science 235: 1156-1167.
- Hart, S.R. 1984. A large-scale isotope anomaly in the Southern Hemisphere mantle. Nature 309: 753-757.
- Hervé, F.; Munizaga, F.; Parada, M.A.; Brook, M.; Pankhurst, R.; Snelling, N.; Drake, R. 1988. Granitoids of the Coast Range of central Chile: geochronology and geologic setting. Journal of South American Earth Sciences 1: 185-194.
- Hildreth, W.; Moorbat, S. 1988. Crustal contribution to the arc magmatism in the Andes of central Chile. Contribution to Mineralogy and Petrology 103: 361-386.
- Howell, J.A.; Schwarz, E.; Spalletti, L.A.; Veiga, G.D. 2005. The Neuquén Basin, Argentina: An Overview. In The Neuquén Basin: a case study in sequence stratigraphy and basin dynamics (Veiga, G.D.; Spalletti, L.A.; Howell, J.A.; Schwarz, E.; editors). Geological Society of London, Special Publications 252: 1-14.
- Klohn, C. 1960. Geología de la Cordillera de los Andes de Chile Central, Provincias de Santiago, O'Higgins, Colchagua y Curicó. Instituto de Investigaciones Geológicas, Boletín 8: 95 p. Santiago.
- Kramer, W.; Siebel, W.; Romer, R.; Haase, G.; Zimmer, M.; Ehrlichmann, R. 2004. Geochemical and isotopic characteristics and evolution of the Jurassic volcanic

- arc between Arica ($18^{\circ}30'S$) and Tocopilla ($22^{\circ}S$), North Chilean Coastal Cordillera. *Chemie der Erde* 65: 47-78.
- Leanza, H.A. 1981. The Jurassic-Cretaceous boundary beds in west central Argentina and their ammonite zones. *Neues Jahrbuch für Geologie und Paläontologie, Abhandlungen* 161: 62-92. Stuttgart.
- Leanza, H.A.; Hugo, C. 1997. Hoja Geológica 3969-III. Picún Leufú. Provincias de Neuquén y Río Negro. Servicio Geológico Minero Argentino, Boletín 218: 135 p.
- Legarreta, L. 1976. Análisis estratigráfico de la Formación Tordillo (Kimmeridgiano superior) entre el Río Diamante y el Río Salado, Departamentos de San Rafael y Malargüe, Provincia de Mendoza, Argentina. Tesis (Unpublished), Universidad de Buenos Aires, Departamento de Geología: 72 p.
- Legarreta, L.; Uliana, M.A. 1999. El Jurásico y Cretácico de la Cordillera Principal y la cuenca Neuquina. I. Facies sedimentarias. In *Geología Argentina (Caminos, R.; editor)*. Servicio Geológico y Minero Argentino, Instituto de Geología y Recursos Minerales, *Anales* 29 (16): 399-416.
- Legarreta, L.; Gulisano, C.A.; Uliana, M.A. 1993. Las secuencias sedimentarias jurásico-cretácicas. In *Geología y Recursos Naturales de Mendoza (Ramos, V.A.; editor)*. Congreso Geológico Argentino, No. 12 y Congreso de Exploración de Hidrocarburos, No. 2, Relatorio: 87-114. Buenos Aires.
- Levi, B.; Aguirre, L.; Nyström, J.O.; Padilla, H.; Vergara, M. 1989. Low-grade regional metamorphism in the Mesozoic-Cenozoic volcanic sequences of the Central Andes. *Journal of Metamorphic Geology* 7: 487-495.
- Le Maitre, R.W. 1989. A classification of igneous rocks and glossary of terms. Blackwell Scientific Publication: 193 p. London.
- López-Gómez, J.; Martín-Chivelet, J.; Palma, R.M. 2009. Architecture and development of the alluvial sediments of the Upper Jurassic Tordillo Formation in the Cañada Ancha Valley, northern Neuquén Basin, Argentina. *Sedimentary Geology* 219: 180-195.
- Lucassen, F.; Franz, G. 1994. Arc related Jurassic igneous and meta-igneous rocks in the Coastal Cordillera of northern Chile/Region Antofagasta. *Lithos* 32: 273-298.
- Lucassen, F.; Escayola, M.; Romer, R.; Voramonte, J.; Koch, K.; Franz, G. 2002. Isotopic composition of Late Mesozoic basic and ultrabasic rocks from the Andes (23° - $32^{\circ}S$) implications for the Andean mantle. *Contributions to Mineralogy and Petrology* 143: 336-349.
- Lucassen, F.; Kramer, W.; Bartsch, V.; Wilke, H.G.; Franz, G.; Romer, R.L.; Dulski, P. 2006. Nd, Pb and Sr isotope composition of juvenile magmatism in the Mesozoic large magmatic province of northern Chile (18° - $27^{\circ}S$): indications for a uniform subarc mantle. *Contributions to Mineralogy and Petrology* 152: 571-589.
- Ludwig, K.R. 2003. User's manual for isoplot 3.00: A geochronological toolkit for Microsoft Excel. Berkeley Geochronological Center, Special Publication 4: 71 p. Berkeley, California.
- Martínez, F.; Arriagada, C.; Mpodozis, C.; Peña, M. 2012. The Lautaro Basin: A record of inversion tectonics in northern Chile. *Andean Geology* 39 (2): 258-278. doi: 10.5027/andgeoV39n2-a04
- Mescua, J.F. 2011. Evolución estructural de la cordillera principal entre Las Choicas y Santa Elena ($35^{\circ}S$), provincia de Mendoza, Argentina. Tesis (Unpublished), Universidad de Buenos Aires: 241 p.
- Mescua, J.F.; Giambiagi, L.B.; Bechis, F. 2008. Evidencias de tectónica extensional en el Jurásico tardío (Kimeridgiano) del suroeste de la provincia de Mendoza. *Revista de la Asociación Geológica Argentina* 63 (4): 512-519.
- Mescua, J.F.; Giambiagi, L.B.; Ramos, V. 2012. Late Cretaceous Uplift in the Malargüe fold-and-thrust belt ($35^{\circ}S$), southern Central Andes of Argentina and Chile. *Andean Geology* 40 (1): 102-116. doi: 10.5027/andgeoV40n1-a05
- Mpodozis, C.; Ramos, V. 2008. Tectónica Jurásica en Argentina y Chile: Extensión, subducción oblicua, rifting, deriva y colisiones? *Revista de la Asociación Geológica Argentina* 63 (4): 481-497.
- Muñoz, M.; Deckart, K.; Charrier, R.; Fanning, M. 2009. New geochronological data on Neogene-Quaternary intrusive rocks from the high Andes of central Chile ($33^{\circ}15'$ - $34^{\circ}00'S$). In *Congreso Geológico Chileno, No. 12, Resúmenes, Sesión 8-008*: 4 p. Santiago.
- Naipauer, M.; García, E.; Marques, J.; Tunik, M.; Rojas, E.; Vujovich, G.; Pimentel, M.; Ramos, V. 2012. Intraplate Late Jurassic deformation and exhumation in western central Argentina: Constraints from surface data and U-Pb detrital zircon ages. *Tectonophysics* 524-525: 59-75.
- Naipauer, M.; Tunik, M.; Marques, J.C.; Rojas, E.; Vujovich, G.; Pimentel, M.; Ramos, V. 2014. U-Pb detrital zircon ages of Upper Jurassic continental successions: implications for the provenance and absolute age of the Jurassic-Cretaceous boundary in the Neuquén Basin. *Geological Society Special Publication*: 399. doi: 10.1144/SP399.1.
- Oliveros, V.; Féraud, G.; Aguirre, L.; Fornari, M.; Morata, D. 2006. The Early Andean Magmatic Province (EAMP):

- ⁴⁰Ar/³⁹Ar dating on Mesozoic volcanic and plutonic rocks from the Coastal Cordillera, Northern Chile. *Journal of Volcanology and Geothermal Research* 157: 311-330.
- Oliveros, V.; Morata, D.; Aguirre, L.; Féraud, G.; Fornari, M. 2007. Jurassic to Early Cretaceous subduction-related magmatism in the Coastal Cordillera of northern Chile (18°30'-24°S): geochemistry and petrogenesis. *Revista Geológica de Chile* 34 (2): 209-232. doi: 10.5027/andgeoV34n2-a03
- Oliveros, V.; Aguirre, L.; Morata, D.; Simonetti, A.; Vergara, M.; Belmar, M.; Calderón, S. 2008. Geochronology of very low-grade mesozoic andean metabasites. An approach through the K-Ar, ⁴⁰Ar/³⁹Ar and U-Pb LA-MC-ICP-MS methods. *Journal of the Geological Society* 165: 579-584.
- Oliveros, V.; Labbé, M.; Rossel, P.; Charrier, R.; Encinas, A. 2012. Late Jurassic paleogeographic evolution of the Andean back-arc basin: new constrains from the Lagunillas Formation, northern Chile (27°30'-28°30'S). *Journal of South American Earth Sciences* 35: 25-40.
- Otamendi, J.; Ducea, M.N.; Tibaldi, A.; de la Rosa, J.; Bergantz, G.; Vujovich, G. 2009. Generation of tonalitic and dioritic magmas by coupled partial melting of gabbroic and metasedimentary rocks within the deep crust of the Famatinian magmatic arc, Argentina. *Journal of Petrology* 50: 841-873. doi: 10.1093/petrology/egp022.
- Pángaro, F.; Ramos, V.A.; Godoy, E. 1996. La faja plegada y corrida de la Cordillera Principal de Argentina y Chile a la latitud del Cerro Palomares (33°35'S). In Congreso Geológico Argentino, No. 13 y Congreso Exploración de Hidrocarburos, No. 3, Actas 2: 315-324. Buenos Aires.
- Parada, M.A.; Nystrom, J.; Levi, B. 1999. Multiple sources for the Coastal batholith of central Chile (31-34°S): geochemical and Sr-Nd isotopic evidence and tectonic implications. *Lithos* 46: 505-521.
- Pearce, J.A. 1982. Trace elements characteristics of lavas from destructive plate boundaries. In *Andesites* (Thorpe, R.S.; Editor). John Wiley and Sons: 525-548. London.
- Pearce, J.A. 1983. Role of the sub-continental lithosphere in magma genesis at active continental margins. In *Continental basalts and mantle xenoliths* (Hawkesworth, C.J.; Norry, M.J.; editors). Shiva, Nentwich: 230-249.
- Pearce, J.A. 1996. A user's guide to basalt discrimination diagrams. In *Trace element geochemistry of volcanic rocks, applications for massive sulphide exploration*, Short Course Notes. (Bailes, A.H.; Christiansen, E.H.; Galley, A.G.; Jenner, G.A.; Keith, Jeffrey D.; Kerrich, R.; Lentz, D.R.; Lesher, C.M.; Lucas, S.B.; Ludden, J.N.; Pearce, J.A.; Peloquin, S.A.; Stern, R.A.; Stone, W.E.; Syme, E.C.; Swinden, H.S.; Wyman, D.A.; editors). Geological Association of Canada 12: 79-113.
- Peate, D.W.; Pearce, J.A.; Hawkesworth, C.J.; Colley, H.; Edwards, C.M.H.; Hirose, K. 1997. Geochemical variations in Vantu arc lavas: the role of subducted materials and a variable mantle wedge composition. *Journal of Petrology* 38: 1331-1358.
- Plank, T. 2005. Constraints from Thorium/Lanthanum on sediments recycling at subduction zones and the evolution of continents. *Journal of Petrology* 46: 921-944.
- Riccardi, A.C. 2008a. The marine Jurassic of Argentina: a biostratigraphic framework. *Episodes* 31 (3): 326-335.
- Riccardi, A.C. 2008b. El Jurásico de la Argentina y sus amonites. *Revista de la Asociación Geológica Argentina* 63 (4): 625-643.
- Ring, U.; Willner, A.; Layer, P.; Richter, P. 2012. Jurassic to Early Cretaceous postaccretional sinistral transpression in northcentral Chile (latitudes 31-32°S). *Geological Magazine* 149 (2): 202-220.
- Robinson, D.; Bevins, R.; Aguirre, L.; Vergara, M. 2004. A reappraisal of episodic burial metamorphism in the Andes of central Chile. *Contributions to Mineralogy and Petrology* 146: 513-528.
- Rossel, P.; Oliveros, V.; Ducea, M.; Charrier, R.; Scaillet, S.; Retamal, L.; Figueroa, O. 2013. The Early Andean subduction system as an analogue to island arcs: evidence from across-arc geochemical variations in northern Chile. *Lithos* 179: 211-230.
- Rudnick, R.L.; Gao, S. 2003. Composition of the continental crust. In *The Crust* (Rudnick, R.L.; editor). Elsevier 3: 1-64.
- SERNAGEOMIN. 2003. Mapa Geológico de Chile: versión digital. Servicio Nacional de Geología y Minería, Publicación Geológica Digital, No. 4 (CD-ROM, versión1.0, 2003). Santiago.
- Scheuber, E.; González, G. 1999. Tectonics of the Jurassic-Early Cretaceous magmatic arc of the north Chilean Coastal Cordillera (22°-26°S): A story of crustal deformation along a convergent plate boundary. *Tectonics* (18): 895-910.
- Stacey, J.S.; Kramers, J.D. 1975. Approximation of terrestrial lead isotope evolution by a two-stage model. *Earth and Planetary Science Letters* 26, 207-221. doi: 10.1016/0012-821X(75)90088-6.
- Stern, C.R. 1991. Role of subduction erosion in the generation of the Andes magmas. *Geology* 19: 78-81.
- Stern, C.R. 2011. Subduction erosion: Rates, mechanism, and its role in arc magmatism and the evolution of the

- continental crust and mantle. *Gondwana Research* 20: 284-308.
- Spalletti, L.A.; Queralt, I.; Matheos, S.D.; Colombo, F.; Maggi, J. 2008. Sedimentary petrology and geochemistry of siliciclastic rocks from the upper Jurassic Tordillo Formation (Neuquén Basin, western Argentina): Implications for provenance and tectonic setting. *Journal of South American Earth Sciences* 25: 440-463.
- Stipanicic, P.N. 1965. El Jurásico en Vega de la Veranada (Neuquén). El Oxfordense y el diastrofismo divesiano (Agassiz-Yaila) en Argentina. *Revista de la Asociación Geológica Argentina* 20 (4): 403-478. Buenos Aires.
- Stipanicic, P.N. 1969. El avance en los conocimientos del Jurásico argentino a partir del esquema de Groeber. *Revista de la Asociación Geológica Argentina* 24 (4): 367-388. Buenos Aires.
- Sun, S.S.; McDonough, W.F. 1989. Chemical and isotopic systematics of oceanic basalts: implications for mantle composition and processes. *Geological Society Special Publication* 42: 313-345.
- Thibodeau, A.M.; Killick, D.J.; Ruiz, J.; Chesley, J.T.; Deagan, K.; Cruxent, J.M.; Lyman, W. 2007. The strange case of the earliest silver extraction by European colonists in the New World. *Proceedings of the National Academy of Sciences of the United States of America* 104: 3663-3666.
- Thiele, R. 1980. Hoja Santiago, Región Metropolitana. Servicio Nacional de Geología y Minería, Carta Geológica de Chile 39: 51 p.
- Vergara, M.; Levi, B.; Nystrom, J.; Cancino, A. 1995. Jurassic and Early Cretaceous island arc volcanism, extension, and subsidence in the Coast Range of central Chile. *Geological Society of America Bulletin* 107: 1427-1440.
- Vicente, J.C. 2005. Dynamic paleogeography of the Jurassic Andean Basin: pattern of transgression and localization of main straits through the magmatic arc. *Revista de la Asociación Geológica Argentina* 60 (1): 221-250.
- Vicente, J.C. 2006. Dynamic Paleogeography of the Jurassic Andean Basin: pattern of regression and general considerations on main features. *Revista de la Asociación Geológica Argentina* 61: 408-437.
- Weaver, C.E. 1931. Paleontology of the Jurassic and Cretaceous of West Central Argentina. University of Washington, Memoir 1: 1-469. Seattle.
- Winchester, J.A.; Floyd, P.A. 1977. Geochemical discrimination of different magma series and their differentiation products using immobile elements. *Chemical Geology* 20: 325-343.
- Yrigoyen, M.R. 1979. Cordillera Principal. In Segundo Simposio de Geología Regional Argentina (Turner, J.C.M.; coordinador). Academia Nacional de Ciencias: I651-I694.
- Zavalá, C.; Martínez Lampe, J.; Fernández, M.; Di Meglio, M.; Ancuri, M. 2008. El Diacronismo entre las formaciones Tordillo y Quebrada del Sapo (Kimeridgiano) en el sector sur de la Cuenca Neuquina. *Revista de la Asociación Geológica Argentina* 63 (4): 754-765. Buenos Aires.

Manuscript received: October 24, 2013; revised/accepted: June 3, 2014; available online: June 3, 2014.

Anexo II

Resúmenes presentados a Congresos y reuniones científicas



ANÁLISIS ESTRUCTURAL DEL SECTOR OCCIDENTAL DE LA FAJA PLEGADA Y CORRIDA DE MALARGÜE EN EL ÁREA DE VALLE GRANDE, REGIÓN DEL MAULE, CHILE (35°23'S)

Felipe Tapia¹ y Marcelo Farías¹

¹Departamento de Geología, Universidad de Chile, ftapia@ing.uchile.cl

Al sur de Santiago, la cordillera disminuye paulatinamente su elevación al mismo tiempo que el volumen y espesor cortical. Esta situación debería estar controlada por una disminución en el acortamiento y acompañado por un cambio en el estilo, mecanismos y cinemática de la deformación neógena. En este trabajo se presenta una actualización de la estratigrafía y un análisis estructural del área de Valle Grande, en el curso superior del río Colorado (35°23'S), en la vertiente chilena del sector occidental de la faja plegada y corrida de Malargüe con el objeto de establecer un modelo y evolución estructural para el área de estudio.

A partir de la descripción de las estructuras superficiales y su interpretación en profundidad, se pudo definir distintos dominios estructurales caracterizados por estructuras de piel gruesa. A pesar de no observarse en superficie, el basamento se encuentra involucrado en la deformación mediante fallas inversas de alto ángulo y reactivación de fallas preexistentes (Fig. 1) agrupadas en dos familias, unas con rumbo NNE y otras con rumbo NNW.

Al comparar las distintas estructuras, se puede observar que sólo el anticlinal de Valle Grande presenta una cinemática de plegamiento por flexura de falla (Fig. 1). La causa de esta diferencia corresponde a la presencia de una estructura extensional previa la cual controla la cinemática que produjo la inversión de la misma. Además, esto se ve favorecido por el contraste de competencia que existe entre las rocas de basamento y la cobertura, lo que genera un desacople y crea un *detachment* en la interfase basamento-cobertura que se propaga horizontal hacia el este. La existencia de este nivel de despegue provoca un traspaso del acortamiento hacia la cobertura. Como consecuencia, se infiere que la interfase basamento-cobertura corresponde a una superficie horizontal no deformada producto de una rápida propagación de la falla de basamento con un alto valor de p/s.

La falla El Novillo también es una estructura preexistente pero no comparte la misma cinemática que las otras estructuras. Esta variación se debe al tipo de basamento de la Cuenca extensional de Abanico, el cual poseería características distintas al basamento involucrado en el anticlinal Valle Grande. Además, no existiría un contraste de competencia suficiente entre las rocas del basamento de la Cuenca de Abanico y la secuencia sedimentaria mesozoica, lo que no favorecería la cinemática de plegamiento por flexura de falla sino una por propagación de falla. Lo anterior apuntaría a que el *pre-rift* de la Cuenca de Abanico y las secuencias sedimentarias mesozoica podrían comportarse mecánicamente igual, llegando a ser lo mismo.

De acuerdo con los datos expuestos, se identifican al menos dos eventos de deformación. El primer evento de deformación (E1) estaría asociado con la formación de los distintos bloques estructurales de los dominios. El segundo evento (E2) corresponde a la actividad que muestra el Sistema de Falla de Calabozos. Este episodio de deformación se habría acomodado al menos desde la última glaciación ya que presenta escarpes en depósitos morrénicos y actualmente exhibe una amplia sismicidad superficial.

Al comparar el estilo de deformación de piel gruesa presente en el área de estudio con otras localidades, se puede observar que existe una correlación. En el sector de las Nacientes del río Teno, Parada (2008) plantea también un estilo de piel gruesa con fallas de alto ángulo tanto para el dominio Cuenca de Abanico y faja plegada y corrida. Ya en territorio argentino, el estilo estructural de la zona de estudio concuerda por el definido para el sector occidental de la faja plegada y corrida de Malargüe, donde bloques de basamento con vergencia este, transfieren el rechazo a la cobertura sedimentaria mesozoica mediante la generación de distintos niveles de despegues. La cinemática de deformación de este sector corresponde a uno por flexión de falla (Giambiagi *et al.*, 2009), lo que muestra la consistencia del modelo cinemático propuesto en este trabajo. Este trabajo es parte del proyecto FONDECYT 11085022

Giambiagi, L., Ghiglione, M., Cristallini, E., y Bottesi, G., 2009. Kinematic models of basement/cover interaction: Insights from the Malargüe fold and thrust belt, Mendoza, Argentina. Journal of Structural Geology, 31: 1443-1457.

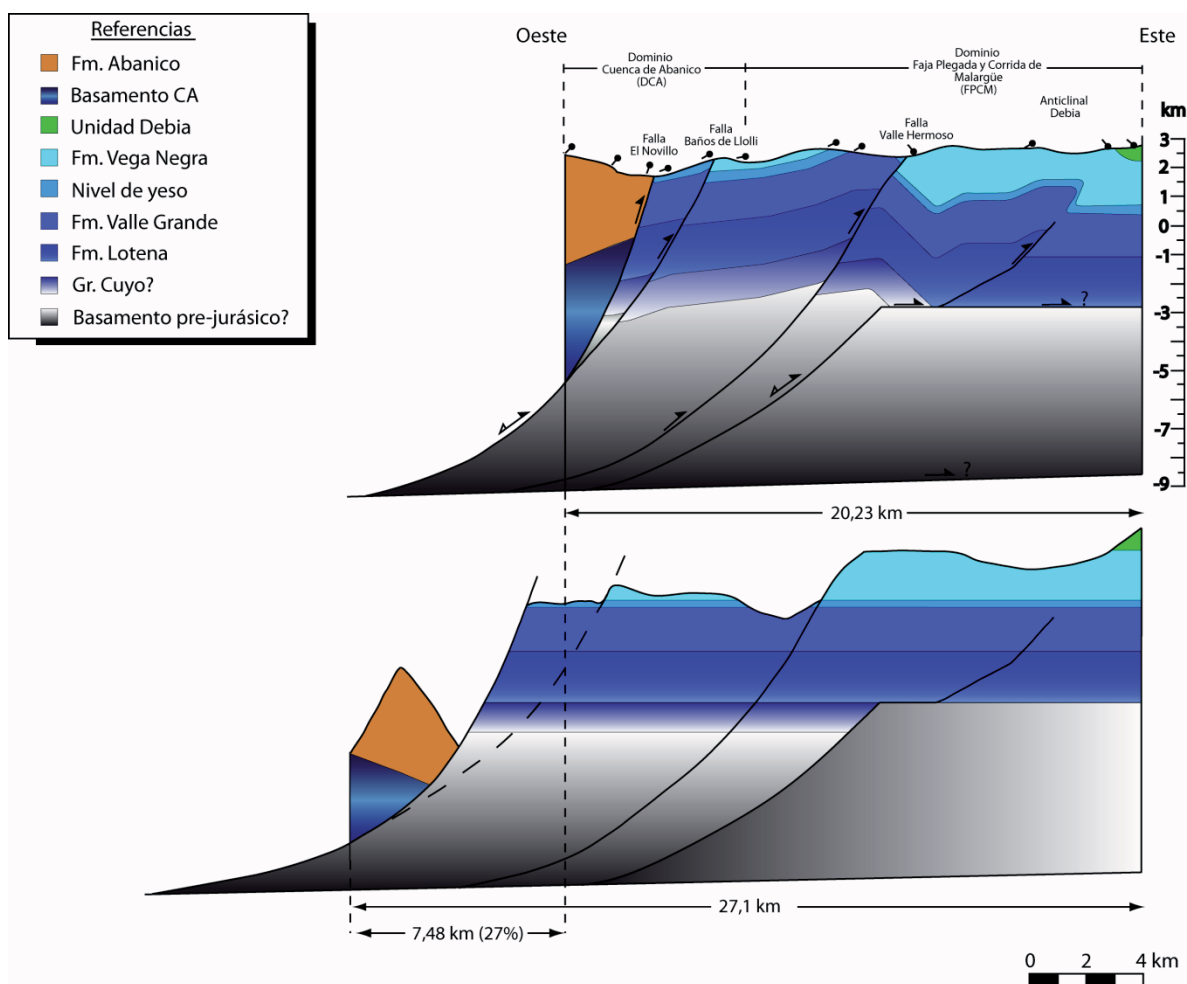


Figura 1. Sección estructural balanceada y restaurada.

Deformación Cretácica-Paleocena y sus evidencias en la Cordillera de los Andes de Chile Central (33,7°-36°S)

Felipe Tapia*, Marcelo Fariñas y Daniela Astaburuaga

Facultad Ciencias Físicas y Matemáticas, Universidad de Chile, Plaza Ercilla 803, Santiago, Chile

*E-mail: ftapia@ing.uchile.cl

Resumen. Las evidencias de la deformación del Cretácico tardío-Paleoceno en Chile Central no han sido directas y por lo tanto no ha sido posible caracterizarla detalladamente, ni mucho menos estimar la contribución que tiene en la construcción Neógena de la Cordillera de los Andes. En la Cordillera Principal de Chile Central (34°-36°S) se han encontrado 3 lugares donde se encuentran en discordancia las secuencias Mesozoicas y Cenozoicas y, en consecuencia, en los cuales se puede cuantificar la deformación K-T. Las evidencias reportadas en este trabajo dan sustento a la existencia de una proto-Cordillera de los Andes en el Paleógeno, además de aportar información para establecer la influencia de esta deformación en la actual configuración de la Cordillera.

Palabras Claves: Discordancia Meso-Cenozoica, proto-Cordillera de los Andes.

1 Introducción

La formación de la corteza continental se puede resumir en períodos de extensión y acortamiento lo que produce una disminución y aumento en el espesor cortical, con el consecuente desarrollo de cuencas y formación de cadenas montañosas, respectivamente. De esta manera se puede establecer que la actual configuración de la cordillera es el resultado de múltiples etapas de deformación que incluyen extensión, inversión y propagación hacia fajas plegadas y corridas.

Los orógenos modernos, como los Andes, comenzaron con su desarrollo durante los primeros tiempos del Mesozoico después de la disgregación del supercontinente Pangea, lo que generó el desarrollo de cuencas extensionales a gran escala, como la Cuenca Neuquina ubicada entre los 32° y 40°S. Durante el Cretácico esta cuenca extensional evolucionó en una cuenca de antepaís durante el cual se depositaron los grupos Neuquén y Malargüe (Ramos, 2010).

En Chile y Argentina, las evidencias de este periodo compresivo sólo son indirectas (Gana y Zentilli, 2000; Parada et al., 2005; Tunik et al., 2010; Sagripanti et al., 2011), por lo que no se ha podido establecer la real contribución e influencia de esta fase a las subsiguientes etapas. Es por eso que este trabajo tiene como objetivo mostrar evidencias estructurales que permitan cuantificar la deformación y de qué manera pudo influir en la formación actual de la Cordillera de los Andes.

2 Evidencias de la deformación Cretácica

A 36°S, en el valle del río Maule, específicamente en el sector de la Mina aflora la parte superior de la secuencia Mesozoica, la cual presenta una inclinación promedio de 45°W. Está compuesta por una unidad marina fosilífera del Neocomiano (González y Vergara, 1962) y por una secuencia roja continental de edad cretácico. Basado en sus relaciones de contacto y correlaciones litológicas esta última se correlacionaría con la Fm. Colimapu (Astaburuaga et al., 2012). En esta misma área, una discordancia angular separa rocas Mesozoicas y Cenozoicas de la Fm. Abanico (Eoceno sup.-Mioceno-inf.) la cual muestra un manto promedio de 22°W (Figura 1). La disposición de las rocas junto con su edad evidencia un periodo de deformación previo al depósito de la Fm. Abanico y posterior al de la secuencia roja Cretácica.

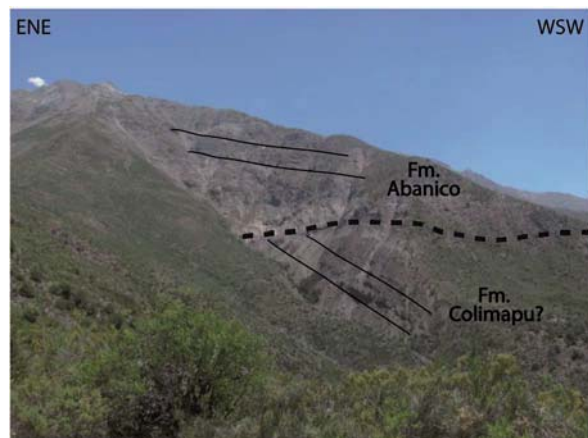


Figura 1: Discordancia entre la Fm. Abanico y la secuencia roja continental en el valle del río Maule.

En el sector de Termas del Flaco, en las nacientes del río Tinguiririca, la secuencia Mesozoica integrada por las formaciones Río Damas y Baños del Flaco (Titoniano-Hauteriviano), además de la unidad B.R.C.U. (Brownish-Red Clastic Unit), se encuentran en contacto con la Fm. Abanico mediante la Falla El Fierro (Figura 2), interpretada como una estructura del borde de la Cuenca de Abanico parcialmente invertida (Charrier et al., 2002). Waite et al. (2005) mediante el análisis de trazas de fisión en circones plantea la existencia de un evento de exhumación en el Cretácico-Paleoceno previo al depósito

del BRCU, situación planteada también por Mescua, (2011) quien muestra que las formaciones Rio Damas y Baños del Flaco pertenecerían al limbo trasero de un gran anticlinal de inversión y el cual presenta depósitos del Gr. Neuquén en el frente oriental asociados a la erosión de la estructura. Es en este contexto que se habría depositado también el BRCU, en el limbo trasero del anticlinal.

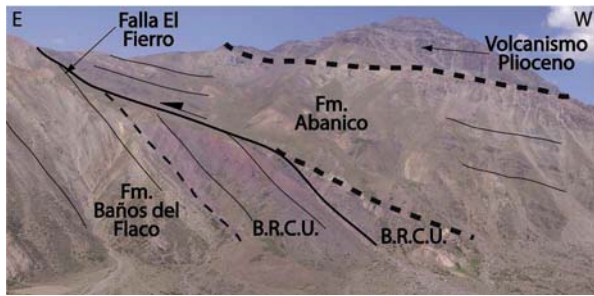


Figura 2: Relaciones estratigráficas entre las secuencias Mesozoicas y Cenozoicas en las nacientes del río Tinguiririca.

La mayor inclinación de las rocas al este de la Falla El Fierro respecto a las ubicadas al oeste ($50\text{--}70^{\circ}\text{W}$ para las rocas Mesozoicas y $20\text{--}40^{\circ}\text{W}$ para la Fm. Abanico) muestra una inconsistencia frente a una deformación en secuencia hacia el este, al momento de restituir cualquier sección estructural del área, evidenciando la naturaleza fuera de secuencia de la falla El Fierro. Sin embargo, la inconsistencia estructural al pensar en una deformación fuera de secuencia, asociada a la Falla El Fierro, se mantiene si se sostiene que el área sólo fue deformada durante el Neógeno, haciendo necesario la hipótesis de la existencia de un periodo previo a la etapa extensional Eocena y simultáneo o posterior al depósito del BRCU, consistente con lo propuesto por otros autores para esta zona.

Algo muy similar sucede en el sector del río Volcán, en el área cordillerana frente a Santiago. En la ladera sur del río Volcán, en la base del Cerro Retumbadero aflora una secuencia rojiza de areniscas con algunas intercalaciones de calizas agrupadas en la Fm. Colimapu, y que se dispone subvertical, consistente con la deformación que presentan el resto de las rocas Mesozoicas hacia el este. Sobre ésta y en discordancia angular se ubica la Fm. Abanico (Fock, 2005) la cual presenta una inclinación de 20°W (Figura 3). Al igual que en el caso anterior, la diferencia entre los manteos que presenta la secuencia mesozoica respecto a la cenozoica no puede ser explicada solamente con una deformación fuera secuencia sino que es necesaria una etapa de deformación previa al depósito de la Fm. Abanico, consistente con una fase compresiva en el Cretácico-Paleoceno.



Figura 3: Vista sur de la discordancia entre las formaciones Abanico y Colimapu en la base del Cerro Retumbadero, valle del río Volcán.

3 Discusión: Implicancias en la construcción de la Cordillera de los Andes

Actualmente, existen dos modelos que plantean distinta configuración y evolución para la porción central Chile y Argentina y donde la diferencia se basa en la relevancia de las estructuras de vergencia oeste y este. Sin embargo, sin poder decir con certeza cual modelo es el correcto, ninguno de los dos considera las etapas compresivas previas y su contribución a la formación actual del orógeno.

Los datos estructurales muestran que las secuencias mesozoicas fueron deformadas previas al Eoceno medio, y con una deformación de vergencia este, igual a la observada y documentada para la fase compresiva neógena en las fajas plegadas y corridas del Aconcagua y Malargüe entre los 34° y 36°S (Giambiagi et al., 2003; Giambiagi et al., 2009). Esta deformación pre-neógena no podría ser explicada como respuesta de la deformación y empuje de la Cordillera Frontal, tal como lo propone Armijo et al., (2010), debido a las evidencias documentadas para la edad de deformación y alzamiento de la misma (Giambiagi et al., 2001). De esta manera, esto podría indicar que esta morfoestructura es más antigua que la edad que se le asigna o bien que las secuencias mesozoicas podrían haberse deformado mediante otro mecanismo antes del Neógeno y el cual podría haber actuado también durante el posterior evento compresivo.

El modelo presentado por Farias et al., (2010) considera la inversión de la Cuenca de Abanico como el factor crítico para la orogenia Andina en el Neógeno y que la geometría es el resultado de un basculamiento al oeste producido por un apilamiento tectónico asociado a una deformación de piel fina con vergencia este. Si bien lo anterior es posiblemente correcto, ellos no consideran la influencia que podría haber ejercido la fase compresiva pre-Eoceno, favoreciendo a través de fallas previas la ubicación de la Cuenca de Abanico y la posterior inversión y propagación de la deformación hacia el este.

Si bien las evidencias documentadas en este trabajo son de suma importancia para poder caracterizar de mejor manera

la fase compresiva pre-Neógeno, también dan sustento a la existencia de una proto-Cordillera de los Andes en el Paleógeno (Charrier et al., 2009). Además, muestra la necesidad de cuantificar la influencia de las etapas de deformación previas para el mejor entendimiento de la evolución de la Cordillera de los Andes.

Agradecimientos

Este trabajo contó con el apoyo del proyecto FONDECYT 11085022 y 1120272 y UNESCO (IGCP 586Y).

Referencias

- Armijo, R., Rauld, R., Thiele, R., Vargas, G., Campos, J., Lacassin, R., and Kausel, E., 2010, The West Andean Thrust, the San Ramón Fault, and the seismic hazard for Santiago, Chile: *Tectonics*, v. 29, p. TC2007.
- Astaburuaga et al., 2012. Geología y estructura del límite Mesozoico-Cenozoico de la Cordillera Principal entre los 35°30' y 36° latitud Sur, Región del Maule, Chile. In Congreso Geológico Chileno, No 13, Actas electrónicas. Antofagasta.
- Charrier, R., Baeza, O., Elgueta, S., Flynn, J.J., Gans, P., Kay, S.M., Munoz, N., Wyss, A.R., and Zurita, E., 2002, Evidence for Cenozoic extensional basin development and tectonic inversion south of the flat-slab segment, southern Central Andes, Chile (33°-36°S.L.): *Journal of South American Earth Sciences* 15: 117-139.
- Charrier, R., Farias, M., and Maksaev, V., 2009, Evolución tectónica, paleogeográfica y metalógénica durante el Cenozoico en los Andes de Chile norte y central e implicaciones para las regiones adyacentes de Bolivia y Argentina: *Revista de la Asociación Geológica Argentina* 65: 05-35.
- Farias, M., Comte, D., Charrier, R., Martinod, J., David, C., Tassara, A., Tapia, F., and Fock, A., 2010, Crustal-scale structural architecture in central Chile based on seismicity and surface geology: Implications for Andean mountain building: *Tectonics* 29: 22.
- Fock, A., 2005, Cronología y tectónica de la exhumación en el Neógeno de los Andes de Chile Central entre los 33° y los 34°S. Tesis de Magíster (Unpublished), Universidad de Chile, Departamento de Geología: 235 p.
- Gana, P., and Zentilli, M., 2000, Historia termal y exhumación de intrusivos de la Cordillera de la Costa de Chile Central. In Congreso Geológico Chileno, No 9, Actas 2: 664-668. Puerto Varas.
- Giambiagi, L., Ghiglione, M., Cristallini, E., and Bottesi, G., 2009, Kinematic models of basement/cover interaction: Insights from the Malargüe fold and thrust belt, Mendoza, Argentina: *Journal of Structural Geology* 31: 1443-1457.
- Giambiagi, L.B., Ramos, V.A., Godoy, E., Alvarez, P.P., and Orts, S., 2003, Cenozoic deformation and tectonic style of the Andes, between 33 degrees and 34 degrees south latitude: *Tectonics* 22: 1041.
- Giambiagi, L.B., Tunik, M.A., and Ghiglione, M., 2001, Cenozoic tectonic evolution of the Alto Tunuyán foreland basin above the transition zone between the flat and normal subduction segment (33° 30' -34° S), western Argentina: *Journal of South American Earth Sciences* 14: 707-724.
- Godoy, E., Yáñez, G., and Vera, E., 1999, Inversion of an Oligocene volcano-tectonic basin and uplifting of its superimposed Miocene magmatic arc in the Chilean Central Andes: First seismic and gravity evidences: *Tectonophysics* 306: 217-236.
- González, O., and Vergara, M., 1962, Reconocimiento geológico de la Cordillera de los Andes entre los paralelos 35° y 38°S: Instituto Geología 24.
- Mescua, J., 2011, Evolución estrucutral de la Cordillera Principal entre las Choicas y Santa Elena (35°S). Provincia de Mendoza, Argentina. Tesis de Doctorado, Universidad de Buenos Aires: 254 p.
- Parada, M.A., Féraud, G., Fuentes, F., Aguirre, L., Morata, D., and Larrodo, P., 2005, Ages and cooling history of the Early Cretaceous Caleu pluton: testimony of a switch from a rifted to a compressional continental margin in central Chile: *Journal of the Geological Society* 162: 273-287.
- Ramos, V.A., 2010, The tectonic regime along the Andes: Present-day and Mesozoic regimes: *Geological Journal* 45: 2-25.
- Sagripanti, L., Naipauer, M., Alvarez, J., Kietzmann, D., Bottesi, G., Folguera, A., and Ramos, V.A., 2011, Análisis y comparación de las cuencas sinorogénicas Cretácicas y Neógenas en el frente orogénico andino entre los 36° y 37°S: Integración de resultados petrográficos y daraciones U/Pb en circones detriticos. In Congreso Geológico Argentino, No 18, Actas electrónicas. Neuquén.
- Tunik, M., Folguera, A., Naipauer, M., Pimentel, M., and Ramos, V.A., 2010, Early uplift and orogenic deformation in the Neuquén Basin: Constraints on the Andean uplift from U-Pb and Hf isotopic data of detrital zircons: *Tectonophysics* 489: 258-273.
- Waite, K., Fügenschuh, B., and Schmidt, S., 2005, Cosntraint from fission track analysis on the evolution of the Rio Tinguiririca valley area in the Main Cordillera of the Andes, Central Chile. In Congress Geoscience Meeting, No 3, Actas electrónicas. Zürich, Switzerland.



DEFORMACIÓN FUERA DE SECUENCIA EN EL SECTOR INTERNO DE LA FAJA PLEGADA Y CORRIDA DE MALARGÜE DURANTE EL MIOCENO SUPERIOR-PLEISTOCENO, CORDILLERA PRINCIPAL, CHILE (35°30'S)

Tapia, Felipe⁽¹⁾; Farias, Marcelo⁽¹⁾ y Naipauer, Maximiliano⁽²⁾

⁽¹⁾ Departamento de Geología, Universidad de Chile, Santiago, Chile. ftapia@ing.uchile.cl

⁽²⁾ Laboratorio de Tectónica Andina. Instituto de Estudios Andinos “Don Pablo Groeber”. Universidad de Buenos Aires, Argentina. Conicet. maxinaipauer@gl.fcen.uba.ar

En el Mioceno inferior, comenzó el principal evento contraccional en los Andes de Chile y Argentina Central, causante de la actual configuración de la cordillera y el cual se caracteriza por la constante migración de la deformación hacia el antepaís (*Giambiagi et al.*, 2003; *Ramos et al.*, 2004). Durante este periodo, se produjo la inversión tectónica de la Cuenca de Abanico y el inmediatamente posterior inicio del desarrollo de las fajas plegadas y corridas que identifican la vertiente oriental de la Cordillera Principal entre 32° y 36°S (*Ramos et al.*, 2004), las cuales acomodaron la mayor cantidad del acortamiento acumulado en esta región Andina (*Giambiagi et al.*, 2003; *Farias et al.*, 2010). La deformación en-secuencia fue interrumpida durante el Mioceno superior-Plioceno inferior por un evento fuera-de-secuencia que afectó a la parte interna de la faja plegada y corrida de Aconcagua (*Giambiagi et al.*, 2003), coincidente con la mayor etapa de alzamiento de la región (*Farias et al.*, 2010). Este trabajo tiene como objetivo mostrar evidencias de un evento de deformación fuera de secuencia equivalente en el sector interno de la faja plegada y corrida de Malargüe, al sur de 34°S.

En una amplia área de la región de estudio, afloran rocas sedimentarias agrupadas dentro de la unidad informal Estratos del Colorado (

Figura 1). Los depósitos corresponden a conglomerados, brechas y areniscas gruesas asociadas a un ambiente aluvial presentando un espesor observado máximo de 500 m en la localidad del Cerro Las Yeguas (

Figura 1). Esta unidad se encuentra deformada y fallada por la falla Llolli y el sistema de falla Calabozos (

Figura 1), el cual además corta a depósitos glaciares recientes. A partir de una muestra tomada en la parte superior de los Estratos del Colorado en el Cerro las Yeguas, se obtuvo una edad mínima U/Pb en minerales de circón detritico de 7 Ma (

Figura 1

Figura 1), lo que representa la edad máxima para el depósito de la unidad. Además, esta edad, junto con los datos encontrados en el campo, acotan la deformación de la falla Llolli y del Sistema de falla Calabozos entre el Mioceno superior y Pleistoceno, evidenciando el carácter fuera de secuencia de la deformación ya que en ese periodo existen evidencias de deformación en el antepaís asociadas al desarrollo del anticlinal Malargüe (*Silvestro et al.*, 2005) y el alzamiento del Bloque San Rafael (*Ramos y Folguera*, 2011), ambos representativos de la continua migración al este del frente de deformación.

Estas evidencias indican que la faja plegada y corrida de Malargüe también desarrolló un evento fuera de secuencia en el Neógeno superior, diferenciándose de la región de Aconcagua en que éste habría continuado hasta el Pleistoceno, inclusive mostrando actividad reciente. Este periodo de deformación también concuerda con lo reportado en la región del río Maule, Región del Maule, Chile (*Astaburuaga et al.*, 2012), y más al sur en la faja plegada y corrida Guañacos, la cual presenta evidencias de deformación desde el Mioceno superior hasta el Cuaternario (*Folguera et al.*, 2006). En base a lo presentado en este trabajo, junto con lo reportado por otros autores, el evento fuera de secuencia parece ser una característica constante en el desarrollo de las fajas plegadas y corridas entre 33° y 37° S.

Si bien, se ha demostrado que la deformación fuera de secuencia en las fajas plegadas y corridas entre ambas regiones tendrían distintos orígenes (*Folguera et al.*, 2006; *Giambiagi et al.*, 2003), la correlación entre tasas de erosión de largo-plazo y la prolongación de la actividad hasta el Presente sugiere que la descarga de material por erosión ejerce un gran control en la dinámica y cinemática de las fajas plegadas y corridas (*Willett*, 1999). En particular, las altas tasas de erosión podrían haber favorecido la localización y activación de deformación a lo largo de estructuras cercanas al *hinterland*, manteniéndola en el tiempo hasta el Presente, consistente con lo observado en modelos análogos y numéricos (*Cruz et al.*, 2011).

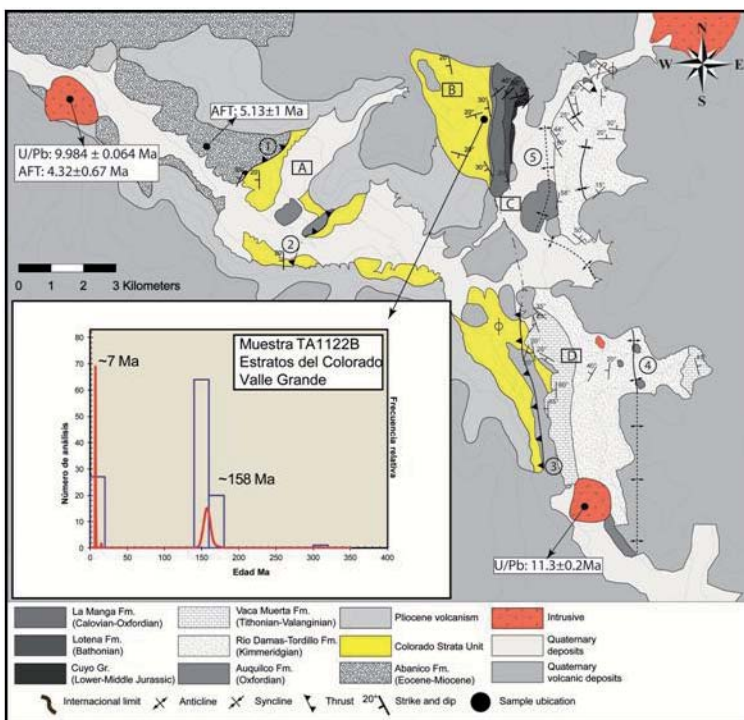


Figura 1: Mapa geológico del área de estudio mostrando la ubicación e histograma de la muestra analizada. En el mapa: 1: Falla El Novillo; 2: Falla LLollí; 3: Sistema de fallas Calabozos; 4: Anticlinal Debía; 5: Anticlinal Valle Grande; A: Quebrada El Novillo; B: Cerro Las Yeguas; C: Valle Grande; D: Cajón del Debía.

Bibliografía:

- Astaburuaga, D., M. Fariñas, R. Charrier, y F. Tapia (2012). Geología y estructuras del límite Mesozoico-Cenozoico de la Cordillera Principal entre 35°30' y 36°S, región del Maule, Chile. 13º Congreso Geológico Chileno, Antofagasta, Chile.
- Cruz, L., J. Malinski, M. Hernandez, A. Take, y G. Hillel (2011). Erosional control of the kinematics of the Aconcagua fold-and-thrust belt from numerical simulations and physical experiments. *Geology* 39(5): 439-442.
- Farias, M., D. Comte, R. Charrier, J. Martinod, C. David, A. Tassara, F. Tapia, y A. Fock (2010). Crustal-scale structural architecture in central Chile based on seismicity and surface geology: Implications for Andean mountain building. *Tectonics* 29: 22.
- Folguera, A., V. A. Ramos, E. F. González Díaz, y R. Hermanns (2006). Miocene to Quaternary deformation of the Guañacos fold-and-thrust belt in the Neuquén Andes between 37°S and 37°30'S. *Geological Society of America Special Papers* 407: 247-266.
- Giambiagi, L. B., V. A. Ramos, E. Godoy, P. P. Alvarez, y S. Orts (2003). Cenozoic deformation and tectonic style of the Andes, between 33 degrees and 34 degrees south latitude. *Tectonics* 22(4): 1041.
- Ramos, V. A., y A. Folguera (2011). Payenia volcanic province in the Southern Andes: An appraisal of an exceptional Quaternary tectonic setting. *Journal of Volcanology and Geothermal Research* 201(14): 53-64.
- Ramos, V. A., E. Zapata, E. Cristallini, y A. Introcaso (2004). The Andean thrust system-Litudinal variations in structural styles and orogenic shortening. En K. R. McClay (ed.) *Thrust tectonics and hydrocarbon system*, AAPG: 30-50.
- Silvestro, J., P. Kraemer, F. Achilli, y W. Brinkworth (2005). Evolución de las cuencas sinorogénicas de la Cordillera Principal entre 35°- 36° S, Malargüe. *Revista de la Asociación Geológica Argentina* 60: 627-643.
- Willett, S. D. (1999). Orogeny and orography: The effects of erosion on the structure of mountain belts. *Journal Geophysical Research* 104(B12): 28957-28981.



NUEVAS EDADES DE U-Pb EN CIRCONES DETRÍTICOS DEL BORDE OCCIDENTAL DE LA CUENCA NEUQUINA: EVIDENCIAS DE LA DINÀMICA DEL ARCO DEL JURÁSICO SUPERIOR

F. Tapia¹, M. Naipauer², M. Farías¹, J. Mescua³, M.M. Pimentel⁴, P. Rossel⁵, V. Oliveros⁵, V.A. Ramos²

¹ Departamento de Geología, Universidad de Chile, Santiago, Chile

² Instituto de Estudios Andinos "Don Pablo Groeber" (FCEN - UBA) and CONICET, Buenos Aires, Argentina

³ Centro Científico y Tecnológico CCT-Mendoza, Consejo Nacional de Ciencia y Tecnología (CONICET), Parque San Martín s/n, 5500 Mendoza, Argentina

⁴ Laboratorio de Geocronología, Universidad de Brasilia, Brasilia, Brasil

⁵ Departamento Ciencias de la Tierra, Facultad de Ciencias Químicas, Universidad de Concepción, Concepción, Chile.

El borde occidental de Gondwana en el Jurásico se caracterizó por una tectónica extensional en la cual se desarrolló un arco magmático en la actual Cordillera de la Costa en Chile (Charrier *et al.* 2007), y la cuenca de tras-arco de Neuquén hacia el este, la cual albergó más de 6000 m de sedimentos marinos y continentales con intercalaciones volcánicas. Recientes trabajos a lo largo de la región central y oriental de la Cuenca Neuquina han reconocido 3 principales fuentes para el relleno jurásico de la cuenca: Grupo Choiyoi (290-240 Ma), volcanismo Precuyano (230-200 Ma) y el arco magmático jurásico (200-145 Ma) (Naipauer *et al.* 2014). En este trabajo se presentan nuevas edades U-Pb en circones detriticos de secuencias jurásicas del borde occidental de la Cuenca Neuquina que muestran el absoluto predominio del arco como área de aporte conforme se asciende en el registro estratigráfico, lo cual podría evidenciar cambios en la dinámica de la construcción del arco magmático contemporáneo.

El área de estudio está ubicada en torno a 35°S y el sector fronterizo de Chile y Argentina (Fig. 1). Se recolectaron tres muestras pertenecientes a las formaciones Lotena, La Manga y Río Damas en la región del río Valle Grande, Chile (Fig. 1); una muestra de la Fm. Río Damas en el sector del río de las Damas, Chile (Fig. 1); dos muestras de la Fm. Tordillo en el área del río Atuel, Argentina (Fig. 1); y dos muestras de la Fm. Tordillo en la región del río Salado, Argentina (Fig. 1). Las dos muestras analizadas pertenecientes a las formaciones Lotena y La Manga muestran una variada distribución de edades donde los picos máximos corresponden a las edades asociadas al arco jurásico (162-200 Ma), destacando de forma secundaria las edades entre 200-220 Ma, 220-300 Ma y 300-330 Ma, indicando un aporte de las rocas del ciclo Precuyano, Gr. Choiyoi y una fuente carbonífera, respectivamente. Es posible identificar aportes occidentales desde el arco magmático jurásico, pero no se puede discriminar las regiones de procedencia de los picos del Precuyano y carboníferos debido a que las zonas de muestreo presentan afloramientos de dicha edad tanto al oeste como al noreste.

En las cuatro muestras pertenecientes a la Formación Tordillo (ríos Atuel y Salado) se puede observar en general distribuciones de edades similares, con la mayor frecuencia perteneciente a los picos de edades asociadas al arco jurásico (149-200 Ma) y de forma subordinada edades del Triásico Tardío, Permo-Triásico y Carbonífero Tardío. Por el contrario, las dos muestras de la Fm. Río Damas (ríos de las Damas y Valle Grande) muestran una distribución unimodal con edades en un rango entre 142-170 Ma que representan sólo aportes del arco magmático jurásico, con la muestra del río Valle Grande presentando edades más jóvenes (142 Ma) que la edad asignada en la literatura para la Formación Río Damas. Si bien esto es materia de mayor análisis y para un estudio más detallado, la posición estratigráfica sobre el yeso de la Fm. Auquilco (González y Vergara 1962) y bajo rocas sedimentarias marinas con fauna fósil del Titoniano (Tapia *et al.* 2011) indican que la secuencia que contiene a la muestra recolectada corresponde a la Fm. Río Damas. Edades U-Pb en circones detriticos en rocas cercanas al techo de la Fm. Río Damas en el río de las Damas (Fig. 1) muestran picos con edades similares (143 Ma) a las encontradas en Valle Grande indicando quizás que el límite superior de esta formación se extiende hasta el Titoniano Medio, siendo al menos 8 myr más joven que lo propuesto anteriormente.

Por otro lado, al integrar toda la información mostrada en este trabajo se puede observar que las muestras ubicadas en la región oeste de la Cuenca Neuquina evidencian un cambio en las fuentes de aporte sedimentario. En la Fm. Río Damas sólo existen aportes desde el arco jurásico contrastando con las muestras más antiguas (formaciones Lotena y La Manga) y con las muestras de las rocas contemporáneas ubicadas en el sector centro-oriental de la Cuenca. La exclusividad de fuente del arco magmático junto con la petrografía altamente volcánica en las muestras de la Fm. Río Damas evidenciarían que para ese tiempo (152-142 Ma), los centros volcánicos se habrían ubicado muy próximos a lo que hoy corresponde al borde occidental de la Cuenca Neuquina en la Cordillera Principal. La ubicación de este volcanismo podría corresponder a: 1) la expansión y/o migración del arco magmático respecto de la ubicación en la Cordillera de la Costa para el Jurásico Inferior y Medio (Charrier *et al.* 2007); o 2) volcanismo de tras-arco al este del arco magmático contemporáneo, similar a lo propuesto para

la Cuenca de Tarapacá (Oliveros *et al.* 2012). Sin embargo, son necesarios más estudios para poder discriminar entre una u otra hipótesis.

Este trabajo contó con el apoyo del proyecto FONDECYT 1120272.

- Charrier, R., Pinto, L., y Rodríguez, M. P. 2007. Tectonostratigraphic evolution of the Andean Orogen. En Moreno T. y Gibbons W. (eds) *The Geology of Chile*, Geol.Soc, Special Publications, 21–114, Londres.
- González O. y Vergara, M. 1962. Reconocimientos geológico de la Cordillera de los Andes entre los paralelos 35° y 38° S. Instituto de Geología 24, 70 p., Santiago.
- Naipauer, M., Tapia, F., Farías, M., Pimentel, M. M. y Ramos, V. 2014. Evolución Mesozoica de las áreas de aporte sedimentario en el sur de los Andes Centrales: El registro de las Edades U-Pb en circones. 19º Congreso Geológico Argentino, Actas electrónicas, Córdoba.
- Oliveros, V., Labbé, M., Rossel, P., Charrier, R. y Encinas, A. 2012. Late Jurassic paleogeographic evolution of the Andean back-arc basin: New constrains from the Lagunillas Formation, northern Chile (27°30'–28°30'S). Journal of South American Earth Sciences 37: 25–40.
- Tapia, F., Farías, M. y Rubilar, A. 2011. Depósitos marinos del Jurásico superior en el curso superior del río Colorado de Lontué (35°23'S), VII Región, Chile. 18º Congreso Geológico Argentino, Actas electrónicas, Neuquén.

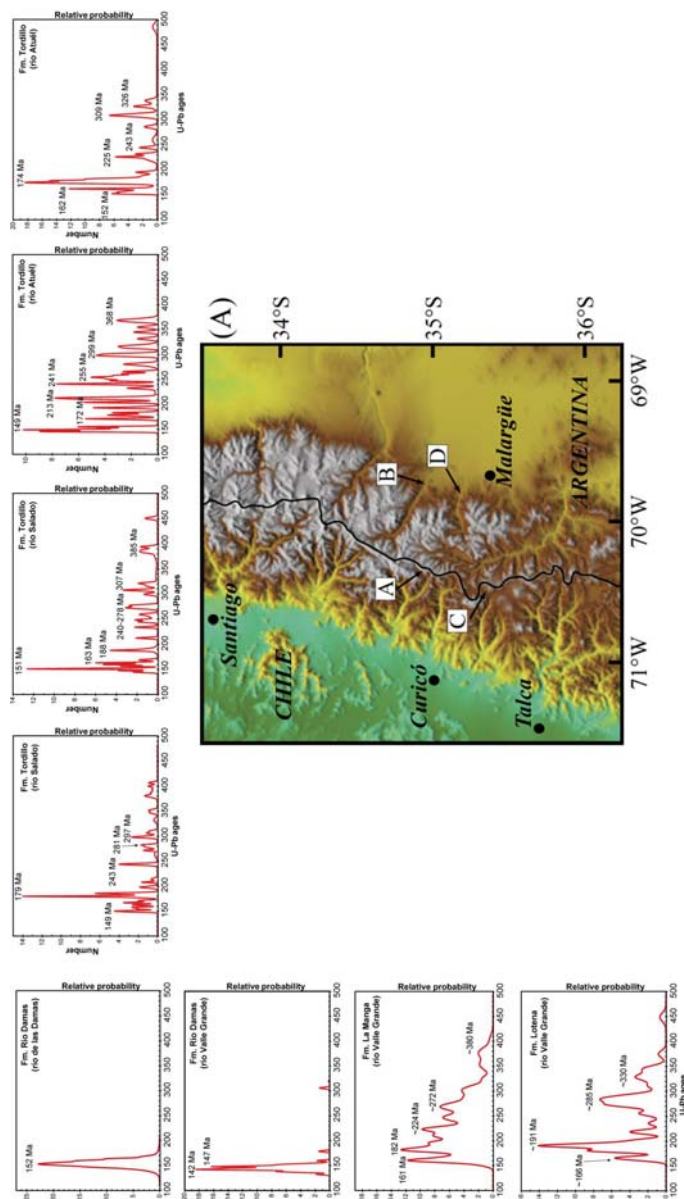


Figura 1: (A) Mapa de ubicación de los lugares donde fueron recolectadas las muestras. a) río de las Damas; b) río Atuel; c) río Salado; d) río Valle Grande. (B) Histogramas de probabilidad relativa de edades U-Pb.

Anexo III

Datos analíticos de dataciones U-Pb en circón

Anexo IV

Material suplementario Tapia et al. En prensa

Appendix A

LA-ICP-MS U-Pb Methodology

The LA-ICPMS method is now widely used for measuring U, Th and Pb isotopic data (e.g. Fryer et al. 1993; Compston 1999; Black et al. 2003; Kosler & Sylvester 2003, Black et al. 2004; Jackson et al. 2004, Chang et al. 2006 Harley & Kelly 2007).

The samples were analyzed in the Department of Geosciences, Arizona geochronology Center e Geochronology and thermochronology Lab, University of Arizona. The Isoprobe is equipped with an ArF Excimer laser ablation system, which has an emission wavelength of 193 nm. The collector configuration allows measurement of ^{204}Pb in an ioncounting channel while ^{206}Pb , ^{207}Pb , ^{208}Pb , ^{232}Th and ^{238}U are simultaneously measured with Faraday detectors. All analyses were conducted in static mode with a laser beam diameter of 35 microns, operated with output energy of w32 mJ (at 23 kV) and a pulse rate of 8 Hz. Each analysis consisted of one 12-s integration on peaks with no laser firing and twenty 1-s integrations on peaks with the laser firing. Hg contribution to the ^{204}Pb mass position was removed by subtracting on-peak background values. Inter-element fractionation was monitored by analyzing an in-house zircon standard (SL-2), which has a concordant ID-TIMS age of 563.5 \pm 3.2 Ma (2s) (Gehrels et al., 2008). This standard was analyzed once for every five unknowns. The lead isotopic ratios were corrected for common Pb, using the measured ^{204}Pb , assuming an initial Pb composition according to Stacey and Kramers (1975) and respective uncertainties of 1.0, 0.3 and 2.0 for $^{206}\text{Pb}/^{204}\text{Pb}$, $^{207}\text{Pb}/^{204}\text{Pb}$, and $^{208}\text{Pb}/^{204}\text{Pb}$. Age of standard, calibration correction from standard, composition of common Pb, decay constant uncertainty are grouped and are known as the systematic error. For these samples the systematic errors are around w1.2e1.7% for $^{206}\text{Pb}/^{238}\text{U}$ and w0.8e1.0 for $^{206}\text{Pb}/^{207}\text{Pb}$. Accordingly, the age probability plots used in this study were constructed using the $^{206}\text{Pb}/^{238}\text{U}$ age for young (<1.0 Ga) zircons and the $^{206}\text{Pb}/^{207}\text{Pb}$ age for older (>1.0 Ga) grains. In old grains, ages with $>30\%$ discordance or $>5\%$ reverse discordance are considered unreliable and were not used. Also analyses with error greater than 10% were rejected.

Table A.1**LA-ICP-MS data of zircons from TA11-22A and TA11-22B samples**

Sample/	Analysis	U (ppm)	Th/U	Isotope ratios				Apparent ages (Ma)				Best age	$\pm 1\sigma$ (Ma)
				$^{238}\text{U}/^{206}\text{Pb}$	$\pm 1\sigma$ (%)	$^{207}\text{Pb}/^{206}\text{Pb}$	$\pm 1\sigma$ (%)	$^{206}\text{Pb}/^{238}\text{U}$	$\pm 1\sigma$ (Ma)	$^{207}\text{Pb}/^{206}\text{Pb}$	$\pm 1\sigma$ (Ma)		
TA11-22B: Colorado Strata													
TA1122BDz-122		207.55	0.82	40.17	0.02	0.06	0.02	158.51	2.90	465.13	35.48	158.51	2.90
TA1122BDz-121		118.09	0.58	40.57	0.02	0.05	0.02	156.97	3.13	140.86	50.64	156.97	3.13
TA1122BDz-120		107.40	0.77	40.10	0.02	0.05	0.02	158.78	3.15	165.22	52.94	158.78	3.15
TA1122BDz-119		214.98	0.84	40.17	0.02	0.06	0.03	158.51	3.00	732.25	68.57	158.51	3.00
TA1122BDz-118		181.33	0.83	857.31	0.05	0.07	0.04	7.51	0.38	1063.87	87.63	7.51	0.38
TA1122BDz-116		165.99	0.87	39.90	0.02	0.05	0.02	159.59	2.99	142.84	44.12	159.59	2.99
TA1122BDz-115		200.89	0.77	39.56	0.02	0.05	0.02	160.94	2.81	365.01	41.95	160.94	2.81
TA1122BDz-114		515.91	0.77	888.86	0.03	0.05	0.04	7.25	0.19	384.71	90.30	7.25	0.19
TA1122BDz-113		135.42	0.70	39.70	0.02	0.05	0.02	160.37	3.23	218.01	43.44	160.37	3.23
TA1122BDz-112		129.20	0.61	38.96	0.02	0.05	0.02	163.38	3.31	250.36	42.29	163.38	3.31
TA1122BDz-111		471.85	0.96	813.06	0.05	0.09	0.08	7.92	0.40	1385.20	137.96	7.92	0.40
TA1122BDz-110		330.91	0.72	898.34	0.03	0.06	0.04	7.17	0.24	716.35	92.58	7.17	0.24

TA1122BDz-109	108.17	0.65	39.16	0.02	0.05	0.02	162.56	3.10	232.61	48.59	162.56	3.10	
TA1122BDz-108	356.52	0.80	812.09	0.03	0.11	0.03	7.93	0.23	1833.47	61.55	7.93	0.23	
TA1122BDz-107	202.79	0.88	39.90	0.02	0.05	0.02	159.56	3.01	213.01	43.28	159.56	3.01	
TA1122BDz-106	108.61	0.63	40.48	0.02	0.05	0.02	157.30	3.09	312.80	51.14	157.30	3.09	
TA1122BDz-104	127.41	0.73	40.60	0.02	0.05	0.02	156.84	3.09	212.19	47.73	156.84	3.09	
TA1122BDz-102	535.62	0.85	40.78	0.02	0.05	0.01	156.18	2.71	220.93	33.14	156.18	2.71	
TA1122BDz-101	93.30	0.60	41.62	0.02	0.05	0.02	153.05	3.58	199.45	54.27	153.05	3.58	
TA1122BDz-99	156.19	0.91	39.79	0.02	0.05	0.02	160.01	2.81	160.82	46.23	160.01	2.81	
TA1122BDz-98	145.90	0.86	40.92	0.02	0.05	0.02	155.65	3.07	202.72	45.60	155.65	3.07	
TA1122BDz-97	237.64	0.79	40.11	0.02	0.05	0.02	158.74	2.99	369.55	40.68	158.74	2.99	
TA1122BDz-96	198.15	0.59	39.47	0.02	0.05	0.02	161.31	2.93	198.57	34.72	161.31	2.93	
TA1122BDz-95	291.49	0.77	40.91	0.02	0.05	0.01	155.69	2.68	229.65	29.84	155.69	2.68	
TA1122BDz-94	450.24	0.93	902.25	0.03	0.06	0.04	7.14	0.23	418.37	91.04	7.14	0.23	
TA1122BDz-93	191.86	0.51	428.55	0.03	0.05	0.04	15.02	0.50	0.12	97.94	15.02	0.50	
TA1122BDz-92	145.13	0.95	40.93	0.02	0.06	0.02	155.62	2.93	559.27	39.27	155.62	2.93	
TA1122BDz-91	692.19	0.85	876.78	0.03	0.07	0.03	7.35	0.19	1021.12	60.79	7.35	0.19	
TA1122BDz-90	699.85	0.99	886.47	0.03	0.06	0.04	7.27	0.19	492.27	75.58	7.27	0.19	
TA1122BDz-89	131.91	0.91	39.64	0.02	0.05	0.02	160.62	3.42	191.12	48.09	160.62	3.42	
TA1122BDz-88	251.76	0.65	41.33	0.02	0.05	0.02	154.12	2.80	129.29	36.51	154.12	2.80	
TA1122BDz-87	1720.03	0.82	38.19	0.02	0.05	0.01	166.61	3.00	158.92	21.33	166.61	3.00	

TA1122BDz-86	143.46	0.93	39.17	0.02	0.06	0.02	162.50	3.01	561.69	44.31	162.50	3.01	
TA1122BDz-85	190.79	1.01	41.24	0.02	0.05	0.02	154.46	3.03	225.18	38.16	154.46	3.03	
TA1122BDz-84	150.17	0.80	42.00	0.02	0.05	0.02	151.70	2.86	267.77	43.00	151.70	2.86	
TA1122BDz-83	211.70	1.08	41.79	0.02	0.05	0.02	152.44	3.14	208.97	36.21	152.44	3.14	
TA1122BDz-82	182.94	1.07	40.83	0.02	0.05	0.02	155.97	2.88	204.76	41.26	155.97	2.88	
TA1122BDz-81	119.58	0.77	40.51	0.02	0.05	0.02	157.21	3.20	249.28	44.83	157.21	3.20	
TA1122BDz-80	123.81	0.73	41.14	0.02	0.06	0.02	154.82	2.91	467.21	47.73	154.82	2.91	
TA1122BDz-79	203.90	1.16	41.94	0.02	0.05	0.02	151.90	2.82	136.76	39.59	151.90	2.82	
TA1122BDz-78	297.77	0.84	41.29	0.02	0.05	0.01	154.27	2.95	211.94	32.06	154.27	2.95	
TA1122BDz-77	134.85	0.83	40.20	0.02	0.05	0.02	158.39	3.15	237.99	47.28	158.39	3.15	
TA1122BDz-76	160.93	0.67	41.56	0.02	0.05	0.02	153.27	2.82	159.75	43.17	153.27	2.82	
TA1122BDz-74	124.51	0.92	40.33	0.02	0.05	0.02	157.91	2.97	207.86	45.68	157.91	2.97	
TA1122BDz-73	295.31	0.90	924.49	0.04	0.09	0.05	6.97	0.27	1496.76	93.41	6.97	0.27	
TA1122BDz-72	2526.65	1.40	38.78	0.02	0.05	0.01	164.13	2.65	154.88	19.46	164.13	2.65	
TA1122BDz-71	130.97	0.88	40.92	0.02	0.05	0.02	155.63	3.13	202.04	43.32	155.63	3.13	
TA1122BDz-70	81.69	0.78	40.54	0.02	0.05	0.03	157.08	3.49	276.45	56.73	157.08	3.49	
TA1122BDz-69	86.68	0.62	41.04	0.02	0.05	0.02	155.20	3.39	305.34	55.06	155.20	3.39	
TA1122BDz-68	220.01	0.55	20.64	0.02	0.05	0.01	304.93	5.66	388.15	29.07	304.93	5.66	
TA1122BDz-67	101.12	0.66	40.61	0.02	0.05	0.02	156.81	3.16	203.71	51.57	156.81	3.16	
TA1122BDz-66	112.77	0.81	39.89	0.02	0.05	0.02	159.61	3.03	124.14	51.33	159.61	3.03	

TA1122BDz-65	370.24	0.76	40.85	0.02	0.05	0.01	155.90	2.67	225.51	32.25	155.90	2.67	
TA1122BDz-64	100.23	0.67	39.35	0.02	0.05	0.02	161.80	3.10	205.59	50.79	161.80	3.10	
TA1122BDz-61	315.28	0.94	42.13	0.02	0.05	0.01	151.21	2.55	205.31	32.05	151.21	2.55	
TA1122BDz-59	211.21	0.86	41.62	0.02	0.05	0.02	153.07	2.59	185.72	39.39	153.07	2.59	
TA1122BDz-58	96.73	0.74	39.98	0.02	0.05	0.02	159.27	3.03	128.40	49.76	159.27	3.03	
TA1122BDz-56	107.40	0.72	39.54	0.02	0.05	0.02	161.02	3.10	151.72	48.54	161.02	3.10	
TA1122BDz-55	233.48	0.78	899.74	0.04	0.07	0.05	7.16	0.27	933.12	89.78	7.16	0.27	
TA1122BDz-53	124.81	0.98	41.11	0.02	0.05	0.02	154.95	2.81	182.27	45.84	154.95	2.81	
TA1122BDz-52	235.47	0.77	41.86	0.02	0.05	0.02	152.20	2.70	217.72	35.50	152.20	2.70	
TA1122BDz-51	109.04	0.61	40.12	0.03	0.06	0.03	158.71	3.95	768.29	57.04	158.71	3.95	
TA1122BDz-49	744.89	0.83	942.99	0.03	0.06	0.03	6.83	0.17	586.67	72.54	6.83	0.17	
TA1122BDz-48	152.53	0.88	40.98	0.02	0.05	0.02	155.43	2.91	154.11	46.95	155.43	2.91	
TA1122BDz-46	181.05	0.88	41.79	0.02	0.05	0.02	152.44	2.67	269.83	38.74	152.44	2.67	
TA1122BDz-45	375.75	0.88	849.04	0.03	0.08	0.05	7.59	0.26	1076.45	88.42	7.59	0.26	
TA1122BDz-43	121.58	0.56	42.24	0.03	0.05	0.03	150.84	5.07	325.10	64.33	150.84	5.07	
TA1122BDz-42	720.63	0.94	900.43	0.03	0.06	0.03	7.16	0.20	479.43	73.16	7.16	0.20	
TA1122BDz-40	171.86	0.99	40.79	0.02	0.05	0.02	156.11	2.92	190.53	42.04	156.11	2.92	
TA1122BDz-38	102.15	0.64	40.90	0.02	0.05	0.02	155.70	3.23	256.33	52.37	155.70	3.23	
TA1122BDz-37	342.45	1.21	40.34	0.02	0.05	0.01	157.85	2.75	235.07	32.59	157.85	2.75	
TA1122BDz-36	563.12	0.90	921.44	0.03	0.05	0.04	6.99	0.18	116.02	87.72	6.99	0.18	

TA1122BDz-35	143.47	0.96	40.36	0.02	0.05	0.02	157.77	3.13	157.57	42.79	157.77	3.13	
TA1122BDz-34	375.05	0.84	858.66	0.04	0.09	0.05	7.50	0.31	1361.72	85.96	7.50	0.31	
TA1122BDz-33	244.51	0.75	42.43	0.02	0.05	0.01	150.15	2.62	171.04	34.35	150.15	2.62	
TA1122BDz-32	127.69	0.73	42.51	0.02	0.06	0.02	149.90	2.81	443.52	40.88	149.90	2.81	
TA1122BDz-31	783.17	0.71	948.06	0.03	0.05	0.03	6.80	0.18	40.23	78.46	6.80	0.18	
TA1122BDz-30	200.05	0.75	39.61	0.02	0.05	0.02	160.72	2.95	148.54	40.27	160.72	2.95	
TA1122BDz-29	570.20	0.90	895.99	0.03	0.05	0.04	7.19	0.19	312.27	82.32	7.19	0.19	
TA1122BDz-28	714.44	0.97	885.22	0.02	0.07	0.03	7.28	0.18	981.45	67.50	7.28	0.18	
TA1122BDz-27	723.04	0.90	870.59	0.03	0.09	0.03	7.40	0.19	1375.55	54.44	7.40	0.19	
TA1122BDz-26	807.87	0.92	893.17	0.02	0.06	0.03	7.21	0.17	520.72	70.02	7.21	0.17	
TA1122BDz-25	240.41	0.87	39.99	0.02	0.05	0.02	159.20	2.63	143.76	35.19	159.20	2.63	
TA1122BDz-24	694.26	0.98	906.22	0.03	0.05	0.04	7.11	0.19	137.41	80.66	7.11	0.19	
TA1122BDz-23	126.57	0.81	40.12	0.02	0.05	0.02	158.70	2.98	97.93	46.43	158.70	2.98	
TA1122BDz-22	144.15	0.92	865.26	0.05	0.09	0.05	7.45	0.34	1335.04	96.90	7.45	0.34	
TA1122BDz-21	188.28	1.01	41.03	0.02	0.05	0.02	155.23	2.88	196.19	39.56	155.23	2.88	
TA1122BDz-20	153.18	0.87	40.34	0.02	0.05	0.02	157.87	2.84	210.69	41.73	157.87	2.84	
TA1122BDz-19	154.66	0.96	40.08	0.02	0.05	0.02	158.87	2.87	107.35	45.67	158.87	2.87	
TA1122BDz-18	88.41	0.90	40.58	0.02	0.05	0.02	156.93	3.01	115.57	54.25	156.93	3.01	
TA1122BDz-17	131.44	0.66	40.25	0.02	0.05	0.02	158.19	2.88	206.90	43.22	158.19	2.88	
TA1122BDz-16	104.11	0.77	40.48	0.02	0.05	0.02	157.33	3.08	129.27	51.75	157.33	3.08	

TA1122BDz-15	77.55	0.72	40.41	0.02	0.05	0.03	157.57	3.44	254.74	62.62	157.57	3.44	
TA1122BDz-14	123.02	0.98	40.94	0.02	0.05	0.02	155.56	2.83	140.37	48.02	155.56	2.83	
TA1122BDz-13	94.69	0.81	40.97	0.02	0.05	0.02	155.44	2.94	166.89	55.01	155.44	2.94	
TA1122BDz-12	141.58	0.91	39.79	0.02	0.05	0.02	160.02	3.19	349.54	37.78	160.02	3.19	
TA1122BDz-11	116.81	1.04	39.85	0.02	0.05	0.02	159.78	3.07	111.03	48.48	159.78	3.07	
TA1122BDz-10	200.11	0.52	40.06	0.02	0.05	0.02	158.94	2.73	233.60	38.69	158.94	2.73	
TA1122BDz-9	150.66	0.67	39.75	0.03	0.05	0.03	160.19	4.07	128.06	79.89	160.19	4.07	
TA1122BDz-8	400.61	0.95	40.14	0.02	0.05	0.01	158.64	2.68	233.27	29.94	158.64	2.68	
TA1122BDz-7	120.03	0.65	41.06	0.02	0.05	0.02	155.13	2.98	128.37	50.11	155.13	2.98	
TA1122BDz-6	739.51	0.92	860.97	0.03	0.09	0.04	7.48	0.26	1498.95	68.08	7.48	0.26	
TA1122BDz-5	199.39	1.33	39.68	0.02	0.05	0.02	160.46	2.94	188.44	36.31	160.46	2.94	
TA1122BDz-4	265.05	0.85	40.96	0.02	0.05	0.01	155.49	2.65	117.75	33.86	155.49	2.65	
TA1122BDz-3	752.46	1.00	905.76	0.03	0.05	0.04	7.11	0.18	381.68	86.95	7.11	0.18	
TA1122BDz-2	405.20	0.88	890.78	0.04	0.05	0.05	7.23	0.27	215.01	118.08	7.23	0.27	
TA1122BDz-1	686.16	0.87	42.27	0.02	0.05	0.01	150.75	2.57	173.47	27.42	150.75	2.57	
TA1122BDz-1	212.48	1.15	924.84	0.04	0.09	0.05	6.97	0.30	1359.09	101.21	6.97	0.30	
TA11-22A: Boulder sized granite fragment													
TA22A_34	304.72	1.03	40.86	0.04	0.06	0.02	155.86	5.44	475.23	44.59	155.86	5.44	
TA22A_33	707.16	1.32	40.78	0.02	0.05	0.01	156.18	2.85	198.79	28.22	156.18	2.85	

TA22A_32	301.68	1.01	41.32	0.02	0.05	0.02	154.16	3.31	184.65	37.29	154.16	3.31	
TA22A_31	179.43	0.70	40.32	0.03	0.05	0.02	157.95	3.97	134.53	41.97	157.95	3.97	
TA22A_30	118.35	0.92	39.92	0.02	0.05	0.02	159.48	3.59	113.82	50.92	159.48	3.59	
TA22A_29	281.04	0.65	41.82	0.02	0.05	0.02	152.34	3.06	175.73	38.72	152.34	3.06	
TA22A_28	134.71	0.69	41.69	0.02	0.05	0.02	152.79	3.35	198.72	47.76	152.79	3.35	
TA22A_27	136.02	0.65	41.50	0.02	0.05	0.02	153.48	3.29	151.18	47.37	153.48	3.29	
TA22A_24	137.85	0.65	41.44	0.03	0.05	0.02	153.72	4.07	127.64	50.56	153.72	4.07	
TA22A_23	162.60	0.59	40.97	0.02	0.05	0.02	155.47	3.21	178.27	43.47	155.47	3.21	
TA22A_22	168.71	0.72	41.21	0.02	0.05	0.02	154.57	3.36	117.98	44.22	154.57	3.36	
TA22A_21	171.43	0.70	40.44	0.02	0.05	0.02	157.48	3.34	194.36	44.71	157.48	3.34	
TA22A_20	718.72	0.32	19.08	0.02	0.05	0.01	329.31	6.00	307.23	23.84	329.31	6.00	
TA22A_19	162.33	0.75	40.50	0.02	0.11	0.03	157.25	3.24	1715.39	52.87	157.25	3.24	
TA22A_18	186.86	0.73	40.86	0.02	0.05	0.02	155.86	3.29	258.51	40.79	155.86	3.29	
TA22A_17	163.75	0.64	41.58	0.02	0.05	0.02	153.19	3.22	147.01	43.82	153.19	3.22	
TA22A_16	231.72	0.66	40.61	0.02	0.06	0.02	156.81	3.15	630.29	42.22	156.81	3.15	
TA22A_15	143.62	0.72	39.95	0.02	0.05	0.02	159.37	3.46	166.28	45.09	159.37	3.46	
TA22A_14	185.40	0.65	41.05	0.02	0.05	0.02	155.14	3.13	223.34	40.27	155.14	3.13	
TA22A_13	130.22	0.63	40.98	0.02	0.05	0.02	155.41	3.24	177.00	49.70	155.41	3.24	
TA22A_12	159.95	0.90	40.01	0.02	0.05	0.02	159.14	2.94	143.22	45.84	159.14	2.94	
TA22A_11	113.00	0.59	41.01	0.02	0.05	0.02	155.31	3.05	246.00	50.57	155.31	3.05	

TA22A_10	69.47	0.52	41.90	0.04	0.05	0.08	152.05	5.87	106.51	171.79	152.05	5.87
TA22A_9	103.05	0.71	41.65	0.02	0.05	0.02	152.94	3.03	192.21	53.12	152.94	3.03
TA22A_8	151.99	0.83	40.93	0.02	0.05	0.02	155.60	3.14	200.28	50.25	155.60	3.14
TA22A_7	214.02	0.79	40.60	0.02	0.05	0.02	156.86	2.91	206.14	39.79	156.86	2.91
TA22A_5	84.62	0.61	40.57	0.02	0.05	0.03	156.98	3.39	205.52	59.66	156.98	3.39
TA22A_4	161.27	0.80	40.21	0.02	0.05	0.02	158.35	2.90	229.88	42.31	158.35	2.90
TA22A_2	115.36	0.56	40.57	0.02	0.05	0.02	156.98	3.25	196.53	51.04	156.98	3.25
TA22A_1	139.60	0.66	40.81	0.02	0.05	0.02	156.06	3.12	297.95	44.65	156.06	3.12

Appendix B

CA-TIMS U-Pb Methodology

Zircon and other U-bearing silicates are separated from bulk rock samples by standard crushing, heavy liquid, and magnetic separation techniques, and are subsequently handpicked under the binocular microscope based on clarity and crystal morphology. In order to overcome the effects of radioactive decay induced crystal defects and associated lead-loss resulting in discordant analyses, zircon grains are pre-treated in one of two ways. Conventional removal of crystal rims is accomplished by abrasion with pyrite inside air-abrasion vessels (Krogh, 1982). Alternatively, the zircon grains are treated by a new method of thermal annealing and chemical leaching (Mattinson, 2003). This method involves heating of zircon inside a furnace at 900°C for 60 hours. The annealed grains are subsequently loaded into FEP Teflon® microcapsules and leached in concentrated HF at 180°C within high-pressure vessels for 12 hours. The partially dissolved sample is then transferred into Savillex® FEP beakers for rinsing. The leached material is decanted with several milliliters of ultra-pure water and by fluxing successively with 4N HNO₃ and 6N HCl on a hot plate and/or in an ultrasonic bath. Air-abraded zircons are cleaned in a similar fashion by fluxing in 4N HNO₃ on the hot plate and in the ultrasonic bath in order to remove surface contaminants. After final rinsing of both air-abraded and annealed/leached zircons with ultra-pure water, zircon grains are loaded back into their microcapsules, spiked with a mixed ²⁰⁵Pb-²³³U-²³⁵U tracer solution and dissolved completely in concentrated HF at 220°C for 48-60 hours. Essentially the high-U parts of the zircon crystals that are associated with Pb-loss are preferentially removed leaving a residue of relatively low U content. After extensive testing we have concluded that this method is the best possible way to obtain the most concordant analyses.

Table B.1

CA TIMS data of zircons from RC-06, RC-08 samples.

Sample fraction (a)	Pb(c) (pg)	Pb*/Pb (b)	Th/U	$^{206}\text{Pb}/^{204}\text{Pb}$ (c)	$^{208}\text{Pb}/^{206}\text{Pb}$ (d)	$^{206}\text{Pb}/^{238}\text{U}$ (e)	$\pm 2\sigma$ (%)	$^{207}\text{Pb}/^{235}\text{U}$ $\pm 2\sigma$ (%)	$^{207}\text{Pb}/^{206}\text{Pb}$ (e)	$\pm 2\sigma$ (%)	$^{206}\text{Pb}/^{238}\text{U}$ (Ma)	$^{207}\text{Pb}/^{235}\text{U}$ (Ma)	$\pm 2\sigma$ (Ma)	
RC-06: Rio Negro pluton														
z1	1.37	5.46	0.85	317.96	0.27	0.002	0.22	0.01	2.96	0.05	2.79	10.21	10.26	0.77
z2	0.95	6.12	0.76	360.33	0.26	0.002	0.16	0.01	2.24	0.05	2.11	9.97	10.45	0.82
z3	0.83	7.61	0.84	434.23	0.28	0.002	0.16	0.01	1.91	0.05	1.81	9.88	10.23	0.68
z5	0.72	18.02	0.47	1103.94	0.16	0.002	0.08	0.01	0.76	0.05	0.72	9.99	10.29	0.56
RC-08: La Gallina pluton														
z1	1.79	3.44	0.99	201.87	0.33	0.001	0.18	0.01	2.41	0.05	2.28	8.69	8.88	0.75
z2	0.71	10.68	0.79	612.27	0.26	0.001	0.15	0.01	1.60	0.05	1.51	8.67	8.78	0.64
z4	3.65	4.77	0.94	278.30	0.30	0.001	0.10	0.01	1.08	0.05	1.02	8.69	8.75	0.62
z5	0.63	4.36	0.85	257.25	0.28	0.003	0.24	0.02	3.45	0.05	3.25	16.82	17.07	0.82

(a) Thermally annealed and pre-treated single zircon.

- (b) Total common-Pb in analyses.
- (c) Measured ratio corrected for spike and fractionation only.
- (d) Radiogenic Pb.
- (e) Corrected for fractionation, spike, blank, and initial common Pb.

Mass fractionation correction of $0.25\%/\text{amu} \pm 0.04\%/\text{amu}$ (atomic mass unit) was applied to single-collector Daly analyses.

Total procedural blank less than 0.5 pg for Pb and less than 0.1 pg for U.

Blank isotopic composition: $^{206}\text{Pb}/^{204}\text{Pb} = 18.31 \pm 0.53$, $^{207}\text{Pb}/^{204}\text{Pb} = 15.38 \pm 0.35$,
 $^{208}\text{Pb}/^{204}\text{Pb} = 37.45 \pm 1.1$.

Corr. coef. = correlation coefficient.

Age calculations are based on the decay constants of Steiger and Jäger (1977).

Common-Pb corrections were calculated by using the model of Stacey and Kramers (1975) and the interpreted age of the sample.

Table B.2**LA-ICP-MS data of zircos from TA11-30 sample.**

Sample/ Analysis	U (ppm)	Th/U	Isotope ratios				Apparent ages (Ma)				Best age	$\pm 1\sigma$ (Ma)	
			$^{238}\text{U}/^{206}\text{Pb}$	$\pm 1\sigma$ (%)	$^{207}\text{Pb}/^{206}\text{Pb}$	$\pm 1\sigma$ (%)	$^{206}\text{Pb}/^{238}\text{U}$	$\pm 1\sigma$ (Ma)	$^{207}\text{Pb}/^{206}\text{Pb}$	$\pm 1\sigma$ (Ma)			
TA1130_34	399.79	1.16	593.96	0.03	0.05	0.04	10.84	0.32	388.98	81.23	10.84	0.32	
TA1130_33	2908.2	5	1.76	552.70	0.02	0.06	0.02	11.65	0.22	496.30	35.54	11.65	0.22
TA1130_32	754.18	1.51	549.75	0.02	0.08	0.03	11.72	0.29	1134.36	56.01	11.72	0.29	
TA1130_31	499.13	1.93	543.15	0.02	0.05	0.04	11.86	0.29	290.15	82.88	11.86	0.29	
TA1130_30	420.64	1.74	578.95	0.03	0.05	0.04	11.13	0.30	179.85	90.86	11.13	0.30	
TA1130_29	643.91	2.03	552.26	0.02	0.05	0.03	11.66	0.25	313.22	77.01	11.66	0.25	
TA1130_27	265.66	1.19	562.84	0.04	0.06	0.04	11.44	0.44	607.17	92.82	11.44	0.44	
TA1130_26	370.75	1.49	561.33	0.03	0.05	0.04	11.47	0.38	242.66	85.91	11.47	0.38	

TA1130_														
25	355.96	1.65	576.00	0.03	0.06	0.04	11.18	0.29	467.13	93.99	11.18	0.29		
TA1130_														
24	813.39	2.06	566.38	0.02	0.05	0.03	11.37	0.25	140.67	70.13	11.37	0.25		
TA1130_														
23	495.33	1.43	545.99	0.03	0.05	0.04	11.80	0.34	168.47	81.86	11.80	0.34		
TA1130_														
22	563.41	1.82	579.36	0.03	0.05	0.03	11.12	0.30	183.61	72.60	11.12	0.30		
TA1130_														
21	273.81	0.99	579.42	0.04	0.07	0.04	11.12	0.39	810.97	90.19	11.12	0.39		
TA1130_														
19	1161.3	7	1.55	556.91	0.02	0.05	0.03	11.56	0.24	250.38	61.81	11.56	0.24	
TA1130_														
18	301.51	1.27	537.78	0.03	0.06	0.04	11.98	0.41	514.75	94.65	11.98	0.41		
TA1130_														
17	453.87	1.41	593.63	0.03	0.07	0.03	10.85	0.29	840.60	70.28	10.85	0.29		
TA1130_														
16	681.08	1.44	552.84	0.02	0.05	0.03	11.65	0.28	321.18	74.40	11.65	0.28		
TA1130_														
15	1177.2	8	1.64	565.58	0.02	0.05	0.03	11.39	0.21	108.74	61.10	11.39	0.21	
TA1130_														
14	645.08	1.62	575.65	0.02	0.05	0.03	11.19	0.25	131.85	72.91	11.19	0.25		
TA1130_														
12	957.41	1.66	561.53	0.02	0.05	0.03	11.47	0.26	322.18	63.07	11.47	0.26		
TA1130_														
10	886.34	2.23	552.20	0.02	0.05	0.03	11.66	0.24	133.52	65.57	11.66	0.24		

TA1130_9	1468.12	0.49	608.93	0.03	0.06	0.04	10.58	0.35	583.88	90.97	10.58	0.35
TA1130_7	779.22	1.67	588.68	0.03	0.06	0.04	10.94	0.31	423.43	78.15	10.94	0.31
TA1130_6	745.45	2.07	584.15	0.02	0.05	0.03	11.03	0.23	139.93	70.61	11.03	0.23
TA1130_5	328.90	1.04	591.45	0.03	0.06	0.04	10.89	0.34	444.61	83.96	10.89	0.34
TA1130_4	446.70	1.23	570.82	0.02	0.05	0.04	11.28	0.28	279.60	86.80	11.28	0.28
TA1130_3	840.29	1.49	572.60	0.03	0.06	0.03	11.25	0.28	651.10	63.43	11.25	0.28
TA1130_2	686.32	1.68	565.95	0.02	0.05	0.03	11.38	0.26	334.77	66.52	11.38	0.26
TA1130_1	168.84	1.06	577.15	0.04	0.06	0.04	11.16	0.50	590.12	94.36	11.16	0.50

Appendix C

U/Th-He Dating Methodology

Most zircon (U-Th)/He ages were performed by Nd: YAG laser heating for He extraction, and sector ICP-MS for U-Th determinations, Apatite and Zircons inc. A few samples. Dated crystals were hand-picked from separates with high power ($160\times$) stereo-zoom microscopes with cross-polarization for screening inclusions. Selected crystals were measured and digitally photographed in at least two different orientations for α -ejection corrections. Crystals were loaded into 1-mm Pt foil tubes, which were then loaded into copper or stainless steel sample planchets with 20–30 sample slots. Planchets were loaded into a ~10-cm laser cell with sapphire (or ZnS for the CO₂ laser) window, connected by high-vacuum flexhose to the He extraction/measurement line. Once in the laser cell and pumped to $<10^{-7}$ – 10^{-8} torr, crystal-bearing foil tubes were individually heated using power levels of 1–5 W on the Nd:YAG, or 5–15 W on the CO₂ laser, for 3 min for apatite or 20 min for zircon. Temperatures of heated foil packets were not measured, but from experiments relating luminosity and step-wise degassing of apatite, we estimate typical heating temperatures of 1000°C for apatite. ⁴He blanks (0.05–0.1 femtomol ⁴He, after correction for spike ⁴He) were determined by heating empty foil packets using the same procedure. Crystals were checked for quantitative degassing of He by sequential reheating. Apatites rarely exhibited residual gas after the first degassing. Gas liberated from samples was processed by: 1) spiking with ~0.4 pmol of ³He, 2) cryogenic concentration at 16K on a charcoal trap (condensation time calibrated for no significant ⁴He/³He fractionation), and purification by release at 37K, and 3) measurement of ⁴He/³He ratios (corrected for HD and H₃ by monitoring H⁺) on a quadrupole mass spectrometer next to a cold Zr-alloy getter. All ratios were referenced to multiple same-day measured ratios and known volumes of ⁴He standards processed in the same way. Linearity of this standard referencing procedure has been confirmed over four orders of magnitude of ⁴He intensity. ⁴He standard reproducibility averages 0.2% on a daily and long-term (tank-depletion corrected) basis. Estimated 2 σ analytical uncertainty on sample He determinations, including precision and accuracy from original manometric ⁴He standard calibrations, is 1–2%.

After degassing, samples were retrieved from the laser cell, spiked with a calibrated ²²⁹Th and ²³³U solution, and dissolved. Apatites were dissolved in situ from Pt tubes in ~30% HNO₃ in Teflon vials. Each sample batch was prepared with a series of acid blanks and spiked normals to check the purity and calibration of the reagents and spikes. Spiked solutions were analyzed as 0.5 mL of ~1–5 ppb U-Th solutions by isotope dilution on a Finnigan Element2 ICP-MS with a Teflon micro-flow nebulizer and double-pass spray chamber. Routine in-run precisions and long-term reproducibilities of standard ²³²Th/²²⁹Th and ²³⁸U/²³³U are 0.1–0.4%, and uncertainty on sample U-Th contents are estimated to be 1–2% (2 σ). α -ejection was corrected using the method of Farley et al. (1996) and Farley (2002). Replicate analyses of Durango apatite and Fish Canyon Tuff zircon during the period of these analyses yielded mean ages of 32.4 ± 1.5 Ma (2 σ , $n = 42$) and 28.3 ± 2.3 Ma (2 σ , $n = 63$), respectively. On the basis of reproducibility of these and other intralaboratory standards, we estimate an analytical uncertainty of 6% for apatite in this study.

Table C.1
(U-Th)/He analyses of the RC-08, RC-06 and RC-05 samples

Sample	Unit	Rock type	Long ($^{\circ}$)	Lat ($^{\circ}$)	Elevation (m)	F_T	He (ncc)	U (ng)	Th (ng)	Age (Ma)	Error $\pm 1\sigma$ (Ma)	Corrected Age (Ma)	Error $\pm 1\sigma$ (Ma)
RC-05 (a)	Abanico Fm.	Tuff	-70.62	-35.35	1708	0.834	0.002	0.008	0.024	0.98	0.59	1.18	0.71
RC-05 (b)	Abanico Fm.		-	-	-	0.79	0.004	0.013	0.036	1.34	0.33	1.70	0.41
RC-06 (a)	Rio Negro pluton	Intrusive	-70.68	-35.33	1289	0.781	0.043	0.075	0.161	3.09	0.10	3.96	0.13
RC-06 (b)	Rio Negro pluton	Intrusive	-	-	-	0.778	0.051	0.1	0.176	2.91	0.08	3.74	0.10
RC-08 (a)	La Gallina pluton	Intrusive	-70.83	-35.31	1023	0.808	0.032	0.047	0.154	3.08	0.09	3.82	0.12
RC-08 (b)	La Gallina pluton	Intrusive	-	-	-	0.676	0.005	0.008	0.027	2.57	0.47	3.81	0.70

Anexo V

Ubicación muestras datadas

Codigo	Unidad o Fm.	Litología	Coordenadas				
			este (m)	norte (m)	lat. (°)	lon. (°)	alt. (m)
RC-05	Abanico	Toba	-	-	-70.62	-35.35	1805
RC-06	Río Negro	Granitoide	-	-	-70.68	-35.33	1278
RC-08	La Gallina	Granitoide	-	-	-70.83	-35.31	1003
TA11-03	Lotena	Arenisca	362031	6088591	-	-	2499
TA11-17	La Manga	Arenisca	361807	6085989	-	-	2477
TA11-22A/B	E. Colorado	Arenisca	360893	6087145	-	-	2885
TA11-30	Potrerillo	Granitoide	364401	6076239	-	-	2462
TF11-04	Río Damas	Arenisca	374390	6132709	-	-	2472
AR-09	Tordillo	Arenisca	-	-	69.69	34.96	1780
AR-11	Tordillo	Arenisca	-	-	69.77	35.20	1696
AR-15	Remoredo	Andesita	-	-	70.28	35.32	2009
Jt-RS-407	Tordillo	Arenisca	-	-	69.88	35.18	-
Jt-CC-429	Tordillo	Arenisca	-	-	69.76	35.00	-
FD12-02	A. Pichuante	Arenisca	359823	6107738	-	-	2552
FD12-03	BRCU	Arenisca	369175	6129736	-	-	1820
FD12-04	BRCU	Arenisca	368998	6129639	-	-	1932
FD12-05	BRCU	Arenisca	368946	6129789	-	-	1829
FD12-06	Colimapu	Arenisca	399426	6255721	-	-	-
FD13-01	Guanaco	Toba	-	-	34.93	70.46	1836
FD13-02	Abanico	Arenisca	-	-	34.94	70.45	1881